Microelectrochemical Transistors Based on Conjugated Organic Polymers: Chemistry, Electrochemistry, and Electronics of Molecule-Based Devices

by

Christopher H. McCoy

B.A. with Honors, Chemistry
Dartmouth College, Hanover, NH
(1987)

SUBMITTED TO THE DEPARTMENT OF CHEMISTRY IN PARTIAL FULFILLMENT OF THE REQUIREMENTS FOR THE DEGREE OF DOCTOR OF PHILOSOPHY

at the

MASSACHUSETTS INSTITUTE OF TECHNOLOGY

June 1995

Signature of Author_____
Department of Chemistry
April 5, 1995

Certified by_____
Mark S. Wrighton
Thesis Supervisor

Accepted by_____
Dietmar Seyferth
Chairman, Departmental Committee on Graduate Students

This doctoral thesis has been examined by a Committee of the Department of Chemistry as follows:

Professor Alan Davison_____
Chairman

Professor Mark S. Wrighton_____
Thesis Supervisor

Professor Robert J. Silbey_____

Microelectrochemical Transistors Based on Conjugated Organic Polymers: Chemistry, Electrochemistry, and Electronics of Molecule-Based Devices

by

Christopher H. McCoy

submitted to the Department of Chemistry on April 5, 1995 in
partial fulfillment of the requirements for the degree of
Doctor of Philosophy in Chemistry

Abstract

Chapter 1

An introduction to microelectrochemical transistors and to conductivity in conjugated polymers is presented. Transistor function in conducing polymer-based devices is explained and compared to that of the conventional MOSFET. The characterization of electrochemistry and conductivity in conjugated organic polymers using microelectrode arrays is reviewed, and factors governing polymer properties are summarized briefly. The references section of the chapter includes the title of each publication cited.

Chapter 2

Characterization of the transconductance, I_D-V_G, and I_D-V_D behavior of polyaniline-based microelectrochemical transistors is reported for a range of values for V_D. The transconductance, I_D-V_G, and especially I_D-V_D characteristics of microelectrochemical transistors are significantly affected by both the magnitude and polarity of drain voltage. The behavior of a microelectrochemical transistor in which a single electrode serves as both source and gate differs markedly from a device in which a separate gate electrode is used. It is found that a device will support drain current as long as one electrode maintains an electrochemical potential at which the device-active material is conducting, even if the other electrodes in contact with the active material are at electrochemical potentials where that material is insulating. The application of microelectrochemical transistors in electronic amplifiers is developed and demonstrated in the form of a polyaniline-based audio amplifier. The method for determination of power gain, consistent with the term as defined for transistors, is described. An improved configuration for power gain measurements at kilohertz frequencies is reported. The procedure for mounting microelectrode array chips onto headers for use in electrochemical experiments is described in the experimental section.

Chapter 3

An inverter gate based on a polyaniline microelectrochemical transistor displays high immunity to input signal noise derived from the characteristic hysteresis in the I_D-V_G response of polyaniline. The inverter is capable of functioning at input signal to noise

ratios of less than 1:1. The design and operating principle of the inverter are described and the noise immunity interpreting in terms of the theoretical basis for hysteresis in conducting polymers. The significant enhancement of noise immunity by hysteresis in the transfer function of an inverter is demonstrated by comparison of the behavior of the polyaniline-based inverter to that of a hysteresis-free standard bipolar transistor inverter constructed such that it displayed a comparable transfer function. The I_D-V_G behavior of polyaniline was characterized in a number of different solvent and supporting electrolyte systems based on H_2O, CH_3CH, CH_3OH, $(CH_3)_3COH$, CH_2Cl_2, $(CH_3)_2SO$ and $LiClO_4$, H_2SO_4, $NaHSO_4$, KCl, $[n\text{-}Bu_4N]PF_6$ and combinations thereof. The specific extent and distribution of hysteresis over the I_D-V_G characteristic varied substantially from one solvent/electrolyte system to the next.

Chapter 4

Conjugated organic polymers display a finite potential window of conductivity yielding the unusual I_D-V_G characteristic of microelectrochemical transistors. This behavior, which is not observed in conventional transistors, yields unique opportunities which are developed as the basis of three families of electronic devices. **I.** The preparation and characterization of a microelectrochemical push-pull amplifier based on one polyaniline transistor and one poly(3-phenylthiophene) transistor which exploits the electrical properties of conducting polymers to achieve freedom from crossover distortion is reported. The two polymers posses I_D-V_G characteristics which overlap, yielding a transistor pair inherently free of the dead zone in response caused by the p-n junction barrier potential in solid state transistors which is the source of crossover distortion. The output waveform of the microelectrochemical push-pull amplifier demonstrates crossover distortion-free operation and is compared to that of the analogous bipolar-transistor based system. **II.** The design of a complementary inverter is described and executed with polyaniline and WO_3 microelectrochemical transistors. This inverter demonstrates operation of a microelectrochemical system without potentiostatic control and in a circuit which utilizes the electrochemical gating process in a configuration, avoiding restrictions that process can incur in multi-transistor circuits. The complementary microelectrochemical transistor inverter achieves true 3-terminal transistor operation and conventional ground-referenced inputs and outputs. **III.** Devices with novel transistor behavior derived from two or more component I_D-V_G characteristics are prepared. By selecting the appropriate degree of overlap between two separate I_D-V_G characteristics, a device in which a plateau region of drain current has been introduced at half of maximum I_D was prepared. This unusual transistor behavior is potentially significant as a molecule-based approach to multiple-state logic devices. A microelectrochemical ternary (3-state) inverter was demonstrated based on an I_D-V_G characteristic designed to be intrinsically suited to 3-state operation.

Chapter 5

Derivatives of 3-phenylthiophene were synthesized by the Ni(II)-catalyzed coupling of 3-bromothiophene and substituted phenylmagnesium bromides. Prepared were 3-(4-R-phenyl)-thiophene, R = methoxy, methyl, chloro, fluoro, trifluoromethyl; 3-(3-methoxyphenyl)-thiophene, 3-(3,5-bis-(trifluoromethyl)phenyl)-thiophene, and 3-(3,4,5-trifluorophenyl)-thiophene. The coupling reaction of 3,4,5-trifluorophenylmagnesium bromide and 3-bromothiophene proceeded in poor yield and pure product was not isolated. The novel 1,4-dithienyl-2,5-difluorobenzene was prepared by the coupling of 1,4-dibromo-2,5-difluorobenzene with 2-thienylmagnesium bromide using $Pd(P\text{Ø}_3)_4$ in 66% yield. Reaction of 1,4-diiodo- or 1,4-dibromo-tetrafluorobenzene with 2-thienylmagnesium bromide using either $Pd(P\text{Ø}_3)_4$ or $Ni(\text{Ø}_2P(CH_2)_3P\text{Ø}_2)Cl_2$ as catalyst gave mainly metal-halogen exchange products. Also prepared was 1,4-dithienylbenzene.

The electrochemistry of each derivative was characterized, and the potential for onset of conduction, relative conductivity, and polymerization characteristics for each of the 3-phenylthiophene polymers is given in Table 1. Both 1,4-dithienylbenzene and 1,4-dithienyl-2,5-difluorobenzene polymerized readily to give polymers of well-behaved electrochemistry. Both polymers showed a window of reductive as well as oxidative conductivity, with the difluoro derivative showing onset of conductivity 100 mV positive of the parent for both windows.

Chapter 6

The reactivity of conjugated organic polymers in electrophilic substitution reactions was examined for aniline, pyrrole, and thiophene-based polymers. Polyaniline displays potential-dependent nucleophilicity in its reaction with trifluoroacetic anhydride and is acylated at nitrogen to yield an insulating, electroinactive polymer. Conducting polyaniline is regenerated by basic hydrolysis. Polypyrrole also displays potential-dependent nucleophilicity in its reaction with trifluoroacetic anhydride but is acylated at the b-carbons to yield a conducting and electroactive polymer which displays onset of conduction 0.5 V positive of polypyrrole. Poly(3-methylthiophene) is chlorinated rapidly by Cl_2 resulting in a striking shift in its potential for onset of conduction from 0.43 to 1.18 V vs. Ag. The chlorinated polymer shows unusually stable electrochemistry to high anodic potentials in CH_3CN. The chlorination of polythiophene, poly(3,4-dimethylthiophene), and polyselenophene were also examined. A microelectrochemical memory device, based on the selective, potential-controlled trifluoroacetylation of polyaniline as the write step and basic hydrolysis to restore conductivity of the acylated memory elements as the erase step is demonstrated. Using the potential-dependent trifluoroacetylations of polyaniline and polypyrrole and the chlorination of poly(3-methylthiophene), the preparation of a 3-state microelectrochemical transistor and a push-pull amplifier with chemically tuned overlap and matched peak conductivity of I_D-V_G characteristics are demonstrated.

Section 6.1

The reaction of electrode-confined polyaniline with trifluoroacetic anhydride in acidified acetonitrile giving insulating and electroinactive trifluoroacetylated polyaniline has been studied by electrochemistry, reflectance IR, and microelectrochemistry. Variation of electrochemical potential from 0.2 V (reduced, most reactive) to 0.6 V (oxidized by 0.5 electrons per repeat unit, unreactive) vs SCE allows control of the reaction rate. Reaction of trifluoroacetic anhydride with aniline oligomers *N*-phenylphenylenediamine and *N, N'*-diphenylphenylenediamine is summarized. Reflectance IR following the potential-dependent growth of CO and CF_3 peaks for macroelectrode films of polyaniline treated with trifluoroacetic anhydride showed similar potential dependence of reactivity as conductivity measurements during trifluoroacetylation of polyaniline-derivatized microelectrode arrays. Polyaniline trifluoroacetylation was accompanied by a symmetric contraction of the potential window of electroactivity and conductivity, and eventual elimination of all conductivity. Trifluoroacetylation of polyaniline terminal amines, rapid at all potentials, does not detectably affect conductivity. Also examined by electrochemistry were the reactions of polyaniline with other anhydrides resulting in the reactivity order $(F_3CCO)_2O > (Cl_3CCO)_2O > (H_2ClCCO)_2O > (HCl_2CCO)_2O >> (H_3CCO)_2O$. IR through polyaniline electrodeposited onto optically transparent Au electrodes shows that essentially complete loss of polyaniline electroactivity occurs when ≈25% of nitrogens are trifluoroacetylated. Electroactivity and conductivity of trifluoroacetylated polyaniline may be recovered by hydrolysis in $K_2CO_3/CH_3OH/H_2O$ solution to regenerate polyaniline. A microelectrochemical erasable-programmable-read-only-memory device has been prepared and characterized in which three polyaniline transistors served as memory elements and selective trifluoroacetylation allowed writing of any 3-bit binary configuration of on and off

states. Hydrolytic de-acylation served as the erase process. A circuit was developed to provide the appropriate digital output. 5 sequential write/read/erase/rewrite steps were carried out on the device.

Section 6.2

Polypyrrole is trifluoroacetylated at the β-carbon sites of the pyrrole ring by trifluoroacetic anhydride. The trifluoroacetylated polypyrrole, which retains electrical conductivity, has a potential for onset of conduction 0.5 V positive of polypyrrole itself. Unlike polypyrrole, the trifluoroacetylated polymer is stable toward aerial oxidation of the reduced state, showing maintained I_D-V_G response after exposure to air. Polypyrrole displayed potential-dependent nucleophilicity. Polypyrrole, at -0.1 V vs Ag where it is fully reduced, is reactive toward trifluoroacetic anhydride. At +0.5 V, were it is partially oxidized, polypyrrole shows no evidence of reaction with the anhydride. Polypyrrole confined to Au electrodes was characterized before and after reaction with trifluoroacetic anhydride. The acylated polymer showed appearance of a CO band with ν_{CO} =1666 cm^{-1}. The trifluoroacetylation of 2,5-dimethylpyrrole, 1,2,5-trimethylpyrrole, and ethyl 3,4-diethyl-5-methyl-2-pyrrolecarboxylate were examined to evaluate the relative nucleophilicities of the pyrrole nitrogen versus the β-carbon sites. Trifluoroacetylation of 2,5-dimethylpyrrole with one equivalent of anhydride or with an excess yielded 3-trifluoroacetyl-2,5-dimethylpyrrole (ν_{CO} = 1678 cm^{-1}) as the major product. Full characterization of this previously unknown compound is reported. Trifluoroacetylation of the β-carbon was also observed for the reaction of 1,2,5-trimethylpyrrole with trifluoroacetic anhydride, while ethyl 3,4-diethyl-5-methyl-2-pyrrolecarboxylate showed low reactivity of nitrogen, as expected for the pyrrole family. Based on the CO stretching frequency observed for the polymer compared to that observed for 3-trifluoroacetyl-2,5-dimethylpyrrole and that reported[14] for N-trifluoroacetylpyrrole (1730 cm^{-1}), the reactivity of pyrrole β-carbons but relative inertness of the pyrrole nitrogen toward trifluoroacetylation under the reaction conditions used demonstrated for the three pyrrole derivatives, it is concluded that polypyrrole reacts with trifluoroacetic anhydride to yield the β-acylated product.

Section 6.3

The reaction of Cl_2 with poly(3-methylthiophene) in CCl_4 at -20°C was investigated by microelectrode conductivity measurements, cyclic voltammetry, and X-ray photoelectron spectroscopy. The chlorinated polymer retains electrical conductivity but displays a striking shift in onset of conduction: from 0.43 to 1.18V vs Ag, corresponding to introduction of ≈ 0.65 chlorine atoms per repeat unit, determined by XPS. Chlorine is proposed to substitute at the 4-position of the thiophene ring in poly(3-methylthiophene) based on the XPS results, the known chlorination patterns of the thiophene family, and the behavior upon chlorination of polythiophene and poly(3,4-dimethylthiophene) which were also characterized. Polythiophene exhibited a 450 mV positive shift in onset of conduction while poly(3,4-dimethylthiophene) showed mainly a rapid loss of conductivity with little shift in oxidation potential. This loss of conductivity, also seen in poly(3-methylthiophene) upon excessive chlorination, is proposed to arise from addition of Cl_2 across double bonds, breaking conjugation. The chlorination of polyselenophene was also examined and resulted in a 0.50 V positive shift in onset of conduction but with loss of most of the polymer conductivity. Control of the *in situ* chlorination of surface-confined poly(3-methylthiophene) yields a series of conducting polymers with potentials for onset of conductivity between 0.43 and 1.18V vs Ag wire. The surprisingly large 750 mV shift in onset of conductivity upon

chlorination is attributed to the combined steric and electron-withdrawing effects from introduction of a chloro substituent.

Section 6.4

Potential-dependent nucleophilicity of polypyrrole was used to allowed selectively trifluoroacetylate of one of two films of polypyrrole. Polypyrrole and β-trifluoroacetylated polypyrrole, which served as parallel source-drain conduction channels for a microelectrochemical transistor, display onset of conductivity 0.5 V apart resulting in more complex overall I_D-V_G behavior for the device and allowing introduction of a "step" at half of maximum drain current. The polypyrrole/β-trifluoroacetylated polypyrrole transistor demonstrates selective electrophilic substitution as an approach to novel I_D-V_G behavior in microelectrochemical transistors. A microelectrochemical push-pull amplifier based on trifluoroacetylated polyaniline and chlorinated poly(3-methylthiophene) has been prepared. Two I_D-V_G characteristics, chemically tuned to have the appropriate degree of overlap for a push-pull amplifier and to have matched peak drain current, were prepared by direct, *in situ* electrophilic substitution reactions on the two device-active materials. The overlap of I_D-V_G characteristics was established by chlorination of poly(3-methylthiophene) with Cl_2/CCl_4 provided a polymer with onset of conduction at 0.8 V vs. Ag. Trifluoroacetylation of polyaniline under electrochemical potential control was used to match the peak drain current of the polyaniline transistor to that of the chlorinated poly(3-methylthiophene) transistor. The pair of transistors was operated and characterized as a push-pull amplifier driving a 470Ω load resistance. These two results demonstrate the use of reaction chemistry in defining the electrical functions of a 3-state transistor and a push-pull amplifier.

Section 6.5

The reactions of polyaniline, polythiophene, and poly(3-methylthiophene) with XeF_2 in CH_3CN, poly(3-methylthiophene) with Br_2 in CH_2Cl_2 under UV irradiation, polyaniline with Cl_2 in CCl_4, and polythiophene under Friedel-Crafts alkylating and acylating conditions were examined. Polyaniline undergoes a decline in conductivity and a contraction of its finite window of conductivity upon reaction with XeF_2 or Cl_2 which closely parallels the effects of trifluoroacetylation on the polymer. Conductivity of chlorinated polyaniline was partially restored upon treatment with CH_3Li. Polythiophene and poly(3-methylthiophene) showed only loss of conductivity upon exposure to XeF_2 in CH_3CN with no change in potential for onset of conduction. Reaction of poly(3-methylthiophene) with Br_2 in CH_2Cl_2 under UV irradiation produced a 400 mV positive shift in onset of conductivity and a broadening of the polymer I_D-V_G characteristic. Reaction of polythiophene under Friedel-Crafts conditions did not produce any evidence of alkylation or acylation in the electrochemistry of the polymer. Attempts to lithiate poly(3-bromothiophene) using alkyllithium reagents and to methylate it with methylmagnesium chloride in the presence of $Ni(Ø_2P(CH_2)_3PØ_2)Cl_2$ were unsuccessful.

Chapter 7

The conjugated organic conductor, poly(2,5-dithienylpyridine), reacts with acid or with methyl trifluoromethanesulfonate to render the polymer completely insulating. The effect, presumed to be the result of quaternization of nitrogen, is reversible. Conducting poly(2,5-dithienylpyridine) can be regenerated by treatment of the protonated polymer with pyridine, and treatment of methylated polymer with $Ø_3P$ in refluxing CH_2Cl_2. The

conductivity of poly(2,5-dithienylpyridine), confined to microelectrode arrays, was switched off by exposure to 0.1 M F_3CCO_2H/CH_2Cl_2 or to HCl (g) and back on by exposure to 0.1 M pyridine/CH_2Cl_2. The cycle of protonation/deprotonation could be carried out repeatedly. Poly(2,5-dithienylpyridine) showed a decline of greater than a factor of 10^4 in conductivity upon exposure to F_3CCO_2H or HCl (g) for less than 10 s. Continuous scanning of the I_D-V_G characteristic of microelectrode-confined poly(2,5-dithienylpyridine) showed complete loss of response in under three 4 s scans upon introduction of HCl(g), demonstrating a high-gain sensor response. A polyaniline transistor, switched between its conducting and insulating states by O_2 and H_2, respectively, was configured to drive a Si bipolar junction transistor which in turn drove a light emitting diode. The circuit showed an overall gain of 6×10^5, 96% of the gain being provided by the polyaniline transistor. The hybrid circuit demonstrates the compatibility of microelectrochemical transistors with conventional semiconductor devices, and the incorporation of a conducting polymer transistor property, that of chemical sensitivity, into a practical application circuit.

Chapter 8

The designs of two circuits based on microelectrochemical transistors are developed based on the results in previous chapters of this thesis. First, a circuit which converts an input voltage into a two-digit binary number is developed based on three partially overlapping finite windows of high conductivity. This circuit is capable of carrying out both analog-to-digital conversion and translation of quaternary logic (4 levels) into binary logic (2-levels). Appropriate polymers for use as the three active materials, provided by the results reported in Chapter 5 and Chapter 6, are selected. Second, a design for a binary adder, capable of adding two one-bit binary numbers, is developed based on conventional logic gates implemented with microelectrochemical transistors. The design of the AND gate as well as the OR gate required by the adder circuit are also developed. The adder design, which uses polyaniline and WO_3 as the active materials, demonstrates a route to a digital function more complex than the single logic gates demonstrated in previous chapters.

Thesis Supervisor: Mark S. Wrighton

Title: Provost and CIBA-GEIGY Professor of Chemistry

Acknowledgements

I remember walking across the Green one afternoon at Dartmouth and thinking that the best outcome of the graduate school admissions process was to be accepted by MIT and to work for Mark Wrighton. I thank Mark for the opportunity to work in his group for the past seven years and for the well-funded and highly independent environment he provided. I have greatly enjoyed my research here and I cannot imagine that I would have found as great an experience anywhere else.

I thank my mother and my father for everything they have done to make this document possible. For letting me choose my career path with their support and encouragement, for their tolerance of the years it took to rid the floors of the last traces of manganese dioxide and graphite tracked all over the house from the basement, and for paying the bill to send me to Dartmouth.

When I was in eighth grade, I took a tour of the laboratories of Polaroid courtesy of Dr. Emmett McCaskill which went a long way in sparking my interest in electrochemistry and I thank him for taking the time to show me around. I have remembered that experience for years since.

My first formal experience with research was in the laboratories of Professor August Witt as summer employment (well, the D-plan version of it, anyway). I thank Professor Witt for all that I learned working for him. I also thank Doug Carlson who directed me when I first started, and Mike Wargo whom I worked for in the summer of '86. To Mike I say we will yet again cover a table at the Muddy with a forest of empty Miller Lite bottles.

In my senior year at Dartmouth it was my privilege and good fortune to carry out my undergraduate thesis research under the direction of Professor David Lemal. His encouragement, guidance, and contagious enthusiasm for chemistry made it a great pleasure to work for him and I thank him for all he taught me and for his interest in my development as a chemist. I thank my professors at Dartmouth for their dedication and talent as teachers and for the excellent chemistry education I received which has been invaluable to me at MIT. Three people from my youth who deserve special mention are David White, my fifth grade teacher; Edward Herlin, my tenth grade chemistry teacher, and Richard Bevilaqua who taught me electronics from eighth to twelfth grade.

The Wrighton group has been a great place to do research, especially in the old days when the labs were alive in the dead of night, the best time to run experiments. To Martin and Oaf, it has never be the same without you. I thank Larry Hancock, Clark Early, and Vince Cammarata for their help when I was new to the group. The Wrighton group was fortunate to have Hal van Ryswyck and Steve Colbran as visiting faculty members. Hal and Steve were a hell of a lot of fun to have in the group and I thank them for the benefit of their knowledge and experience. I thank the two group members I collaborated with, Ivan Lorkovic with whom the work in section 6.1 was a joint effort, and Larry Rozsnyai who obtained the XPS data presented in this thesis. I also thank Mike Wolf for the synthesis of 2,5-dithienylpyridine.

The work in Chapter 3 came about as a result of a discussion with Dr. Mark Hollis of MIT Lincoln Labs and I gratefully acknowledge him for valuable conversations. Thanks to Lee Ward and Joan LaValle at MIT Graphic Arts for their work on illustrations in this thesis.

For their interest in my progress and all that they have done to help me over the years my thanks to Alan Davison and Joe Dhosi. I thank Joe for his encouragement and support of my interest in science over many years and for all he has done on my behalf. Alan's influence and concern for students goes well beyond his own group. I thank Alan for his interest in my research, his advice and help throughout my time at MIT, and for his support when it came time to look for a job. It was an honor to be present at Alan's Bachelor Party, an event which will reign unequaled for a long time to come.

I shared my time here with many people that I thank for making the experience worthwhile. The Defenders of the Faith: Krissy Kreutzer, Chris Willoughby, and Mike Absalon. Larry "I gotta go to sleep, I gotta sleep RIGHT NOW" Rozsnyai, Joel Freundlich - one day you'll be able to smell phosphines again Joel, Ivan Lorkovic - a good friend and a great guy to work with, Mary Bailey - whose departure was a real loss to the group, Mike "Sparky" Reed, Chad "face it, I'll always be stronger, leaner, - and more modest, than you are" Mirkin who introduced me to lifting, Eric Lee for his Canadian Detachment, Tayhas Palmore because only she could be Tayhas, and Richard Giasson. I thank the members of the MIT Korean Karate Club. Tae Kwon Do has many rewards and I am particularly grateful for three friends I made through it: Chris Dennis, Brent Phillips, and Dave Gray.

Ronald R. Duff, Jr., a man who defies description. Ron was a great labmate and a defining influence in the Wrighton Group experience. His approach to life of hardened, practical, absolute sanity punctuated with spikes of explosive rancidity is really something to experience. Ron's neurochemistry may contain the most potent autocatalysis mechanism in existence. Foremost innovatör of his generation in english vocabulary and grammar, merciless proponent of the philosophy of *be ineffective - PAY THE PRICE*, Mastür of the highest order, and one of the best mechanics I have ever met, I salute you Ron. If they get any bigger, you'll never get them through you're garage door.

It was a pleasure to work with the crew of the undergraduate chemistry office as a teaching assistant, and even more fun to just stop in and say hi. Thanks to Launa Callender and Peter Floyd for letting me to wander into the office and inflict my need to goof off on them. To Melinda Cerny my profound gratitude for making that office the great place that it is, for her friendship, and for her combination of understanding and support balanced with firm-handed advice when I needed it.

To the people that have meant the most to me over the course of my time at MIT, I thank you for your friendship and for being the exceptional people you are. In a sort of chronological order, Dave Ofer, Martin Schloh, Ann Roseberry, Rob Toreki, Caroline Gil, Tim Gardner, Helen Tatistcheff, Linda Doerrer, Chris Dennis, Brent Phillips, and Barbara Erickson. I will never forget you.

Finally, a special acknowledgement to Dave Ofer. Hard-core member of the night shift, master of the SO_2 line, and a man of wisdom and extraordinary patience. Dave's doctoral research is an important foundation of the work described in this thesis. I have always referred to the finite window of high conductivity as "The Oferian behavior of conducting polymers". It was from Dave that I first learned about conducting polymers, what they were and why, how to make them, and how to work with them. I thank him for helping me get started and for all the invaluable guidance he provided over the years. For his friendship and his unfailing concern for my welfare at times when that was not an easy undertaking, Dave has my deepest gratitude. I will always remember what Dave said after a weekend of continuous fishing on Martha's Vinyard: "it's just as well, if we'd caught anything, it only would have violated the purity of the experience".

TABLE OF CONTENTS

ABSTRACT 3

ACKNOWLEDGEMENTS 9

TABLE OF CONTENTS 11

LIST OF FIGURES 15

LIST OF SCHEMES 24

LIST OF TABLES 29

CHAPTER 1 30

Introduction 31

Conducting polymers 31

Microelectrochemical transistors 34

References (with titles) 46

CHAPTER 2 58

Electrochemistry and Electrical Characteristics of Microelectrochemical Transistors

Introduction 60

Results and Discussion 63

Experimental Section 97

References 102

CHAPTER 3 103

An Inverter Gate with High Noise Immunity Based on a Polyaniline Microelectrochemical Transistor

Introduction 105

Hysteresis in conducting polymers 105

Logic gates 113

Results and Discussion 114

Experimental Section 158

References 159

CHAPTER 4 161

Finite Windows of High Conductivity Yield Unique Opportunities for Molecule-Based Devices: A Microelectrochemical Push-Pull Amplifier Based on Two Different Conducting Polymer Transistors, Devices with Novel Drain Current-Gate Voltage Characteristics, and Complementary Microelectrochemical Digital Logic

Introduction 163

Results and Discussion 171

Experimental Section 208

References 212

CHAPTER 5 214

The Synthesis of Substituted 3-Phenylthiophenes and 1,4-Dithienylbenzenes and their Polymers: Substituent Effects on Polymer Electrical Characteristics and on Monomer Reactivity in Anodic Polymerization

Introduction 216

Results and Discussion 221

Experimental Section 246

References 258

CHAPTER 6 261

Electrophilic Substitution Reactions of Conjugated Organic Polymers

Section 6.0 263

General Introduction to Chapter 6 264

References 269

Section 6.1 271

The Potential-Dependent Nucleophilicity of Polyaniline

Introduction 273

Results and Discussion 274

Experimental Section 311

References 314

Section 6.2 317

The Trifluoroacetylation and Potential-Dependent Nucleophilicity of Polypyrrole

Introduction 319

Reactivity of the pyrrole ring 320

Acylation reactions of pyrrole 323

Results and Discussion 326

Experimental Section 347

References 351

Section 6.3 353

The Chlorination of Poly(3-Methylthiophene)

Introduction 355

Results and Discussion 358

Experimental Section 382

References 385

Section 6.4 387

Chemically-Tuned Microelectrochemical Electronics: Using Reaction Chemistry in Defining Electrical Function

Introduction 389

Results 394

Discussion 412

Experimental Section 414

References 415

Section 6.5 416

Investigations of Other Reactions on Conducting Polymers

Introduction 418

Results and Discussion 418

Experimental Section 423

References 424

CHAPTER 7 425

The Effect of Quaternization of Nitrogen on the Charge Transport Properties of Poly(2,5-dithienylpyridine) and a Chemically-Gated Polyaniline Microelectrochemical/Silicon Bipolar Transistor Hybrid Circuit with Very High Gain.

Introduction 427

Results and Discussion 429

Experimental Section 446

References 449

CHAPTER 8 450

Design of Conducting Polymer Electronics: Analog-to-Digital Conversion, Quaternary to Binary Translation, and a Circuit for the Addition of Two Numbers

Introduction 452

Results and Discussion 453

References 464

LIST OF FIGURES

CHAPTER 1

Figure 1. 35
An n-channel metal-oxide semiconductor field-effect transistor.

Figure 2. 38
A microelectrochemical transistor

Figure 3. 39
A microfabricated array of 8 individually addressable band microelectrodes approximately 1.5 μm wide, 1.5 μm apart, and 80 μm long.

Figure 4. 40
Cyclic voltammetry and Drain current as a function of gate voltage (transistor characteristic) for a polyaniline-based microelectrochemical transistor. The device, as shown at the top of the figure, uses a commonly employed configuration where a single electrode serves as both source and gate connection.

CHAPTER 2

Figure 1. 64
I_D-V_G characteristic and device transconductance for a polyaniline transistor at V_D = 25 mV.

Figure 2. 66
I_D-V_G and transconductance characteristics for a polyaniline microelectrochemical transistor at V_D = 400 mV.

Figure 3. 69
Gate voltage, drain current, and gate current waveforms for a polyaniline microelectrochemical transistor.

Figure 4. 78
I_D-V_D behavior for a polyaniline microelectrochemical transistor using a combined gate/source electrode (Scheme V, configuration B) and with V_D applied positive side to the source, negative side to the drain.

Figure 5. 80
I_D-V_D behavior for a polyaniline microelectrochemical transistor using a combined gate/source electrode (Scheme V, configuration B) and with V_D applied negative side to the source, positive side to the drain.

Figure 6. 82
I_D-V_D behavior for a polyaniline microelectrochemical transistor using a separate gate electrode (Scheme V, configuration A).

Figure 7. 86
Transfer characteristic (output voltage as a function of input voltage) for a polyaniline microelectrochemical transistor with a 10 KΩ drain resistor at V_{DD} = 50, 300, 600 and 1000 mV. An output voltage of 0 corresponds to the fully conducting state of polyaniline, an output voltage of V_{DD} corresponds to the fully insulating state.

Figure 8. 88
Operation of a polyaniline transistor in the circuit shown in Figure 7 demonstrating response with reduced hysteresis.

Figure 9. 90
Transfer characteristic (output voltage as a function of input voltage) for a polyaniline microelectrochemical transistor with a 10 KΩ drain resistor at V_{DD} = -50, -300, and -600 mV. An output voltage of 0 corresponds to the fully conducting state of polyaniline, an output voltage of V_{DD} corresponds to the fully insulating state.

Figure 10. 92
Transfer characteristic (output voltage as a function of input voltage) for a polyaniline microelectrochemical transistor with a 10 KΩ drain resistor at V_{DD} = 500 mV scanned over the entire window of conductivity for polyaniline.

CHAPTER 3

Figure 1. 106
Drain Current-Gate Voltage (I_D-V_G) characteristic of a polyaniline transistor. 0.5 M H_2SO_4, V_D = 400 mV, 200 mV/s The unusually high potential for onset of oxidative insulation is due to the high value of drain voltage (400 mV) suitable for microelectrochemical logic gates. The arrows indicate the forward and return scan of V_G.

Figure 2. 115
Schematic (top) and output voltage as a function of input voltage (bottom, known as the *transfer function*) of an inverter gate based on a polyaniline microelectrochemical transistor. The arrows indicate the forward and return scans.

Figure 3. 119
Characterization of a microelectrochemical inverter based on a polyaniline microelectrochemical transistor operated in 0.5M H_2SO_4. Shown are the input voltage (top) a square wave switching between the gate potentials corresponding to logic LOW and logic HIGH, drain current through the circuit (middle), and output voltage.

Figures 4a - 4f: 123
Characterization of the noise immunity of an inverter gate based on a polyaniline microelectrochemical transistor using the circuit shown in Figure 2. The transistor was operated in 0.5 M H_2SO_4 with V_{DD} = 400 mV. Input waveforms were generated using the equipment configuration shown in Scheme VI.

Figure 5. 137
Transfer functions and assigned logic levels for a silicon bipolar transistor inverter (top) and a polyaniline transistor-based inverter (bottom). *Silicon-based inverter*: schematic shown Scheme VII, characterization of noise immunity shown Figures 6a-f. *Polyaniline-based inverter (described above)*: schematic shown Figure 2, characterization of noise immunity shown Figures 4a-f.

Figures 6a - 6f: 140
Characterization of the noise immunity of an inverter gate based on a standard silicon bipolar transistor using the circuit shown in Scheme VII. V_{CC} = 5 V Input waveforms were generated using the equipment configuration shown in Scheme VI.

Figure 7a-7d. 153
I_D-V_G characteristic of a polyaniline transistor in different solvent/electrolyte media showing variation in the specific character of hysteresis.

Figure 7e - 7g. 155
I_D-V_G characteristic of a polyaniline transistor in different solvent/electrolyte media showing variation in the specific character of hysteresis.

CHAPTER 4

Figure 1. 164
(top) Cross-sectional view of a microelectrochemical transistor. The electrodes are functionalized with a film of polymer by electropolymerization of the appropriate monomer. (bottom) I_D-V_G characteristic of a polythiophene transistor. The neutral (no shading) and highly oxidized (dark shading) states of the polymer film are insulating. High conductivity occurs in the partially oxidized state (medium shading).

Figure 2. 166
Log(I_D) as a function of gate potential for a polyaniline microelectrochemical transistor (solid line) and a theoretical MOSFET of comparable parameters showing the insulation to conduction transition for a MOSFET and the insulation to conduction to insulation transition of a conducting polymer-based microelectrochemical transistor.

Figure 3. 172
Schematic and output waveform of a silicon bipolar push-pull amplifier. The distortion as the output crosses zero is due to the 0.6V p-n junction barrier potential in the silicon devices.

Figure 4. 177
Cyclic voltammogram and I_D-V_G characteristic of polyaniline in 0.1 M $LiClO_4/F_3CCO_2H/CH_3CN$.

Figure 5. 182
Micrograph of a push-pull amplifier device based on polyaniline (blue polymer) and poly[3-phenylthiophene] (red polymer).

Figure 6. 183
I_D-V_G characteristics of polyaniline(V_D=50mV) and poly[3-phenylthiophene](V_D=35mV) in the window of push-pull operation. The transistors were fabricated on a single microelectrode array and characterized in 0.1M $LiClO_4$/0.4M F_3CCO_2H/CH_3CN.

Figure 7. 184
Output waveform for a polyaniline/poly(3-phenylthiophene) push-pull amplifier driven by a triangular wave, illustrating the clean zero-crossing of the device. V^+ = 150 mV, V^- = 25 mV, V_{rest} set for zero output current at zero input voltage, operated in 0.1 M $LiClO_4$/ 0.4 M F_3CCO_2H/CH_3CN).

Figure 8. 191
(top) I_D-V_G characteristics for polyaniline and WO_3 in 0.5 M H_2SO_4. (bottom) Input and output waveforms for a polyaniline/WO_3-based complementary microelectrochemical transistor inverter. The input voltage was switched manually. The microfabricated WO_3 transistor showed some background conduction not associated with WO_3 electrochemistry, resulting in the positive offset of the I_D-V_G characteristic and loading of the inverter in the HIGH output state. As a result, the inverter output was 320 mV in the HIGH state instead of the full 400 mV value of V_{DD}.

Figure 9. 200
Complex I_D-V_G characteristics generated by parallel connection of two polyaniline transistors under independent potential control, Scheme VIII, such that the I_D-V_G behavior of each individual device could be offset from the other. The middle characteristic demonstrates a transistor based on two contributing I_D-V_G characteristics configured to introduce a region of constant I_D at an intermediate value of V_G between onset of conduction and peak conductivity. The conductivity of device 1 was approximately twice that of device 2.

Figure 10. 202
(left) Schematic of a ternary (3-state) microelectrochemical inverter and a table showing the relationship of input state to output state.[23] (right) Operation of the ternary inverter at V_{DD} = 50 mV. The transistor device was the pair of polyaniline transistors described above, operated to provide the I_D-V_G characteristic shown Figure 9 (middle).

Figure 11. 204
Experimental (solid) and modeled (dashed) I_D-V_G characteristics for a polyaniline microelectrochemical transistor.

Figure 12. 205
Simulated I_D-V_G characteristics for a device modeled after the results of Figure 9 using equation (1).

Figure 13. 206
I_D-V_G-ΔV_G plot for a hypothetical device based on four contributing finite potential windows of high conductivity. ΔV_G is incremented by 50 mV for each curve.

CHAPTER 5

Figure 1a. 225
GC/MS of 1,4-dithienyl-2,5-difluorobenzene.

Figure 1b. 227
^{1}H-NMR (300 MHz, $CDCl_3$) 1,4-dithienyl-2,5-difluorobenzene.

Figure 2. 233
Cyclic voltammetry and I_D-V_G characteristic of poly(3-(4-trifluoromethylphenyl)-thiophene)

Figure 3. 237
Hammett constant (σ_p) vs. potential for onset of conduction for para-substituted poly(3-phenylthiophene)

Figure 4. 238
Dual substituent parameter equation treatment of potentials for onset of conduction of poly[3-(4-R-phenyl)-thiophene] derivatives.

Figure 5. 241
Cyclic voltammetry and I_D-V_G characteristic of poly(1,4-dithienylbenzene).

Figure 6. 243
Cyclic voltammetry and I_D-V_G characteristic of poly(1,4-dithienyl-2,5-difluorobenzene).

Figure 7. 250
^{1}H-NMR (d_6-acetone, 300 MHz) of 3-(3-methoxyphenyl)-thiophene.

Figure 8. 252
Mass spectrum of 3-(3-methoxyphenyl)-thiophene.

CHAPTER 6

Section 6.1

Figure 1. 277
Cyclic voltammetry of polyaniline deposited onto flat gold electrodes ($\Gamma = 1 \times 10^{-6}$ moles of aniline cm^{-2}) before and after exposure to trifluoroacetic anhydride under potential control at 0.2 V vs SCE (top) and 0.5 V vs SCE (bottom).

Figure 2. 279
Cyclic voltammetry and I_D-V_G characteristics for polyaniline deposited onto three adjacent electrodes on a microelectrode array before and after treatment of the electrode-confined polymer with 1.0 M trifluoroacetic anhydride in 0.2 M F_3CCO_2H/ 0.1 M $LiClO_4$/ CH_3CN.

Figure 3. 282
Reflectance IR spectra for electrodeposited polyaniline on flat Au electrodes over the course of exposure to 1.0 M trifluoroacetic anhydride in 0.2 M F_3CCO_2H/ 0.1 M $LiClO_4$/ CH_3CN at 0.2 V vs SCE (top) and 0.4 V vs SCE (bottom). Spectral changes corresponding to nitrogen trifluoroacetylation are seen for both electrodes.

Figure 4. 284
Evolution of -log(R/R_0) over the course of reaction of polyaniline on Au electrodes with trifluoroacetic anhydride at different potentials. The carbonyl band "absorbance" is shown as normalized to the absorbance of the unchanging polyaniline 818 cm^{-1} band.

Figure 5. 287
Plot of the rate of CO absorbance growth from Figure 4 versus polyaniline state of charge, in electrons per repeat unit. The polyaniline state of charge was obtained by averaging the anodic and cathodic current of the dashed CV in Figure 3 integrated to the potentials at which the samples were held. It was assumed that the degree of oxidation after the second anodic wave is 1 electron per repeat unit. The dashed line is a hypothetical reaction rate which is linearly dependent on the polyaniline oxidation state.

Figure 6. 290
Progression of the normalized peak drain current observed in the I_D-V_G characteristics of a series of polyaniline-derivatized microelectrode arrays held at the potentials indicated over the course of exposure to 1.0 M trifluoroacetic anhydride in 0.2 M F_3CCO_2H/ 0.1 M $LiClO_4$/ CH_3CN.

Figure 7. 296
Peak carbonyl stretching frequency for polyaniline treated with trifluoroacetic anhydride as a function of extent of trifluoroacetylation. Data taken from results shown in Figure 4.

Figure 8. 302
RIR spectra following the hydrolysis of trifluoroacetylated polyaniline on flat Au electrodes, showing disappearance of the CO and CF_3 bands and the regeneration of polyaniline.

Figure 9. 304
Color micrograph and I_D-V_G characterization of a microelectrode array showing functionalized with three independent polyaniline transistors.

Figure 10. 306
Selective trifluoroacetylation of polyaniline transistors on a microelectrode array using electrochemical potential control. Transistors labeled X and Z are trifluoroacetylated or "written" by holding at 0.2 V vs SCE, while transistor Y is protected from reaction by being held oxidized, at 0.5 V vs SCE. Trifluoroacetylated polyaniline of transistors X and Z are then hydrolyzed by immersion in potassium carbonate in aqueous methanol, thereby "erasing" the device, restoring the conductivity of each transistor.

Section 6.2

Figure 1. 328
^{1}H-NMR spectrum (300 MHz, $CDCl_3$) of 3-trifluoroacetyl-2,5-dimethylpyrrole.

Figure 2. 330
FTIR spectrum ($CDCl_3$) of 3-trifluoroacetyl-2,5-dimethylpyrrole.

Figure 3. 332
Gas chromatogram (top) and mass spectrum (bottom) of 3-trifluoroacetyl-2,5-dimethylpyrrole.

Figure 4. 336
I_D-V_G characteristics of polypyrrole before and after exposure to 1M $(F_3CCO)_2O$/0.1 M [*n*-Bu_4N]PF_6/CH_3CN for 20 minutes under active potential control at 0.5 V vs. Ag (top) and -0.1 V (bottom)

Figure 5. 339
Specular reflectance FTIR of electrochemically deposited polypyrrole prior to exposure to trifluoroacetic anhydride.

Figure 6. 341
Specular reflectance FTIR of polypyrrole following 20 minutes immersion in 1M $(F_3CCO)_2O$/0.1 M [*n*-Bu_4N]PF_6/CH_3CN at -0.2 V vs. Ag.

Section 6.3

Figure 1. 359
Cyclic voltammetry (top) and I_D-V_G characteristic (bottom) of microelectrode-confined poly(3-methylthiophene) before (dashed) and after (solid) chlorination.

Figure 2. 361
Chlorination of microelectrode-confined poly(3-methylthiophene) using 1 mM Cl_2/CCl_4 at -20°C until t = 307 s at which point Cl_2 concentration was raised to 10 mM, noted by an asterisk (*) on the figure. The polymer was characterized at 13 points over the 382 s reaction time in 0.1 M [*n*-Bu_4N]PF_6/CH_3CN, V_D = 25 mV, 200 mV/S. The top section shows the progression of the I_D-V_G characteristic to more positive potential for onset of conduction. For clarity only 7 of the 13 characterizations are shown. The bottom graph shows the change in potential for onset of conduction as a function of reaction time for the same poly(3-methylthiophene) film.

Figure 3. 364
Chlorination of microelectrode array-confined polythiophene. (top) I_D-V_G characteristic of the polymer before chlorination (dashed), and after chlorination at room temperature had shifted the potential for onset of conduction had shifted approximately 0.3 V positive of its original value. (solid). (bottom) Graph of potential for onset of conduction as a function of reaction time for the chlorination of polythiophene (confined to 4 microelectrodes) at -20°C with 10 mM Cl_2/CCl_4.

Figure 4. 366
Effects of chlorination on the conductivity of polythiophene. (top) Peak drain current as a function of potential for onset of conduction. (bottom) Peak drain current as a function of reaction time for the same device. See also the graph at the bottom of Figure 3 for a plot of potential for onset of conduction as a function of reaction time for this device. Polythiophene was deposited and characterized on 4 electrodes, thus drain current represents conduction across three interelectrode gaps instead of the usual single gap. Therefore the drain current should be compared to other figures at 1/3 its value.

Figure 5. 369
XPS data for the chlorination of poly(3-methylthiophene) on Au electrodes. Chlorine peaks for 6 electrodes chlorinated under the conditions noted. The highest peak corresponds to a sample chlorinated at +27°C in 200 mM Cl_2/CCl_4 for 60 s while the lower five show peaks for samples chlorinated in 10 mM Cl_2/CCl_4 at -20°C for 5, 15, 30, 60, and 180 s. (inset) Plot of chlorine atoms per repeat unit (see text) for the five samples chlorinated in 10 mM Cl_2/CCl_4 at -20°C.

Figure 6. 372
Plot of maximum transconductance (dI_D/dV_G) as a function of potential for onset of conduction for the data shown in Figure 2 for the chlorination of microelectrode-confined poly(3-methylthiophene).

Figure 7. 375
Change in cyclic voltammetry and I_D-V_G characteristic upon chlorination of microelectrode-confined poly(3,4-dimethylthiophene). Shown after 0, 7, and 12 s in 10 mM Cl_2/CCl_4 at -20°C. V_D = 25 mV

Figure 8. 379
Chlorination of microelectrode-confined polyselenophene at -20 °C in 10 mM Cl_2/CCl_4. Main: Onset of polymer conduction, V vs. Ag wire, as a function of reaction time. Inset: Peak drain current as a function of reaction time. Characterization of I_D-V_G characteristic carried out in 0.1 M [*n*-Bu_4N]PF_6/CH_3CN, V_D = 25 mV, 200 mV/s.

Section 6.4

Figure 1. 396
Operation of polypyrrole and trifluoroacetylated polypyrrole transistors in parallel yielding a more complex net I_D-V_G characteristic. The resistor controls the magnitude of the drain current contribution from the polypyrrole device.

Figure 2. 399
Chemical tuning of the potential for onset of conductivity in poly(3-methylthiophene), and the relationship of the I_D-V_G characteristics obtained to that of polyaniline (dashed line) which has been overlaid. For clarity only the forward scans are shown. The I_D-V_G characteristics of chlorinated poly(3-methylthiophene) are from the work described in section 6.3.

Figure 3. 404
Preparation of a chemically-tuned push-pull amplifier. (top) Chlorination of poly(3-methylthiophene) to obtain onset of conductivity at 0.8 V. (bottom) A polyaniline transistor has been deposited onto the array, and the I_D-V_G characteristics for polyaniline and the now chlorinated poly(3-methylthiophene) are shown.

Figure 4. 406
Preparation of a chemically-tuned push-pull amplifier. (top) The I_D-V_G characteristics of chlorinated poly(3-methylthiophene) and as-deposited polyaniline. (bottom) The peak drain currents have been matched by controlled attenuation of the conductivity of the polyaniline transistor by trifluoroacetylation.

Figure 5. 408
A chemically-tuned push-pull amplifier based on chlorinated poly(3-methylthiophene) and trifluoroacetylated polyaniline: I_D-V_G characteristics in the range of V_G for amplifier operation.

Figure 6. 410
Output waveform for the chlorinated poly(3-methylthiophene)/ trifluoroacetylated polyaniline push pull amplifier, driven over it entire operating range.

CHAPTER 7

Figure 1. 431
I_D-V_G response of poly(2,5-dithienylpyridine) following alternate protonation with F_3CCO_2H and deprotonation with pyridine.

Figure 2. 434
I_D-V_G response of poly(2,5-dithienylpyridine). Top: before exposure to HCl(g). Middle: After exposure to HCl(g). Bottom: After exposure to 0.1 M pyridine.

Figure 3. 436
I_D-V_G response of poly(2,5-dithienylpyridine) scanned continuously while HCl(g) was passed over the surface of the electrolyte solution.

Figure 4. 440
Schematic (top) and diagram of operation (bottom) of a chemically-gated hybrid circuit based on a polyaniline microelectrochemical transistor and a Si bipolar junction transistor.

Figure 5. 442
Operation of the chemically-gated hybrid circuit shown in Figure 3 showing drain current through the polyaniline device (top) and collector current through the Si device (bottom) as the polyaniline device is alternately exposed to O_2 and H_2.

LIST OF SCHEMES

CHAPTER 1

Scheme I. 32
Examples of conducting polymers

Scheme II. 44
Structure of the 3-substituted polythiophene family.

CHAPTER 2

Scheme I. 67
Representation of transistor response to an oscillation in gate potential.

Scheme II. 72
Bipotentiostat configuration suitable for measurement of power gain at frequencies up to 500 Hz (for a Pine Instruments RDE4 bipotentiostat). A signal source such as a function generator drives both working electrodes. An offset voltage applied to K2 provides V_D.

Scheme III. 73
Improved experimental configuration for power gain measurements.

Scheme IV. 74
An audio amplifier based on a polyaniline microelectrochemical transistor.

Scheme V. 76
Four drain, source, and gate electrode configurations for microelectrochemical transistors.

Scheme VI. 85
Electrochemical potentials in a microelectrochemical transistor amplifier.

CHAPTER 3

Scheme I. 107
Benzenoid (a) and quinoid (b) resonance forms for the polyaromatic family of conducting polymers.

Scheme II. 108
Representations of changes in the π-manifold and electronic band structure for a polyheteroaromatic upon oxidation. a) The neutral polymer in the benzenoid ground state. b) Removal of an electron results in a quinoid distortion to minimize total energy. A new, half-occupied electronic state appears in the band gap as a result. c) Upon further removal of charge, polarons combine to form bipolarons and a stronger distortion to quinoid form. As the number of cationic sites increases the new energy levels overlap sufficiently to become narrow bands.

Scheme III. 112
Representation of oxidation of polyaniline and concurrent evolution of electronic band structure resulting in hysteresis in the I_D-V_G characteristic.

Scheme IV. 113
An AND gate (top) and an INVERTER (bottom) and the relationship of output to input for each gate.

Scheme V. 117
Current flow in a microelectrochemical transistor-based inverter. Top: input LOW, output HIGH. Bottom: input HIGH, output LOW.

Scheme VI. 122
The sweep generator of an RDE4 potentiostat was used to modulate the square wave connected to the IN terminals of the potentiostat. The working electrode potential is the sum of the two waveforms allowing generation of square waves with an arbitrary noise signal component.

Scheme VII. 136
An inverter based on a standard bipolar transistor configured to provide a transfer function comparable to the polyaniline-based inverter shown in Figure 2.

CHAPTER 4

Scheme I. 168
Representations of the (a) neutral, (b) partially oxidized, and (c) fully oxidized (one electron per repeat unit) states for a polyheteroaromatic conductor.

Scheme II. 175
A microelectrochemical push-pull amplifier.

Scheme III. 180
Electrochemical procedure for the deposition of two different transistors on one array.

Scheme IV. 187
Schematic of a CMOS inverter gate.

Scheme V. 189
A complementary inverter gate based on microelectrochemical transistors.

Scheme VI. 190
Electrochemical potentials of drain, source, and gate electrodes in the LOW and HIGH output states of a complementary inverter gate based on microelectrochemical transistors.

Scheme VII. 197
A transistor based on two contributing I_D-V_G characteristics, simulated using equation (1) as described below.

Scheme VIII. 199
Experimental configuration for two polyaniline microelectrochemical transistors operated with drain and source electrodes in parallel and separate potential control for each device. The I_D-V_G characteristics of the two devices can be offset from each other by an arbitrary potential.

CHAPTER 5

Scheme I. 217
Possible steps in the mechanism of anodic polymerization.

Scheme II. 221
Synthesis of substituted 3-phenylthiophenes.

Scheme III. 222
Synthesis of 1,4-dithienylbenzene.

Scheme IV. 223
Synthesis of 1,4-dithienyl-2,5-difluorobenzene.

Scheme V. 224
Side reactions in the attempted synthesis of 1,4-dithienyl-tetrafluorobenzene.

Scheme VI. 229
Polymerization of substituted 3-phenylthiophenes.

Scheme VII. 235
Positions of activation in 3-(3-methoxyphenyl)-thiophene.

CHAPTER 6

Section 6.0

Scheme I. 267
Generalized representation of substitution to less than one group per repeat unit.

Section 6.1

Scheme 1. 273
Structures of neutral, partially oxidized, and fully oxidized polyaniline.

Scheme 2. 275
Reactions of oligomeric analogs of polyaniline with trifluoroacetic anhydride.

Scheme 3. 295
Potential dependence of the reaction of terminal vs. internal amine groups in the trifluoroacetylation of polyaniline.

Scheme 4. 309
A circuit used to read the configuration of a polyaniline/trifluoroacetylated polyaniline-based erasable programmable read only memory providing an output of zero for acylated devices and V_{DD} for non-acylated devices at outputs X, Y, and Z. The optimal value for V_G was 0.225 V vs SCE which is within the window of conductivity for polyaniline but slightly negative of onset of conducting for trifluoroacetylated polyaniline.

Section 6.2

Scheme 1. 321
Resonance forms for pyrrole.

Scheme 2. 321
Resonance structures for an intermediate arising from electrophilic attack at carbons α (top) and β (bottom) to nitrogen.

Scheme 3. 322
Percent trifluoroacetylation at the 2 vs. 3 positions for a series of N-substituted pyrroles bearing increasingly sterically demanding groups.

Scheme 4. 327
Trifluoroacetylation products from 2,5-dimethylpyrrole, 1,2,5-trimethylpyrrole, and ethyl 3,4-diethyl-5-methyl-2-pyrrolecarboxylate. Reaction time was 20 minutes.

Scheme 5. 345
Resonance stabilization by the backbone of polypyrrole of the σ-complex resulting from electrophilic attack at a β-carbon.

Section 6.3

Scheme I. 356
Examples of chlorination of thiophene derivatives.

Scheme II. 378
Proposed reactions of chlorine with (top) poly(3-methylthiophene), reacting by substitution for the 4-hydrogen; (middle) polythiophene, reacting by substitution with either the 3 or 4 hydrogen; and (bottom) poly(3,4-dimethylthiophene) with addition across a double bond.

Section 6.4

Scheme I. 395
Deposition of two polypyrrole transistors followed by selective acylation of one device by reaction of the two under potential control. At 0.5 V polypyrrole is partially oxidized and non-nucleophilic. At -0.1 V polypyrrole is fully reduced and reacts with trifluoroacetic anhydride.

Scheme II. 402
Preparation of a chemically tuned push-pull amplifier.

Section 6.5

Scheme I. 419
Summary of results from miscellaneous reactions of conducting polymers.

CHAPTER 7

Scheme I. 430
Methylation and de-methylation of poly(2,5-dithienylpyridine)

Scheme II. 438
Protonated poly(2,5-dithienylpyridine).

CHAPTER 8

Scheme I. 455
Design for a microelectrochemical analog-to-digital converter/quaternary to binary translator based on three different windows of high conductivity.

Scheme II. 456
Overlap of the finite windows of high conductivity of trifluoroacetylated polyaniline, poly(3-(4-methoxyphenyl)-thiophene), and chlorinated polythiophene.

Scheme III. 458
Logic gate diagram of a circuit for the addition of two binary numbers.

Scheme IV. 459
Design for a microelectrochemical OR gate.

Scheme V. 460
Design for a microelectrochemical AND gate.

Scheme VI. 463
Complete design for a microelectrochemical binary adder.

LIST OF TABLES

CHAPTER 5

Table 1. 231
Polymerization characteristics of substituted 3-phenylthiophenes and potential for onset of conduction, stability, and relative conductivity of poly(3-phenylthiophene)s obtained.

CHAPTER 6

Section 6.1

Table 1. 299
X-Ray Photoelectron Spectroscopy Data for **V**, **VI**, and for polyaniline trifluoroacetylated at 0.2 V and 0.5 V vs SCE.

Section 6.4

Table 1. 391
Electrophilic substitution reactions of conducting polymers and resulting effects on polymer electrical characteristics.

Table 2. 392
Comprehensive compilation of potentials for onset of conductivity for polymers characterized in this thesis. The characterizations were carried out using the same Ag reference electrode as reference in 0.1 M [*n*-Bu_4N]PF_6/CH_3CN for all polymers. Since electrochemistry of polyaniline requires a proton source, 0.5 M F_3CCO_2H was added to the electrolyte medium.

CHAPTER 8

Table 1. 457
Sum of two numbers X and Y in binary and decimal.

Chapter 1

Introduction

Microelectrochemical transistors are electronic devices which derive function from insulator-conductor transitions undergone by molecular reagents such as a redox material or conjugated organic polymer.[1-20] In 1984 White, Kittlesen, and Wrighton reported a transistor device based on an array of microelectrodes derivatized with a film of the organic conductor polypyrrole[1] and Pickup and Murray described preparation of a diode-like device by modification of a macroscopic electrode with a redox polymer sandwiched between a Pt disk and a porous Au film.[2] Two earlier results in the area of transistors based on electrochemical events were devices in which chemical species, rather than electrons and holes, were the charge carriers.[21,22] Since the initial report 11 years ago, microelectrochemical transistors have been developed extensively in the Wrighton Group. This thesis describes work carried out over the past 5 years on the microelectrochemistry, synthesis, and reactivity of conjugated organic polymers and the development of molecule-based electronic amplifiers, sensors, and digital logic.[23-28]

Conducting Polymers

Conjugated organic polymers[29,30] display electrical conductivity derived from the mobility of charge along their extended π-manifolds. Polyacetylene is the prototypical conducting polymer and its high conductivity upon treatment with an oxidant was discovered in 1977[29] setting off a wave of research into polymers with extended π-conjugated backbones which has continued to the present day. The five polymers shown in Scheme I are prominent members of the family of conjugated organic conductors and numerous derivatives have been prepared based on these backbones. Examples of other systems which have been investigated range from the more esoteric relatives of the thiophene family polyselenophene,[31] polyfuran,[32] and even polytellurophene,[33] to materials based on more complex repeat units such as poly(1,4-dithienylbenzene),[34] poly(4,4'-diphenylenediphenylvinylene),[35] and polyisothianaphthene.[36] These examples

are only a small sample of a vast array of materials which have been prepared and characterized.

Scheme I

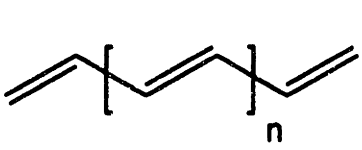

trans-polyacetylene

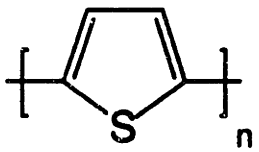

polythiophene

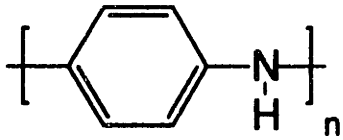

polyaniline

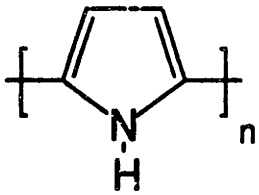

polypyrrole

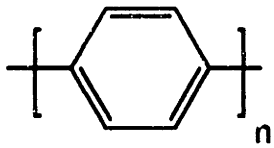

poly(*para*-phenylene)

The majority of conducting polymers have chain architecture centered on what is essentially a polyacetylene backbone consisting of alternating single and double carbon-carbon bonds. Polyaniline is an important exception where a nitrogen p-orbital is part of the conjugated backbone. Conductivity in conjugated organic polymers[29,30,37,38] is thought to proceed via motion of delocalized charge sites both along polymer chains and from one chain to another, the latter being rate-limiting. Maximum conductivity occurs in the partially oxidized, "mixed valency" state and conducting polymers actually become insulating again when more highly oxidized leading to what has been termed a "finite potential window of high conductivity". This behavior, in which a polymer is conducting over a finite range of electrochemical potential (oxidation state), has been shown to be a general feature of charge transport in conjugated organic polymers.[39-45] As the π-system of a polymer is depopulated and the density of holes on the backbone becomes high, motion of holes both along the backbone and from one polymer chain to another becomes

unfavorable. An insulating state is achieved in highly oxidized polymers when holes become localized and immobile and as such cannot support conduction. While the highest conductivity for conjugated organic polymers is observed in the partially oxidized state, these material can also conduct when reduced and a finite window of conductivity is also observed for reductive conduction.[41,43,44] Reductive conductivity is typically two orders of magnitude lower than oxidative conductivity for a given polymer. Polymers which are stable to both oxidation and reduction from their neutral state can function as either "*p*-type" materials where conduction is brought about by depopulation the π molecular orbitals of the polymer backbone (the valence band), or "*n*-type" materials where conductivity is attained by population of the π^* orbitals (the conduction band) by electrons.

Conducting polymers have been studied to both better understand their properties[29-73] and to develop potential applications.[74-95] (References 47-73 and 74-95 are ordered by year of publication within each group and the title of each publication is included.) Synthesis,[16,29-34,36,45-47,56-58,60,62,64,68,69,71-73,91,94,96,97] conductivity, electrochemical and electrical characteristics,[1,4,5,8,29-34,36-46,48-53,55,65,69,74,78,94] solubility properties,[30,54,57,68,92] optical characteristics,[5,35,40,43,61,81,88,91,92,95] and substituent effects[29,30,34,36,40,46,49,50,59,64,68,69,91,92,94,95] are examples of fundamental properties of conjugated organic polymers which have been examined. Conducting polymers have been investigated for application in sensors,[8,10-12,19,72,76,75,84] drug release systems,[76] battery electrodes,[69,77,80] capacitors,[86,94] diodes,[74,78] photovolatics,[87] light emitting diodes,[88,91,92,95] and field-effect[78,79,82,83,85,90,93] and microelectrochemical transistors.[1,3-20] The utility of an inexpensive, highly conducting, and processable polymeric substitute for metallic conductors like copper is obvious. Processability and extended durability remain major obstacles to the use of conducting polymers in applied settings but considerable progress has been made in developing processable polymer or polymer precursors. Durability remains an under-addressed issue.

Conducting polymers can synthesized either via chemical means[29,30] or by the widely used method of anodic polymerization.[31,68,96,97] This electrochemical synthetic method yields electrode-confined films for a wide range of polymers which is convenient as conducting polymers are usually insoluble and intractable. In Electrochemical polymerization, oxidation of the appropriate monomer generates reactive radical cations which couple to form oligomers. When the oligomers become long enough to be insoluble they precipitate onto the electrode surface. This description is probably an oversimplification because the mechanism of anodic polymerization is considered to be complex and far from fully understood.[68] Anodic polymerization is suitable for preparation of many polymers and is tolerant of a modest range of functionalities although nucleophilic or highly electron-withdrawing groups must generally be avoided.[68,96] Thiophenes, anilines, pyrroles, and many other families of monomers are reactive in anodic polymerization. Special conditions are required for monomers which are more difficult to oxidize such as benzene[48] and conditions have yet to be found under which polyacetylene can be prepared electrochemically.

Microelectrochemical Transistors

A transistor[98-100] is a device with a conducting channel through which electrical current can flow and a control electrode which governs the extent to which that channel is open or closed. A transistor is therefore a valve to control a flow of electrons. The essence of transistor function is that a smaller quantity of power (power is the product of current and voltage) applied to the control electrode governs a larger amount of power passing through the main channel of the device. This is the basis of amplification. Note that the transistor does not "make a large signal out of a small one" which, of course, would violate conservation of energy, but rather uses a small signal to control the flow of power from another source, referred to as the power supply. Transistors are the single most important electronic device and are the basis of amplifiers, digital logic, control electronics, and a host

of other applications.[101] The transistor was discovered in 1947 at Bell Laboratories and was described by Bardeen and Brattain[98] and by Schockley[99] in papers which introduced the device.[100] The first transistor was based on Ge and was a bipolar device, so named because both electrons and holes participate in device operation.

Following discovery of the bipolar transistor, field-effect devices were developed.[100,102] Microelectrochemical transistors are most closely related to a member of the field-effect family, the enhancement-mode metal-oxide semiconductor field-effect transistor (MOSFET). Figure 1 shows the layout of an n-channel MOSFET.[100,102] The device is called a field-effect transistor because transistor action is brought about by a field-

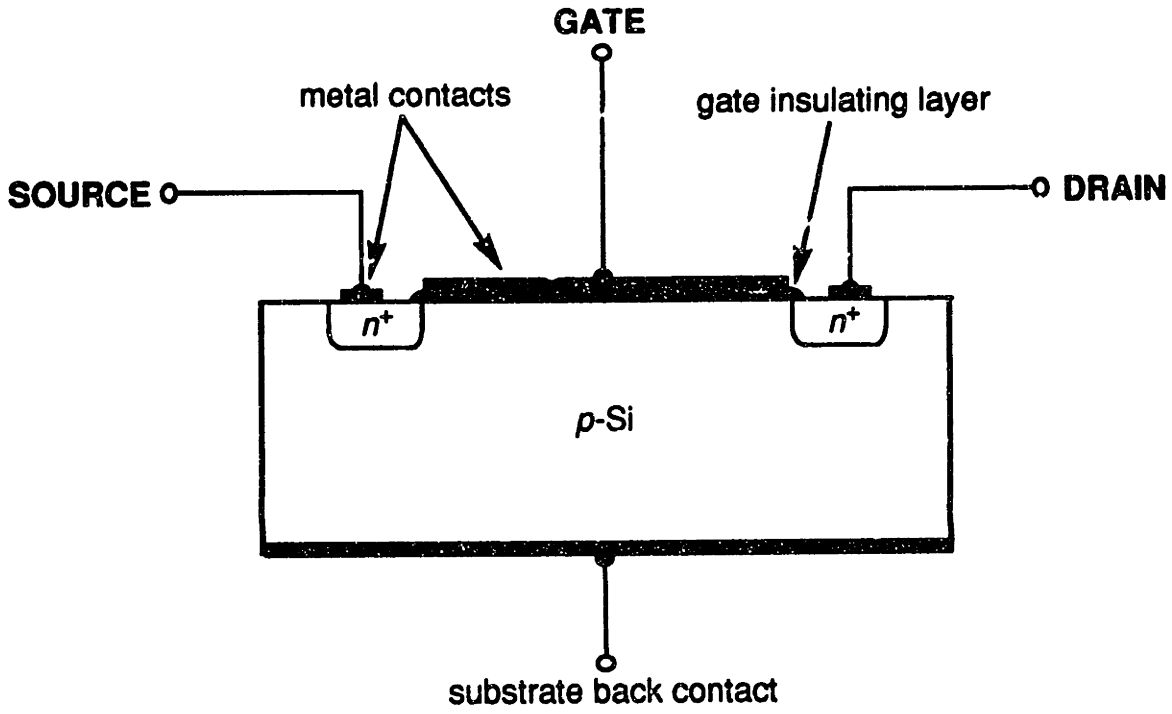

Figure 1. An n-channel metal-oxide semiconductor field-effect transistor.

induced redistribution of carriers in the bulk of the device. The conducting channel in a FET is the path between the *source* and *drain* terminals, which in an *n*-channel device are heavily doped *n*-type regions implanted into the *p*-type bulk of the device. The control electrode is referred to as the *gate* and gate voltage V_G is usually applied between the gate

and source terminals, with the fourth contact (the back of the substrate) connected to the source electrode. Alternatively, V_G can be applied to the gate with respect to the substrate back contact alone. With no gate voltage applied, the source-to-drain path consists of two back-to-back *p-n* junctions and as such one will be reversed-biased regardless of the polarity of V_{DS} and no current will flow. To bring the transistor into drain-source conduction, a positive voltage is applied to the gate causing electrons to be drawn from the *p*-bulk of the device to its interface with the SiO_2 gate insulating layer. This field-induced redistribution of charge produces an *inversion layer*, an *n*-type region at the surface of the *p*-bulk between the drain and source regions. The inversion layer bridges the two n^+ regions forming a continuous conducting channel through which drain current, I_D, can flow. The fact that the device is off when no gate voltage is applied and that the field effect induces conduction is the source of the term *enhancement-mode*. (A *depletion-mode* MOSFET is fully conducting when no gate voltage is applied and the field effect serves to reduce, rather than enhance, device conductivity.) The magnitude of V_G controls the flow of drain current through the device by controlling the extent to which the inversion layer which connects the source and drain is created. This is the means by which a MOSFET achieves transistor function. The device is essentially a voltage-controlled resistor in which V_G sets R_{DS}. Indeed, the name *transistor* is a contraction of *transfer resistor*[100] which is an apt name for the device since a transistor's function is to transfer a control signal to main-channel conductivity and current flow.

The terms "*p*-type", "*n*-type", "conduction band" and "valence band" come from the solid state physics of conductivity in conventional inorganic semiconductors like Si but they translate reasonably to conjugated organic polymers. However, throughout the conducting polymer literature the term "doping" is ubiquitous and is used as a general term to describe treatment of a polymer with a chemical oxidant or reductant, as well as other classes of reagents. It has been pointed out that the term is ambiguous and misleading.[37] In conventional semiconductors, doping is the addition of a very small concentration (one

part in 10^3 to one part in 10^8) of an impurity such as B or As to generate a slight excess or deficiency of electrons in the lattice of the material.[103] The level of acceptor required for peak conductivity in conjugated organic polymers ranges from one part in ten to one part in two.[40] More importantly, a critical difference between conventional semiconductors and conducting polymers is the strong coupling in the latter of injection of charge with structural distortions of the polymer backbone resulting in a reconfiguration of orbital interactions and changes in the electronic band structure of the material.[37,38,104] Further confusion would arise if the term "doping" were employed in description of microelectrochemical transistor processes. In the author's opinion, the analogy between doping of inorganic semiconductor lattice and oxidation or reduction of a conducting polymer is a poor one and is indeed ambiguous and misleading. Since the terms "oxidation" and "reduction" as they are defined in the field of chemistry are complete, unambiguous, and rigorously accurate for the describing a change in state of charge of a conducting polymer, these terms will be used to describe those processes throughout this thesis.

The device architecture of a typical microelectrochemical transistor is shown in Figure 2. Devices are usually prepared by electrochemical deposition of the active material onto a microelectrode array. Figure 3 shows an optical micrograph of an MS17 array consisting of 8 individually addressable band microelectrodes approximately 1.5 μm wide, 1.5 μm apart, and 80 μm long. The arrays are fabricated by standard photolithographic and metallization techniques using Au or Pt as the electrode material.[3,20] A conducting polymer-based transistor is prepared by electrochemical polymerization of a monomer such as aniline, 3-methylthiophene, or pyrrole to obtain a film of polymer on the electrodes of sufficient thickness to occupy the intervening gaps. The device consists of a set of electrodes functionalized with a polymer film, or other redox material, and a reference/counter electrode which provides a fixed reference of electrochemical potential. All of these are in contact with an electrolyte medium which provides the source of charge-

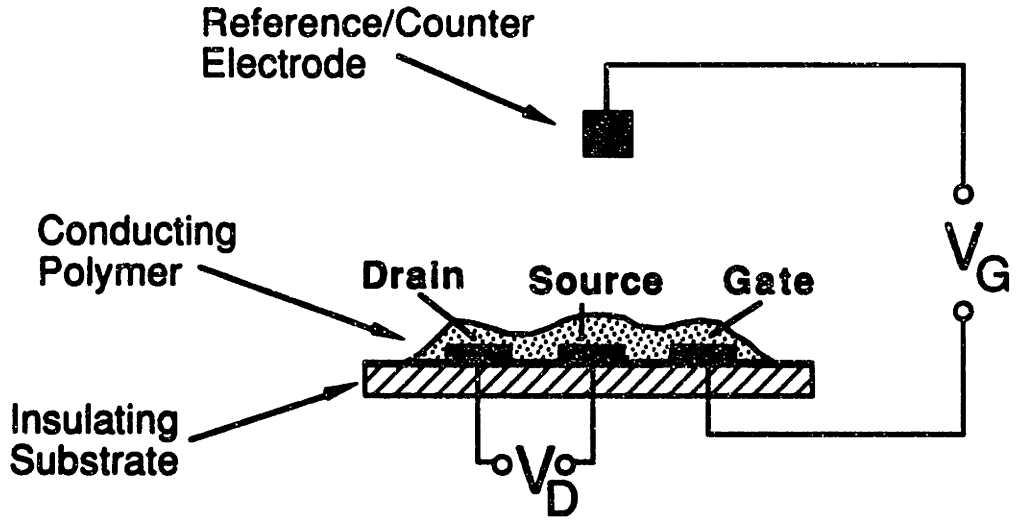

Figure 2. A microelectrochemical transistor

compensating counterions required for oxidation and reduction of the device-active material. The electrodes are designated drain, source, and gate by analogy with the MOSFET, the closest solid-state relative of the microelectrochemical transistor. The polymer occupying the gap between the source and drain electrodes forms the main channel of the transistor. When partially oxidized and conducting, the polymer supports flow of drain current through the device. The oxidation state of the conducting polymer is controlled by application of gate voltage V_G. Gate current is the flow of electrons due to oxidation and reduction of the device-active material and these electrons are consumed or supplied by a countering electrochemical process at the reference/counter electrode. Figure 4 shows the cyclic voltammetry for polyaniline on a microelectrode array. Positive current corresponds to oxidation of the polymer while negative current corresponds to reduction. If a drain voltage (V_D) is applied, drain current (I_D) will flow when the polymer is in its partially oxidized, conducting state. By scanning V_G and monitoring I_D, a profile of conductivity as a function of polymer oxidation state is measured, seen in Figure 4 for a polyaniline microelectrochemical transistor. This profile, the I_D-V_G characteristic of the device, shows the changes in conductivity which accompany oxidation and re-reduction of

Figure 3. A microfabricated array of 8 individually addressable band microelectrodes approximately 1.5 μm wide, 1.5 μm apart, and 80 μm long.

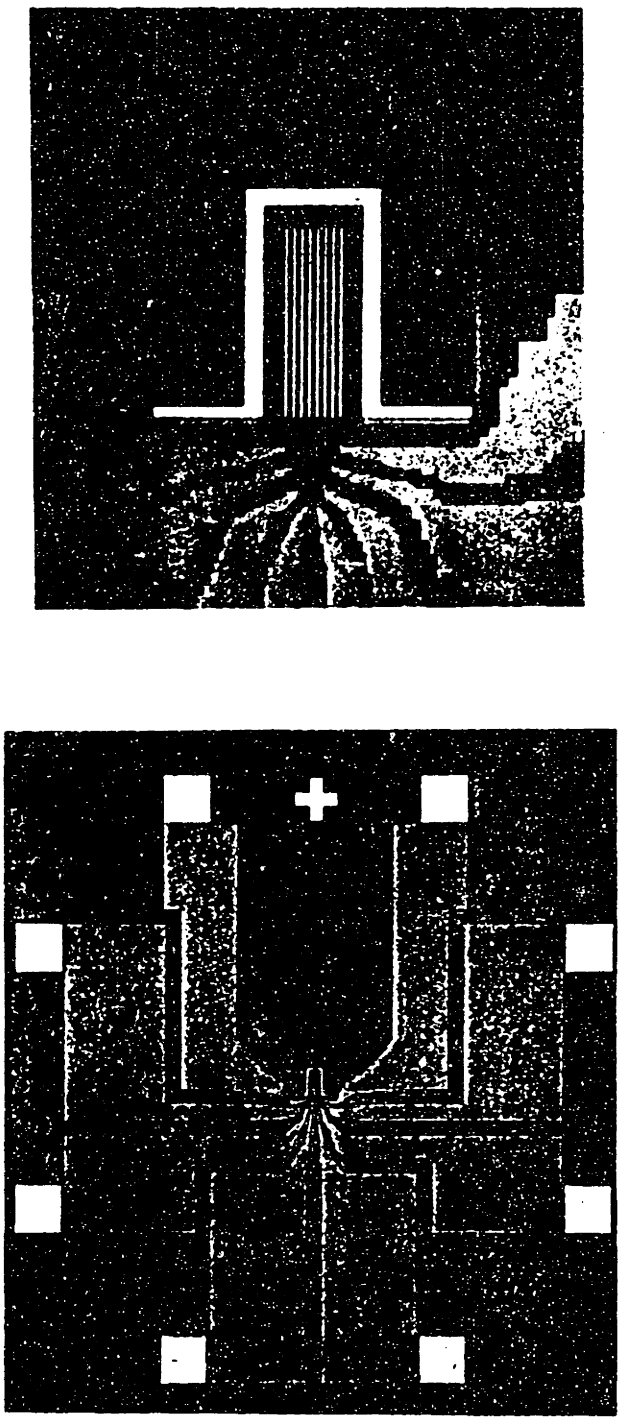

Figure 4. Cyclic voltammetry and Drain current as a function of gate voltage (transistor characteristic) for a polyaniline-based microelectrochemical transistor. The device, as shown at the top of the figure, uses a commonly employed configuration where a single electrode serves as both source and gate connection.

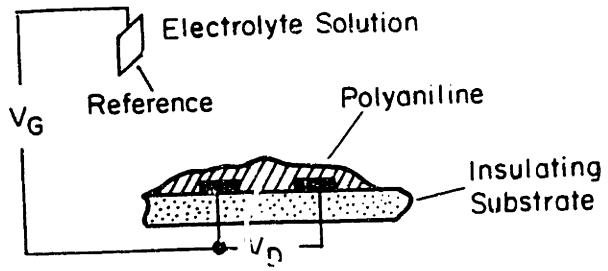
Electrolyte Solution
Reference
V_G
Polyaniline
Insulating Substrate
V_D

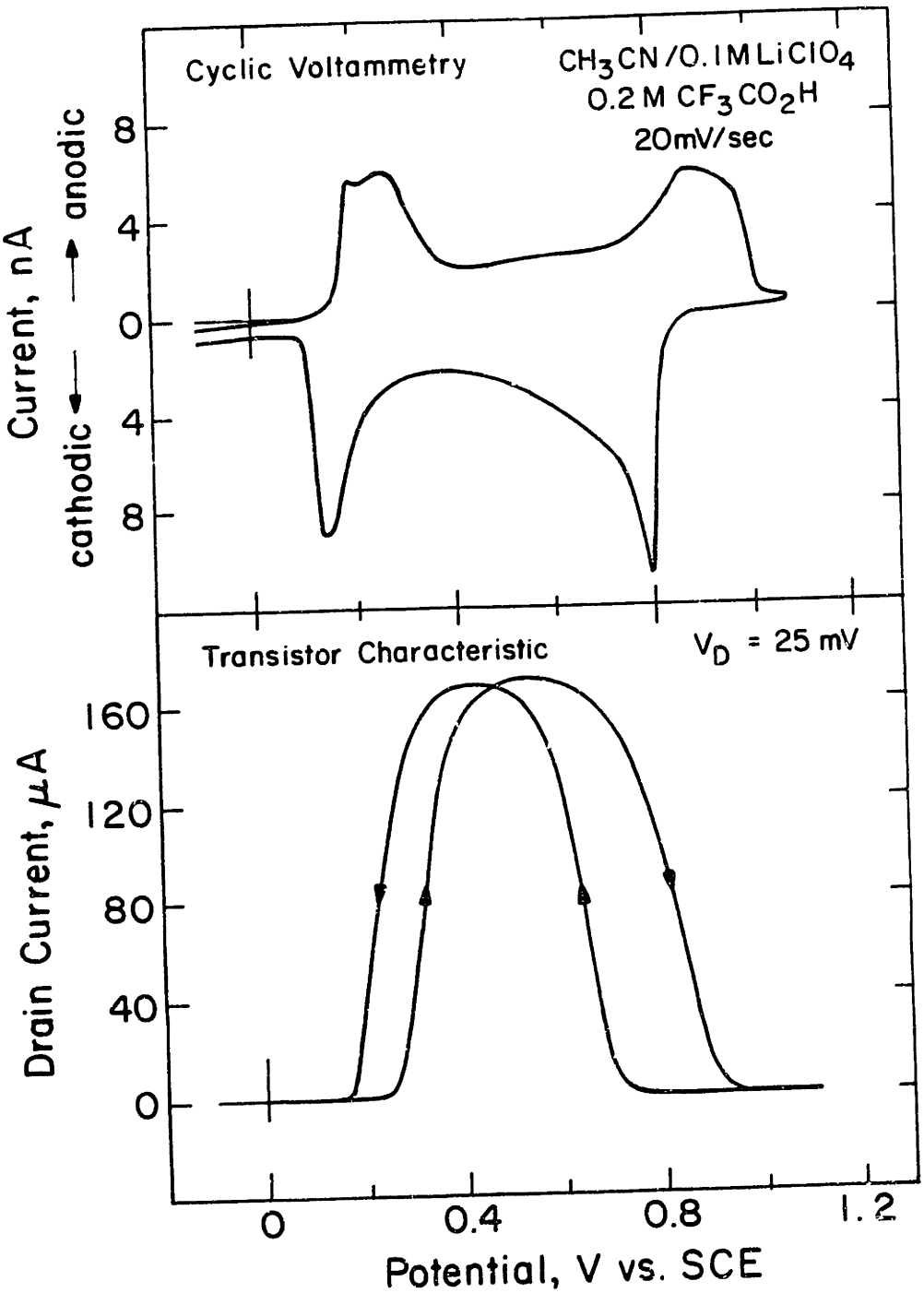
Cyclic Voltammetry
$CH_3CN/0.1M LiClO_4$
$0.2 M CF_3CO_2H$
20mV/sec
Current, nA
anodic
cathodic
8
4
0
4
8
Transistor Characteristic
V_D = 25 mV
Drain Current, μA
160
120
80
40
0
0
0.4
0.8
1.2
Potential, V vs. SCE

the polymer. As V_G is scanned positive, electrons are withdrawn from polyaniline, as seen in the cyclic voltammogram, and onset of conduction is observed in the I_D-V_G characteristic. This is followed by a rise in drain current to a maximum that occurs when the polymer is in the partially oxidized, "mixed valency" state. From this point, further oxidation results in a fall in conductivity and finally onset of oxidative insulation. In the cyclic voltammogram, onset of oxidative insulation corresponds to a second wave in which charge exits abruptly, completing oxidation of polyaniline to the extent of one electron per repeat unit. The I_D-V_G behavior of polyaniline illustrates the finite potential window of high conductivity observed for conjugated organic polymers. The hysteresis in the scan (the return scan does not re-trace the forward scan) has been attributed to an evolution of polymer electronic band structure upon oxidation resulting from the coupling of charge injection to structural distortion of the polymer backbone.[37,40] This feature is not indicative of any degradation of the polymer and is typical of conjugated organic conductors. The theoretical basis of hysteresis is introduced in greater detail in Chapter 3, and the finite window of conductivity in Chapter 4. Hysteresis requires specifying parameters such as potential for onset of conduction or potential of peak conductivity for one scan direction or the other, so by convention the *forward scan* of I_D-V_G characteristics will be used.

Transistor action in microelectrochemical devices is based oxidation and reduction of the device-active material. While this is usually accomplished electrochemically, it can also occur by electron transfer between the device-active material and a species in solution. A microelectrochemical transistor can therefore respond to both electrical and chemical signals. The ability to be gated chemically allows microelectrochemical transistors to function as highly sensitive chemical sensors.[8,10-12,19]

Because gating of a microelectrochemical transistor is based on oxidation and reduction of the device-active material, it occurs accompanied by diffusion of counterions. When a polymer is oxidized, anions must diffuse into the bulk of the polymer film from the

electrolyte solution to compensate the cationic sites generated on the polymer chain. Upon reduction these anions must be expelled. Since diffusion is a slow process compared to electronic conduction, microelectrochemical transistors are slow compared to conventional solid state devices.[7]

The microelectrochemical transistor (MET) has many important parallels with the conventional solid state MOSFET. Both transistors are charge-controlled devices where a fixed number of electrons must be moved through the gate terminal to switch the device between two given states of conduction. Therefore, both METs and MOSFETs draw dynamic gate current only. Once V_G has been established by passing the required quantity of gate charge, no further gate current flows. Both METs and MOSFETs will support drain current in both directions, i.e. from source to drain or from drain to source. These characteristics of MOSFETs and METs differ from conventional bipolar transistors which are current controlled devices which draw a steady current at their control electrode, known as the base, and allow current flow in only one direction between their emitter and collector electrodes.[101]

The term "molecule-based transistor" introduced by Wrighton is meant to emphasize the molecular as opposed to solid-state nature of the active material of the device. The semiconducting properties of Si arise to a large extent from the long-range order of Si atoms in a crystalline lattice. Si can be made an *n*-type or *p*-type semiconductor, but beyond that it is essentially a single material with a single set of properties. The III-V semiconductors of which GaAs is an example, or ternary materials like $Hg_xCd_{1-x}Te$[105,106] or $Ga_zIn_{1-x}As$,[107] offer more flexibility since there are several options for each component element and a range of stoichiometries possible in the case of the II-VI ternary semiconductors. When the constraints of a crystalline lattice are removed, and a material becomes molecular in nature rather than solid state, the possibilities become vast indeed. In a conducting polymer, properties are strongly influenced by the molecular structure and composition of the polymer chain and long range order is not a requirement,

although it can enhance conductivity.[29-73] With the number of repeat units, combinations of repeat units, and derivatives of the backbones created from those units to choose from, it is hardly surprising that so many different conducting polymers have been reported to date. Scheme II shows an important class of polymers, the 3-substituted polythiophenes. The

Scheme II

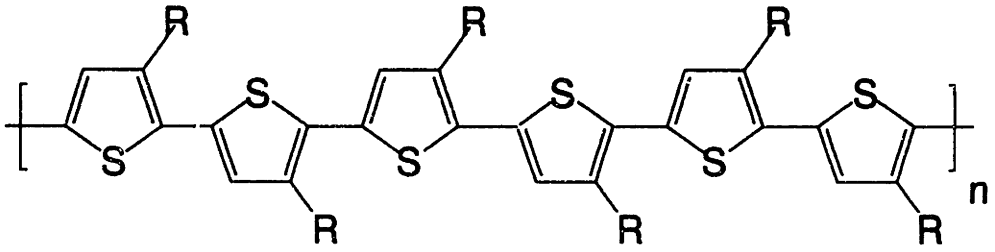

R-group influences electrochemical, electrical, optical, and physical properties of the polymer.[5,8,23,26,30,40,49-51,53,64,69,95] Chemical functionalities and chemical sensitivity can be incorporated as a pendant group as well.[56] Thus, the polythiophene backbone is parent to a large family of polymers of diverse and varied properties. Such is the flexibility inherent in molecular materials, and one expression of this flexibility is the range of different electrical and chemical properties attainable in microelectrochemical transistors. What is really interesting about conducting polymers is not how highly they can ultimately be made to conduct or how closely they can be made to mimic conventional semiconductor devices, but all of the things they can do as a result of their molecular nature that Si or GaAs *cannot.*

Presented in this thesis are results on the chemistry and reactivity of conjugated organic polymers in electrophilic substitution reactions, the electrochemistry of these materials in microelectrochemical transistors, and on molecule-based amplifiers and logic circuits which derive their function from the powerful combination of the finite window of

high conductivity of conjugated organic polymers and the ability to tune electrical characteristics of those materials by modification of their structure at the molecular level.

References

1. White, H. S.; Kittlesen, G. P.; Wrighton, M. S. *J. Am. Chem. Soc.*, **1984**, *196*, 5375. "Chemical Derivatization of an Array of Three Gold Microelectrodes with Polypyrrole: Fabrication of a Molecule-Based Transistor"
2. Pickup, P. G.; Murray, R. W. *J. Electrochem. Soc.*, **1984**, *131*, 833. "Redox Conduction: Its Use in Electronic Devices"
3. Kittlesen, G. P.; White, H. S.; Wrighton, M. S. *J. Am. Chem. Soc.*, **1984**, *106*, 7389. "Chemical Derivatization of Microelectrode Arrays by Oxidation of Pyrrole and N-Methylpyrrole: Fabrication of Molecule-Based Electronic Devices"
4. Paul, E. W.; Ricco, A. J.; Wrighton, M. S. *J. Phys. Chem.*, **1985**, *89*, 1441. "Resistance of Polyaniline Films as a Function of Electrochemical Potential and the Fabrication of Polyaniline-Based Microelectronic Devices"
5. Thackeray, J. W.; White, H. S.; Wrighton, M. S. *J. Phys. Chem.*, **1985**, *89*, 5133. "Poly-3-Methylthiophene Coated Electrodes: Optical and Electrical Properties as a Function of Redox Potential and Amplification of Electrical and Chemical Signals Using Poly-3-Methylthiophene-Based Microelectrochemical Transistors"
6. Kittlesen, G. P.; White, H.S.; Wrighton, M. S. *J. Am. Chem. Soc.*, **1985**, *107*, 7373. "A Microelectrochemical Diode Based on the Connection of Two Microelectrodes Using Dissimilar Redox Polymers: A Two-Terminal Electrochemical Device with Submicron Contact Spacing"
7. Lofton, E. P.; Thackeray, J. W.; Wrighton, M. S. *J. Phys. Chem.*, **1986**, *90*, 6080. "Amplification of Electrical Signals with Molecule-Based Transistors: Power Amplification up to a Kilohertz Frequency and Factors Limiting Higher Frequency Operation"

8. Thackeray, J. W.; Wrighton, M. S. *J. Phys. Chem.*, **1986**, *90*, 6674. "Chemically Responsive Microelectrochemical Devices Based on Platinized Poly(3-Methylthiophene): Variation in Conductivity with Variation in Hydrogen, Oxygen, or pH in Aqueous Solution"

9. Jernigan, J. C.; Wilbourn, K. O.; Murray, R. W. *J. Electroanal. Chem.* **1987**, *222*, 193. "A Benzimidazobenzophenanthroline Polymer Molecular Transistor Fabricated Using Club Sandwich Electrodes"

10. Natan, M. J.; Mallouk, T. E.; Wrighton, M. S. *J. Phys. Chem.*, **1987**, *91*, 648. "pH-Sensitive WO_3-Based Microelectrochemical Transistors"

11. Natan M. J.; Bélanger, D.; Carpenter, M. K.; Wrighton, M. S. *J. Phys. Chem.*, **1987**, *91*, 1834. "pH-Sensitive $Ni(OH)_2$-Based Microelectrochemical Transistors"

12. Bélanger, D.; Wrighton, M. S. *Anal. Chem.*, **1987**, *59*, 1426. "Microelectrochemical Transistors Based on Electrostatic Binding of Electroactive Metal Complexes in Protonated Poly(4-Vinylpyridine): Devices that Respond to Two Chemical Stimuli"

13. Chao, S.; Wrighton, M. S. *J. Am. Chem. Soc.*, **1987**, *109*, 2197. "Solid State Microelectrochemistry: Electrical Characteristics of a Solid State Microelectrochemical Transistor Based on Poly(3-Methylthiophene)"

14. Jones, E. T. T.; Chyan, O. M.; Wrighton, M. S. *J. Am. Chem. Soc.*, **1987**, *109*, 5526. "Preparation and Characterization of Molecule-Based Transistors with a 50 Nanometer Source-Drain Separation Using Shadow Deposition Techniques: Towards Faster, More Sensitive Molecule-Based Devices"

15. Chao, S.; Wrighton, M. S. *J. Am. Chem. Soc.*, **1987**, *109*, 6627. "Characterization of a "Solid State" Polyaniline-Based Transistor: Water Vapor-Dependent Characteristics of a Device Employing a Polyvinylalcohol/Phosphoric Acid Solid State Electrolyte"

16. Shu, C.-F.; Wrighton, M. S. *J. Phys. Chem.*, **1988**, *92*, 5221. "Synthesis and Charge Transport Properties of Polymers Derived from Oxidation of 1-H-1´-(6-(pyrrol-1-yl)hexyl-4,4´-bipyridinium Bis(hexafluorophosphate) and Demonstration of a pH Sensitive Microelectrochemical Transistor Derived from the Redox Properties of a Conventional Redox Center"

17. Schloh, M. O.; Leventis, N.; Wrighton, M. S. *J. Appl. Phys.*, **1989**, *66*, 965. "Microfabrication of WO_3-Based Microelectrochemical Devices"

18. Leventis, N.; Schloh, M. O.; Natan, M. J.; Hickman, J. J.; Wrighton, M. S. *Chemistry of Materials*, **1990**, *2*, 568. "Characterization of a "Solid-State" Microelectrochemical Diode Employing a Poly(vinyl alcohol)/Phosphoric Acid Solid-State Electrolyte: Rectification at Junctions between WO_3 and Polyaniline"

19. Huang, J.; Wrighton, M. S. *Anal. Chem.*, **1993**, *65*, 2740. "Microelectrochemical Multitransistor Devices Based on Electrostatic Binding of Electroactive Anionic Metal Complexes in Protonated Poly(4-vinylpyridine): Devices That Can Detect and Distinguish up to Three Species Simultaneously"

20. Schloh, Martin O. *Doctoral Thesis*, Massachusetts Institute of Technology, 1990. Novel Microelectrochemical Devices: Diodes and Transistors Based on Microfabrication and Electrochemical Derivatization of Microelectrodes with Redox Materials"

21. Letaw, Jr., H.; Bardeen, J. *J. Appl. Phys.* **1954**, *25*, 600. "Electrolytic Analog Transistor"

22. Hetrick, R. E.; Vassell, W. C. *Appl. Phys. Lett.* **1980**, *37*, 494. "An electrochemical transistor using a solid electrolyte"

23. McCoy, C. H.; Wrighton, M. S. *Chem. Mater.*, **1993**, *5*, 914. "Potential-Dependent Conductivity of Conducting Polymers Yields Opportunities for Molecule-Based Devices: A Microelectrochemical Push-Pull Amplifier Based on Two Different Conducting Polymer Transistors"

24. McCoy, C. H.; Wrighton, M. S. *submitted*, "An Inverter Gate With High Noise Immunity Based On A Conducting Polymer Microelectrochemical Transistor"

25. McCoy, C. H.; Lorkovic, I. M.; Wrighton, M. S. *J. Am. Chem. Soc.* in press, "Potential-Dependent Nucleophilicity of Polyaniline"

26. McCoy, C. H.; Rozsnyai, L. F.; Wrighton, M. S. *submitted* "Direct Chemical Tuning of the Electrical Properties of Poly(3-Methylthiophene) by Chlorination"

27. McCoy, C. H.; Wrighton, M. S. *in preparation* (Direct Trifluoroacetylation and Potential-Dependent Nucleophilicity of Polypyrrole)

28. McCoy, C. H.; Wolf, M. O.; Wrighton, M. S. *in preparation* (pH Dependence of the Conducting Properties of Poly(2,5-dithienylpyridine): A Chemically Sensitive Polymer)

29. *Handbook of Conducting Polymers*; Skotheim, T. A., Ed.; Marcel Dekker: New York, 1986

30. *Conjugated Polymers*, Brédas, J. L.; Silbey, R. Eds.; Kluwer Academic Publishers: Boston, 1991

31. Glenis, S.; Ginley, D. S.; Frank, A. J. *J. Appl. Phys.* **1987**, *62*, 190. "Solid-state and electrochemical properties of polyselenophene". Chorro, C.; Moukala, B.; Lere-Porte, J.-P.; Petrissans, J. *Mol. Cryst. Liq. Cryst.* **1990**, *187*, 199. "Optimisation of the electrosynthesis of polythiophene and polyselenophene"

32. Glenis, S.; Benz, M.; LeGoff, I; Schindler, J. L.; Kannewurf, C. R.; Kanatzidis, M. G. *J. Am. Chem. Soc.* **1993**, *115*, 12519. "Polyfuran: A New Synthetic Approach and Electronic Properties"

33. Sugimoto, R.; Yoshino, K.; Inoue, S.; Tsukagoshi, K. *Jpn. J. Appl. Phys. Part 2* **1985**, *24*, 425. "Preparation and property of polytellurophene and polyselenophene"

34. Reynolds, J. R.; Ruiz, J. P.; Child, A. D.; Nayak, K.; Marynick, D. S. *Macromolecules* **1991**, *24*, 678. "Electrically Conducting Polymers Containing Alternating Substituted Phenylene and Bithiophene Repeat Units"

35. Feast, W. J.; Millichamp, I. S.; Friend, R. H.; Horton, M. E.; Phillips, D.; Rughooputh, S. D. D. V.; Rumbles, G. *Synth. Met.* **1985**, *10*, 181. "Optical absorption and luminescence in poly(4,4'-diphenylenediphenylvinylene)"

36. King, G.; Higgins, S. J. *J. Chem. Soc. Chem. Comm.* **1994**, 825. "Novel Substituted Poly(benzo[*c*]thiophenes); Controlling n- and p-Doping Potentials"

37. Brédas, J.-L.; Street, G. B. *Accs. Chem. Res.* **1985**, *18*, 309. "Polarons, Bipolarons, and Solitons in Conducting Polymers"

38. Chance, R. R.; Boudreaux, D. S.; Brédas, J.-L.; Silbey, R. in reference 29, Chapter 24. "Solitons, Polarons, and Bipolarons in Conjugated Polymers"

39. Ofer, D.; Wrighton, M. S. *J. Am. Chem. Soc.*, **1988**, *110*, 4467. "Potential Dependence of the Conductivity of Poly(3-methylthiophene) in Liquid SO_2/Electrolyte: A Finite Potential Window of High Conductivity"

40. Ofer, D.; Crooks, R. M.; Wrighton, M. S. *J. Am. Chem. Soc.*, **1990**, *112*, 7869. "Potential Dependence of the Conductivity of Highly Oxidized Polythiophenes, Polypyrroles, and Polyaniline: Finite Windows of High Conductivity"

41. Ofer, D.; Park, L. Y.; Schrock, R. R.; Wrighton, M. S. *Chemistry of Materials*, **1991**, *3*, 573. "Potential Dependence of the Conductivity of Polyacetylene: Finite Potential Windows of High Conductivity"

42. Park, L. Y.; Ofer, D.; Gardner, T. J.; Schrock, R. R.; Wrighton, M. S. *Chemistry of Materials*, **1992**, *4*, 1388. "Effect of Chain Length on the Conductivity of Polyacetylene. Potential Dependence of the Conductivity of a Series of Polyenes Prepared by a Living Polymerization Method"

43. Ofer, David. *Doctoral Thesis*, Massachusetts Institute of Technology, 1991. "Electrochemical Studies of Conjugated Polymers; Finite Potential Windows of High Conductivity"

44. Crooks, R. M.; Chyan, O. M. R.; Wrighton, M. S. *Chemistry of Materials*, **1989**, *1*, 2. "Potential Dependence of the Relative Conductivity of Poly(3-methylthiophene): Electrochemical Reduction in Acetonitrile and Liquid Ammonia"

45. Ofer, D; Swager, T. M.; Wrighton, M. S. *Chem. Mater.* **1995**, *7*, 418 "Solid-State Ordering and Potential Dependence of Conductivity in Poly(2,5-dialkoxy-*p*-phenyleneethynylene)

46. Storrier, G. D.; Colbran, S. B.; Hibbert, D. B. *Synth. Met.* **1994**, *62*, 179 "Chemical and electrochemical syntheses, and characterization of poly(2,5-dimethoxyaniline) (PDMA): a novel, soluble, conducting polymer"

47. Edwards, J. H.; Feast, J. W. *Polymer* **1980**, *21*, 595. "A new synthesis of poly(acetylene)"

48. Rubinstein, I. *J. Electrochem. Soc.* **1983**, *130*, 1506. "Electrochemistry of Polyphenylene Films Deposited Anodically on Platinum or Glassy Carbon Electrodes in HF-Benzene System"

49. Tourillon, G.; Garnier, F. *J. Electroanal. Chem.* **1984**, *161*, 51. "Structural effect on the electrochemical properties of polythiophene and derivatives"

50. J. M. Bureau, M. Gazard, M. Champagne, and J. C. Dubois, *Mol. Cryst. Liq. Cryst.* **1985**, *118*, 235. "Influence of 3-4 substitutions on properties of five membered polyheterocycles"

51. Brédas, J. L.; Street, G. B.; Thémans, B.; André, J. M. *J. Chem. Phys.* **1985**, *83*, 1323. "Organic polymers based on aromatic rings (polyparaphenylene, polypyrrole, polythiophene): Evolution of the electronic properties as a function of the torsion angle between adjacent rings"

52. Huang, W.-S.; Humphrey, B. D.; MacDiarmid, A. G. *J. Chem. Soc., Faraday Trans. 1* **1986**, *82*, 2385. "Polyaniline, a Novel Conducting Polymer"

53. Roncali, J.; Garnier, F.; Lemaire, M.; Garreau, R. *Synth. Met.* **1986**, *15*, 323. "Poly mono-, bi-, and trithiophene: effect of oligomer chain length on the polymer properties"

54. Patil, A. O.; Ikenoue, Y.; Wudl, F.; Heeger, A. J. *J. Am. Chem. Soc.* **1987**, *109*, 1858. "Water-Soluble Conducting Polymers"

55. Kaplan, S.; Conwell, E. M.; Richter, A. F.; MacDiarmid, A. G. *J. Am. Chem. Soc.* **1988**, *110*, 7647. "Solid-State ^{13}C NMR Characterization of Polyanilines"

56. Shu, C.-F.; Wrighton, M. S. *ACS Symposium Series*, No 378, "Electrochemical Surface Science: Molecular Phenomena at Electrode Surfaces", ed. Manuel P. Soriaga, American Chemical Society, Washington, **1988**. "Synthesis and Electrochemical Properties of the Polymer Derived from Oxidation of 1-Methyl-1'-(3-thiophene-3-yl-propyl)-4,4'-bipyridinium Bis-Hexafluorophosphate: Charge Transport via the Viologen Subunits and Properties of the Polythiophene"

57. Rehahn, M.; Schlüter, A.-D.; Wegner, G.; Feast, W. J. *Polymer*, **1989**, *30*, 1054. "Soluble poly(*para*-phenylene)s. 1. Extension of the Yamamoto synthesis to dibromobenzenes substituted with flexible side chains"

58. Rühe, J.; Ezquerra, T. A.; Wegner, G. *Synth. Met.* **1989**, *28*, C177. "New conducting polymers from 3-alkylpyrroles"

59. Manohar, S. K.; MacDiarmid, A. G.; Cromack, K.; Ginder, J. M.; Epstein, A. J. *Synth. Met.* **1989**, *29*, E349. "N-substituted derivatives of polyaniline"

60. Leclerc, M.; Guay, J.; Dao, L. H. *Macromolecules* **1989**, *22*, 649. "Synthesis and Characterization of Poly(alkylanilines)"

61. Lacroix, J. C.; Kanazawa, K. K.; Diaz, A. *J. Electrochem. Soc.* **1989**, *136*, 1308. "Polyaniline: A Very Fast Electrochromic Material"

62. Ando, M.; Watanabe, Y.; Iyoda, T.; Honda, K.; Shimidzu, T. *Thin Solid Films* **1989**, *179*, 225. "Syntheses of conducting polymer Langmuir-Blodgett multilayers"

63. Geniès, E. M.; Noël, P. *J. Electroanal. Chem.* **1990**, *296*, 473. "Oxidation of 2,5-dimethylaniline in $NH_4F{\cdot}2.35$ HF medium Characteristics of the resulting conducting polymer"

64. Lemaire, M.; Garreau, R.; Delabouglise, D.; Roncali, J.; Youssoufi, H. K.; Garnier, F. *New J. Chem.* **1990**, *14*, 359. "Design and synthesis of polythiophene containing phenyl substituents"

65. Paloheimo, J.; Stubb, H.; Yli-Lahti, P.; Kuivalainen, P. *Synth. Met.* **1991**, *41-43*, 563. "Field-effect conduction in polyalkylthiophenes"

66. Fabre, P.-L.; Dalger, A. *J. Chem. Research (S)* **1991**, 16 *(M)* **1991**, 0255. "Functionalization of Poly(3-methylthiophene) Film Electrodes: Doping of Iron-Thiolate Complexes"

67. Ochmanska, J.; Pickup, P. *Can. J. Chem.* **1991**, *69*, 653. "Synthesis, electrochemistry, and ligand substitution reactions of conducting copolymer films of ruthenium polypyridine complexes of aromatic heterocycles"

68. Roncali, J. *Chem. Rev.* **1992**, *92*, 711. "Conjugated Poly(thiophenes): Synthesis, Functionalization, and Applications"

69. Ritter, S. K.; Noftle, R. E.; Ward, A. E. *Chem. Mater.* **1993**, *5*, 752. "Synthesis, Characterization, and Oxidative Polymerization of 3-(Fluoromethyl)thiophenes"

70. Wolf, M.; Wrighton, M. S. *Chem. Mater.* **1994**, *6*, 1526. "Tunable Electron Density at a Rhenium Carbonyl Coordinated to the Conducting polymer Poly(5,5'-(2-thienyl)-2,2'-bithiazole)"

71. Ono, N.; Hironaga, H.; Simizu, K.; Ono, K.; Kuwano, K.; Ogawa, T. *J. Chem. Soc. Chem. Comm.* **1994**, 1019. "Synthesis of pyrroles annulated with polycyclic aromatic compounds; precursor molecules for low band gap polymers"

72. Marsella, M. J.; Carroll, P. J.; Swager, T. M. *J. Am. Chem. Soc.* **1994**, *116*, 9347 "Conducting Pseudopolyrotaxanes: A Chemoresistive Response via Molecular Recognition"

73. Ferraris, J. P.; Bravo, A.; Kim, W.; Hrncir, D. C. *J. Chem. Soc. Chem. Comm.* **1994**, 991. "Reduction of steric interactions in thiophene-pyridino[*c*]thiophene copolymers"

74. Aizawa, M.; Yamada, T.; Shinohara, H.; Akagi, K.; Shirakawa, H. *J. Chem. Soc. Chem. Comm.* **1986**, *1315*. "Electrochemical Fabrication of a Polypyrrole-Polythiophene p-n Junction Diode"

75. Malmros, M. K.; Gulbinski III, J.; Gibbs Jr., W. B. *Biosensors* **1987/88**, *3*, 71. "A Semiconductive Polymer Film Sensor for Glucose

76. Miller, L.; Zhou, Q. X. *Macromolecules* **1987**, *20*, 1594. "Poly(N-methylpyrrolylium) Poly(styrenesulfonate). A Conductive, Electrically Switchable Cation Exchanger That Cathodically Binds and Anodically Releases Dopamine"

77. Naegele, D.; Bittihn, R. *Solid State Ionics* **1988**, *28-30*, 983. "Electrically conductive polymers as rechargeable battery electrodes"

78. Burroughes, J. H.; Jones, C. A.; Friend, R. H. *Nature* **1988**, *335*, 137. "New semiconductor device physics in polymer diodes and transistors"

79. Oyama, N.; Yoshimura, F.; Ohsaka, T.; Koezuka, H.; Ando, T. *Jpn. J. Appl. Phys., Part 2* **1988**, *27*, L448. "Characteristics of a Field-Effect Transistor Fabricated with Electropolymerized Thin Film"

80. Shacklette, L. W.; Jow, T. R.; Maxfield, M.; Hatami, R. *Synth. Met.* **1989**, *28*, C655. "High energy density batteries derived from conducting polymers"

81. Mastragostino, M.; Marinangeli, A. M.; Corradini, A.; Giacobbe, S. *Synth. Met.* **1989**, *28*, C501. "Conducting Polymers as Electrochromic Materials"

82. Horowitz, G.; Fichou, D.; Peng, X.; Xu, Z.; Garnier, F. *Solid State Commun.* **1989**, *72*, 381. "A field-effect transistor based on conjugated alpha-sexithienyl"

83. Assadi, A.; Svensson, C.; Willander, M.; Inganäs, O. *Synth. Met.* **1989**, *28*, C863. "Field effect mobility in thin films of poly(3-alkylthiophene)"

84. Fortier, G.; Brassard, E.; Bélanger, D.; *Biosens. Bioelectron.* **1990**, *5*, 473. "Optimization of a polypyrrole glucose oxidase biosensor"

85. Paloheimo, J.; Kuivalainen, P.; Stubb, H.; Vuorimaa, E.; Yli-Lahti, P. *Appl. Phys. Lett.* **1990**, *56*, 1157. "Molecular field-effect transistors using conducting polymer Langmuir-Blodgett films"

86. Rosner R. B.; Rubner, M. F. *Mat. Res. Soc. Symp. Proc.* Vol. **1990**, *173*, 363. "Evaluation of thing film capacitors fabricated from heterogeneous polypyrrole based Langmuir-Blodgett films"

87. Sailor, M. J.; Ginsburg, E. J.; Gorman, C. B.; Kumar, A.; Grubbs, R. H.; Lewis, N. S. *Science* **1990**, *249*, 1146. "Thin Films of *n*-Si/Poly-$(CH_3)_3Si$-Cyclooctatetraene: Conducting-Polymer Solar Cells and Layered Structures"

88. Burroughes, J. H.; Bradley, D. D. C.; Brown, A. R.; Marks, R. N.; Mackay, K.; Friend, R. H.; Burns, P. L.; Holmes, A. B. *Nature* **1990**,*347*, 539. "Light-emitting diodes based on conjugated polymers"

89. Punkka, E.; Rubner, M. F. *Synth. Met.* **1991**, *41-43*, 1509. "Formation of rectifying contacts to Langmuir-Blodgett films of poly(3-hexylthiophene)"

90. Dyreklev, P.; Gustafsson, G.; Inganäs, O.; Stubb, H. *Solid State Commun.* **1992**, *82*, 317. "Aligned Polymer Chain Field Effect Transistors"

91. Burn, P. L.; Holmes, A. B.; Kraft, A.; Bradley, D. D. C.; Brown, A. R.; Friend, R. H.; Gymer, R. W. *Nature* **1992**, *356*, 47. "Chemical tuning of electroluminescent copolymers to improve emission efficiencies and allow patterning"

92. Gustafsson, G.; Cao, Y.; Treacy, G. M.; Klavetter, F.; Colaneri, N.; Heeger, A. J. *Nature* **1992**, *357*, 477. "Flexible light emitting diodes made from soluble conducting polymers"

93. Koezuka, H.; Tsumura, A.; Fuchigami, H.; Kuramoto, K. *Appl. Phys. Lett.* **1993**, *62*, 1794. "Polythiophene field-effect transistor with polypyrrole worked as source and drain electrodes"

94. Rudge, A.; Raistrick, I.; Gottesfeld, S.; Ferraris, J. P. *Electrochimica Acta* **1994**, *39*, 273. "A study of the electrochemical properties of conducting polymers for application in electrochemical capacitors"

95. Berggren, M.; Inganäs, O.; Gustafsson, G.; Rasmusson, J.; Andersson, M. R.; Hjertberg, T.; Wennerström, O. *Nature*, **1994**, *372*, 444. "Light-emitting diodes with variable colours from polymer blends"

96. Diaz, A. F.; Bargon, J. in reference 29, Chapter 3. "Electrochemical Synthesis of Conducting Polymers"

97. Waltman, R. J.; Bargon, J. *Can. J. Chem.* **1986**, *64*, 76. "Electrically conducting polymers: a review of the electropolymerization reaction, of the effects of chemical structure on polymer film properties, and of applications towards technology"

98. Bardeen, J.; Brattain, W. H. *Phys. Rev.* **1948**, *74*, 230. "The Transistor, A Semiconductor Triode"

99. Schockley, W. *Bell Syst. Tech. J.* **1949**, *28*, 435. "The Theory of *p-n* Junctions in Semiconductors and *p-n* Junction Transistors"

100. Sze, S. M. *Physics of Semiconductor Devices*, Wiley: New York, 1981

101. Horowitz, P.; Hill, W. *The Art Of Electronics*; Cambridge University Press: New York, 1989

102. Pierret, R. F. *Field Effect Devices*, Addison-Wesley: Reading, Massachusetts, 1990

103. Pierret, R. F. *Semiconductor Fundamentals*, Addison-Wesley: Reading, Massachusetts, 1990

104. Heeger, A. J. In reference 29 "Polyacetylene: New Concepts and New Phenomena"

105. Specht, L. T.; Hoke, W. E.; Oguz, S.; Lemonias, P. J.; Kreismanis, V. G.; Korenstein, R. *Appl. Phys. Lett.* **1986**, *48*, 417. "High performance HgCdTe photoconductive devices grown by metalorganic chemical vapor deposition"

106. Irvine, S. J. C.; Giess, J.; Gough, J. S.; Blackmore, G. W.; Royle, A.; Mullin, J. B.; Chew, N. G.; Cullis, A. G. *J. Crystal Growth* **1986**, *77*, 437

107. Ludowise, M. J. *J. Appl. Phys.* **1985**, *58*, R31. "Metalorganic chemical vapor deposition of III-V semiconductors"

Chapter 2

Electrochemistry and Electrical Characteristics of Microelectrochemical Transistors

Abstract

Characterization of the transconductance, I_D-V_G, and I_D-V_D behavior of polyaniline-based microelectrochemical transistors is reported for a range of values for V_D. The transconductance, I_D-V_G, and especially I_D-V_D characteristics of microelectrochemical transistors are significantly affected by both the magnitude and polarity of drain voltage. The behavior of a microelectrochemical transistor in which a single electrode serves as both source and gate differs markedly from a device in which a separate gate electrode is used. It is found that a device will support drain current as long as one electrode maintains an electrochemical potential at which the device-active material is conducting, even if the other electrodes in contact with the active material are at electrochemical potentials where that material is insulating. The application of microelectrochemical transistors in electronic amplifiers is developed and demonstrated in the form of a polyaniline-based audio amplifier. The method for determination of power gain, consistent with the term as defined for transistors, is described. An improved configuration for power gain measurements at kilohertz frequencies is reported.

Introduction

The work presented in this thesis began with the demonstration that a microelectrochemical transistor could amplify an audio signal and drive a pair of headphones. This result and the background associated with it is an appropriate introduction to molecule-based transistors functioning in electronic circuits because it demonstrates the concepts of gain, frequency response, basic transistor function and its extension to the complete electrical function of an amplifier. Indeed, upon the discovery of the transistor[1] one of the first tests made of the device was the demonstration of its ability to amplify an audio signal to drive a speaker. This chapter provides a further introduction to the specifics of microelectrochemical transistors, for which the abbreviation MET will be used, and then moves into new results concerning fundamental device characteristics and the electrochemistry of conducting polymer devices in electronic circuits.

The closest solid-state relative of the MET, as described in Chapter 1, is the metal-oxide semiconductor field-effect transistor, or MOSFET. There are a number of important comparisons to be made between the MET and the MOSFET. Both devices are charge-controlled meaning that a fixed number of electrons must be moved into or out of the gate terminal to switch the device between two given states of conduction. Therefore, both devices draw dynamic gate current only and once the necessary charge has been passed to establish V_G, no further gate current flows. The description of voltage-controlled resistor is an apt one for both devices. For both devices, the faster V_G is switched between two values, the high I_G is since the same quantity of charge must be passed in a shorter period of time. Both devices have four terminals: drain, source, and gate, and the substrate back for a MOSFET and the counter/reference electrode for a microelectrochemical transistor. A critical difference is that while the substrate back contact and source terminal in a MOSFET can be connected together and V_G applied between gate and source, in a microelectrochemical transistor the counter/reference electrode must remain independent so that the electrochemical potential of the device-active material can be varied with respect to

the counter/reference electrode. While the MOSFET has a specific structure associated with its gate (the metal contact separated from the bulk of the device by the gate insulating layer), the microelectrochemical transistor does not. Any electrode can serve as gate if that electrode can effect oxidation or reduction of the polymer. Indeed, it is common to use only two microelectrodes rather than three in a device and simply employ one electrode as both source and gate. The role of the counter/reference electrode and the ability of any electrode to serve as gate are minor distinctions when characterizing a single transistor but become absolutely critical in the preparation of systems employing more than one device. Part of this thesis is devoted to understanding and developing the necessary design approaches to account for the unusual gate properties of electrochemical devices.

Like MOSFETs, a microelectrochemical transistor brought into conduction will allow drain current to flow either from source to drain or drain to source, since no rectifying junctions are present. In MOSFETs, the threshold value of V_G for onset of transistor conduction is subject to manufacturing variability. In microelectrochemical transistors, onset potential is an inherent property of the device-active material which is not subject to variability from one device to the next. The threshold voltage for a microelectrochemical transistor can be chosen by selecting the appropriate reference electrode, if desired, but for a given device active material/reference system combination onset potential is highly reproducible.

While METs have many characteristics in common with MOSFETs, and indeed it will be shown in Chapter 4 that METs can often function in a directly parallel fashion, The differences in the processes by which the two devices achieve transistor action can be critical. Because the ability of microelectrochemical transistors to act as a valve and control the flow of an electrical current is based on oxidation and reduction of a molecular reagent, the electrical characteristics are strongly linked to the electrochemistry of the gating process. Further, the device geometry of the microelectrochemical transistor is unusual in that unlike bipolar junction transistors or the field-effect transistor family, the control electrode is

simply an additional connection to the device-active material. Since the device configuration consists of two or more electrodes in contact with a molecular reagent which can display conductivity, *the electrode functions of source, drain, and gate are defined only by external circuit connections and not by device architecture.* As a result, any electrode in contact with the device-active material can serve as a gate electrode and give rise to gating electrochemical processes. This distinction is a critical one if two or more transistors are to be used in concert or if interelectrode potentials become significant, both situations being inevitable when METs are placed in application environments. The microelectrochemistry of a conducting polymer serving as the device-active material controlling a power supply of as much as 1500 mV is essential to understanding and preparing circuits based on conducting polymer transistors. This chapter is a detailed investigation of a wide range of basic transistor characteristics and the manner in which they change according to the specific and sometimes complex conditions of electrochemical potential control which inevitable arise from circuit requirements of amplifiers and logic gates.

Results and Discussion

Transconductance

The drain current-gate voltage (I_D-V_G) characteristic is fundamental expression of transistor function. It illustrates the governing of conduction through the device by control voltage V_G. Transconductance is the change in drain current resulting from a change in gate voltage, in other words the first derivative of the I_D-V_G characteristic.[2,3] As with MOSFETs, since channel conduction in METs is set by V_G, transconductance is a natural gain parameter. It is usually specified in units of mS per mm of gate width. (Gate *length* is the source-drain separation, gate *width* is the length of a source/drain electrode in an MET). Maximum transconductance values for METs have been reported for polyaniline[4] and poly(3-methylthiophene).[5] Figure 1 shows plots of drain current and device transconductance as a function of gate potential. METs are unusual in that they display a region of negative transconductance, a result of the unique finite window of high conductivity displayed by conducting polymers. Device transconductance can be increased by increasing V_D to obtain higher values of I_D, but a concurrent widening of the window of V_G over which the device conducts results in a shallower slope. For example, at V_D = 400 mV, polyaniline reaches oxidative insulation at 1.2 V vs. SCE instead of 0.8 V, and a maximum transconductance of about 30 mS/mm is attained on the forward scan, Figure 2. This dependence of the I_D-V_G characteristic on the magnitude of V_D, seen by comparison of Figures 1 and 2, is one example of the effect of drain voltage which is not small.

A high value for transconductance is desirable because it corresponds to high device gain. Choosing polymers of high conductivity such as poly(3-methylthiophene) as the device-active material is one route to obtaining good transconductance values, but polymers of only moderate conductivity can also compete. The primary requirement is a steep I_D-V_G characteristic. Thus a polymer which can provide only 20 μA of drain current in a microelectrochemical transistor but undergoes the 0 to 20 μA transition in 100 mV yields

Figure 1. I_D-V_G characteristic and device transconductance for a polyaniline transistor at $V_D = 25$ mV.

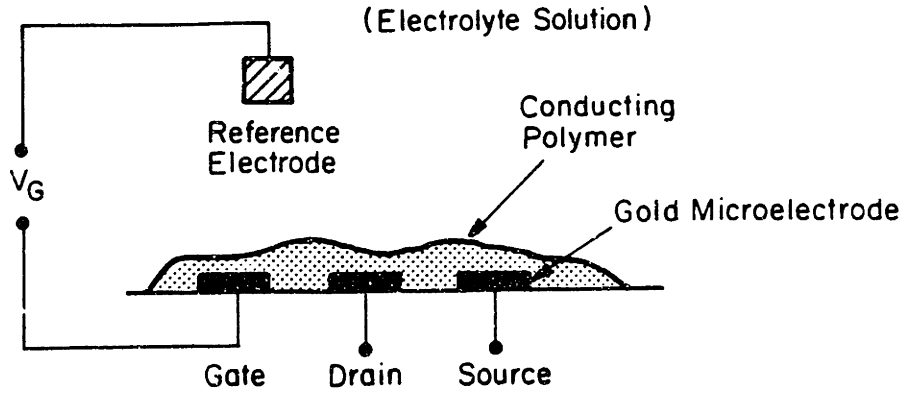
(Electrolyte Solution)
Reference Electrode
Conducting Polymer
V_G
Gold Microelectrode
Gate
Drain
Source

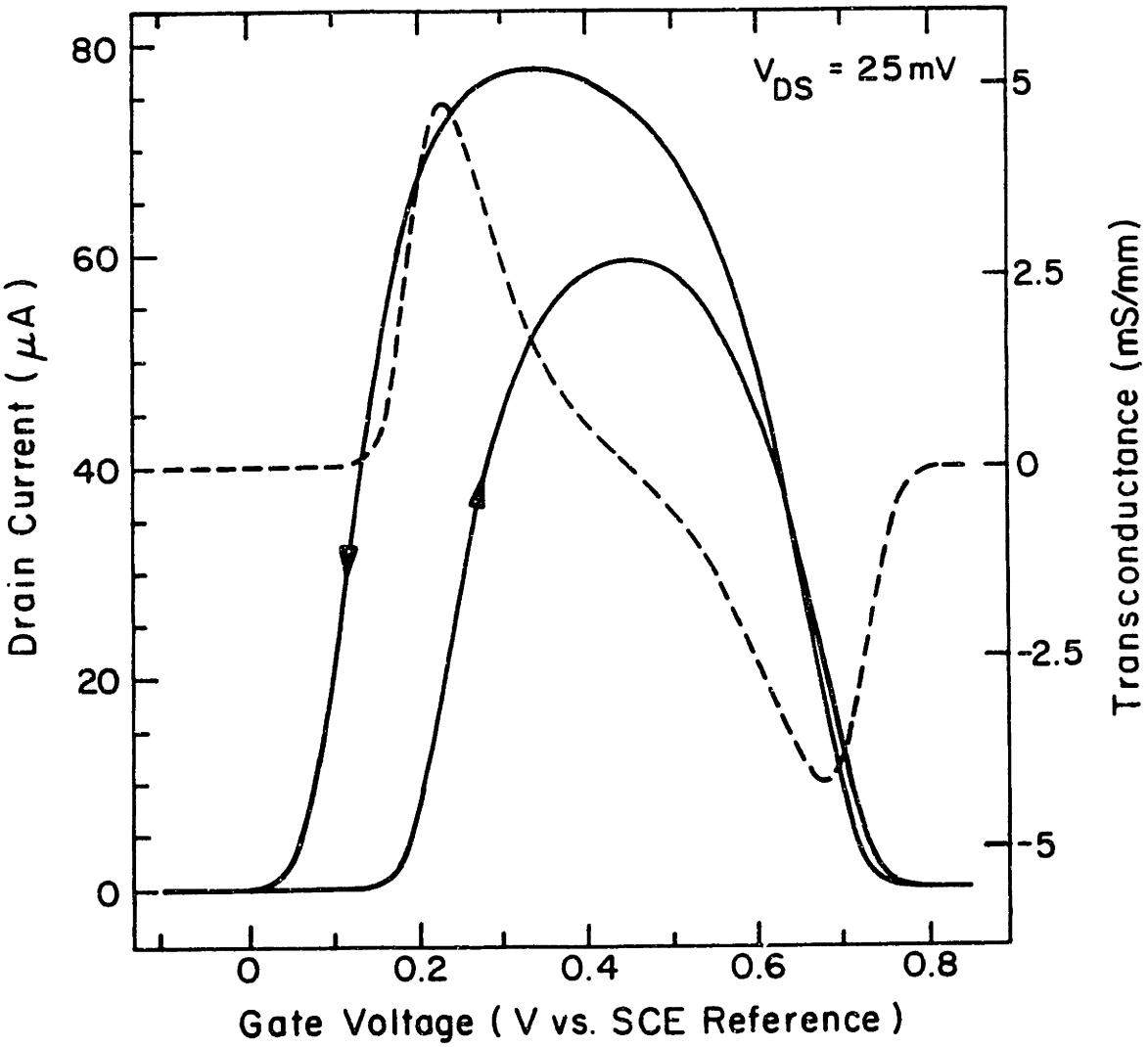
V_{DS} = 25 mV
Drain Current (μA)
Transconductance (mS/mm)
Gate Voltage (V vs. SCE Reference)
80
60
40
20
0
5
2.5
0
-2.5
-5
0
0.2
0.4
0.6
0.8

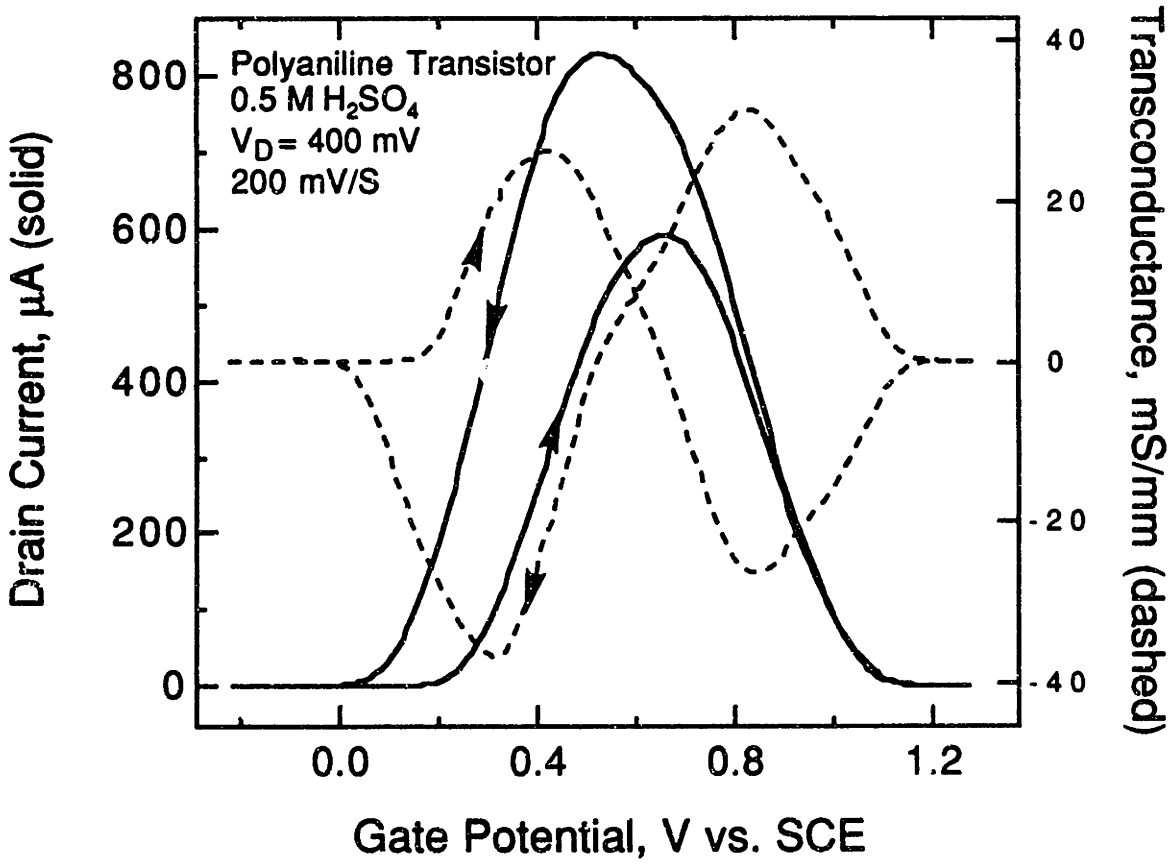

Figure 2. I_D-V_G and transconductance characteristics for a polyaniline microelectrochemical transistor at V_D = 400 mV.

the same transconductance as a polymer which provides a 100 µA swing over 500 mV. While maximum conductivity is clearly a central attribute of conducting polymers, it is only one property relevant to electronic devices.

Operating parameters for amplification

Amplification is the process by which a signal of smaller voltage and/or current is used to control a larger voltage and/or current. Scheme I shows a generalized representation of how a transistor functions in the amplification of a signal. The variation in V_G oxidizes and reduces the device-active material drawing gate current, I_G. The change

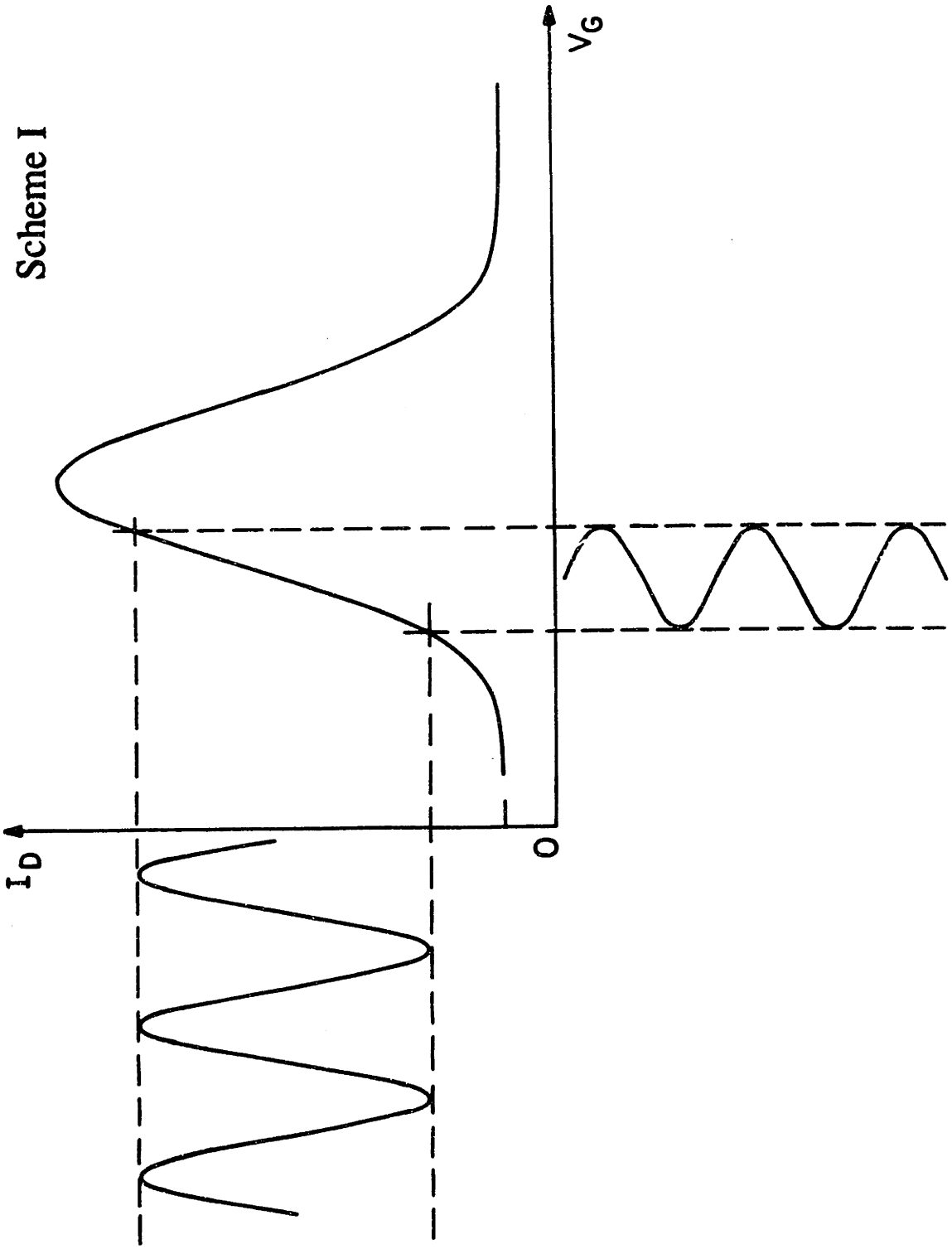
Scheme I
V_G
I_D
O

in conductivity resulting from this gate process gives rise to a variation in I_D. Current and power gain are realized because the current required to oxidize and reduce the polymer is small compared to the change in drain current which results. Note that operation is confined to a range of V_G well within the bounds of onset of conduction and peak conductivity. If this were not the case, and these limits were exceeded, the transistor would badly distort the electrical signal being amplified. A triangular wave is used as a test waveform, since a deviation (distortion) from its sharp peaks and linear ramp in the output waveform are more readily detected by inspection that would be the case for a sine wave. An example of a polyaniline transistor operated as represented in Scheme I is shown in Figure 3. The variation in drain current is a clean triangular wave like the gate waveform driving it. The distortion arising from the hysteresis in the I_D-V_G behavior of polyaniline can be seen upon close inspection of the drain current waveform manifesting itself as a slight bowing of the triangular wave. The gate current waveform shows the withdrawal and injection of charge as V_G ramps positive and negative, with sharp switching between oxidative and reductive current as the scan of gate voltage changes direction, and a maintained current as polyaniline is oxidized or reduced between the limits of the scan of gate potential. It is important to note that while I_D-V_G characteristics are not linear (for METs or MOSFETs) a linear relationship between input and output voltage can be introduced by the design of specific amplifier circuits.[2]

Power Gain

Power gain values have previously been reported for microelectrochemical transistors[6-10] according to a convention which is consistent, but incorrect in several respects. The peak positive values (measured with respect to baseline) of I_D and I_G were used to calculate gate and drain power, which neglects negative gate current, and is not meaningful for an oscillating drain current offset from zero. Power gain, as defined for transistors, is determined as the *change in drain power resulting from a change in gate*

Figure 3. Gate voltage, drain current, and gate current waveforms for a polyaniline microelectrochemical transistor.

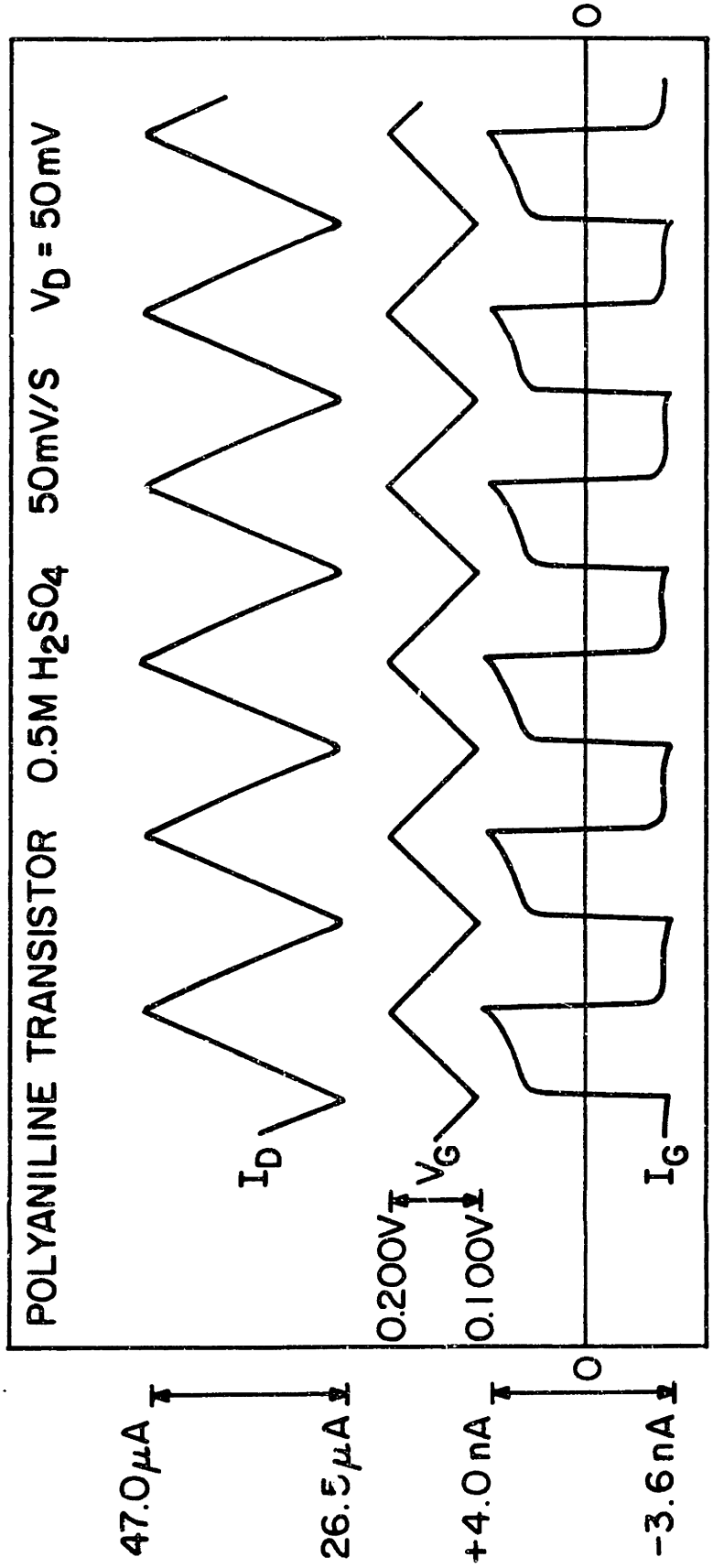
POLYANILINE TRANSISTOR 0.5M H_2SO_4 50mV/S V_D = 50mV
I_D
V_G
I_G
0.200V
0.100V
0
0
47.0μA
26.5μA
+4.0nA
-3.6nA

power.[11,12] In other words, the *peak to peak amplitude* of the appropriate waveforms. In Figure 3, these amplitudes have been pointed out. The current gain of the device is given by equation (1) and power gain by equation (2).

$$A_I = (I_{D,\,max} - I_{D,\,min})/(I_{G,\,max} - I_{G,\,min}) \qquad (1)$$

$$A_P = \Delta I_D V_D/\Delta I_G \Delta V_G = A_I(V_D/\Delta V_G) \qquad (2)$$

For the device data shown in Figure 3, the current and power gain were:

$A_I = (47\ \mu A - 26.5\ \mu A)/(0.004\ \mu A - (-.0036\ \mu A)) = 2697$

$A_P = (20.5\ \mu A)(50\ mV)/(0.0076\ \mu A)(100\ mV) = 1348$

A further point is that voltage gain is taken to be the ratio of drain voltage to gate voltage to allow comparison to the published gain figures. However, while current gain can be measured without a load in the circuit, voltage gain cannot. With no load present, no voltage variation controlled by the transistor is occurring and voltage gain has no meaning. Therefore, the measurement of power gain should be conducted with a load present in the drain circuit. With a load resistance equal to the minimum drain-source resistance achieved by the transistor, a voltage variation of $V_D/2$ would be obtained as the output of a conventional amplifier circuit consisting of the transistor with a load resistor in the drain circuit and the output voltage taken to be V_{DS}. The resistor in the drain circuit would also half maximum drain current, reducing power gain by a factor of 4 compared to that calculated above in equation (2).

Power gain has previously been measured using the same bipotentiostat configuration used to make I_D-V_G measurements, Scheme II. This method is convenient but is not suitable for use at higher frequencies. The design of a bipotentiostat does not use two identical circuits to drive the two working electrodes but instead drives one with respect to the reference electrode and the second referenced to the other working

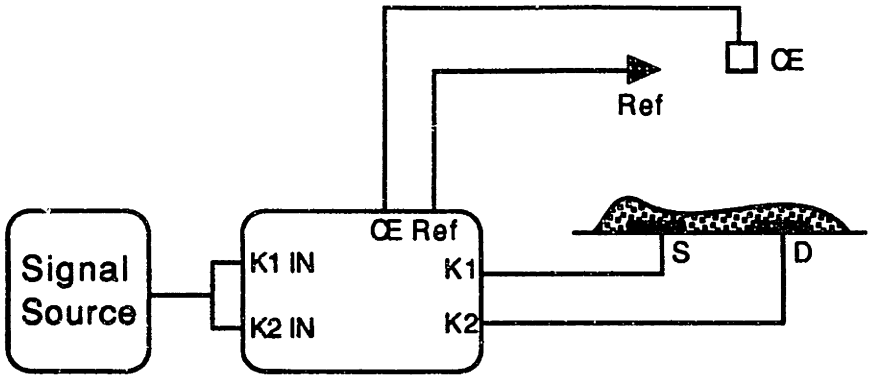

Scheme II. Bipotentiostat configuration suitable for measurement of power gain at frequencies up to 500 Hz (for a Pine Instruments RDE4 bipotentiostat). A signal source such as a function generator drives both working electrodes. An offset voltage applied to K2 provides V_D.

electrode.[13] As a result, the two circuits are expected to have different frequency response characteristics and in fact they do. The frequency response of a Pine Instruments RDE4 bipotentiostat was characterized and K2 is faster and its response rolls off at higher frequency than K1. As a result, even through K1 and K2 were swept together, they responded differently, especially in the 10 - 30 KHz range. This results in an oscillation in V_D, because one electrode tracks the drive signal while the other lags it, increasing the positive peak and attenuating the negative peak of I_D. The effect was significant enough to cause a resistor to appear to have 80 μA of power gain at 30 KHz! Such an error is serious on the current scale of MET measurements and the alternative configuration shown in Scheme III is a solution. In this set-up, V_D is applied by a second, independent source. A convenient independent source is simply a potentiostat with its counter and reference electrode terminals connected together, since this provides V_D and also a current follower to conveniently measure I_D. This configuration in Scheme III cannot give inflated results, and allows the use of faster potentiostats for V_G, such as the ubiquitous PAR 173 the frequency response of which was found to be flat to 100 KHz. A load has been added to the drain circuit to allow correct measurement of power gain. Voltage gain is the ratio of

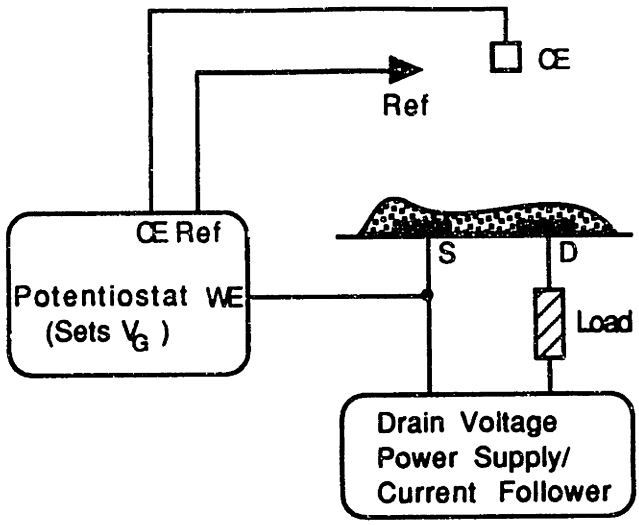

Scheme III. Improved experimental configuration for power gain measurements.

the peak-to-peak variation in voltage across the load to the peak-to-peak variation in gate voltage.

A Polyaniline-Based Audio Amplifier

An audio amplifier based on a polyaniline transistor was prepared as shown in Scheme IV. A power supply is provided capable of delivering sufficient voltage and current to drive the load (a pair of headphones). The polyaniline transistor serves to control the flow of power through the headphones, increasing and decreasing it in response to the amplitude of the audio input signal. Since an audio signal swings both positive and negative of zero, it is necessary to provide room for drain current to both increase and decrease in response. This is accomplished by choosing a fixed offset voltage that centers operation at one-half of maximum drain current, as represented at the bottom left of Scheme IV. This is a general consideration of one-transistor amplifiers and is not specific to microelectrochemical transistors. The audio signal controls the oxidation state, and therefore conductivity, of the polyaniline and governs the flow of drain current through the headphones. Dedicated gate electrodes were used so that gate current could not flow through the headphones. (This is irrelevant at low frequencies since I_G is so small, but

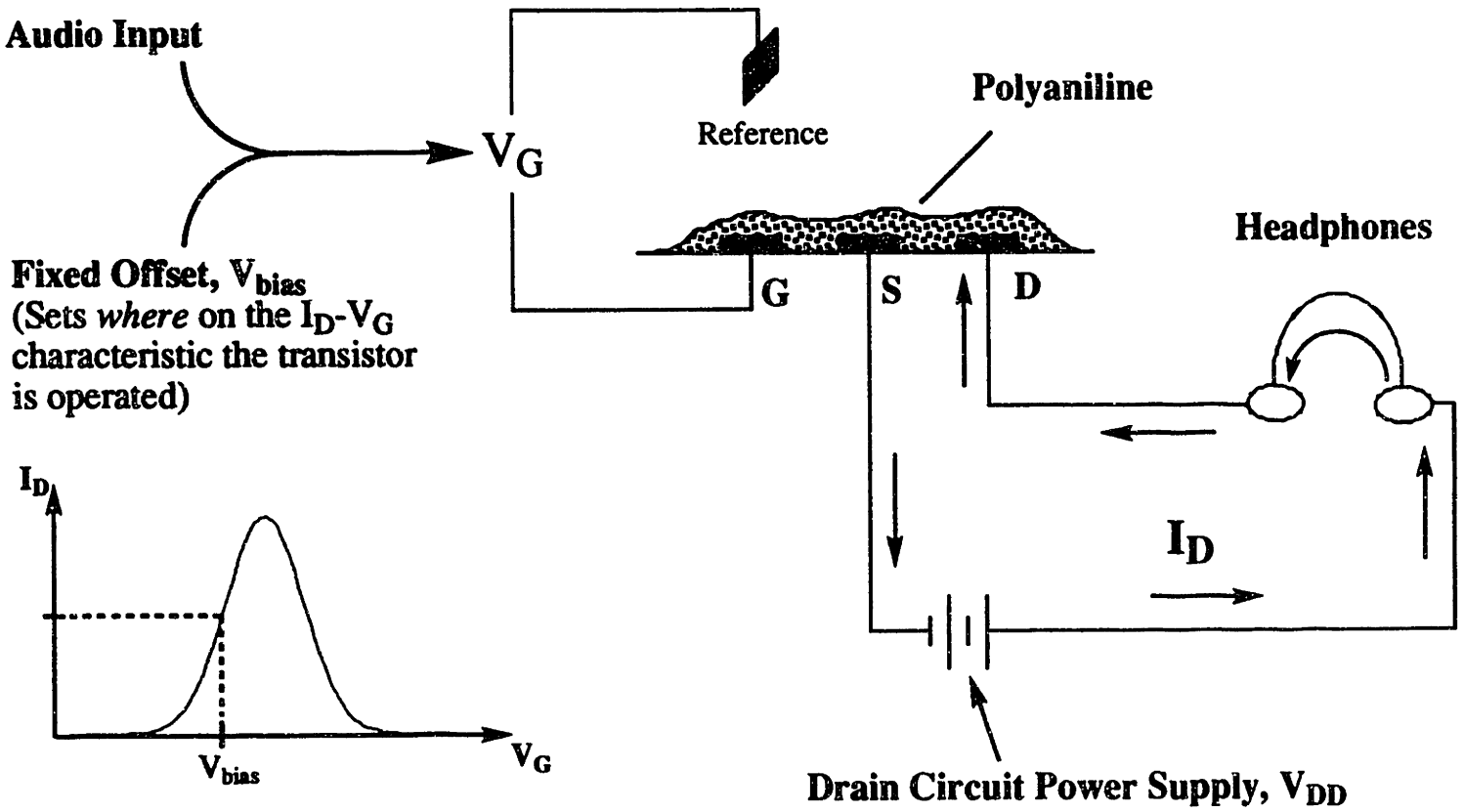

Scheme IV. Amplification of an audio signal by a polyaniline microelectrochemical transistor. A working amplifier was characterized based on a polyaniline device operated in 0.5 M H_2SO_4/0.25 M $NaHSO_4$ (aq) with V_{DD} = 500 mV and16Ω headphones. To increase drain current capability, two of each, D, S, and G were used in the configuration G/S/D/S/D/G.

significant in the KHz range were I_G becomes comparable to I_D) The large drain voltage of 500 mV is required to provide adequate drain current to produce an audible response in the headphones, which are a highly demanding load for a transistor of the device dimensions used, requiring polyaniline to sustain a current density of 10^3 A/cm^2. The frequency response limitations were evident in the increasing attenuation of higher frequencies and complete loss of frequencies above 10 KHz. The power gain of the circuit declined to unity by 1 KHz so the device was only able to amplify the lower portion of the audio spectrum. The configuration of the device, which used a total of six electrodes (2 each, drain, source, and gate) was chosen for high output current and not speed. Faster device configurations have been demonstrated which should provide improved frequency response.[6,9]

I_D-V_D Relationships

In the polyaniline audio amplifier described above it was necessary to use a comparatively large drain voltage. This requirement is inevitable as will be seen in the chapters which follow. When using the microelectrochemical transistor experiment to measure electrical characteristics of conducting polymers or other materials, the magnitude of V_D is intentionally kept small, 25 mV being a typical value. In this way, electrochemical potential control is not significantly perturbed by V_D. However, since large drain voltages which do perturb potential control are unavoidable in most transistor application environments, it became necessary to understand the electrochemistry of conducting polymer transistors under the more complex conditions of multielectrode potential control at high interelectrode potential differences. The magnitude and polarity of the applied drain voltage, as well as the specific arrangement of source, drain, and gate electrodes, all exert a marked effect on transistor electrical characteristics.

There is more than one possible choice of electrode configuration for an MET. Four important variations are shown in Scheme V. If V_D is kept small, potential control of the

Scheme V

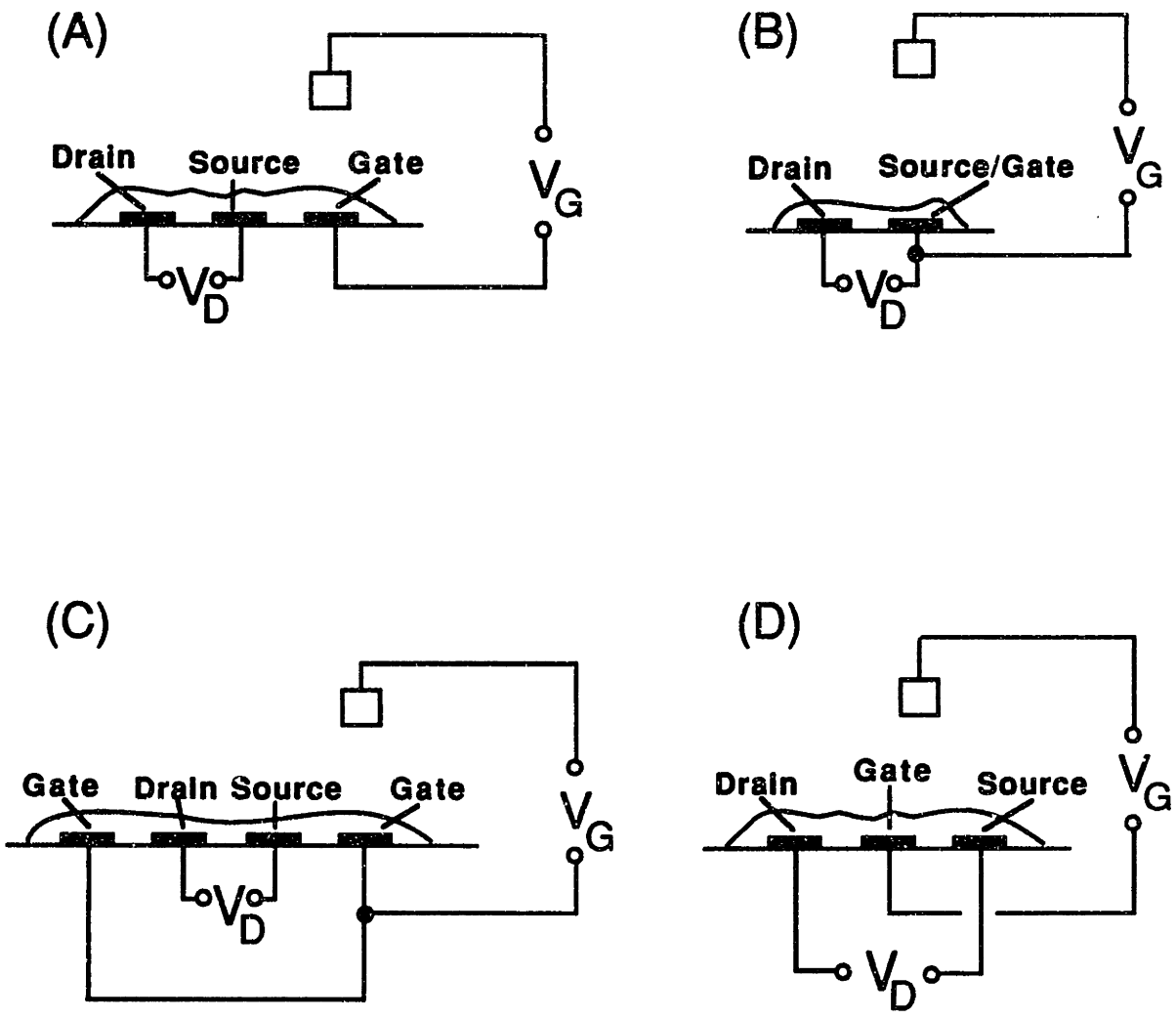

device active material is essentially due solely to gate potential V_G and the four configurations yield the same device characteristics. However, when V_D is large, the electrochemical potential of the drain and source electrodes can deviate substantially from V_G. As a result, each configuration has its own set of characteristics. I_D-V_D characteristics are commonly used in the characterization of transistors. The most important electrode configurations in Scheme V are A and B. In configuration B, it can be seen that the electrochemical potential of the drain electrode is equal to (V_G + V_D). V_D therefore has a direct effect on device behavior. In configuration A, the gate electrode is independent and

the effect of V_D is less direct. Figure 4 shows the I_D-V_D behavior for a polyaniline transistor of configuration B. In Figure 4, V_D is applied with the positive side connected to the source. Thus, the drain electrode is shifted negative of V_G by V_D. I_D increases linearly at first and then plateaus when the device-active material reaches its maximum rate of charge transport, known as saturation. Up to $V_G = 0.7$ V, the curves are analogous to a conventional MOSFET. However, at V_G greater than 0.7 V there is a lag in onset of drain current as V_D is scanned positive. Figure 5 shows the same device but with V_D applied with the positive side connected to the drain, thus shifting the drain electrode positive of V_G. The I_D-V_D behavior in Figures 4 and 5 are consistent with the precept that as long as either the source or drain electrode is at an electrochemical potential at which polyaniline is conducting, drain current is supported even if the other electrode or electrodes are at a potential where polyaniline is insulating. At 0.8, 0.9 and 1.0 V vs. SCE, polyaniline is insulating, being sufficiently oxidized to have reached oxidative turn-off. However, in Figure 4, as the magnitude of V_D is increased, the electrochemical potential of the drain electrode (V_G - V_D) is moved back into the window of conductivity of polyaniline. The more positive V_G, the larger V_D must be before this occurs, reflected in the positive progression in onset of drain current from $V_G = 0.8$ to 0.9 to 1.0 V. Notice that the saturation value of I_D does *not* follow the trend expected from the I_D-V_G characteristic of polyaniline where maximum conductivity occurs at about $V_G = 0.35$ V vs. SCE. Instead, maximum drain current occurs for the I_D-V_D characteristic scanned at $V_G = 0.8$ V.

In Figure 5, the polarity of V_D is reversed. At $V_G = -0.2$ V, polyaniline is insulating. However, when V_D reaches about 0.4 V, onset of drain current is observed. The potential for onset of conduction is 0.18 V vs. SCE for polyaniline, so this is consistent with the above precept. When V_D is 0.4 V, then the electrochemical potential of the drain electrode is (V_G + V_D) or 0.2 V. At progressively more positive V_G, a smaller magnitude of V_D is required to move the drain electrode into the range of potential where polyaniline is conducting. The data shown in both Figure 4 and Figure 5 indicate that even though one

Figure 4. I_D-V_D behavior for a polyaniline microelectrochemical transistor using a combined gate/source electrode (Scheme V, configuration B) and with V_D applied positive side to the source, negative side to the drain.

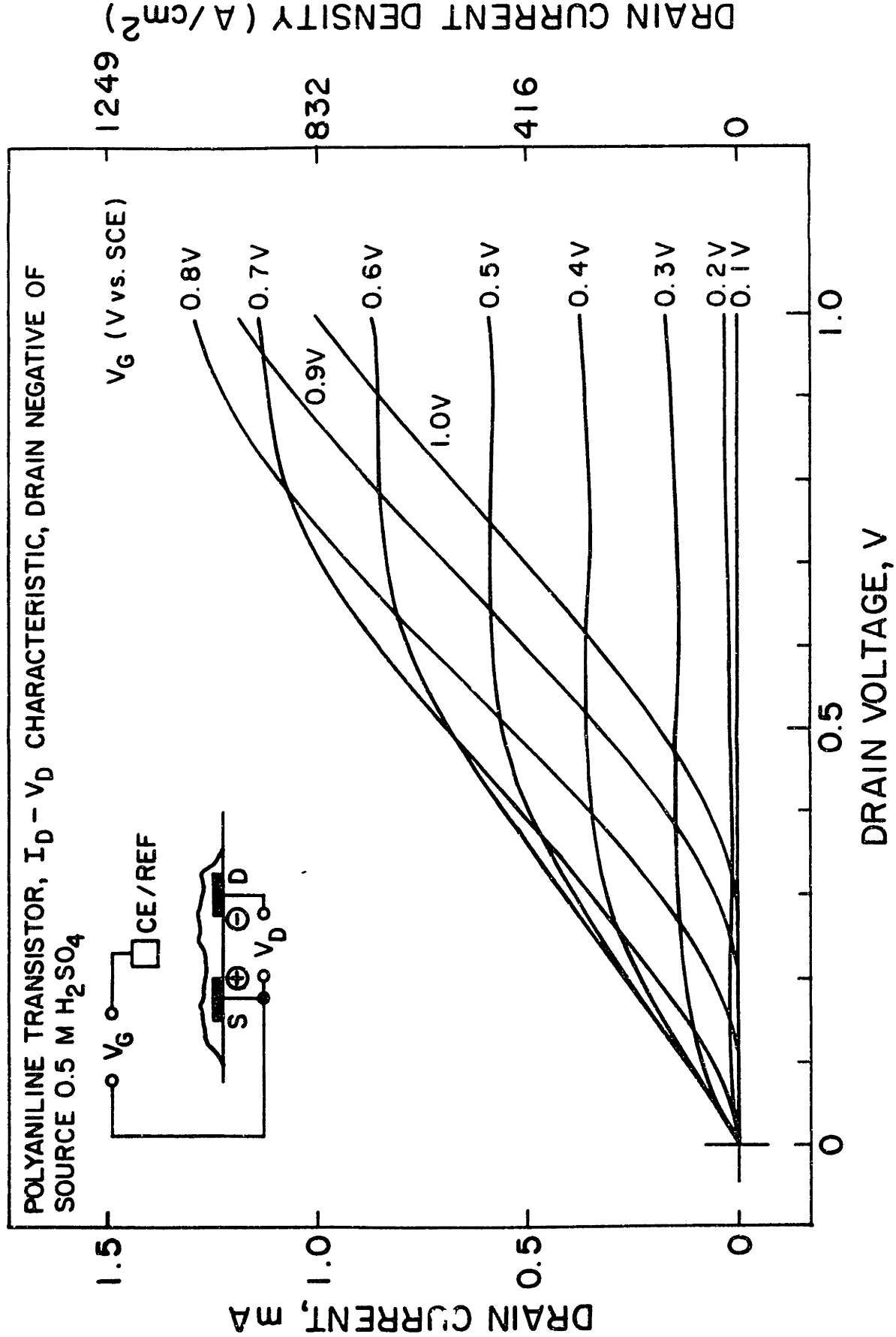
POLYANILINE TRANSISTOR, $I_D - V_D$ CHARACTERISTIC, DRAIN NEGATIVE OF SOURCE 0.5 M H_2SO_4
V_G (V vs. SCE)
0.8V
0.7V
0.9V
0.6V
1.0V
0.5V
0.4V
0.3V
0.2V
0.1V
V_G
CE/REF
S
D
V_D
DRAIN CURRENT, mA
1.5
1.0
0.5
0
DRAIN CURRENT DENSITY (A/cm^2)
1249
832
416
0
0
0.5
1.0
DRAIN VOLTAGE, V

Figure 5. I_D-V_D behavior for a polyaniline microelectrochemical transistor using a combined gate/source electrode (Scheme V, configuration B) and with V_D applied negative side to the source, positive side to the drain.

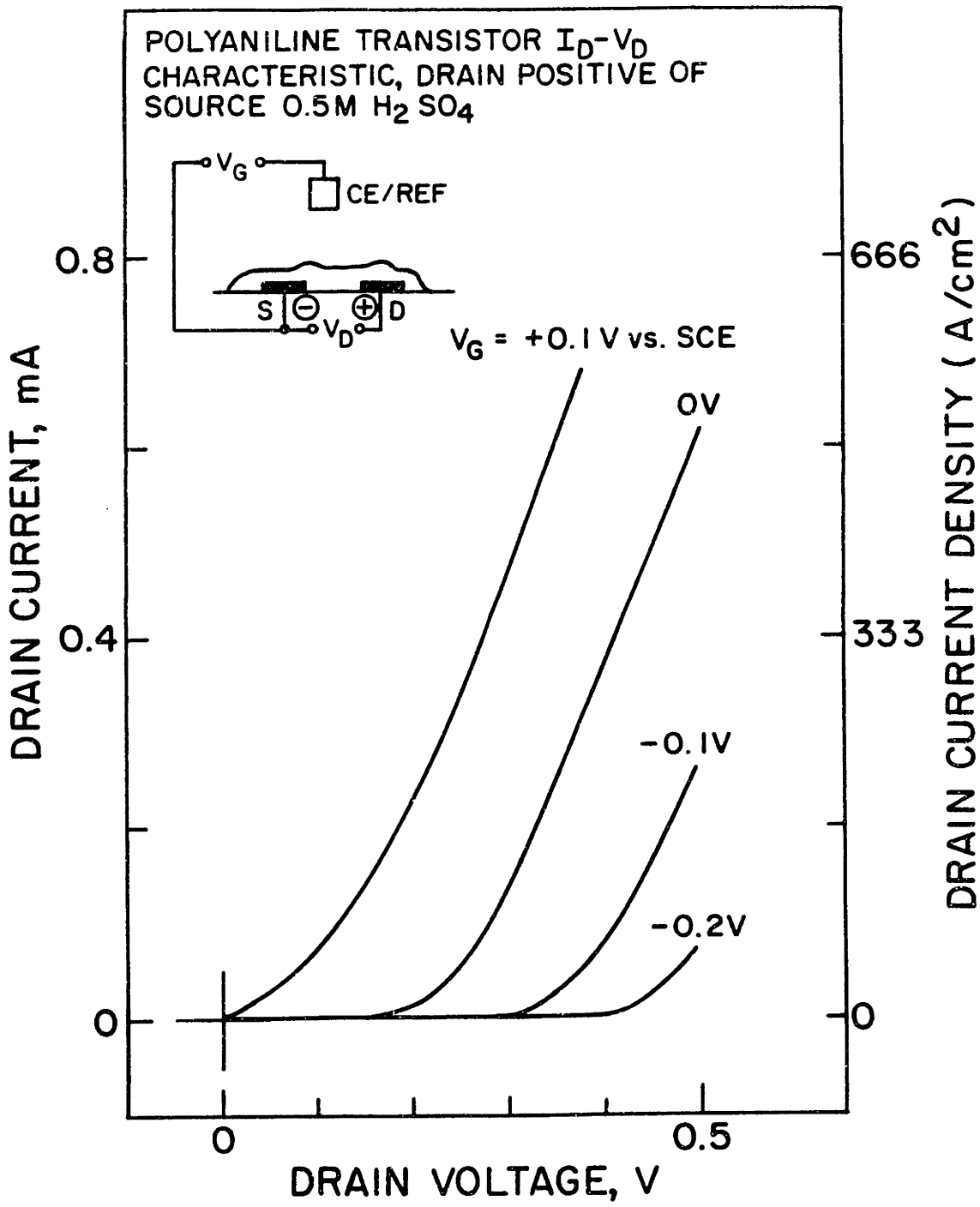
POLYANILINE TRANSISTOR I_D-V_D CHARACTERISTIC, DRAIN POSITIVE OF SOURCE 0.5M H_2SO_4
V_G
CE/REF
S
D
V_D
V_G = +0.1 V vs. SCE
0V
-0.1V
-0.2V
0.8
0.4
0
666
333
0
0
0.5
DRAIN CURRENT, mA
DRAIN CURRENT DENSITY (A/cm^2)
DRAIN VOLTAGE, V

Figure 6. I_D-V_D behavior for a polyaniline microelectrochemical transistor using a separate gate electrode (Scheme V, configuration A).

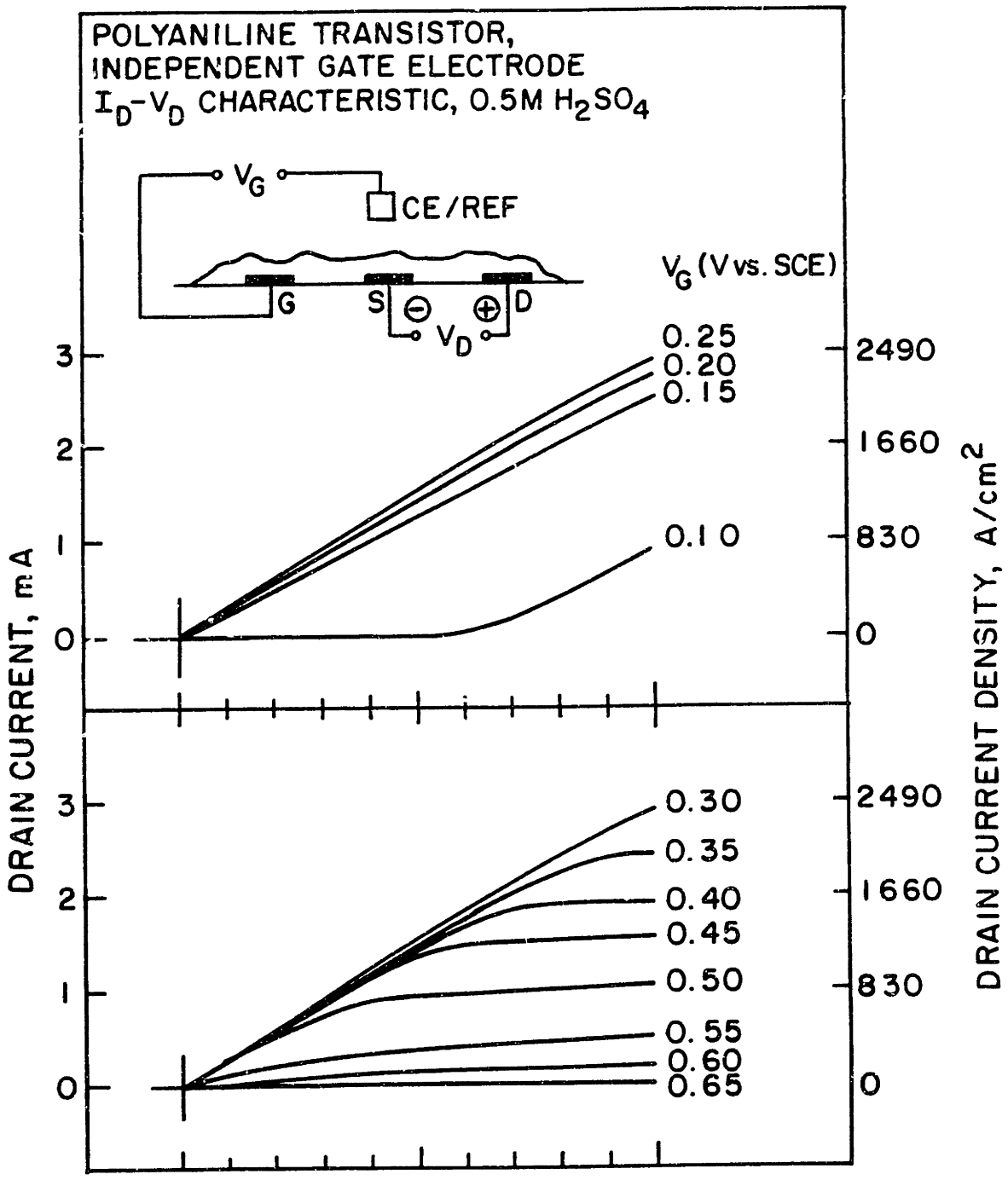
POLYANILINE TRANSISTOR,
INDEPENDENT GATE ELECTRODE
I_D-V_D CHARACTERISTIC, 0.5M H_2SO_4
V_G
CE/REF
G
S
D
V_D
V_G (V vs. SCE)
0.25
0.20
0.15
0.10
0.30
0.35
0.40
0.45
0.50
0.55
0.60
0.65
DRAIN CURRENT, mA
DRAIN CURRENT DENSITY, A/cm^2
3
2
1
0
2490
1660
830
0

electrode may be at an electrochemical potential where polyaniline is insulating, I_D still flows as long as the other electrode is within the finite window of conductivity of polyaniline.

The profile of I_D-V_D characteristics for a polyaniline MET of configuration A, where a dedicated gate electrode is used, is shown in Figure 6. The I_D-V_D behavior seen in Figure 6 differs substantially from that seen in Figure 4 and more closely follows the expectations derived from the I_D-V_G characteristic of polyaniline: drain current increases at first as V_G is raised, reaches a maximum at $V_G = 0.3$ V where saturation is not yet attained at $V_D = 1$ V, and then declines as V_G is made more positive. While in device configuration B the electrochemical potential of both electrodes is known, the three-electrode arrangement allows specification only of the electrochemical potential of the gate electrode. The drain and source are not directly tied to V_G and a large magnitude of V_D does not result in so large a perturbation in behavior. The overall transistor behavior obtained with device configuration A was found to be significantly less effected by the magnitude of V_D However, device configuration B showed higher gain and faster response in the inverter described in Chapter 3. Electrode configurations C and D in Scheme V yield further differences in I_D-V_D behavior from both A and B, probably derived from the different tendencies of the drain and source electrodes to equilibrate with the gate electrode or electrodes.

The effects of drain voltage and electrode configuration on overall transistor behavior occur, and are important, in circuit environments. The circuit building block consisting of a transistor with a drain resistor is fundamental to both amplifiers and logic gates.[2] The behavior of this system is affected by both the magnitude and polarity of V_D. Scheme VI shows the circuit and the relationship of electrode potentials to circuit parameters, which has become more complex with the insertion of a resistor in the drain circuit. When no drain current flows, the electrochemical potential of the drain electrode, ε_D, is $(V_G + V_D)$. When the transistor is fully conducting, the electrochemical potential of

Scheme VI

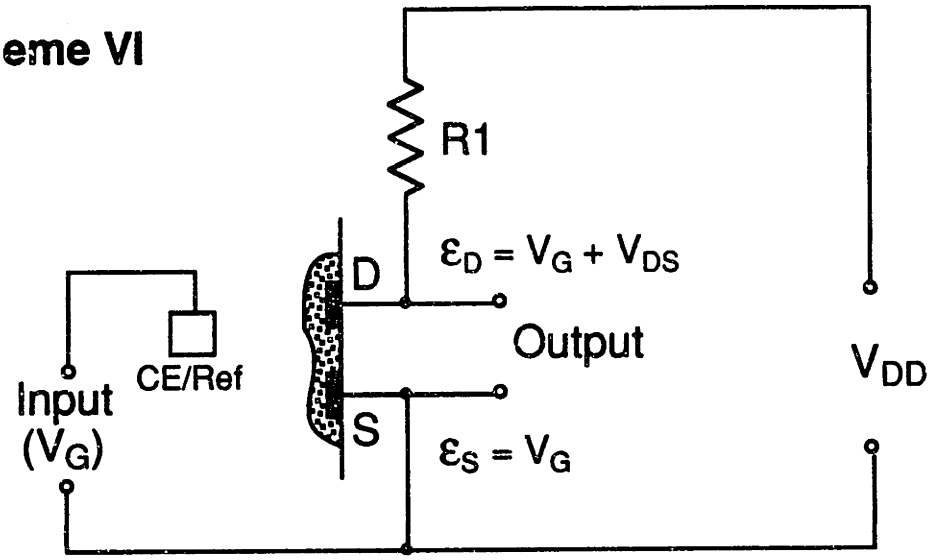

$$V_{DS} = V_{DD} - I_D R1$$

the drain electrode is close to V_G as long as R is large compared to the drain-source resistance of the device, R_{DS}, at full conduction. Figure 7 shows the voltage transfer characteristic at different values of V_{DD} (fix figure). (The double D notation signifies a circuit power supply voltage, as opposed to V_D, which is used to specify a voltage applied directly between the drain and source of a transistor.) The transfer characteristic is output voltage (V_{DS}) as a function of input voltage (V_G) and resembles the inversion of the I_D-V_G characteristic. When the transistor is insulating, the output voltage is equal to V_{DD} since device resistance is extremely high and all of V_{DD} is dropped across the drain-source gap of the transistor. When the transistor is fully conducting, output is near zero since R_{DS} is small compared to the 10 KΩ resistor. The difference in the two values of V_G corresponding to these points becomes larger as V_{DD} is made larger. This can be understood in terms of the same principle introduced above, which stated that as long as one electrode is within the window of conductivity of polyaniline, the transistor will allow drain current to pass. In the results shown in Figure 7, V_{DD} is applied such that it shifts the electrochemical potential of the drain electrode positive of V_G. As V_G is scanned negative and the transistor approaches turn-off, the drain electrode approaches an electrochemical

Figure 7. Transfer characteristic (output voltage as a function of input voltage) for a polyaniline microelectrochemical transistor with a 10 KΩ drain resistor at V_{DD} = 50, 300, 600 and 1000 mV. An output voltage of 0 corresponds to the fully conducting state of polyaniline, an output voltage of V_{DD} corresponds to the fully insulating state.

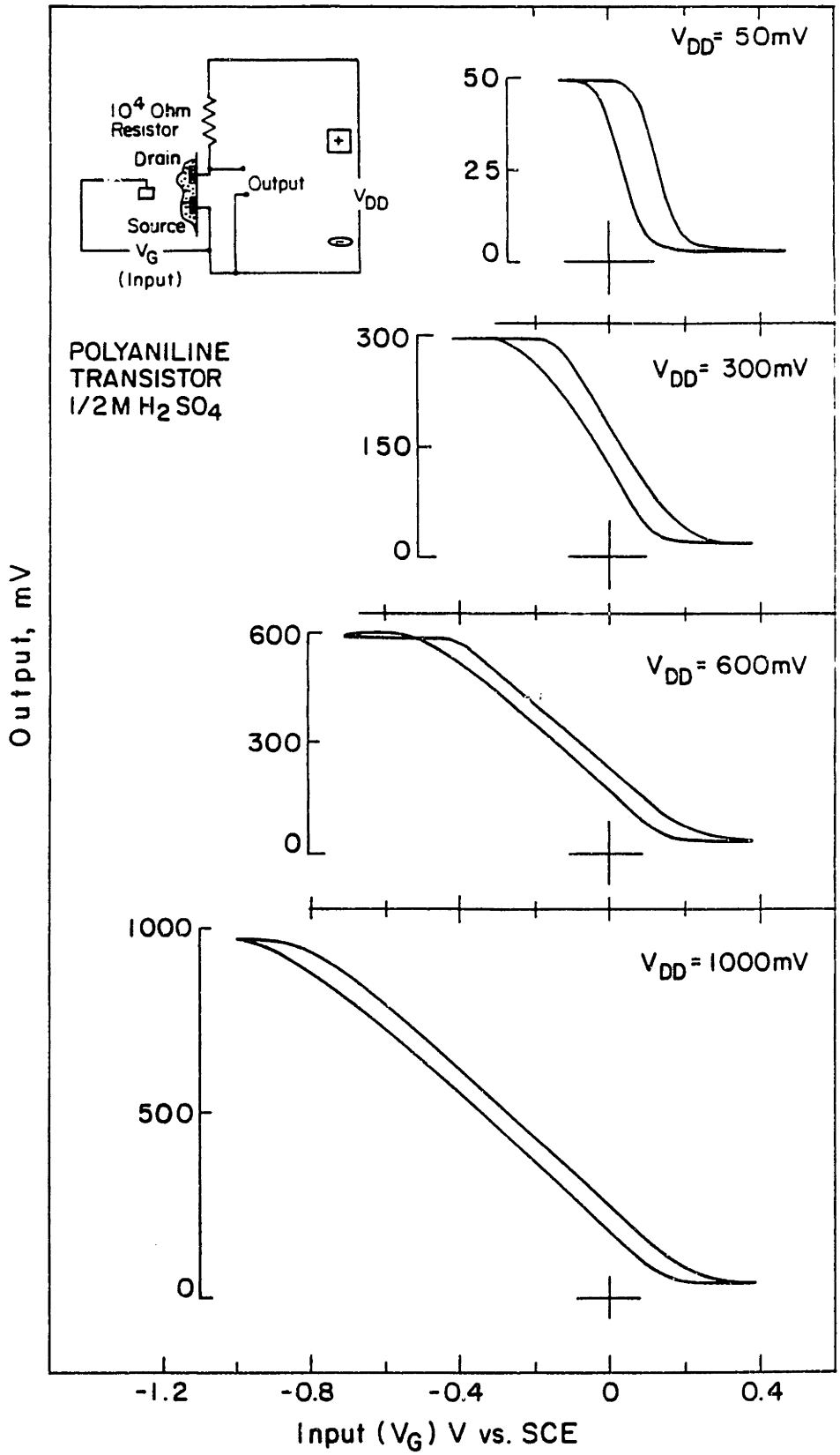
10^4 Ohm Resistor
Drain
Source
V_G (Input)
Output
V_{DD}
POLYANILINE TRANSISTOR 1/2M H_2SO_4
V_{DD}= 50mV
50
25
0
V_{DD}= 300mV
300
150
0
V_{DD}= 600mV
600
300
0
V_{DD}= 1000mV
1000
500
0
Output, mV
-1.2
-0.8
-0.4
0
0.4
Input (V_G) V vs. SCE

Figure 8. Operation of a polyaniline transistor in the circuit shown in Figure 7 demonstrating response with reduced hysteresis.

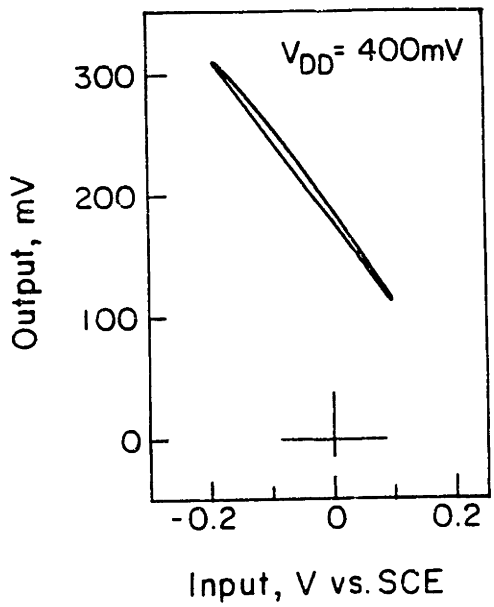
V_{DD}= 400mV
300
200
100
0
Output, mV
-0.2
0
0.2
Input, V vs. SCE

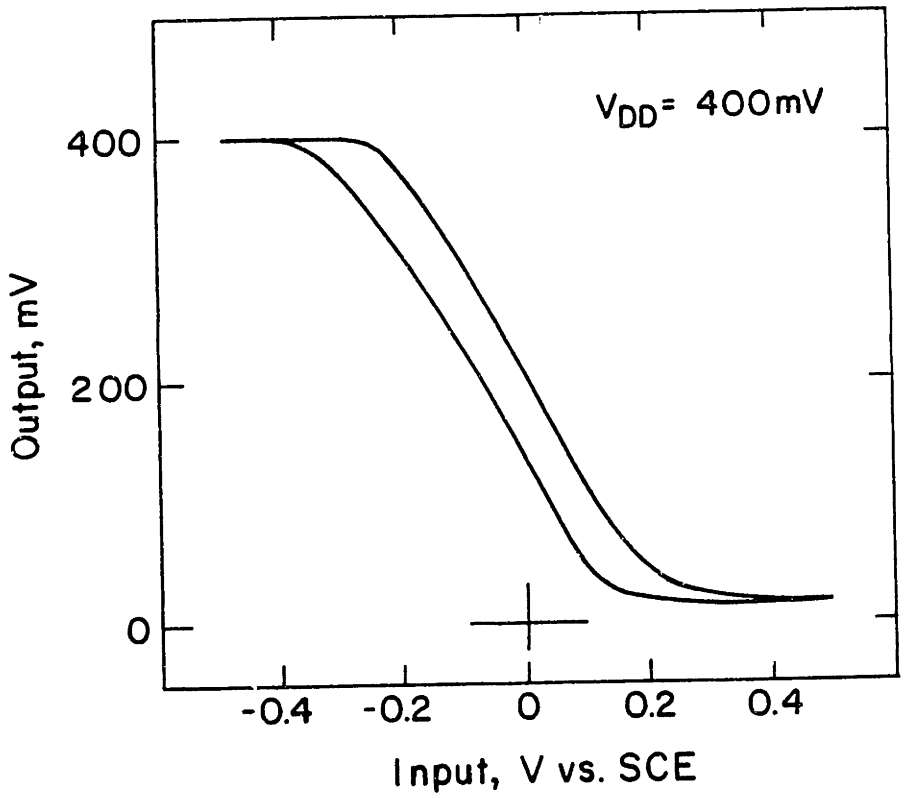
V_{DD}= 400mV
400
200
0
Output, mV
-0.4
-0.2
0
0.2
0.4
Input, V vs. SCE

Figure 9. Transfer characteristic (output voltage as a function of input voltage) for a polyaniline microelectrochemical transistor with a 10 KΩ drain resistor at V_{DD} = -50, -300, and -600 mV. An output voltage of 0 corresponds to the fully conducting state of polyaniline, an output voltage of V_{DD} corresponds to the fully insulating state.

POLYANILINE TRANSISTOR
0.5M H_2SO_4

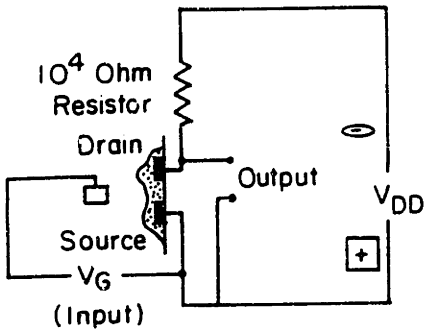

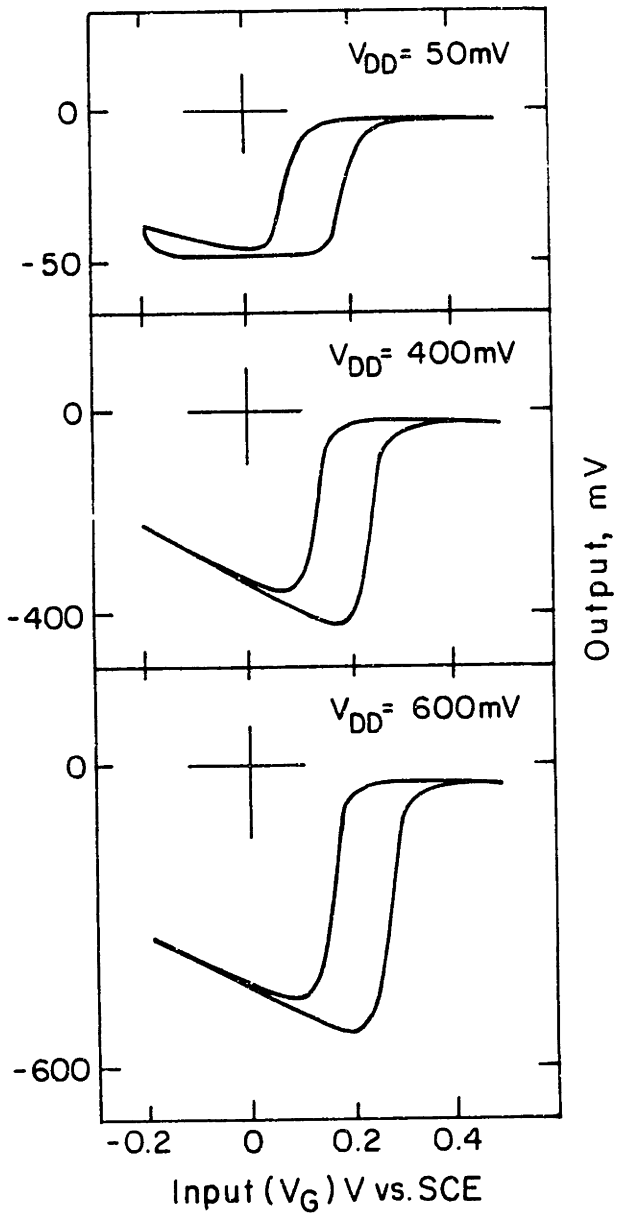

Figure 10. Transfer characteristic (output voltage as a function of input voltage) for a polyaniline microelectrochemical transistor with a 10 KΩ drain resistor at V_{DD} = 500 mV scanned over the entire window of conductivity for polyaniline.

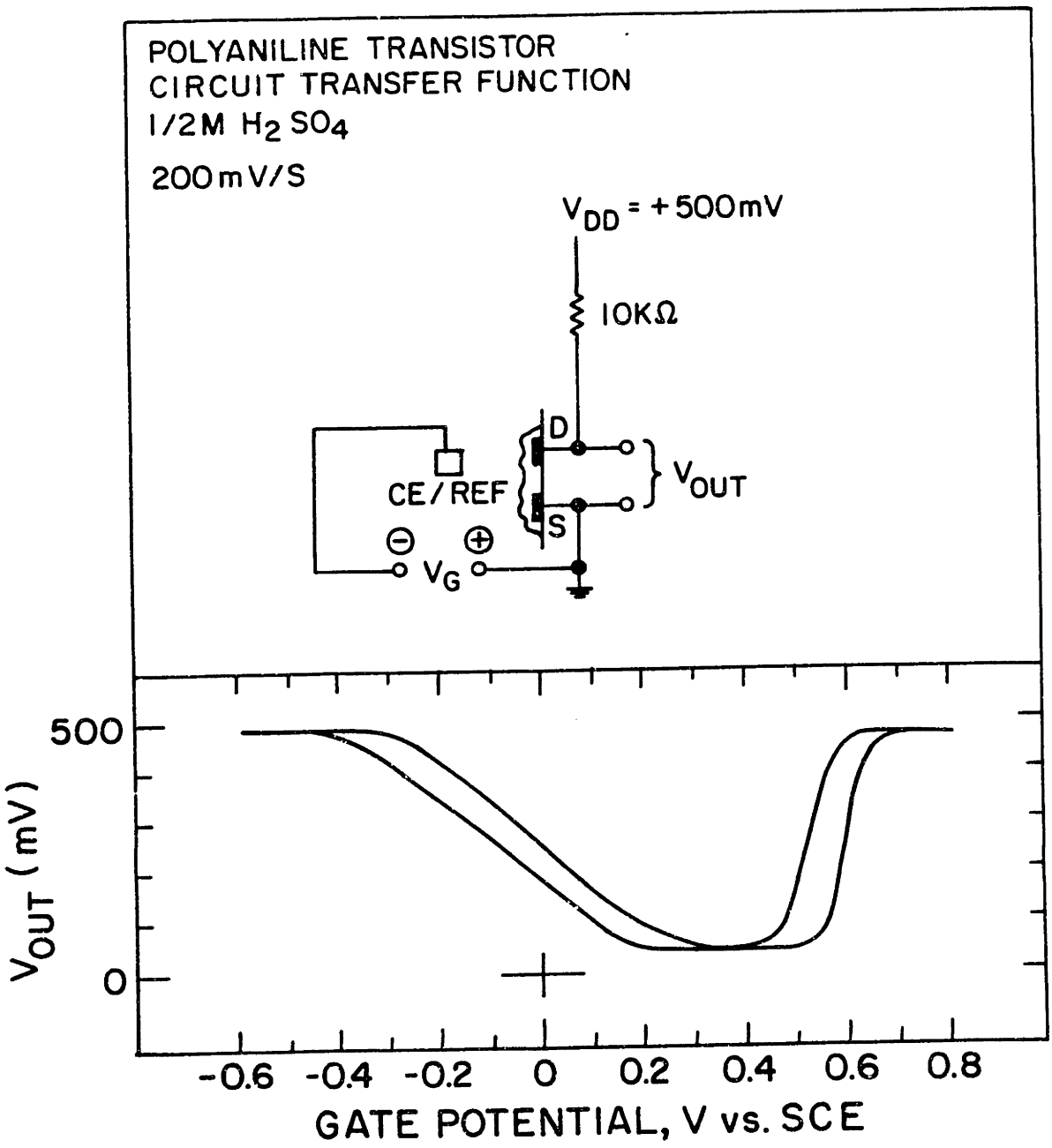
POLYANILINE TRANSISTOR
CIRCUIT TRANSFER FUNCTION
1/2M H_2SO_4
200mV/S
V_{DD} = +500mV
10KΩ
D
S
CE/REF
V_{OUT}
V_G
500
0
V_{OUT} (mV)
-0.6 -0.4 -0.2 0 0.2 0.4 0.6 0.8
GATE POTENTIAL, V vs. SCE

potential of ($V_G + V_{DD}$). The larger V_{DD} is, the farther negative V_G must be scanned to bring the electrochemical potential of the drain electrode negative of onset of conduction for polyaniline. The expansion of the range of V_G over which the transistor is switched from insulation to peak conduction allows operation of a transistor with very low hysteresis, Figure 8. The low hysteresis and linear change in output voltage with V_G is well suited to amplifier operation and an important result since hysteresis is a source of distortion when METs are used as amplifiers.

Figure 9 shows characterization of the circuit under the same conditions as in Figure 7 but with the polarity of V_{DD} reversed. Here, the width of the zone between zero and maximum output does not change. However, a tailing off of output voltage, indicating device conduction, is observed as V_G is moved negative of zero. Here, V_{DD} shifts the electrochemical potential of the drain electrode negative of V_G. As V_{DD} becomes large, this probably moves the drain electrode sufficiently negative to engage an electrochemical process such as reduction of protons from the sulfuric acid electrolyte. Figure 10 shows the transfer function of the circuit scanned through the entire window of conductivity for polyaniline. If V_{DD} were small, the transfer characteristic in Figure 10 would closely resemble an inverted I_D-V_G characteristic. Instead, the large value of V_{DD} results in onset of transistor conduction at about -0.4 V, where the electrochemical potential of the drain electrode is essentially -0.4 V + V_{DD}, expanding the range of V_G corresponding to the transition from onset of conduction to full conductivity. The transition from peak conductivity to oxidative insulation is not as significantly effected, indicating that while the drain electrode may be held well positive of V_G in electrochemical potential, it does not perturb potential control of the bulk of the polymer.

The I_D-V_G characteristic for a microelectrochemical transistor is also effected by the magnitude of V_D in exactly the way expected from the results described above. If V_D is applied such that the drain electrode lags V_G in potential, then onset of conduction will be observed at the expected potential but onset of oxidative insulation will not occur until the

potential of the drain electrode (V_G - V_D) reaches the potential for onset of oxidative insulation. The effects of V_D on I_D-V_G and I_D-V_D characteristics of METs and on transfer characteristics for MET circuits are consistent with a previous report[14] in which it was demonstrated that if two microelectrodes of a polypyrrole-derivatized array are held under active potential control at different potentials, almost all of the potential difference is dropped at the electrode held at a reducing potential where polypyrrole is insulating. In other words, the bulk of the polymer remains oxidized, so it is reasonable to assume that a relatively thing insulating layer is generated in the vicinity of the reducing electrode. The high resistance of the reduced polymer naturally drops most of the applied potential difference. In the results described above, it is true in each case that the electrode at a potential where polyaniline is conducting set the potential for the bulk of the polymer. This may also explain the higher speed of the two electrode configuration with a combined source and gate as compared to the three electrode case. In the latter, the entire bulk of the polymer must be oxidized and reduced to effect drain current. In the two-electrode case, the generation of a thin insulating layer of reduced material around the source/gate electrode is all that is required to attenuate drain current.

Conclusions

The transconductance of a polyaniline MET has been characterized over the complete window of high conductivity for the polymer. A maximum value of 30 mS/mm at V_D = 400 mV. While increasing drain voltage increases drain current and transconductance, a concurrent widening of the window of V_G over which the transistor conducts partly offsets that increase. The implementation of a complete amplifier circuit was described including consideration of appropriate circuit parameters for the use of a microelectrochemical device in a one-transistor amplifier. An audio amplifier, capable of driving standard headphones, was demonstrated using a polyaniline microelectrochemical transistor as the active device. The magnitude and polarity of drain voltage in microelectrochemical transistors significantly

alter I_D-V_G, I_D-V_D, and circuit transfer characteristics. The effect is markedly different for different drain, source, and gate electrode configurations. As the value of V_D is increased beyond about 100 mV, the electrochemistry of a polymer characterized at a small value of V_D becomes an increasingly poor description of device behavior. However, the effects of V_D on device characteristics can be understood and predicted by assuming that as long as the electrochemical potential control of one electrode in contact with the device-active material is within the window of conductivity for that material, the device will support drain current, even if the other electrodes are at potentials where the device-active material is insulating.

Experimental and General Experimental for Microelectrochemical Transistors

[This experimental section covers general procedures for the preparation of microelectrochemical transistors, referred to as "general experimental section" in subsequent chapters.]

Microelectrode arrays

Arrays of 8 individually addressable Au or Pt band microelectrodes 1.5 μm wide, 80 μm long, and 1.5 μm apart on 3 x 3 mm chips were mounted with a drop of clear epoxy on a standard 8-pin gold-plated header mounted on a ≈ 3 cm length of glass tubing. Under a stereoscopic microscope: The edges of the chip and surface of the header were then insulated with a coat of clear epoxy, cured for 30 min at 100 °C. The microelectrode array chip is insulated with clear epoxy except for the array itself, and the 8 bonding pads which terminate the leads from each of the electrodes. This is accomplished with a highly sharpened wooden applicator stick which had previously been coated with epoxy and heated to provide a sharp, stiff tip. The posts of the header (the termination of the leads) were cleaned with a razor blade and a connection was made from each of the 8 bonding pads of the microelectrode chip to one of the posts of the header with conductive silver epoxy, cured at 150 °C for 2 h. The entire header/chip assembly is coated with white epoxy except for the array of microelectrodes and cured at room temperature overnight and at 2 h at 120 °C. The room temperature cure avoids fouling of the array which can occur as a result of thermally accelerated curing. The mounted arrays are cleaned either by a 10 min Ar, 5 min O_2, 3 min H_2 plasma clean series, or by placing one drop of freshly prepared 10:3 H_2SO_4:30% H_2O_2 on the array, rinsing well with deionized water after 3-5 seconds, blowing the array dry under a stream of N_2, and repeating this procedure twice more. The chemical etch is preferred for more heavily fouled arrays unless a powerful plasma etcher is available. Pt,

because of the distinctive hydride wave signature in 0.5 M H_2SO_4 for a clean surface, was found to be superior to gold for the work in this thesis, except where the lowest possible device lead resistance is required. Immediately prior to use, each electrode of the array is cycled from -0.3 V to 1.2 V vs. SCE in 0.5 M H_2SO_4 until a good cyclic voltammetric response is obtained. The lower limit is adjusted so that the H_2 evolution current spike is not too large, -0.27 being a typical value.

Polyaniline

Polyaniline microelectrochemical transistors are used throughout this thesis. Aniline can be used as received, but for regular use very pure material which is resistant to degradation and yields excellent results can be prepared according to a published procedure.[15] Aniline is distilled from CaH_2, this is best carried out under Ar or N_2 and in the dark. The distilled material is stirred with stannous chloride and filtered. The completely colorless liquid is stored under argon in the dark and will remain colorless for over a year. If polyaniline is to be prepared from an aqueous solution of the monomer only, the CaH_2 drying agent can be omitted from the distillation step. It should be noted that aniline is quite toxic in addition to being carcinogenic.

Polyaniline is prepared by oxidation of aniline from a solution of 0.20 ml aniline, 20 ml 0.25 M $NaHSO_4$, and 0.5 - 1 ml H_2SO_4. Microelectrodes are scanned from 0 to 0.9 V vs. SCE at 100 mV/s over the course of which the cyclic voltammogram grows as polyaniline is deposited on the surface. For a pair of microelectrodes, a peak anodic current of 8 nA for the polymer oxidation wave at about 0.2 V corresponds to a thin film of polyaniline while 20 nA will yield a heavy film. After the last scan is underway, the lower limit is set to -0.2 V and the scan is stopped at that limit. The polyaniline film is characterized by its cyclic voltammetry and I_D-V_G response from -0.2 to -0.4 V vs. SCE in the deposition solution.

I_D-V_G characteristics

The I_D-V_G characteristics of polymers were typically obtain using a Pine Instruments model RDE4 bipotentiostat. Working electrode terminals K1 and K2 are connected to adjacent, polymer-derivatized microelectrodes. An offset voltage of -25 mV is set for K2 (this is V_D) and the two electrodes are both swept together over the desired range of V_G. Polyaniline is characterized from -0.2 to +0.5 V in the deposition solution. Conductivity is calculated using the entire exposed area of a microelectrode as the cross-section through which current flows. While this may yield overly pessimistic values since the cross section of polymer which supports the majority of current flow is probably less, it avoids speculation and provides a consistent standard.

I_D-V_D characteristics

The characteristic can be obtained by holding one microelectrode at a fixed potential (V_G) and sweeping a second, adjacent electrode using an RDE4 potentiostat as in the I_D-V_G measurement, except that here the potential of only one electrode is swept.

Transconductance

Transconductance plots were generated by recording the I_D-V_G characteristic using a digital storage oscilloscope and differentiating it using suitable software. For example, data recorded on a Nicolet 4094 digital storage oscilloscope was read using the commercial software ***vupoint***, saved as a text file, and differentiated using the commercial software *Igor*.

Circuits

Circuit construction and characterization has been described above for each specific case. It is important to consider possible unwanted connections between equipment resulting from ground connections between instruments. It is almost universal that the working electrode of a potentiostat is grounded through the potentiostat's internal circuitry

and in equipment such as the PAR 173 potentiostat the working electrode is actually connected to power line ground. This must be accounted for when setting up many of the circuits described in this chapter. The RDE4 is a convenient instrument because its "DC Common" terminals (i.e. internal power supply ground) are not connected to power line ground.

Drain voltages were supplied either by shorting the counter and reference electrode terminals of a potentiostat, which converts the potentiostat to operation as a regulated power supply, or by a power supply constructed for the purpose. A power supply was constructed capable of providing 0 - 5 V with millivolt precision. A ten-turn potentiometer was used as a voltage divider to provide a precise voltage which was buffered by a TL071 operational amplifier the output of which was augmented by a bipolar push-pull follower (2N4400, 2N4401). The feedback to the inverting input of the op amp was taken from the output of the push-pull stage to eliminate crossover distortion from the complementary pair. A power supply of standard linear design based on the 7800 and 7900 series regulators provided +7.5 V and -7.5 V. From these supplies were configured precise reference voltages (which had trimmer potentiometers for the purpose of calibration) which fed the ten-turn voltage divider potentiometer.

Polyaniline Transistor Audio Amplifier

An array of microelectrodes as derivatized with polyaniline and electrodes 3 and 5 were used as sources, 4 and 6 as drains, and 2 and 7 as gate electrodes. A drain voltage of 500 mV was provided and a set of Koss model TNT 55 headphones (33 Ω) were used as load with the left and right channel connected in parallel. A potentiostat provided V_G and a fix offset corresponding to approximately 1/2 maximum drain current was established. An audio signal of 200 mV peak to peak amplitude was connected to the external signal input of the potentiostat. The source material was the masterwork "Big Bottom" written and performed by the legendary *Spinal Tap*.[16] The heavy use of bass in this piece is further

enhanced by the high gain of microelectrochemical transistors at low frequency. Once amplifier operation was established, V_{bias} was adjusted to allow maximum output swing without clipping, as determined by monitoring the output waveform on an oscilloscope. Power gain was determined from gate current swing, gate voltage swing, and the current and voltage swing developed at the headphones.

References

1. Bardeen, J.; Brattain, W. H. *Phys. Rev.*, **1948**, *74*, 230

2. Horowitz, P.; Hill, W. *The Art Of Electronics*; Cambridge University Press: New York, 1989

3. Pierret, R. F. *Field Effect Devices*, Addison-Wesley: Reading, Massachusetts, 1990

4. Paul, E. W.; Ricco, A. J.; Wrighton, M. S. *J. Phys. Chem.* **1985**, *89*, 1441

5. Thackeray, J. W.; White, H. S.; Wrighton, M. S. *J. Phys. Chem.* **1985**, *89*, 5133

6. Lofton, E. P.; Thackeray, J. W.; Wrighton, M. S. *J. Phys. Chem.*, **1986**, *90*, 6080.

7. Natan M. J.; Bélanger, D.; Carpenter, M. K.; Wrighton, M. S. *J. Phys. Chem.*, **1987**, *91*, 1834

8. Natan, M. J.; Mallouk, T. E.; Wrighton, M. S. *J. Phys. Chem.*, **1987**, *91*, 648

9. Jones, E. T. T.; Chyan, O. M.; Wrighton, M. S. *J. Am. Chem. Soc.*, **1987**, *109*, 5526

10. Chao, S.; Wrighton, M. S. *J. Am. Chem. Soc.*, **1987**, *109*, 6627

11. Ludwig, R. H. *Illustrated Handbook of Electronic Tables, Symbols, Measurements, and Values, 2nd ed.*, Prentice-Hall: Englewood Cliffs, N. J., 1984 pp. 315-323

12. Mandl, M. *Electronic Data Reference Manual*, Reston Publishing Co. (Prentice-Hall): Reston, VA. 1979

13. Bard, A. J.; Faulkner, L. R. *Electrochemical Methods*, John Wiley and Sons: New York, 1980. Chapter 13

14. Kittlesen, G. P.; White, H. S.; Wrighton, M. S. *J. Am. Chem. Soc.*, **1984**, *106*, 7389

15. Perrin, D. D.; Armarego, W. L. F.; Perrin, D. R. *Purification of Laboratory Chemicals, 2nd ed.* Pergamon Press: New York, 1980. pp. 108-109

16. © Polymer Records

Chapter 3

An Inverter Gate with High Noise Immunity Based on a Polyaniline Microelectrochemical Transistor

Abstract

An inverter gate based on a polyaniline microelectrochemical transistor displays high immunity to input signal noise derived from the characteristic hysteresis in the I_D-V_G response of polyaniline. The inverter is capable of functioning at input signal to noise ratios of less than 1:1. The design and operating principle of the inverter are described and the noise immunity interpreting in terms of the theoretical basis for hysteresis in conducting polymers. The significant enhancement of noise immunity by hysteresis in the transfer function of an inverter is demonstrated by comparison of the behavior of the polyaniline-based inverter to that of a hysteresis-free standard bipolar transistor inverter constructed such that it displayed a comparable transfer function. The I_D-V_G behavior of polyaniline was characterized in a number of different solvent and supporting electrolyte systems based on H_2O, CH_3CH, CH_3OH, $(CH_3)_3COH$, CH_2Cl_2, $(CH_3)_2SO$ and $LiClO_4$, H_2SO_4, $NaHSO_4$, KCl, [*n*-Bu_4N]PF_6 and combinations thereof. The specific extent and distribution of hysteresis over the I_D-V_G characteristic varied substantially from one solvent/electrolyte system to the next.

Introduction

Hysteresis in Conducting Polymers

Polyaniline, as with all conjugated organic polymers, displays pronounced hysteresis in its I_D-V_G characteristic, Figure 1. Hysteresis in the electrical characteristics of conducing polymers is a consequence of the coupling of introduction of charge sites to geometric distortions of the polymer backbone.[1] This is not the case in conventional solid state semiconductors where introduction of charge carriers does not cause a structural distortion of the crystal lattice or alter the band structure of the material.

> The unique and truly essential feature (when compared and contrasted with traditional semiconductors) is the two-fold coordination, characteristic of the chainlike structures of conducting polymers and the resulting inherent coupling of the electronic excitations to structural distortions.[1a]

Hysteresis in the response of a conducting polymer-based microelectrochemical transistor is therefore one of the electrical characteristics which arises from the molecular, rather than solid-state, nature of the device-active material. An interesting potential benefit of hysteresis in transistor response is that it can endow logic gates with enhanced immunity to noise.[2] The preparation and characterization of a microelectrochemical inverter gate was undertaken to explore the consequences of this aspect of conducting polymer behavior.

Hysteresis, the differing of the return scan from the forward scan in the I_D-V_G characteristic of a conducting polymer, is an inherent feature of the electrical characteristics of conjugated organic conductors.[3,4] Figure 1 shows the I_D-V_G characteristic of polyaniline. Onset of conduction occurs at more positive gate potential on the forward scan than onset of insulation on the return scan. The effect is not indicative of degradation of the polymer and is re-traced on each scan. Because hysteresis does not vary with scan rate it cannot be attributed to sluggish kinetics of the polymer redox processes. The basis of hysteresis is an evolution in the electronic states of the polymer upon oxidation resulting

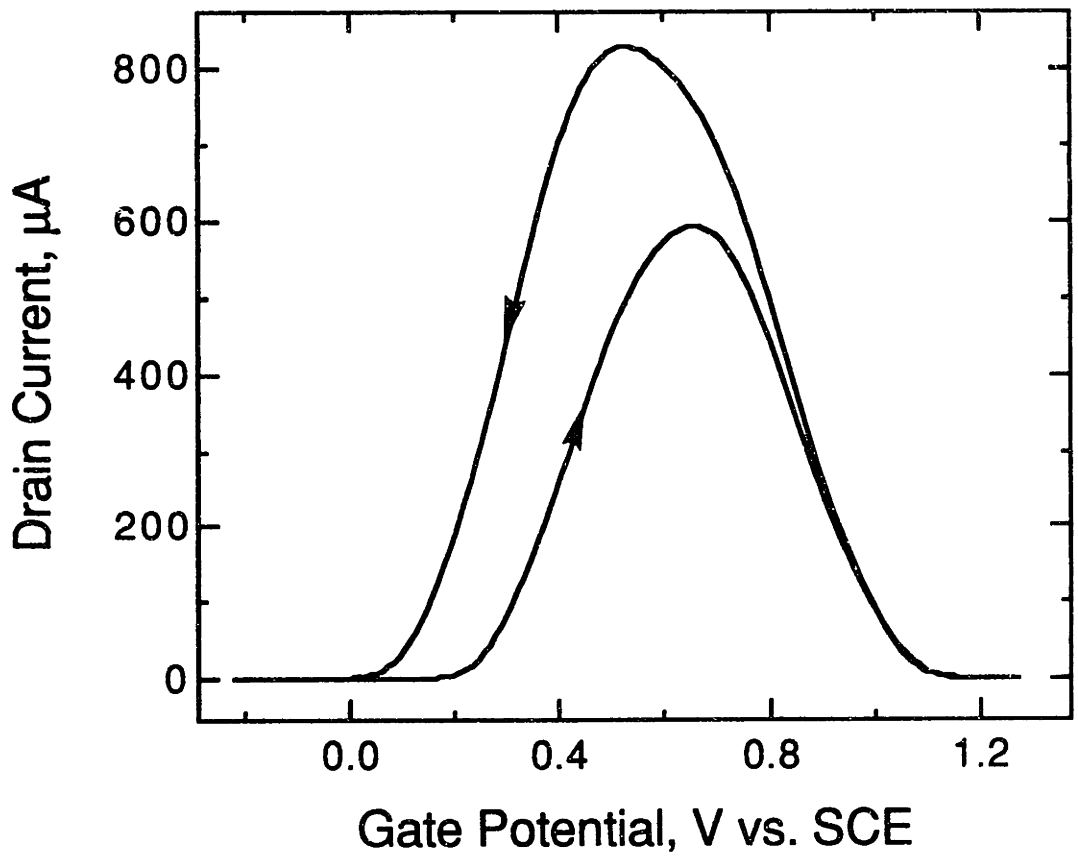

Figure 1: Drain Current-Gate Voltage (I_D-V_G) characteristic of a polyaniline transistor. 0.5 M H_2SO_4, V_D = 400 mV, 200 mV/s The unusually high potential for onset of oxidative insulation is due to the high value of drain voltage (400 mV) suitable for microelectrochemical logic gates. The arrows indicate the forward and return scan of V_G.

from structural distortions from ground-state geometry and changes in the π-manifold of the polymer which occur as the polymer adopts the lowest-energy upon introduction of charge. For polyaromatics there are two possible resonance forms for the ground state: one benzenoid and one quinoid in character, Scheme I. The two configurations are not

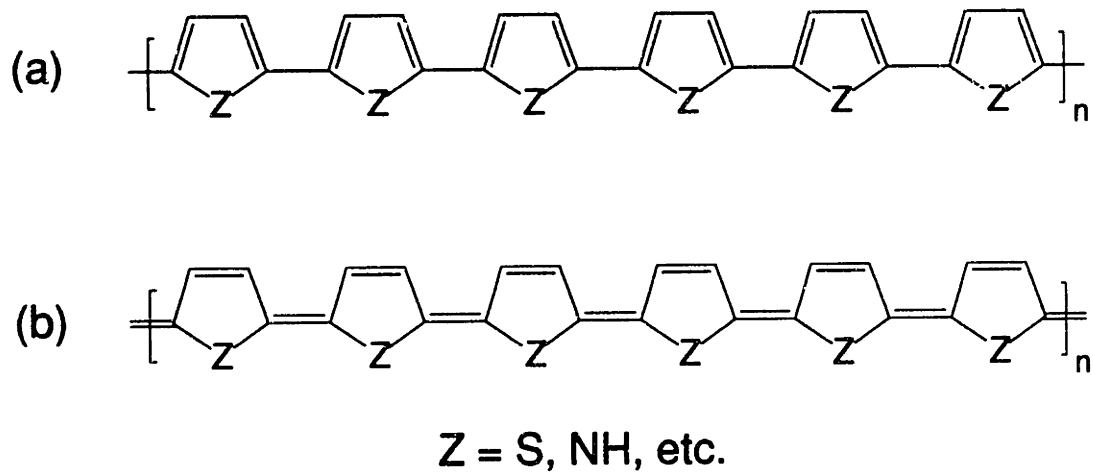

Scheme I. Benzenoid (a) and quinoid (b) resonance forms for the polyaromatic family of conducting polymers.

degenerate. The benzenoid form has been calculated to be lower in energy than the quinoid form for the ground (neutral) state of the polymer. The quinoid structure has been calculated to have a higher affinity for charge than the benzenoid form and is energetically favored for support of charge sites.[4,5] Therefore, adoption of quinoid character in the vicinity of charge sites minimizes overall energy. Scheme II is a representation of the resulting evolution of polymer band structure upon oxidation. Scheme II (a) represents the neutral, ground state of the polymer with a filled valence band and empty conduction band. Upon removal of an electron, a cationic center and an unpaired electron are created, known as a polaron.[4,6] To accommodate the charge and minimize total energy the polymer adopts quinoid character in the region of the charge site resulting in distortion of interatomic distances and an alteration of the π-manifold in the vicinity of the charge. The distortion is thought to extend over four rings in polypyrrole[4] and is represented in (b) as a partial shift

Scheme II. Representations of changes in the π-manifold and electronic band structure for a polyheteroaromatic upon oxidation. a) The neutral polymer in the benzenoid ground state. b) Removal of an electron results in a quinoid distortion to minimize total energy. A new, half-occupied electronic state appears in the band gap as a result. c) Upon further removal of charge, polarons combine to form bipolarons and a stronger distortion to quinoid form. As the number of cationic sites increases the new energy levels overlap sufficiently to become narrow bands.

(a)

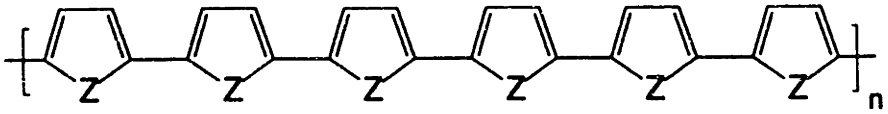
Z
n

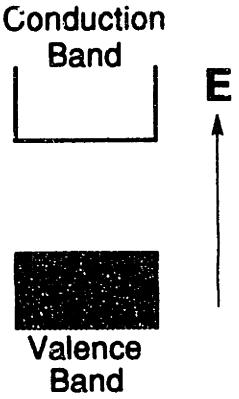
Conduction Band
E
Valence Band

(b)

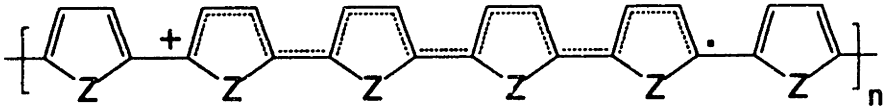
+
Z
n

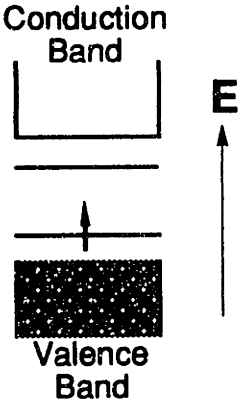
Conduction Band
E
Valence Band

(c)

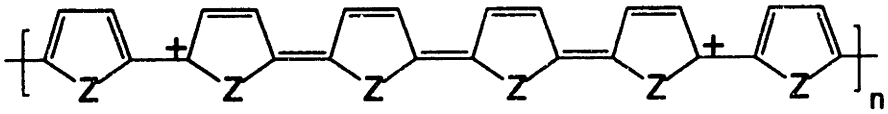
+
Z
n

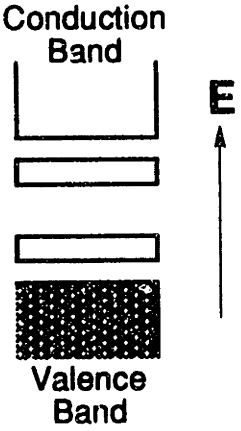
Conduction Band
E
Valence Band

toward quinoid form. Accompanying structural distortion is the appearance of a new energy level in the band gap, represented as a half-filled state in the band diagram for Scheme II (b). Upon further removal of charge the polymer adopts more quinoid character represented in Scheme II (c) where a bipolaron, a pair of charges and the result of the combination of two polarons, is shown. As with the polaron the distortion arising from support of a bipolaron is also thought to extend over four repeat units (calculated for polypyrrole) but the quinoid distortion is stronger for the bipolaron and for this reason Scheme II (c) is intended to represent fully quinoid character for support of a bipolaron while Scheme II (b) is intended to represent only a partial adaptation of quinoid form. In the band diagram for (b) a single new state is shown. However, as the density of charge sites on the backbone increases, the energy levels appearing in the band gap begin to overlap sufficiently to become narrow bands unto themselves, represented as the narrow bands in the band gap in (c). For a full discussion of electronic states in conducting polymers the topic is the subject of excellent reviews by Brédas and Street[4] and Chance, Boudreaux, Brédas and Silbey.[6]

Because the actual band structure (and not just band population) is altered as a polymer is oxidized and reduced, the electronic states present on the forward and return scan of gate potential are different, resulting in differences in charge transport characteristics and conductivity. On the forward scan of V_G, electrons are removed from the valence band. The holes created result in quinoid distortions and a corresponding set of new, unoccupied energy levels comprising a new band at higher energy than the valence band. Since this new band is more difficult to reduce than the valence band from which the electrons were originally withdrawn, it requires a more negative potential to neutralize the holes that created upon initial oxidation and return the polymer to its reduced, insulating state. This can be seen in the I_D-V_G characteristic shown in Figure 1 where onset of conductivity on the forward scan of V_G occurs at a potential positive of onset of insulation on the return scan.

The theoretical explanation of hysteresis, described quantitatively for polypyrrole, and generalized to derivatives of polypyrrole, polythiophene, and polyparaphenylene by Brédas and Street,[4] can be extended to polyaniline as shown in Scheme III. Polyaniline differs from other conducting polymers which have a continuos carbon skeleton because it possesses nitrogens between rings with participation by the nitrogen p-orbital in the π-manifold of the backbone. However, given the similarity of I_D-V_G characteristic and hysteresis observed for polyaniline to that observed for many other conducting polymers including polypyrrole, polythiophene, and their derivatives,[3] and the further importance of the quinoid form in oxidized polyaniline,[7] it seems completely reasonable to include polyaniline in the group of polymers for which hysteresis is explained by the structure shown in Scheme II. Scheme III shows the valence structures and evolution of band structure which can be envisioned for polyaniline upon oxidation. The extent of protonation of polyaniline in its various oxidation states depends on the medium in which the electrochemistry is carried out. Polyaniline oxidized to the extent of one electron per repeat unit (Scheme III, bottom) is drawn in the fully deprotonated form, and at pH 0 in aqueous acid polyaniline has been described as existing in the completely deprotonated state.[7] In contrast, in liquid SO_2 polyaniline is thought to remain fully protonated throughout the oxidation-reduction cycle.[3] The degree of protonation depends on solution pH,[7] and in organic solvents it is not clear to what extent polyaniline is protonated in a given state of charge. The possible significance of protonation will be discussed below with regard to variations in the specific character of hysteresis from one medium to the next.

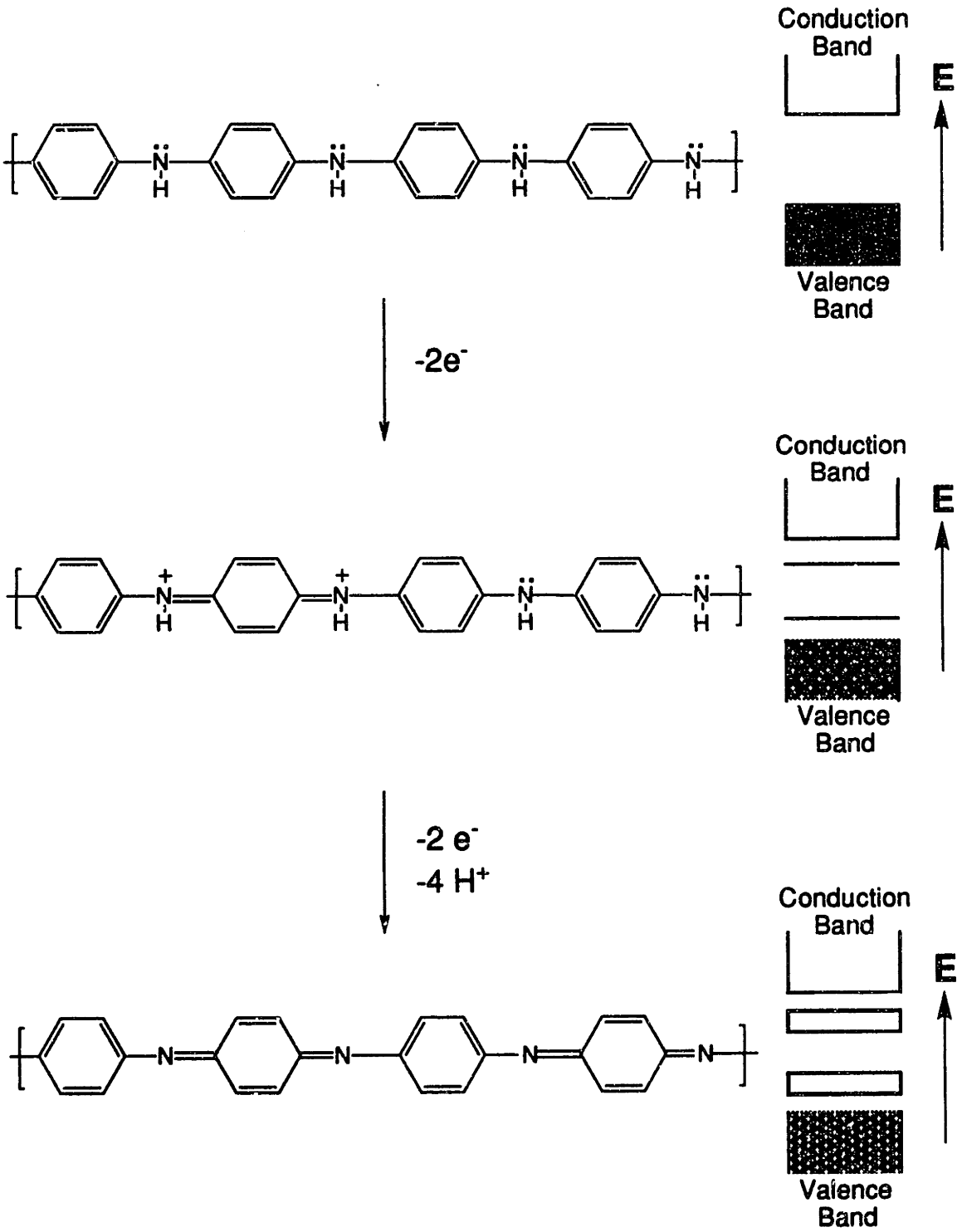

Scheme III. Representation of oxidation of polyaniline and concurrent evolution of electronic band structure resulting in hysteresis in the I_D-V_G characteristic.

Logic Gates

Logic gates are the basic decision-making element on which higher order functions in digital electronics are based.[8a] Digital logic circuits operate in binary using two different voltages, a LOW one and a HIGH one, referred to as logic LOW and logic HIGH, to represent 0 and 1, respectively. [For a general introduction to logic gates and their design and use, see reference 8a.] The function of a logic gate is to respond to certain combinations of input states with specific output states. An example is the AND gate, the function of which is to deliver a HIGH output if and only if input A *AND* input B of the AND gate are HIGH, Scheme IV (top).

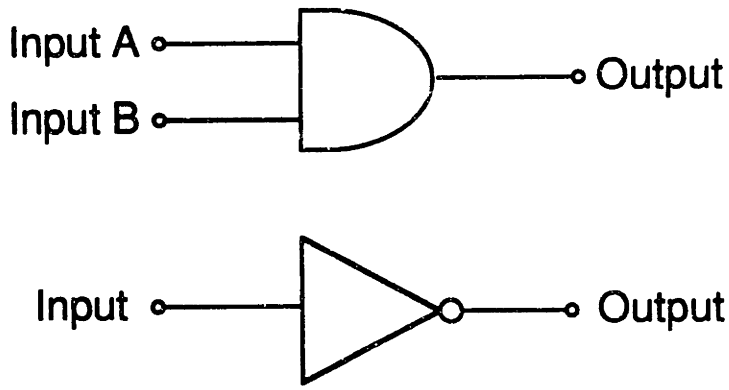

A	B	Output
0	0	0
0	1	0
1	0	0
1	1	1

Input	Output
0	1
1	0

Scheme IV. An AND gate (top) and an INVERTER (bottom) and the relationship of output to input for each gate.

The simplest of all gates is the inverter which possesses only one input and one output, Scheme IV (bottom). Its function is to give an output which is the inversion of the input, i.e. LOW in, HIGH out; HIGH in, LOW out. The inverter is an important building block of higher circuit functions and can also serve to evaluate the performance of a transistor in digital circuits in general.[9] More complex logic gates based on microelectrochemical transistors are also possible and are described in Chapters 4 and 8 of this thesis.

Results and Discussion

An inverter gate based on a polyaniline microelectrochemical transistor

The most basic execution of the inverter gate requires one transistor and one resistor. An inverter circuit based on a polyaniline microelectrochemical transistor is shown in Figure 2 with the corresponding output voltage versus input voltage characteristic, known as the *transfer function*, of the inverter. While many conducting polymers are suitable for use as the device active material, polyaniline offers a combination of desirable attributes. It is a highly rugged polymer with the fastest switching speed of any conducting polymer known as a result of reliance on diffusion of protons upon oxidation and reduction as opposed to more bulky counterions.[10] It can be deposited onto microelectrodes with superior precision and can support current densities of 10^3 A/cm.[11] Polyaniline is highly durable in aqueous sulfuric acid and most of the hysteresis in the I_D-V_G response occurs between onset of conduction and peak conductivity in this medium, the potential range over which the device will be operated.

Before describing operation of the circuit it is necessary to define the voltages corresponding to logic HIGH and LOW. In general, HIGH should turn the transistor fully on and LOW fully off. The potential of peak conductivity is the clear choice for logic HIGH but logic LOW can be anything negative of onset of conduction (0.18V vs. SCE in 0.5M H_2SO_4) that the polymer will withstand. The power required to switch a device scales with the voltage gap between HIGH and LOW so the smaller the voltage difference between the two logic levels the lower the power consumption of the inverter. The most demanding test of noise immunity occurs when the HIGH-LOW gap is set as small as possible (about 400mV for polyaniline) because the smaller the gap, the more significant a fixed amplitude of noise becomes. The gate potentials corresponding to HIGH and LOW are indicated in Figure 2 on the transfer function of the inverter and have been chosen close to the minimum gap allowable.

Figure 2. Schematic (top) and output voltage as a function of input voltage (bottom, known as the *transfer function*) of an inverter gate based on a polyaniline microelectrochemical transistor. The arrows indicate the forward and return scans.

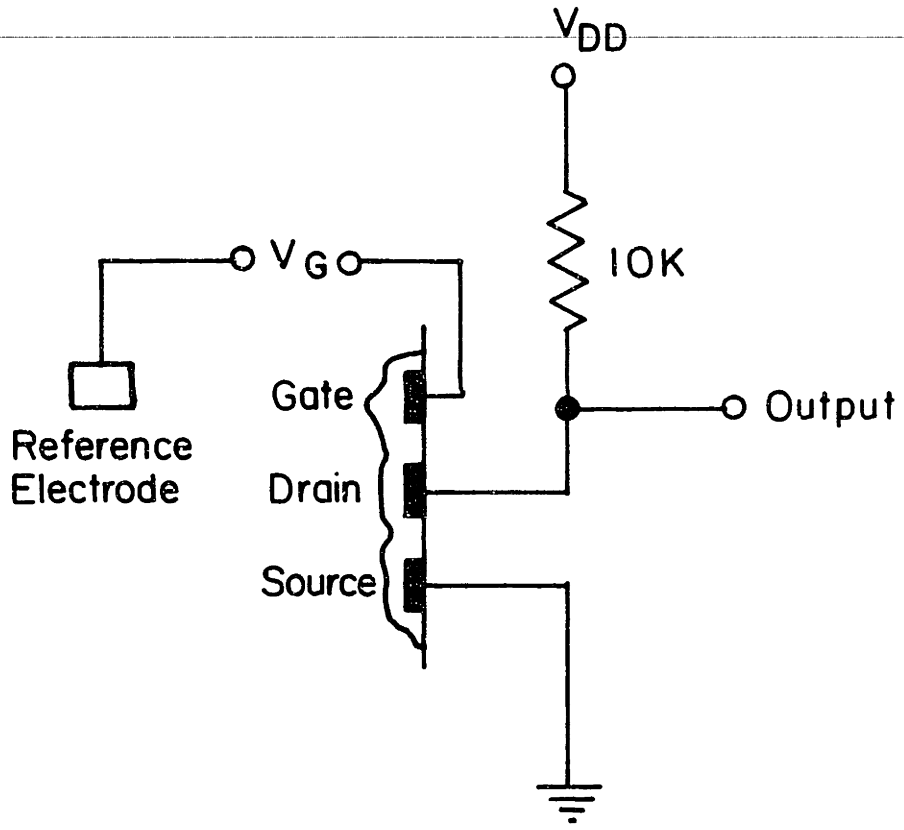
V_{DD}
10K
V_G
Output
Gate
Drain
Source
Reference
Electrode

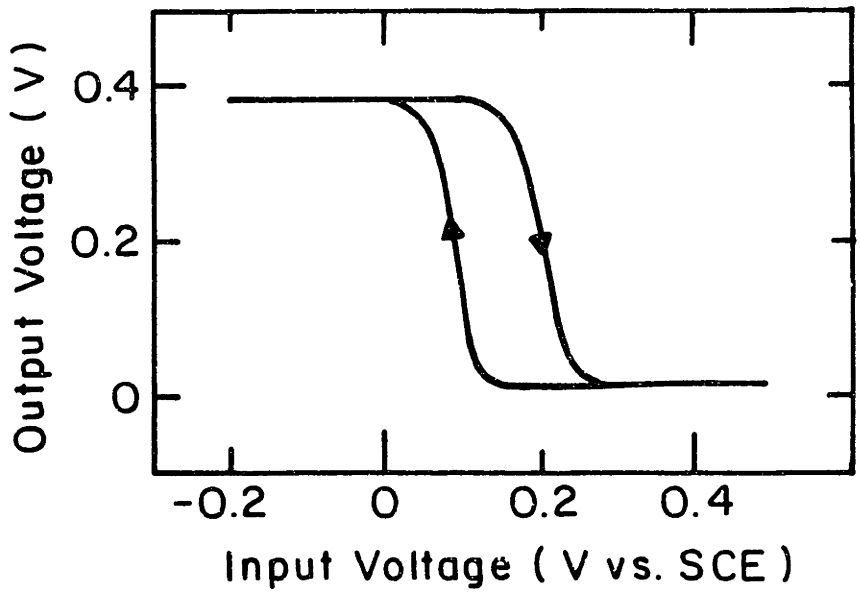
Output Voltage (V)
0.4
0.2
0
-0.2
0
0.2
0.4
Input Voltage (V vs. SCE)

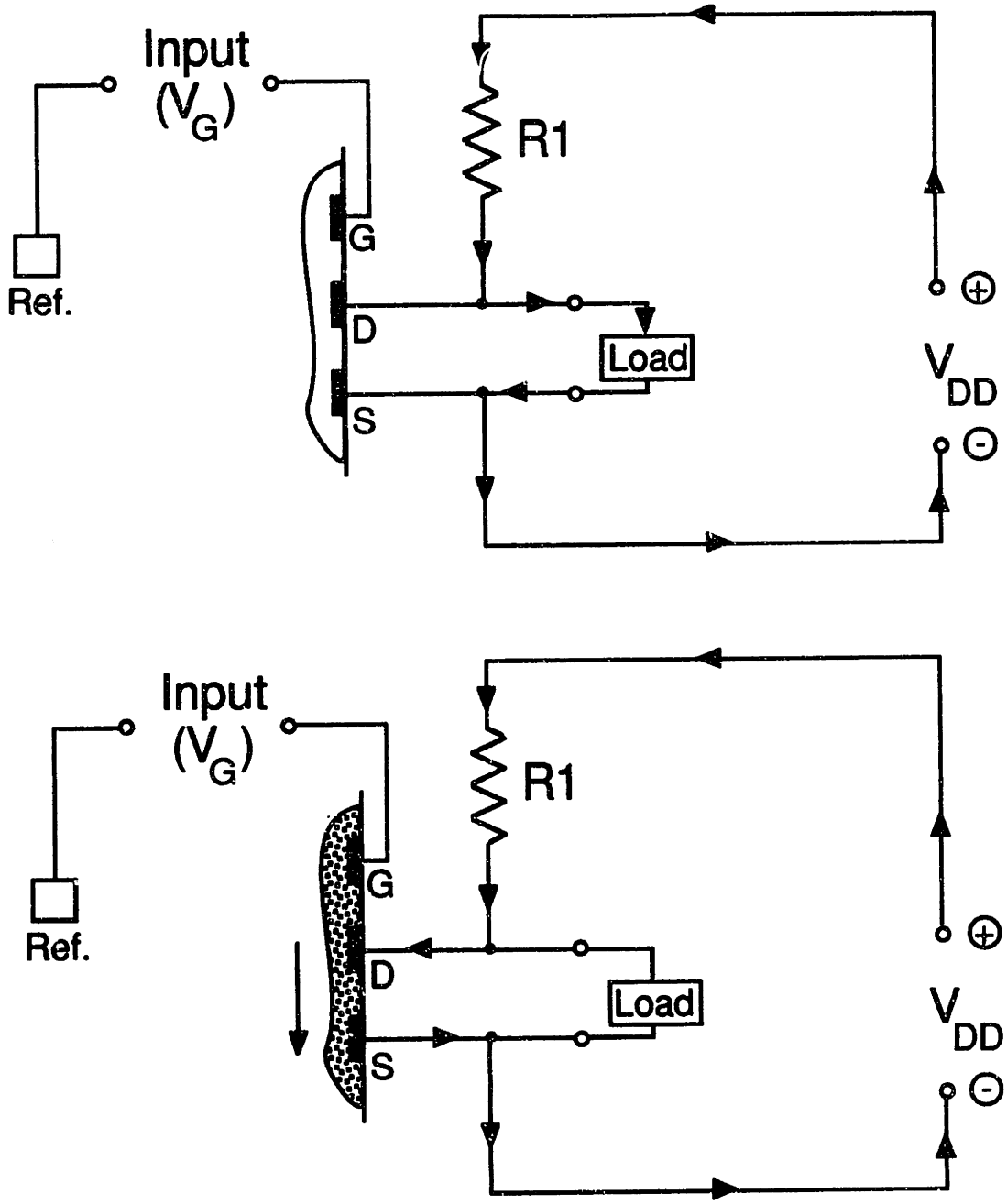

Scheme V. Current flow in a microelectrochemical transistor-based inverter. Top: input LOW, output HIGH. Bottom: input HIGH, output LOW.

The circuit accomplishes the function of inversion according to Scheme V. V_{DD} is the circuit supply voltage where the double D notation signifies a circuit power supply voltage rather than a voltage applied directly across the drain-source gap which is universally referred to as V_D in this thesis. The circuit is a voltage divider comprised of a fixed resistance, R1, and a transistor the resistance of which is switched by the input voltage between a value which is either small or large compared to R1. A HIGH input switches the transistor to full conduction, where its resistance is low and the voltage drop across it is close to zero (output LOW). A logic LOW input voltage results in full insulation by the polyaniline transistor so its resistance is extremely high and all of V_{DD} is dropped across the drain-source gap of the transistor (output HIGH). An equivalent description of inverter operation is indicated by the arrows denoting current flow in Scheme V.[12] At the top of Scheme V, the input is LOW and polyaniline is insulating. Current flows from the power supply around through the resistor and out the output terminal through the load and back to the other side of the power supply, in other words the output is HIGH. Scheme V (bottom) is the case where the input is HIGH and polyaniline is conducting. The transistor now provides a low resistance path back to the other side of the power supply causing current flow to bypass the output and the load, so the output is LOW.

Operation of a polyaniline-based microelectrochemical inverter is shown in Figure 3. The input signal is a square wave which alternates between logic LOW and HIGH (top waveform). The middle waveform of Figure 3 is the drain current through the transistor, switched on and off by the input signal. The bottom waveform is the output of the inverter gate: a square wave switching between 0 and V_{DD} 180 degrees out of phase with the input square wave, i.e. the inversion of the input. Figure 3 shows that the inverter operates as expected and correctly inverts the input. In this early version of the inverter, R1 was 4.7 KΩ and V_{DD} = 100mV. The value of R1 proved low since the output voltage when the transistor was on was slightly above zero. In subsequent experiments R1 was 10 KΩ,

Figure 3. Characterization of a microelectrochemical inverter based on a polyaniline microelectrochemical transistor operated in 0.5M H_2SO_4. Shown are the input voltage (top) a square wave switching between the gate potentials corresponding to logic LOW and logic HIGH, drain current through the circuit (middle), and output voltage.

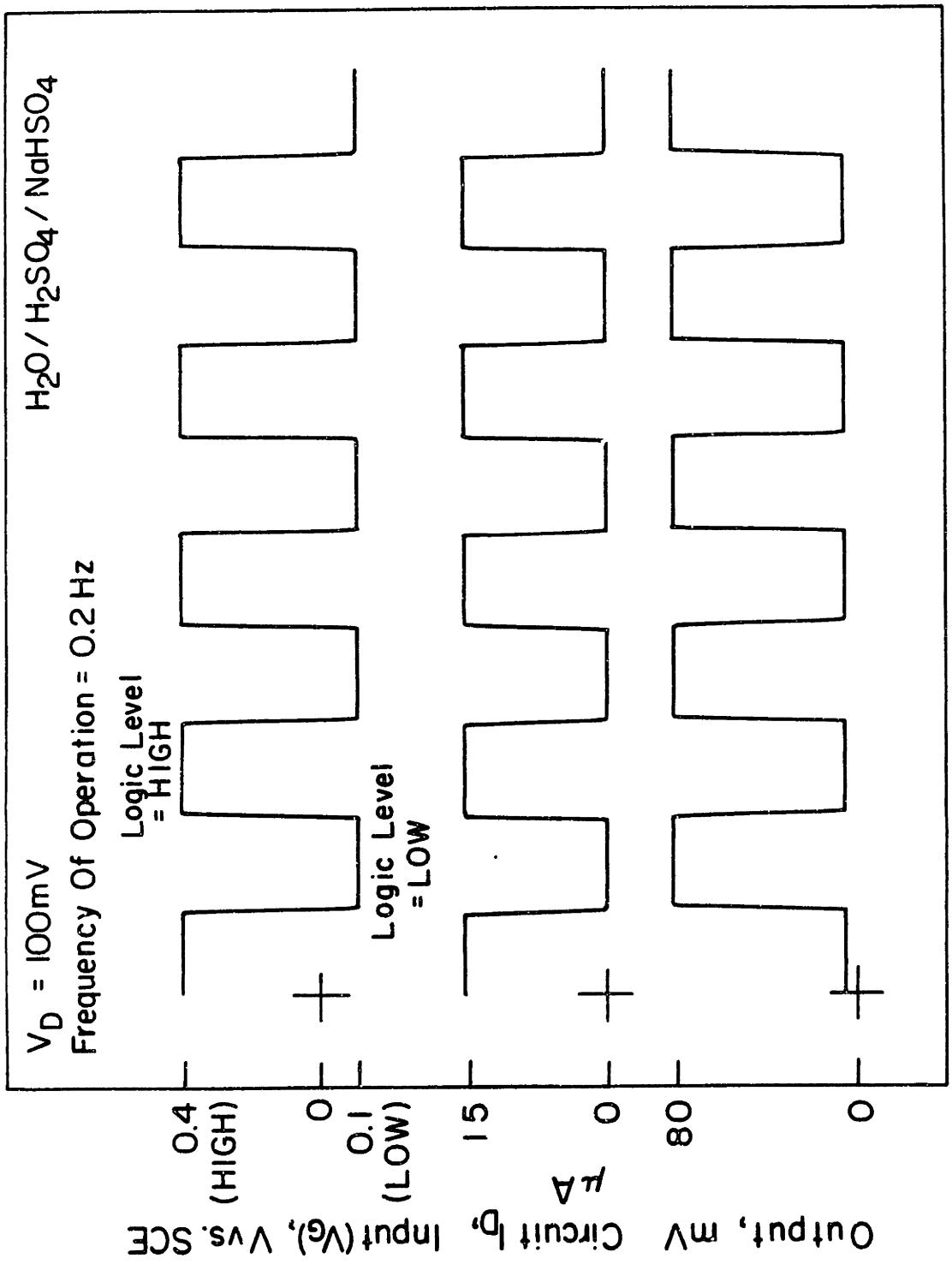
V_D = 100mV
Frequency Of Operation = 0.2 Hz
H_2O / H_2SO_4 / $NaHSO_4$
Logic Level = HIGH
Logic Level = LOW
0.4 (HIGH)
0
0.1 (LOW)
15
0
80
0
Input (V_G), V vs. SCE
Circuit I_D, μA
Output, mV
Time

found to be the optimal value. It should be noted that the value of R1 must be large enough to drop essentially all of V_{DD} when the polyaniline transistor is fully conducting, but at the same time small enough to allow reasonable current flow to drive a load (Scheme V, top).

It is normal in characterization conducting polymers to keep V_D in a transistor experiment small, usually 25-50 mV, so that V_D does not significantly effect potential control of the polymer. However, in the case of a logic gate a further consideration arises: one logic gate must be able to switch another. Therefore the output must be able to swing over a voltage range sufficient to switch another transistor between the fully on and fully off states, i.e. 400 mV for the logic levels selected above. This requires the circuit supply voltage V_{DD} to be 400mV. The large drain voltage substantially perturbs potential control by V_G *depending on the electrode configuration and the polarity arrangement of* V_{DD}. The investigation and characterization of this issue was dealt with in detail in Chapter 2 the results of which indicate use of a 3-electrode configuration employing a dedicated gate electrode.

In Figure 3 the input voltage is a clean square wave. To allow characterization of the noise immunity of the polyaniline-based inverter, a means of driving the gate with a "noisy" input signal was required. The configuration shown in Scheme VI allows the modulation of the square wave with a second waveform serving to represent noise. Because a square wave is employed to characterize operation of the inverter, the sweep generator of the potentiostat is not required and is free to provide a convenient source of "noise". This allows the introduction of an arbitrary component of noise by choosing the amplitude of the triangular wave produced by the potentiostat sweep generator. The waveform represented at the working electrode terminal in Scheme VII still alternates between logic HIGH and LOW as in Figure 3, but now the HIGH and LOW information content of the waveform is obscured by the introduction of noise. Figures 4 a-f show the response of the inverter circuit shown in Figure 2 to inputs of signal-to-noise ratios (S/N) ranging from

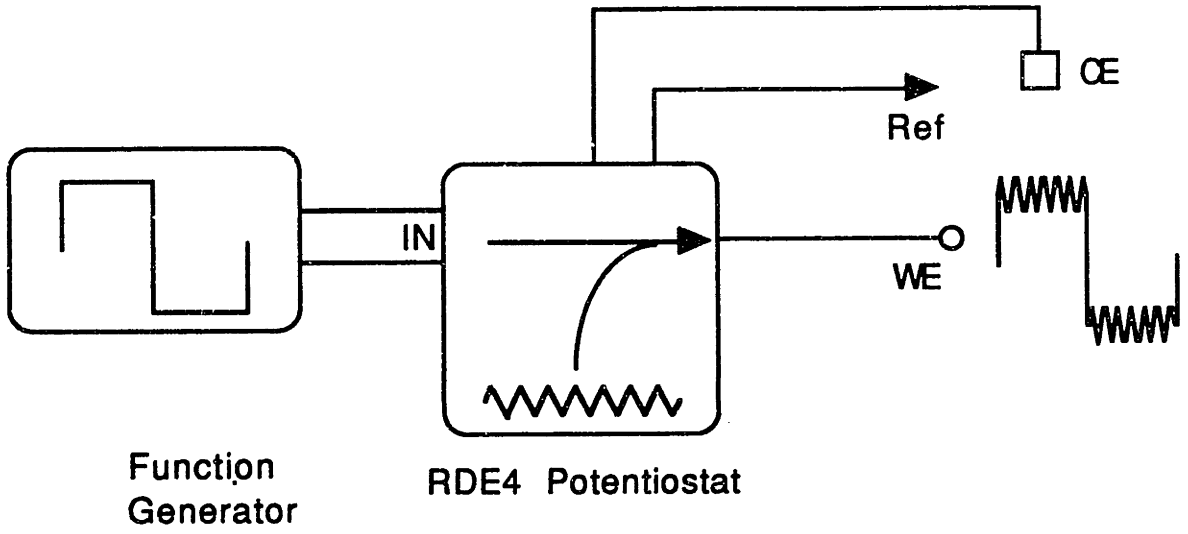

Scheme VI. The sweep generator of an RDE4 potentiostat was used to modulate the square wave connected to the IN terminals of the potentiostat. The working electrode potential is the sum of the two waveforms allowing generation of square waves with an arbitrary noise signal component.

4.2:1 to 0.70:1. At S/N of 4.2, 2.1, and 1.4 (Figure 4a,b,and c) the inverter is completely immune to the noise in the input signal. The output waveform remains a clean square wave as the inverter correctly discerns HIGH and LOW inputs and generates noise-free LOW and HIGH outputs in spite of the input signal noise. At S/N of 1.05:1 (Figure 4d) the noise in the input signal begins to manifest itself in the output waveform. By S/N of 0.84:1 (Figure 4e) the output has become significantly noisy but note than another polyaniline-based logic gate accepting this output waveform would still be immune to this noise level. Thus, a pair of inverters back-to-back could provide a noise filter which would provide a clean output from an input which actually has more noise than signal. It is only at 0.70:1 (Figure 4f) that the noise immunity of the inverter is finally overcome and the output becomes unusable.

Figures 4a - 4f: Characterization of the noise immunity of an inverter gate based on a polyaniline microelectrochemical transistor using the circuit shown in Figure 2. The transistor was operated in 0.5 M H_2SO_4 with V_{DD} = 400 mV. Input waveforms were generated using the equipment configuration shown in Scheme VI.

Figure 4a. Input and output waveforms for a polyaniline-based inverter at an input waveform signal-to-noise ratio of 4.2:1.

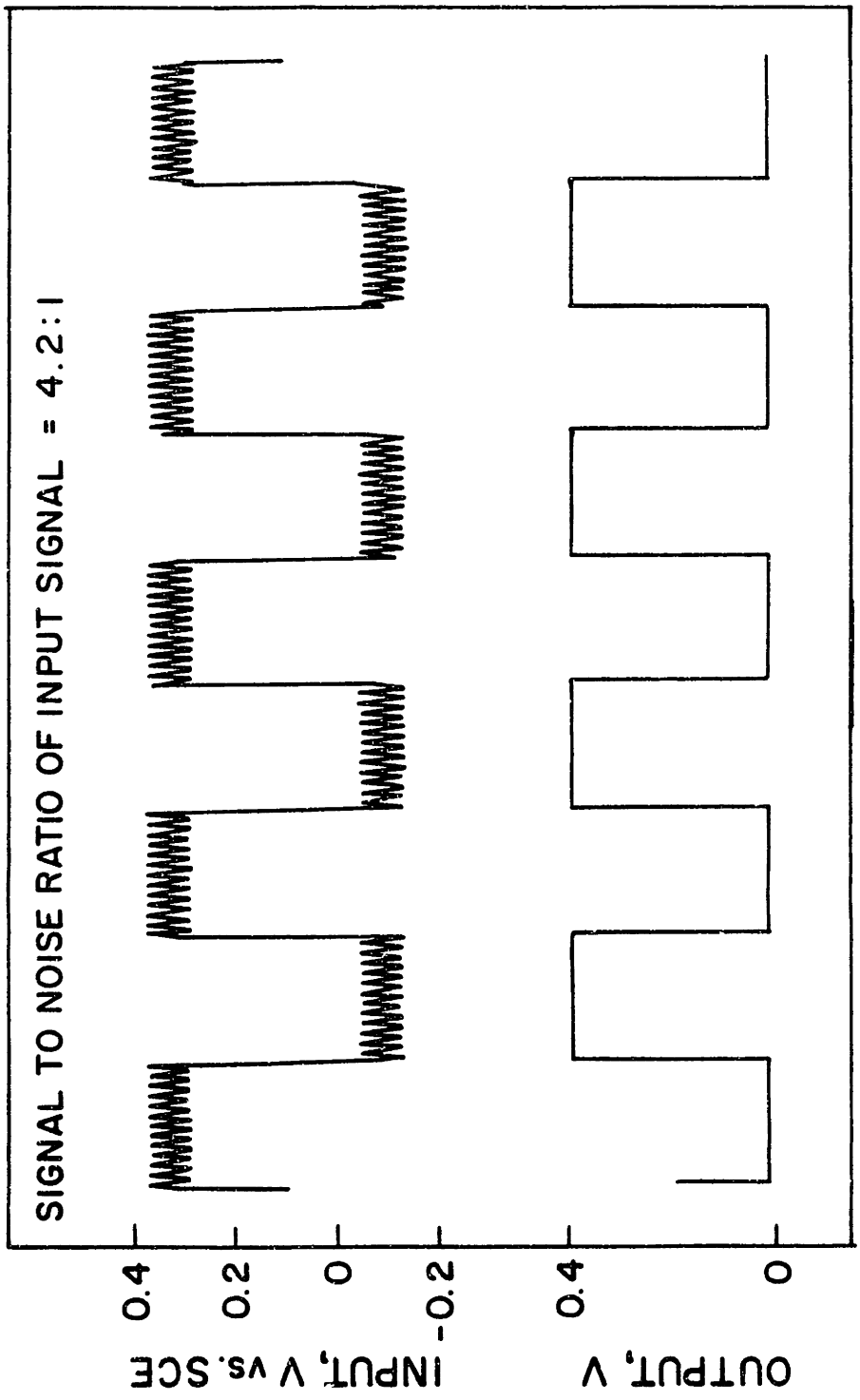
SIGNAL TO NOISE RATIO OF INPUT SIGNAL = 4.2:1
OUTPUT, V
INPUT, V vs. SCE
0.4
0.2
0
-0.2
0.4
0

Figure 4b. Input and output waveforms for a polyaniline-based inverter at an input waveform signal-to-noise ratio of 2.1:1.

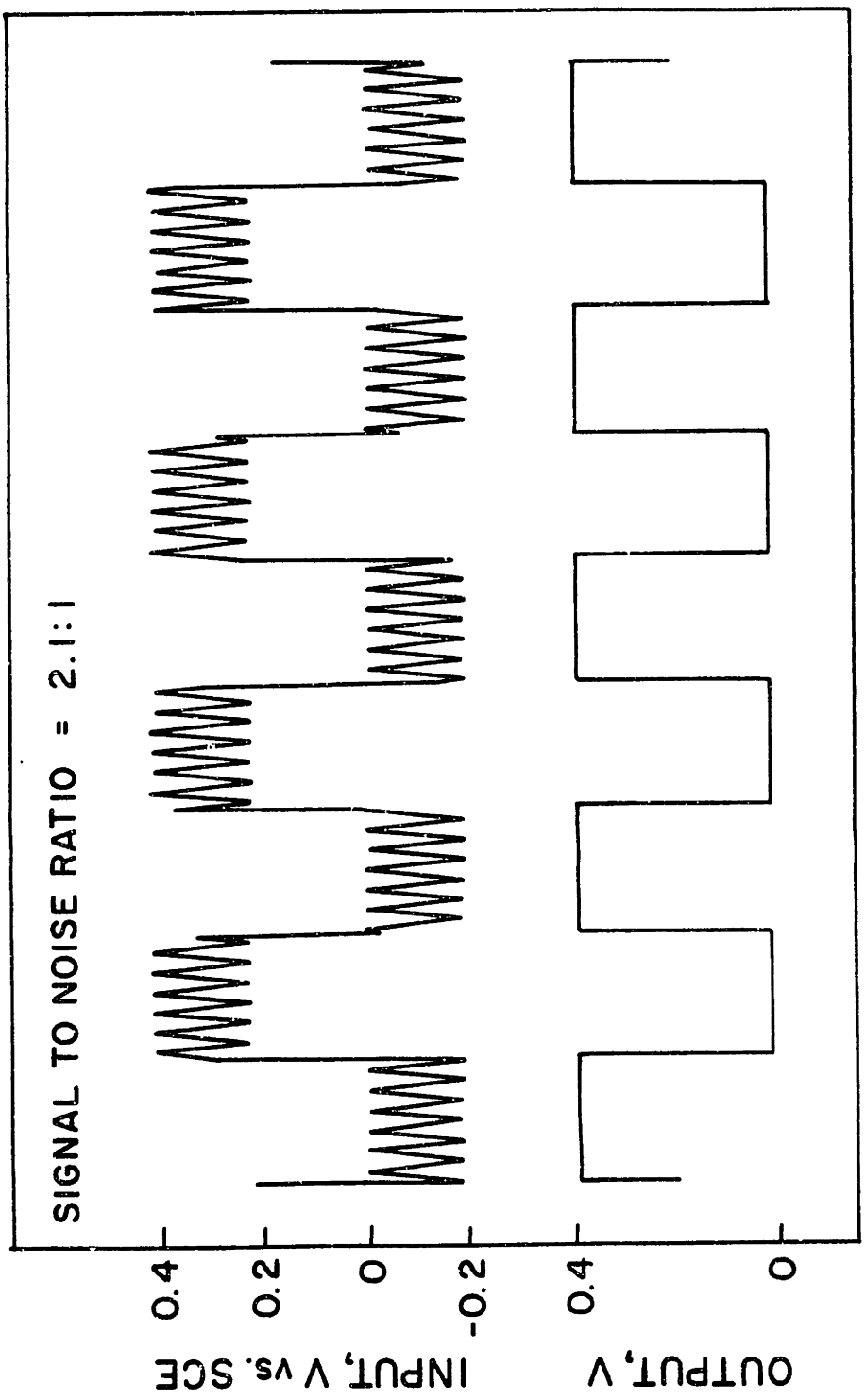
SIGNAL TO NOISE RATIO = 2.1:1
INPUT, V vs. SCE
0.4
0.2
0
-0.2
OUTPUT, V
0.4
0

Figure 4c. Input and output waveforms for a polyaniline-based inverter at an input waveform signal-to-noise ratio of 1.4:1.

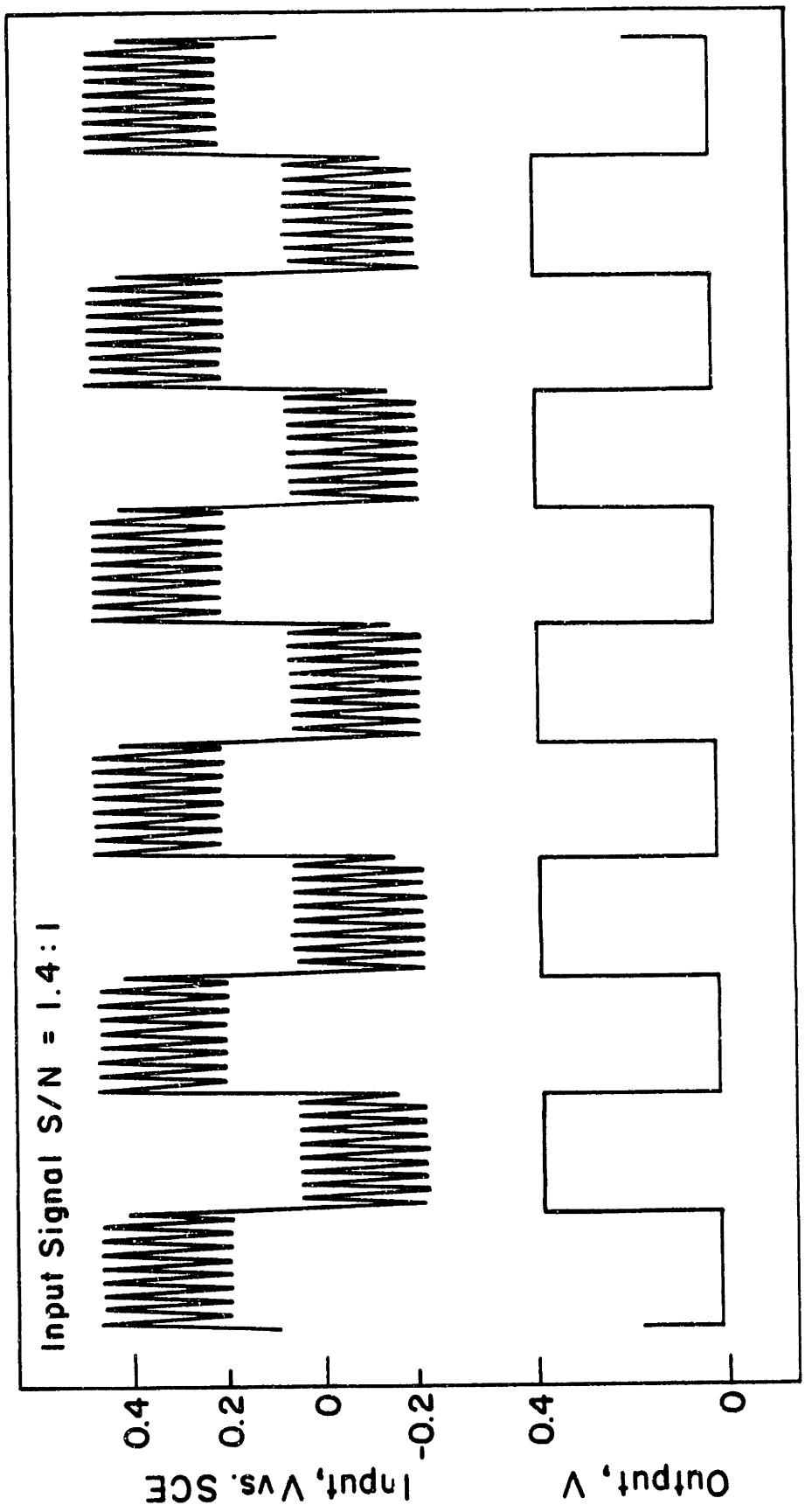
Input Signal S/N = 1.4 : 1
0.4
0.2
0
-0.2
Input, V vs. SCE
0.4
0
Output, V

Figure 4d. Input and output waveforms for a polyaniline-based inverter at an input waveform signal-to-noise ratio of 1.05:1.

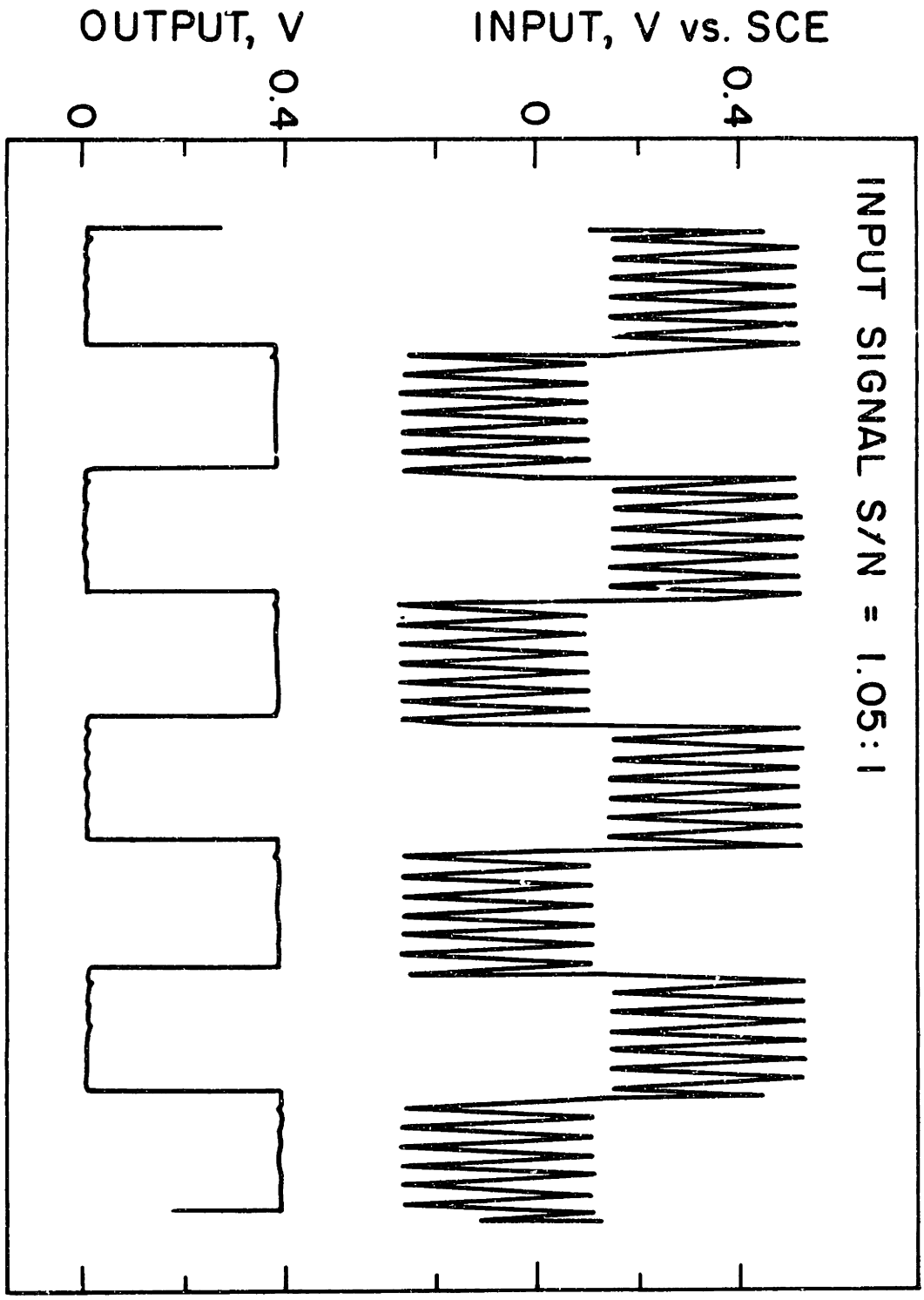
OUTPUT, V
0
0.4
INPUT, V vs. SCE
0
0.4
INPUT SIGNAL S/N = 1.05:1

Figure 4e. Input and output waveforms for a polyaniline-based inverter at an input waveform signal-to-noise ratio of 0.84:1.

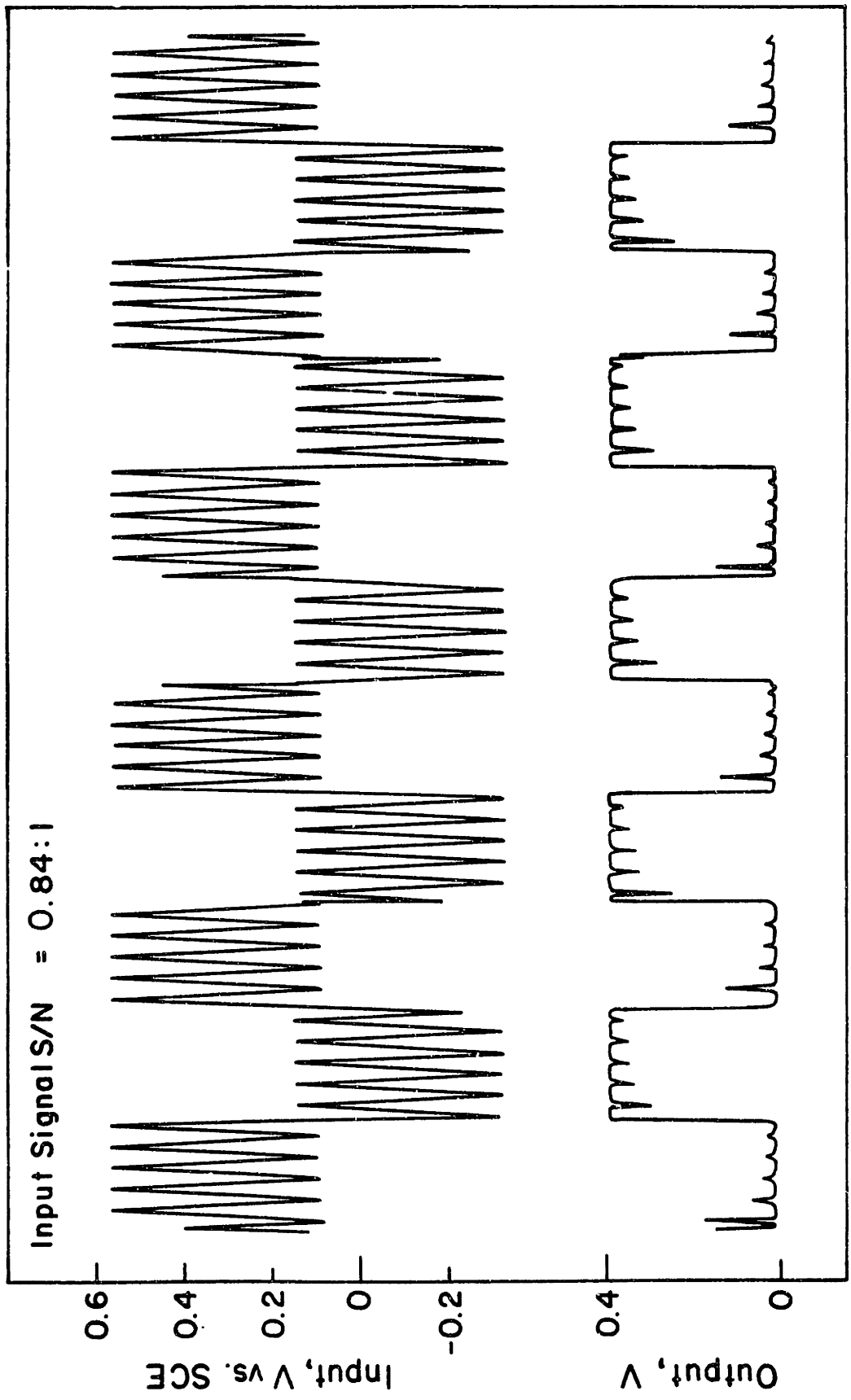
Input Signal S/N = 0.84:1
0.6
0.4
0.2
0
-0.2
Input, V vs. SCE
0.4
0
Output, V

Figure 4f. Input and output waveforms for a polyaniline-based inverter at an input waveform signal-to-noise ratio of 0.70:1.

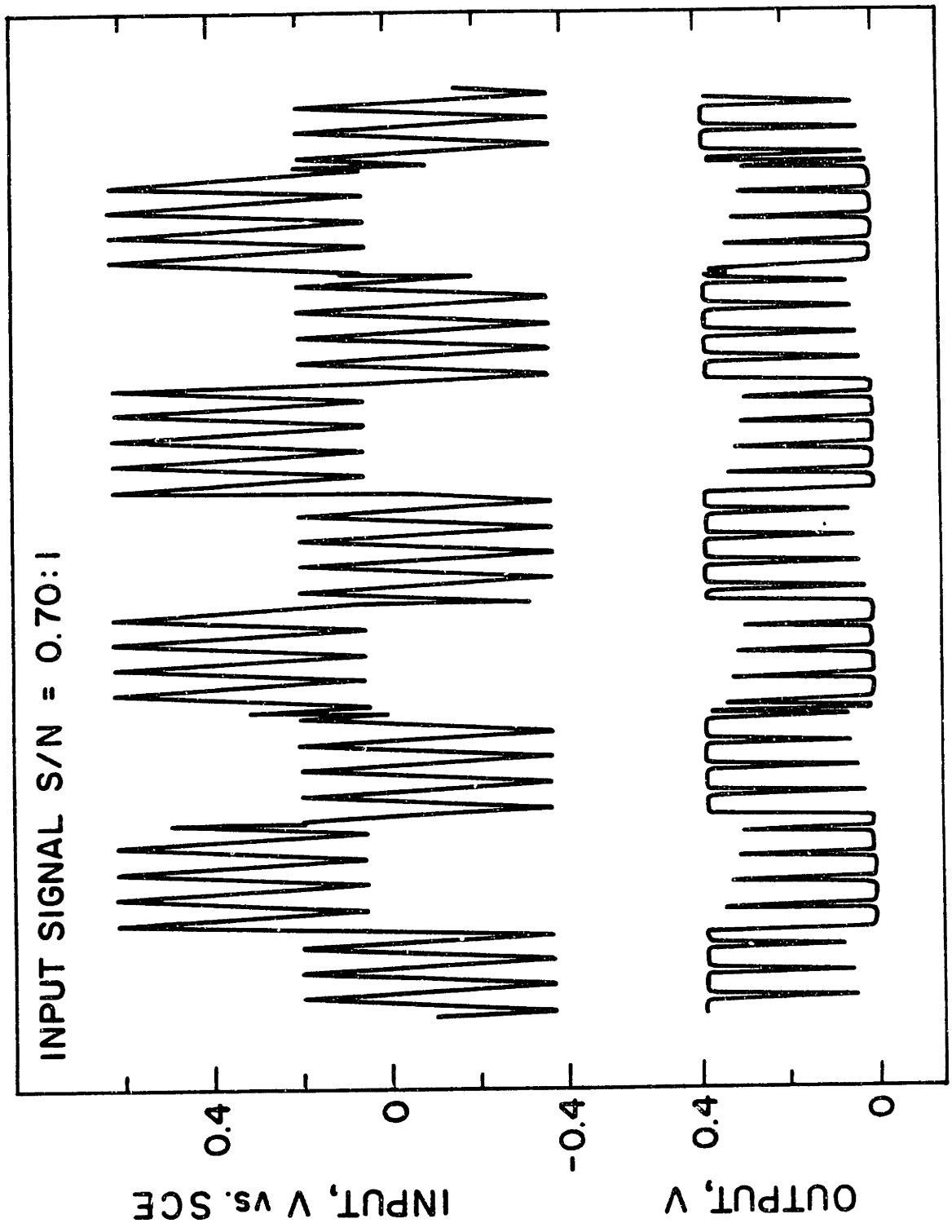
INPUT SIGNAL S/N = 0.70:1
0.4
0
-0.4
INPUT, V vs. SCE
0.4
0
OUTPUT, V

The remarkable immunity to high noise levels of the polyaniline-based inverter gate is a result of the hysteresis in the inverter transfer function. Inspection of Figure 2 shows that whether switching from LOW to HIGH or HIGH to LOW, *once either output state is achieved it is necessary to back-track by about 150mV in input voltage before any effect on the output voltage is observed.* This latching effect provides a buffer zone which is responsible for enhancing the noise immunity of the inverter gate. A HIGH input voltage switches the transistor on so the output is LOW and in terms of the evolving band structure explanation of hysteresis described in the introduction, the oxidation which has occurred generates quinoid states in the polymer and a new energy band. The new electronic states are more difficult to reduce than the valence band states from which the electrons were originally withdrawn, so the input voltage must be moved further negative to force re-injection of those electrons - about a 150mV difference for polyaniline. A LOW input voltage switches the transistor off (so the output is HIGH) and eliminates the more easily oxidized quinoid band responsible for the presence of holes supporting conduction at gate potentials negative of 0.18 V. Ionization of the valence band is required to re-introduce holes and this does not occur until the 0.18 V onset potential.

The polyaniline transistor proved durable when operated continuously in an inverter circuit. As a test of its ruggedness, a polyaniline inverter was switched continuously at 0.2 Hz for 96 hours, over 6.8 X 10^4 oxidation-reduction cycles for polyaniline, with 98% retention of initial drain current. Prolonged switching at 5 KHz showed continued good performance after over 500 million cycles. Inverter operation at greater than 50 KHz was possible using a two-electrode transistor configuration with one electrode serving as both source and gate. The inverter functioned correctly but gate current exceeded drain current at 50 KHz. Unity current gain is the limit of practical operation since below it the gate would be unable to provide sufficient output current to drive a second gate.

Characterization of a hysteresis-free inverter gate based on a conventional transistor

The question of how the polyaniline-based inverter would behave if no hysteresis in response were present was addressed by construction and characterization of a bipolar transistor-based inverter since conventional solid-state transistors do not display hysteresis. For a direct comparison of the behavior of two inverters in this regard the width of their transfer functions must be the same. The inverter circuit shown in Scheme VII operates in the same manner as the polyaniline-based inverter but can be configured to provide a transfer function comparable to that of the polyaniline-based inverter described above by selecting appropriate component values. The transistor used was a standard small-signal silicon bipolar transistor. Unlike field-effect transistors or microelectrochemical transistors, bipolar devices draw continuous current at their control electrode, known as the *base*, which is analogous to the gate in a field effect device. Resistor R2 limits base current and also allows adjustment of the width of the transfer function.

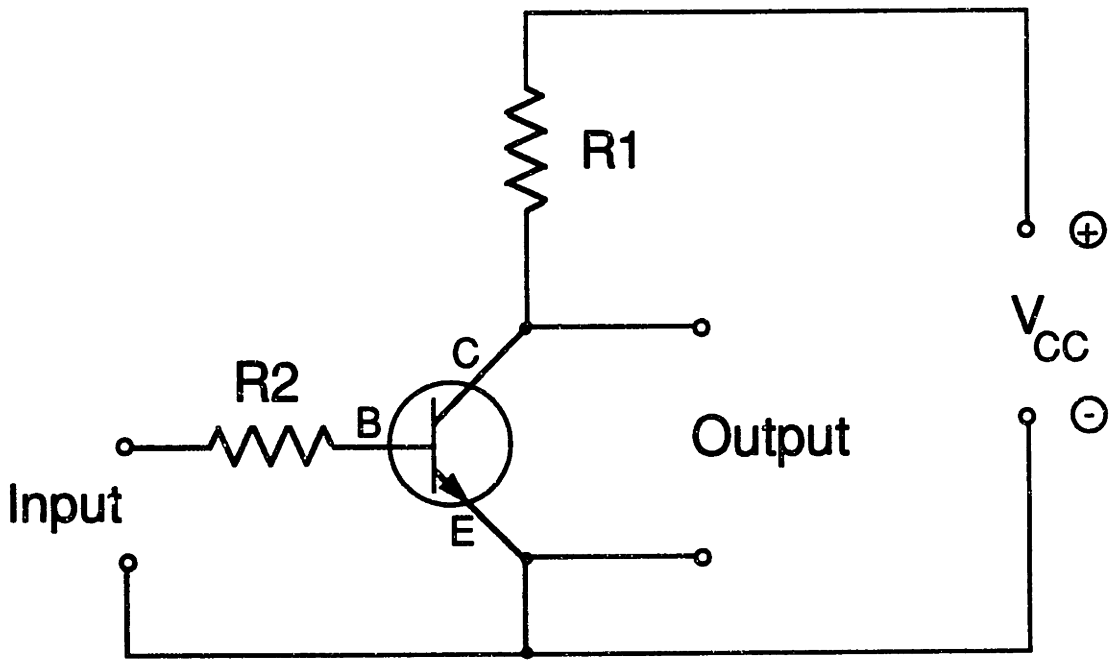

Scheme VII. An inverter based on a standard bipolar transistor configured to provide a transfer function comparable to the polyaniline-based inverter shown in Figure 2.

Figure 5. Transfer functions and assigned logic levels for a silicon bipolar transistor inverter (top) and a polyaniline transistor-based inverter (bottom). *Silicon-based inverter*: schematic shown Scheme VII, characterization of noise immunity shown Figures 6a-f. *Polyaniline-based inverter (described above)*: schematic shown Figure 2, characterization of noise immunity shown Figures 4a-f.

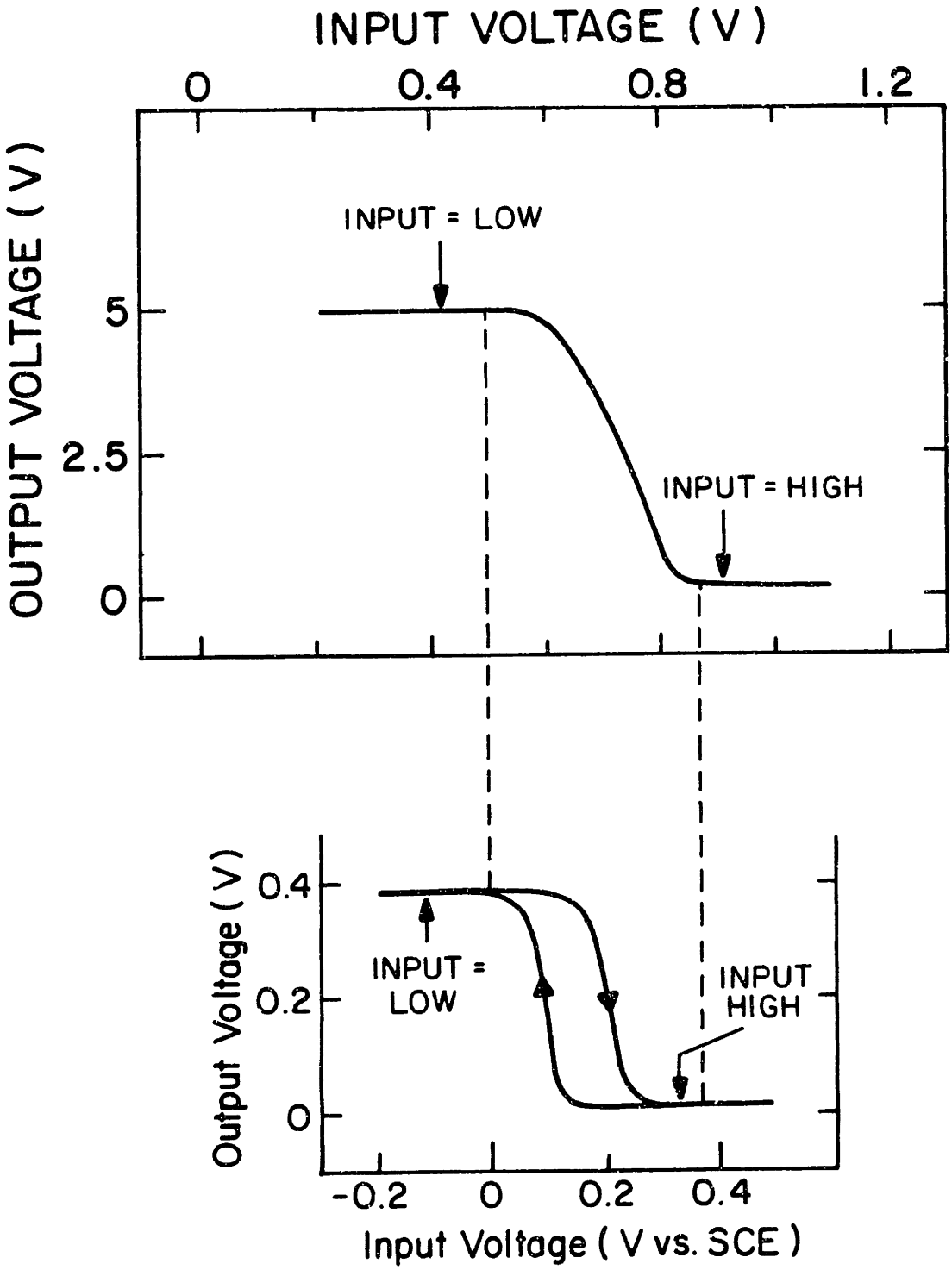
INPUT VOLTAGE (V)
0
0.4
0.8
1.2
OUTPUT VOLTAGE (V)
5
2.5
0
INPUT = LOW
INPUT = HIGH
Output Voltage (V)
0.4
0.2
0
INPUT = LOW
INPUT HIGH
-0.2
0
0.2
0.4
Input Voltage (V vs. SCE)

The transfer function of the silicon-based inverter is shown in Figure 5. R1 is 10 KΩ, the same value used for the polyaniline-based inverter. By varying R2, the transfer function was adjusted to closely match that of the polyaniline-based inverter in width (i.e. input voltage range between HIGH and LOW output). The transfer function of the polyaniline-based inverter is included at the bottom of Figure 5 for comparison. It should be noted that the purpose of this experiment was to characterize noise immunity under equivalent conditions but in the absence of hysteresis and the results should be viewed as such and not as a direct overall competition experiment between polyaniline and silicon as device materials.

The noise immunity of the solid state inverter was characterized in the same manner as that of the polyaniline-based inverter. Figure 6 a-f show the response of the silicon bipolar transistor-based inverter to input waveforms with signal to noise ratios from 4.7:1 to 0.78:1. In each case, some noise was present in the output waveform since without hysteresis an inverter gate cannot completely reject noise when the logic levels are set close to boundaries of the region where output voltage changes with response to changing input voltage, as is clear from inspection of the transfer function for the silicon transistor-based inverter in Figure 5. At S/N of 1.57:1, Figure 6c, the output contains substantial noise while the polyaniline-based inverter shows a clean output waveform at an input S/N of 1.4:1, Figure 4c. At a S/N of 0.94:1, Figure 6e, the solid state inverter is overwhelmed by the noise in the input while the polyaniline-based inverter still remains operative at S/N of 0.84:1, Figure 4e. However, once noise in the input signal drives the transistor beyond the hysteresis-derived buffer zone both inverters behave similarly, seen in Figures 3f and 6f where a large noise component is present in both output waveforms.

Figures 6a - 6f: Characterization of the noise immunity of an inverter gate based on a standard silicon bipolar transistor using the circuit shown in Scheme VII. V_{CC} = 5 V Input waveforms were generated using the equipment configuration shown in Scheme VI.

Figure 6a. Input and output waveforms for a silicon bipolar transistor-based inverter at an input waveform signal-to-noise ratio of 4.70:1.

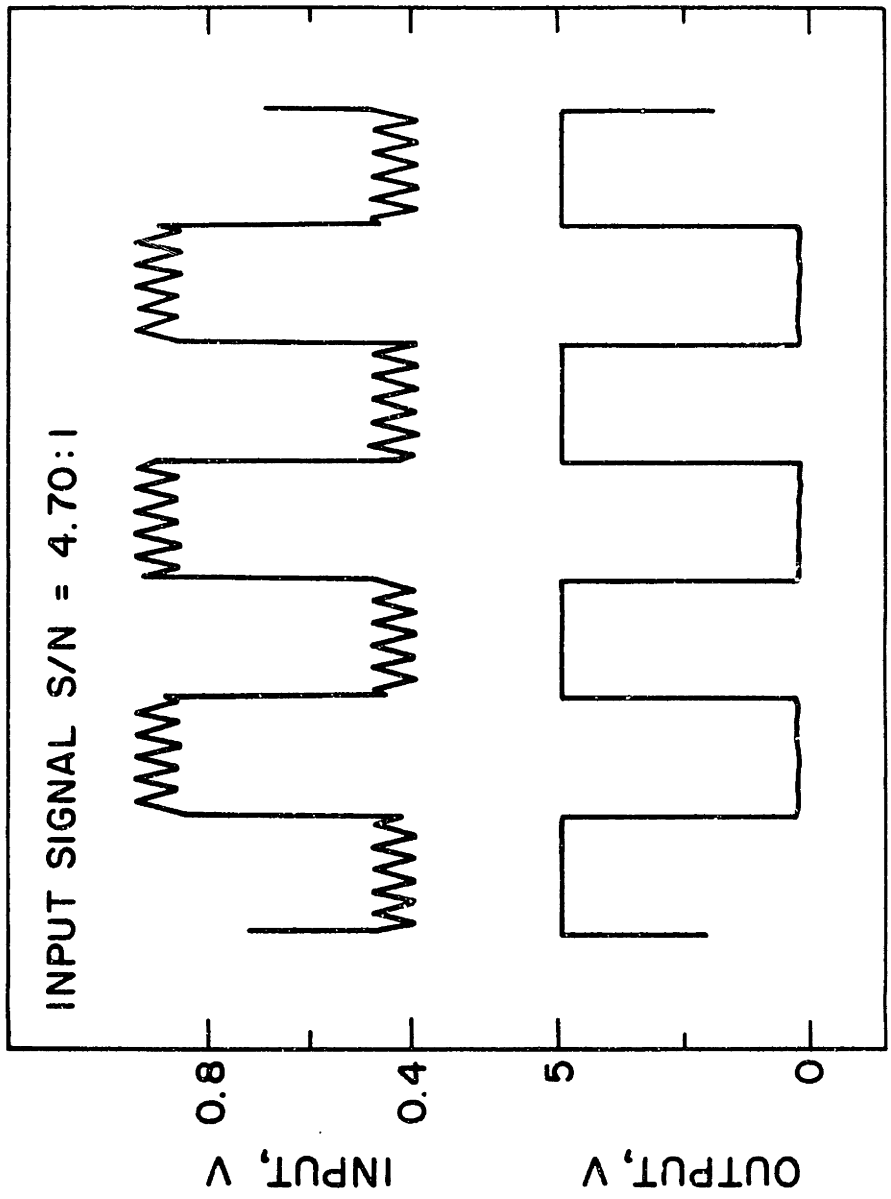
INPUT SIGNAL S/N = 4.70:1
0.8
0.4
INPUT, V
5
0
OUTPUT, V

Figure 6b. Input and output waveforms for a silicon bipolar transistor-based inverter at an input waveform signal-to-noise ratio of 2.35:1.

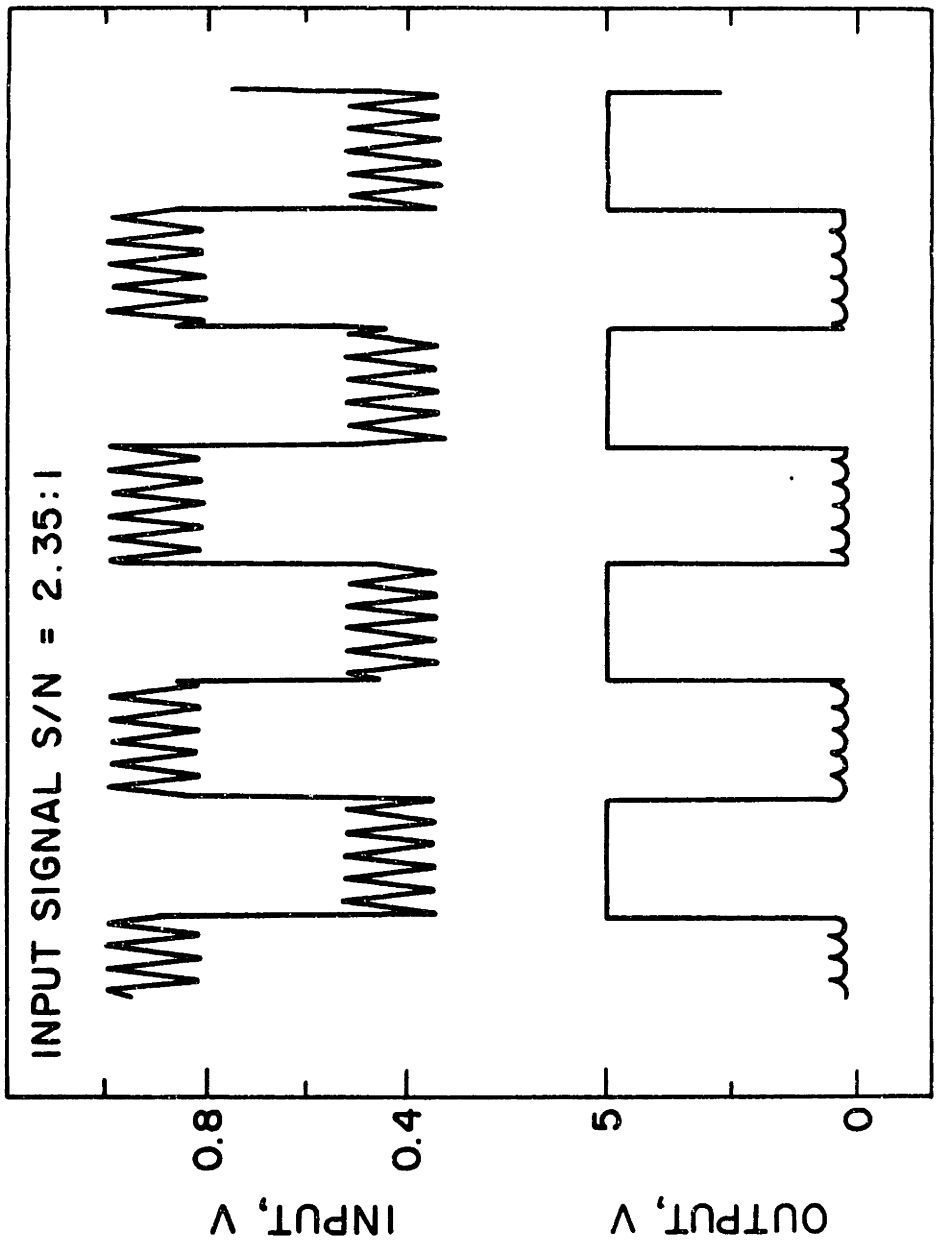
INPUT SIGNAL S/N = 2.35:1
0.8
0.4
INPUT, V
5
0
OUTPUT, V

Figure 6c. Input and output waveforms for a silicon bipolar transistor-based inverter at an input waveform signal-to-noise ratio of 1.57:1.

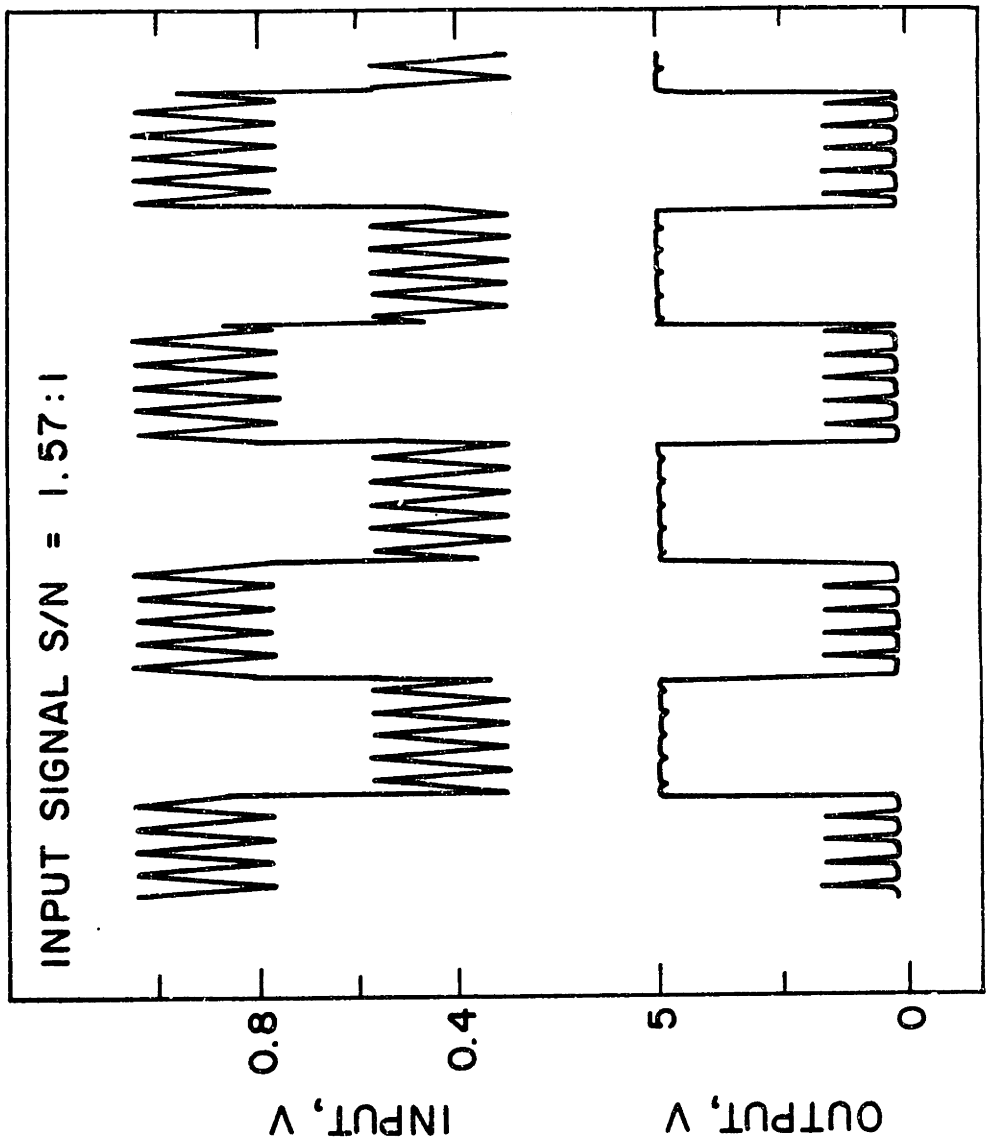
INPUT SIGNAL S/N = 1.57:1
0.8
0.4
INPUT, V
5
0
OUTPUT, V

Figure 6d. Input and output waveforms for a silicon bipolar transistor-based inverter at an input waveform signal-to-noise ratio of 1.18:1.

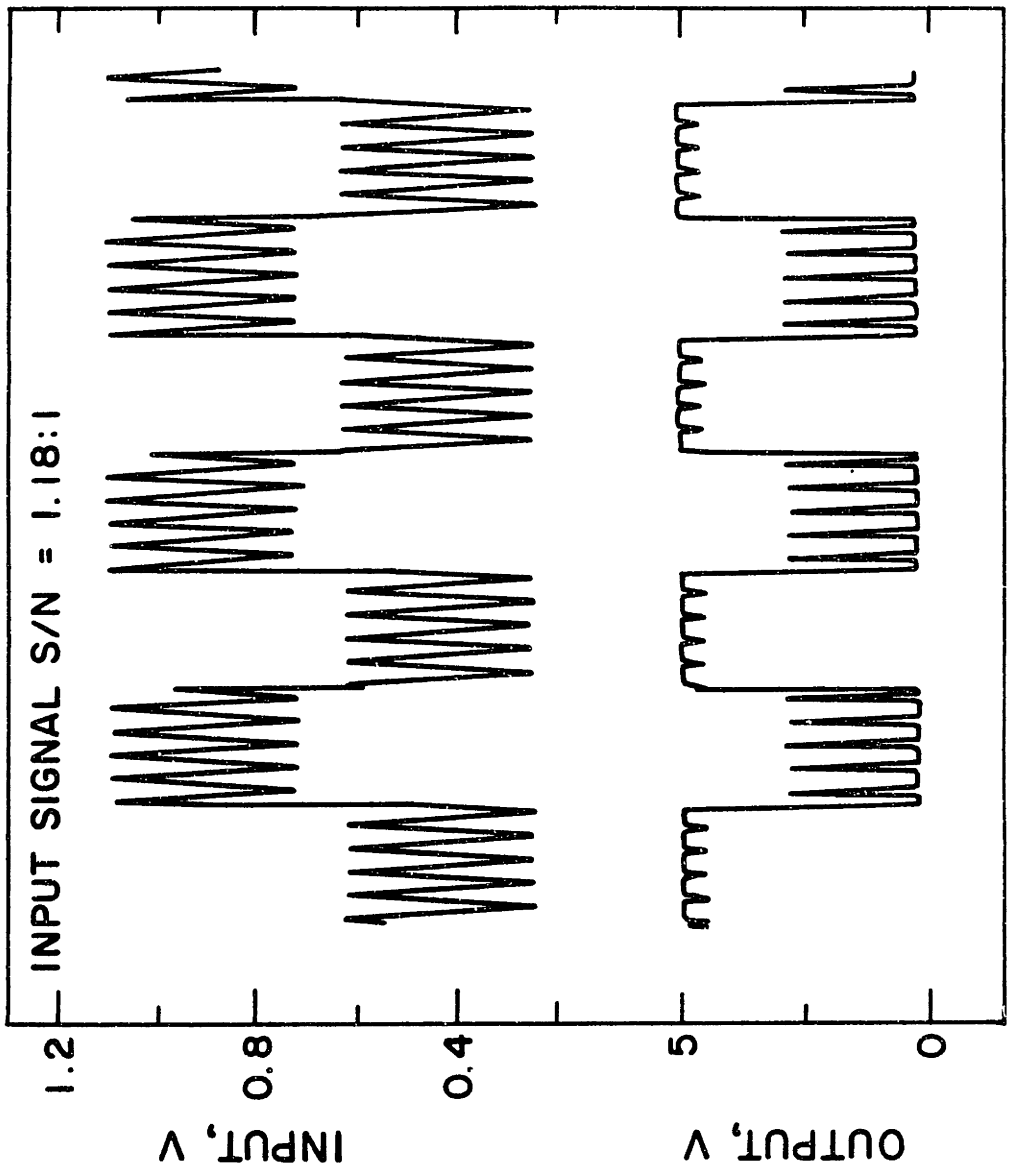
INPUT SIGNAL S/N = 1.18:1
1.2
0.8
0.4
INPUT, V
5
0
OUTPUT, V

Figure 6e. Input and output waveforms for a silicon bipolar transistor-based inverter at an input waveform signal-to-noise ratio of 0.94:1.

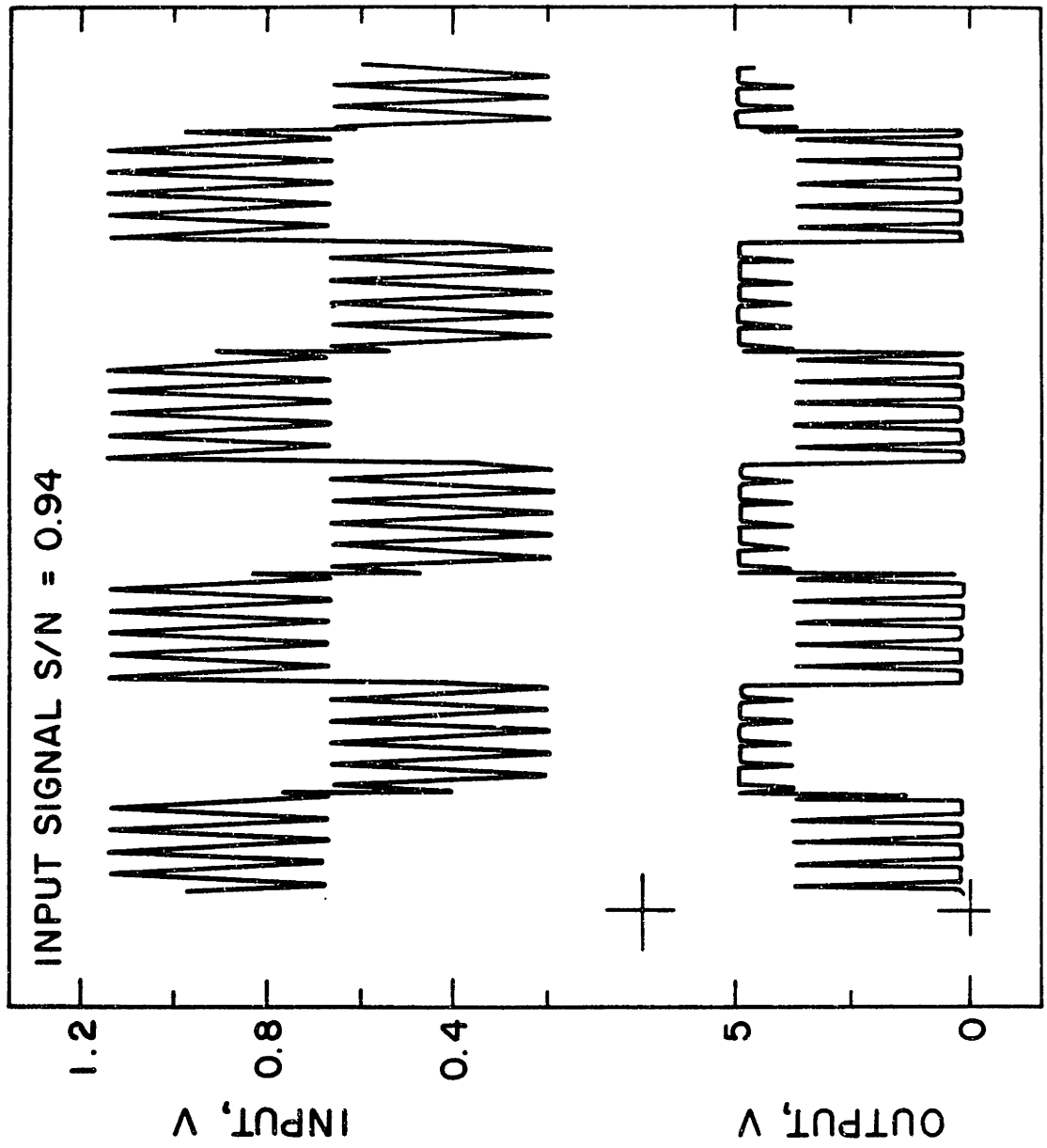
INPUT SIGNAL S/N = 0.94
1.2
0.8
0.4
INPUT, V
5
0
OUTPUT, V

Figure 6f. Input and output waveforms for a silicon bipolar transistor-based inverter at an input waveform signal-to-noise ratio of 0.78:1.

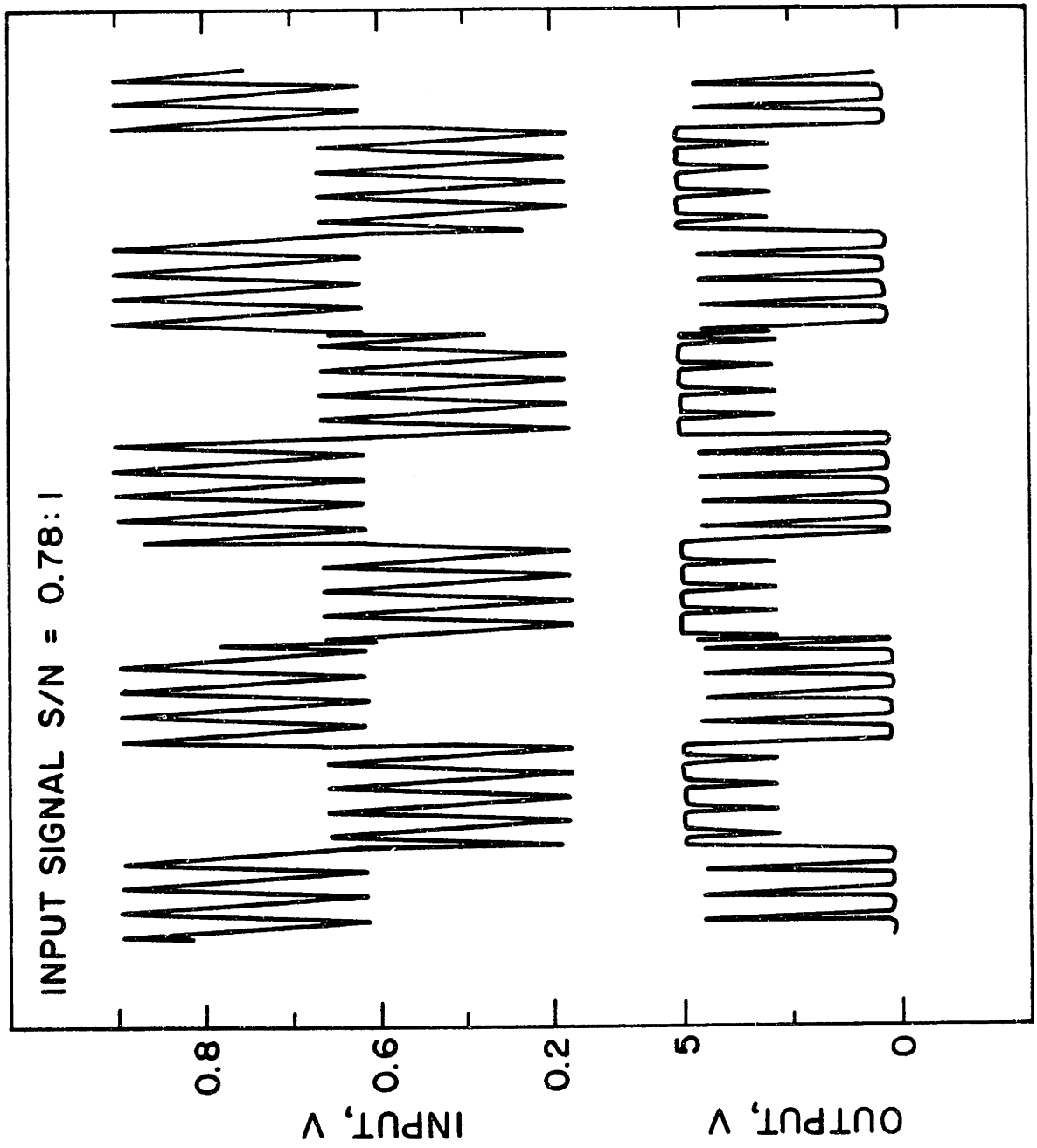
INPUT SIGNAL S/N = 0.78:1
0.8
0.6
0.2
INPUT, V
5
0
OUTPUT, V

Solvent and Electrolyte Effects on Hysteresis

Over the course of working with polyaniline microelectrochemical transistors it had been observed that differences is hysteresis from one solvent/electrolyte system to another were considerable. The importance of hysteresis in the results described above led to the examination of the electrochemistry of polyaniline in a number of electrolyte systems. Figure 7 a-g shows the results. Trifluoroacetic acid provided the required proton source for the organic solvent media. In general, polyaniline displayed the highest conductivity in aqueous acid or acidified CH_3CN. Differences in solvent, supporting electrolyte, or both resulted in differences in hysteresis. In Figure 7a almost all of the hysteresis occurs between 0 and +0.6 V and a significant portion of the I_D-V_G characteristic between peak conductivity and oxidative insulation is nearly free of hysteresis. A concentration of hysteresis on the side of the I_D-V_G characteristic negative of peak conductivity was observed when the solvent system was partly or completely aqueous. In Figure 7f, a H_2O-CH_3CN mixture, the same effect is seen to a degree, as in Figure 7g when H_2O was added to the electrolyte system. In organic solvents hysteresis is substantial throughout the entire I_D-V_G characteristic. Electrolyte choice alone exerts an effect, seen in Figure 7b vs. 6e, the only difference being $LiClO_4$ versus [*n*-Bu_4N]PF_6 as supporting electrolyte. Alcohols proved acceptable solvents for the electrochemistry of polyaniline as well. Because $LiClO_4$ is insoluble in $(CH_3)_3COH$, 10% CH_3OH was added. In Figure 7g a highly symmetrical distribution of hysteresis over the I_D-V_G characteristic was obtained using a mixture of the electrolyte systems from (d) and (e). Interestingly, polyaniline showed essentially no I_D-V_G characteristic in CH_2Cl_2 or $(CH_3)_2SO$ (also acidified with trifluoroacetic acid). Examination of the data in Figure 7 indicates that for an inverter where maximum hysteresis over the range of gate potential between onset of conductivity and peak conductivity in polyaniline is desirable, 0.5 M H_2SO_4 or acidified $LiClO_4$ /CH_3CN are the best choices for operating medium.

Figure 7a-7d. I_D-V_G characteristic of a polyaniline transistor in different solvent/electrolyte media showing variation in the specific character of hysteresis.

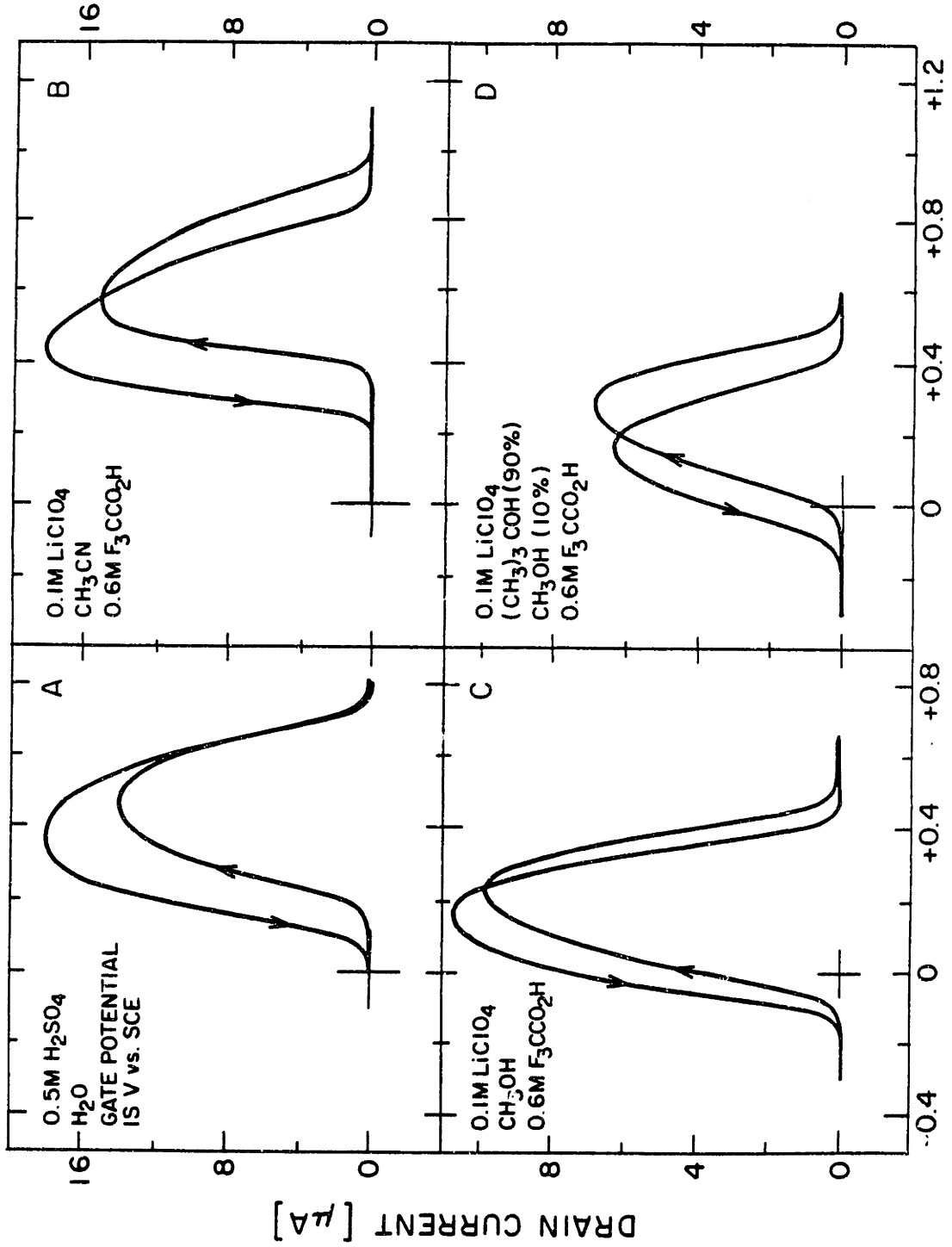
A
0.5M H_2SO_4
H_2O
GATE POTENTIAL IS V vs. SCE
B
0.1M $LiClO_4$
CH_3CN
0.6M F_3CCO_2H
C
0.1M $LiClO_4$
CH_3OH
0.6M F_3CCO_2H
D
0.1M $LiClO_4$
$(CH_3)_3COH$(90%)
CH_3OH (10%)
0.6M F_3CCO_2H
DRAIN CURRENT [μA]
GATE POTENTIAL [V vs. Ag Wire for B, C, D; V vs. SCE for A]

Figure 7e - 7g. I_D-V_G characteristic of a polyaniline transistor in different solvent/electrolyte media showing variation in the specific character of hysteresis.

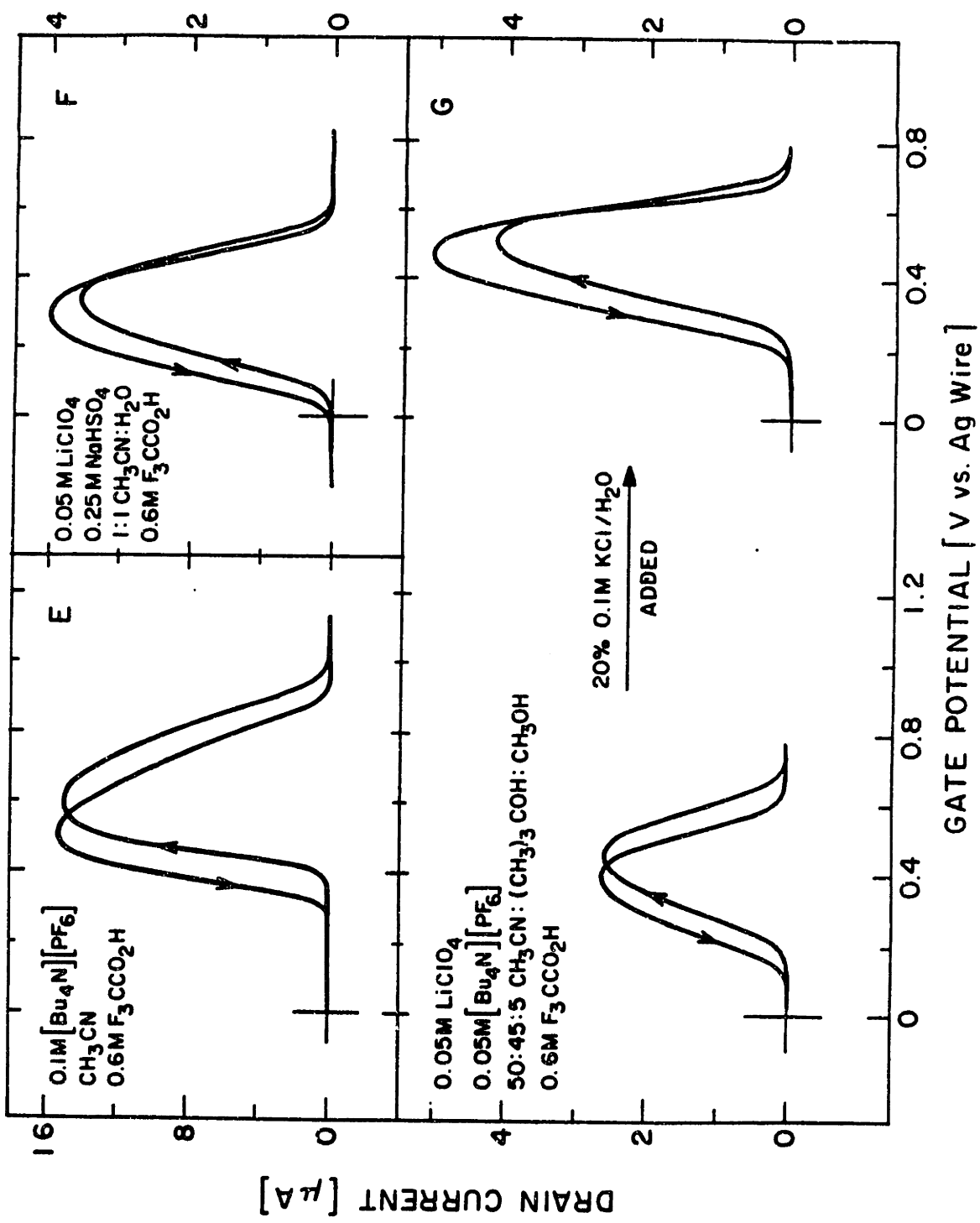
E
F
G
0.1M [Bu4N][PF6]
CH3CN
0.6M F3CCO2H
0.05 M LiClO4
0.25 M NaHSO4
1:1 CH3CN:H2O
0.6M F3CCO2H
0.05M LiClO4
0.05M [Bu4N][PF6]
50:45:5 CH3CN: (CH3)3 COH: CH3OH
0.6M F3CCO2H
20% 0.1M KCl/H2O
ADDED
DRAIN CURRENT [μA]
GATE POTENTIAL [V vs. Ag Wire]

It is reasonable to expect some variation from one medium to another in the hysteresis exhibited by polyaniline since solvation and the nature of the charge-compensating counterion are expected to affect the energetics of charge sites in the polymer. Because protonation and deprotonation of nitrogen plays a role in the redox chemistry of polyaniline, solvent effects may be more pronounced for this polyaniline than for other polymers. A good I_D-V_G response for polyaniline is observed in 0.1M [*n*-Bu_4N]PF_6/ CF_3CO_2H/ CH_3CN but an extremely poor response with three orders of magnitude less drain current was obtained if CH_2Cl_2 was the solvent. Poly(3-methylthiophene), however, shows good electrochemical response and conductivity in either solvent. Since the majority of positive charge in polyaniline is thought to be supported on the nitrogens,[13] solvent and counterion effects on the extent of protonation of those nitrogens may significantly affect hysteresis in the I_D-V_G characteristic. The best conductivity and electrochemistry were observed in polar solvents: H_2O, CH_3CN, and alcohols. Dichloromethane is not a reasonable choice of solvent for acid-base reactions and this may be the source of the poor electroactivity of polyaniline in that solvent.

In conclusion, the hysteresis which is characteristic of conducting polymer I_D-V_G response enhances the noise immunity of an inverter gate based on a polyaniline microelectrochemical transistor allowing operation at signal to noise ratios of less than 1:1 for the input waveform. It has been demonstrated that this would not be possible without hysteresis in the transfer function of the inverter. The distribution of hysteresis over the I_D-V_G characteristic of polyaniline was found to change according to choice of solvent and supporting electrolyte leading to preferred choices of operating medium in which hysteresis between onset of conduction and peak conductivity was maximum thereby resulting in the largest expected noise immunity. A polyaniline transistor-based inverter gate was operated continuously for greater than 5×10^8 inversions with sustained correct performance.

Experimental

Materials

[*n*-Bu_4N]PF_6 and $LiClO_4$ (Aldrich) were recrystallized from ethyl acetate and dried at 150°C under vacuum prior to use. CH_3CH, CH_3OH, $(CH_3)_3COH$, CH_2Cl_2, $(CH_3)_2SO$, KCl, H_2SO_4 (Mallinkrodt or Aldrich) and $NaHSO_4$ (Fluka) were used as received.

Electrochemistry

Polyaniline was deposited onto Pt microelectrode arrays as described in Chapter 2, general experimental section. Electrochemistry was carried out with a Pine Instruments RDE4 bipotentiostat using a saturated calomel or silver wire reference electrode. The inverter circuit power supply voltage, V_{DD} was supplied by using a second RDE4 potentiostat with counter and reference electrode connections shorted which allows the instrument to serve as a simple regulated power supply. *It is critical when using this set up to make no connections of the two instruments' DC common terminals to chassis ground. Because potentiostat design has the working electrode at circuit ground* [14] *("DC common" on an RDE4) this effectively connects the working electrodes of the two instruments, an unwanted situation leading to ground loops, unwanted current paths, and interference with measurements.* A 2N3904 (Si, NPN) transistor was used in the silicon bipolar transistor-based inverter circuit, Scheme VII. Data was recorded on a Kipp and Zonen model BD91 XYY' recorder or on a Nicolet model 4094 digital storage oscilloscope. A Hewlett-Packard model 3311A function generator was used as a square wave source.

References

1. Heeger, A. J. In *Handbook of Conducting Polymers*; Skotheim, T. A., Ed.; Marcel Dekker: New York, 1986; p. 729 a) p. 749

2. The author gratefully acknowledges Dr. Mark Hollis of MIT/Lincoln Laboratory for valuable discussions and for pointing out the potential benefits of hysteresis to noise rejection in logic gates, which led to the experiments presented in this chapter.

3. Ofer, D.; Crooks, R. M.; Wrighton, M. S. *J. Am. Chem. Soc.* **1990**, *112*, 7869

4. Brédas, J.-L.; Street, G. B. *Accs. Chem. Res.* **1985**, *18*, 309

5. Brédas, J.-L.; Thémans, B.; Fripiat, J. G.; André, J. M.; Chance, R. R. *Phys. Rev. B: Condens. Matter* **1984**, *29*, 6761

6. Chance, R. R.; Boudreaux, D. S.; Brédas, J.-L.; Silbey, R. in *Handbook of Conducting Polymers*; Skotheim, T. A., Ed.; Marcel Dekker: New York, 1986. Chapter 24

7. Huang, W.-S.; Humphrey, B. D.; MacDiarmid, A. G. *J. Chem. Soc., Faraday Trans. 1* **1986**, *82*, 2385

8. Horowitz, P.; Hill, W. *The Art of Electronics*; Cambridge University Press: New York, 1989 a) chapter 8; b) chapters 2,3

9. Hollis, M. A.; Murphy, R. A. in *High Speed Semiconductor Devices*, Sze, S. M. ed., John Wiley and Sons, 1990

10. Lofton, E. P.; Thackeray, J. W.; Wrighton, M. S. *J. Phys. Chem.* **1986**, *90*, 6080

11. this thesis, Chapter 2.

12. The arrows denoting flow of current conform to the (unfortunate) standard convention whereby current is depicted as the flow of positive charge, rather than the flow of electrons.

13. Kaplan, S.; Conwell, E. M.; Richter, A. F.; MacDiarmid, A. G. *J. Am. Chem. Soc.* **1988**, *110*, 7647.

14. Bard, A. J.; Faulkner, L. R. *Electrochemical Methods*, John Wiley and Sons: New York, 1980, Chapter 13

Chapter 4

Finite Windows of High Conductivity Yield Unique Opportunities for Molecule-Based Devices: A Microelectrochemical Push-Pull Amplifier Based on Two Different Conducting Polymer Transistors, Devices with Novel Drain Current-Gate Voltage Characteristics, and Complementary Microelectrochemical Digital Logic

Abstract

Conjugated organic polymers display a finite potential window of conductivity yielding the unusual I_D-V_G characteristic of microelectrochemical transistors. This behavior, which is not observed in conventional transistors, yields unique opportunities which are developed as the basis of three families of electronic devices. **I.** The preparation and characterization of a microelectrochemical push-pull amplifier based on one polyaniline transistor and one poly(3-phenylthiophene) transistor which exploits the electrical properties of conducting polymers to achieve freedom from crossover distortion is reported. The two polymers posses I_D-V_G characteristics which overlap, yielding a transistor pair inherently free of the dead zone in response caused by the p-n junction barrier potential in solid state transistors which is the source of crossover distortion. The output waveform of the microelectrochemical push-pull amplifier demonstrates crossover distortion-free operation and is compared to that of the analogous bipolar-transistor based system. **II.** The design of a complementary inverter is described and executed with polyaniline and WO_3 microelectrochemical transistors. This inverter demonstrates operation of a microelectrochemical system without potentiostatic control and in a circuit which utilizes the electrochemical gating process in a configuration, avoiding restrictions that process can incur in multi-transistor circuits. The complementary microelectrochemical transistor inverter achieves true 3-terminal transistor operation and conventional ground-referenced inputs and outputs. **III.** Devices with novel transistor behavior derived from two or more component I_D-V_G characteristics are prepared. By selecting the appropriate degree of overlap between two separate I_D-V_G characteristics, a device in which a plateau region of drain current has been introduced at half of maximum I_D was prepared. This unusual transistor behavior is potentially significant as a molecule-based approach to multiple-state logic devices. A microelectrochemical ternary (3-state) inverter was demonstrated based on an I_D-V_G characteristic designed to be intrinsically suited to 3-state operation.

Introduction

A unique aspect of conjugated organic polymers as electronic materials is their *finite potential window of high conductivity*,[1-6] a property not found in conventional inorganic semiconductor materials. Polymers such as polythiophene,[2-4] polypyrrole,[3,4] polyaniline,[1,3,4] and polyacetylene[4-6] while insulating in their neutral form, become highly conducting upon partial oxidation. The polymers become insulating again when further oxidized, yielding the unusual I_D-V_G characteristic illustrated in Figure 1 for a polythiophene-based transistor. This behavior, in which conductivity is observed over a finite window of gate potential, is an electrical characteristic which has been shown to be a general feature of conjugated organic polymers.[3,4] As a result of it, microelectrochemical transistors have unique I_D-V_G behavior. In contrast to conventional transistors[7,8,9] where a control voltage governs an off-to-on transition, microelectrochemical transistors based on conducting polymers display an off-to-on-to-off progression as a consequence of the finite window of conductivity. This capability is not shared by conducting polymer-based field-effect transistors[10-13] or more conventional devices such as MOSFETs,[7-9] where I_D reaches a maximum and plateaus as V_G is increased rather than returning to zero yielding an off to on transition only. This difference in behavior is illustrated in Figure 2 by the characteristics of a polyaniline transistor and a theoretical[8a] MOSFET. The push-pull amplifier, involving two different conducting polymers, demonstrates a new way to utilize the materials properties of conducting polymers which give rise to the unusual electrical characteristics of polymer-based microelectrochemical transistors.[14] The device possibilities arising from the finite window of high conductivity are developed further in the preparation of a complementary microelectrochemical transistor inverter, and the demonstration of transistors based on two or more contributing I_D-V_G characteristics in order to produce more complex I_D-V_G behavior. In this way, devices intrinsically suited to use in multiple-level logic circuits can be prepared.

Figure 1. (top) Cross-sectional view of a microelectrochemical transistor. The electrodes are functionalized with a film of polymer by electropolymerization of the appropriate monomer. (bottom) I_D-V_G characteristic of a polythiophene transistor. The neutral (no shading) and highly oxidized (dark shading) states of the polymer film are insulating. High conductivity occurs in the partially oxidized state (medium shading). The I_D-V_G characteristic of polythiophene taken in liquid SO_2 appears here courtesy of Dr. David Ofer, who measured it.

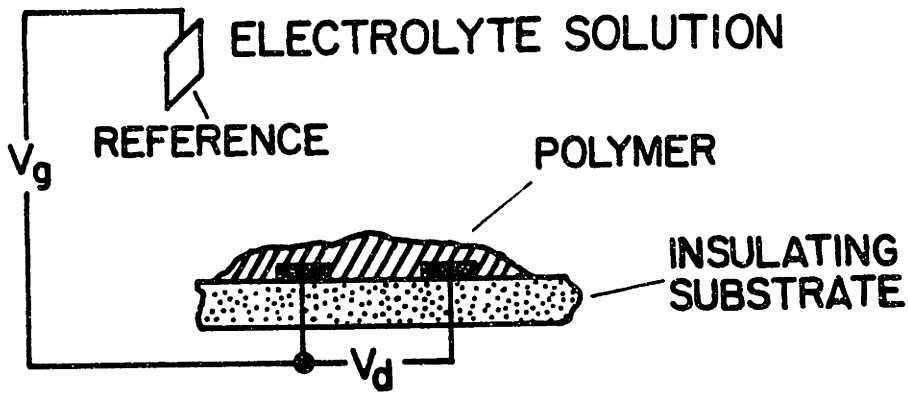
ELECTROLYTE SOLUTION
REFERENCE
V_g
POLYMER
INSULATING SUBSTRATE
V_d

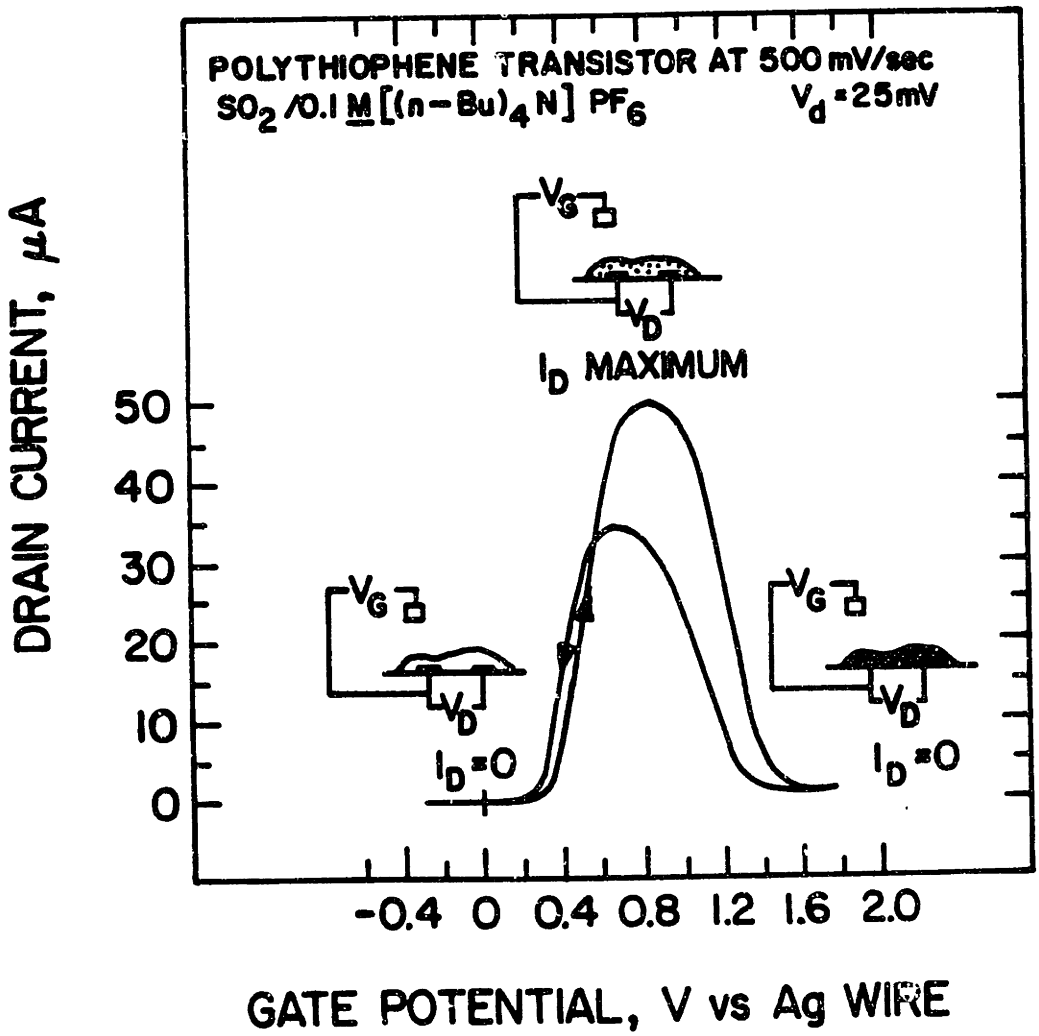
POLYTHIOPHENE TRANSISTOR AT 500 mV/sec
SO_2 /0.1 M $[(n-Bu)_4N]$ PF_6
V_d =25mV
V_G
V_D
I_D MAXIMUM
I_D=0
I_D=0
DRAIN CURRENT, μA
50
40
30
20
10
0
-0.4 0 0.4 0.8 1.2 1.6 2.0
GATE POTENTIAL, V vs Ag WIRE

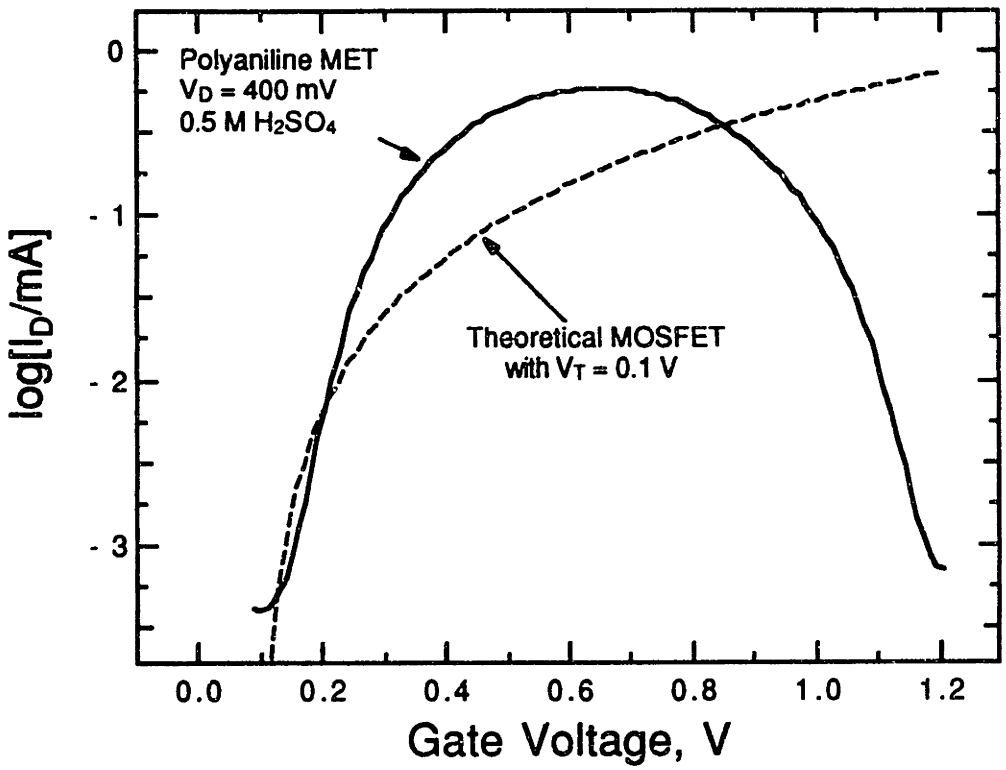

Figure 2. Log(I_D) as a function of gate potential for a polyaniline microelectrochemical transistor (solid line) and a theoretical MOSFET of comparable parameters showing the insulation to conduction transition for a MOSFET and the insulation to conduction to insulation transition of a conducting polymer-based microelectrochemical transistor.

A microelectrochemical transistor consists of a film of polymer deposited onto two Pt or Au microelectrodes which serve as the source and drain of the transistor.. A cross-sectional view of this device configuration is shown in Figure 1. The oxidation state of the polymer is controlled by application of gate voltage, V_G, with respect to a reference electrode in the electrolyte solution. Gate current, I_G, corresponds to withdrawal from, or injection into, the polymer of electrons (oxidation or reduction) which controls the polymer conductivity. A drain potential, V_D, is applied across the polymer film and drain current, I_D, flows when the polymer is in its conducting state. Transistor action occurs because a small change in V_G gives rise to a large change in I_D. In Figure 1 the I_D-V_G characteristic

for a polythiophene-based transistor is shown. The finite potential window of high I_D and the hysteresis in the scan are both typical of conducting polymer-based devices. The high value of I_D corresponds to the partially oxidized, conducting state of polythiophene.[3]

The Finite Window of High Conductivity

The finite window of high conductivity has been shown to be a general feature of conjugated organic polymers and is the subject of a report by Ofer, Crooks, and Wrighton[3] which includes an extensive discussion of conducting polymer I_D-V_G behavior. Finite window behavior has been shown for polyaniline,[1,3,4] polypyrrole and derivatives,[3,4] polythiophene and derivatives,[2-4] polyacetylene,[4-6] as well as other polymer systems. In the course of the work reported in this thesis finite windows of high conductivity have been characterized for a series of para-substituted poly(3-phenylthiophene)s, poly(1,4-dithienylbenzene), poly(1,4-dithienyl-2,5-difluorobenzene), polyselenophene, poly(3,4-dimethylthiophene), and poly(3-methoxyaniline) including characterization of finite windows of conductivity upon reduction from the neutral state for poly(1,4-dithienylbenzene), poly(1,4-dithienyl-2,5-difluorobenzene), and poly[3-(4-trifluoromethyl-phenyl)-thiophene).

The I_D-V_G behavior of conducting polymers shows that these materials sustain charge transport when partially oxidized but not in the neutral or highly oxidized states. Scheme I shows representations[15-18] of a conjugated polymer in the neutral, partially oxidized, and highly oxidized states. In Scheme I (a), the polymer is in its neutral state. Its valence band is fully populated, its conduction band is empty, and with no charge carriers present the polymer is insulating. In Scheme I (b) a quinoid distortion, known as a bipolaron has been introduced.[15,16] The quinoid structure, extending over four rings, has been calculated to be the overall energy-minimized π-configuration for support of the positive charge,[15,17] as discussed in more detail in the introduction to Chapter 3. The bipolaron is mobile. Resonance forms can be drawn in which the bipolaron distortion is

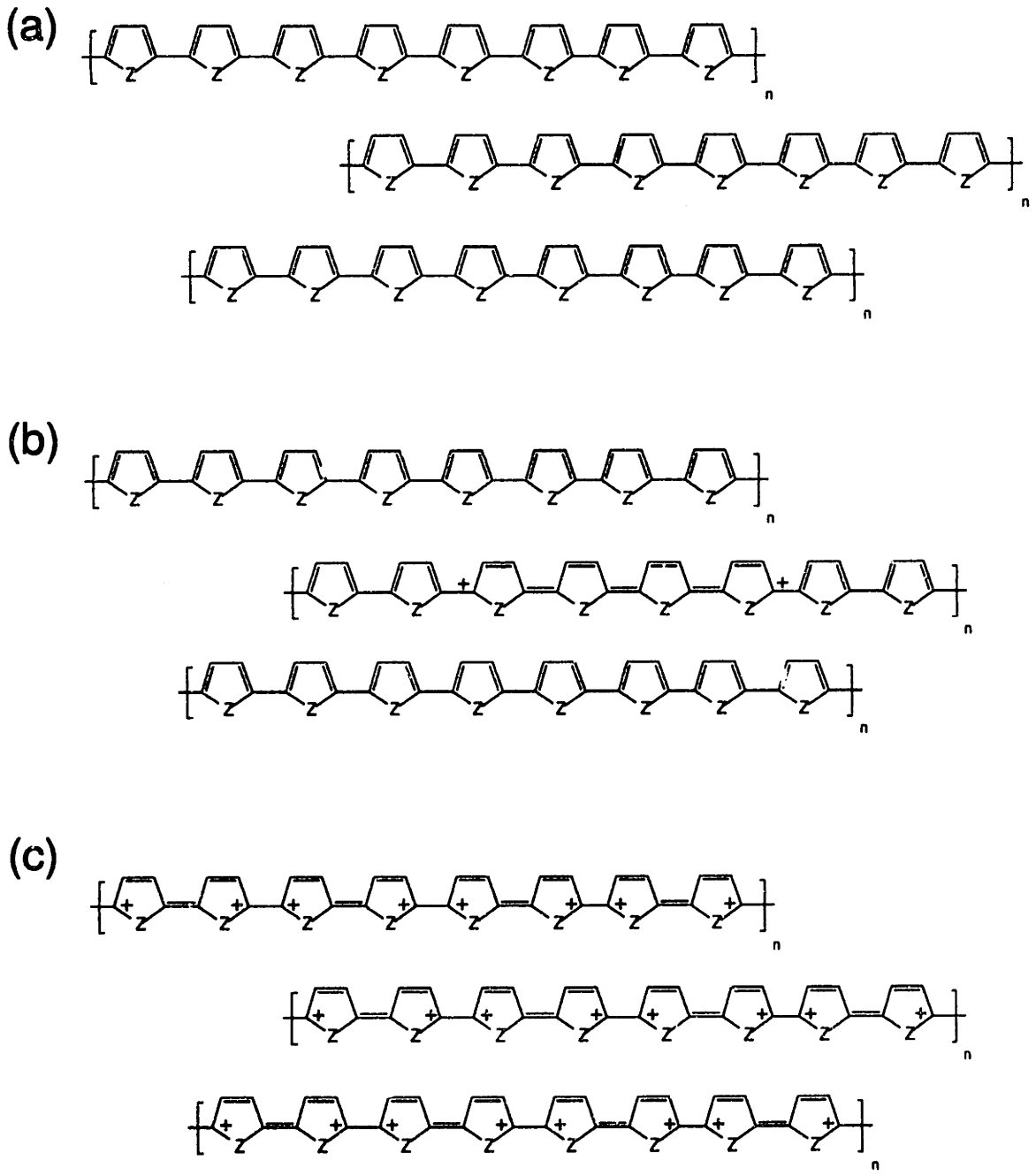

Scheme I. Representations of the (a) neutral, (b) partially oxidized, and (c) fully oxidized (one electron per repeat unit) states for a polyheteroaromatic conductor.

shifted left or right along the polymer chain. Further, Scheme I (b) shows two neighboring chains present representing expanses of neutral polymer to which a cationic site can jump. Thus, in Scheme I (b), the charged sites are mobile both along polymer

chains and from one chain to another and in this state the polymer is electrically conducting. In Scheme I (c) the polymer chain is represented as oxidized to one electron per repeat unit. In this valence structure, resonance forms for shifting of the charges along the polymer chain would be highly coulombically strained and unreasonable. Holes cannot jump from chain to chain without generating dicationic repeat units. It is thus reasonable to expect that at high oxidation levels the holes on a conducting polymer backbone become localized and do not support condution.[3,4] A similar argument can be made for conduction in the reduced state where anionic sites are the carriers.

The extent of oxidation corresponding to peak conductivity varies from a low of 0.1 electrons per repeat unit for polyacetylene to a high of 0.5 for polyaniline.[3,4,5] Polyaniline is a special case which deserves commentary. Typically, conducting polymers are highly vulnerable to attack and degradation if their π-manifolds are depopulated sufficiently to achieve oxidative insulation. To study the entire window of high conductivity for many materials it is necessary to work in a medium which is both non-nucleophilic and can support the very positive electrochemical potentials required to attain the highly oxidized states of materials such as polythiophene or polyacetylene at which oxidative insulation is observed. For this purpose, liquid SO_2 has proven a useful electrochemical solvent. However, even under the most favorable conditions polymers of the pyrrole, thiophene, and acetylene families have limited durability when very highly oxidized.[3] The coulombic strain and expected highly reactive nature of a species of the type represented in Scheme I (c) has already been pointed out.[3] Polyaniline is a significant exception to the generally limited stability of very highly oxidized conducting polymers. Polyaniline reaches peak conductivity at 0.5 electrons per repeat unit[19] (an extent of oxidation where polythiophenes and polypyrroles degrade rapidly) and is so durable that its entire window of conductivity can be characterized in aqueous sulfuric acid with modest stability of I_D-V_G response. This stability is probably due to the fact that it is primarily the nitrogens of the backbone which bear the burden of supporting positive charge. This favorable situation allows polyaniline

to be reversibly oxidized to the extent of one electron per repeat unit.[3,4,19,20] This is perhaps the most pronounced difference in the behavior of polyaniline from the pyrrole, thiophene, phenylene, acetylene, and other polymer families which have continuous carbon backbones.

The finite window of high conductivity yields the unusual I_D-V_G characteristic in conducting polymer-based microelectrochemical transistors. Since vacuum tubes, bipolar junction transistors, junction field-effect transistors, and MOSFETs are all devices which provide an off-to-on transition, the unique behavior of microelectrochemical transistors affords an opportunity to explore new roles for a transistor which displays an off-to-on-to-off transition. The results presented in this chapter demonstrate that the finite window of high conductivity is a versatile electrical characteristic leading to unique molecule-based approaches to a diverse range of electronic devices.

Results and Discussion

I. A Microelectrochemical Push-Pull Amplifier

A push-pull amplifier serves applications where a load must be driven both positive and negative of ground.[8b] It can be seen in the polyaniline-based audio amplifier described in Chapter 2 that a one-transistor amplifier configuration is best suited to supplying current in only one direction. This is the nature of one-transistor amplifiers since they have only a single active device and a single power supply.[8] A load such as a speaker can and should be driven with current in both directions since the speaker cone is intended to undergo displacement both forward of and behind its equilibrium point. The purpose of a push-pull amplifier is to provide an output which can drive a load positive and negative of zero, in other words to be able to "push", or "pull", current at its output. The push-pull amplifier, shown in Figure 3 in its most basic form,[8b] sees wide use as the output stage in audio amplifiers, operational amplifiers, potentiostats, and countless other circuits. (The circuit in Figure 3 is also commonly implemented with MOSFETs, one *p*-channel and one *n*-channel.) One transistor handles the positive side of operation and the other the negative side. The NPN transistor (the designation *NPN* signifies a bipolar device constructed of an *n*-type/*p*-type/*n*-type arrangement[7]) conducts only in response to a positive input voltage, causing current from the positive supply, V^+, to flow, while the PNP transistor conducts only in response to a negative input, causing V^- current to flow. In this way the load can be driven both positive and negative of ground. The response of a push-pull amplifier based on silicon bipolar transistors is shown in Figure 3. Notice that the amplifier output shows a dead zone as it crosses zero, commonly referred to as "crossover distortion".[8b] The crossover distortion is due to the *p-n* junction barrier potential, 0.6 V in Si, which must be exceeded before a bipolar device begins to turn on. The result is a dead zone between +0.6 and -0.6 V in input voltage where neither transistor conducts giving rise to

Figure 3. Schematic and output waveform of a silicon bipolar push-pull amplifier. The distortion as the output crosses zero is due to the 0.6V p-n junction barrier potential in the silicon devices.

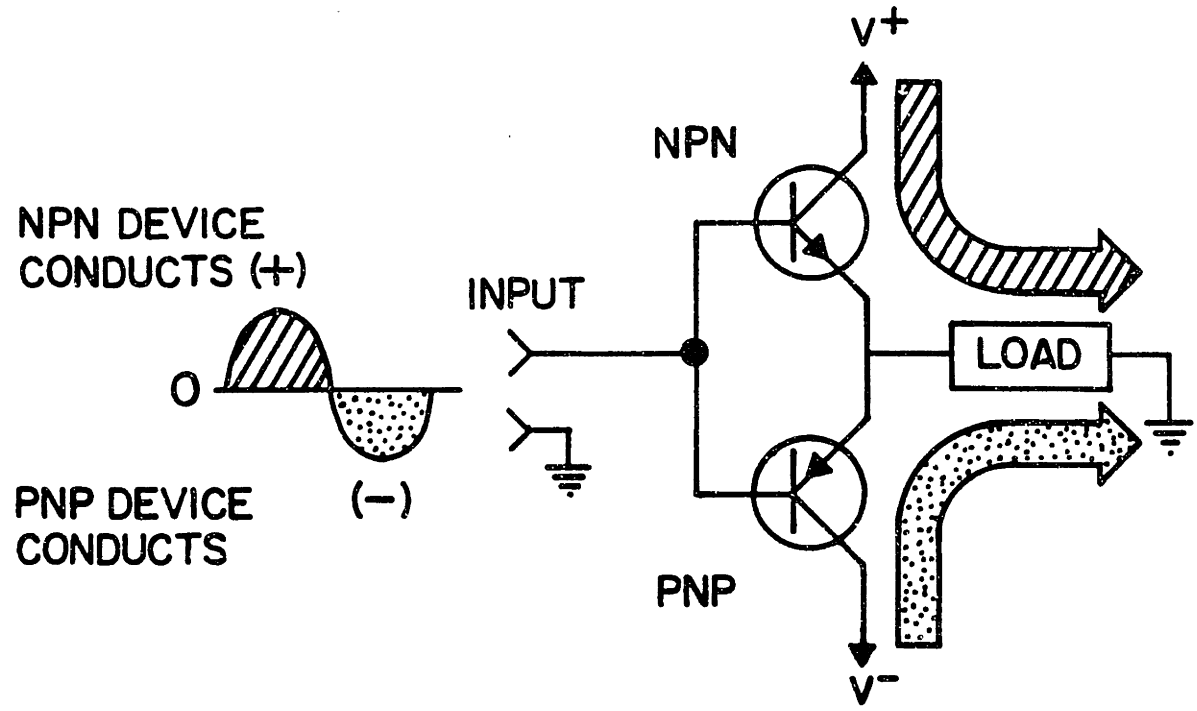
V+
NPN
NPN DEVICE
CONDUCTS (+)
INPUT
LOAD
0
(−)
PNP DEVICE
CONDUCTS
PNP
V−

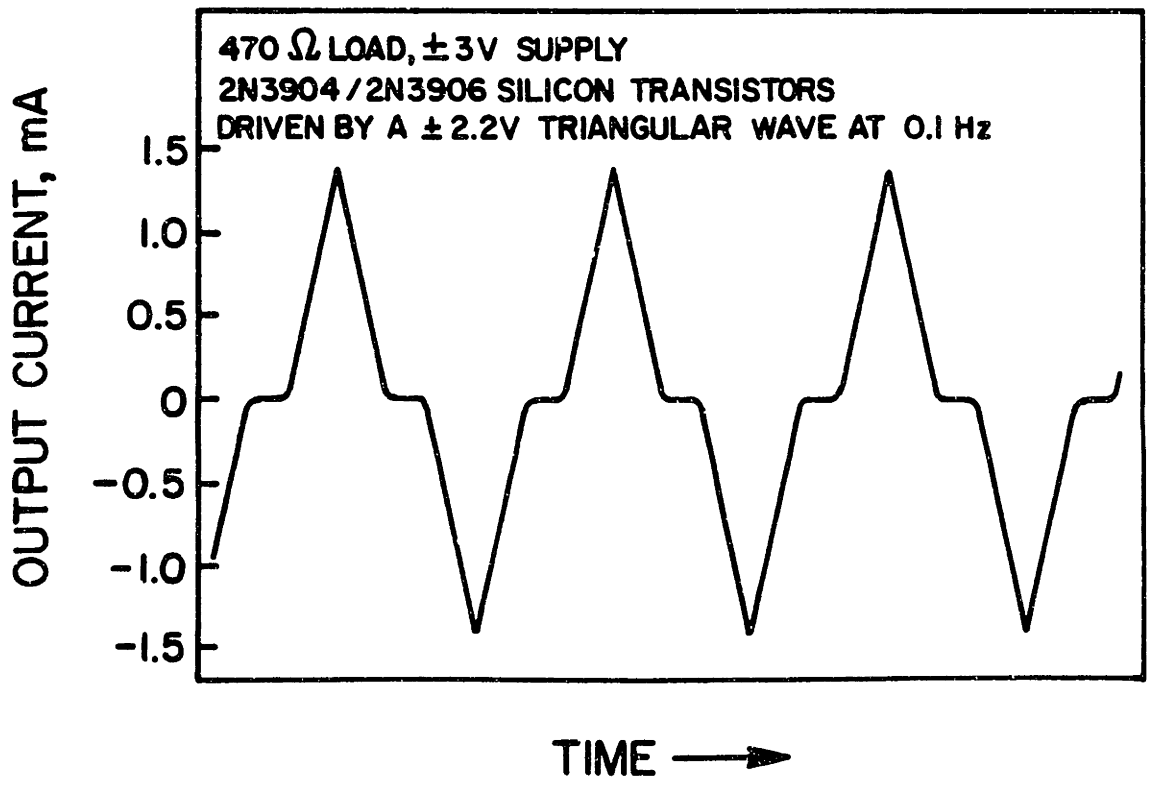
470 Ω LOAD, ±3V SUPPLY
2N3904 / 2N3906 SILICON TRANSISTORS
DRIVEN BY A ±2.2V TRIANGULAR WAVE AT 0.1 Hz
OUTPUT CURRENT, mA
1.5
1.0
0.5
0
−0.5
−1.0
−1.5
TIME

the plateau in the output as it crosses zero. (In the MOSFET version of the push-pull amplifier, gate threshold potential (V_T) rather than a junction barrier potential is responsible for crossover distortion) In most applications this crossover distortion is undesirable and is typically overcome by additional circuitry which holds both transistors slightly above their turn-on threshold.[8b]

The unusual I_D-V_G characteristic of conducting polymers allows conducting polymer-based microelectrochemical transistors to be operated on *either side* of the peak in the I_D-V_G characteristic. As a result, a positive or negative dI_D/dV_G can be selected for a given application by the range of V_G over which the transistor is operated. Further, a number of conducting polymers with different potential windows of high conductivity are available. The significance of these two materials properties is that the manner in which two transistors complement each other electrically in a commonly-gated pair can be determined by the conducting polymers selected as the device-active materials. Currently known conducting polymers can accommodate requirements ranging from transistor pairs with windows of conductivity overlapping completely to windows separated by a significant gap. A push-pull amplifier requires that one device to respond to the positive half of the input waveform and the other to respond to the negative half. Scheme II shows an approach to implementing a push-pull amplifier with microelectrochemical transistors. By choosing two conducting polymers with I_D-V_G characteristics overlapping as shown in Scheme II, the transistor responses appropriate for a push-pull amplifier are obtained. The principle of operation of the microelectrochemical push-pull amplifier is essentially the same as the solid state version in Figure 3. From the potential at which the I_D-V_G characteristics cross, V_{rest} in Scheme II, moving negative drives polymer 1 into conduction and polymer 2 into a range of V_G where it is reduced and insulating. Moving positive of V_{rest} results in conduction by polymer 2 and insulation by polymer 1. In this way, the amplifier drives the load with power from the positive or negative supply as the input signal moves positive or negative of zero, respectively.

Scheme II

A Microelectrochemical Transistor-Based Push-Pull Amplifier

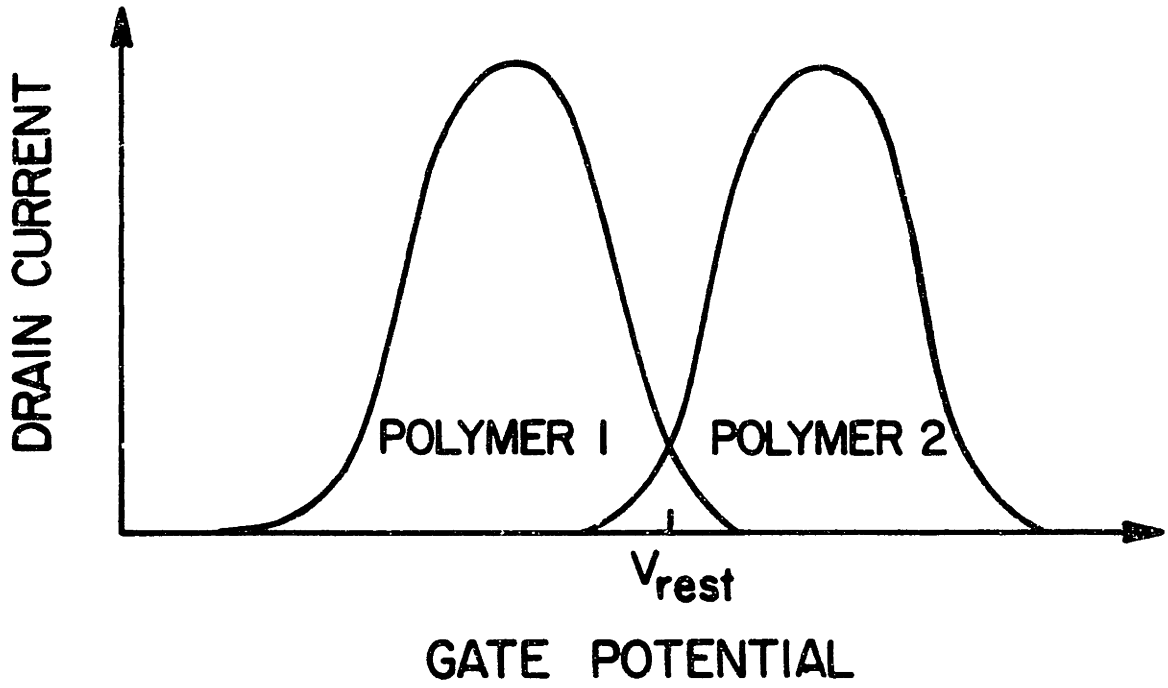

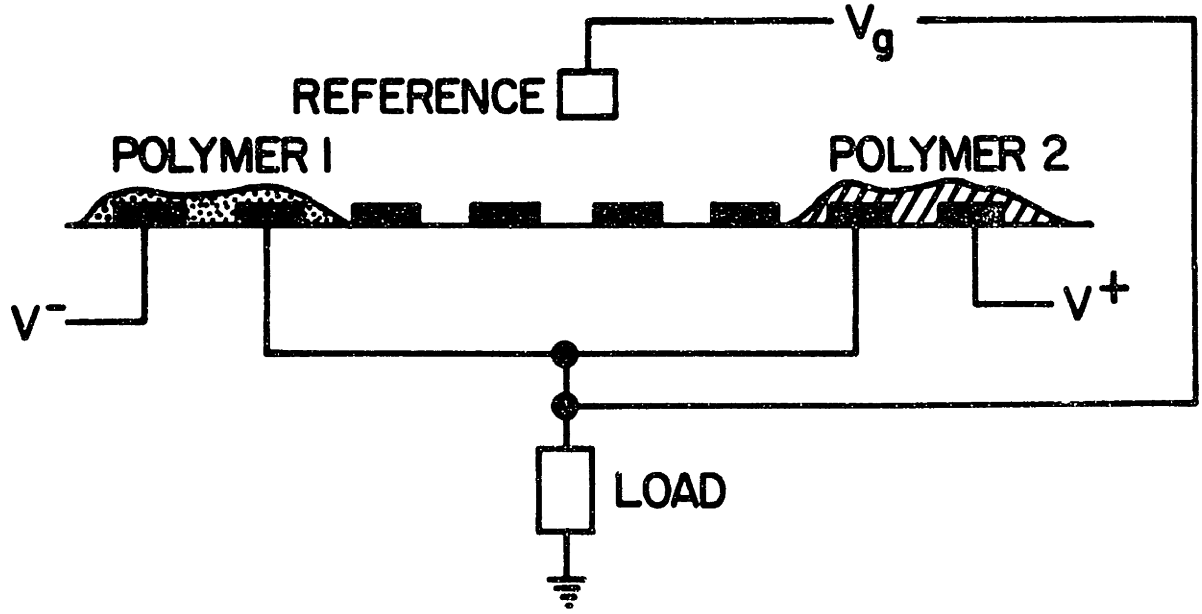

In selecting a pair of polymers for demonstration of a microelectrochemical push-pull amplifier the following criterion had to be met. The approach summarized in Scheme II requires Polymer 1 to sustain a high level of oxidation, since the transistor based on Polymer I will be driven into oxidative insulation when Polymer 2 is in conduction. The robust electrochemistry of polyaniline make it a clear choice for Polymer 1. Figure 4 shows the cyclic voltammetry and I_D-V_G characteristic of polyaniline in acidified CH_3CN. If the electrolyte medium is dry, the electrochemistry of polyaniline is stable well beyond the onset of oxidative insulation . Polymer 2 must have the appropriate potential for onset of conduction to obtain the relationship of I_D-V_G characteristics shown in Scheme II. Thus, the choice of polyaniline as Polymer 1 requires that Polymer 2 be a material with a potential for onset of conduction close to polyaniline's potential for onset of oxidative insulation. Poly(3-phenylthiophene) was chosen for Polymer 2 since its potential for onset of conduction of 0.68 V vs. Ag made it a promising match for polyaniline. Finally, the two polymers must be compatible with a single electrolyte medium if they are to be operated side-by-side on a single microelectrode array. A suitable electrolyte medium is 0.1 M $LiClO_4$/0.4 M F_3CCO_2H/CH_3CN. This provides a non-aqueous environment, required because in its oxidized state poly(3-phenylthiophene) is very sensitive to water, a proton source which polyaniline requires for electroactivity, and an electrolyte medium in which both polymers display good I_D-V_G response.

Preparation of the device led to initial difficulties in deposition of both polymers onto the same array. Following electrochemical polymerization of either aniline or 3-phenylthiophene onto a fraction of the 8 electrodes of a microelectrode array, the remaining microelectrodes of the array were found to be passivated, preventing deposition of a second polymer transistor. A further problem was the poor confinement to the driven electrodes of the polymer obtained from electrochemical polymerization of 3-phenylthiophene from CH_3CN. A device such as the one sought here places special requirements on the deposition characteristics of a conducting polymer. A monomer must not simply

Figure 4. Cyclic voltammogram and I_D-V_G characteristic of polyaniline in 0.1 M $LiClO_4/F_3CCO_2H/CH_3CN$.

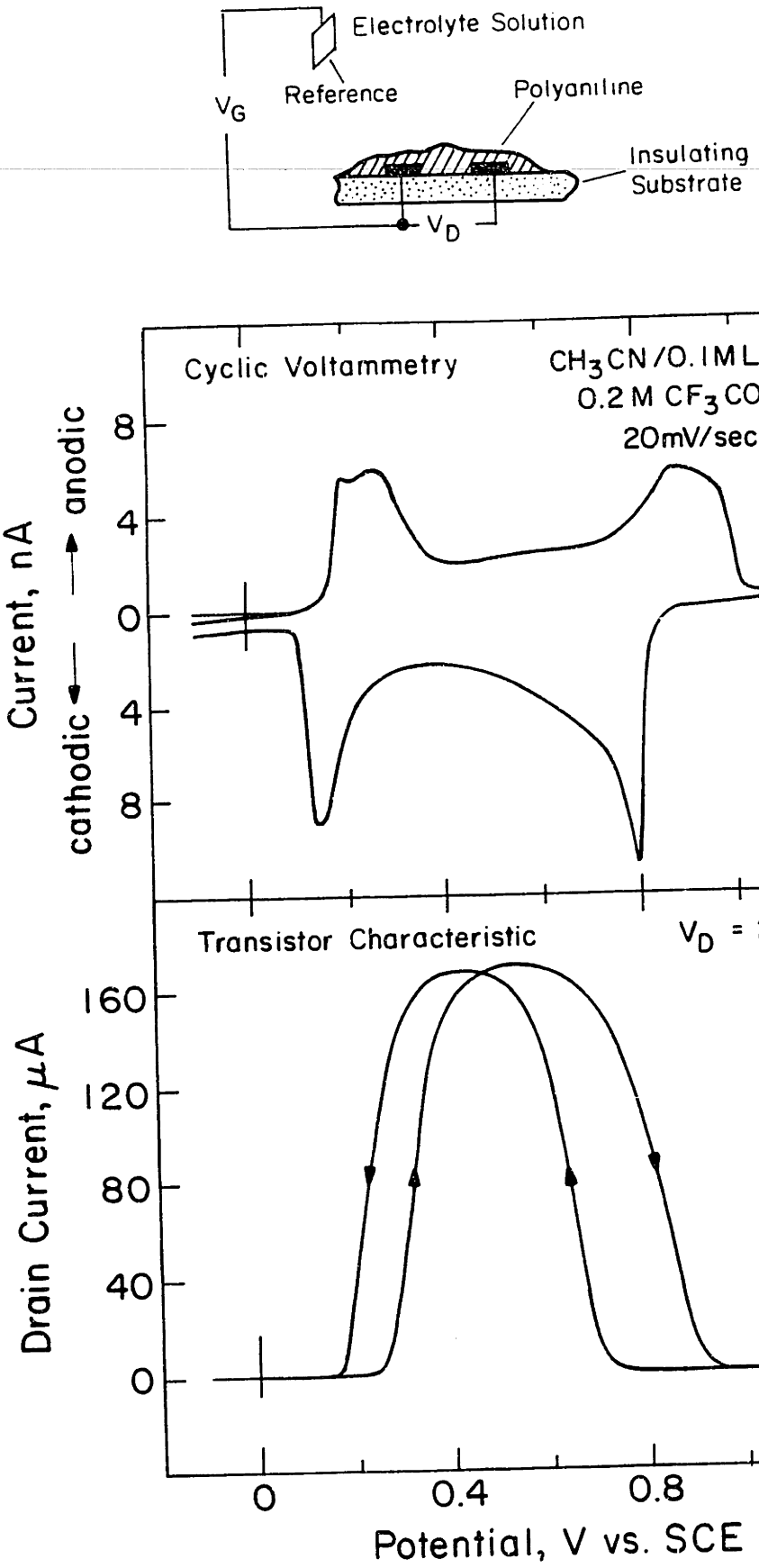
Electrolyte Solution
Reference
V_G
Polyaniline
Insulating Substrate
V_D
Cyclic Voltammetry
CH_3CN/0.1M $LiClO_4$
0.2 M CF_3CO_2H
20mV/sec
Current, nA
anodic
cathodic
8
4
0
4
8
Transistor Characteristic
V_D = 25 mV
Drain Current, μA
160
120
80
40
0
0
0.4
0.8
1.2
Potential, V vs. SCE

polymerize readily but must polymerize with good control such that a film is obtained only on the intended electrodes of the array. If the polymer (which deposits in the oxidized and conducting state) contacts adjacent electrodes during deposition thereby bringing them under potential control, polymer growth will jump from one electrode to the next. Not only did 3-phenylthiophene tend to deposit over the entire array, but it also deposited poorly in the gap between a pair of driven electrodes. Apparently, a monomer depletion zone is created in the immediate vicinity of the microelectrodes at which 3-phenylthiophene oxidation is taking place, such that the quantity of polymer deposited into the gap between the electrodes was insufficient to produce an electrical connection. Instead, adjacent gaps between electrodes which were not under active potential control became connected by poly(3-phenylthiophene). This behavior was reproducible. Examination of over 20 devices by optical microscopy made it clear that 3-phenylthiophene oligomers could diffuse a comparatively long distance in CH_3CN before precipitating from solution. Often, a gradient of red film could be seen which was centered on the electrodes driven during polymerization and extended well beyond the array. Since the source of the deposition behavior appeared to be that 3-phenylthiophene oligomers are too soluble in CH_3CN, deposition from CH_2Cl_2 was examined. It was expected that the polycationic oligomers formed in the polymerization reaction would be less soluble in CH_2Cl_2 and give better confinement of the polymer film to the electrodes at which monomer oxidation was occurring. When polymerized from CH_2Cl_2 3-phenylthiophene yielded a film of granular appearance which remained tightly confined to the electrodes at which it was oxidized. Optimal deposition was obtained by polymerization from a 100 mM solution of 3-phenylthiophene in 4:1 CH_2Cl_2:CH_3CN and these conditions were employed for preparation of push-pull amplifier devices. For a more detailed discussion of electrochemical polymerization, see Chapter 5.

The problem of passivation of electrodes during deposition of the first of the two polymers was solved by introduction of a cleaning step following preparation of the first

Scheme III

Electrochemical Procedure for the Deposition of Two Different Transistors on One Array

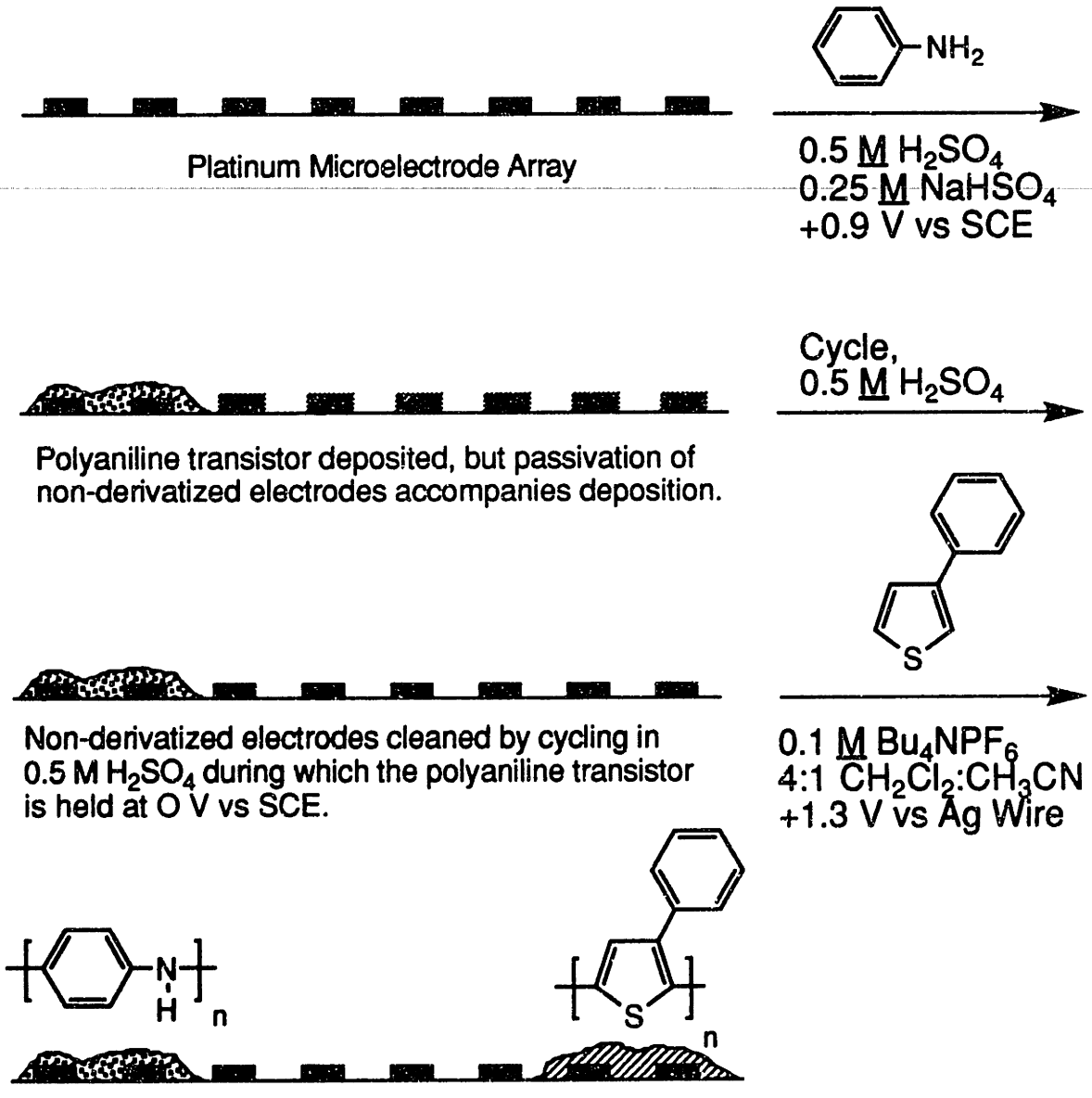

Com leted two-transistor array

transistor in which the remaining non-derivatized electrodes were cycled in 0.5 M H_2SO_4 until a sharp H_2 evolution spike appeared and hydride waves were visible in the cyclic voltammogram, i.e. the cleaning procedure for microelectrode arrays described in the general experimental section of Chapter 2. Following this cleaning step, the second polymer was deposited. This procedure allowed deposition of polyaniline and poly(3-phenylthiophene), in either order, onto microelectrode arrays. Scheme III shows the fabrication steps for a polyaniline/poly(3-phenylthiophene) device and Figure 5 shows a color micrograph of a working microelectrochemical push-pull amplifier chip prepared according to the procedure.

The I_D-V_G characteristics for the two transistors in a working microelectrochemical push-pull amplifier are shown in Figure 6. To characterize amplifier operation, the microelectrochemical push-pull amplifier was provided with a triangular wave as an input signal, and a 4.7 KΩ resistor as a load. A triangular wave was used as a diagnostic because it has sharp peaks, useful for judging onset of sluggish amplifier response, and linear ramps in between which allow detection of distortion by inspection more readily than would be the case with a sine wave. This system responds to an input signal, added to V_{rest}, in the same manner as the conventional push-pull amplifier in Figure 3 but with an important difference: there is no crossover distortion since the overlap of the I_D-V_G characteristics of the two transistors is chosen such that at V_{rest} both transistors are in partial conduction, and no dead zone intervenes where the transition between conduction by one transistor to conduction by the other occurs. Figure 7 shows the response of the polyaniline/ poly(3-phenylthiophene) push-pull amplifier, driven by a triangular wave, demonstrating clean zero-crossing of the output. The poly(3-phenylthiophene) transistor, operating on the side of its I_D-V_G negative of peak drain current, drives the load during positive excursions of the output while negative output current corresponds to conduction by the polyaniline transistor, operating on the side of its I_D-V_G positive of peak drain current. Interestingly, despite the unusual hysteresis in the I_D-V_G characteristics for the

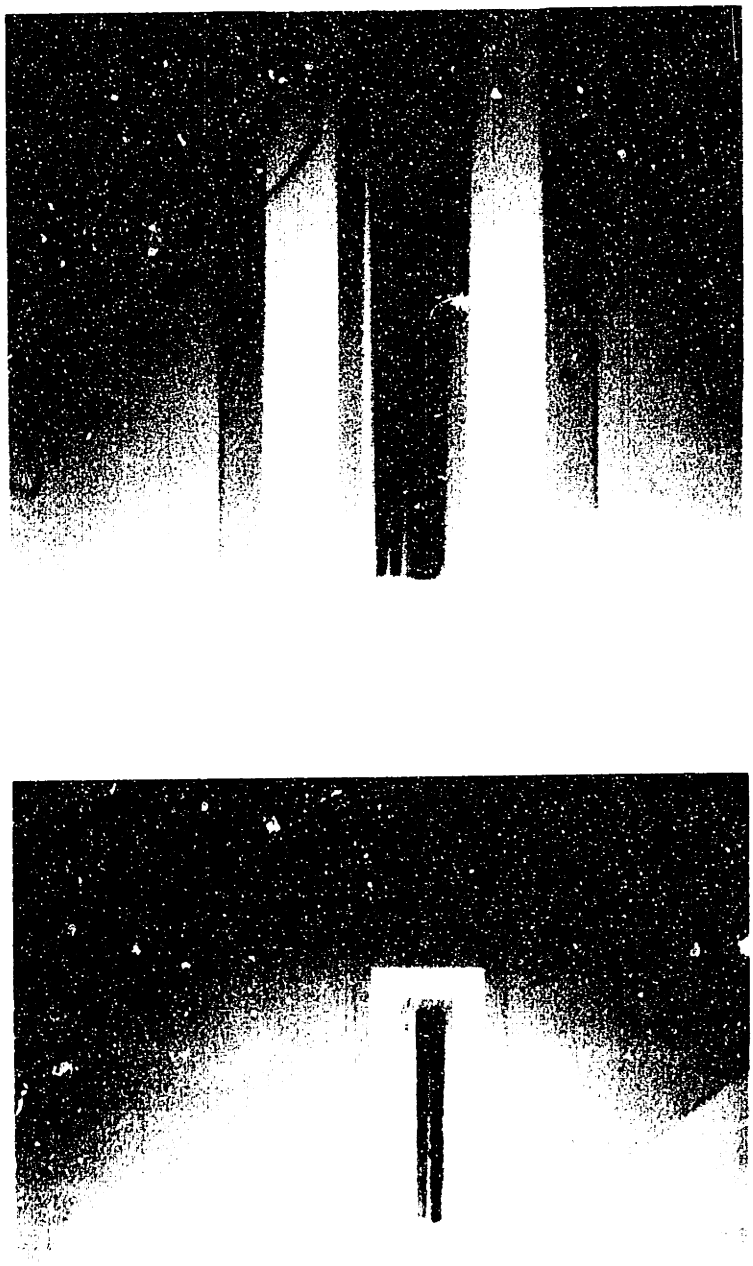

Figure 5. Micrograph of a push-pull amplifier device based on polyaniline (blue polymer) and poly[3-phenylthiophene] (red polymer).

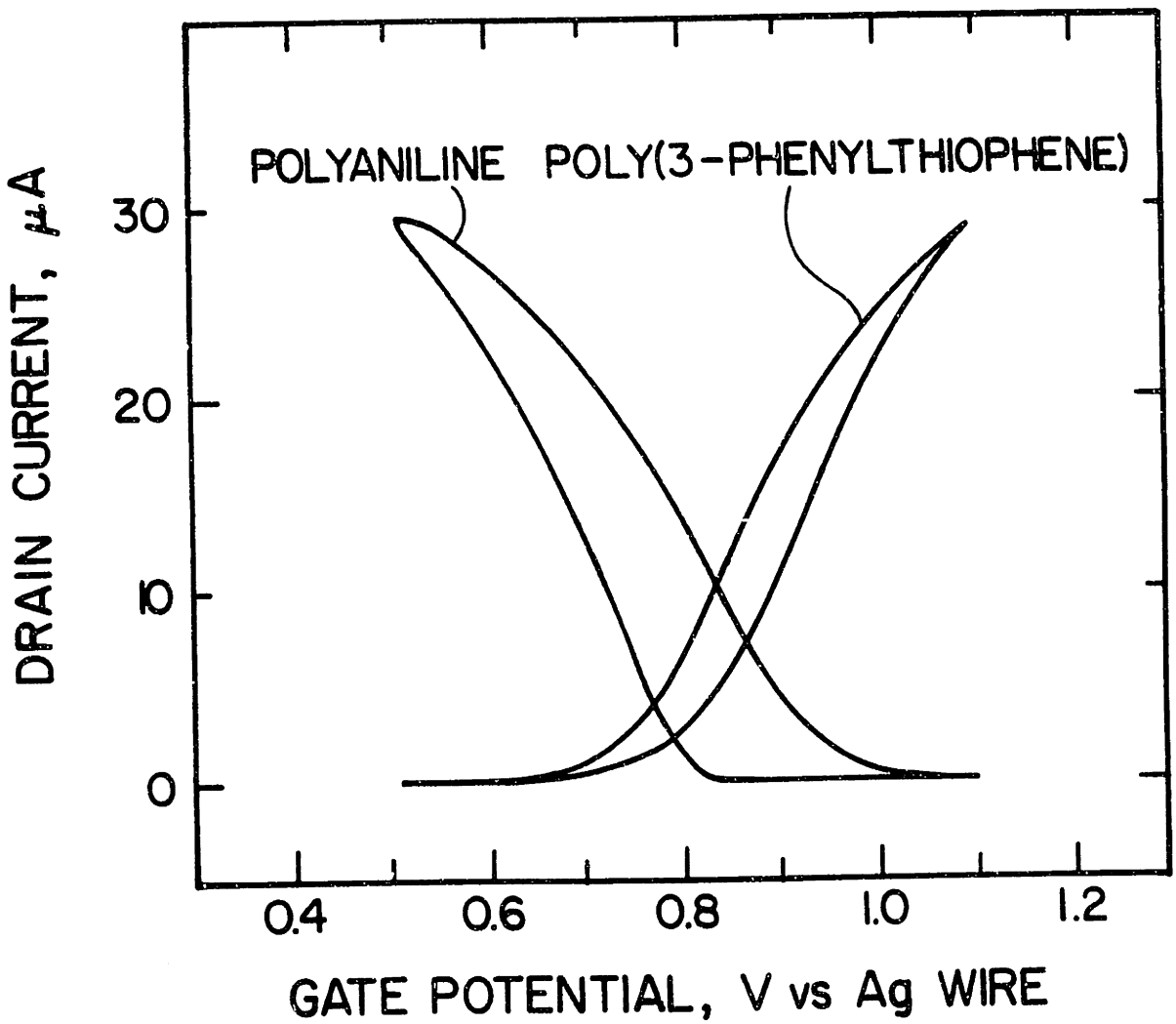

Figure 6. I_D-V_G characteristics of polyaniline(V_D=50mV) and poly[3-phenylthiophene](V_D=35mV) in the window of push-pull operation. The transistors were fabricated on a single microelectrode array and characterized in 0.1M $LiClO_4$/0.4M F_3CCO_2H/CH_3CN.

Figure 7. Output waveform for a polyaniline/poly(3-phenylthiophene) push-pull amplifier driven by a triangular wave, illustrating the clean zero-crossing of the device. V^+ = 150 mV, V^- = 25 mV, V_{rest} set for zero output current at zero input voltage, operated in 0.1 M $LiClO_4$/ 0.4 M F_3CCO_2H/CH_3CN).

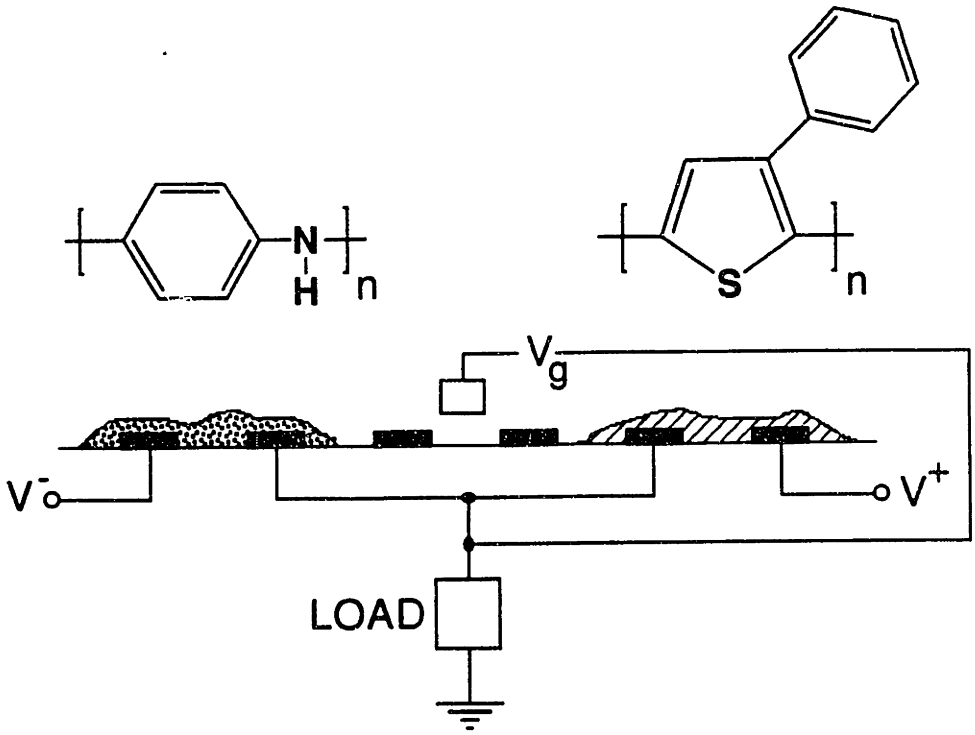
N
H
n
S
n
V_g
V^-
V^+
LOAD

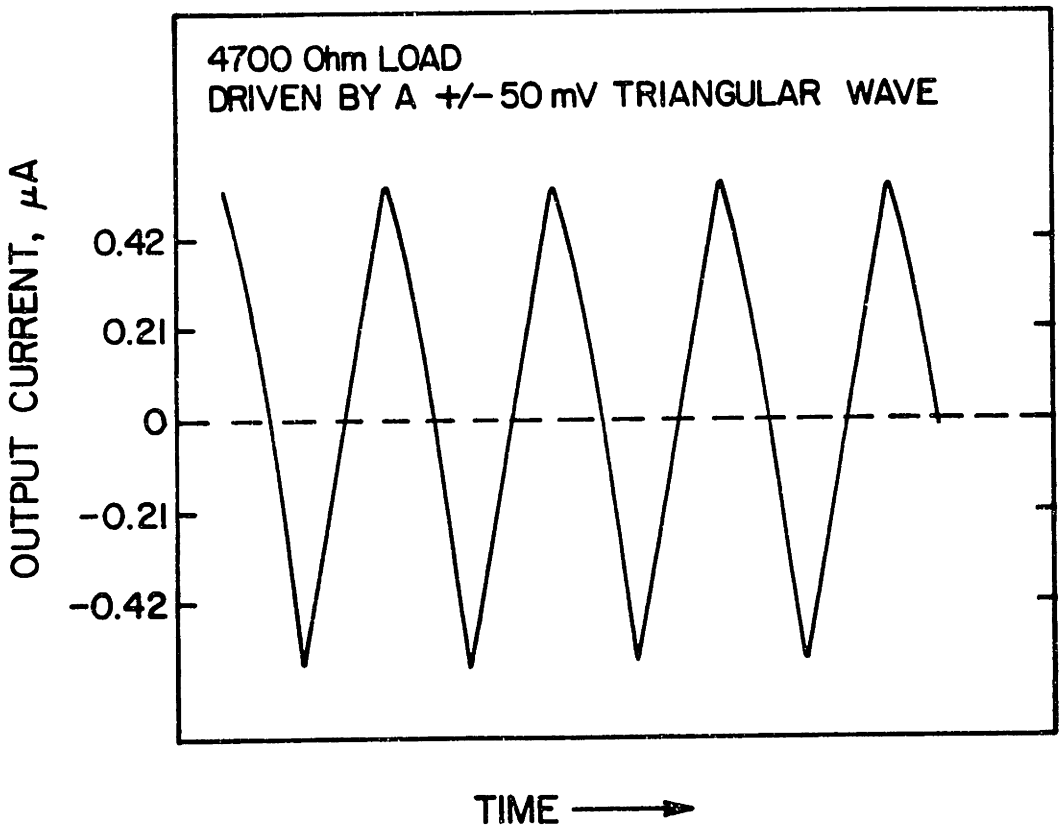
4700 Ohm LOAD
DRIVEN BY A +/- 50 mV TRIANGULAR WAVE
OUTPUT CURRENT, μA
0.42
0.21
0
-0.21
-0.42
TIME

transistors, the push-pull amplifier shows fidelity amplification of the triangular wave driving it. There is a noticeable "bowing" of the output waveform, but it is surprisingly small. Note, however, that ΔV_G is only 100mV and hysteresis in polymer response declines as ΔV_G is reduced. Moreover, the hysteresis effects in the two I_D-V_G characteristics actually *oppose* each other, which reduces distortion arising from hysteresis (see Figure 6).

The significant finding in the demonstration of the microelectrochemical push-pull amplifier is that it utilizes two different polymers with different potential windows of conductivity, selected such that the pair of transistors comprises an amplifier inherently free of crossover distortion. The polyaniline device functions in a unique transistor role where it is always operating in the range of gate potential beyond peak conductivity. The manner in which the two microelectrochemical transistors complement each other electrically is established by the choice of polyaniline and poly(3-phenylthiophene) as the device-active materials because of the overlap of I_D-V_G characteristics those polymers provide. The finite window of high conductivity is an unusual an interesting dimension of microelectrochemical transistors which expands the contribution that a single device makes to achieving overall circuit electrical function.

II. A Complementary Microelectrochemical Transistor Inverter Gate

The two transistors in a push-pull amplifier are often referred to as a complementary pair. In both solid state and microelectrochemical push-pull amplifiers the two transistors "complement" each other in their respective responses. A closely related role for such a complementary pair is seen in logic gates. MOSFETs see extensive use in modern digital logic in the CMOS (complementary metal-oxide semiconductor) family of logic gates. MOSFETs were introduced in Chapter 1, and logic gates in Chapter 3, both topics being of relevance to the results presented here. The operation of a CMOS inverter gate suggested the interesting possibility of implementation with microelectrochemical transistors. The

schematic of a CMOS inverter is shown in Scheme IV and it operates as follows. For an explanation of logic levels see the introduction to Chapter 3.

If the source and gate of a MOSFET are at the same potential, the transistor is off and passes no drain current. A *p*-channel MOSFET conducts when the gate is negative of the source, while an *n*-channel MOSFET conducts when the gate is positive of the source. When V_{in} is LOW (grounded), the gate of the *n*-channel device is at the same potential as the source, so the *n*-channel device is off while the source of the *p*-channel device is V_{DD} volts positive of the gate. Thus, the gate is negative of the source and the *p*-channel device turns on, connecting the V_{out} terminal to V_{DD} and the output is HIGH. Thus, inversion has taken place: LOW in, HIGH out. When V_{in} is HIGH (V_{DD} volts with respect to

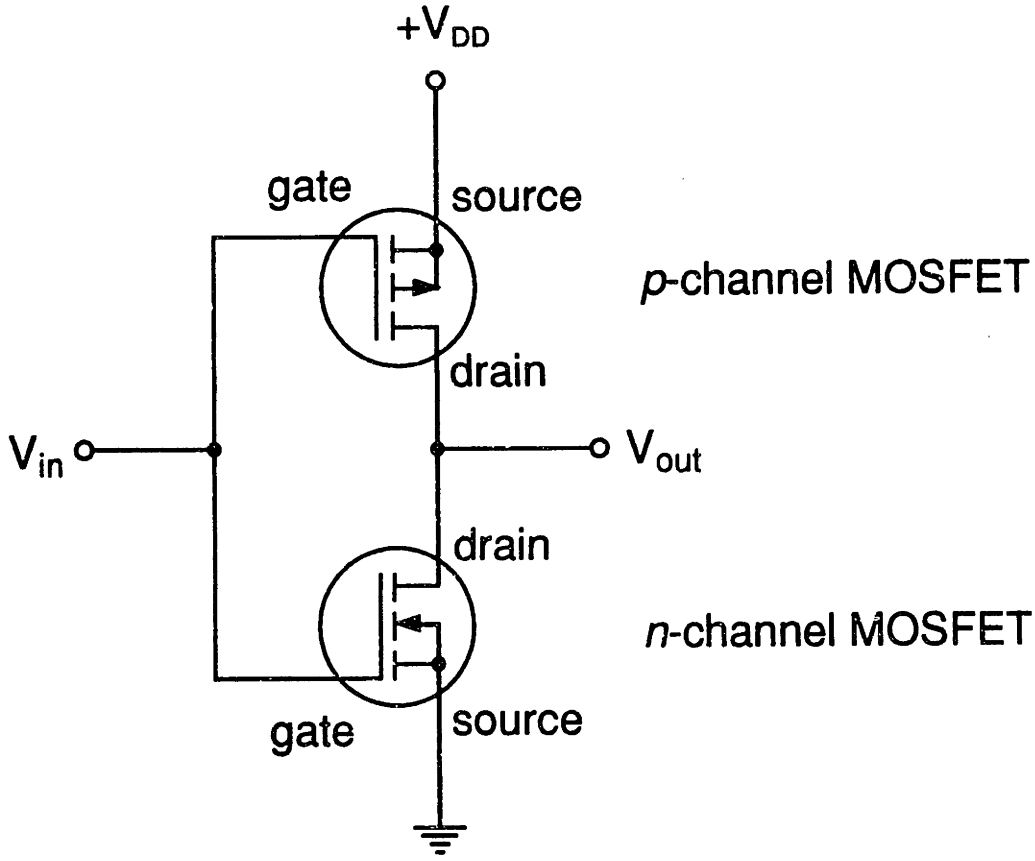

Scheme IV. Schematic of a CMOS inverter gate.

ground) then the source and gate of the *p*-channel device are both at V_{DD} so the *p*-channel device is off, while the gate of the *n*-channel device is positive of the grounded source electrode and the *n*-channel device conducts, grounding the V_{out} terminal so that the output is LOW. Again, inversion has occurred: HIGH in, LOW out. Only one transistor conducts at a time, so the only path from the power supply to ground is through a load connected to V_{out}. As such, CMOS logic gates draw less current than logic gates of the type described in Chapter 3, which have a steady-state flow of current in the HIGH output state even if no load is connected.

In most of the work on microelectrochemical transistors, the devices are operated using electrochemical instrumentation to control gate voltage. It was undertaken to create a design in which an electronic function beyond simple transistor action was accomplished with microelectrochemical transistors without the use of such instrumentation. Several results from Chapter 2 are particularly important to the design and preparation of a microelectrochemical complementary inverter gate. Recall that large drain voltages perturb and complicate potential control of the oxidation state of the device-active material because the circuit power supply can also drive oxidation and reduction processes. It becomes complex and completely unrealistic to isolate each transistor in a multi-transistor circuit by providing it with independent gate voltage control and its own power supply. Further, connections between transistors which are part of the overall circuit will inevitable cause unwanted electrochemical events. This all arises from subtle difference of microelectrochemical transistors from solid state devices that V_G and V_D are applied separately and not with respect to a common ground. There are two solutions. The obvious one is keep V_D small and avoid the whole situation. This is only a partial solution and a logic gate is of little value if it cannot drive another like itself, therefore an output voltage which can fully switch another logic gate on and off must be produced and large circuit power supply voltages are unavoidable. The second solution is to find a design in which a circuit functions with conventional ground-referenced inputs and outputs. Scheme

V presents a such a design in which the large power supply voltage is *intentionally utilized to switch the transistors* and in which no potentiostat is used to set gate potentials. The circuit is a direct parallel to the CMOS inverter shown in Scheme IV in configuration and function. This is a significant accomplishment because the input and output of the complementary microelectrochemical transistor (CMET) inverter are ground-referenced allowing it to be used as a building block for more complex circuits without any need to consider complicated problems of unwanted gate current paths or perturbation of potential control.

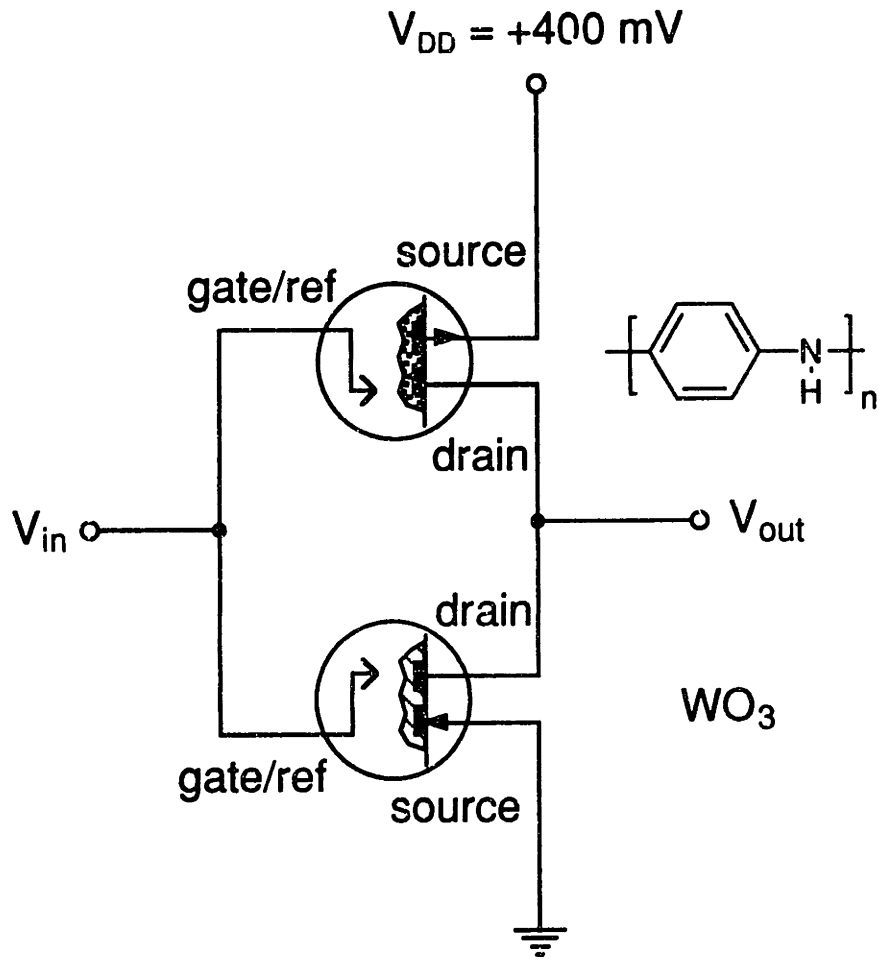

Scheme V. A complementary inverter gate based on microelectrochemical transistors.

The CMET inverter in Scheme V is based on polyaniline, a *p*-type conductor, and tungsten trioxide, an *n*-type redox conductor which displays conductivity when reduced.[21]

Both transistors use a saturated calomel electrode (SCE) as a combined reference and counter electrode, referred to in the CMET inverter as the gate/reference electrode. As described in Chapter 2, it was found that an MET will support drain current as long as the electrochemical potential of at least one of its microelectrodes is within the bounds of the finite window of conductivity for the active material of the device. The I_D-V_G characteristics of polyaniline and WO_3 are shown in Figure 8. The CMET inverter operates in the following manner. Because there are two independent devices with two independent SCE reference electrodes, potentials will be specified with respect to circuit ground to avoid confusion. Several conditions always apply: the source of the WO_3 device is grounded and therefore is always at 0 V vs. ground; the source of the polyaniline device is connected to V_{DD} so it is always 400 mV positive of ground; the input and output voltages are applied and measured vs. ground; the V_{in} terminal and both SCE gate/reference electrodes are

Scheme VI

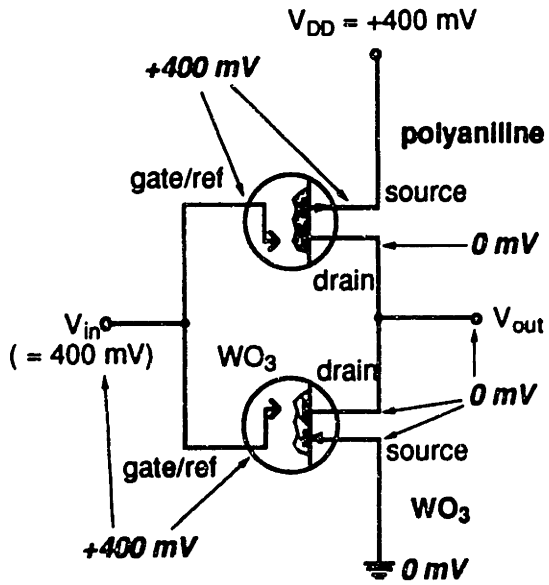

a) HIGH input voltage, source of WO_3 device 400 mV negative of SCE, WO_3 conducts. Source of polyaniline device at 0 vs SCE, polyaniline insulating, Output grounded through WO_3 device, V_{out} is 0 (LOW).

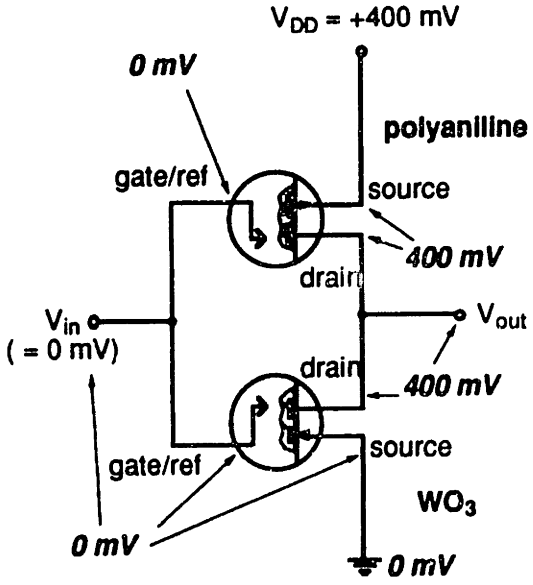

b)LOW input voltage, source of polyaniline device 400 mV postive of SCE, polyaniline conducts. Source of WO_3 device at 0 vs SCE, WO_3 insulating. Output connected to V_{DD} through polyaniline device, V_{out} is 400 mV (HIGH).

Figure 8. (top) I_D-V_G characteristics for polyaniline and WO_3 in 0.5 M H_2SO_4. (bottom) Input and output waveforms for a polyaniline/WO_3-based complementary microelectrochemical transistor inverter. The input voltage was switched manually. The microfabricated WO_3 transistor showed some background conduction not associated with WO_3 electrochemistry, resulting in the positive offset of the I_D-V_G characteristic and loading of the inverter in the HIGH output state. As a result, the inverter output was 320 mV in the HIGH state instead of the full 400 mV value of V_{DD}.

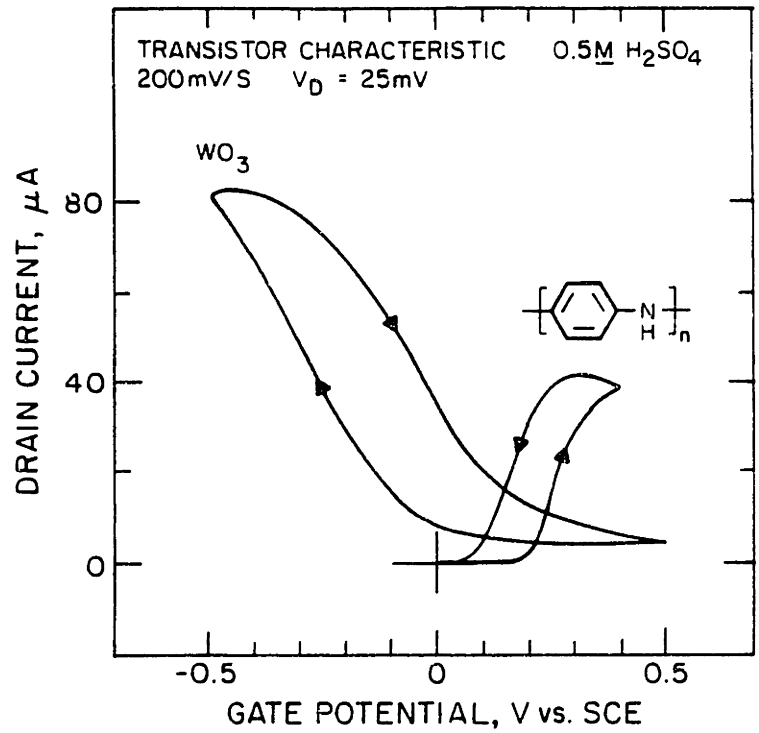
TRANSISTOR CHARACTERISTIC 0.5M H_2SO_4
200mV/S V_D = 25mV
WO_3
DRAIN CURRENT, μA
80
40
0
-0.5
0
0.5
GATE POTENTIAL, V vs. SCE
N
H
n

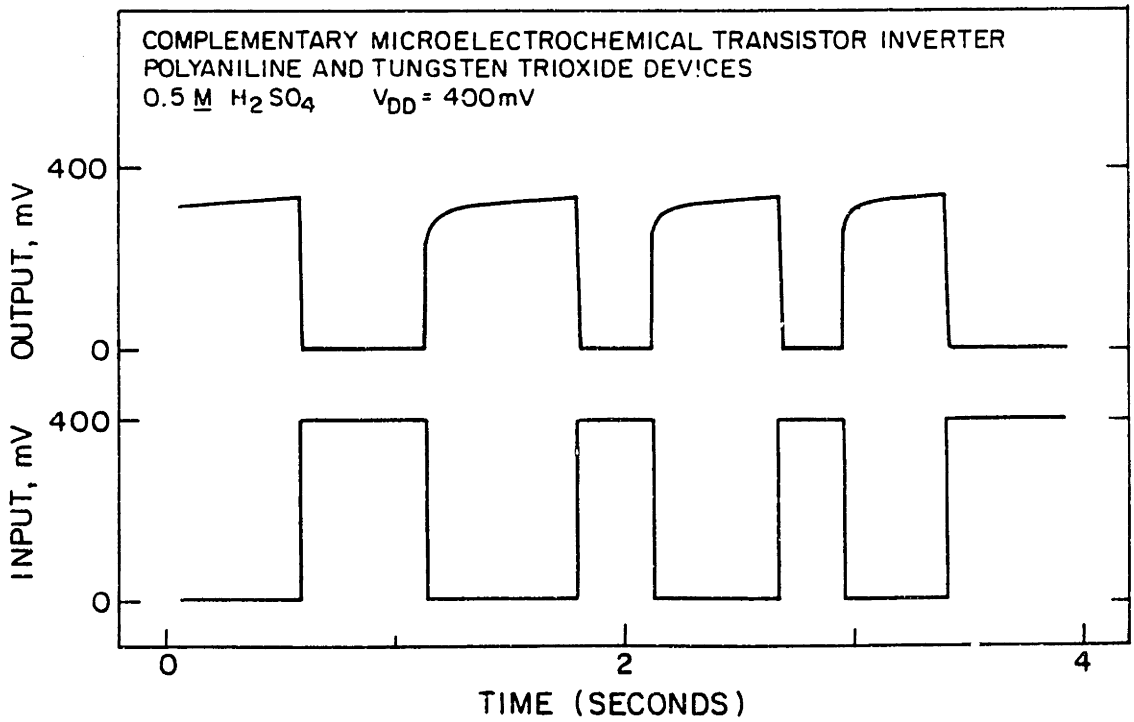
COMPLEMENTARY MICROELECTROCHEMICAL TRANSISTOR INVERTER
POLYANILINE AND TUNGSTEN TRIOXIDE DEVICES
0.5 M H_2SO_4 V_{DD} = 400mV
OUTPUT, mV
400
0
INPUT, mV
400
0
0
2
4
TIME (SECONDS)

connected together and must therefore be at the same potential; similarly, the V_{out} terminal and both drain electrodes are connected together and must be at the same potential.

When V_{in} is set to zero(ground), Scheme VIa, the source of the polyaniline transistor is held 400 mV positive of the SCE gate/reference electrode by power supply voltage V_{DD}. At 400 mV positive of SCE, polyaniline is conducting so the polyaniline transistor turns on, connecting the output to V_{DD}, so V_{out} is HIGH. Under this condition, the drain of the WO_3 device is 400 mV positive of the SCE gate/reference electrode of the WO_3 device, while the source is grounded, so both the source and the gate/reference are at the same potential with respect to ground. Therefore, the source of the WO_3 device is at 0 V vs. the SCE gate/reference of the WO_3 device while the drain is at +400 mV vs. SCE. WO_3 is insulating at both these potentials so the WO_3 device is off. Inversion thus occurs: input LOW (ground), output HIGH (V_{DD}).

If V_{in} is set HIGH (V_{DD}, +400 mV), Scheme VIb, then the gate/reference electrode of the WO_3 device is held 400 mV positive of the source of the WO_3 device. At -400 mV vs SCE WO_3 is conducting and the WO_3 device turns on, connecting the output terminal to ground. The source of the polyaniline transistor is at 400 mV vs. ground as is the SCE gate electrode so the electrochemical potential of the source electrode is 0 V vs SCE while the drain electrode is 400 mV negative of SCE. Polyaniline is not conducting at either of those potentials so the polyaniline transistor is off. Note what occurs in each case, the electrochemical potential of the source electrodes of the transistors are swung positive or negative of SCE by V_{DD} volts. As such, V_{DD} must be chosen according to the I_D-V_G characteristics of the two active materials. It can be seen in Figure 8 that 400 mV positive of SCE is well into the conducting range of polyaniline and 400 mV negative of SCE is well into the conducting range of WO_3 and therefore 400 mV is a reasonable value for V_{DD}.

Input and output waveforms for operation of the CMET inverter is shown in the lower half of Figure 8. The input terminal was switched manually between ground and

V_{DD}. The output waveform shows inversion of the input demonstrating inverter function. The WO_3 device used for in these experiments was prepared completely by microfabrication with a final step of photolithography and electron-beam deposition of WO_3 in a process developed and executed by Martin Schloh.[22] The particular devices used were the remnants of a years old batch and showed some background conductivity, as can be seen in the positive offset of the WO_3 I_D-V_G in Figure 8. Since the background conduction prevented the WO_3 transistor from achieving full insulation, the CMET inverter output does not fully achieve V_{DD} as its HIGH output state. However, the drain current capability of the polyaniline transistor is sufficiently to mostly overcome this limitation.

While polyaniline and WO_3 are a well-suited complementary pair because they both operate with excellent stability and performance in aqueous acid, the use of the *n*-type molecular conductor is an option, not a requirement. By utilizing the finite window high conductivity and operating one transistor of on the negative transconductance side of its I_D-V_G characteristic, two *p*-type conducting polymers can provide the pair of transistors needed for a CMET inverter. The approach is a minor modification to the push-pull amplifier developed above. In the push-pull amplifier, a partial overlap of I_D-V_G characteristics is optimal. The degree of overlap most appropriate for a CMET device is complete separation of the windows of conduction which polyaniline and WO_3 did not provide. Polyaniline, paired with a derivative of polythiophene of more positive onset of conduction than poly(3-phenylthiophene) would be suitable for this finite windows-based approach to a CMET inverter. The synthesis and characterization of suitable polymers is reported in Chapter 5 and Chapter 6.

The complementary microelectrochemical transistor inverter is significant in that it requires no special allowances for the electrochemical gating process by which the transistors operate in its incorporation in larger circuits. Operating speed remains a significant limitation as with other microelectrochemical devices. However, the CMET inverter demonstrates microelectrochemical transistors functioning in a true 3-terminal

arrangement, without the use of electrochemical instrumentation, and in an important class of digital logic.

III. Transistor Devices with Complex Drain Current-Gate Voltage Characteristics

Part of the versatility of the finite window of conductivity is that different polymers conduct over different ranges of electrochemical potential as demonstrated by the polyaniline/poly(3-phenylthiophene) push-pull amplifier. Given the large number of different I_D-V_G characteristics available from the many different families of conducting polymers, many different combinations of windows of conductivity which overlap to varying degrees can be envisioned. A single I_D-V_G characteristic represents a smooth transition from onset of conduction, to a maximum in drain current, to onset of oxidative insulation. However, by combining two or more I_D-V_G characteristics, a wide range of more complex device behaviors could be created. Such a device can be realized by using two or more different polymers as source-drain conduction channels connected in parallel. One specific area where a device of fundamentally altered I_D-V_G behavior is potentially significant is that of multiple-valued logic, which refers to logic systems with more than two states.[23,24] Ternary (3-state) logic is an example. A ternary device operates at three logic levels (voltages) to represent the digits 0, 1, and 2.[25]

Conventional transistors are intrinsically suited to functioning as on-off switches. It is for this reason that electronic logic evolved in binary and not, say, decimal in which we normally think, work, and carry out math. That is not to say that higher order electronic logic is not possible. Indeed, the greater information density of operating in multiple state logic makes it potentially attractive.[25] A single binary digit specifies one of two possibilities while a single decimal digit specifies one of ten. However, trying to implement ten-level logic is considerable more challenging than implementing binary logic,

which comes back to the fundamentally two-state nature of a conventional transistor. The issue is described by Vranesic and Smith in the following way.[26]

> It is unquestionable clear that the greatest hindrance to multi-valued systems design is the lack of a trivially simple physical element, which would naturally exhibit *R* stable states where *R* is considerable greater than 2. The discovery of such an element would probably help resolve most of the present difficulties in practical applications.[26]

Approaches to ternary logic based on conventional transistors become rather complex because they are limited by the two-state nature of standard transistors.[23,24,26] Circuit complexity increases further for higher order logic, as might be expected. This has led, in part, to research in devices which are better suited to multi-state operation.[23] It was undertaken here to prepare a microelectrochemical transistor device which was intrinsically suited to multi-state logic with the specific goal of introducing a plateau or well in the I_D-V_G response of a device at a point intermediate between onset of conduction and peak conductivity to provide a third, stable state. A concise, direct route to such a device is provided by the finite window of high conductivity displayed by conjugated polymers.

The approach to a transistor device which has been intentionally altered to display an I_D-V_G characteristic designed for ternary logic is shown in Scheme VII. The device derives its overall I_D-V_G characteristics from two contributing polymers of different potentials for onset of conduction and different peak conductivities. The overall I_D-V_G characteristic is a function of the extent of overlap and relative conductivity of the two contributing I_D-V_G components from Polymer X and Polymer Y. Thus, by selecting the appropriate conducting polymers, a device of the desired characteristics can be prepared by derivatizing a microelectrode array as shown in Scheme VII and connecting the two pairs of polymer-modified electrodes in parallel so that device drain current is the sum of drain current due to Polymer X and Polymer Y.

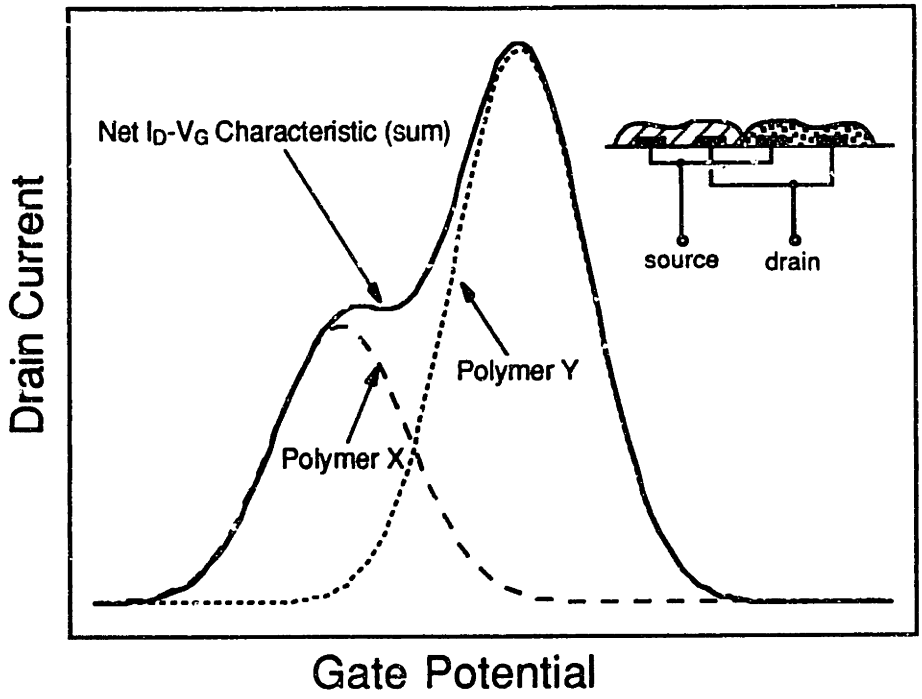

Scheme VII. A transistor based on two contributing I_D-V_G characteristics, simulated using equation (1) as described below.

In order to characterize the full range of possible I_D-V_G characteristics accessible by the approach shown in Scheme VII, an experiment was designed in which a pair of polyaniline transistors provided two I_D-V_G characteristics which could be offset from each other and thus combined with an arbitrary degree of separation. This was chosen as the initial investigation of complex I_D-V_G devices because of the time-consuming nature of the alternative, preparing a large number of individual devices bearing different combinations of polymers. The experimental configuration shown in Scheme VIII operates two microelectrochemical transistors in separate cells under independent potential control. The source and drain electrodes of each device are connected in parallel such that observed drain current is the net drain current through both transistors. A drain voltage is applied, which can be conveniently provided by a third potentiostat operated as a power supply by connecting its counter and reference electrode terminals together. Gate voltage is provided

by the sweep generator of the third potentiostat which drives potentiostat 1 and potentiostat 2 via their external signal inputs. In this particular experimental context, gate voltage V_G is taken to mean applied gate voltage from potentiostat 3, as shown in Scheme VIII. The reference electrode for each cell is an SCE. An offset voltage can be introduced by either potentiostat 1 or potentiostat 2, or both, such that device 1 is held at (V_G + offset 1) and device 2 at (V_G + offset 2). From the perspective of potentiostat 3 which scans the net I_D-V_G characteristic, device 1 and device 2 display onset of conduction at the same value of V_G if no offsets are applied, but at different values of V_G if offset voltages are applied by potentiostat 1 and potentiostat 2. In this way, the degree of overlap between the apparent I_D-V_G characteristics of device 1 and device 2 can be set arbitrarily. For example, polyaniline shows onset of conduction at 180 mV vs SCE. If an offset of +100 mV is applied by potentiostat 1, then device 1 will show onset of conduction when V_G reaches 80 mV since device 1 is held 100 mV above V_G. In this way it is possible to conveniently explore the combined I_D-V_G characteristic of the two devices as a function of the separation of the two contributing I_D-V_G components. Figure 9 shows 3 of the many I_D-V_G characteristics produced by this approach. The top plot shows the result of offsetting device 1 by +200 mV resulting in a net I_D-V_G characteristic which is the sum of two polyaniline I_D-V_G characteristics shifted 200 mV apart in gate potential. The bottom of Figure 9 shows an I_D-V_G characteristics in which a deep well has been introduced, obtained by a 500 mV combined offset of the two polyaniline transistors.

In the middle section of Figure 9, the goal of deliberately introducing a plateau is realized using a 300 mV separation of the two I_D-V_G characteristics. This behavior provides a 200 mV wide range of V_G over which I_D is constant, which would allow a logic level to be assigned in the center of this range where it would have a 100 mV margin for error in either direction. Using the pair of polyaniline devices configured for I_D-V_G characteristic shown in the middle Figure 9 and a 4.7 KΩ drain resistor, ternary inverter

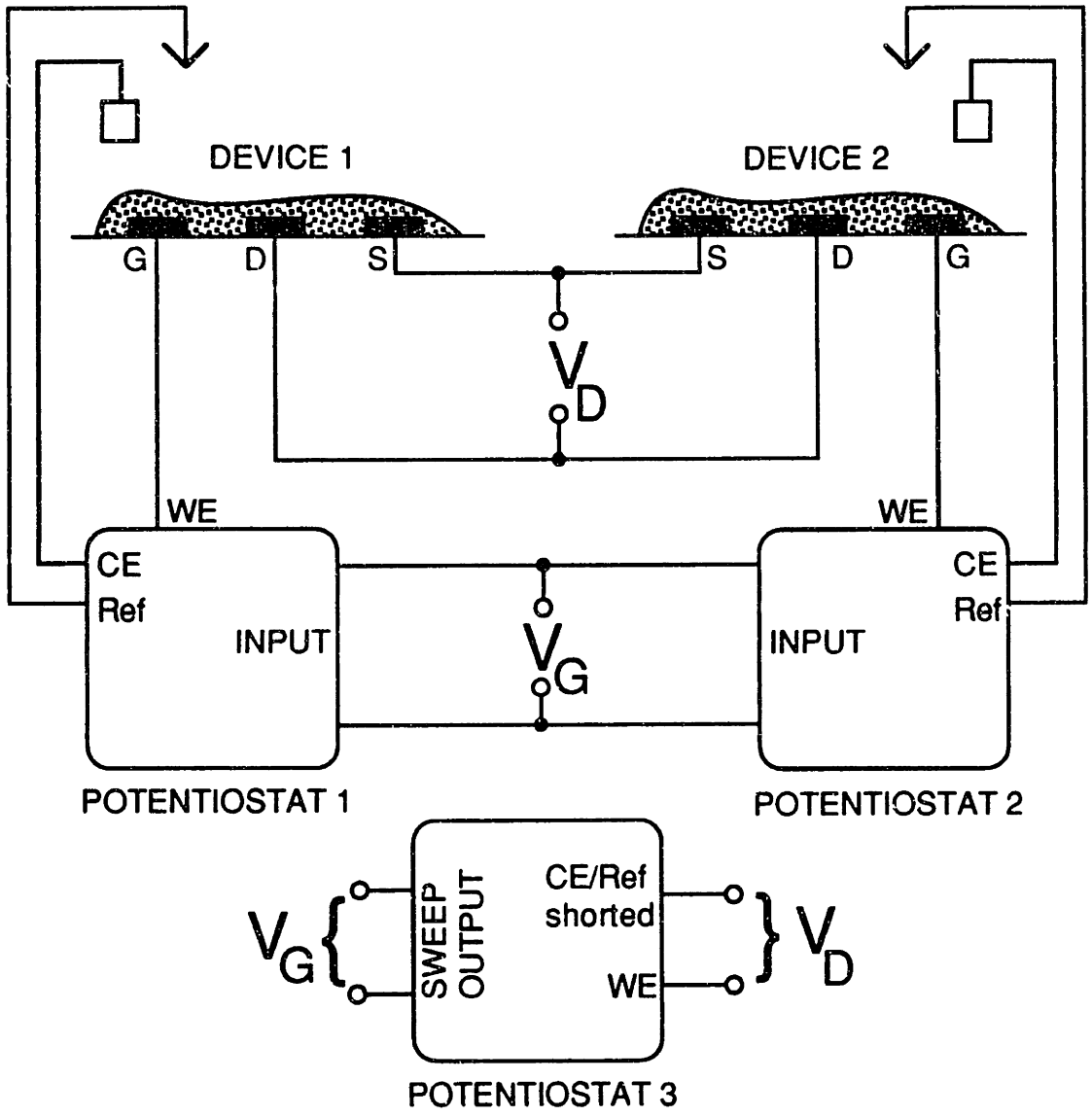

Scheme VIII. Experimental configuration for two polyaniline microelectrochemical transistors operated with drain and source electrodes in parallel and separate potential control for each device. The I_D-V_G characteristics of the two devices can be offset from each other by an arbitrary potential.

Figure 9. Complex I_D-V_G characteristics generated by parallel connection of two polyaniline transistors under independent potential control, Scheme VIII, such that the I_D-V_G behavior of each individual device could be offset from the other. The middle characteristic demonstrates a transistor based on two contributing I_D-V_G characteristics configured to introduce a region of constant I_D at an intermediate value of V_G between onset of conduction and peak conductivity. The conductivity of device 1 was approximately twice that of device 2.

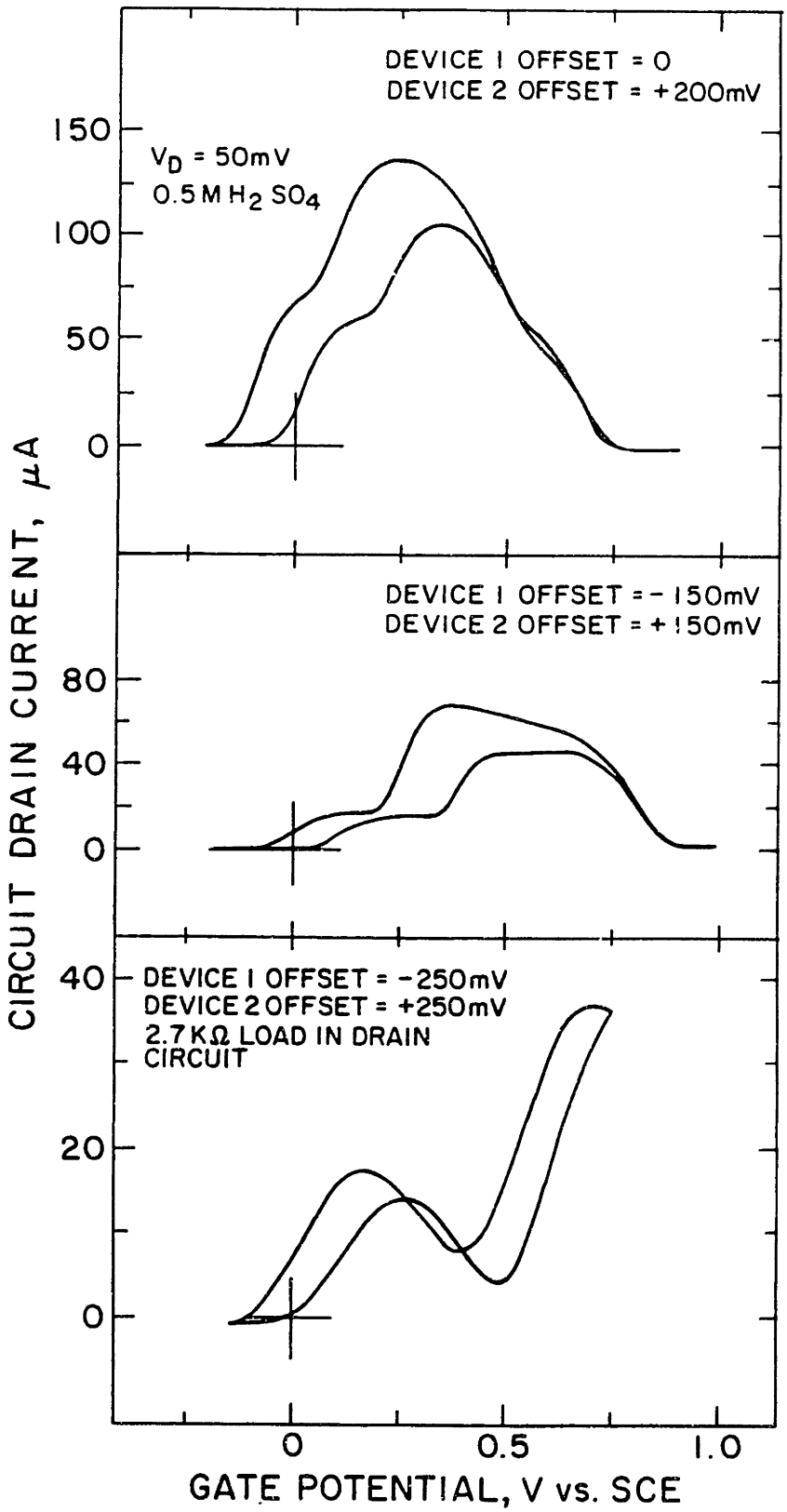
DEVICE 1 OFFSET = 0
DEVICE 2 OFFSET = +200mV
V_D = 50mV
0.5 M H_2 SO_4
150
100
50
0
DEVICE 1 OFFSET = - 150mV
DEVICE 2 OFFSET = + 150mV
80
40
0
DEVICE 1 OFFSET = -250mV
DEVICE 2 OFFSET = +250mV
2.7 KΩ LOAD IN DRAIN CIRCUIT
40
20
0
CIRCUIT DRAIN CURRENT, μA
0
0.5
1.0
GATE POTENTIAL, V vs. SCE

function was demonstrated qualitatively. Figure 10 shows a simplified schematic, a table specifying the ternary inverter logic function, and a table of the input and output voltages determined for the working circuit. The pair of polyaniline transistors are represented simply as two polymers connected in parallel. Referring to the logic levels 0, 1, and 2 as LOW, MEDIUM and HIGH, respectively, the ternary inverter function is realized in that the LOW input, HIGH output; MEDIUM input, MEDIUM output; HIGH input, LOW output required is observed, albeit qualitatively. The ternary inverter was not optimized as part of this set of experiments since the goal was to probe the scope of complex I_D-V_G behavior possible through the approach of combining two individual I_D-V_G characteristics. However, the data in Figure 10 make the required alterations clear. V_{DD} should be increased to 600 mV so that the HIGH output is the same as the 600 mV input required for

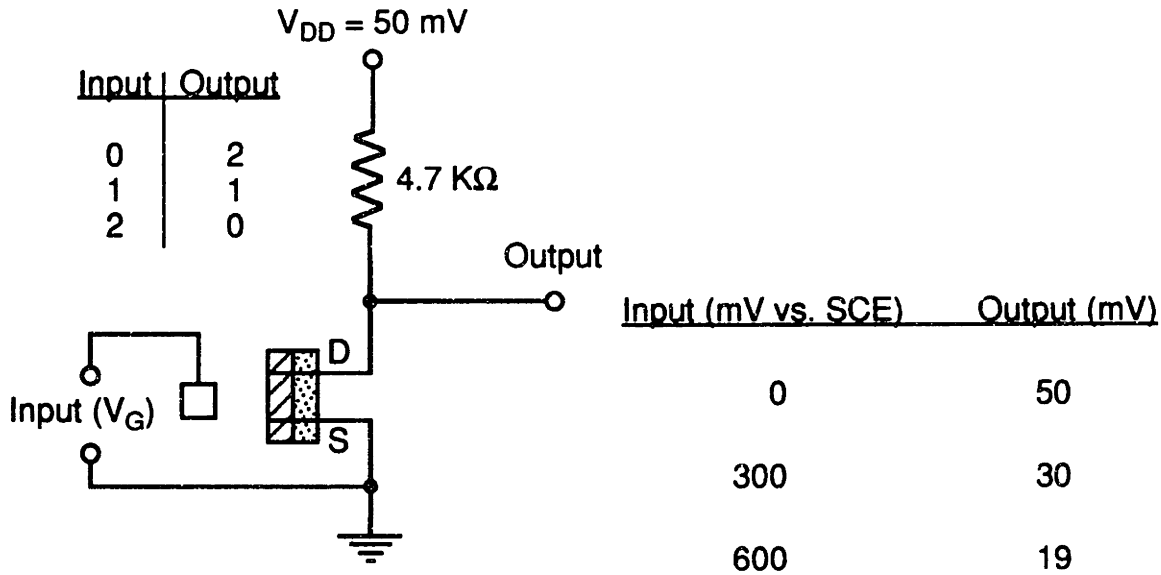

Figure 10. (left) Schematic of a ternary (3-state) microelectrochemical inverter and a table showing the relationship of input state to output state.[23] (right) Operation of the ternary inverter at V_{DD} = 50 mV. The transistor device was the pair of polyaniline transistors described above, operated to provide the I_D-V_G characteristic shown Figure 9 (middle).

maximum conduction, the plateau should correspond to a transistor drain-source resistance equal to the resistor used so that the MEDIUM output state is half of V_{DD}, i.e. 300 mV, and the drain-source resistance of the transistor in the fully conducting state should be small compared to the resistor used, so that the LOW output state is close to zero. The lack of sufficient conductivity to achieve near-zero output was a result of previous characterization of the system at extremely high offset 1 and offset 2 values, driving polyaniline to potentials where it begins to show degradation in water.

The middle I_D-V_G characteristic in Figure 9 upon which the ternary inverter is based displays the usual hysteresis. Thus, the ternary inverter should display the same excellent noise immunity as the binary inverter of Chapter 3. Significantly, the ternary inverter uses the same circuit as the binary inverter of Chapter 3. Only the transistor behavior has been changed. Thus, a ternary logic function is achieved without resorting to a more complex circuit. Indeed, if a transistor device were prepared suitable for quaternary or quinternary operation it would still require only the basic inverter circuit of Figure 10. In section 6.4, a device based on two different polymers, obtained by the selective *in situ* trifluoroacetylation of polypyrrole to alter its potential for onset of conduction, is presented which is also suitable for the ternary inverter shown in Figure 10 and does not involve the experimental set-up of Scheme VIII. While it must be noted that microelectrochemical transistors suffer the unfortunate drawback of low switching speed due to the dependence on diffusion of counterions in the electrochemical gating process, multi-state operation can be achieved with these devices in a direct manner with high flexibility in attaining specific target responses.

The experimental configuration of Scheme VIII allows many combinations of two I_D-V_G characteristics to be profiled with ease and rapidity. An approach to profiling more complex combinations of I_D-V_G characteristics, such as would be required in development of a quinternary (5-state) inverter, is to model I_D-V_G combinations mathematically. Both MOSFET I_D-V_G and bipolar junction transistor I_C-V_{BE} relationships have quantitative

models.[8a,d] If a model were available for conducting polymer I_D-V_G characteristics it would be possible to simulate complex I_D-V_G behavior of all kinds. Such an equation was developed, based on the observation that the log(I_D)-V_G relationship for a polyaniline transistor, Figure 2, closely conforms to an inverted parabola. Proceeding from this assumption, equation (1) can be derived (a full description and commentary follow the

$$I_D = I_D^{max}\, 10^{\left[\frac{\log\left[I_D(V_{onset})/\, I_D^{max}\right]}{(V_{onset} - V_{peak\ con})^2}\,(V_G - V_{peak\ con})^2\right]} \qquad (1)$$

experimental section). Specifying the appropriate parameters for polyaniline, equation (1) provides a reasonable representation of a polyaniline I_D-V_G characteristic, as seen in Figure 11.

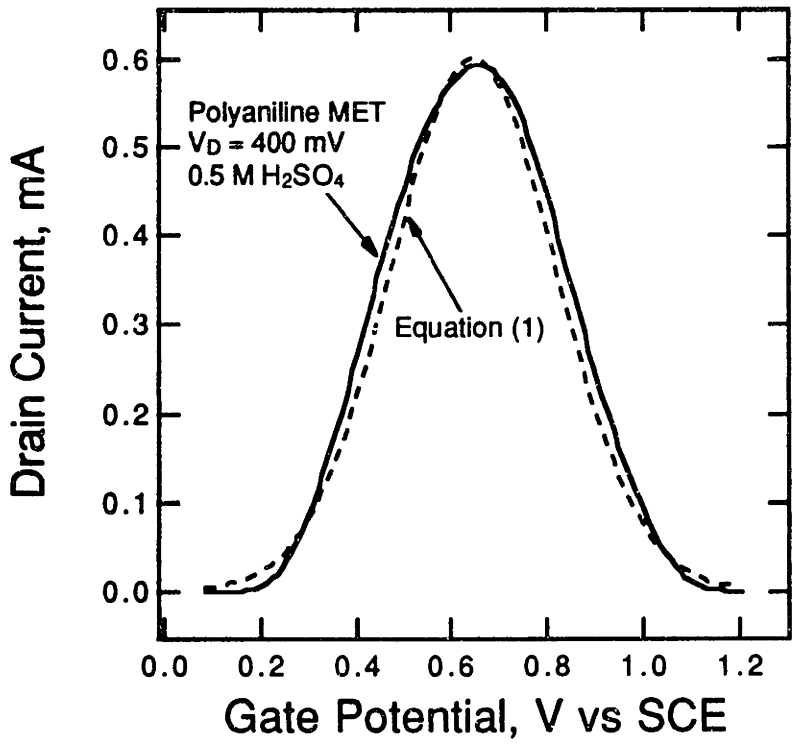

Figure 11. Experimental (solid) and modeled (dashed) I_D-V_G characteristics for a polyaniline microelectrochemical transistor.

Equation (1) can serve to represent different polymer I_D-V_G characteristics by using the appropriate values of V_{onset} and $V_{peak\ con}$ for known or hypothetical polymers, although it does not model hysteresis or allow for asymmetry about $V_{peak\ con}$. Since it provides a mathematical expression for I_D-V_G characteristics it can be used to profile possible combinations of I_D-V_G characteristics to produce devices of the type demonstrated by the results in Figure 9. Figure 12 shows a simulation using equation (1) of the forward

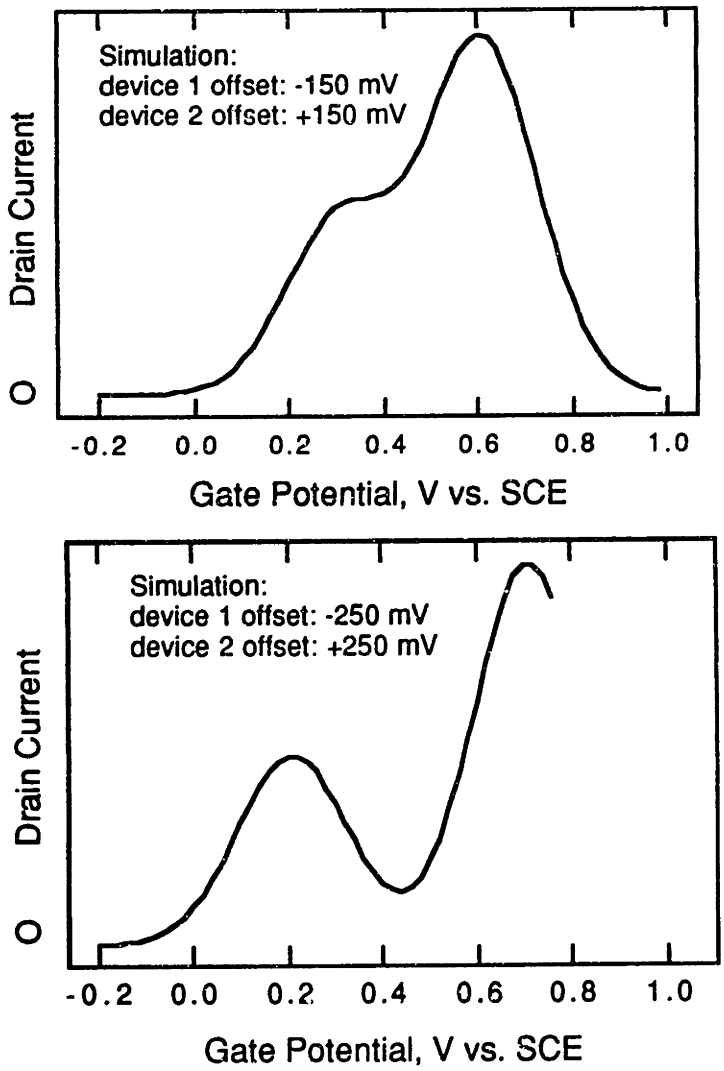

Figure 12. Simulated I_D-V_G characteristics for a device modeled after the results of Figure 9 using equation (1).

scans of I_D-V_G characteristics suitable for molecule-based ternary devices shown in Figure 9, middle and bottom.

If a device for a quinternary inverter were sought, it would be necessary to introduce 3 steps in the I_D-V_G characteristic spaced at 25, 50, and 75% of maximum drain current. Figure 13 shows a simulation of the I_D-V_G characteristic as a function of ΔV_G for a hypothetical device deriving behavior from 4 component I_D-V_G responses of relative amplitudes 0.25, 0.5, 0.75, and 1, offset from each other by 0, 33, 66, and 100%, respectively, of the offset for the component of amplitude 1. The simulation approach is

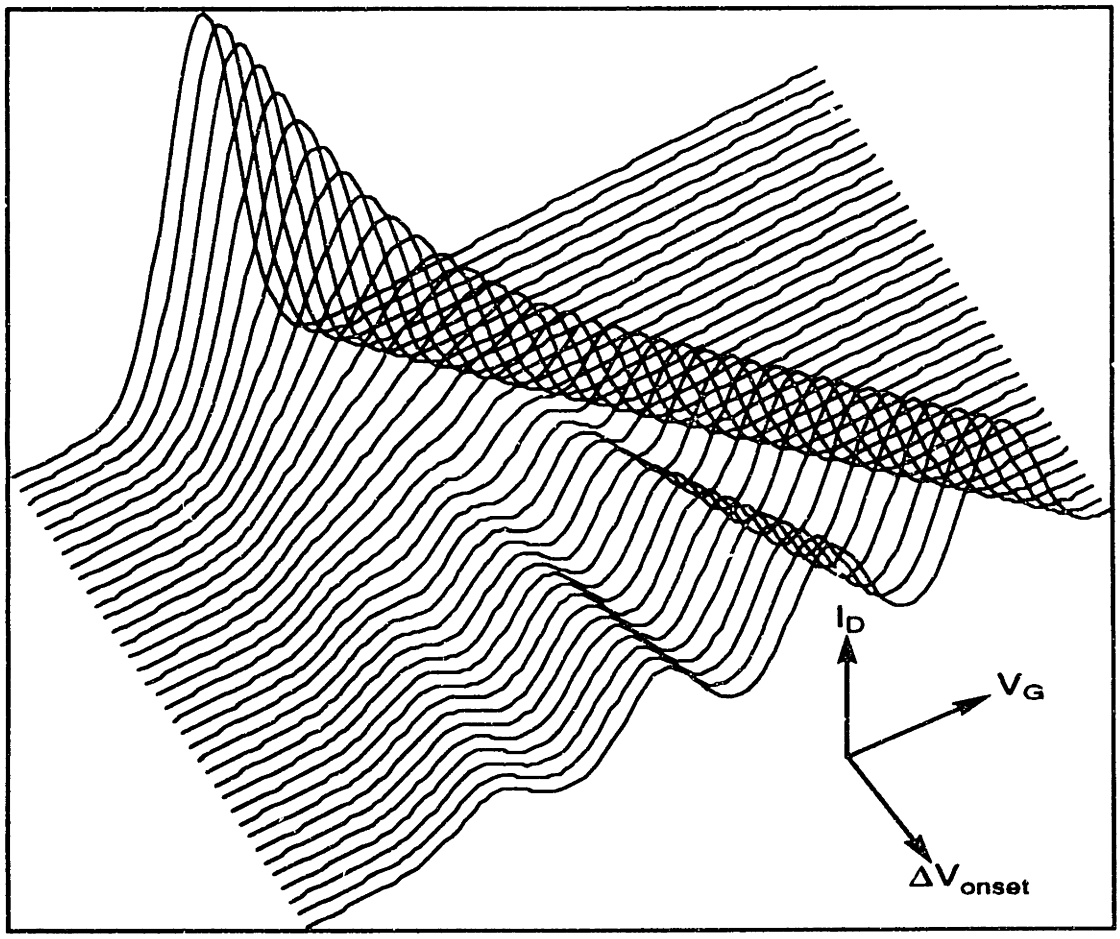

Figure 13. I_D-V_G-ΔV_G plot for a hypothetical device based on four contributing finite potential windows of high conductivity. ΔV_G is incremented by 50 mV for each curve.

useful for more complex systems since it would be difficult to generate comprehensive profiles of the effects of varying the many parameters on which overall device behavior rests by an experimental approach. Equation (1) offers the option of evaluating different possible approaches to obtaining a given complex I_D-V_G characteristic.

Conclusions

A push-pull amplifier, a complementary inverter gate, or a transistor with an I_D-V_G characteristic suitable for a ternary invert gate were all prepared using a pair of appropriately chosen conducting polymers as the active materials. The degree of overlap between the finite potential windows of conductivity of the two polymers plays a major role in defining overall circuit electrical function, demonstrating the versatility derived from the unusual characteristics of microelectrochemical transistors. A push-pull amplifier requires just enough overlap to yield a smooth transition between conduction by one transistor to conduction by the other. A complementary inverter gate requires complete separation of I_D-V_G characteristics for best results. A device based on two polymers providing a transistor designed for ternary logic requires more extensive overlap of two windows of conductivity where the extent of that overlap will be dictated by the specific net I_D-V_G characteristic sought. Therefore, it is clear that being able to chemically tune polymer electrical characteristics is an integral part of developing polymer electronic devices. The next two chapters focus extensively on this issue, culminating in Chapter 6.4 which presents a highly flexible, chemically tunable pair of polymers which can be used to prepare *all* of the molecule-based devices demonstrated in this chapter.

Experimental

Materials

Aniline (Aldrich) was distilled prior to use; CH_3CN, CH_2Cl_2 (Mallinkrodt) and F_3CCO_2H were used as received. [*n*-Bu_4N]PF_6 (Aldrich) was recrystallized from ethyl acetate and $LiClO_4$ was recrystallized from CH_3CH_2OH prior to use. 3-phenylthiophene was synthesized by Dr. Timothy Miller via the Ni(II) catalyzed coupling of phenyl Grignard and 3-bromothiophene and was sublimed prior to use. Chapter 5 details this procedure for preparation of 3-phenylthiophenes. WO_3-derivatized microelectrode arrays were fabricated by Martin Schloh as reported in the literature.[22]

Electrochemistry

Arrays of 8 platinum microelectrodes were cleaned prior to use by cycling each electrode in Ar-purged 0.5 M H_2SO_4 from -.3 to +1.2 V vs. SCE until hydride waves were evident in the cyclic voltammogram. Arrays which upon inspection under a microscope appeared excessively dirty were first etched 3 times for 3-5 s in 10:3 H_2SO_4: 30% H_2O_2; following each etch the array was rinsed thoroughly in deionized water and blown dry under a stream of N_2. All electrochemistry was carried out using Pine Instruments RDE4 bipotentiostats. Power supply voltages were supplied by an RDE4 with its counter and reference electrode terminals connected together as one side of the supply. Thus configured, the RDE4 can supply both V^+ and V^- as required for push-pull amplifier experiments at its K1 and K2 working electrode terminals. Electrochemical and circuit data were recorded on a Kipp and Zonen model BD90 XY recorder.

Polyaniline was deposited by cycling the potential of three adjacent microelectrodes between 0 and +0.90 V vs SCE in 0.1 M aniline in 0.25 M $NaHSO_4$/ 0.5 M H_2SO_4 until the anodic peak for the polymer (0.2 V) reached 20 nA. Poly(3-phenylthiophene) was deposited from a 100 mM solution of the monomer in 0.1 M [*n*-Bu_4N]PF_6 in 4:1

CH_2Cl_2:CH_3CN by scanning the potential of several adjacent microelectrodes positive from 0 V vs Ag at 20 mV/s until the abrupt onset of current (approximately 1.3 V) at which point the potential was held for 1/3 - 1/2 s and then switched to 0 V. Cyclic voltammetry, I_D-V_G measurements, and optical microscopy were used to characterize the deposited polymers.

Preparation of a typical microelectrochemical push-pull amplifier device

Onto electrodes 1,2, and 3 of an 8-electrode array was deposited polyaniline until the peak anodic current for the first polymer oxidation wave at 0.2 V vs SCE reached 20 nA. Holding electrodes 1-3 at 0 V vs SCE, electrodes 5-8 of the array were cycled from -0.3V-1.2V vs SCE at 500 mV/s in Ar-purged 0.5 M H_2SO_4 until hydride waves became evident in the cyclic voltammetry. Poly(3-phenylthiophene) was then deposited driving electrodes 5-8. The device is connected as shown in Figure 7 with the power supply voltages being provided by an RDE4 potentiostat with the shorted counter and reference electrode terminals serving as ground, K1 providing V^+ and K2 providing V^-. A dry electrolyte medium of 0.1 M $LiClO_4$ in CH_3CN acidified with F_3CCO_2H is used for amplifier operation.

Solid-state push-pull amplifier characterization

A standard push-pull amplifier was constructed with 2N3904 and 2N3906 Si bipolar junction transistors according to the schematic in Figure 3. The power supply voltages were provided by an RDE4 potentiostat with the shorted counter and reference electrode terminals serving as ground, K1 providing V^+ and K2 providing V^-. The input waveform was supplied by a Hewlett-Packard model 3311A function generator. (The sweep generator of an RDE4 potentiostat could also provide the triangular wave used.)

Simulations

Simulations were carried out on a Macintosh IIsi by means of a straight-forward program written in True Basic which used equation (1) to produce I_D-V_G characteristics. Appropriate offset and scaling factors were used to adjust onset potentials and relative peak drain currents as required for each simulation.

Development of Equation (1) and Comments

Upon inspection of Figure 2 in which the log of drain current for a polyaniline transistor is plotted as a function of gate potential, it may be observed that the curve is parabolic in nature. It was found that the log(I_D)-V_G characteristic can indeed be modeled as an inverted parabola, from which can be derived equation (1). The equation expresses

$$I_D = I_D^{max}\, 10^{\left[\frac{\log\,[I_D(V_{onset})/\, I_D^{max}]}{(V_{onset} - V_{peak\ con})^2}\,(V_G - V_{peak\ con})^2\right]} \qquad (1)$$

drain current I_D in terms of gate potential V_G and uses the potential for onset of conduction, V_{onset}, and the potential of peak conductivity, $V_{peak\ con}$, as parameters. V_{onset} is specified for a value of I_D such as 0.1, 1, or 10% of maximum. The equation is a model for the I_D-V_G characteristic which assumes that log(I_D) versus V_G is an inverted parabola centered on $V_{peak\ con}$, hence $V_{peak\ con}$ is subtracted from V_G yielding the basic format given in equation (2) which states that log(I_D) is equal to the subtraction from the maximum value of log(I_D)

$$\log(I_D) = \log(I_D^{max}) - k(V_G - V_{peak\ con})^2 \qquad (2)$$

of a parabolic dependence of I_D on V_G centered at $V_{peak\ con}$. The constant *k* was obtained by using a value of V_{onset} where onset of conduction is specified as occurring at a fraction

of maximum drain current, i.e. the equation is fitted to two points: the point of peak conduction and a specified onset point. The equation was then converted to specify I_D instead of $\log(I_D)$ to yield equation (1). Figure 11 shows the I_D-V_G characteristic for a polyaniline transistor and the modeling of it using equation (1). The parabolic fit for $\log(I_D)$-V_G is a good one for all but the tailing edges of that curve, so it is better to specify V_{onset} at 10% of maximum I_D, which is out of the tail-off region, than at 0.1%, for example. The value of *k* in equation (2) can, of course, be varied at will to optimize the fit if optimal results for a single I_D-V_G characteristic are desired. While the I_D-V_G characteristic of polyaniline is widened by large value of V_D, equation (1) still provided a reasonable fit at various values of V_D as long as the appropriate parameters for each case were inserted into the equation.

Interestingly, in the region of the I_D-V_G characteristic roughly between the two half-maximum points, the cyclic voltammogram for polyaniline is essentially flat showing steady anodic current as V_G is scanned, as seen in Figure 4. Therefore, polymer state of charge varies linearly with V_G in this region. It is this same region of the I_D-V_G characteristic were the parabolic fit of $\log(I_D)$-V_G closely matches the I_D-V_G characteristic. Thus, conductivity in this region oft he I_D-V_G characteristic is exponentially dependent on the inverse square of the deviation from the state of charge corresponding to $V_{peak\ con}$.

References

1. Paul, E. W.; Ricco, A. J.; Wrighton, M. S. *J. Phys. Chem.*, **1985**, *89*, 1441

2. Ofer, D.; Wrighton, M. S. *J. Am. Chem. Soc.*, **1988**, *110*, 4467

3. Ofer, D.; Crooks, R. M.; Wrighton, M. S. *J. Am. Chem. Soc.*, **1990**, *112*, 7869

4. Ofer, David. *Doctoral Thesis*, Massachusetts Institute of Technology, 1991

5. Ofer, D.; Park, L. Y.; Schrock, R. R.; Wrighton, M. S. *Chemistry of Materials*, **1991**, *3*, 573

6. Park, L. Y.; Ofer, D.; Gardner, T. J.; Schrock, R. R.; Wrighton, M. S. *Chemistry of Materials*, **1992**, *4*, 1388

7. Sze, S. M. *Physics of Semiconductor Devices*, Wiley: New York, 1981

8. Horowitz, P.; Hill, W. *The Art Of Electronics*; Cambridge University Press: New York, 1989. a) p. 121; b) pp. 91-94; c) pp. 484-487; d) p. 80

9. Pierret, R. F. *Field Effect Devices*, Addison-Wesley: Reading, Massachusetts, 1990

10. Burroughes, J. H.; Jones, C. A.; Friend, R. H. *Nature* **1988**, *335*, 137.

11. Oyama, N.; Yoshimura, F.; Ohsaka, T.; Koezuka, H.; Ando, T. *Jpn. J. Appl. Phys., Part 2* **1988**, *27*, L448

12. Horowitz, G.; Fichou, D.; Peng, X.; Xu, Z.; Garnier, F. *Solid State Commun.* **1989**, *72*, 381

13. Assadi, A.; Svensson, C.; Willander, M.; Inganäs, O. *Synth. Met.* **1989**, *28*, C863

14. McCoy, C. H.; Wrighton, M. S. *Chem. Mater.*, **1993**, *5*, 914

15. Brédas, J.-L.; Street, G. B. *Accs. Chem. Res.* **1985**, *18*, 309

16. Chance, R. R.; Boudreaux, D. S.; Brédas, J.-L.; Silbey, R. in *Handbook of Conducting Polymers*; Skotheim, T. A., Ed.; Marcel Dekker: New York, 1986

17. Brédas, J.-L.; Thémans, B.; Fripiat, J. G.; André, J. M.; Chance, R. R. *Phys. Rev. B: Condens. Matter* **1984**, *29*, 6761

18. Brédas, J.-L.; Chance, R. R.; Silbey, R. *Mol. Cryst. Liq. Cryst.* **1981**, *77*, 319

19. Orata, D; Buttry, D. A.; *J. Am. Chem. Soc.* **1987**, *109*, 3574

20. Huang, W.-S.; Humphrey, B. D.; MacDiarmid, A. G. *J. Chem. Soc., Faraday Trans. 1* **1986**, *82*, 2385

21. Natan, M. J.; Mallouk, T. E.; Wrighton, M. S. *J. Phys. Chem.*, **1987**, *91*, 648

22. Schloh, M. O.; Leventis, N.; Wrighton, M. S. *J. Appl. Phys.*, **1989**, *66*, 965

23. *Computer Science and Multiple-Valued Logic: Theory and Applications 2nd ed.*; Rine, D. C., ed.; Elsevier Science Publishing Co.: New York, 1984

24. Lee, S. C. *Modern Switching Theory and Digital Design*; Prentice-Hall: Englewood Cliffs, NJ, 1978. Chapter 5

25. Moraga, C. "A Monograph on Ternary Threshold Logic"; in reference 23

26. Vranesic, Z. G.; Smith, K. C. "Electronic Circuits for Multi-Valued Digital Systems"; in reference 23

Chapter 5

The Synthesis of Substituted 3-Phenylthiophenes and 1,4-Dithienylbenzenes and their Polymers: Substituent Effects on Polymer Electrical Characteristics and on Monomer Reactivity in Anodic Polymerization

Abstract

Derivatives of 3-phenylthiophene were synthesized by the Ni(II)-catalyzed coupling of 3-bromothiophene and substituted phenylmagnesium bromides. Prepared were 3-(4-R-phenyl)-thiophene, R = methoxy, methyl, chloro, fluoro, trifluoromethyl; 3-(3-methoxyphenyl)-thiophene, 3-(3,5-bis-(trifluoromethyl)phenyl)-thiophene, and 3-(3,4,5-trifluorophenyl)-thiophene. The coupling reaction of 3,4,5-trifluorophenylmagnesium bromide and 3-bromothiophene proceeded in poor yield and pure product was not isolated. The novel 1,4-dithienyl-2,5-difluorobenzene was prepared by the coupling of 1,4-dibromo-2,5-difluorobenzene with 2-thienylmagnesium bromide using $Pd(P\emptyset_3)_4$ in 66% yield. Reaction of 1,4-diiodo- or 1,4-dibromo-tetrafluorobenzene with 2-thienylmagnesium bromide using either $Pd(P\emptyset_3)_4$ or $Ni(\emptyset_2P(CH_2)_3P\emptyset_2)Cl_2$ as catalyst gave mainly metal-halogen exchange products. Also prepared was 1,4-dithienylbenzene. The electrochemistry of each derivative was characterized, and the potential for onset of conduction, relative conductivity, and polymerization characteristics for each of the 3-phenylthiophene polymers is given in Table 1. Both 1,4-dithienylbenzene and 1,4-dithienyl-2,5-difluorobenzene polymerized readily to give polymers of well-behaved electrochemistry. Both polymers showed a window of reductive as well as oxidative conductivity, with the difluoro derivative showing onset of conductivity 100 mV positive of the parent for both windows.

Introduction

The molecular nature of conducting polymers results in a strong link between their electrical characteristics and their specific molecular structure and composition. A host of derivatives of basic conducting polymer backbones have been prepared and studied[1-19] in an effort to understand and utilize the structure-property relationships of these materials. Anodic polymerization of a substituted monomer has been and remains a major synthetic method for preparation of conducting polymers and is the subject of major reviews[20-22] one of which is devoted exclusively to the thiophene family.[22] The preparation of substituted derivatives of a polymer backbone is a clear approach both to probing the conduction characteristics and other properties of a polymer and to learning how to manipulate or tune those properties. Substituents also, of course, affect the reactivity of a monomer as well to a significant and sometimes dominant extent. Thus, if the effect of a methyl group is to be evaluated in the polymer obtained from thiophene as compared to the polymer obtained from 3-methylthiophene, the effect of the methyl group on polymerization must be considered in addition to its possible effects on the thiophene backbone conduction properties.

As a major route to conducting polythiophenes, anodic polymerization warrants introduction and discussion. The mechanism of anodic polymerization, also referred to as oxidative polymerization, electrochemical polymerization, and electropolymerization in the literature, is only partly understood and is considered to be highly complex.[22] A general representation of the process of anodic polymer synthesis is shown at the top of Scheme I. It is certain that electron transfer from the π-system of the monomer to the electrode is the first step in the reaction,[20-22] but the farther along one gets in considering the fate of that radical cation, the more complex and speculative things become. The top of Scheme I summarizes the generally accepted aspects of the mechanism. Overall, a monomer is oxidized to generate a radical cation which is reactive and couples with itself to form a

dimer following loss of two protons. The dimer is easier to oxidize than the monomer on account of the greater resonance stabilization of the resulting cation so it is quickly oxidized at the electrode surface and undergoes a second coupling step to yield a trimer which is

Scheme I

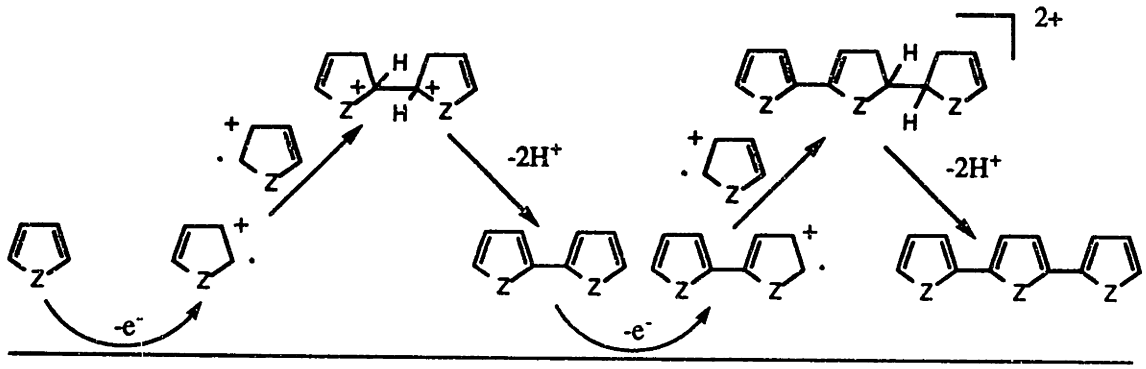

electrode surface

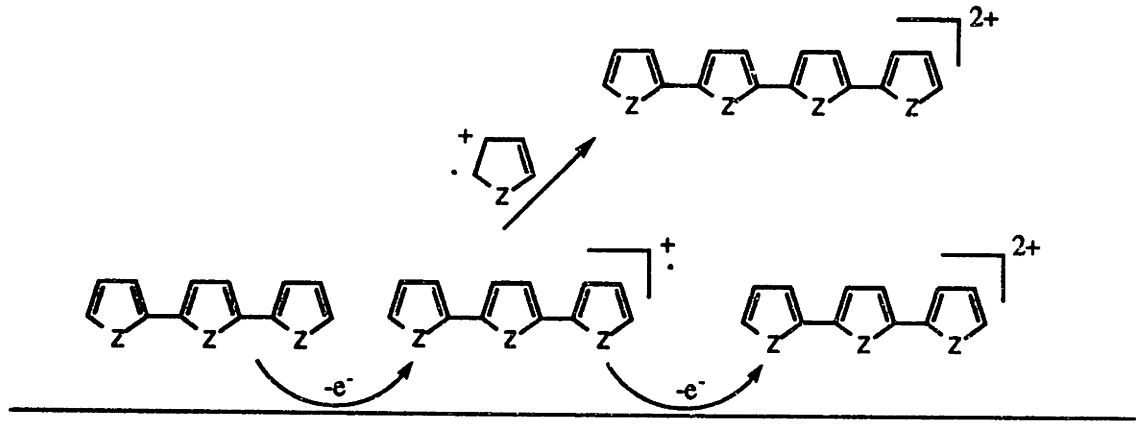

electrode surface

oxidized more easily still. This process continues until the oligomers become long enough to be insoluble and precipitate onto the electrode. Many questions remain regarding details of the suitability of this description.[22]

Several steps after initiation of polymerization, consideration of all of the possible mechanistic pathways becomes increasingly complex. As longer oligomer form, predicting

their fate becomes more difficult because they can interact with any of the number of possible species in solution as well as with the electrode surface. Since the longer the oligomer the more easily it supports charge, a trimer may, for example, undergo loss of a second electron to form a dication as a competing process with coupling to form a tetramer, as shown at the bottom of Scheme I. The reactivity of the initial radical cation is critical. It is reasonable to expect and has been proposed[20-22] that there exists an optimal range of radical cation reactivity for efficient coupling and polymerization. The oxidized monomer must be sufficiently reactive to undergo coupling and oligomer growth before it diffuses too far away from the electrode surface. Too stable a radical cation is detrimental. An example of this is terthiophene. The polymer obtained from it is several orders of magnitude less conducting than the polymer obtained from thiophene.[23] This is attributed the delocalization of the terthiophene cation which leads to α–β coupling of monomers, unfavorable for conductivity, instead of the desired α–α linkages. Indeed, conductivity declines by several orders of magnitude going from polythiophene, to polybithiophene, to polyterthiophene.[22,23] While bithiophene and terthiophene are α–α linked starting materials, the stabilization of the terminal α sites by delocalization and statistical advantage gained by the β-sites in the polycyclic monomers results in a decline in preferential reaction at the α-carbons, increasing the rate of linking errors.[22-24]

While a monomer which produces too stable a radical cation is undesirable, so is a monomer which results in a highly reactive species. In the thiophene family it is a general trend that electron-withdrawing groups at the 3-position such as halogens result in poor polymerization while a nitro, cyano, or carboxylic acid group prevent it.[20-22] If the radical cation is so reactive that it undergoes intramolecular decomposition or attacks the solvent or electrolyte, poor polymerization or a complete lack of it can result.[20-22] Solvent, electrolyte, monomer concentration, and potentiostatic versus galvanostatic deposition are other factors which can also be important in determining polymer properties.[20-22]

The synthesis of the molecules described in this chapter was undertaken in an effort to examine substituent effects on the electrical characteristics of thiophene-based polymers important to microelectrochemical transistors . The investigation of the 3-phenylthiophene family of polymer arose from the use of poly(3-phenylthiophene) in the push-pull amplifier of Chapter 4. An investigation of substitution of the phenyl ring was made particularly attractive given the extensive existing knowledge of substituent effects in aryl systems and the large body of quantitative data available in the form of Hammett equation substituent constants.[25] One goal was to develop a means of predicting the potential for onset of conduction for a series of 3-phenylthiophene polymers bearing substituents on the phenyl ring based on a Hammett-type treatment of the data on the polymers prepared. The focus on potential for onset of conduction is a result of the microelectrochemical device opportunities based on the finite window of high conductivity described in Chapter 4. This parameter, which is the negative boundary of the finite window of conductivity, is defined here to be the potential at which the I_D-V_G characteristic first deviates from baseline on the forward scan of V_G from the fully reduced state of the polymer. The potential for onset of conduction is not only a critical electrical parameter but is a good property for study because it is highly reproducible.

The 3-phenylthiophenes prepared in this chapter were all synthesized using the Ni-catalyzed coupling of 3-bromothiophene with the appropriate Grignard reagent,[26,27] a reaction which has seen wide application in the synthesis of substituted thiophenes. The substituents chosen are time-honored standards of varied electronic character: methoxy, methyl, hydrogen, chloro, fluoro, and trifluoromethyl.

Following the work on the phenylthiophene family, other polymer systems were sought which would allow preparation of derivatives of varied electronic character. In choosing a polymer architecture suited to tuning properties via use of different substituents, it is sensible to look for systems which offer wide substitutional flexibility. Poly(3-phenylthiophene) is such a case because of the range of substitution possible on the

pendant phenyl ring. If an aryl ring were incorporated into a polythiophene backbone, substituents on it would exert a direct effect on carbons which participate in the conducting π-manifold. An example of this is poly(1,4-dithienylbenzene).[8,28,30,31] The parent 1,4-dithienylbenzene and its 2,5-dimethyl and 2,5-dimethoxy derivatives and their polymers are the subject of a comprehensive study which is described in an excellent and detailed report.[8] Both 1,4-dithienylbenzene and 1,4-dithienyl-2,5-dimethylbenzene were accessible via the Ni-catalyzed coupling reaction described above, provided that the aryl diiodide is used for coupling with 2-thienyl Grignard as the dibromoarene is insufficiently activated. Synthesis of 1,4-dithienyl-2,5-dimethoxy was reported to require the more nucleophilic 2-thienylcopper in place of the Grignard.[8] Interestingly, while the parent and the dimethoxy polymers had conductivities on the order of 1 S/cm, the dimethyl derivative was six orders of magnitude less conducting and also calculated to have a much higher torsion angle between the thiophene and phenyl rings.[8] Thus, sterically demanding groups are expected to markedly reduce conjugation and must be avoided if conductivity is to be maintained in this system. While a number of alkyl and alkoxy derivatives of 1,4-dithienylbenzene are known, substitution with electron-withdrawing groups was limited to the single example of the 2-nitro derviative.[28] The latter section of this chapter is devoted to the development of the synthesis of fluorine-substituted 1,4-dithienylbenzenes and their polymers, previously unknown.

Results and Discussion

Synthesis of 3-Phenylthiophenes bearing subtituents on the aryl ring

Nine derivatives of 3-phenylthiophene were prepared by the coupling of 3-bromothiophene with substituted phenylmagnesium bromides catalyzed by [1,3-*bis*-diphenylphosphinopropane]nickel(II) chloride,[26] Scheme II. The chloro, fluoro, and

Scheme II

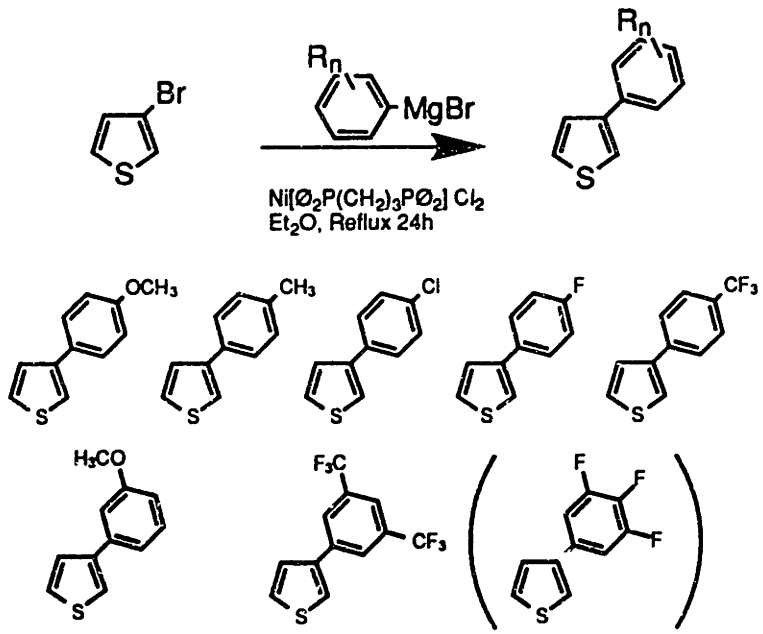

methyl derivatives of phenylmagnesium bromide are commercially available whereas the Grignards of 4-methoxy-, 3-methoxy-, 4-trifluoromethyl-, 3,5-*bis*-trifluoromethyl-, and 3,4,5-trifluoro-bromobenzene were prepared from the bromoarene and magnesium as their diethyl ether solutions. The 4-trifluoromethyl-, 3,5-*bis*-trifluoromethyl-, and 3,4,5-trifluoro derivatives of bromobenzene react with magnesium with great vigor and rapid initiation while the methoxy Grignards are tedious to prepare, requiring several hours of reflux with stirring. Unknown prior to this work were 3-(4-methoxyphenyl)-thiophene, 3-(3,5-*bis*-trifluoromethylphenyl)-thiophene, and 3-(3,4,5-trifluorophenyl)-thiophene.

While the trifluorophenyl Grignard was readily prepared, the coupling reaction proceeded in such poor yield that the product could not be isolated in acceptable purity and was not characterized further. The Ni-catalyzed coupling reaction proved generally applicable for the rest of the substrates giving acceptable yields for all of the reactions except for that of 3,4,5-trifluorophenylmagnesium bromide with 3-bromothiophene. The loading of the phenyl ring with electron-withdrawing substituents in two of the derivatives was in pursuit of thiophene backbones with depleted π-systems for very positive potentials for onset of conduction. All of the para-substituted derivatives sublimed beautifully and this proved the best method for their purification. Gas chromatography/mass spectrometry (GC/MS) was used to monitor the progress of reactions and identify reaction side products. Because the phenyl and thienyl regions in the ^{1}H-NMR often overlap yielding complex and often uninterpretable spectra, GC/MS proved particularly useful in identifying reaction side-products for this class of molecules.

Synthesis of 1,4-dithienylbenzenes and related chemistry

For the most part, synthesis of the derivatives of 3-phenylthiophene was straight-forward. The synthetic chemistry of dithienylbenzenes, however, is more varied as described above and this trend held in attempts to expand this family of molecules to fluorinated derivatives. The parent molecule was prepared according to the literature[8] by the same Ni-catalyzed coupling reaction used above, Scheme III. Reaction is satisfactory

Scheme III

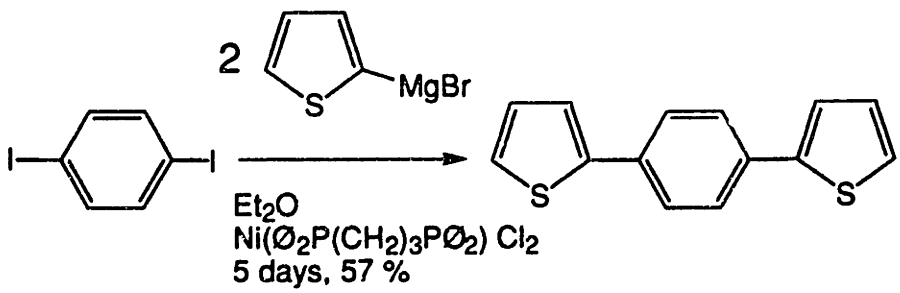

with 1,4-diiodobenzene but proceeded extremely poorly with 1,4-dibromobenzene. The pursuit of fluoro derivatives of dithienylbenzene was arrived at by consideration of the following criteria. First, dithienylbenzenes bearing electron withdrawing groups are interesting because they represent an uncharacterized class of molecule and also because of microelectrochemical device possibilities arising from conducting polymers with potentials for onset of conduction positive of onset of oxidative insulation in polyaniline. Second, from the poor conductivity of the 2,5-dimethyl[8] derivative it was concluded that steric demand must be kept to a minimum. Third, the required starting arene must be accessible. Fluorine was a clear choice of substituent because it electronically potent yet sterically undemanding, and mono, di, and tetrafluorodihalobenzenes are commercially available. The first reaction undertaken was the coupling of 2-thienylmagnesium bromide (readily prepared from 2-bromothiophene and magnesium) with 1,4-dibromo-2,5-difluorobenzene, Scheme IV. While an aryl diiodide was indicated as the preferred substrate for the reaction in Scheme IV given the poor coupling of dibromobenzene with 2-thienylmagnesium

Scheme IV

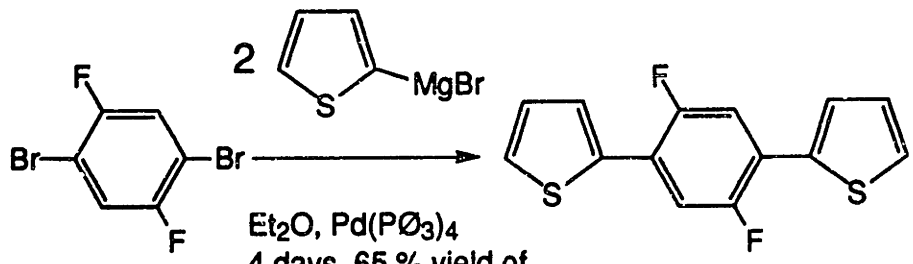

bromide found above and in the literature,[8] 1,4-diiodo-2,5-difluorobenzene was not commercially available. However, just as the methoxy groups of 1,4-diiodo-2,5-dimethoxybenzene deactivate the aryl dihalide toward attack thus requiring a more nucleophilic thienyl equivalent for reaction,[8] it was hoped that the fluoro groups might

sufficiently activate the dibromide to allow reaction. Reaction of 1,4-dibromo-2,5-difluorobenzene with two equivalents of 2-thienylmagnesium bromide in ether in the presence of $Ni(Ø_2P(CH_2)_3PØ_2)Cl_2$ showed no coupling product whatsoever after 24 hours at reflux. In the hope that a Pd(0) species might succeed where the Ni catalyst had not, some $Pd(PØ_3)_4$ was added to the reaction mixture. After 4 days a sample of the reaction mixture was analyzed by GC/MS and it was discovered that the reaction had proceeded to completion. Work-up afforded the novel 1,4-dithienyl-2,5-difluorobenzene in 66 % yield for the refined product. The pure compound is a white crystalline solid. Its ^{1}H-NMR and GC/MS are shown in Figure 1. In the synthesis of both the 2,5-difluoro and parent dithienylbenzenes, virtually no monothienylated products were observed.

The third of the dithienylbenzenes sought was the 2,3,5,6-tetrafluoro derivative. The successful synthesis of 1,4-dithienyl-2,5-difluorobenzene using $Pd(PØ_3)_4$ as catalyst prompted use of the same approach to the tetrafluoro derivative. In stark contrast, the major products obtained were those attributable to metal-halogen exchange,[25a,29] Scheme V. GC/MS of the reaction mixtures showed bithiophene, conclusively identified by its

Scheme V

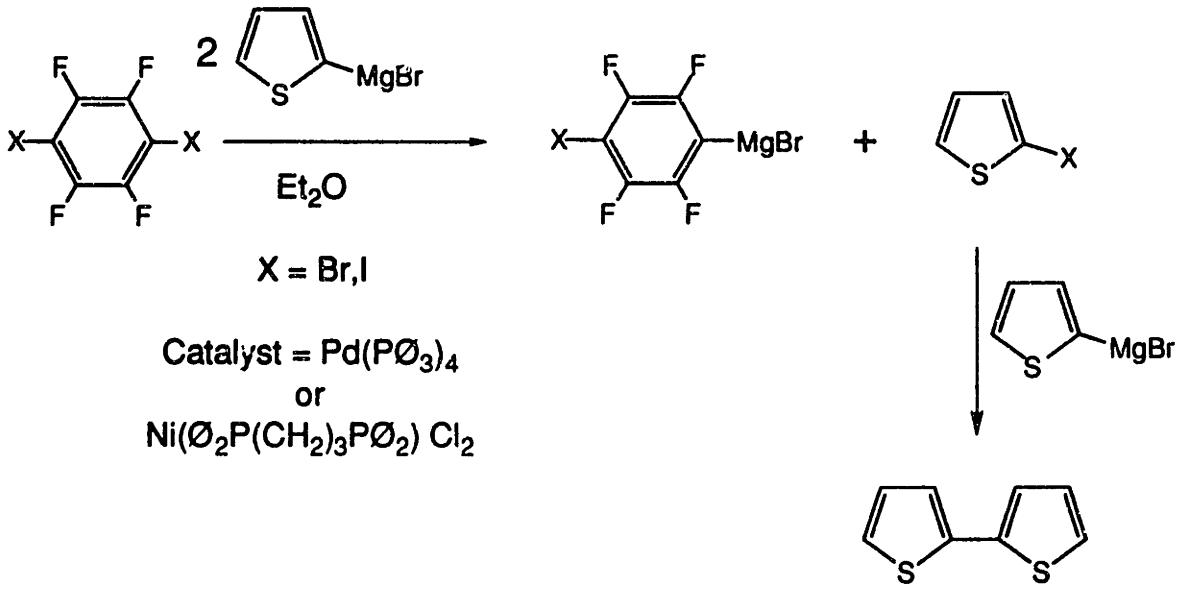

Figure 1a. GC/MS of 1,4-dithienyl-2,5-difluorobenzene.

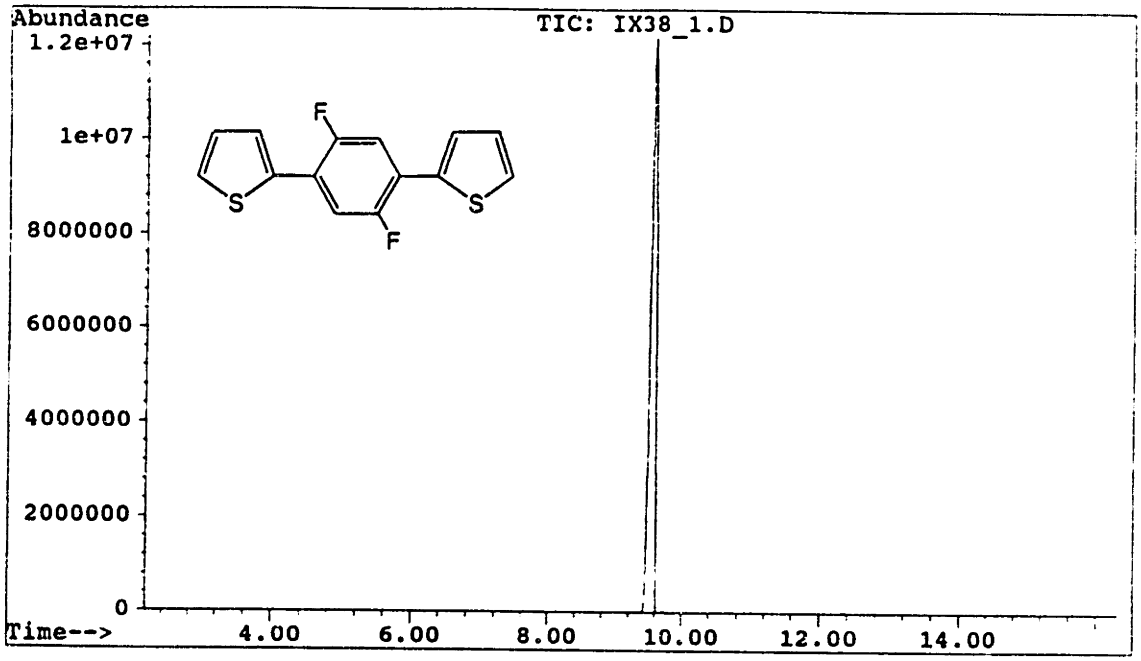
Abundance
TIC: IX38_1.D
1.2e+07
1e+07
8000000
6000000
4000000
2000000
0
Time-->
4.00
6.00
8.00
10.00
12.00
14.00
F
S
S
F

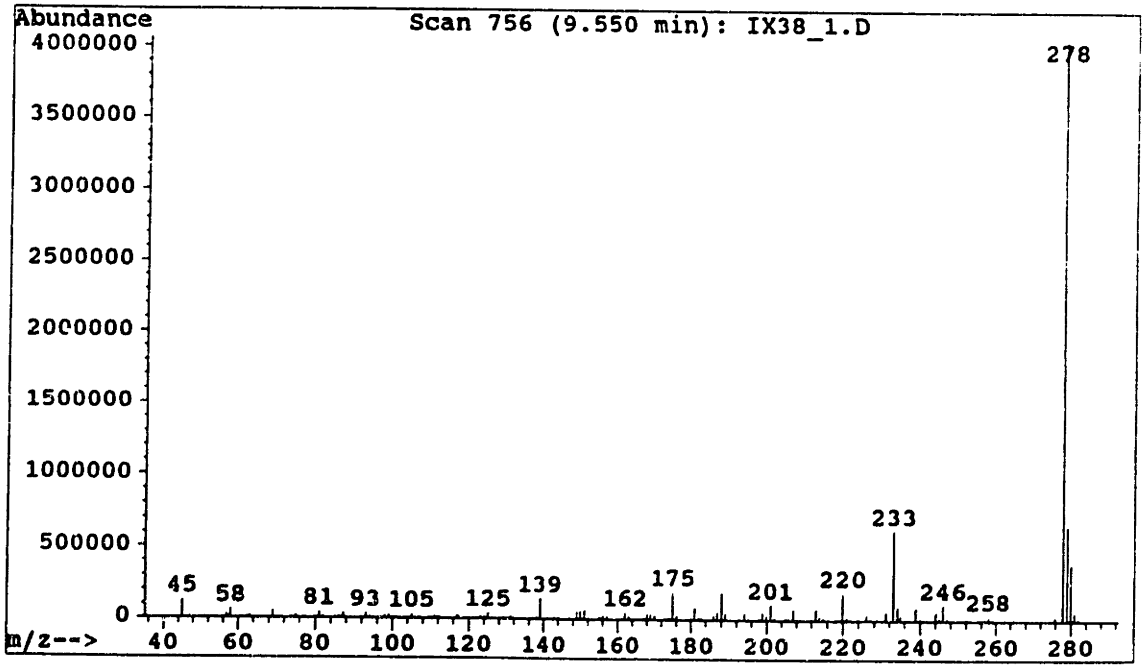
Abundance
Scan 756 (9.550 min): IX38_1.D
4000000
3500000
3000000
2500000
2000000
1500000
1000000
500000
0
m/z-->
278
233
45
58
81
93
105
125
139
162
175
201
220
246
258
40
60
80
100
120
140
160
180
200
220
240
260
280

Figure 1b. ^{1}H-NMR (300 MHz, $CDCl_3$) 1,4-dithienyl-2,5-difluorobenzene.

^{1}H-NMR, 300 MHz, $CDCl_3$

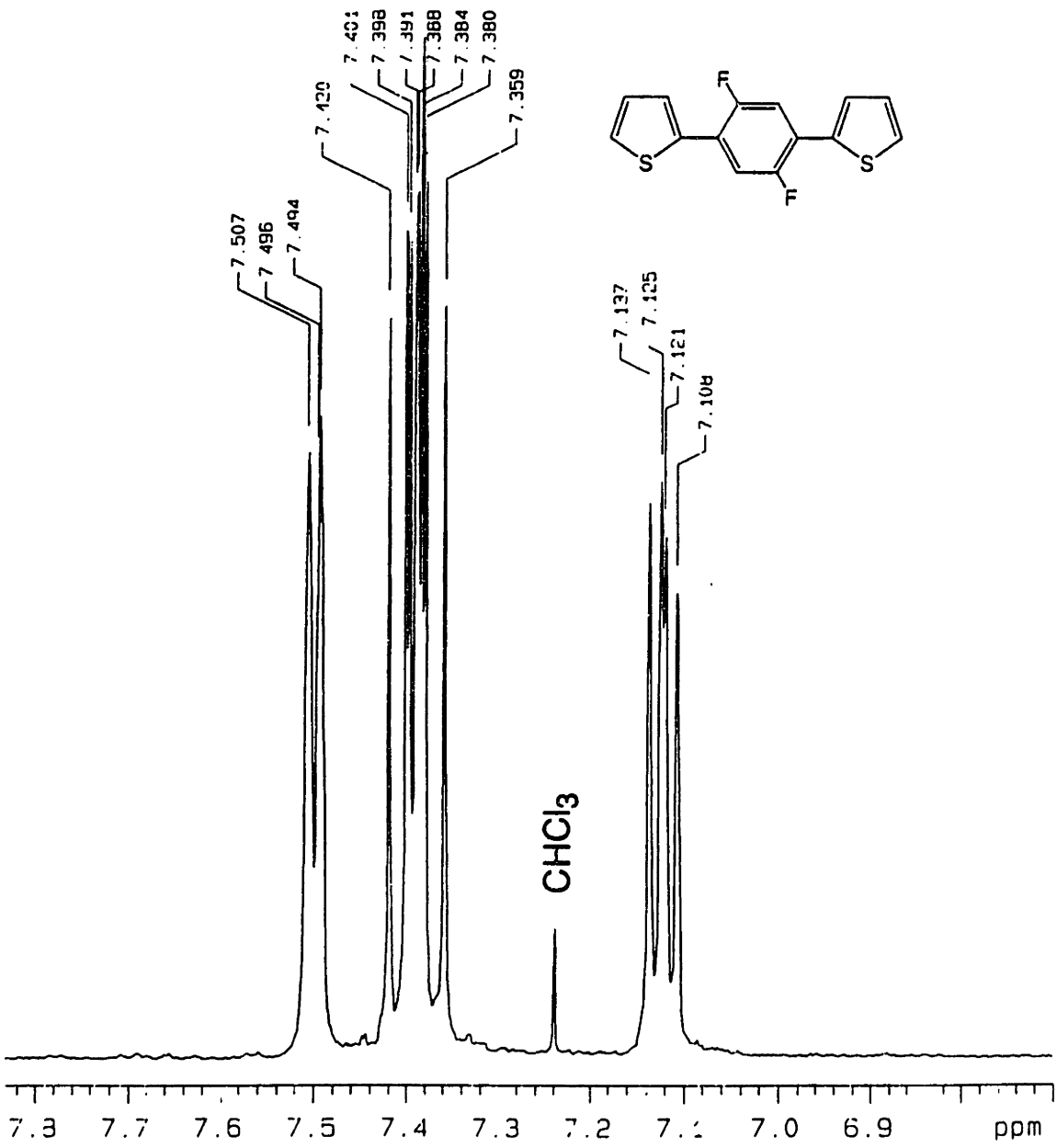

mass spectrum and retention time compared to an authentic sample, iodothiophene and iodotetrafluorobenzene when the diiodo substrate was used, and bromothiophene and bromotetrafluorobenzene when the dibromo substrate was used. Similar results were obtained whether 1,4-dibromotetrafluorobenzene or the diiodo derivative was used as substrate, and whether $Ni(Ø_2P(CH_2)_3PØ_2)Cl_2$ or $Pd(PØ_3)_4$ was used as catalyst although a small amount of the desired dithienyltetrafluorobenzene was detected from reaction of the diiodo substrate using the nickel catalyst. It is conceivable that a tedious, low yield synthesis might be carried out in this way, but this was not pursued.

Electrochemistry of Derivatives of 3-Phenylthiophene

Derivatives of 3-phenylthiophene were characterized by oxidation at microelectrode arrays from a 100 mM solution of the monomer in 0.1 M [*n*-Bu_4N]PF_6/CH_2Cl_2. The majority of the derivatives produced electroactive and conducting polymers, Scheme VI.

Scheme VI

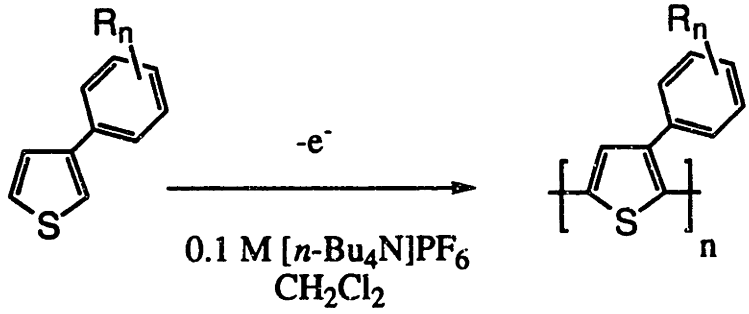

The high concentration made certain that monomers which polymerized with difficulty would still have a reasonable chance of providing films for characterization. Because 3-phenylthiophene itself polymerizes with much better results from CH_2Cl_2 than CH_3CN (see Chapter 4, push-pull amplifier preparation), CH_2Cl_2 was chosen as the solvent for polymerization. Polymerization on microelectrode can be carried out three ways. First, slowly scanning the potential of the electrode positive until onset of current is observed at which point the current is allowed to rise to approximately 0.5-1 μA per pair of 2 x 80 μm microelectrodes and after a approximately 0.5 s the potential is switched to zero. The time

for which the potential is held determines film thickness. For a highly reactive monomer like thiophene, the deposition voltammogram is a step function where avalanche onset of anodic current is observed and film growth is very rapid, while a more stabilized radical cation such as that obtained from terthiophene results in more moderate growth. The second approach is to cycle the electrode between 0 and a potential at which the monomer is oxidized. This is appropriate for mildly reactive monomers such as terthiophenes but can yield poor results at microelectrodes for thiophene, 3-methylthiophene, or any monomer which undergoes sudden, rapid polymerization. The final approach, used as a last resort for difficult monomers, is to step the potential of the electrode to a high potential just below the point at which the solvent begins to oxidize. This can succeed in cases where the monomer tends to passivate the electrode before polymerization sets in. 3-bromothiophene is a monomer for which this approach succeeds. A good predictor of the ultimate polymerizability of a monomer is to scan potential positive at a slow rate (10 mV/s) and halt the scan 200 mV positive of the first point at which anodic current is observed. A rapid increase in current, especially where current continues to increase at constant potential, is characteristic of a polymerizable monomer which will readily yield polymer films. If instead, a gradual increase in current to a low value (as compared to that observed for a reactive monomer which polymerizes well) and an immediate decline in anodic current once the sweep is halted is observed, the monomer was almost always found to yield no polymer under other conditions either.

Each of the derivatives prepared above were subjected to oxidation at microelectrode arrays. The results are summarized in Table 1. The derivatives which polymerized easily, quickly covering and connecting a pair of electrodes, were 3-phenylthiophene and its 4-chloro, 4-fluoro, and 4-trifluoromethyl derivatives. The latter three polymerized particularly smoothly to readily give uniform films which covered and connected the electrodes of the array at which the monomer was oxidized. The methyl derivative was difficult to polymerize, but good polymer growth was obtained by stepping

Table 1. Substituted 3-Phenylthiophenes as Polymer Precursors

Polymer[1]	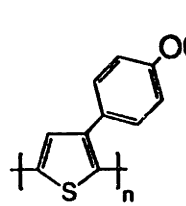	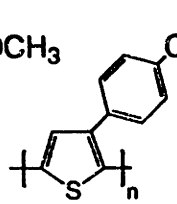	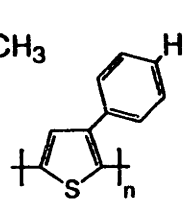	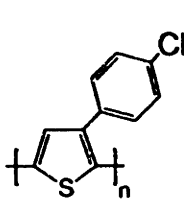	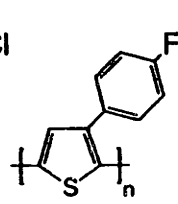	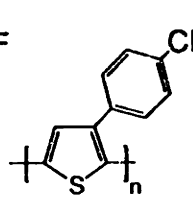	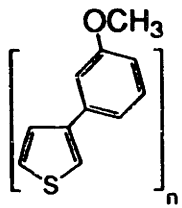	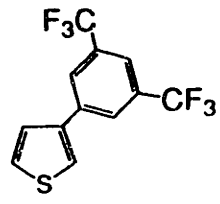
Onset of Conduction, V vs Ag	+0.65	+0.60	+0.68	+0.73	+0.74	+1.0	—	—
Deposition behavior	poor	difficult	fair-good	good	very good	good	fair	none
Relative Conductivity	0.06	0.7	1	2.3	1.2	0.2	0	—
Stability	low	fair	good	very good	very good	fair	—	—

Deposition: anodic polymerization from 100mM monomer in 0.1M $[n\text{-}Bu_4N]PF_6/CH_2Cl_2$ onto an 8-microelectrode array.

Characterization: 0.1M $[n\text{-}Bu_4N]PF_6/CH_3CN$

1. 3-(3-methoxyphenyl)-thiophene polymerized to yield a thick, red film which was electrochemically inactive. 3-(3,5-bis-trifluoromethylphenyl)-thiophene showed irreversible oxidation only with no depostition of any material onto the electrode surface.

the potential of the electrode to 2.2 V vs Ag. Difficulty in the polymerization of a thiophene containing a para-tolyl group attached to thiophene via an ether linkage has been reported and attributed to a side reaction resulting from the lower oxidation potential of a methyl-substituted phenyl ring.[10] This had been considered, and the polymerization of poly(3-methylthiophene) in the presence of toluene and also cumene was examined to see if the alkylbenzenes had any effect on polymer formation, but polymerization occurred as usual despite the presence of the two potential radical interceptors. 3-(4-Methoxyphenyl)-thiophene polymerized poorly. A very thin reddish film was all that could be obtained no matter how long sustained current was passed. The film did grow sufficiently to connect the electrodes of the array, however, so that the I_D-V_G characteristic and cyclic voltammogram could be fully characterized. The 4-trifluoromethyl derivative also polymerized easily, and the cyclic voltammetry and I_D-V_G characteristic are shown in Figure 2. The polymer, which had the highest potential for onset of conduction observed for the derivatives of 3-phenylthiophene, showed some loss of peak drain current on repeated scanning of the I_D-V_G characteristic, a behavior often observed in polymers which are difficult to oxidize. This is not surprising given that the higher the oxidation potential of a polymer, the more electrophilic and reactive the cationic sites generated are expected to be. The fluoro and chloro derivatives, on the other hand, showed better polymerization, higher conductivity, and better stability than all of the other derivatives.

The good polymerization characteristics of the monomers bearing electron-withdrawing groups and difficult polymerizations of the 4-methyl and 4-methoxy derivatives suggested that if the phenyl ring is made too electron rich that it interferes with polymerization. One possibility is that if the phenyl ring is substituted with donating substituents, it better stabilizes the radical cationic thiophene ring leading to insufficient reactivity for effective coupling and polymerization. A test case for this hypothesis is provided by the methoxy group because it is donating by resonance in the para position but inductively withdrawing from the meta position. The meta derivative, where the methoxy

Figure 2. Cyclic voltammetry and I_D-V_G characteristic of poly(3-(4-trifluoromethylphenyl)-thiophene)

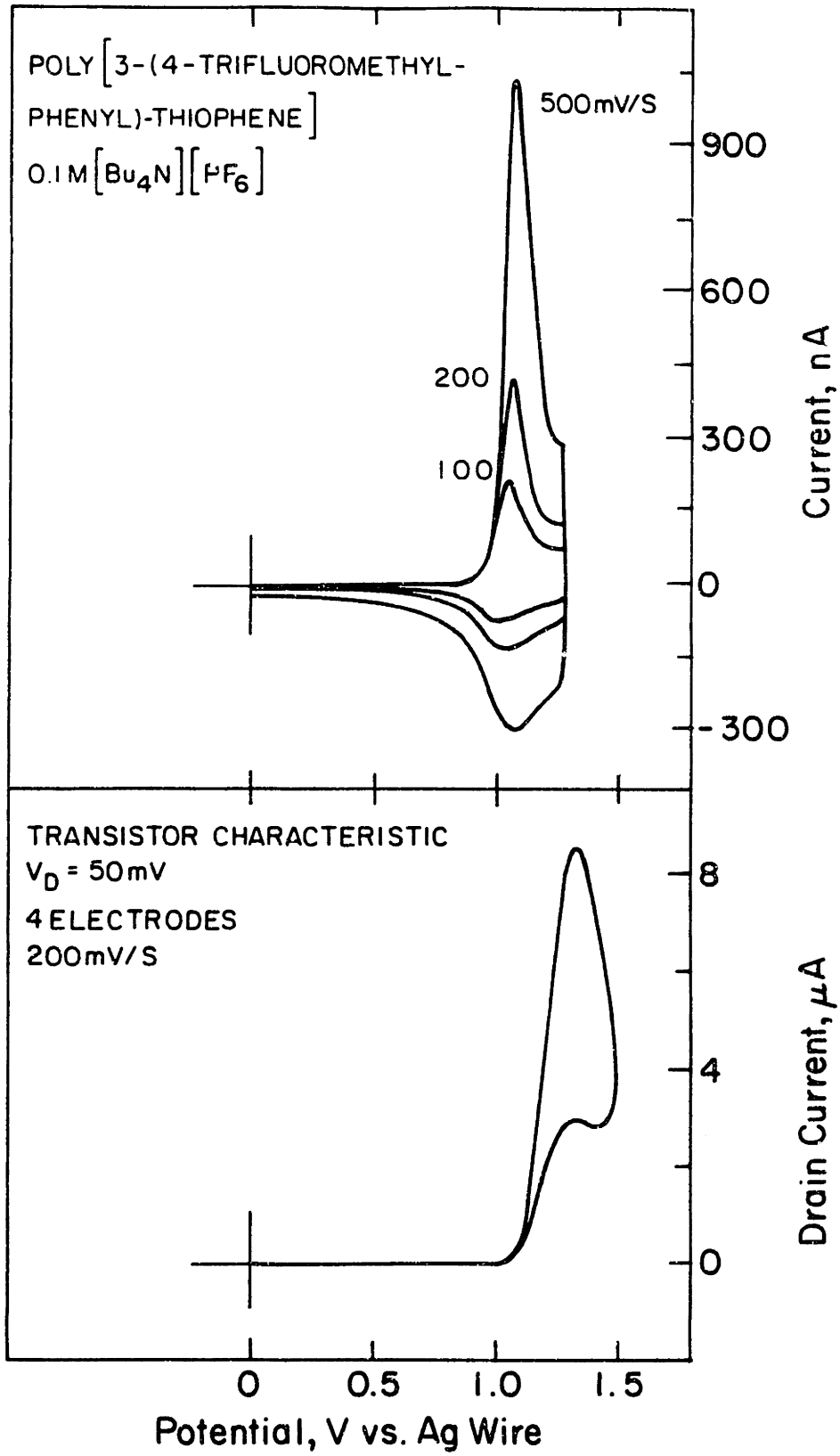
POLY [3-(4-TRIFLUOROMETHYL-
PHENYL)-THIOPHENE]
0.1M [Bu4N][PF6]
500mV/S
200
100
900
600
300
0
-300
Current, nA
TRANSISTOR CHARACTERISTIC
VD = 50mV
4 ELECTRODES
200mV/S
8
4
0
Drain Current, μA
0
0.5
1.0
1.5
Potential, V vs. Ag Wire

group is mildly electron-withdrawing toward the thiophene ring, should have better polymerization characteristics than the para derivative. To this end, 3-(3-methoxyphenyl)-thiophene was prepared. Oxidation readily yielded a red film on the microelectrode array but it showed poor cyclic voltammetry, an anodic wave with little cathodic current on the return scan, and no I_D-V_G characteristic. The fact that a thick film could be grown indicates that the material obtained has some minimal conductivity during deposition, but several trials yielded the same results and it is possible that a polythiophene backbone is not even produced by oxidation of 3-(3-methoxyphenyl)-thiophene. While the methoxy group is mildly electron withdrawing toward the thiophene ring from the meta position, it is ortho to the 4-position of the phenyl ring and activates it by resonance, an effect augmented further by the thiophene ring which is para to the 4-position, Scheme VII.

Scheme VII

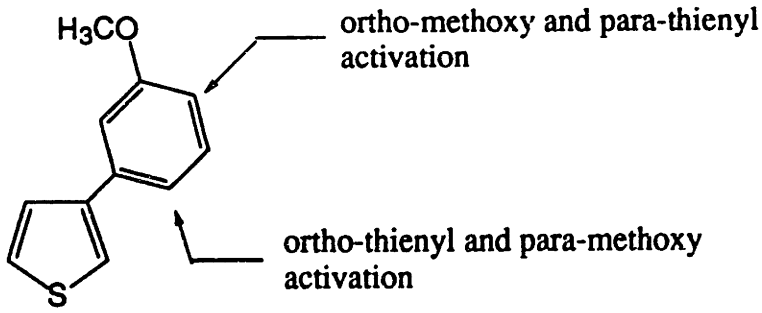

By the same token, the 6-position of the phenyl ring is activated by the combination of the para-methoxy and ortho-thienyl substituents. This activation may promote polymerization with coupling at the phenyl ring as a significant pathway. One undesirable consequence possible from such polymerization is that a polymer linked from the 5-position of the thiophene ring to the 4-position of the phenyl ring does not allow a resonance form to be drawn in which each bond is shifted one position along the chain. Thus, the meta-methoxy group may promote a polymerization pathway that leads to a poorly conjugated material.

Only an irreversible oxidation with no detectable deposition of material onto the electrode surface was obtained with 3-(3,5-*bis*-trifluoromethylphenyl)-thiophene. Repeated attempts on fresh microelectrode arrays yielded the same results. While 3-(3,5-*bis*-trifluoromethylphenyl)-thiophene yielded no polymer, 3-methylthiophene polymerized normally at the arrays after the attempted deposition of the former, confirming that the electrodes of the array were not in any way impaired. Thus, the 3,5-*bis*-trifluoromethylphenyl group may be too electron-withdrawing and fall into the category of other withdrawing substituents which prevent polymerization.[20-22]

The conductivities in Table 1 are given relative to the parent polymer, poly(3-phenylthiophene) which has an absolute conductivity measured at microelectrode arrays of about 0.05 S/cm. The chloro and fluoro derivatives were the best two polymers in deposition characteristics, conductivity, and stability. The more electronegative trifluoromethyl group or the donating meta or para-methoxy substituents resulted in a general decline in overall properties. With the exception of the trifluoromethyl derivative, the effect of a para substituent on the potential for onset of conduction is quite modest. Figure 3 shows a plot of the respective Hammett substituent coefficient[32] against potential for onset of conduction for the series of para-substituted 3-phenylthiophene polymers. The fit to a straight line is clearly not tight enough to provide more than reasonable guide in terms of what to expect for onset potential. The σ_p^+ set of Hammett coefficients intended for reactions in which the substituent can enter into resonance interaction with the reaction site might be considered more appropriate for the polymer conductivity situation because of the importance of delocalization to conduction, but these constants actually give a more, not less, scattered fit than the standard σ_p coefficients used in Figure 3.

It is interesting that the para-methoxy derivative has an onset potential which is positive of the methyl derivative. On the basis of the donating nature of a para-methoxy substituent it was expected that poly(3-(4-methoxyphenyl)-thiophene) would be the easiest of the derivatives prepared to oxidize and have the lowest onset of conductivity. However,

a complicating factor is the possibility of variation from one substituent to the next in the degree of coplanarity of the phenyl and thiophene rings. From steric considerations and

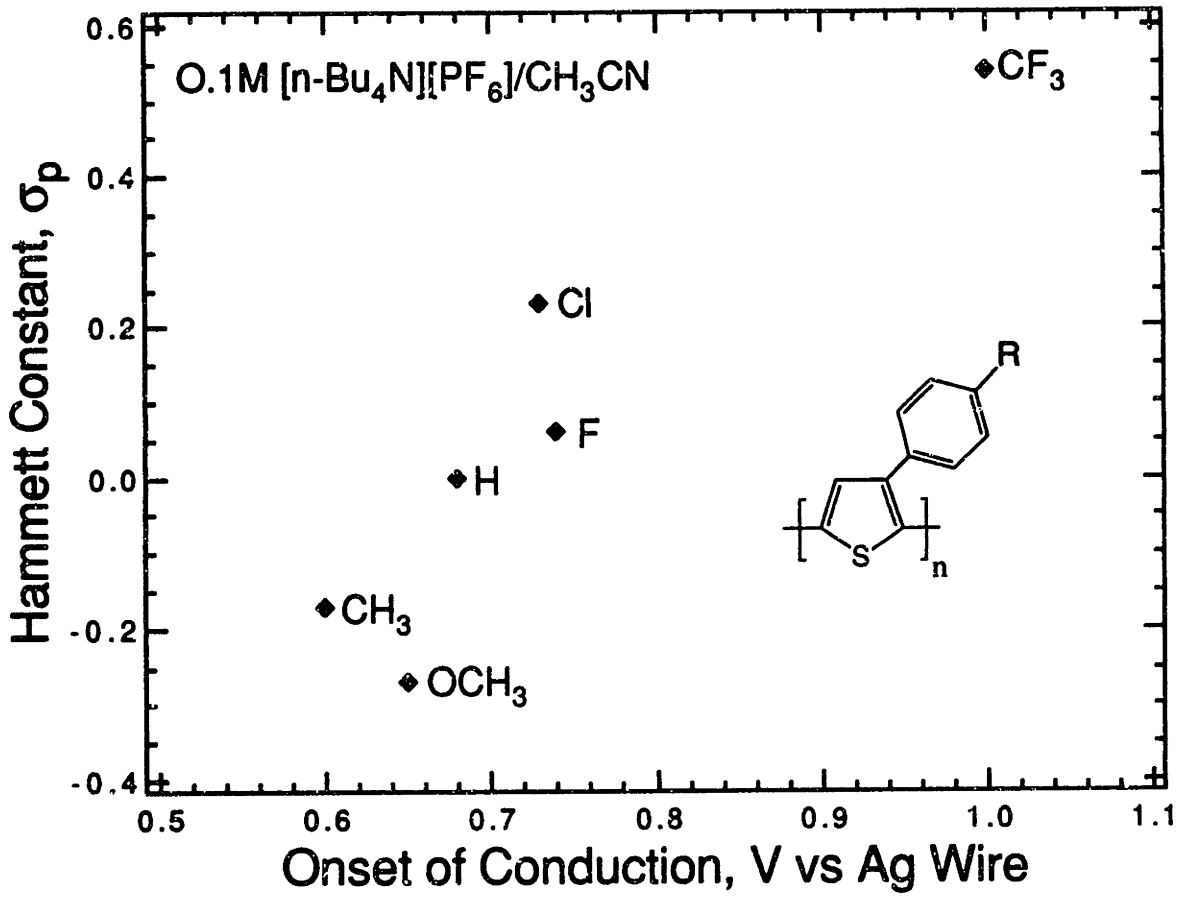

Figure 3. Hammett constant (σ_p) vs. potential for onset of conduction for para-substituted poly(3-phenylthiophene)

what is reported about other polymer systems in the literature,[8,33] it is clear that the phenyl ring and the thiophene will not be coplanar. Since the steric influence of the phenyl ring varies with the degree of coplanarity of the thiophene and phenyl rings, the effect of a para-substituent which changes that degree of coplanarity exerts a steric as well as an electronic effect on potential for onset of conduction since the degree of coplanarity between thiophene rings influences oxidation potential.[10,33] Further, the greater the coplanarity of the thiophene and phenyl rings, the more strongly the resonance effect of a given para-

substituent is communicated to the thiophene backbone. According to this precept, the electronic character of a substituent is transmitted to the thiophene backbone in proportion to its tendency to bring about greater or less coplanarity of the phenyl ring with the thiophene ring it is attached to. Electron-withdrawing substituents on the phenyl ring should bring about greater coplanarity of the rings to allow the electron-rich thiophene π-system to compensate for depletion of the phenyl π-system by the withdrawing group. Donating substituents, on the other hand, may not provide enough benefit to overcome the steric

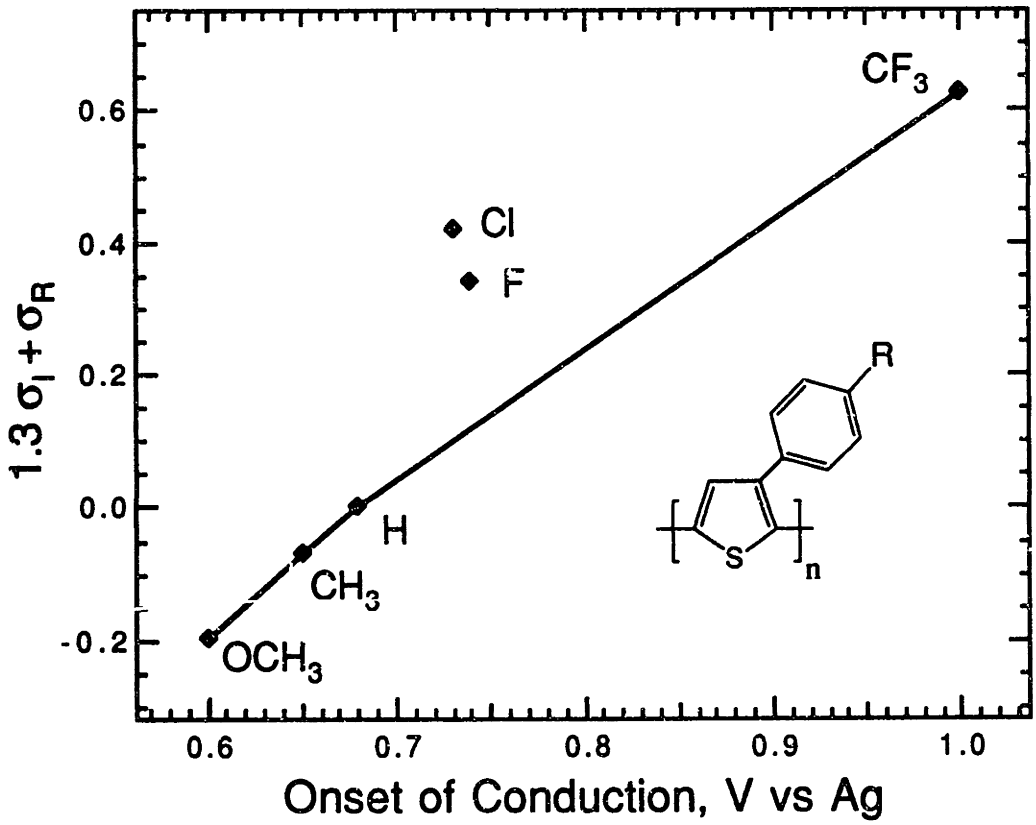

Figure 4. Dual substituent parameter equation treatment of potentials for onset of conduction of poly[3-(4-R-phenyl)-thiophene] derivatives.

unfavorability of moving toward greater coplanarity. A improved fit to the data is obtained by using a dual substituent parameter approach[34,35] which allows for separate coefficients for resonance and inductive effects. Instead of the usual Hammett equation, an equation of the type shown, equation (1), is used. Figure 4 shows a plot of the dual substituent

$$\log(k/k_0) = \rho_I\sigma_I + \rho_R\sigma_R^0 \qquad (1)$$

parameter sum against potential for onset of conduction with coefficients of $\rho_I = 1.3$ and $\rho_R = 1$. While a set of coefficients bringing the chloro and fluoro derivatives more in line could not be found, it was possible to obtain a very good fit for the remaining points with the dual substituent parameter approach.

The conclusions drawn from electrochemical characterization of the derivatives of 3-phenylthiophene which have been synthesized are that a moderately but not strongly electron-withdrawing substituent on the phenyl ring yields the best deposition characteristics, conductivity, and stability. Despite the structural similarity of the monomers, a wide variation in polymerization characteristics was observed which consistent with the importance of electronic effects on monomer reactivity. The para-methoxy and *bis*-trifluoromethyl derivatives may define the limits of what is too donating and too withdrawing a phenyl ring for obtaining good polymerization of a 3-phenylthiophene. Hammett equation substituent constants as well as a dual substituent parameter approach provide a reasonable guide in predicting potentials for onset of conduction but these treatments indicate that quantitative interpretation requires a more sophisticated approach. All of the polymers for which I_D-V_G characteristics could be obtained displayed a finite window of high conductivity with rapid degradation of the polymer in the highly oxidized state.

Electrochemistry of 1,4-dithienylbenzene and 1,4-dithienyl-2,5-difluorobenzene

Both 1,4-dithienylbenzene and the novel 1,4-dithienyl-2,5-difluorobenzene were polymerized from 100 mM solutions from 0.1 M [*n*-Bu_4N]PF_6/CH_2Cl_2. The difluoro derivative, like the parent, polymerized readily to give excellent quality films on microelectrode arrays. Figure 5 shows the cyclic voltammogram and I_D-V_G characteristics

for the parent polymer, which has been shown by IR spectroscopy to be α-linked.[8] Poly(1,4-dithienylbenzene) displayed significant reductive as well as oxidative conduction with surprisingly stability. The conductivity in the reduced state was about two orders of magnitude lower than in the oxidized state which is comparable to what is observed for poly(3-methylthiophene) and polyacetylene.[36,37] The cyclic voltammetry and I_D-V_G characteristic of poly(1,4-dithienyl-2,5-difluorobenzene) are shown in Figure 6. It also displays a window of reductive conductivity as well as the usual window of oxidative conduction. The conductivity and stability of the difluoro derivative was lower than that of poly(1,4-dithienylbenzene) for both oxidative and reductive conduction. The polymer showed some loss of peak drain current upon repeated scanning of its I_D-V_G characteristic. The potential for onset of oxidative conduction is 100 mV positive of that of poly(1,4-dithienylbenzene) and the potential for onset of reductive conduction is also 100 mV positive of the value observed in the parent polymer. Thus, the fluoro substituents lower the energy of the filled π orbitals rendering the poly(1,4-dithienyl-2,5-difluorobenzene) harder to oxidize by easier to reduce than the parent. The lower conductivity of the difluoro derivative compared to the parent may be the result of differences in polymerization, the enhancement of the difference in energy difference between the π-systems of the benzene and thiophene rings by the fluoro groups making hole transport through the difluorophenyl ring more difficult, or a combination of both. Both polymers are the usual polythiophene red in appearance.

From the effects of substitution on potential for onset of conduction in both the 3-phenylthiophene and 1,4-dithienylbenzene systems it is clear that a strong electronic effect is required to obtain a shift of several hundred millivolts. However, the use of strongly donating or strongly withdrawing substituents is limited to those which do not lead to very poor polymerization and low conductivity. It is also clear that the magnitude of the shift can be difficult to predict and in a series of substituents may not come in the order expected. Since the completion of most of the work described in this chapter several reports have

Figure 5. Cyclic voltammetry and I_D-V_G characteristic of poly(1,4-dithienylbenzene).

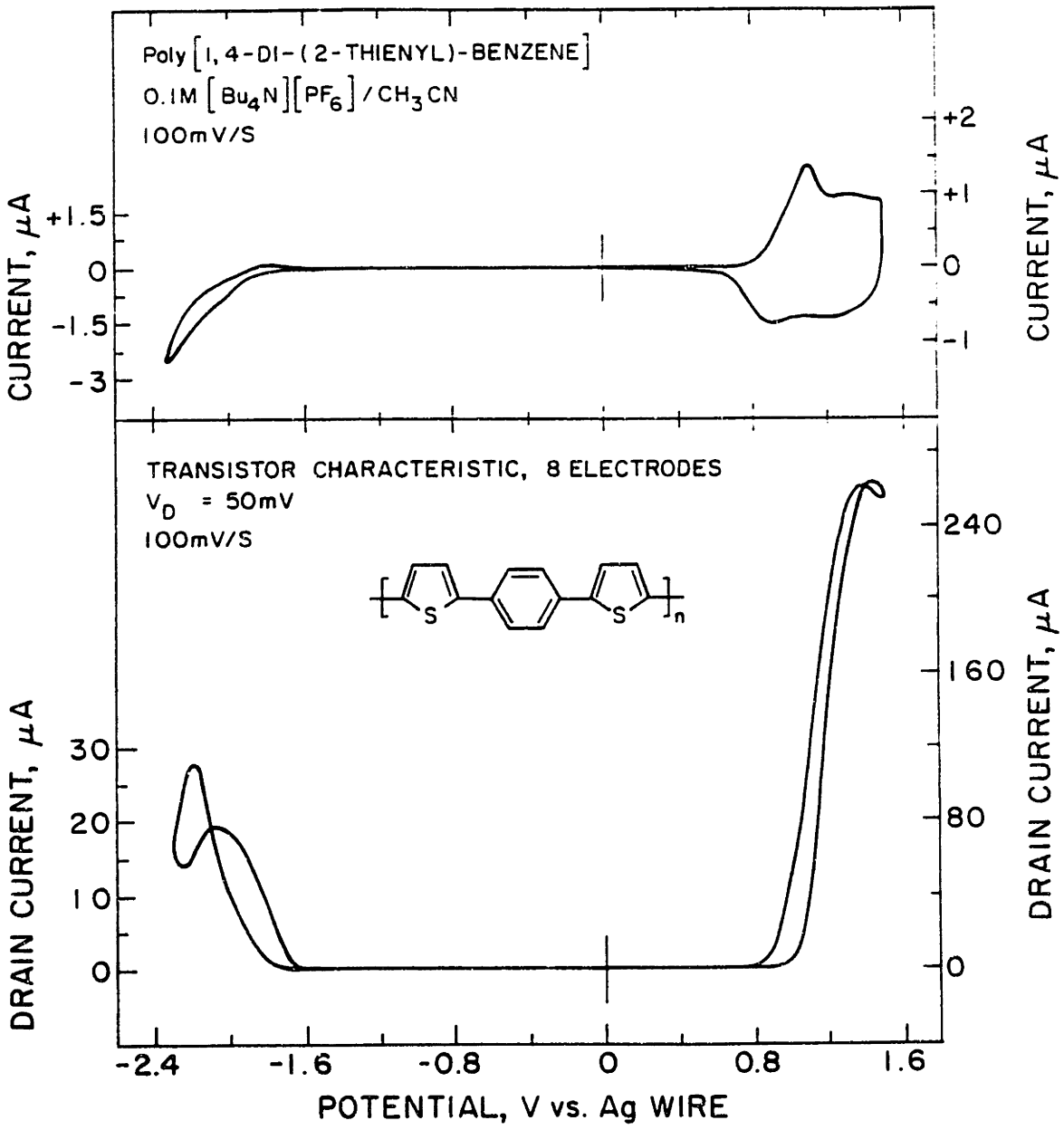
Poly [1, 4-DI-(2-THIENYL)-BENZENE]
0.1M [Bu4N][PF6] / CH3CN
100mV/S
CURRENT, μA
+1.5
0
-1.5
-3
+2
+1
0
-1
CURRENT, μA
TRANSISTOR CHARACTERISTIC, 8 ELECTRODES
VD = 50mV
100mV/S
DRAIN CURRENT, μA
30
20
10
0
240
160
80
0
DRAIN CURRENT, μA
-2.4
-1.6
-0.8
0
0.8
1.6
POTENTIAL, V vs. Ag WIRE

Figure 6. Cyclic voltammetry and I_D-V_G characteristic of poly(1,4-dithienyl-2,5-difluorobenzene).

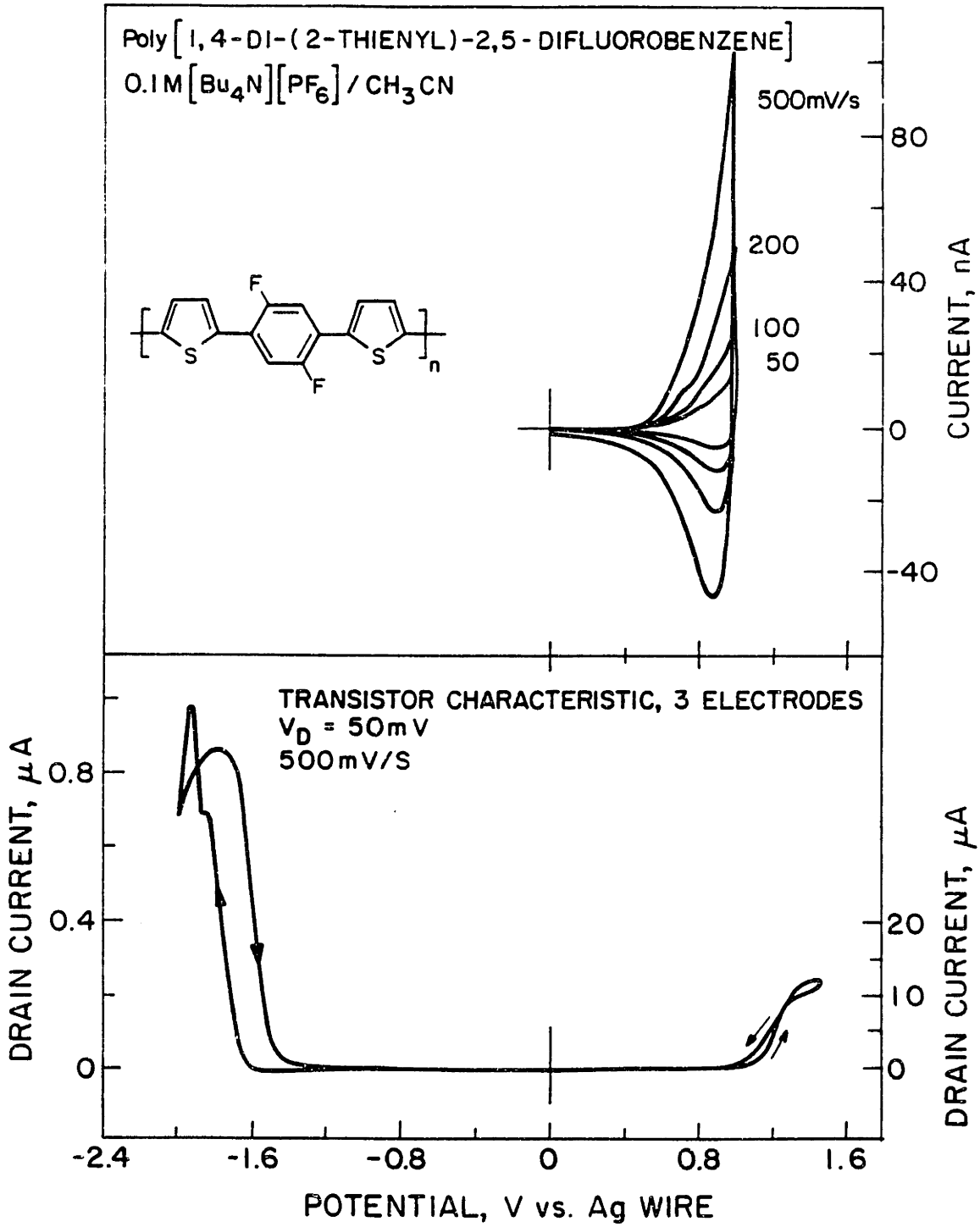
Poly [1,4-DI-(2-THIENYL)-2,5-DIFLUOROBENZENE]
0.1M [Bu4N][PF6] / CH3CN
500mV/s
200
100
50
80
40
0
-40
CURRENT, nA
F
S
S
F
n
TRANSISTOR CHARACTERISTIC, 3 ELECTRODES
VD = 50mV
500mV/S
DRAIN CURRENT, μA
0.8
0.4
0
20
10
0
DRAIN CURRENT, μA
-2.4
-1.6
-0.8
0
0.8
1.6
POTENTIAL, V vs. Ag WIRE

appeared in the literature in which other workers have experienced similar results with other systems. For example, the oxidation potentials of poly(3-methylthiophene), poly(3-(fluoromethyl)-thiophene), poly(3-(difluoromethyl)-thiophene) become progressively higher in that order, as expected but the trifluoromethyl derivative is considerably *easier* to oxidize than either the mono or difluoro derivatives.[6] In another report, a series of substituted poly(benzo[*c*]thiophenes) were prepared and it was found that while variation in substitution had little effect on oxidation potential it had a marked effect on reduction potential.[2]

The polymers characterized and reported here demonstrate that substituents exert a strong effect on monomer reactivity in anodic polymerization. The para-substituted 3-phenylthiophene polymers provide a set of materials with potentials for onset of conduction ranging from 0.60 V to 1.0 V vs Ag and a guide for selecting other substituents to obtain other specific potentials. Both the para-chloro and para-fluoro derivatives of poly(3-phenylthiophene) are suitable for use in a push-pull amplifier. They are each an improvement over the parent polymer in that they are more conducting and have potentials for onset of conductivity about 50 mV higher, which should be ideal. The synthesis, polymerization, and characterization of previously unknown 1,4-dithienyl-2,5-difluorobenzene shows that this 3-ring monomer system will tolerate fluoro substituents and its derivatives bear further examination. Poly(1,4-dithienyl-2,5-difluorobenzene) provides a polymer with the high potential for onset of conduction suitable for demonstration of a complementary inverter gate with polyaniline as the other material.

Experimental

All materials were used as received from Aldrich Chemical except for anhydrous diethyl ether which was used as received from Mallinkrodt, or distilled from sodium benzophenone ketyl. Tetrabutylammonium hexafluorophosphate was recrystallized from ethyl acetate. 3-phenylthiophene (sublimed) was synthesized by Dr. Timothy Miller by the same procedure used below. 1H-NMR spectra were obtained on a Varian XL-300 or Bruker AC-250 spectrometer. Gas chromatography/mass spectrometry was performed on a Hewlett-Packard Model HP5890 Series II Gas Chromatograph equipped with a 5971 Series Mass Selective Detector. Electrochemical measurements were performed using a Pine Instruments model RDE4 bipotentiostat and a Kipp and Zonen model BD90 XY recorder. A silver wire was used as reference electrode and a platinum wire as counterelectrode.

3-(4-chlorophenyl)-thiophene

Into a 250 ml 3-necked round bottom flask equipped with a septum, a magnetic stir bar, and a reflux condenser bearing a gas inlet was placed 50 mg $Ni(Ø_2P(CH_3)_2PØ_2)Cl_2$. The system was purged with dry argon and 50 ml 1.0 M 4-chlorophenylmagnesium bromide in diethyl ether (Aldrich) was added by syringe followed by 6.45 g (40 mM) 3-bromothiophene in 20 ml dry ether. The mixture was stirred at reflux for 24 hours. 1M HCl was added. The layers were separated and the organic phase washed with two portions of 1M HCl. The combined aqueous washes were extracted with two portions of ether and the combined organic phase was dried over Na_2SO_4. Ether was removed by rotary evaporation and the crude product recrystallized from ethanol/water followed by chromatographing over silica gel eluted with 30/70 ether/hexane. The chromatographed product was sublimed to yield 3-(4-chlorophenyl)-thiophene, a white solid which was pure by GC/MS. ^{1}H-NMR ($CDCl_3$, 250 MHz) 7.26 (s), 7.3-7.4 (m), 7.51 (m) MS: m/z (relative abundance) 196(42), 194(100), 158(9), 149(14), 115(18), 114(7), 79(6)

3-(4-methylphenyl)-thiophene

Into a 250 ml 3-necked round bottom flask was placed 55 mg $Ni(Ø_2P(CH_3)_2PØ_2)Cl_2$ along with 8.15 g (50 mM) 3-bromothiophene in 30 ml ether and a stir bar. The flask was fitted with a septum and a condenser bearing an argon inlet and purged. 50 ml (50 mM) 1 M p-tolylmagnesium bromide (Aldrich) was added by syringe. A vigorous reaction accompanied addition of the first 25 ml and the reaction mixture turned deep red-brown. The mixture was stirred at reflux for 36 hours and then hydrolyzed with 1M HCl. The layers were separated and the aqueous phase extracted with two portions of ether. The combined organic layers were dried over Na_2SO_4 and the ether removed by rotary evaporation. The crude product (8.19 g, 94%) was recrystallized from ethanol/water and a portion chromatographed over silica gel eluted with 20% dichloromethane in hexanes. This product was re-chromatographed on silica gel eluted with petroleum ether to yield 3-(4-methylphenyl)-thiophene. m.p. 111-111.5°C (lit. 112[38]) MS: m/z(relative abundance) 175(16), 174(100), 173(54)

3-(4-fluorophenyl)-thiophene

3.27 g (20 mM) 3-bromothiophene in 10 ml ether was placed in a 50 ml 3-necked flask with a stir bar and 20 mg $Ni(Ø_2P(CH_3)_2PØ_2)Cl_2$. The flask was fitted with a septum and a reflux condenser bearing an argon inlet. 10 ml (20 mM) 2M 4-fluorophenylmagnesium bromide (Aldrich) was added slowly by syringe. The amber -colored reaction mixture was brought to reflux. After stirring 28 hours at reflux, the mixture was cooled and hydrolyzed with 1M HCl. The layers were separated and the organic layer was washed with a second portion of 1M HCl. The combined aqueous layers were extracted twice with ether. The combined organic layers were dried over Na_2SO_4. The ether was removed by rotary evaporation affording a yellow solid which was dried under vacuum. Yield was 3.17 g (17.8 mM, 89%). A portion of the product was sublimed

under vacuum to yield a white solid. mass spectrum: m/z(relative abundance) 178(100), 158(3), 146(11), 134(8), 133(39), 120, 107, 89, 83, 69, 57 (low abundances). GC/MS also showed some contamination by bithiophene.

3-(4-methoxyphenyl)-thiophene

Into an oven-dried 100 ml 3-necked flask equipped with a reflux condenser bearing a gas inlet was placed 0.975 g (40 mM) Mg turnings followed by an immediate purge with dry argon. 7.49 g (40 mM) 4-bromoanisole in 12 ml ether was added. The Grignard reaction was slow to initiate and some of the Mg turnings were crushed with a stirring rod and the reaction mixture warmed gently. The reaction accelerated to a moderate rate, but then slowed. The mixture was stirred at reflux for 4 hours but some Mg remained unreacted. 6.53 g (40 mM) 3-bromothiophene in 20 ml dry ether was added with 60 mg $Ni(Ø_2P(CH_3)_2PØ_2)Cl_2$. The reaction mixture was stirred at reflux for 24 hours. Aqueous work-up as above yielded the crude product, 5.02 g (66 %). The crude product was recrystallized from ethanol and a portion of this sublimed to yield a white solid. ^{1}H-NMR (300 MHz, $CDCl_3$) 3.82 (s, 3H, OCH_3); 6.90, 6.93 (d, 2H, phenyl); 7.31-7.36 (m, 3H, thienyl); 7.49, 7.52 (d, 2H, phenyl). MS: m/z(relative abundance) 190(100), 175(71), 147(41)

3-(3-methoxyphenyl)-thiophene

Previous attempts had shown that the required Grignard for this reaction was difficult to make. 5.5 g Mg turnings were stirred under dry Ar for 36 hours in a 100 ml 3-necked flask yielding partial conversion to a gray powder. 30 ml dry ether was added with 0.5 ml 1,2-dibromoethane to further activate the magnesium. 5.72 g (40 mM) 3-bromoanisole was added slowly by syringe. After 2 hours stirring at reflux, an off-white solid mass had formed at the bottom of the flask which prevented the intended cannula transfer of the Grignard solution leaving the excess Mg behind. However, 3-

bromothiophene does not react readily with Mg. A catalytic amount of $Ni(Ø_2P(CH_3)_2PØ_2)Cl_2$ was added followed by dropwise addition of 4.95 g (30 mM) 3-bromothiophene. The reaction mixture became dark brown and the solid mass quickly dissolved. Standard aqueous work-up yielded a yellow oil, 5.85 g (101%). GC/MS showed minor contaminants of methoxybenzene, bithiophene, and dimethoxybiphenyl. The oil was sublimed yielding a white solid which reverted to an oil upon warming the cold finger of the sublimator to room temperature. This product was chromatographed over silica gel eluted with pentane. Bithiophene eluted first followed by the product which moved slowly on the column. The ^{1}H-NMR and MS of this previously unknown derivative of phenylthiophene are shown in Figures 7 and 8.

3-(3,5-bis-trifluoromethylphenyl)-thiophene

0.77 g Mg turnings were placed in a 250 ml 3-necked flask equipped with a stir bar, anaerobic addition funnel, and a reflux condenser bearing an argon inlet. The system was heated to 120 °C and purged with dry argon. 30 ml of dry diethyl ether was placed in the addition funnel and about half of it added to the flask. 8.79 g (30 mM) 3,5-bis(trifluoromethyl)-bromobenzene was added to the addition funnel. The ether solution of the aryl bromide was added dropwise to the flask. Application of heat initiated the Grignard reaction which was vigorous and consumed almost all of the Mg yielding a clear, dark brown solution. 50 mg $Ni(Ø_2P(CH_3)_2PØ_2)Cl_2$ was added followed by 4.89 g (30 mM) 3-bromothiophene in 10 ml dry diethyl ether which was added dropwise by means of the addition funnel. The reaction mixture turned a deep, striking blood-red in color. The reaction mixture was stirred at reflux. After 30 h, GC/MS analysis of the reaction mixture showed remaining starting material. After 48 h, standard aqueous work-up yielded a dark, red-brown oil which was filtered through a plug of silica gel. 1 ml of the crude product was chromatographed over silica gel eluted with pentane but separation from remaining 3-bromothiophene was poor. Since a solvent system yielding acceptable separation of the

Figure 7. ^{1}H-NMR (d_6-acetone, 300 MHz) of 3-(3-methoxyphenyl)-thiophene.

^{1}H-NMR, 300 MHz, d_6-acetone

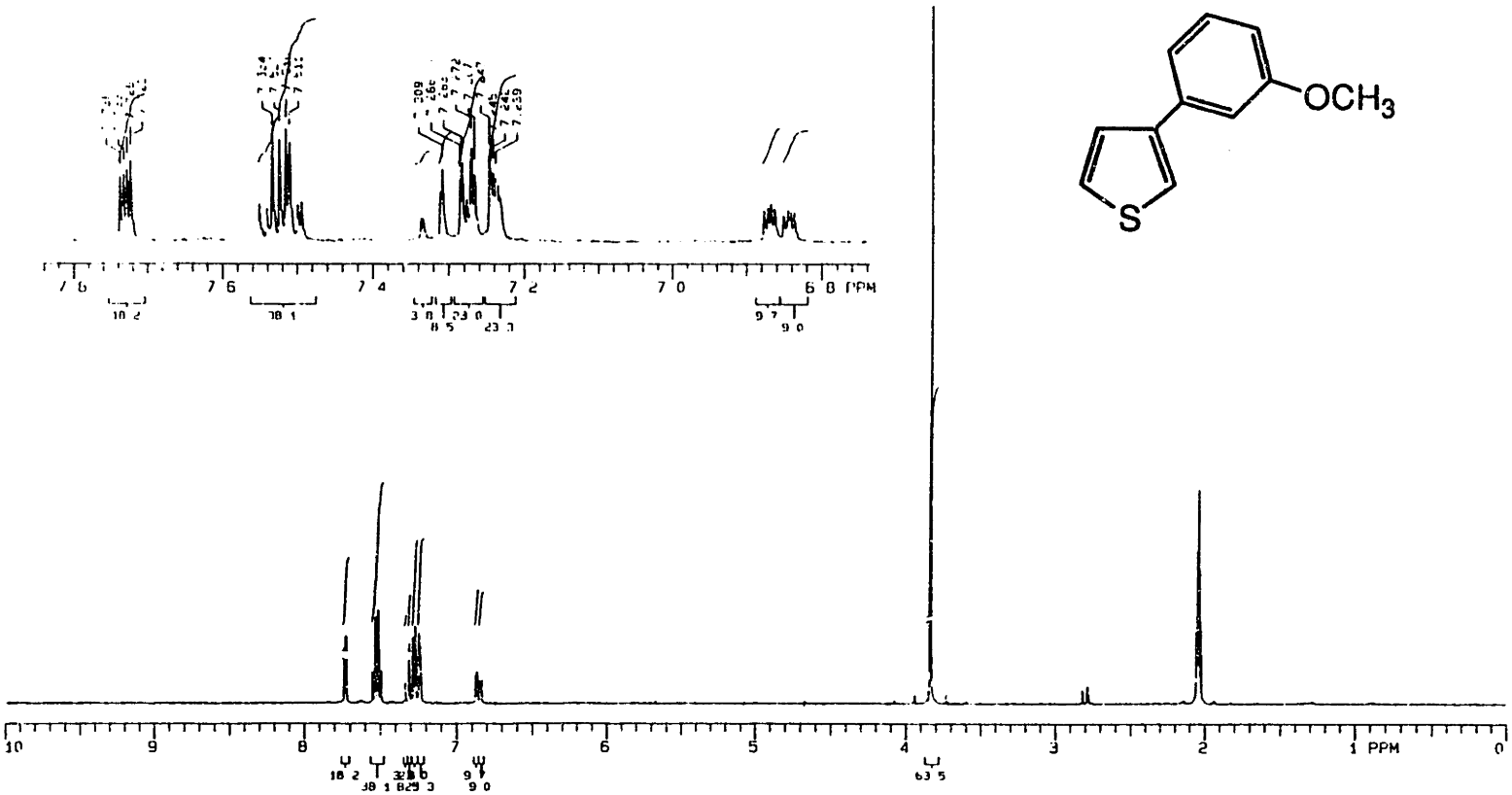

Figure 8. Mass spectrum of 3-(3-methoxyphenyl)-thiophene.

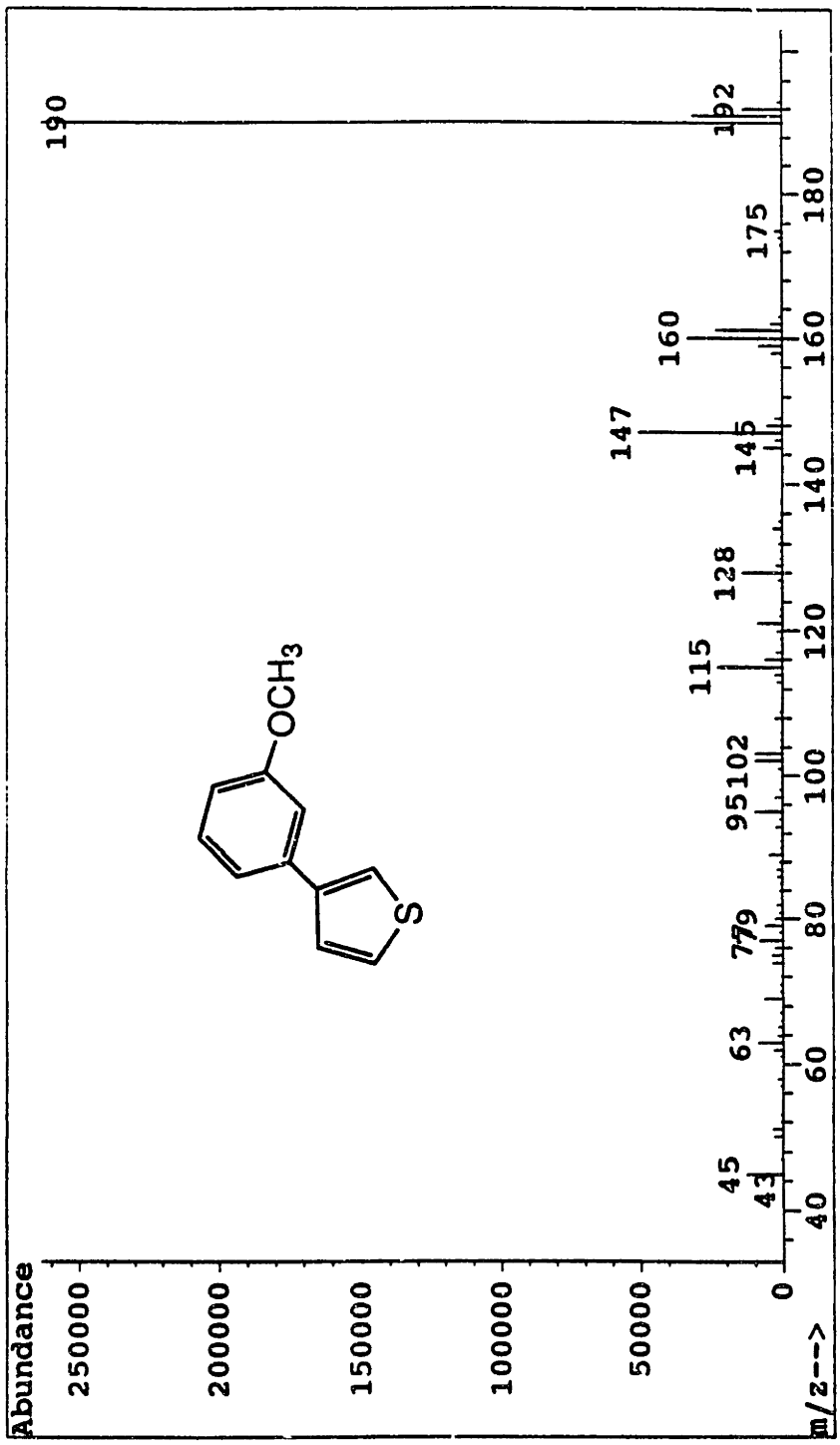
Abundance
250000
200000
150000
100000
50000
0
m/z-->
40
60
80
100
120
140
160
180
43
45
63
77
79
95
102
115
128
145
147
160
175
190
192
OCH3
S

contaminants was not found, the product was sublimed. The sublimed solid (white crystals) was a mixture of 3-(3,5-bis-trifluoromethylphenyl)-thiophene (80%) and tetra(trifluoromethyl)biphenyl (20%) which both sublimed at room temperature. A means of separating the contaminant could not be found, but it was considered to be electrochemically inert. Mass spectrum of 3-(3,5-bis-trifluoromethylphenyl)-thiophene: Figure 9.

3-(3,4,5-trifluorophenyl)-thiophene

0.513 g (21 mM) Mg was placed in a 50 ml 3-necked flask equipped with a stir bar and reflux condenser (glassware was dried in a 125 °C oven prior to use). 2.39 ml (4.22 g, 20 mM) 1-bromo-3,4,5-trifluorobenzene in 11 ml dry diethyl ether was added to the flask. The Grignard reaction initiated within a few minutes and became extremely vigorous. The reaction rate was moderated by cooling with an ice bath. When the reaction had ceased, the mixture was brought to reflux briefly and then 3.29 g (20 mM) 3-bromothiophene was added followed by a catalytic amount of $Ni(Ø_2P(CH_3)_2PØ_2)Cl_2$. When the mixture was brought to reflux again, a vigorous reaction ensued and the gray-brown reaction mixture turned the red-brown color typical of most of these reactions. After 26 hours of stirring at reflux a standard aqueous work-up yielded a yellow-orange oil which analysis by GC/MS showed to contain 3-(3,4,5-trifluorophenyl)-thiophene with a large amount of 3-bromothiophene. Flash chromatography over silica gel eluted with petroleum ether yielded several fractions of a colorless oil still contaminated by 3-bromothiophene which did not separate well. The remainder of the crude product was distilled at aspirator pressure through a short-path distillation apparatus. A product of satisfactory purity was not obtained. While not pursued further, this synthesis could probably be developed to proceed successfully. A longer reaction time, excess Grignard, and larger scale to allow work up by fractional distillation are indicated.

3-(4-trifluoromethylphenyl)-thiophene

7.0 g Mg (0.288 mole) was placed in a 250 ml 3-necked flask with a stir bar. The flask was fitted with a septum, condenser bearing a gas inlet, and an addition funnel. The system was heated to 125 °C under dry Ar purge. After the reaction set-up was allowed to cool, 12.38 g (55 mM) 1-bromo-4-trifluoromethyl-benzene ("4-bromobenzotrifluoride") was placed in the addition funnel with 20 ml dry diethyl ether. This solution was added in portions to the magnesium. A water bath was used to moderate the vigorous reaction which ensued. A deep brown solution was obtained. GC/MS showed complete conversion of the substrate to 4-trifluoromethylphenylmagnesium bromide. A second 3-necked flask was equipped with a septum and a condenser bearing a gas inlet. Approximately 50 mg $Ni(Ø_2P(CH_3)_2PØ_2)Cl_2$ was placed in the second flask with a stir bar. 8.15 g (50 mM) 3-bromothiophene in 20 ml dry diethyl ether was added to the flask. The solution of the Grignard was transferred into the second flask by cannula over several minutes and a water bath was used to moderate the exothermic reaction. The reaction mixture was stirred at reflux for 34 h and then hydrolyzed with 1M HCl. A stubborn emulsion due to presence of a fine brown solid made work up tedious. Repeated washes of the organic layer with 1M HCl and extractions of the aqueous layer with ether were used to accomplish full separation. The ether layer was filtered through a plug of silica gel and dried over Na_2SO_4. Ether was removed by rotary evaporation and the crude solid dried under vacuum at 0°C to suppress sublimation but allow removal of any 3-bromothiophene present. Yield of the crude product was 77 %. Following this, the solid was taken up into hot ethanol. The hot ethanolic solution was filtered through celite and allowed to crystallize overnight in the freezer. Concentration of the mother liquor yielded a second crop. The combined recrystallized product was sublimed in batches to yield a white solid which was pure by NMR and GC/MS. ^{1}H-NMR (d_6-acetone) 7.55-7.64 (m, 2H, phenyl); 7.69-7.76 (m, 2H, phenyl); 7.85-7.96 (m, 3H, thienyl). mass spectrum: m/z(relative abundance) 229(14), 228(100),

209(7), 189 (3), 183(12), 164(5), 158(3), 133(5), 115(9), 114(5), 89(15), 69(4), 58(5), 45(14)

2-thienylmagnesium bromide

24 g (1 mole) Mg turnings was placed into a 500 ml 3-necked flask fitted with a large condenser bearing a gas inlet and a 250 ml anaerobic addition funnel fitted with a septum. The system was heated to 170 °C and evacuated and back-filled with dry Ar four times to eliminate water. 250 ml of dry diethyl ether were placed in the addition funnel and about 50 ml was added to the flask to make room for 44.15 g 2-bromothiophene (0.2708 mol) which was placed in the addition funnel by syringe. The ether solution of 2-bromothiophene was added to the magnesium over 45 min. Once the vigorous Grignard reaction initiated, a gentle reflux was established by adjusting the rate of addition of the substrate. The solution was stirred at reflux for an additional 3 h and then cooled to room temperature. A septum was installed on a neck of the flask and the green-brown solution transferred to a 500 ml round bottom flask, rejecting the solid residue at the bottom of the reaction vessel. GC/MS analysis of a hydrolyzed sample showed the no 2-bromothiophene or bithiophene were present. The Grignard solution is completely stable and was stored in a dry box for future use. [The solution showed full activity 6 months after its preparation]

1,4-di-(2-thienyl)-benzene

3.29 g (10 mM) 1,4-diiodobenzene and 60 mg $Ni(Ø_2P(CH_3)_2PØ_2)Cl_2$ were placed into a 100 ml 3-necked flask with a stir bar. The flask was fitted with a stopper, reflux condenser bearing a gas inlet, and a septum. The system was purged with Ar, 15 ml of dry diethyl ether was added, and 25 ml of 0.9 M 2-thienylmagnesium bromide in diethyl ether was transferred into the flask by cannula. The mixture was stirred at reflux and reaction progress was monitored by GC/MS. After 5 days standard aqueous work-up yielded 1.39 g of orange crystals. (57%). The product was dissolved in CH_2Cl_2, evaporated onto silica

gel, and placed on a column packed with silica gel. The column was eluted with pentane which yielded good separation of 4 bands (starting material, bithiophene, product, heavy reaction residues) but a low R_f value for the product. The product, a white solid, was isolated by rotary evaporation of a large volume of pentane. ^{1}H-NMR (250 MHz, $CDCl_3$) 7.08-7.12 (dd, 2H, thienyl), 7.29-7.35 (4 doublets, 4H, thienyl), 7.63 (s, 4H, phenyl). [for full assignments, see reference 8] MS m/z(relative abundance) 244(10), 243(16), 242(100), 197(10), 121(8), and minor peaks at 184, 171, 152, and 139

1,4-di-(2-thienyl)-2,5-difluorobenzene

In a dry box, 30 ml of 0.9 M 2-thienylmagnesium bromide in diethyl ether was placed in a 100 ml 3-necked flask fitted with a septum, stopper, and a condenser bearing a gas inlet. The assembly was brought out of the dry box and connected to an Ar bubbler. 2.72 g (10 mM) 1,4-dibromo-2,5-difluorobenzene and 40 mg $Ni(Ø_2P(CH_3)_2PØ_2)Cl_2$ were added in 15 ml dry diethyl ether. The reaction mixture turned dark brown. The reaction mixture was stirred at reflux and after 36 hours analysis by GC/MS showed almost no conversion of the substrate. As an experiment, a spatula tip of $Pd(PØ_3)_4$ was added. After 4 days GC/MS showed complete consumption of the starting material and the presence of a peak assigned as 1,4-di-(2-thienyl)-2,5-difluorobenzene. The reaction mixture was filtered through celite and standard aqueous work-up yielded a yellow-brown solid which was recrystallized from methanol. This product was chromatographed over silica gel eluted with pentane yielding white crystals of pure 1,4-di-(2-thienyl)-2,5-difluorobenzene. The latter end of the product band from the column was yellowish in color, but still pure by NMR and GC/MS. Yield of chromatographed product was 1.80 g (65%). The ^{1}H-NMR and GC/MS of this previously unknown compound are shown in Figure 1. ^{1}H-NMR ($CDCl_3$, 300 MHz) 7.11-7.14 (dd, 2H, thienyl), 7.36-7.42 (overlapping multiplets, 4H, thienyl), 7.49,7.51 (d, 2H, phenyl protons, split by fluorines) MS m/z(relative abundance) 280(8), 279(16), 278(100), 233(16), and minor peaks as shown, Figure 1.

References

1. Ono, N.; Hironaga, H.; Simizu, K.; Ono, K.; Kuwano, K.; Ogawa, T. *J. Chem. Soc. Chem. Comm.* **1994**, 1019

2. King, G.; Higgins, S. J. *J. Chem. Soc. Chem. Comm.* **1994**, 825

3. Ferraris, J. P.; Bravo, A.; Kim. W.; Hrncir, D. C. *J. Chem. Soc. Chem. Comm.* **1994**, 991

4. Rudge, A.; Raistrick, I.; Gottesfeld, S.; Ferraris, J. P. *Electrochimica Acta* **1994**, *39*, 273

4. Berggren, M.; Inganäs, O.; Gustafsson, G.; Rasmusson, J.; Andersson, M. R.; Hjertberg, T.; Wennerström, O. *Nature*, **1994**, *372*, 444

5. McCoy, C. H. and Wrighton, M. S *Chemistry of Materials*, **1993**, *5*, 914

6. Ritter, S. K.; Noftle, R. E.; Ward, A. E. *Chem. Mater.* **1993**, *5*, 752

7. Burn, P. L.; Holmes, A. B.; Kraft, A.; Bradley, D. D. C.; Brown, A. R.; Friend, R. H.; Gymer, R. W. *Nature* **1992**, *356*, 47

8. Reynolds, J. R.; Ruiz, J. P.; Child, A. D.; Nayak, K.; Marynick, D. S. *Macromolecules* **1991**, *24*, 678

9. Gustafsson, G.; Inganäs, O.; Salaneck, W. R.; Laasko, J.; Loponen, M.; Taka, T.; Österholm, J.-E.; Stubb, H.; Hjertberg, T. in *Conjugated Polymers*, Brédas, J. L.; Silbey, R. Eds.; Kluwer Academic Publishers: Boston, 1991; pp 315-362

10. Lemaire, M.; Garreau, R.; Delabouglise, D.; Roncali, J.; Youssoufi, H. K.; Garnier, F. *New J. Chem.* **1990**, *14*, 359

11. Rehahn, M.; Schlüter, A.-D.; Wegner, G. *Polymer*, **1989**, *30*, 1054

12. Rühe, J.; Ezquerra, T. A.; Wegner, G. *Synth. Met.* **1989**, *28*, C177

13, Brédas, J.-L. *Synth. Met.* **1987**, *17*, 115

14. Patil, A. O.; Ikenoue, Y.; Wudl, F.; Heeger, A. J. *J. Am. Chem. Soc.* **1987**, *109*, 1858

15. Feast, W. J.; Millichamp, I. S.; Friend, R. H.; Horton, M. E.; Phillips, D.; Rughooputh, S. D. D. V.; Rumbles, G. *Synth. Met.* **1985**, *10*, 181

16. Bureau, J. M.; Gazard, M.; Champagne, M.; Dubois, J. C. *Mol. Cryst. Liq. Cryst.* **1985**, *118*, 235

17. Waltman, R. J.; Diaz, A. F.; Bargon, J. *J. Electrochem. Soc.* **1984**, *131*, 1452

18. Tourillon, G.; Garnier, F. *J. Electroanal. Chem.* **1984**, *161*, 51

19. Edwards, J. H.; Feast, J. W. *Polymer* **1980**, *21*, 595

20 Diaz, A. F.; Bargon, J. In *Handbook of Conducting Polymers*; Skotheim, T. A., Ed.; Marcel Dekker: New York, 1986; Chapter 3

21. Waltman, R. J.; Bargon, J. *Can. J. Chem.* **1986**, *64*, 76

22. Roncali, J. *Chem. Rev.* **1992**, *92*, 711

23. Yumoto, Y.; Yoshimura, S. *Synth. Met.* **1985**, *13*, 185. Roncali, J.; Garnier, F.; Lemaire, M.; Garreau, R. *Synth. Met.* **1986**, *15*, 323.

24. Waltman, R. J.; Bargon, J. *Tetrahedron*, **1984**, *40*, 3963

25. March, J. *Advanced Organic Chemistry, 4th ed.*, John Wiley & Sons: New York, **1992**. a) p.625 b) p. 278-286

26. Tamao, K.; Kodama, S.; Nakajima, I.; Kumada, M. *Tetrahedron*, **1982**, *38*, 3347

27. Monthéard, J.-P.; Delzant, J.-F. *Synth. Commun.* **1984**, *14*, 289

28. Pelter, A.; Maud, J. M.; Jenkins, I.; Sadeka, C. Coles, G. *Tet. Lett.* **1989**, *30*, 3461

29. Zakharkin, L. I.; Okhlobystin, O. Yu.; Bilevitch, K. A. *J. Organomet. Chem.* **1964**, 2, 309

30. Tanaka, S.; Sato, M.-A.; Kaeriyama, K. *J. Macromol. Sci. Chem.* **1987**, *A24*, 749

31. Mitsuhara, T.; Tanaka, S.;Kaeriyama, K. *Makromol. Chem.* 1988, *189*, 1755

32. Dean, J. A. *Handbook of Organic Chemistry* McGraw-Hill: New York, 1987. p. 7-2 to p. 7-9

33. Brédas, J. L.; Street, G. B.; Thémans, B.; André, J. M. *J. Chem. Phys.* **1985**, *83*, 1323

34. Ehrenson, S.; Brownlee, R. T. C.; Taft, R. W. *Prog. Phys. Org. Chem.* **1973**, *10*, 1

35. Bromilow, J.; Brownlee, R. T. C.; Lopez, V. O.; Taft, R. W. *J. Org. Chem.* **1979**, *44*, 4766

36. Ofer, D.; Park, L .Y.; Schrock, R. R.; Wrighton, M. S. *Chem. Mater.* **1991**, *3*, 573

37. Crooks, R. M.; Chyan, O. M. R.; Wrighton, M. S. *Chem. Mater.* **1989**, *1*, 2

38. Chrzaszczewska, A. *Rocz. Chem.* **1925**, *5*, 33; *C.A.* **1926**, *20*, 1078

Chapter 6

Electrophilic Substitution Reactions of Conjugated Organic Polymers

General Abstract

The reactivity of conjugated organic polymers in electrophilic substitution reactions was examined for aniline, pyrrole, and thiophene-based polymers. Polyaniline displays potential-dependent nucleophilicity in its reaction with trifluoroacetic anhydride and is acylated at nitrogen to yield an insulating, electroinactive polymer. Conducting polyaniline is regenerated by basic hydrolysis. Polypyrrole also displays potential-dependent nucleophilicity in its reaction with trifluoroacetic anhydride but is acylated at the b-carbons to yield a conducting and electroactive polymer which displays onset of conduction 0.5 V positive of polypyrrole. Poly(3-methylthiophene) is chlorinated rapidly by Cl_2 resulting in a striking shift in its potential for onset of conduction from 0.43 to 1.18 V vs. Ag. The chlorinated polymer shows unusually stable electrochemistry to high anodic potentials in CH_3CN. The chlorination of polythiophene, poly(3,4-dimethylthiophene), and polyselenophene were also examined. A microelectrochemical memory device, based on the selective, potential-controlled trifluoroacetylation of polyaniline as the write step and basic hydrolysis to restore conductivity of the acylated memory elements as the erase step is demonstrated. Using the potential-dependent trifluoroacetylations of polyaniline and polypyrrole and the chlorination of poly(3-methylthiophene), the preparation of a 3-state microelectrochemical transistor and a push-pull amplifier with chemically tuned overlap and matched peak conductivity of I_D-V_G characteristics are demonstrated.

Section 6.0
General Introduction

Conjugated organic polymers conduct electricity as a result of their extended π-systems and most of the attention devoted to these materials has focused on their charge transport properties and the consequences of those properties for electronic and optical devices. Many families of polymer architectures have been explored and many more can be envisioned, thus making the synthesis and derivatization of those architectures a major component of exploring polymer electronic devices. However, the extended π-system and electrical conductivity of conjugated polymers makes them an unusual and interesting class of substrates for chemical reactions. Because the population of the π manifold of a conjugated organic polymer is varied by oxidation and reduction, the π electron density along the backbone can be directly controlled electrochemically. Thus, conducting polymers represent a class of substrates where π electron density can be tuned over a continuos range. This chapter is divided into four sections beginning with this section which provides a general introduction. Section 6.1 and 6.2 describe the trifluoroacetylation and potential-dependent nucleophilicity of polyaniline and polypyrrole, respectively. Section 6.3 reports the chlorination of poly(3-methylthiophene) and other thiophene polymers, and section 6.4 demonstrates the versatility of these reactions in the preparation of novel microelectrochemical electronic devices created by chemically tuning polymer electrical characteristics via the *in-situ* acylation and halogenation of the conducting polymers serving as the device-active materials. Our interest in the reactivity of conducting polymer began with the observation that polyaniline appeared to react readily with trifluoroacetic anhydride *but only in the reduced state.* We found the possibility of directly controlling reactivity by altering the electronic nature of a substrate at the molecular level with a dial on an instrument a fundamentally interesting and intriguing opportunity.

Initially, it might be assumed that a conducting polymer substrate would display low reactivity due to difficulty of reacting species diffusing into the polymer, steric hindrance of the reaction sites by adjacent rings, and the fact that the most reactive sites of the component ring system have already been utilized to form the ring to ring bonds of the

polymer chain. While these factors may sometimes be significant limitations, the reactions described in sections 6.1-6.3 demonstrate conducting polymer substrates undergoing facile substitutions. Indeed, initial assumptions that reactivity would be low led to bludgeoning of the unfortunate polymer with unduly aggressive conditions. The substrates polyaniline, polypyrrole, poly(N-methylpyrrole), poly(3-methylthiophene), polythiophene, poly(3,4-dimethylthiophene) and polyselenophene were examined. The aniline, pyrrole, and thiophene families of polymers represent three varied classes of reactivity by analogy with their monomeric analogs, heteroatom reactivity and π-aromaticity being different for each family. Electrophiles employed were primarily trifluoroacetic anhydride and molecular chlorine, but also examined were the milder tri, di, and monochloroacetic anhydrides, acetic anhydride, bromine, the powerful xenon difluoride, and standard Friedel-Crafts alkylating and acylating conditions. The two main reactions which are the subject of this chapter, acylation and chlorination, are classic organic transformations which have each been studied for well over a century. While there is little data on conducting polymer reactivity available from the literature, there is of course a large body of information about the reactivity of the ring systems the conducting polymer backbones are based on. The aromaticity, reactivity, and substitution patterns of 5-membered heterocycles is introduced in sections 6.2 and 6.3.

The changes in electrical characteristics induced by electrophilic substitution reactions were of prime interest for molecule-based devices. The molecular, rather than solid-state, nature of conducting polymers results in a strong link between the composition and structure of these materials and their properties. While silicon, for example, is a single material with a specific band gap, *p-n* junction potential, and other such inherent fixed properties, a conducting backbone such as polythiophene can be viewed as a foundation which can be extensively modified by adding any of the wide array of substituents polythiophene tolerates to produce a very diverse battery of results. Such substitution

changes the properties of the backbone and with sufficient understanding of these effects it becomes possible to intentionally alter or "chemically tune" polymer behavior.

Many derivatives of polymers of the thiophene, aniline, acetylene, pyrrole, phenylene, and phenylene vinylene families have been prepared and characterized in an effort to understand the nature of substitution effects in these materials[1-9] and to modify polymer behavior.[10-20] Introduction of solubility and processablility,[10-15] chemical tuning of optical properties for light emitting diodes,[15-17] chemical tuning of electrical characteristics,[6,18-20] and introduction of chemical sensistivity[21,22] are some examples of exploiting this flexibility in conducting polymer behavior. In Chapter 4, three families of novel microelectrochemical devices were presented which all require a specific degree of overlap between the windows of conductivity of two different conducting polymers. The greater the range and precision with which the electrical characteristics of polymers can be tuned, the broader and more sophisticated are the electrical functions which can be achieved.

The conventional approach to different polymers involves synthesis of a number of monomers bearing different substituents followed by chemical or electrochemical polymerization. Substituents on the monomer exert not only the steric and electronic effects in the resulting polymer but also affect the polymerization reaction by which the material is prepared.[23-25] As a result, compatibility of a substituted monomer with good polymerization is an important consideration. In oxidative polymerization, substituents which are electron withdrawing, sterically demanding, or reactive toward the radical cation of the monomer can preclude efficient monomer coupling resulting in poor polymerization or a complete lack of it.[23,24] Therefore, certain functionalities cannot be introduced prior to polymerization. Examples of these limitations ranging from monomer synthesis difficulties, to lack of polymerizability, to wide variation in conductivity of derivatives of the same backbone can be found in Chapter 5 which describes the synthesis and characterization of derivatives of 3-phenylthiophene and of 1,4-dithienylbenzene and their polymers.

An alternative to introduction of substituents at the monomer stage is substitution by direct reaction of a polymer with a suitable reagent *after* polymerization. This approach is attractive from several standpoints. Since the polymer has already been formed, substituents which are detrimental or incompatible with polymerization can be introduced. Also, introducing a substituent onto an already-formed backbone bypasses speculation on what effects the introduction of a substituent has on the polymerization reaction versus charge transport in the polymer. Further, in tailoring the properties of a polymer by substitution it is sometimes desirable to be able introduce an effect to varying degrees. This can be accomplished by controlling the fraction of available sites on the backbone which are substituted, Scheme I.

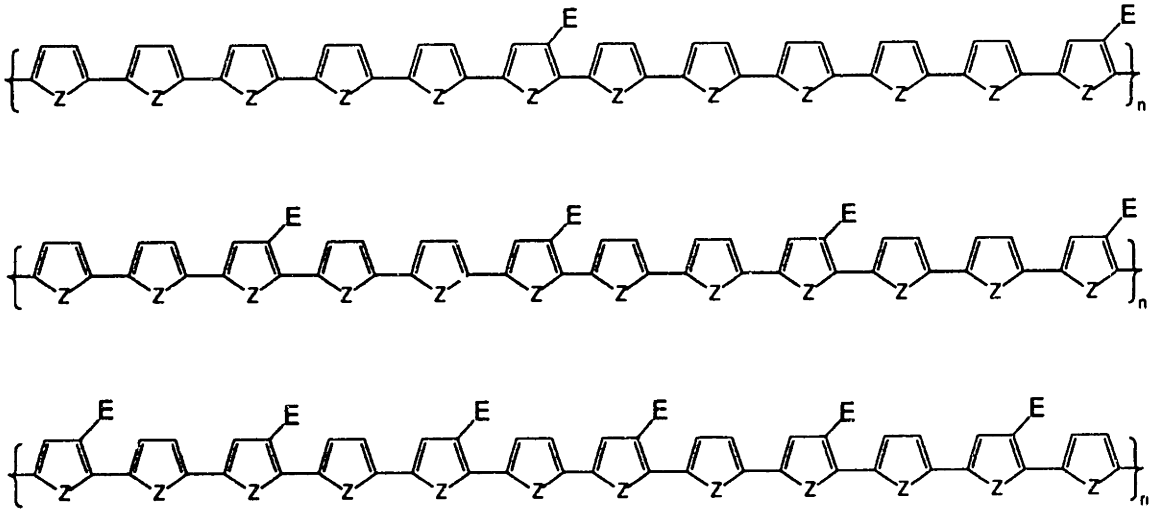

Scheme I. Generalized representation of substitution to less than one group per repeat unit.

In the conventional approach where a monomer provides only the fully substituted (one group per repeat unit) polymer, different substituents are used to provide, say, a more or less electron-withdrawing effect. Fractional substitution by direct reaction on the polymer allows a single substituent to provide a range of effect by introducing a greater or lesser number of them. The potential for onset of conductivity is a parameter where access to a

continuos range of tuning is more useful than a discrete set of polymers with specific turn-on potentials.

Reactions on conducting polymers in which new substituents are introduced onto the polymer backbone have not been investigated to a very great extent, but some interesting examples include the methylation of polyaniline,[26] a preliminary report of the sulfonation and nitration of polyphenylene,[27] a two-step reaction on poly(3-methylthiophene) to introduce a thiol functionality (a group too easily oxidized to survive polymerization)[28] and ligand substitution reactions on metal centers incorporated into thiophene[29] and pyrrole[30] polymers. While full characterization of the product of a reaction on polymeric substrate can be more difficult than for a monomeric substrate, these reports point to a number of exciting possibilities in this relatively unexplored area. We now report direct electrophilic substitution reactions on conducting polymer substrates which display potential-dependent nucleophilicity and demonstrate direct chemical tuning of electrical characteristics, and the application of that tuning to the preparation of the three families of microelectrochemical devices developed and characterized in Chapter 4.

References

1. *Handbook of Conducting Polymers*; Skotheim, T. A., Ed.; Marcel Dekker: New York, 1986

2. *Conjugated Polymers*, Brédas, J. L.; Silbey, R. Eds.; Kluwer Academic Publishers: Boston, 1991

3. Diaz, A. F.; Bargon, J. In *Handbook of Conducting Polymers*; Skotheim, T. A., Ed.; Marcel Dekker: New York, 1986; Chapter 3

4. Reynolds, J. R.; Ruiz, J. P.; Child, A. D.; Nayak, K.; Marynick, D. S. *Macromolecules* **1991**, *24*, 678

5. Lemaire, M.; Garreau, R.; Delabouglise, D.; Roncali, J.; Youssoufi, H. K.; Garnier, F. *New J. Chem.* **1990**, *14*, 359

6. Ritter, S. K.; Noftle, R. E.; Ward, A. E. *Chem. Mater.* **1993**, *5*, 752

7. Rühe, J.; Ezquerra, T. A.; Wegner, G. *Synth. Met.* **1989**, *28*, C177

8. Roncali, J. *Chem. Rev.* **1992**, *92*, 711 and references therein.

9. Tourillon, G.; Garnier, F. *J. Electroanal. Chem.* **1984**, *161*, 51

10. Gustafsson, G.; Inganäs, O.; Salaneck, W. R.; Laasko, J.; Loponen, M.; Taka, T.; Österholm, J.-E.; Stubb, H.; Hjertberg, T. in *Conjugated Polymers*, Brédas, J. L.; Silbey, R. Eds.; Kluwer Academic Publishers: Boston, 1991; pp 315-362

11. Rehahn, M.; Schlüter, A.-D.; Wegner, G.; Feast, W. J. *Polymer*, **1989**, *30*, 1054

12. Patil, A. O.; Ikenoue, Y.; Wudl, F.; Heeger, A. J. *J. Am. Chem. Soc.* **1987**, *109*, 1858

13. Feast, W. J.; Millichamp, I. S.; Friend, R. H.; Horton, M. E.; Phillips, D.; Rughooputh, S. D. D. V.; Rumbles, G. *Synth. Met.* **1985**, *10*, 181

14. Edwards, J. H.; Feast, W. J. *Polymer* **1980**, *21*, 595

15. Burroughes, J. H.; Bradley, D. D. C.; Brown, A. R.; Marks, R. N.; Mackay, K.; Friend, R. H.; Burns, P. L.; Holmes, A. B. *Nature*, **1990***347*, 539

16. Burn, P. L.; Holmes, A. B.; Kraft, A.; Bradley, D. D. C.; Brown, A. R.; Friend, R. H.; Gymer, R. W. *Nature* **1992**, *356*, 47

17. Berggren, M.; Inganäs, O.; Gustafsson, G.; Rasmusson, J.; Andersson, M. R.; Hjertberg, T.; Wennerström, O. *Nature*, **1994**, *372*, 444

18. Ono, N.; Hironaga, H.; Simizu, K.; Ono, K.; Kuwano, K.; Ogawa, T. *J. Chem. Soc. Chem. Comm.* **1994**, 1019

19. King, G.; Higgins, S. J. *J. Chem. Soc. Chem. Comm.* **1994**, 825

20. Rudge, A.; Raistrick, I.; Gottesfeld, S.; Ferraris, J. P. *Electrochimica Acta* **1994**, *39*, 273

21. Chapter 7, this Thesis, pH gating of poly(2,5-dithienylpyridine)

22. M. J. Marsella, P. J. Carroll, T. M. Swager, *J. Am. Chem. Soc.* **116**, 9347 (1994)

23. Diaz, A. F.; Bargon, J. In *Handbook of Conducting Polymers*; Skotheim, T. A., Ed.; Marcel Dekker: New York, 1986; Chapter 3

24. Roncali, J. *Chem. Rev.* **1992**, *92*, 711 and references therein.

25. Roncali, J.; Garnier, F.; Lemaire, M.; Garreau, R. *Synth. Met.* **1986**, *15*, 323

26. Manohar, S. K.; MacDiarmid, A. G. *Synth. Met.* **1989**, *29*, E349

27. Rubinstein, I. *J. Electrochem. Soc.* **1983**, *130*, 1506

28. Fabre, P.-L.; Dalger, A. *J. Chem. Research (S)* **1991**, 16 *(M)* **1991**, 0255

29. Wolf, M.; Wrighton, M. S. *Chem. Mat.* **1994**, *6*, 1526

30. Ochmanska, J.; Pickup, P. *Can. J. Chem.* **1991**, *69*, 653

Section 6.1

The Potential-Dependent Nucleophilicity of Polyaniline

Abstract

The reaction of electrode-confined polyaniline with trifluoroacetic anhydride in acidified acetonitrile giving insulating and electroinactive trifluoroacetylated polyaniline has been studied by electrochemistry, reflectance IR, and microelectrochemistry. Variation of electrochemical potential from 0.2 V (reduced, most reactive) to 0.6 V (oxidized by 0.5 electrons per repeat unit, unreactive) vs SCE allows control of the reaction rate. Reaction of trifluoroacetic anhydride with aniline oligomers *N*-phenylphenylenediamine and *N, N'*-diphenylphenylenediamine is summarized. Reflectance IR following the potential-dependent growth of CO and CF_3 peaks for macroelectrode films of polyaniline treated with trifluoroacetic anhydride showed similar potential dependence of reactivity as conductivity measurements during trifluoroacetylation of polyaniline-derivatized microelectrode arrays. Polyaniline trifluoroacetylation was accompanied by a symmetric contraction of the potential window of electroactivity and conductivity, and eventual elimination of all conductivity. Trifluoroacetylation of polyaniline terminal amines, rapid at all potentials, does not detectably affect conductivity. Also examined by electrochemistry were the reactions of polyaniline with other anhydrides resulting in the reactivity order $(F_3CCO)_2O > (Cl_3CCO)_2O > (H_2ClCCO)_2O > (HCl_2CCO)_2O >> (H_3CCO)_2O$. IR through polyaniline electrodeposited onto optically transparent Au electrodes shows that essentially complete loss of polyaniline electroactivity occurs when ≈25% of nitrogens are trifluoroacetylated. Electroactivity and conductivity of trifluoroacetylated polyaniline may be recovered by hydrolysis in $K_2CO_3/CH_3OH/H_2O$ solution to regenerate polyaniline. A microelectrochemical erasable-programmable-read-only-memory device has been prepared and characterized in which three polyaniline transistors served as memory elements and selective trifluoroacetylation allowed writing of any 3-bit binary configuration of on and off states. Hydrolytic de-acylation served as the erase process. A circuit was developed to provide the appropriate digital output. 5 sequential write/read/erase/rewrite steps were carried out on the device.

Introduction

We present results demonstrating electrochemical potential control over the reactivity of the conjugated organic conductor polyaniline. Polyaniline reacts with trifluoroacetic anhydride resulting in partial *N*-trifluoroacetylation. In this reaction, polyaniline displays a continuum of states of nucleophilicity determined by the degree of oxidation of the polymer, allowing electrochemical potential control of the rate of trifluoroacetylation, and thus control of polymer conductivity and electroactivity. In addition, the *N*-trifluoroacetyl moieties may be hydrolyzed to re-form the original conducting polymer.

Polyaniline,[1-6] while insulating in its colorless polybenzenoid "leucoemeraldine" reduced state, becomes conducting in acidic media when partially oxidized. The "emeraldine salt" state of polyaniline, corresponding to oxidation by 0.5 electrons per repeat unit, exhibits maximum conductivity. Further oxidation to 1 electron per repeat unit gives

Scheme 1

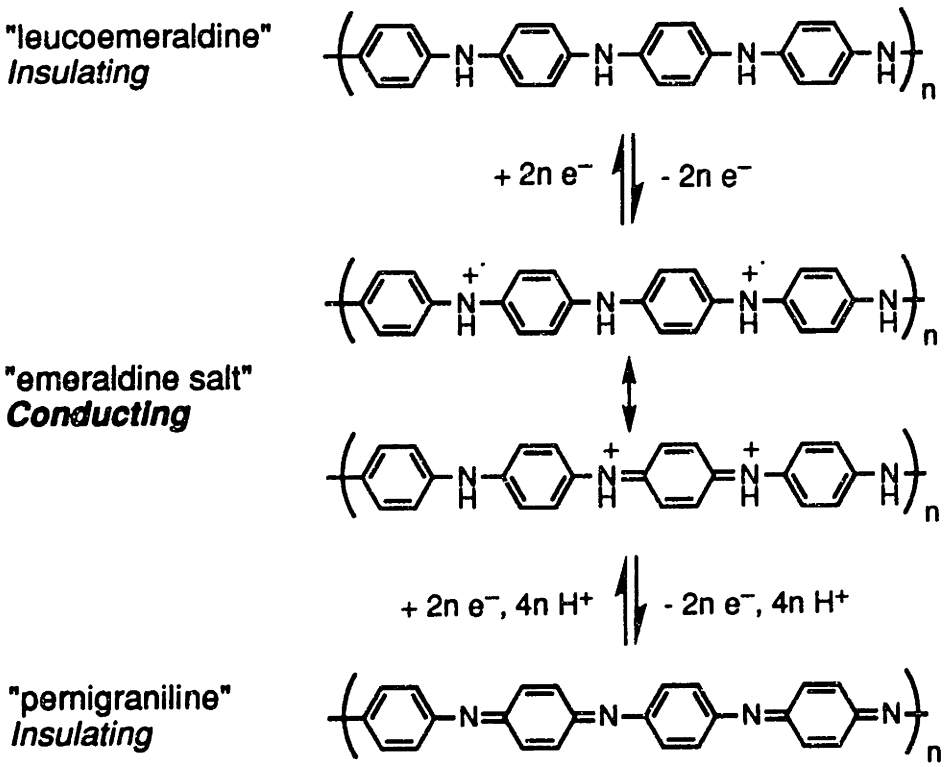

the insulating blue-black polyquinoid "pernigraniline" state, which in all but the most anhydrous non-nucleophilic media is deprotonated.[7-13] Polyaniline is a rugged polymer which is distinguished by stability over its entire finite window of high conductivity.[9] Electrochemical potential control of the oxidation state of a conducting polymer allows the electron density along the backbone to be varied continuously leading to the possibility of tuning reactivity of the polymer substrate by means of an applied voltage. Since polyaniline supports positive charge primarily by residence on the nitrogens,[13] electron density at those sites is expected to be strongly coupled to the electrochemical potential of the polymer. We became interested in the nucleophilicity of polyaniline upon observing that its peak conductivity decayed in the presence of trifluoroacetic anhydride if the polymer was held reduced but was completely stable when highly oxidized. Our interest in molecules possessing electrochemically tunable reactivity and in the connection between molecular structure and polymer electrical characteristics led the author and Ivan Lorkovic to investigate the potential-dependent reaction of polyaniline with trifluoroacetic anhydride using a combination of electrochemistry and infrared spectroscopy.[14]

Results and Discussion

Reactivity of aniline oligomers. To assess the merit of our hypothesis that the degradation of electrochemistry of polyaniline exposed to trifluoroacetic anhydride was due to nucleophilic attack of the polymer nitrogens on the anhydride, the reactivity towards trifluoroacetic anhydride of two simple oligomeric analogs to polyaniline, *N*-phenylphenylenediamine, **I**, and *N,N'*-diphenylphenylenediamine, **II** was examined. The results[14,15] are summarized in Scheme 2. Both oligomers reacted quantitatively with Trifluoroacetic anhydride with introduction of the first trifluoroacetyl group occurring quickly followed by slower substitution of the remaining site. Importantly, acylation of the terminal amine in *N*-phenylphenylenediamine occurs first, followed by substitution of the internal nitrogen. In contrast to the reactivity of pyrrole and polypyrrole towards

trifluoroacetic anhydride under similar conditions,[16] there were no products detected resulting from electrophilic aromatic substitution at carbon.

Scheme 2

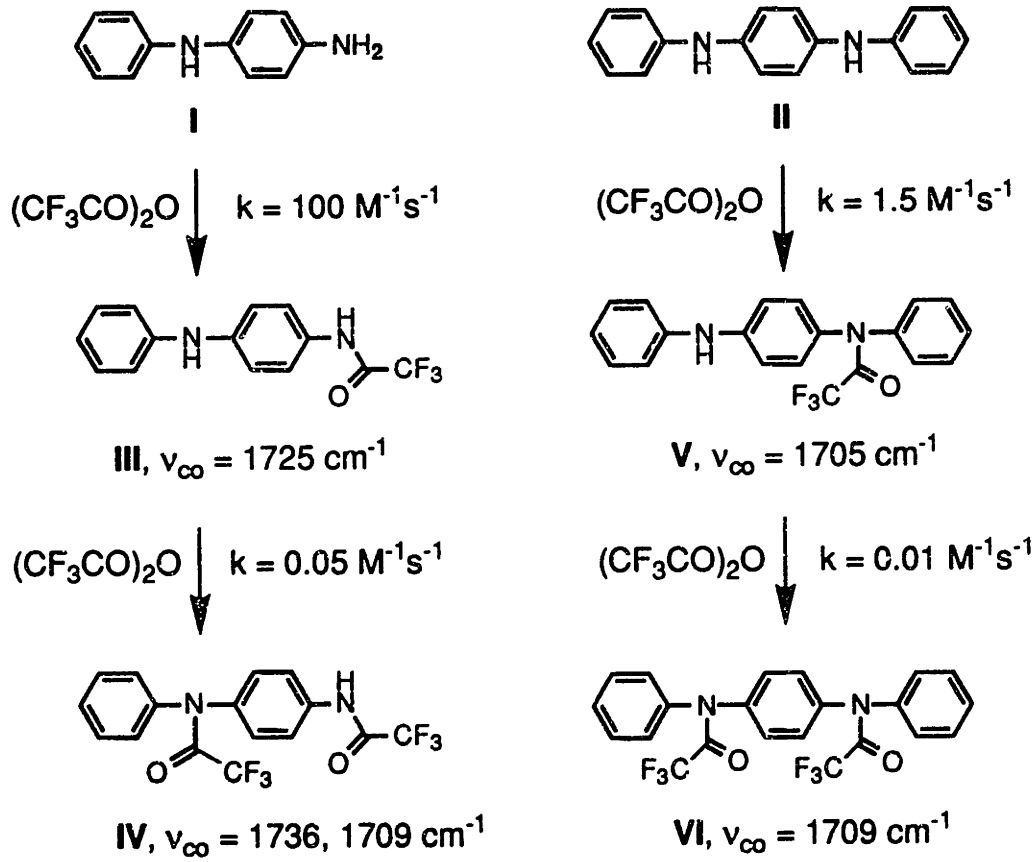

Having established that polyaniline-like species in solution react with trifluoroacetic anhydride at nitrogen, we examined the reaction of electrode-confined polyaniline itself with trifluoroacetic anhydride. To accomplish this, polyaniline was deposited electrochemically onto flat Au macroelectrodes and onto Pt microelectrode arrays. The resulting electrode-confined polymer allowed potential control of the oxidation state of polyaniline during reaction with trifluoroacetic anhydride, and characterization of the reaction product by cyclic voltammetry, specular reflectance FTIR (RIR), and microelectrochemical conductivity measurements.

Figure 1 shows cyclic voltammetry of polyaniline electrodeposited onto two Au macroelectrodes before and after immersion under potential control into a 0.1 M $LiClO_4$/0.2 M CF_3CO_2H/CH_3CN solution containing 1.0 M trifluoroacetic anhydride. The polyaniline held at 0.2 V vs SCE showed loss of most of its voltammetric response (without polymer loss, as demonstrated by RIR (*vide infra*)). When held at 0.5 V, however, polyaniline showed virtually no loss in response. While cyclic voltammetry of macroelectrodes provides a guide to the loss of electroactivity of the polyaniline films, characterization of the polymer by I_D-V_G response is more definitive and revealing. Figure 2 shows the cyclic voltammetry and I_D-V_G of microelectrode-confined polyaniline before and after treatment of the reduced polymer with trifluoroacetic anhydride. Changes in the cyclic voltammogram are not as dramatic as those observed in Figure 1 owing to a lesser degree of trifluoroacetylation; there is a contraction of the electroactive region of the polymer by about 100 mV and some loss in total charge passed. The I_D-V_G, however, is more dramatically affected; the peak conductivity decreases by a factor of fifty, and the region of V_G over which the polymer is conducting contracts symmetrically by about 200 mV. The greater sensitivity of the I_D-V_G characteristic is not surprising as it has been observed that in many other conducting polymers the I_D-V_G characteristic is effected long before any interpretable change appears in the cyclic voltammogram. This is not unexpected, however, when the effect of removal of an electroactive site is considered. If a polymer chain has 50 conjugated sites, rendering 10 of them inactive is only a 20 % loss in electroactivity and thus gives rise to a minor loss of cyclic voltammetric response. The possible effect on conductivity is a very different issue. Substitution at regular intervals would reduce maximum conjugation length from 50 sites to 5 which is expected to cause a major loss of conductivity.[17] The changes in polyaniline electrochemistry upon reaction at nitrogen with trifluoroacetic anhydride are in stark contrast to those of polypyrrole upon reaction with trifluoroacetic

Figure 1. Cyclic voltammetry of polyaniline deposited onto flat gold electrodes (Γ = 1 x 10^{-6} moles of aniline cm^{-2}) before and after exposure to trifluoroacetic anhydride under potential control at 0.2 V vs SCE (top) and 0.5 V vs SCE (bottom).

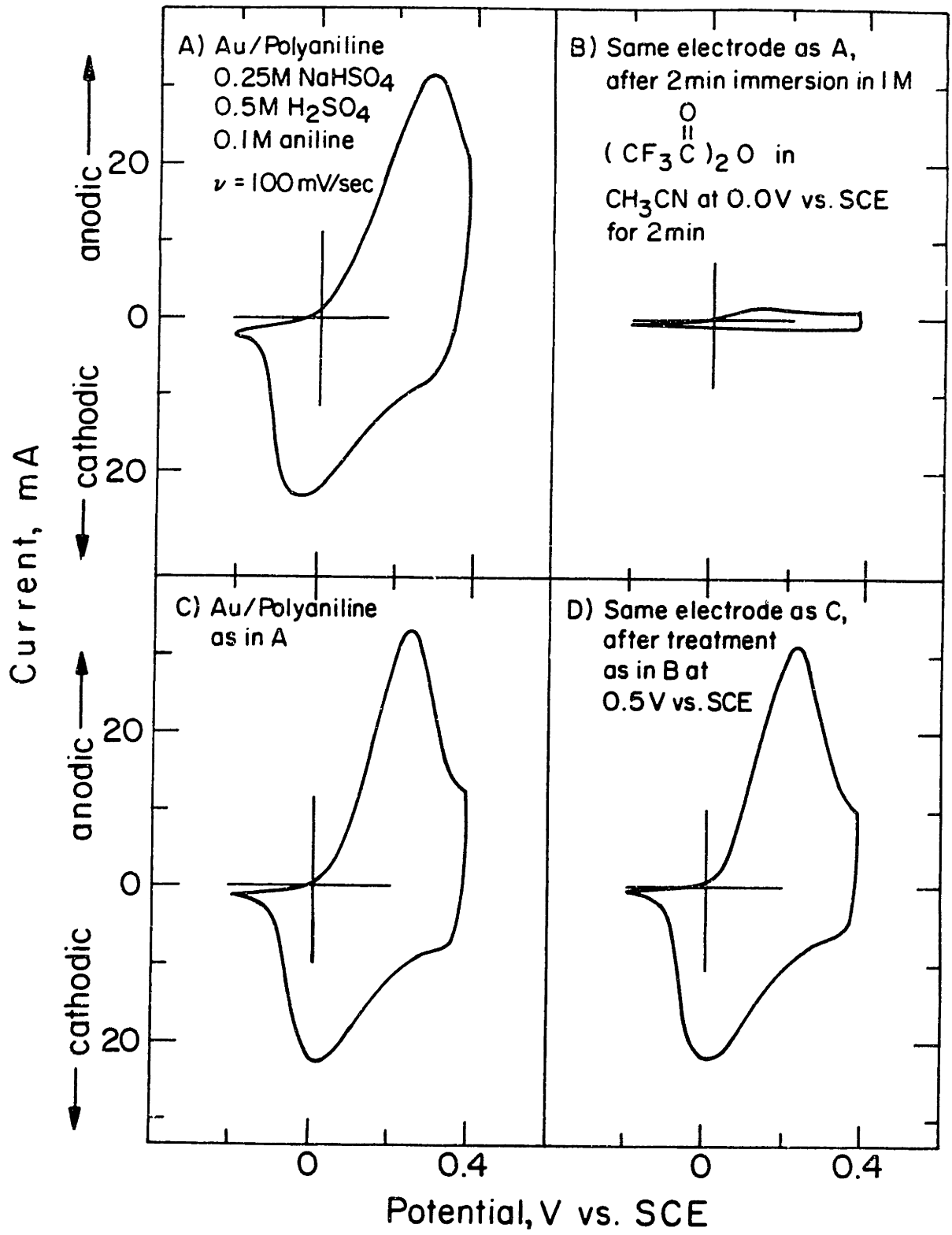
A) Au/Polyaniline
0.25M NaHSO4
0.5M H2SO4
0.1M aniline
ν = 100 mV/sec
B) Same electrode as A,
after 2min immersion in 1M
(CF3C(=O))2O in
CH3CN at 0.0V vs. SCE
for 2min
C) Au/Polyaniline
as in A
D) Same electrode as C,
after treatment
as in B at
0.5V vs. SCE
anodic
cathodic
20
0
20
anodic
cathodic
20
0
20
0
0.4
0
0.4
Current, mA
Potential, V vs. SCE

Figure 2. Cyclic voltammetry and I_D-V_G characteristics for polyaniline deposited onto three adjacent electrodes on a microelectrode array before and after treatment of the electrode-confined polymer with 1.0 M trifluoroacetic anhydride in 0.2 M F_3CCO_2H/ 0.1 M $LiClO_4$/ CH_3CN.

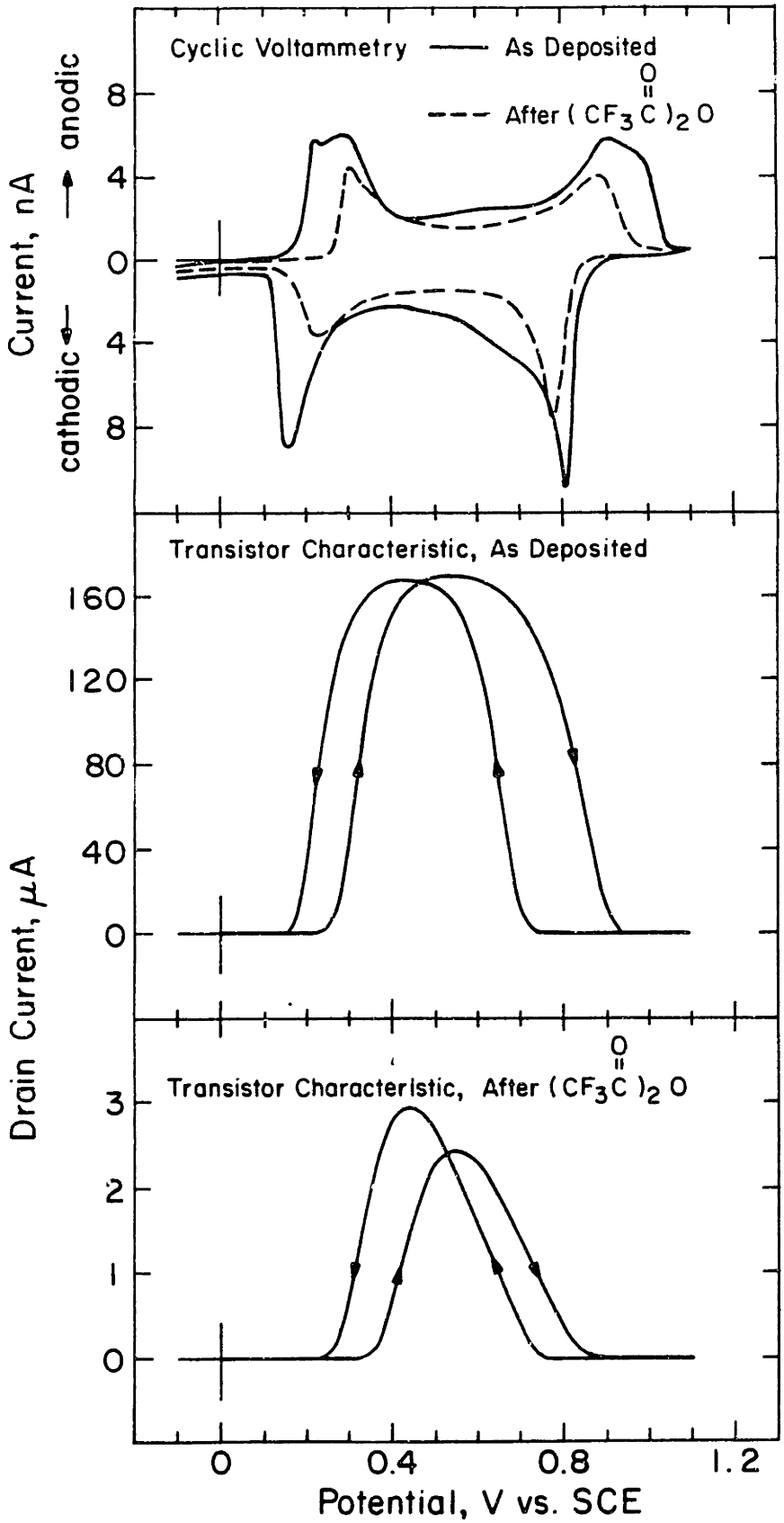
Cyclic Voltammetry
As Deposited
After (CF3 C)2 O
Current, nA
anodic
cathodic
8
4
0
4
8
Transistor Characteristic, As Deposited
160
120
80
40
0
Transistor Characteristic, After (CF3C)2 O
Drain Current, μA
3
2
1
0
0
0.4
0.8
1.2
Potential, V vs. SCE

anhydride[16] and poly(3-methylthiophene) with Cl_2.[18] In both of the latter cases, reaction of the electrophile with the polymer results in potential shifts of up to 0.8 V in the potential of conductivity onset but a comparatively small loss in conductivity and no loss in cyclic voltammetric response (see sections 6.2 and 6.3 of this chapter)

The evolution of RIR spectra for reaction of macroelectrode-confined polyaniline at 0.2 and 0.4 V vs SCE is shown in Figure 3. Bands at 1700 (CO) and 1225, 1200, and 1155 cm^{-1} (CF_3) grow in consistent with N-trifluoroacetylation of polyaniline. Trifluoroacetylation for 150 s at 0.2 V vs SCE is accompanied by a decline in cyclic voltammetric response equivalent to that seen in Figure 1 for the electrode held at 0.2 V. Note that while the reaction proceeds relatively quickly at 0.2V vs SCE, acetylation is an order of magnitude slower at 0.4V vs SCE where polyaniline is partially oxidized. Despite the fact that the RIR spectra in Figure 3 were taken after full electrochemical reduction of the surface confined polyaniline, the spectra resemble those of emeraldine from other reports on the basis of the broad featureless absorbance, increasing at higher frequency (removed by baseline correction for Figure 3) and the high relative intensity of the peak at 1600 cm^{-1}.[19-22] Spectra of fully reduced polyaniline have a flat baseline and a very weak absorbance at 1600 cm^{-1}. We believe that some oxidation of the polyaniline occurs rapidly after taking the electrode out of potential control, by exposure to oxygen during rinsing and drying of the electrode.[23,24] The grass-green color of the dried polymer films is consistent with partial oxidation of polyaniline. There was no noticeable evolution of the RIR spectra over 30 min once the electrode was placed in the FTIR sample chamber. Figure 4 shows plots of the trifluoroacetamide carbonyl peak absorbance as a function of trifluoroacetic anhydride exposure time over a range of electrochemical potentials. There is clearly a range of states of polyaniline reactivity with trifluoroacetic anhydride; the more polyaniline is oxidized the less reactive it becomes. The most obvious changes in reactivity on the laboratory timescale occur at potentials near 0.35 V vs SCE. Since the absorbance of radiation reflected from the films varied from sample to sample, we used the absorbance of the peak at 818 cm^{-1} (para-

Figure 3. Reflectance IR spectra for electrodeposited polyaniline on flat Au electrodes over the course of exposure to 1.0 M trifluoroacetic anhydride in 0.2 M F_3CCO_2H/ 0.1 M $LiClO_4$/ CH_3CN at 0.2 V vs SCE (top) and 0.4 V vs SCE (bottom). Spectral changes corresponding to nitrogen trifluoroacetylation are seen for both electrodes.

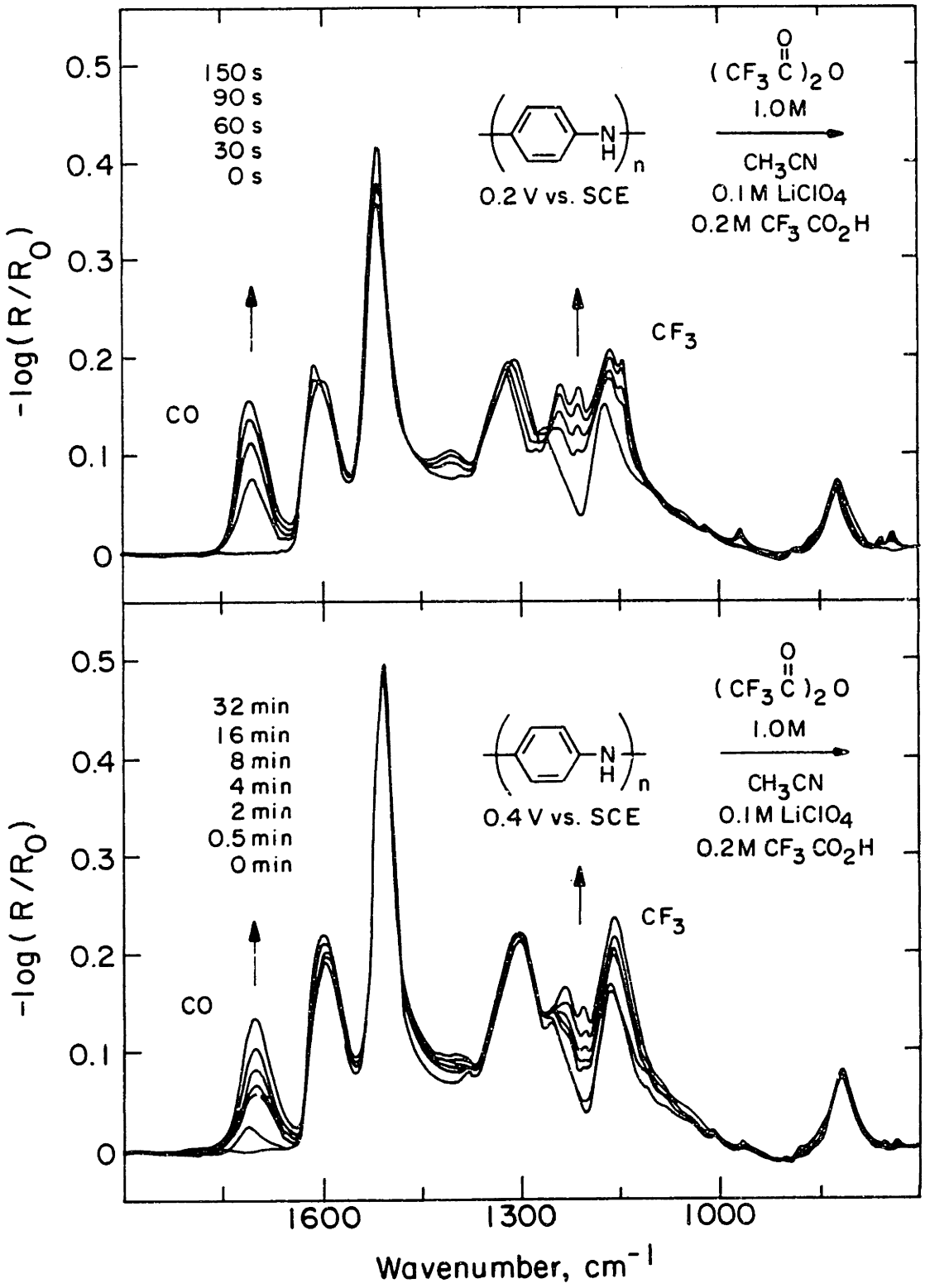
150 s
90 s
60 s
30 s
0 s
CO
CF3
0.2 V vs. SCE
(CF3C)2O
1.0M
CH3CN
0.1 M LiClO4
0.2M CF3CO2H
-log(R/R0)
32 min
16 min
8 min
4 min
2 min
0.5 min
0 min
0.4 V vs. SCE
1600
1300
1000
Wavenumber, cm-1

Figure 4. Evolution of -log(R/R_0) over the course of reaction of polyaniline on Au electrodes with trifluoroacetic anhydride at different potentials. The carbonyl band "absorbance" is shown as normalized to the absorbance of the unchanging polyaniline 818 cm^{-1} band.

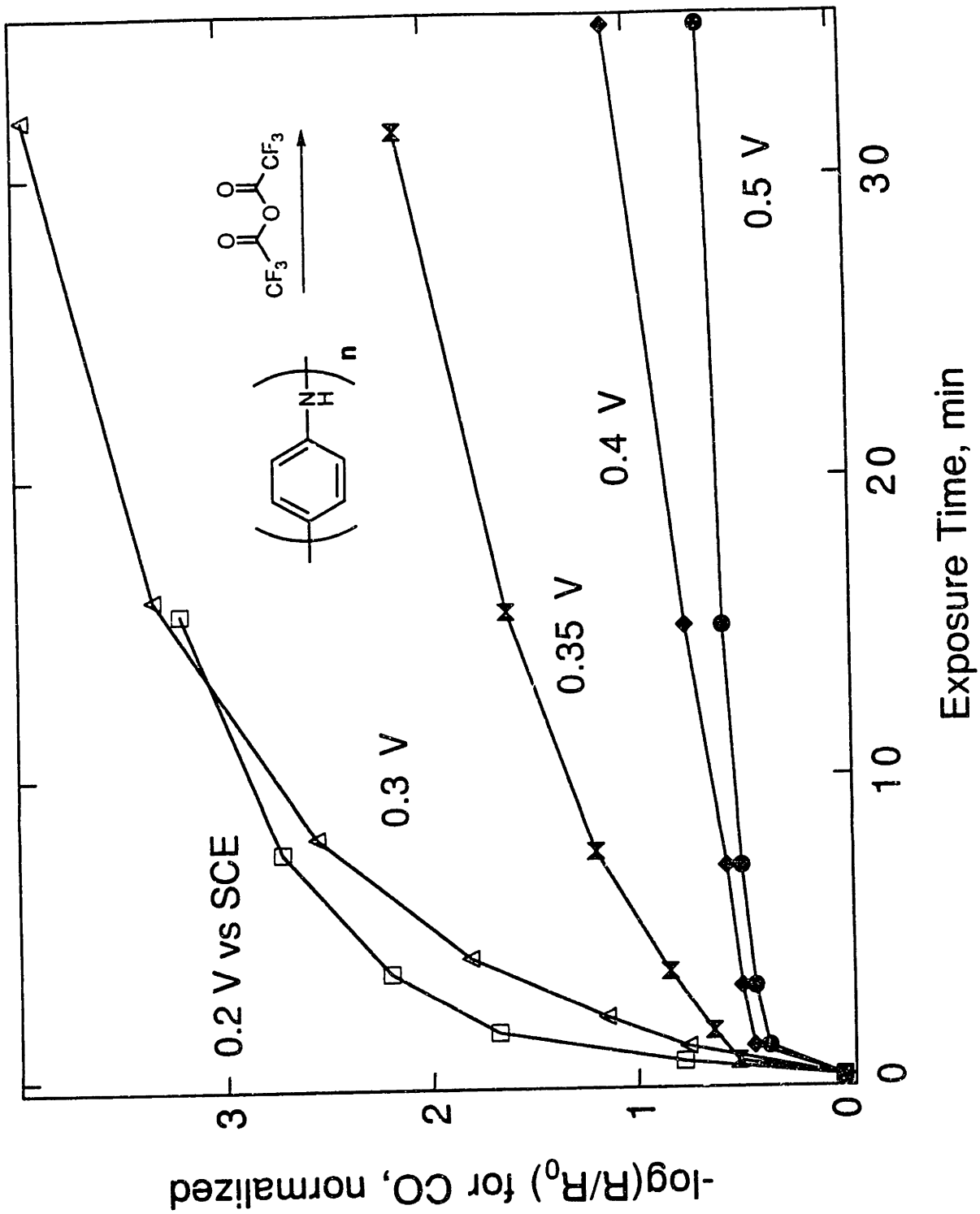
-log(R/R0) for CO, normalized
Exposure Time, min
0
1
2
3
0
10
20
30
0.2 V vs SCE
0.3 V
0.35 V
0.4 V
0.5 V
n
CF3
CF3

substituted arene CH "flapping" mode) as an internal standard for the degree of polyaniline trifluoroacetylation, since, as Figure 3 demonstrates, absorbance of this peak changes very little over the course of trifluoroacetylation. Hence the carbonyl absorbance is shown as normalized absorbance, the ratio of the carbonyl absorbance to that of the peak at 818 cm^{-1}.

There is some confusion as to whether polyaniline, when partially oxidized in acidic media, is best described as having access to a continuum of states of charge on a molecular level, ranging from 0 to 1 electrons per aniline repeat unit, or whether there are only three states: leucoemeraldine, emeraldine salt (0.5 electrons per repeat unit), or pernigraniline (1 electron per repeat unit), and "phase separated" mixtures thereof.[8,20,25-32] The nucleophilicity of polyaniline may shed some light on this problem. Figure 5 shows the relative rate of CO absorbance rise in Figure 4 plotted as a function of the polyaniline state of charge, The dashed curve showing hypothetical initial reaction rate linearly dependent on degree of oxidation is included for comparison. A complication encountered in generating Figure 5 is that polyaniline at a given potential becomes more reduced with a higher degree of trifluoroacetylation, especially at potentials in the vicinity of the peak current of the first redox process, as seen in Figure 2, due to anodic shift in the oxidation potential of the polymer over the course of the reaction. We estimated the fractional oxidation state of polyaniline using the dashed cyclic voltammogram, representing trifluoroacetylated polymer, of Figure 2 since we felt it would best represent an average of degrees of trifluoroacetylation which are followed in Figure 4.

We find that polyaniline reactivity with trifluoroacetic anhydride has a higher than first order dependence on polyaniline state of charge. The discrete states of charge picture makes an unambiguous prediction of a first-order dependence of reaction rate on polymer state of charge. If the discrete states picture of the electronic structure of polyaniline at fractional oxidation states were appropriate, the rate of reaction between trifluoroacetic anhydride and polyaniline would be linearly dependent on the mole fraction of leucoemeraldine, assuming no mass-transport limitations. That is, polyaniline oxidized to

Figure 5. Plot of the rate of CO absorbance growth from Figure 4 versus polyaniline state of charge, in electrons per repeat unit. The polyaniline state of charge was obtained by averaging the anodic and cathodic current of the dashed CV in Figure 3 integrated to the potentials at which the samples were held. It was assumed that the degree of oxidation after the second anodic wave is 1 electron per repeat unit. The dashed line is a hypothetical reaction rate which is linearly dependent on the polyaniline oxidation state.

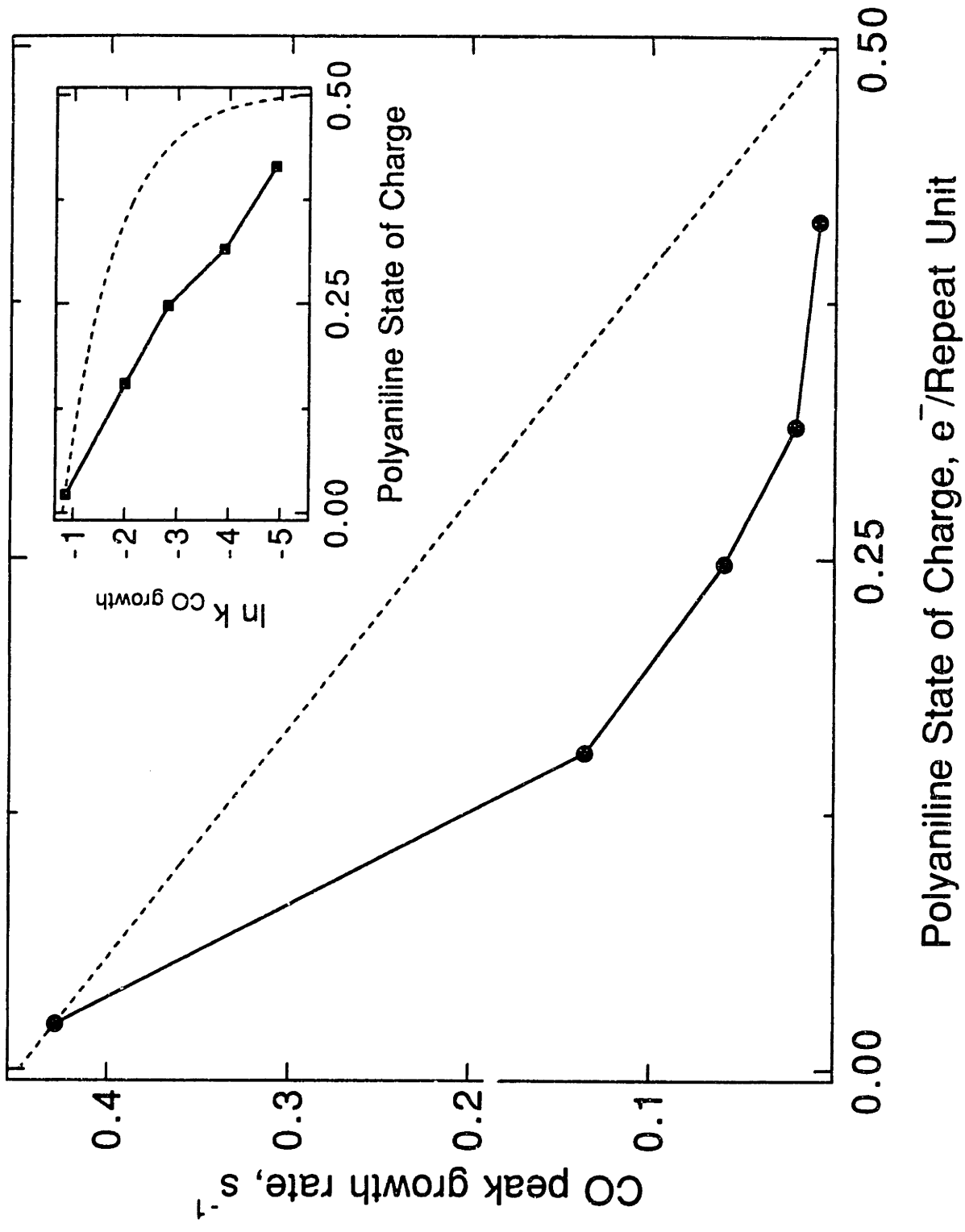
CO peak growth rate, s-1
0.4
0.3
0.2
0.1
0.00
0.25
0.50
Polyaniline State of Charge, e-/Repeat Unit
ln k CO growth
-1
-2
-3
-4
-5
0.00
0.25
0.50
Polyaniline State of Charge

0.25 electrons per repeat unit, "protoemeraldi..., [3] should initially react 1/2 as rapidly with trifluoroacetic anhydride as fully reduced leucoemeraldine. If, on the other hand, the degree of polymer oxidation is distributed evenly over the nitrogens of each monomer unit, the state-of-charge dependence of reaction rate should be more logarithmic, and therefore more sensitive to fractional oxidation state. Our results are therefore more consistent with the view that partially oxidized polyaniline in acidified CH_3CN has access to a continuum of charge states, rather than mixtures of the three shown in Scheme 1.

In a set of experiments carried out under identical conditions to the RIR study, the change in conductivity of polyaniline upon exposure to trifluoroacetic anhydride as a function of time was determined for a series of electrochemical potentials of the polymer. The results are shown in Figure 6. Notice that loss of conductivity observed here corresponds well to the trend in degree of trifluoroacetylation as determined by RIR. The conductivity loss occurs at a faster rate than the rise in the CO absorbance in Figure 4, indicating that even after the film is rendered insulating, further reaction with trifluoroacetic anhydride occurs. Again the transition from quick to sluggish reactivity occurs over the 0.3 to 0.4 V range. At 0.6 V >99.9% of the original conductivity was observed after 40 min exposure to trifluoroacetic anhydride. While potentials higher than 0.6 V were not included in Figure 6, the I_D-V_G characteristic of polyaniline was stable when scanned continuously from 0.6 to 1.2 V vs SCE in the presence of trifluoroacetic anhydride. The more negative of 0.6 V the lower limit, the greater the loss in conductivity observed on each scan, as expected from the data in Figure 6. While it is possible to continuously monitor conductivity of the polyaniline during reaction with trifluoroacetic anhydride by simply applying a drain voltage across the two microelectrodes and monitoring drain current, such a measurement is complicated by the positive shift in the potential for onset of drain current upon trifluoroacetylation seen in Figure 2, a consequence of the contraction of the window of conductivity. This shift in the I_D-V_G characteristic means that the drain current observed at a given gate voltage will shift as the potential for onset of conductivity and I_D-

Figure 6. Progression of the normalized peak drain current observed in the I_D-V_G characteristics of a series of polyaniline-derivatized microelectrode arrays held at the potentials indicated over the course of exposure to 1.0 M trifluoroacetic anhydride in 0.2 M F_3CCO_2H/ 0.1 M $LiClO_4$/ CH_3CN.

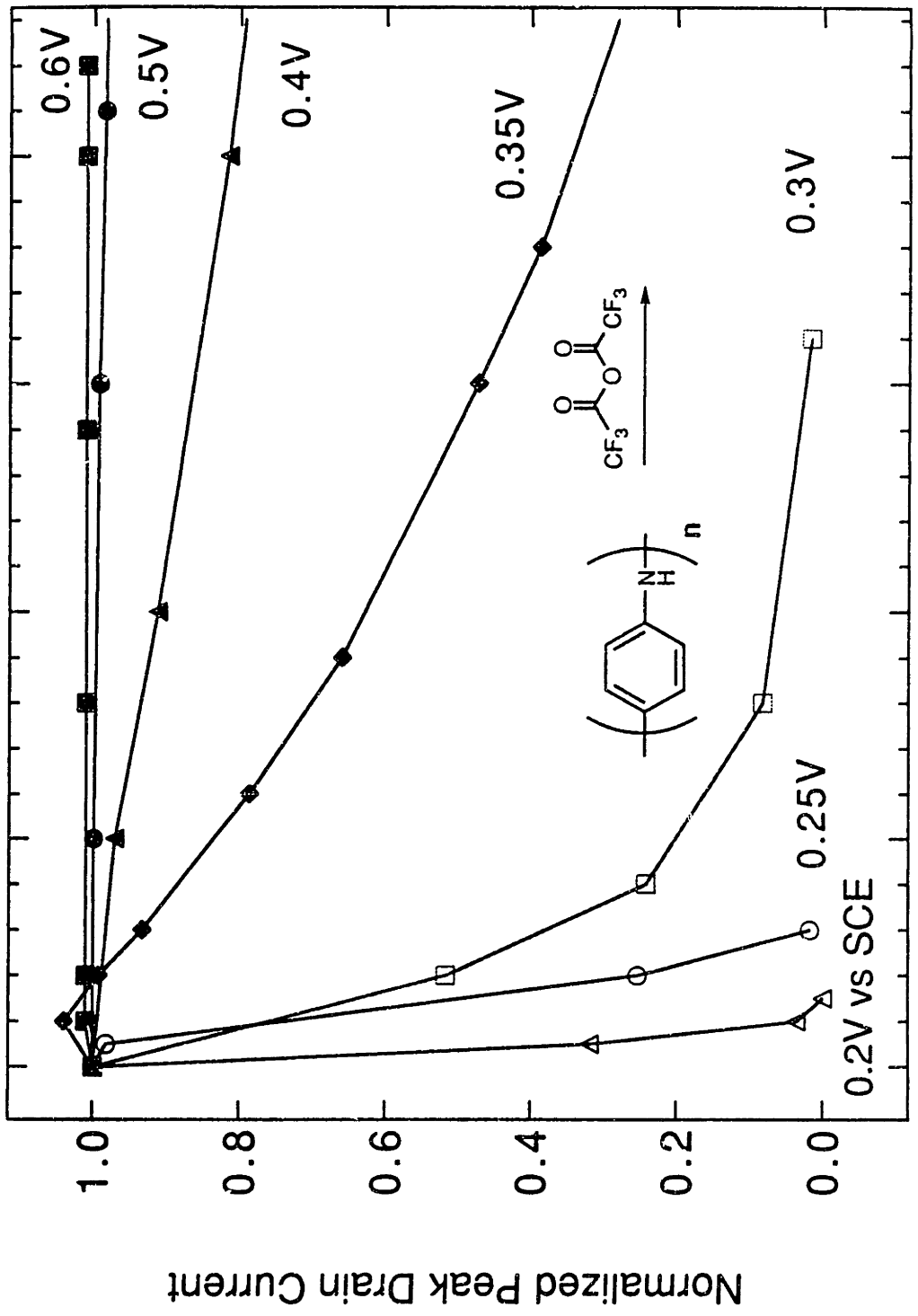
Normalized Peak Drain Current
1.0
0.8
0.6
0.4
0.2
0.0
0
5
10
15
20
Exposure Time, min
0.6V
0.5V
0.4V
0.35V
0.3V
0.25V
0.2V vs SCE
CF3
CF3
n

V_G characteristic of the polymer shift. The observed change in drain current will thus be the combination of this effect , quite pronounced in the 0.2-0.35 V range of V_G, and the loss of conductivity due to trifluoroacetylation of nitrogen. This complication is avoided by instead removing the polyaniline transistor from the anhydride cell, rinsing with water, and scanning the I_D-V_G characteristic in the absence of trifluoroacetic anhydride to determine peak conductivity of the polymer at periodic intervals, a procedure which also parallels the treatment of electrodes in the RIR experiments.

Figure 2 shows that polyaniline exhibits peak conductivity at 0.6 V in acidified CH_3CN, where it is oxidized to the extent of 0.5 electrons per repeat unit. The detectable changes in polyaniline reactivity with trifluoroacetic anhydride occur at more negative potentials, or lower oxidation states. Under the same conditions used for trifluoroacetylation, a more powerful or weaker electrophile than trifluoroacetic anhydride may require respectively higher or lower degrees of polyaniline oxidation to noticeably or controllably slow nucleophilic attack by the polyaniline nitrogen. The reactivity of polyaniline toward acetic anhydride and its mono, di, and trichloro derivatives was characterized by microelectrode conductivity experiments in which polyaniline was exposed to a 1.0 M solution of anhydride in 0.1 M $LiClO_4/CH_3CN$ acidified to 0.2 M of the corresponding acid (e.g. chloroacetic anhydride and chloroacetic acid). Using the rate of loss of conductivity as indicative of reaction, the following order of polyaniline reactivity with acetic anhydrides was found: trifluoro > trichloro > chloro > dichloro >> acetic anhydride. Trifluoromethanesulfonic anhydride, a more powerful electrophile than trifluoroacetic anhydride, resulted in complete loss of polymer from the electrode, precluding characterization. The electrochemistry and conductivity of polyaniline were stable in the presence of acetic anhydride, irrespective of oxidation state of the polymer. As the methyl group of the anhydride becomes less electron withdrawing reactivity is expected to decline as a result of the lower electrophilicity of the carbonyl carbon and the poorer stabilization of the acetate leaving group. This order was observed with the exception that

chloroacetylation was faster than dichloroacetylation, perhaps a result of the greater bulk of the dichloromethyl group. In all cases, polyaniline was stable when held well oxidized. With the less reactive anhydrides, a lesser degree of oxidation was required to render polyaniline inert to acylation. For example, if the I_D-V_G characteristic of polyaniline is scanned in the presence of 1.0 M trifluoroacetic anhydride it is stable provided the lower limit is at least 0.6 V vs SCE. In the case of dichloroacetic anhydride 0.3 V was sufficient and nearly complete reduction of polyaniline was required before loss of conductivity from one scan to the next became evident.

The cyclic voltammetry and I_D-V_G characteristic for polyaniline shown in Figure 2 display pronounced hysteresis, another feature typical of conjugated organic polymers which, unlike sluggish kinetics or other sources of quasi-reversibility, is essentially independent of scan rate and arises from an evolution of electronic states upon oxidation.[9,33] On the return scan, it is necessary to go to a more negative potential to achieve the fully reduced state of the polymer. (A more detailed discussion of the theory of origin of hysteresis can be found in the introduction to Chapter 3) With thick films there is also the expected normal kinetic component to response which does vary with scan rate. For polyaniline, in acidified CH_3CN, the hysteresis approaches a lower limit of about 100 mV in gate potential at scan rates down to 0.2 mV/s. For all of the potential-dependent reactivity we report here, the potential was approached from the positive side, that is, during polymer re-reduction, where more negative potentials are required for full reduction of polyaniline. We expected hysteresis to cause polyaniline held at 0.35 V, where we find the greatest observable change in reactivity for potential change, approached from the reduced (negative) side to have a more negative state of charge, and therefore higher nucleophilicity, than a polymer held at 0.35 V approached from the oxidized side. We observe, contrarily, that two polyaniline-derivatized electrodes held at 0.35 V vs SCE, one brought to that potential cathodically and one anodically, have indistinguishable reactivity with trifluoroacetic anhydride over periods of up to 10 min. The implication is that, contrary to

the slow scan rate cyclic voltammetry results, on the timescale of a few minutes the oxidation state of polyaniline equilibrates to a single level from the initially different states of charge arising from the hysteresis observed in the normal regime of electrochemical scan rates. Charge integration of the cyclic voltammograms in Figure 2 before and after trifluoroacetylation reveal that maximal hysteresis of 0.15 electrons per repeat unit occurs at 0.2 to 0.25 V for the freshly deposited polyaniline, and at 0.25 to 0.3 V for the partially trifluoroacetylated polymer, while hysteresis at 0.35 V is lower, 0.02 and 0.09 electrons per repeat unit for the polymer before and after trifluoroacetylation, respectively. Thus, polyaniline reactivity with a less reactive anhydride such as dichloroacetic anhydride may yet display hysteresis effects since the potentials for maximum observable change in reactivity for potential shift are lower, and overlap more with the region of maximum polyaniline hysteresis, where trifluoroacetic anhydride reacts too rapidly to permit examination of hysteresis effects.

An interesting difference between the RIR and microelectrode conductivity data is the fact that IR reveals a rapid, but only partial, reaction with trifluoroacetic anhydride under all conditions, but conductivity declines only when the polymer is in the more reduced states. In RIR we observe an initial, comparatively rapid appearance of a carbonyl band at ~1710 cm^{-1} in the IR spectra of polyaniline electrodes which does not appear to depend on the electrochemical potential of the polymer. The expectation from a microelectrochemical measurement of conductivity would be a rapid, initial loss of drain current, and yet this is not observed. Instead, polyaniline shows only a slight and gradual loss of conductivity at 0.5 V and no loss whatsoever at 0.6 V even after 40 min. We propose that the initial potential-independent trifluoroacetylation is occurring at terminal amino groups of polyaniline, Scheme 3, and support this proposition with the following observations. First, reaction of **I** with 1 equivalent of trifluoroacetic anhydride produces only **III**, suggesting that terminal amino groups in polyaniline are also more reactive nucleophiles than their internal counterparts. Second, ν_{CO} for the terminally trifluoroacetylated polyaniline analog

III is 1725 cm^{-1}, about 20 cm^{-1} higher than for **IV**. Figure 7 shows a plot of trifluoroacetamide carbonyl peak frequency versus "normalized absorbance" for every data point in Figure 4. When the degree of trifluoroacetylation is low, either for short

Scheme 3

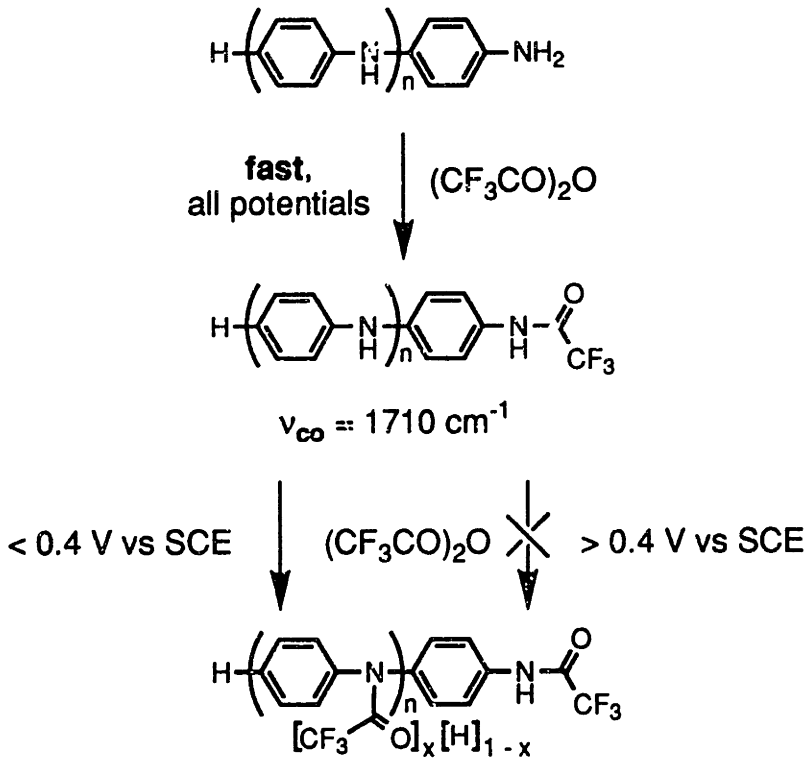

trifluoroacetic anhydride exposure periods of polyaniline held reduced or for longer periods with polyaniline held oxidized, the peak frequency is high, about 1710 cm^{-1}. Intermediate degrees of trifluoroacetylation give a lower peak frequency, down to 1692 cm^{-1}, while more extensive trifluoroacetylation, accompanied by complete loss of polymer electroactivity, yields gradually higher peak frequencies. Consideration of the reactivity towards trifluoroacetic anhydride of **I** and **II** and the spectral features of **III-VI** leads us to conclude that the initial rapid trifluoroacetylation resulting in a higher ν_{CO} is occurring at terminal nitrogens only, and that the subsequent trifluoroacetylation of internal nitrogens in

Figure 7. Peak carbonyl stretching frequency for polyaniline treated with trifluoroacetic anhydride as a function of extent of trifluoroacetylation. Data taken from results shown in Figure 4.

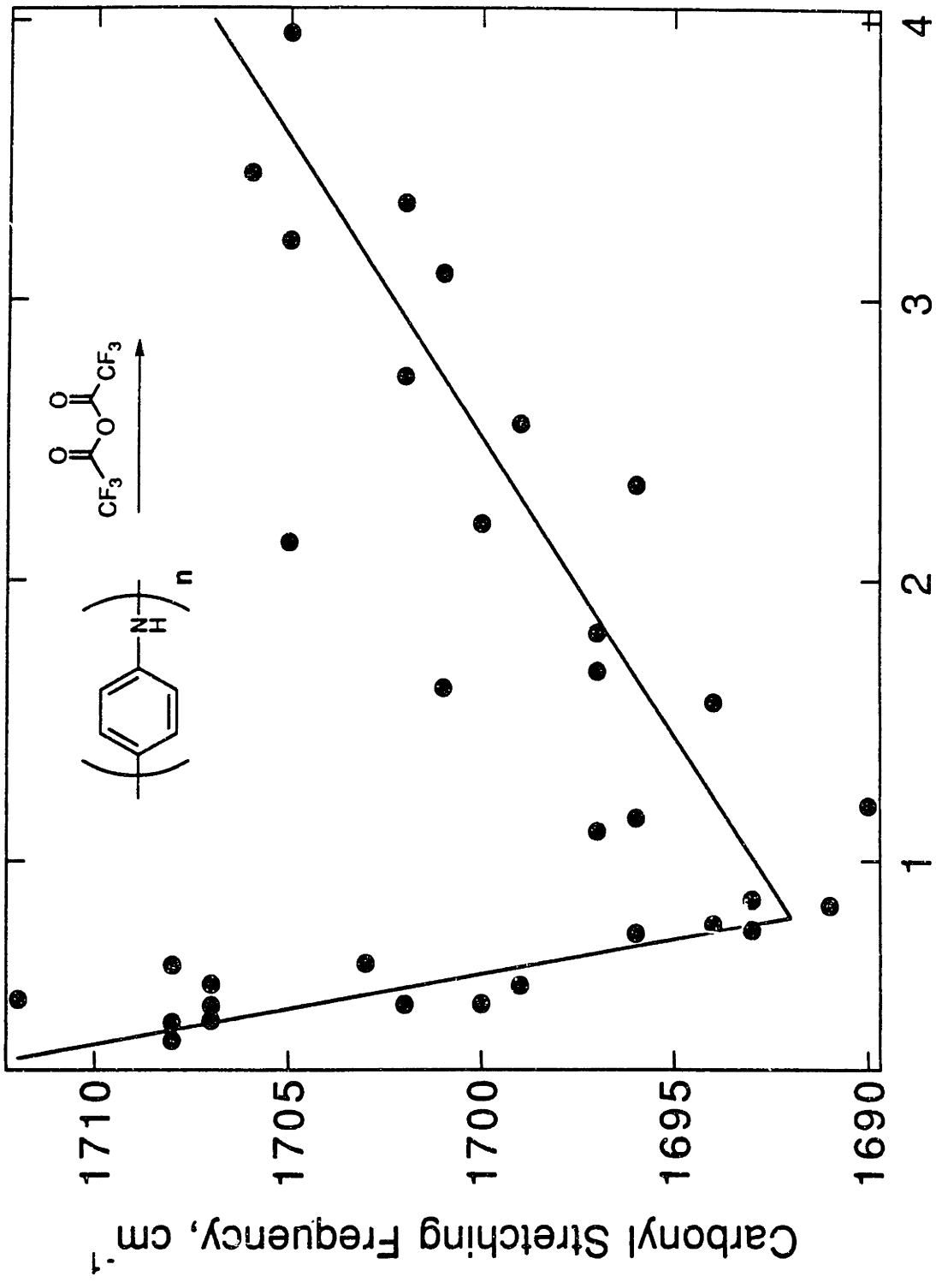
Carbonyl Stretching Frequency, cm-1
1710
1705
1700
1695
1690
1
2
3
4
-log(R/R0), normalized
CF3
O
O
O
CF3
N
H
n

polyaniline gives initially low and gradually increasing peak frequency as trifluoroacetylation makes the polyaniline backbone when fully reduced progressively more electron withdrawing.

In partially oxidized polyaniline most of the charge associated with the polymer oxidation is supported on the nitrogen atom, as depicted in Scheme 1.[13] Substitution at nitrogen is therefore expected to have a powerful effect on the conducting properties of the polymer. The drastic loss of conductivity upon trifluoroacetylation of nitrogen is much greater than the effect of substitution observed in N-alkyl or ring substituted polyanilines.[34-45] Electrochemical characterization of oligomers **I-VI**.[14,15] showed that the greater the degree of trifluoroacetylation of the oligomeric analogs, the more positive and irreversible their electrochemical oxidations. The fully trifluoroacetylated oligomers have redox potentials about 1.5 V more positive of their protonated precursors. The data indicate that oxidation of trifluoroacetylated polyaniline nitrogen gives a much higher energy radical cation than a protonated, or methylated nitrogen radical cation, and thus presents a barrier to hole transport. This line of reasoning, along with the fact that **I**, which contains a terminal amine, has a higher redox potential than **II**, may also explain the potential independence of what we propose is the initial trifluoroacetylation of polyaniline terminal amino groups and the insensitivity of conductivity to terminal amine trifluoroacetylation. A terminal amino group is afforded the least delocalization of any site on a polyaniline chain. It is the highest energy and least favorable location for a hole to reside. The terminal amino groups are therefore less coupled to the overall degree of oxidation of the polyaniline chain and might retain charge density and nucleophilicity even when the polymer is partially oxidized. Similarly, if a terminal nitrogen is the least favorable site for a hole and is the least important contributor to the π-manifold of the polymer, its loss upon trifluoroacetylation may be irrelevant to conductivity.

An interesting question of broad relevance to conduction in organic polymers is what fraction of the nitrogens are trifluoroacetylated at the point at which the polymer has lost

most of its electroactivity. We first attempted to address this question by X-Ray photoelectron spectroscopy, XPS. Results are shown in Table 1. We used compounds V and VI as standards since they have similar chemical structure to trifluoroacetylated polyaniline. The samples "0.2 V" and "0.5 V" are the same ones studied by RIR in Figure 4, and were held in the trifluoroacetic anhydride for 16 and 32 min, respectively. By comparison with the oligomeric standards, the degree of trifluoroacetylation for the samples held at 0.2 V and 0.5 V vs SCE is about 60% to 20%, respectively.

Table 1. X-Ray Photoelectron Spectroscopy Data for **V**, **VI**, and for polyaniline trifluoroacetylated at 0.2 V and 0.5 V vs SCE.

	XPS Integrations[a]		
sample	C_{1s} (expected)	N_{1s}	F_{1s} (expected)
V[b]	13.0 (10.0)	1	1.24 (1.5)
VI[b]	14.3 (11.0)	1	2.26 (3.0)
0.2 V	11.4, 10.3[c]	1	1.44, 1.36
0.5 V	11.0, 7.8[c]	1	0.56, 0.40

[a] Corrected for element sensitivity.

[b]Average of two runs.

[c]Not including CO and CF_3 carbons.

One limitation of XPS analysis for studying the composition of relatively thick films is that the electron mean free path limits quantitation to only the top 10-50 Å of the surface.[46] The lack of good self-consistency of the overall XPS results for **V** and **VI** did not recommend quantitative interpretation of the results for polymer samples. A more unambiguously quantitative technique for coverage measurement is transmission IR. Use of electrodes bearing a very thin layer (50-100 Å) of gold allows transmission IR,[47] but the resistance of the electrode itself gives rise to a voltage drop which results in a gradient of film thickness evident to the naked eye. Beer's law therefore does not obtain. To deposit

polyaniline more uniformly, electrodes were prepared with a border of conductive silver epoxy to minimize voltage drop. Polyaniline coverage was determined by cyclic voltammetry, and the electrode-confined polymer was subsequently trifluoroacetylated as above until >85% of the voltammetric response disappeared. The trifluoroacetyl coverage groups was determined by integrating the absorbance of the trifluoroacetyl peak and dividing by the average integrated extinction coefficient per carbonyl of **III-VI** (determined in CH_3CN) in the same frequency region. The results for 2 experiments were that 20 and 33% of the nitrogens in polyaniline are trifluoroacetylated when the electrochemical response is <15% of the non-trifluoroacetylated polyaniline. Since the transmission IR is sampling the entire thickness of the film, while XPS is sampling only the top 10-50 Å, we believe the coverage calculated based on cyclic voltammetry and transmission IR to be more reliable. While the comparison of XPS and IR data seem to point to a depth-dependent gradient in extent of trifluoroacetylation, preliminary RIR experiments on polyaniline-derivatized macroelectrodes having different thicknesses of electrodeposited polyaniline ranging over a factor of four, showed essentially the same potential-dependent rate of normalized CO absorbance rise shown in Figure 4, independent of thickness. We conclude that loss of >99% of conductivity occurs when ≈25% of the nitrogens are trifluoroacetylated.

According to Figure 4, the "normalized" value for $-\log(R/R_0)_{CO}$ is five times larger for polyaniline films held reduced for extended periods in the presence of trifluoroacetic anhydride than for those held oxidized. Using the trifluoroacetyl coverage calculated above, and assuming that all of the terminal amino and no internal amino groups are trifluoroacetylated, we estimate that 5-6% of the nitrogens in polyaniline as we prepare it are terminal. We propose that reaction of oxidized polyaniline of known molecular weight and polydispersity in an acidic medium with trifluoroacetic anhydride followed by IR could serve as a good assay for branching,[48-51] since only terminal amino groups will react under these conditions.

While trifluoroacetylation of polyaniline results in nearly complete loss of electroactivity and conductivity of the polymer, the trifluoroacetyl group can be chemically removed to regenerate polyaniline. Amines are often protected as their trifluoroacetamide derivatives.[52] Trifluoroacetamide hydrolysis can be accomplished with potassium carbonate in 30% aqueous methanol.[53] This reagent was found to cleave the carbon-nitrogen bond in trifluoroacetylated polyaniline and return the polymer to its initial state displaying a typical I_D-V_G characteristic and cyclic voltammetry for polyaniline. Figure 8 shows the RIR spectral changes accompanying the cleavage reaction on a trifluoroacetylated polyaniline-coated electrode. The RIR spectrum prior to immersion in the cleavage reagent (t = 0) shows the CO and CF_3 bands as seen in Figure 3. At the times noted, the electrode was removed from the cleavage solution, rinsed, dried, and characterized by RIR. Note that over the course of exposure to the cleavage reagent the carbonyl and trifluoromethyl absorptions disappear completely, while the cyclic voltammetric response returns. When the trifluoroacetylated polyaniline hydrolysis reaction has proceeded to >80% completion, ν_{CO} remains at a low frequency (1689 cm^{-1}), indicating that only internal trifluoroacetamides remain after longer hydrolysis periods and that the terminal amide groups are therefore hydrolyzed at least as rapidly as internal amides.

To see if the conductivity returned to polyaniline upon trifluoroacetamide hydrolysis, a microelectrode array derivatized with polyaniline was trifluoroacetylated until an I_D-V_G showed the peak conductivity to be less than 1% of its initial value. Immersion in the cleavage reagent for 12 h resulted in nearly complete return of conductivity. Most of the conductivity of trifluoroacetylated samples returned in the first 6 h of immersion while 18 h provided maximum recovery. Heating the cleavage solution to 50° C gave only a minor increase in the rate of conductivity return. The recovery of conductivity in polyaniline rendered insulating by trifluoroacetylation is interesting in the context of a device known as an EPROM, or erasable-programmable-read-only-memory, the function of which is to provide semi-permanent set of information to be read and used as required but with the

Figure 8. RIR spectra following the hydrolysis of trifluoroacetylated polyaniline on flat Au electrodes, showing disappearance of the CO and CF_3 bands and the regeneration of polyaniline.

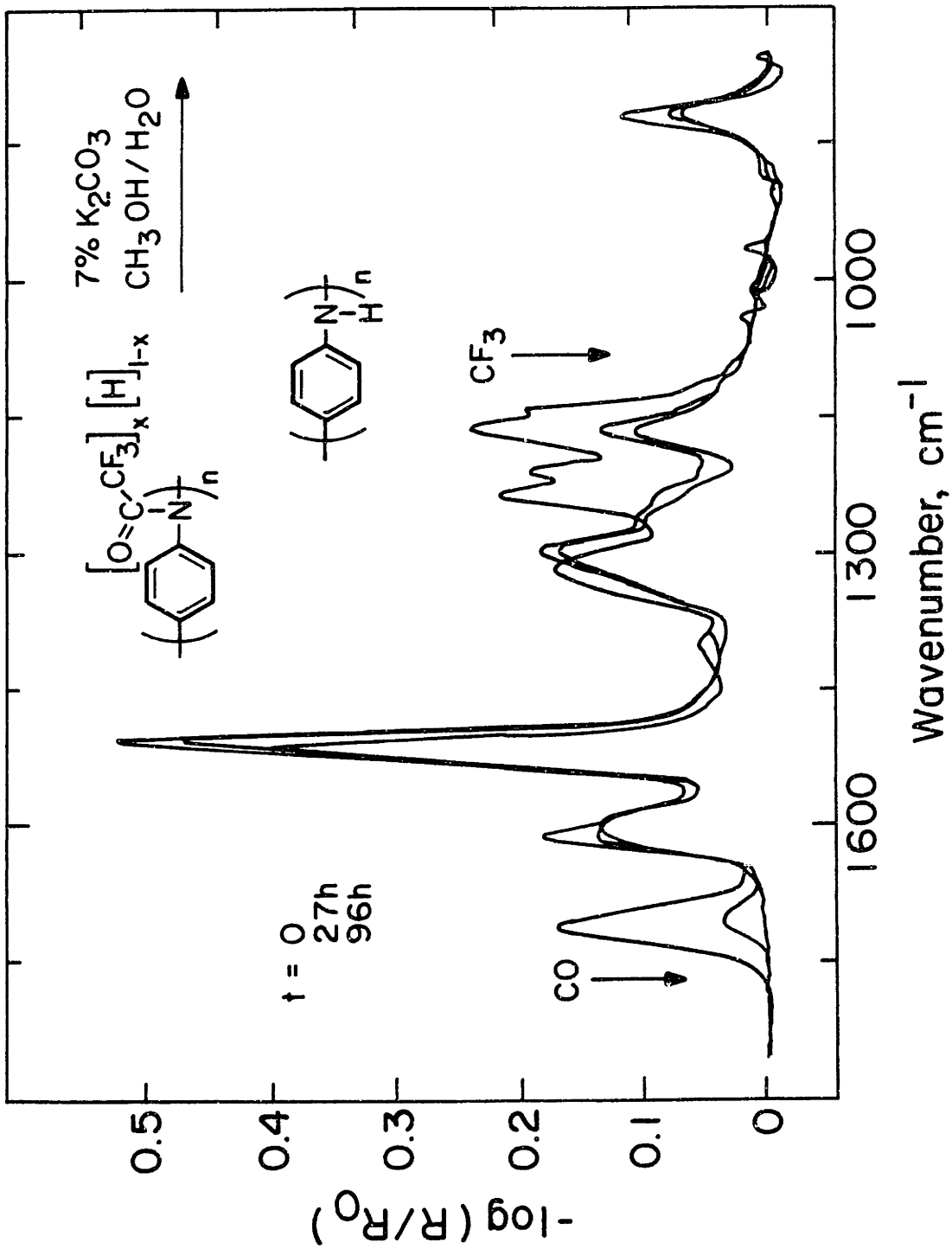
7% K_2CO_3
CH_3OH / H_2O
$[O=C(CF_3)]_x [H]_{1-x}$
t = 0
27h
96h
CO
CF_3
-log (R/R$_o$)
Wavenumber, cm^{-1}
0
0.1
0.2
0.3
0.4
0.5
1600
1300
1000

Figure 9. Color micrograph and I_D-V_G characterization of a microelectrode array showing functionalized with three independent polyaniline transistors.

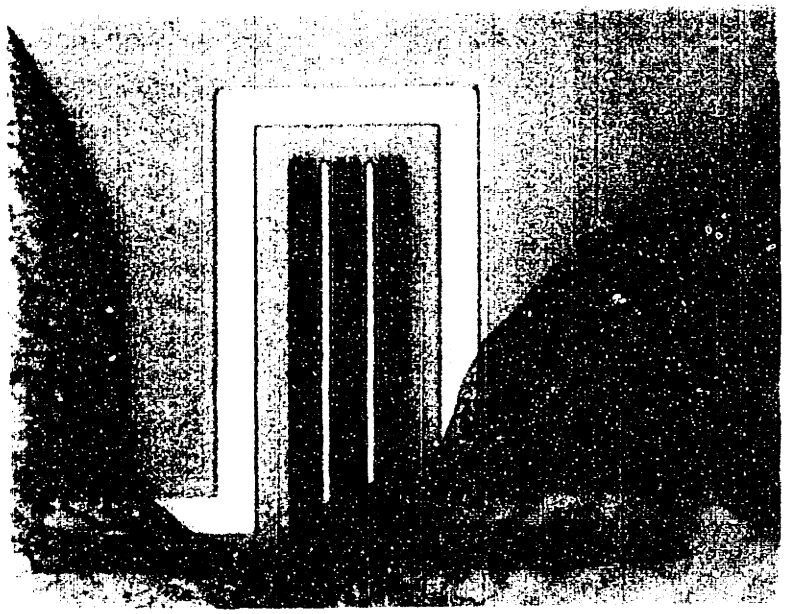

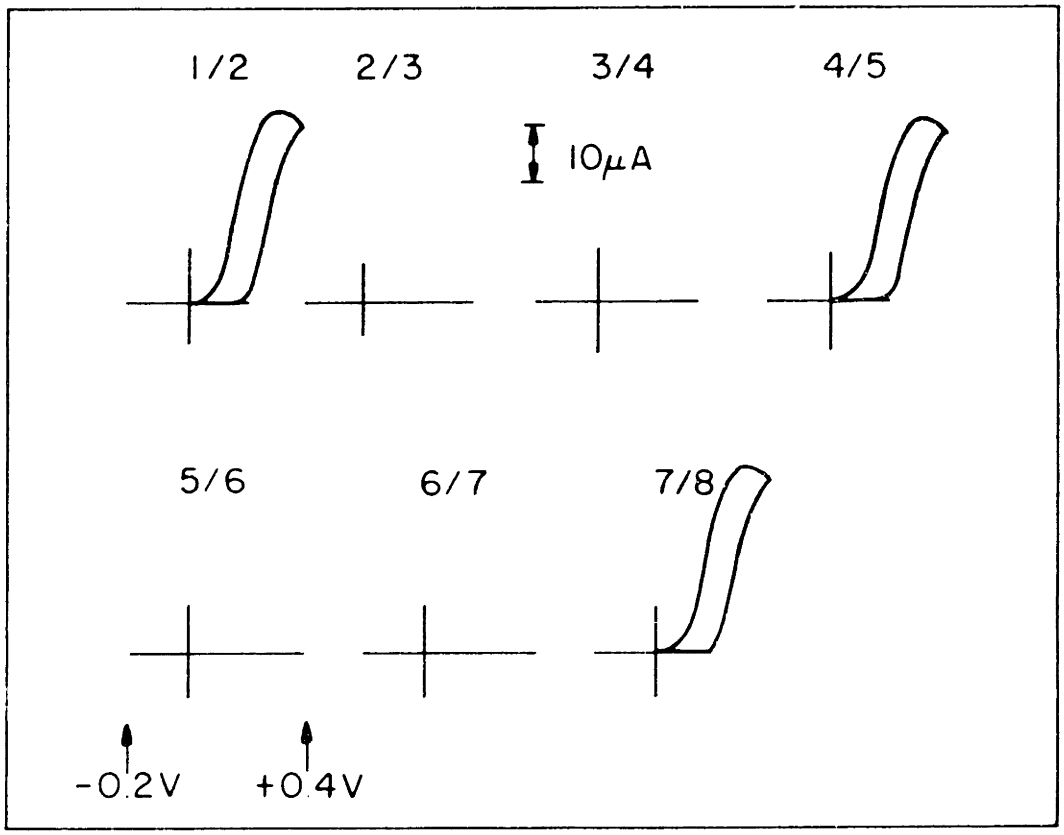
1/2
2/3
3/4
4/5
10μA
5/6
6/7
7/8
-0.2V
+0.4V

Figure 10. Selective trifluoroacetylation of polyaniline transistors on a microelectrode array using electrochemical potential control. Transistors labeled X and Z are trifluoroacetylated or "written" by holding at 0.2 V vs SCE, while transistor Y is protected from reaction by being held oxidized, at 0.5 V vs SCE. Trifluoroacetylated polyaniline of transistors X and Z are then hydrolyzed by immersion in potassium carbonate in aqueous methanol, thereby "erasing" the device, restoring the conductivity of each transistor.

AN ERASABLE PROGRAMMABLE READ-ONLY MEMORY (EPROM) BASED ON THE REVERSIBLE TRIFLUOROACYLATION OF POLYANILINE

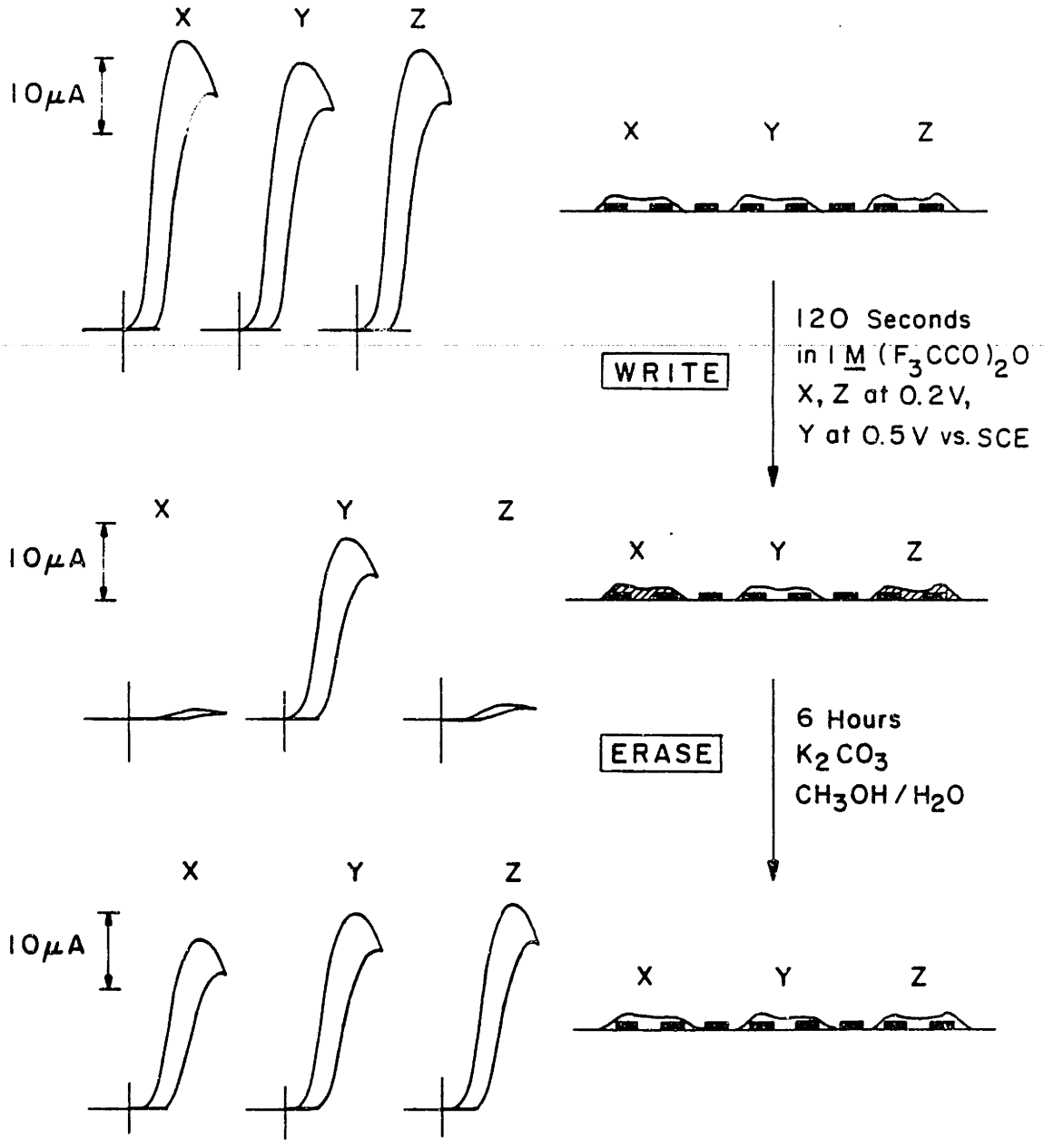

option of erasing and re-writing.[54] Shown in Figure 9 are a color micrograph and I_D-V_G characterization of an array which has been functionalized with three independent polyaniline transistors. The effect of trifluoroacetylation on conductivity provides a means of "writing" off states by shutting down conductivity and the potential dependence of the reaction allows it to be done selectively on only the desired devices. This was demonstrated as shown in Figure 10 using the device shown in Figure 9. The transistors are referred to as devices X, Y, and Z. The array was immersed in the same 1M trifluoroacetic anhydride solution used above with transistors X and Z held at 0.2V while transistor Y was held at 0.5V, thus resulting in the selective trifluoroacetylation of devices X and Z. The I_D-V_G characteristics of X and Z declined while device Y maintained its response. Immersion of the array in the same K_2CO_3/MeOH/H_2O solution used in Figure 8 for 6 h restored conductivity to transistors X and Z (a full 12 hours is required for maximum recovery). The process of trifluoroacetylation followed by hydrolysis can be repeated although the polymer does not recover complete conductivity in each cycle. Selective introduction of trifluoroacetyl groups provides a means of attenuating conductivity of any combination of specific devices allowing electrochemical "writing" of any configuration of states. The states stored as acylated and non-acylated polyaniline can be read by characterization of the I_D-V_G characteristics but instead the more realistic method shown in Scheme 4 was used. A fixed gate potential is applied and if a memory element is trifluoroacetylated no current flows and the output voltage (the voltage drop across the resistor) is zero. If the memory element is not acylated and is conducting, drain current flows and essentially all of the supply voltage is dropped across the resistor so the output is high. Thus outputs X, Y, and Z are either zero or V_{DD} with respect to ground, providing the appropriate digital output for a memory device. Because V_G is held at a single value at all times in the circuit shown in Scheme 4, no motion of counterions is required for its operation and thus it does not experience the response speed limitations associated with oxidation and reduction of polyaniline. The microelectrochemical circuit in Scheme 4 does not experience the usual

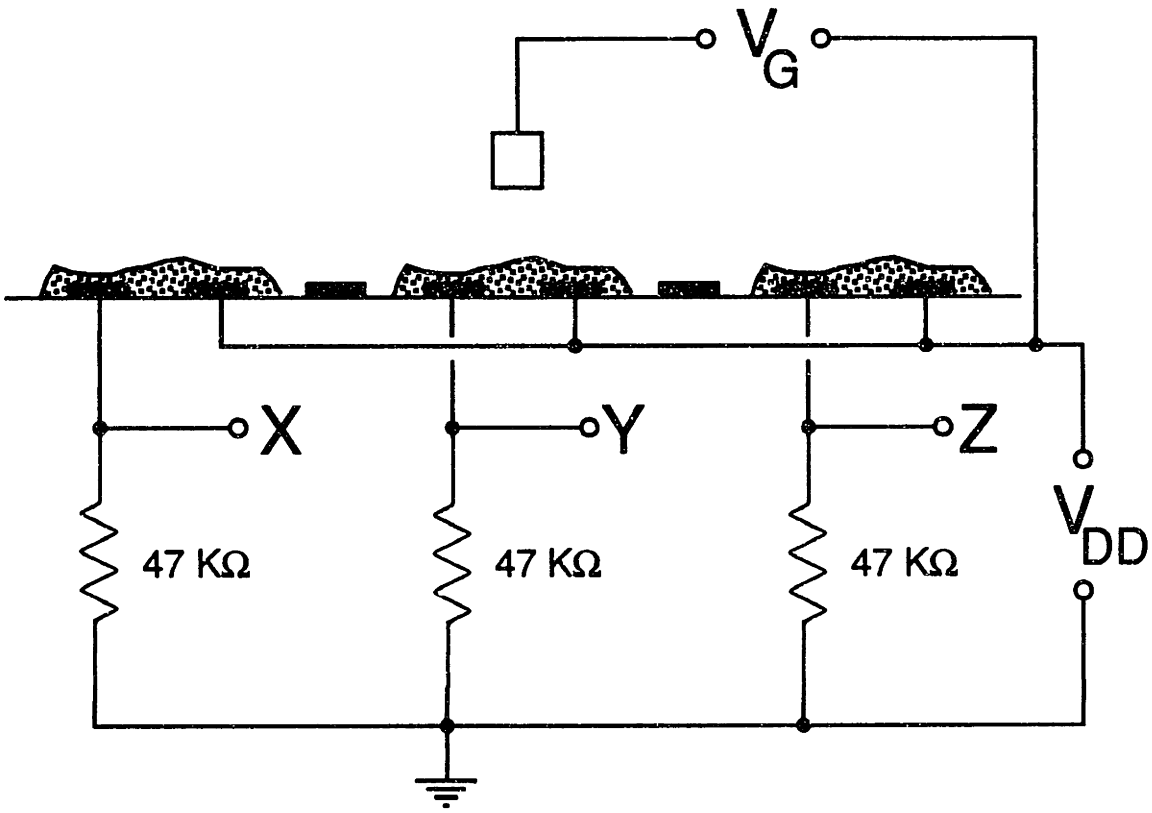

Scheme 4. A circuit used to read the configuration of a polyaniline/trifluoroacetylated polyaniline-based erasable programmable read only memory providing an output of zero for acylated devices and V_{DD} for non-acylated devices at outputs X, Y, and Z. The optimal value for V_G was 0.225 V vs SCE which is within the window of conductivity for polyaniline but slightly negative of onset of conducting for trifluoroacetylated polyaniline.

ionic motion since no variation of V_G is required to obtain the output voltages, i.e. this is entirely a static measurement. Setting V_G just positive of onset of conduction for polyaniline to read the device capitalizes on the contraction of the window of conductivity and positive shift in onset of conduction upon trifluoroacetylation, requiring less extensive reaction to obtain a fully off response from the read circuit. This was found to be optimal since heavy trifluoroacetylation, resulting in complete insulation by polyaniline, could not be fully reversed by the hydrolysis step. Immersion in the cleavage reagent "erases" the device, by restoring conductivity to the acetylated transistors and allowing a new

configuration to be written. The polyaniline-based EPROM device was successfully taken through five write/read/erase/ re-write cycles before one of the devices could no longer be sufficiently revived by the cleavage reagent.

In summary, we find that reaction of trifluoroacetic anhydride with the conducting polymer polyaniline confined to electrode surfaces gives trifluoroacetylation of nitrogen. The effect of polyaniline trifluoroacetylation is a drastic loss of conductivity accompanied by a symmetric contraction of the potential window of conductivity. The rate of trifluoroacetylation can be attenuated over a range of reactivities by partial oxidation of polyaniline, with a much higher than first order dependence of reactivity on polymer state of charge. Only terminal amine trifluoroacetylation is proposed to occur if polyaniline is held oxidized to 0.5 electrons per repeat unit at which potential no effect of exposure to trifluoroacetic anhydride on conductivity was observed. The trifluoroacetylated polyaniline can be hydrolyzed by base to reform the original polymer with restoration of its conductivity and electroactivity.

Experimental

All starting materials and solvents (reagent grade or better) were purchased from commercial sources and used as received except for aniline, which was distilled from CaH_2. All infrared spectroscopy was performed on a Nicolet 60SX FTIR spectrometer equipped with a liquid nitrogen cooled $Hg_xCd_{1-x}Te$ detector. Electrochemical measurements were performed using a Pine Instruments RDE4 bipotentiostat with a saturated calomel reference electrode and platinum counterelectrode, and a Kipp and Zonen BD90 XY recorder. X-ray photoelectron spectroscopy (XPS) was performed using a Surface Science Instruments (Fisons) SSL-100 spectrometer with an Al $K_{\alpha 1,2}$ source and a quartz monochromator. The author thanks Larry Rozsnyai for XPS characterization of polymer-modified electrodes.

Infrared Spectroscopy and Reactivity Under Electrochemical Potential Control. Polycrystalline Au films for RIR were prepared by electron beam deposition of a 50 Å Ti adhesion layer followed by 1000 Å of Au on Si_3N_4 coated Si wafers. Electrodes were sonicated in acetone followed by isopropanol prior to use. Polyaniline was electrodeposited onto the bottom 2 cm of 4X1.5 cm pieces of these wafers by cycling the potential of the immersed electrode from 0 to 0.9 V vs SCE at 100 mV/s in a freshly prepared aqueous solution of aniline (0.1 M), $NaHSO_4$ (0.25 M), and H_2SO_4 (0.5 M) until the peak anodic current at 0.2 V reached 20 mA. After cyclic voltammetric characterization of the polyaniline film by potential cycling between -0.2 and 0.4 V, an RIR spectrum of the fuzzy light green film on the electrode was obtained after emmersion, copious rinsing with water, and drying under a stream of nitrogen. RIR spectra of the polyaniline films on Au were acquired with a 74° angle of incidence at 4 cm^{-1} resolution. The spectra were linearly (binomial) baseline corrected, first between 2000 and 1400 cm^{-1}, forcing the region between 2000 and 1750 cm^{-1} to follow the baseline and then between 2000 to 700 cm^{-1}. By this method a constant is added to the absorbance at the frequencies outside the baseline correction window to retain spectral continuity. Prior to exposure to trifluoroacetic

anhydride, the electrode was held briefly at the electrochemical potential to be studied in 0.1 M $LiClO_4/CH_3CN$ acidified with F_3CCO_2H to set the oxidation state of the polymer prior to any opportunity to react with the anhydride. The electrode was then quickly immersed under potential control in a solution, temperature controlled to 25.0° C, containing 1.0 M trifluoroacetic anhydride in a 0.2 M trifluoroacetic acid/0.1 M $LiClO_4/CH_3CN$ solution. After the desired immersion interval, the electrode was removed from the cell and immediately washed thoroughly with water to quench residual anhydride. The cyclic voltammogram of the electrode was recorded in the aqueous deposition solution and an RIR spectrum of the rinsed, dried electrode was obtained. The electrode was then subjected to repeated cycles of exposure to trifluoroacetic anhydride and characterization allowing the progress of the reaction to be followed. The rise in CO absorbance at potentials 0.35 V and more negative was fit to a single exponential. The curves for 0.4 and 0.5 V were fit to a line. All curves were fit excluding the time zero point, since the initial absorbance rise is potential independent. Optically transparent Au films for Transmission FTIR were prepared by electron beam deposition of a 50 Å Cr adhesion layer followed by 100 Å of Au onto a Si wafer. a Cu wire lead was attached to one border of 2 X 2 cm squares of such a wafer using silver epoxy, which was also applied around the entire perimeter of the square. After curing, the silver epoxy border was covered with insulating white epoxy, leaving an effective electrode of dimensions 14 X 14 mm. Polyaniline deposition and reaction under potential control was performed as described above for the reflectance electrodes.

Trifluoroacetamide cleavage reactions were carried out by immersion of the trifluoroacetylated polyaniline-coated electrode in 7% K_2CO_3/5:2 $CH_3OH:H_2O$ at room temperature. Over the course of the reaction the polymer gradually turned deep purple. After exposure to the cleavage reagent, the electrode was rinsed with water and characterized in 0.5 M H_2SO_4 where the normal electrochromic response expected for polyaniline was observed.

Microelectrochemistry. Arrays of 8 individually addressable, platinum band microelectrodes, 1.5 X 80 μm separated by 1.5 μm were fabricated by conventional photolithographic and metallization techniques as described in Chapter 1. The electrodes were cleaned prior to derivatization by cycling in 0.5 M H_2SO_4 from -0.3 to 1.2 V vs SCE. Polyaniline was deposited onto pairs of adjacent electrodes as described above until current for the polymer oxidation wave reached 12 nA. I_D-V_G characteristics were obtained as usual by sweeping the potential of the two adjacent polyaniline-coated microelectrodes between 0 and +1.1 V vs SCE with a 25 mV drain voltage applied as a negative offset on K2 of an RDE4 bipotentiostat. Polyaniline deposited onto microelectrodes was trifluoroacetylated and subsequently hydrolyzed under the same conditions as the macroelectrodes. The microelectrode device represented in Figure 9 was prepared by simultaneous deposition of polyaniline onto three pairs of electrodes leaving the third and sixth electrodes unmodified to obtain three independent transistors. Reactions with other anhydrides were carried out at room temperature in solutions of 1.0 M anhydride and 0.2 M of the corresponding acid in 0.1 M $LiClO_4/CH_3CN$.

Oligomer Synthesis and Reactivity. The study of the oligomeric analogs of polyaniline was the work of Ivan Lorkovic. Further details and experimental can be found in references 14 and 15.

References

1. Letheby, H. *J. Chem. Soc.* **1862**, 161-3.

2. Willstätter, R.; Dorogi, S. *Chem. Ber.* **1909**, *42*, 2147.

3. Willstätter, R.; Dorogi, S. *Chem. Ber.* **1909**, *42*, 4118.

4. Green, A. G.; Woodhead, A. E. *J. Chem. Soc.* **1910**, 2388

5. Green, A. G.; Woodhead, A. E. *J. Chem. Soc.* **1912**, 1117.

6. Mohilner, D. M.; Adams, R. N.; Argersinger, W. J., Jr. *J. Am. Chem. Soc.* **1962**, *84*, 3618.

7. Paul, E. W.; Ricco, A. J.; Wrighton, M. S. *J. Phys. Chem.* **1985**, *89*, 1441.

8. Huang, W.-S.; Humphrey, B. D.; MacDiarmid, A. G. *J. Chem. Soc. Faraday Trans. 1* **1986**, *82*, 2385.

9. Ofer, D.; Crooks, R. M.; Wrighton, M. S. *J. Am. Chem. Soc.* **1990**, *112*, 7869.

10. Focke, W. W.; Wnek, G. E.; Wei, Y. *J. Phys. Chem.* **1987**, *91*, 5813.

11. Salaneck, W. R.; Lundström, I.; Huang, W.-S.; MacDiarmid, A. G. *Synth. Met.* **1986**, *13*, 291.

12. Genies, E. M.; Boyle, A.; Lapkowski, M.; Tsintavis, C. *Synth. Met.* **1990**, *36*, 139.

13. Kaplan, S.; Conwell, E. M.; Richter, A. F.; MacDiarmid, A. G. *J. Am. Chem. Soc.* **1988**, *110*, 7647.

14. McCoy, C. H.; Lorkovic, I. M.; Wrighton, M. S. *J. Am. Chem. Soc.* in press

15. Lorkovic, I. M. *Doctoral Thesis*, Massachusetts Institute of Technology, 1995; Chapter 4

16. Section 6.2 of this thesis; McCoy, C. H.; Wrighton, M. S. manuscript in preparation

17. Brédas, J.-L. in *Handbook of Conducting Polymers*; Skotheim, T. A., Ed.; Marcel Dekker: New York, 1986; Chapter 25

18. Section 6.3, this thesis; McCoy, C. H.; Rozsnyai, L. F.; Wrighton, M. S. submitted for publication.

19. Lu, F.-L.; Wudl, F.; Nowack, M.; Heeger, A. J. *J. Am. Chem. Soc.* **1986**, *108*, 8311.

20. Shacklette, L. W.; Wolf, J. F.; Gould, S.; Baughman, R. H. *J. Chem. Phys.* **1988**, *88*, 3955.

21 Tang, J.; Jing, X.; Wang, B.; Wang, F. *Synth. Met.* **1988**, *24*, 231.

22. Quillard, S.; Louarn, G.; Buisson, J. P.; Lefrant, S.; Masters, J.; MacDiarmid, A. G. *Synth. Met.* **1993**, *55-57*, 475.

23. Mengoli, G.; Musiani, M. M.; Zotti, G.; Valcher, S. *J. Electroanal. Chem.* **1986**, *202*, 217.

24. Wei, Y.; Hsueh, K.-F.; Jang, G.-W. *Macromolecules* **1994**, *27*, 518.

25. Wudl, F.; Angus, R. O., Jr.; Lu, F. L.; Allemand, P. M.; Vachon, D. J.; Nowack, M.; Liu, Z. X.; Heeger, A. J. *J. Am. Chem. Soc.* **1987**, *109*, 3677.

26. Baughman, R. H.; Wolf, J. F.; Eckhardt, H.; Shacklette, L. W. *Synth. Met.* **1988**, *25*,

121.

27. Javadi, H. H. S.; Treat, S. P.; Ginder, J. M.; Wolf, J. F.; Epstein, A. J. *J. Phys. Chem. Solids* **1990**, *51*, 107.

28. Travers, J. P.; Genoud, F.; Menardo, C.; Nechtschein, M. *Synth. Met.* **1990**, *35*, 159.

29. Shacklette, L. W.; Baughman, R. H. *Mol. Cryst Liq. Cryst.* **1990**, *189*, 193.

30. Glarum, S. H.; Marshall, J. H. *J. Phys. Chem.* **1986**, *90*, 6076.

31. Genies, E. M.; Lapkowski, M. *Synth. Met.* **1987**, *21*, 117.

32. MacDiarmid, A. G.; Chiang, J. C.; Richter, A. F.; Epstein, A. J. *Synth. Met.* **1987**, *18*, 285.

33. Brédas, J.-L.; Street, G. B. *Accs. Chem. Res.* **1985**, *18*, 309

34. Wang, S.; Wang, F.; Ge, X. *Synth. Met.* **1986**, *16*, 99.

35. Snauwaert, P. H.; Lazzaroni, R.; Riga, J.; Verbist, J. J. *Synth. Met.* **1987**, *21*, 181.

36. Comisso, N.; Daolio, S.; Mengoli, G.; Salmaso, R.; Zecchin, S.; Zotti, G. *J. Electroanal. Chem.* **1988**, *255*, 97.

37. Dao, L. H.; Leclerc, M.; Guay, J.; Chevalier, J. W. *Synth. Met.* **1989**, *29*, E377.

38. Leclerc, M.; Guay, J.; Dao, L. H. *Macromolecules*, **1989**, *22*, 649.

39. MacDiarmid, A. G.; Epstein, A. J. *Farad. Discuss. Chem. Soc.*, **1989**, *88*, 317.

40. Wang, Z. H.; Ehrenfreund, E.; Ray, A.; MacDiarmid, A. G.; Epstein, A. J. *Mol. Cryst. Liq. Cryst.* **1990**, *189*, 263.

41. Wei, Y.; Hariharan, R.; Patel, S. A. *Macromolecules* **1990**, *23*, 758.

42. Yue, J.; Wang, Z. H.; Cromack, K. R.; Epstein, A. J.; MacDiarmid, A. G. *J. Am. Chem. Soc.* **1991**, *113*, 2665.

43. D'Aprano, G.; Leclerc, M.; Zotti, G. *Macromolecules* **1992**, *25*, 2145.

44. D'Aprano, G.; Leclerc, M.; Zotti, G. *J. Electroanal. Chem.* **1993**, *351*, 145.

45. Storrier, G. D.; Colbran, S. B.; Hibbert, D. B. *Synth. Met.* **1994**, *62*, 179.

46. Seah, M. P.; Dench, W. A. *Surf. Interface Anal.* **1979**, *83*, 391.

47. Kang, D.; Wrighton, M. S. *Langmuir* **1991**, *7*, 2169.

48. Genies, E. M.; Tsintavis, C. *J. Electroanal. Chem.* **1985**, *195*, 109.

49. Genies, E. M.; Lapkowski, M. *J. Electroanal. Chem.* **1987**, *220*, 67.

50. Lapkowski, M. *Synth. Met.* **1990**, *35*, 169.

51. Toshima, N.; Yan, H.; Ishiwatari, M. *Bull. Chem. Soc. Jpn.* **1994**, *67*, 1947

52. Greene, T. W.; Wuts, P. G. W. *Protecting Groups in Organic Synthesis* Wiley: New York, 1991 pp. 353-354.

53. Newman, H. *J. Org. Chem.* **1965**, *30*, 1287.

54. Horowitz, P.; Hill, W. *The Art Of Electronics*; Cambridge University Press: New York, **1989**. pp. 816-817.

Section 6.2

The Trifluoroacetylation and Potential-Dependent Nucleophilicity of Polypyrrole

Abstract

Polypyrrole is trifluoroacetylated at the β-carbon sites of the pyrrole ring by trifluoroacetic anhydride. The trifluoroacetylated polypyrrole, which retains electrical conductivity, has a potential for onset of conduction 0.5 V positive of polypyrrole itself. Unlike polypyrrole, the trifluoroacetylated polymer is stable toward aerial oxidation of the reduced state, showing maintained I_D-V_G response after exposure to air. Polypyrrole displayed potential-dependent nucleophilicity. Polypyrrole, at -0.1 V vs Ag where it is fully reduced, is reactive toward trifluoroacetic anhydride. At +0.5 V, were it is partially oxidized, polypyrrole shows no evidence of reaction with the anhydride. Polypyrrole confined to Au electrodes was characterized before and after reaction with trifluoroacetic anhydride. The acylated polymer showed appearance of a CO band with ν_{CO} =1666 cm^{-1}. The trifluoroacetylation of 2,5-dimethylpyrrole, 1,2,5-trimethylpyrrole, and ethyl 3,4-diethyl-5-methyl-2-pyrrolecarboxylate were examined to evaluate the relative nucleophilicities of the pyrrole nitrogen versus the β-carbon sites. Trifluoroacetylation of 2,5-dimethylpyrrole with one equivalent of anhydride or with an excess yielded 3-trifluoroacetyl-2,5-dimethylpyrrole (ν_{CO} = 1678 cm^{-1}) as the major product. Full characterization of this previously unknown compound is reported. Trifluoroacetylation of the β-carbon was also observed for the reaction of 1,2,5-trimethylpyrrole with trifluoroacetic anhydride, while ethyl 3,4-diethyl-5-methyl-2-pyrrolecarboxylate showed low reactivity of nitrogen, as expected for the pyrrole family. Based on the CO stretching frequency observed for the polymer compared to that observed for 3-trifluoroacetyl-2,5-dimethylpyrrole and that reported[14] for N-trifluoroacetylpyrrole (1730 cm^{-1}), the reactivity of pyrrole β-carbons but relative inertness of the pyrrole nitrogen toward trifluoroacetylation under the reaction conditions used demonstrated for the three pyrrole derivatives, it is concluded that polypyrrole reacts with trifluoroacetic anhydride to yield the β-acylated product.

Introduction

Polypyrrole is an interesting substrate for electrophilic substitution reactions. From the chemistry of the pyrrole ring, polypyrrole is expected to be reactive toward an electrophile such as trifluoroacetic anhydride. However, whereas polyaniline has a reactive nitrogen and deactivated carbons, polypyrrole has a deactivated nitrogen and more electron-rich and nucleophilic ring carbons. A further contrast between polypyrrole and polyaniline as substrates for trifluoroacetylation is that while substitution of nitrogen blocks hole transport and conductivity in polyaniline, both N- and β-substituted polypyrroles are conducting. Therefore, polypyrrole offers a system in which trifluoroacetylation, if successful, could be used to tune the potential for onset of polymer conductivity.

The success encountered in the *in situ* trifluoroacetylation of polyaniline led to the consideration of other conducting polymers which might be suitable substrates for the reaction. Polypyrrole was a clear candidate on account of its expected reactivity toward trifluoroacetic anhydride but in terms of the *site* of acylation and effects of substitution on electrical characteristics polypyrrole is a very different substrate from polyaniline. Acylation of pyrrole itself is facile but the most reactive site is the α-carbon and not nitrogen. In polypyrrole, the α-carbons are already occupied in inter-ring bonds leaving nitrogen and the β-carbons as the potential sites for reaction. Since both N- and β-substituted polypyrroles are conducting, it was thought that trifluoroacetylation of polypyrrole might provide a reaction in which the potential for onset of conduction of a polymer substrate could be shifted by substitution with retention of conductivity, an important goal for microelectrochemical devices of the types described in Chapter 4.

Polypyrrole is among the most extensively studied of conducting polymers. The discovery of its conducting properties came not long after the observation of high conductivity in polyacetylene.[1] The conductivities of polypyrrole reported in the literature are usually in the range of 100 S/cm.[1a] Pyrrole, with its electron-rich π-system, reacts

readily in anodic polymerization yielding a polymer which is particularly easy to oxidize.[1a] Polypyrrole is vulnerable to aerial oxidation which results in a permanent, highly conducting state. The polypyrrole backbone is tolerant of both β- and N-substitution, offering a particularly diverse range of substitution options. Conductivities of N-substituted polypyrroles, however, are usually four orders of magnitude lower than polypyrrole itself and many β-substituted polypyrroles . Steric effects arising from substitution at nitrogen are reported to be responsible for the lower conductivities.[1b]

Reactivity of the Pyrrole Ring

The chemistry of pyrrole is a field spanning over a century of research. It has been broadly and extensively studied and is the subject of a number of comprehensive reviews.[2,3,4,5] The acetylation of pyrrole, the parent reaction to the chemistry described in this chapter, was first reported by Ciamician and Dennstedt in 1883.[6] This introduction discusses aspects of the reactivity of pyrroles pertinent to evaluating the expected reactivity of polypyrrole in electrophilic substitution and especially trifluoroacetylation.

Pyrrole is an aromatic heterocycle. Participation of the nitrogen p-orbital in the π-system of the ring results in a basicity of nitrogen which is very low compared to typical secondary amine.[2b] However, pyrrole is less aromatic than benzene or thiophene[2c] and its carbons are more nucleophilic and reactive than a carbon site in a strongly aromatic ring such as benzene. This aspect of pyrrole reactivity, and the strong activation of the α-carbons (usually the most reactive site in 5-membered heterocycles) can be understood in terms of the resonance forms for the pyrrole ring shown in Scheme 1.[2,3,5] The Zwitterionic forms constitute a redistribution of the nitrogen lone pair over the four carbons, enhancing their nucleophilicity at the expense of electron density at nitrogen. This explains the low basicity of the nitrogen in pyrrole compared to other secondary amines and why the most nucleophilic site in pyrrole is a carbon and not nitrogen.[5a] Pyrrole is sufficiently activated

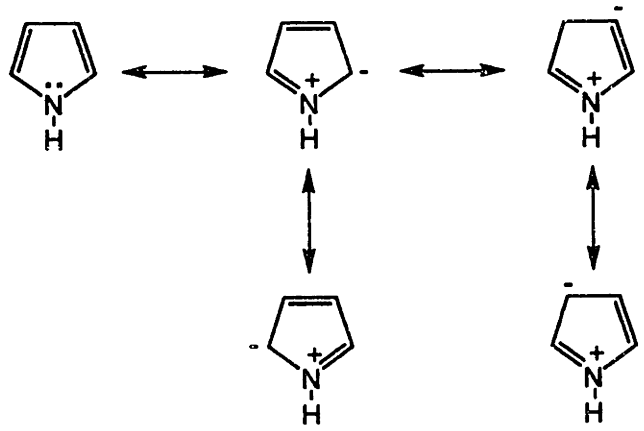

Scheme 1. Resonance forms for pyrrole.

to undergo reaction with many electrophiles without need of a catalyst[2d,4a] unlike benzene for which alkylation, acylation, and halogenation usually require a Lewis acid catalyst to enhance the electrophilicity of the attacking reagent.[7] Like other 5-membered heterocycles pyrrole undergoes electrophilic substitution preferentially at the 2-position where resonance stabilization of the σ-complex formed by attack is greater than at the 3-position, Scheme 2. However, in a polymer backbone such as polypyrrole, the α-carbons of the heterocycle are

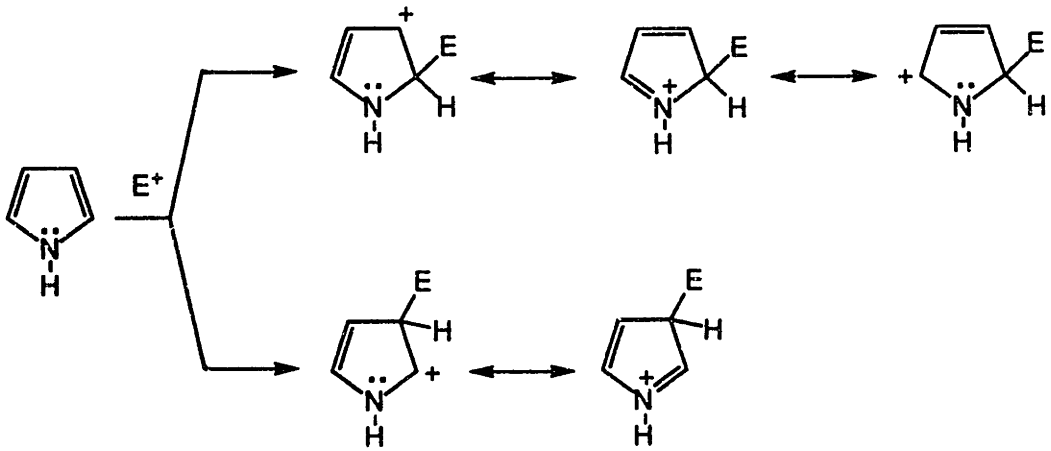

Scheme 2. Resonance structures for an intermediate arising from electrophilic attack at carbons α (top) and β (bottom) to nitrogen.

already substituted by virtue of the inter-ring bonds which form the chain. Thus the reactivity of the β-carbons is of special importance in conducting polymer substrates. In polypyrrole, the possibility of reactivity at both the β-carbons and at nitrogen make the chemistry of polypyrrole particularly interesting.

Reactions at the β-carbons and at nitrogen in pyrrole and its derivatives

While in pyrrole itself 3-substitution is rarely a major pathway, reaction at a β-carbons is facile if α-substitution is made unfavorable or impossible. Direction of substitution to the 3-position can be accomplished by placing a sterically demanding group on nitrogen, thereby hindering attack at the α-carbons[8,9,10,11] Scheme 3 summarizes the results of Chadwick, Meakins, and Rhodes.[8] The overall yields for all of the reactions

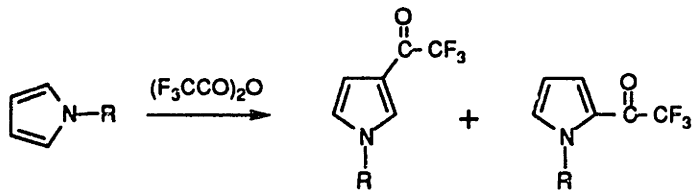

N–CH3	0	100
N–	15	85
N–	90	10
N–	100	0

Chadwick, D. J.; Meakins, G. D.; Rhodes, C. A. *J. Chem. Res. (S)* **1980**, 42

Scheme 3. Percent trifluoroacetylation at the 2 vs. 3 positions for a series of N-substituted pyrroles bearing increasingly sterically demanding groups.

were high. For example, 98% in the case of N-adamantylpyrrole.[8] Therefore, it is clear that even though the α-carbons of the pyrrole ring are the most reactive sites, the β-carbons which are of special interest in the reactivity of polypyrrole, are also quite nucleophilic and might also display such nucleophilicity in polypyrrole.

An interesting side note to the above strategy for obtaining β-substitution is the use of a fluoride-cleavable N-triisopropylsilyl group as the steric director which can be removed after substitution of the 3-position. This has been developed preparatively as a route to 3-substituted pyrroles[9-11] which, of course, are precursors to derivatives in the polypyrrole family of conductors.

Acetylation of Pyrrole

Pyrrole is acetylated by acetic anhydride to yield 2-acetylpyrrole as the major, but not sole, product.[12] There has been some debate over the extent of concurrent 3- and N-substitution occurring in the process.[2d,5,12] While the dominance of reaction at the α-carbon of pyrrole emphasizes the relatively low nucleophilicity of the pyrrole nitrogen, reaction does occur at nitrogen under certain circumstances. In general, conversion to the pyrrole anion as its sodium or potassium salt is required.[2a,2e,13a,14,15] However, pyrrole can be acetylated without resorting to the anion if the reaction is carried out under basic conditions. In the reaction of acetic anhydride with pyrrole, the presence of triethylamine raises the degree of N-substitution to 80%.[16] An interesting preparatively useful route to a range of N-acetylpyrroles is reaction of the pyrrole with acetic anhydride in the presence of triethylamine and 4-(dimethylamino)-pyridine as catalyst. This procedure is reported to show no traces of acetylation at carbon.[17] Overall, then, specific conditions control the extent to which N-acetylation competes with or dominates α-acetylation.

Trifluoroacetylation of Pyrrole

While acetylation of pyrrole by acetic anhydride requires heating, trifluoroacetic anhydride trifluoroacetylates pyrrole readily at 0°C, equation (1).[18] The only product reported in this

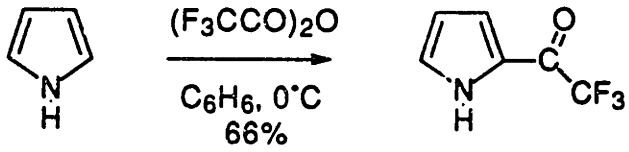

Cooper, W. D. *J. Org. Chem.* **1958**, *23*, 1382 (1)

reaction is 2-trifluoroacetylpyrrole. However, since "electrophilic substitution at the nitrogen atom of the pyrrole ring normally occurs only under strongly basic conditions"[2a] it seems less likely that N-substitution would compete given that reaction with trifluoroacetic anhydride generates an equivalent of strong acid as the byproduct of substitution. Preparation of N-trifluoroacetylpyrrole has been reported in 30% yield using trifluoroacetic anhydride and the potassium salt of pyrrole, equation (2)[14], and in "low yield" from the sodium salt.[15]

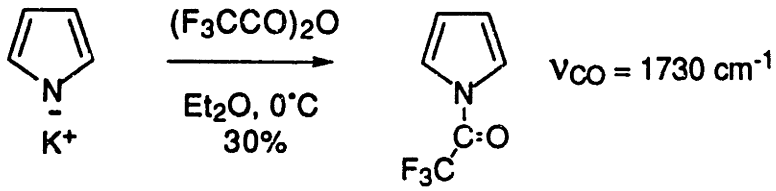

Cipiciani, A.; Linda, P.; Savelli, G.; Bunton, C. A.
J. Am. Chem. Soc. **1981**, *103*, 4874 (2)

Overall, the electronic nature of the pyrrole ring and the acylation patterns of pyrroles make a prediction that trifluoroacetylation of polypyrrole will proceed via β-substitution. However, the prediction from the literature considered left some room for speculation. One important piece of data which was not obtained from the literature cited

was a direct competition experiment between the nitrogen and the β-carbons of polypyrrole for reaction with trifluoroacetic anhydride. It was undertaken as part of this investigation, therefore, to examine the relative nucleophilicity of the two potentially reactive sites in polypyrrole by examination of monomeric systems as models, and to establish at which site trifluoroacetylation of polypyrrole occurred.

Results and Discussion

Trifluoroacetylation of derivatives of pyrrole: substitution at nitrogen versus carbon

The trifluoroacetylation of three substituted pyrroles was undertaken in order to specifically examine β-carbon versus nitrogen nucleophilicity toward trifluoroacetic anhydride. A convenient test case for β-carbon versus nitrogen nucleophilicity is 2,5-dimethylpyrrole which like polypyrrole has its α-sites blocked by electron-donating substituents allowing it to serve as a model for the polymer, although the methyl groups don't provide the resonance delocalization possible in the polypyrrole backbone. Also included in this study of trifluoroacetylation of pyrrole derivatives were 1,2,5-trimethylpyrrole which has the nitrogen as well as the α-carbons blocked leaving only the β-carbons as available sites, and ethyl 3,4-diethyl-5-methyl-2-pyrrolecarboxylate, a tetra-substituted pyrrole with only nitrogen available as a site for electrophilic attack, chosen for its combination of 2,3,4,5-substitution and commercial availability. The reactions were carried out by addition of one equivalent of trifluoroacetic anhydride to the pyrrole in CD_2Cl_2 at 0°C (25°C for the tetra-substituted pyrrole). The reaction mixtures, following a brief $NaHCO_3$ wash and drying over Na_2SO_4, were analyzed by ^{1}H-NMR spectroscopy and gas chromatography/mass spectrometry (GC/MS). Because both the 3- and N-trifluoroacetyl derivative of 2,5-dimethylpyrrole were unknown in the literature, the product of the trifluoroacetylation of 2,5-dimethylpyrrole was isolated and fully characterized by IR, NMR, GC/MS, and high-resolution MS. Scheme 4 shows the products of the three reactions, determined by ^{1}H-NMR and GC/MS, and also IR spectroscopy in the case of 2,5-dimethylpyrrole. The ^{1}H-NMR spectrum, FTIR spectrum, gas chromatogram, and mass spectrum of 3-trifluoroacetyl-2,5-dimethylpyrrole are shown in Figures 1-3. While ^{1}H-NMR is as expected for substitution at the 3-position of 2,5-dimethylpyrrole, conjugation of the trifluoroacetyl group with the pyrrole π-system can result in coplanarity and discrete syn and anti isomers.[8] Thus, inequivalency of the methyl

group resonances might occur in the N-acylated as well as the β-acylated product and therefore does not in and of itself establish the site of substitution. However, the presence of the strong N-H stretch at 3445 cm^{-1} in the IR spectrum resolves any doubt that the product is the 3-substituted derivative.

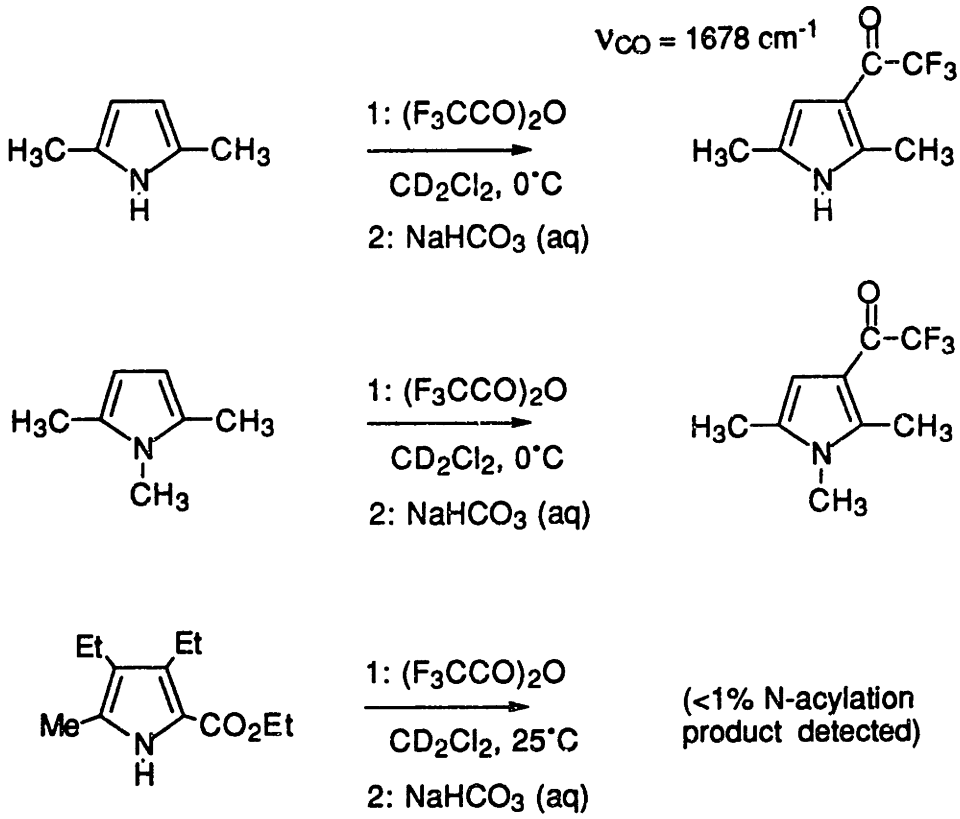

Scheme 4. Trifluoroacetylation products from 2,5-dimethylpyrrole, 1,2,5-trimethylpyrrole, and ethyl 3,4-diethyl-5-methyl-2-pyrrolecarboxylate. Reaction time was 20 minutes.

In the reaction of 2,5-dimethylpyrrole, the singlet corresponding to the α-methyl groups disappeared and was replaced by a pair of singlets further downfield. The resonance for the β-hydrogen also shifted downfield as did the very broad resonance due to the N-hydrogen. If the reaction mixture was examined by NMR prior to washing with aqueous bicarbonate, the same results were obtained so it does not appear that

Figure 1. ^{1}H-NMR spectrum (300 MHz, $CDCl_3$) of 3-trifluoroacetyl-2,5-dimethylpyrrole.

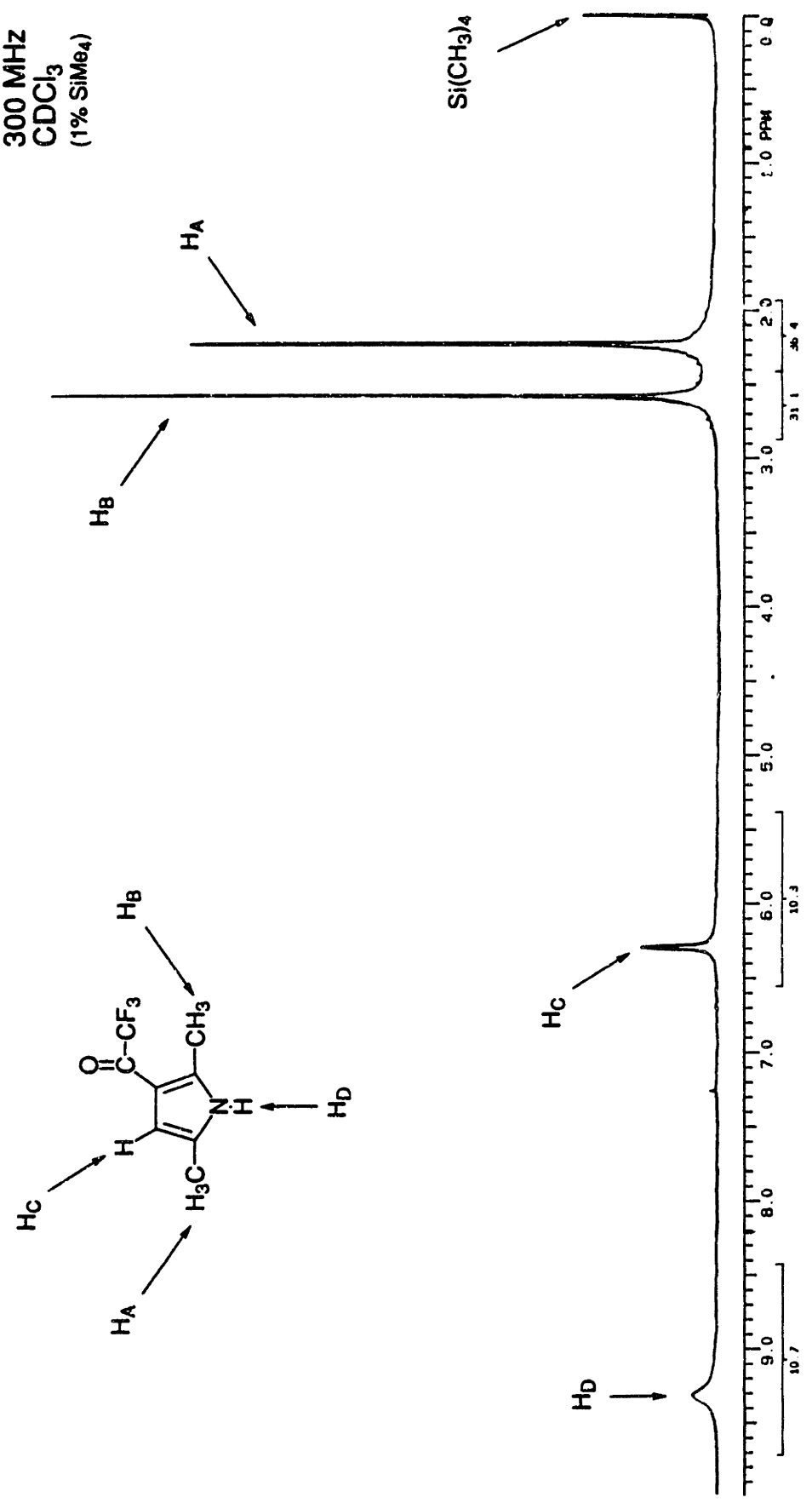
300 MHz
CDCl3
(1% SiMe4)
Si(CH3)4
HA
HB
HC
HD
HB
CH3
C–CF3
O
N
H
HD
HC
H3C
HA
9.0
8.0
7.0
6.0
5.0
4.0
3.0
2.0
1.0 PPM
0.0

Figure 2. FTIR spectrum ($CDCl_3$) of 3-trifluoroacetyl-2,5-dimethylpyrrole.

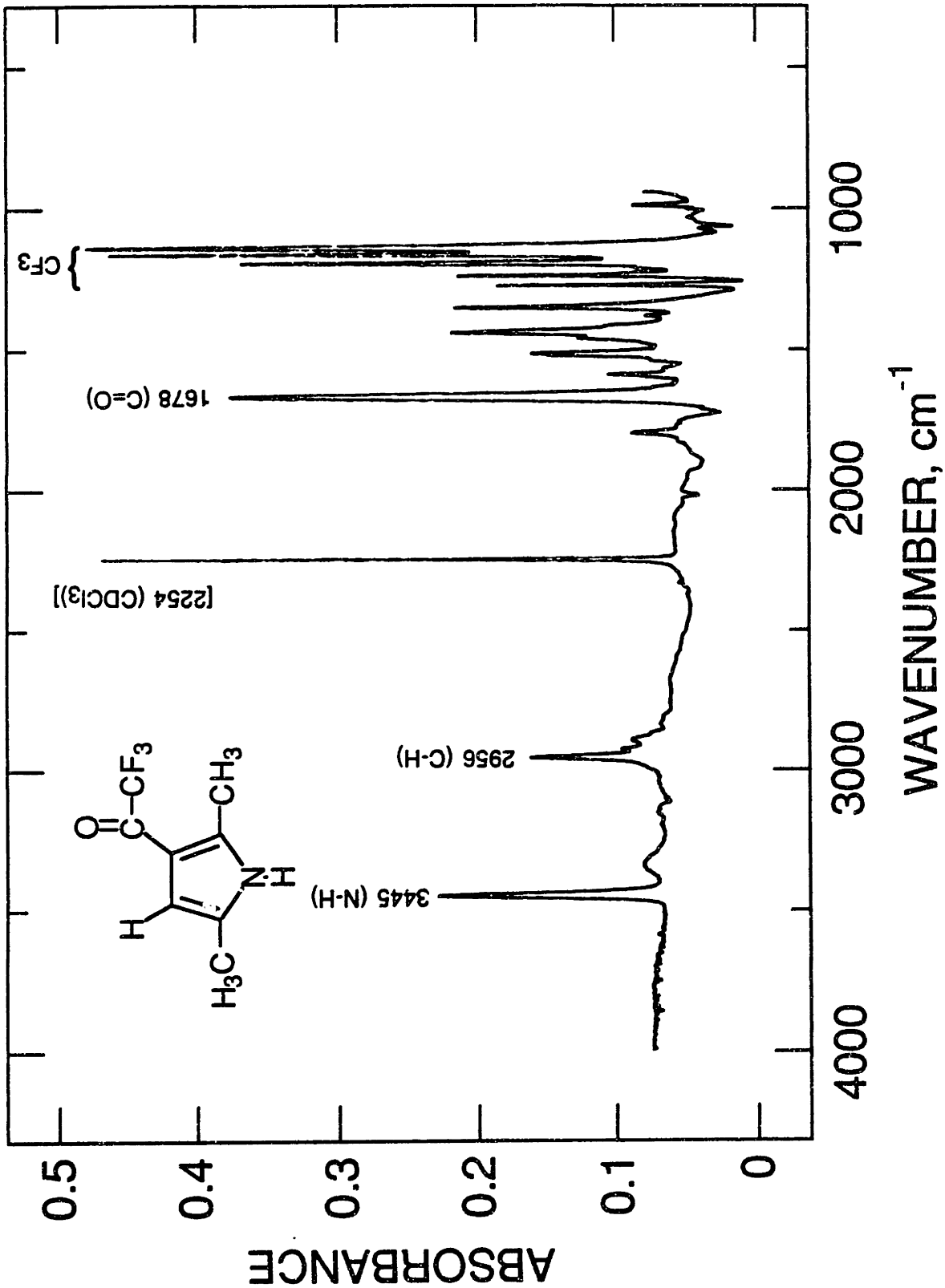
ABSORBANCE
0.5
0.4
0.3
0.2
0.1
0
4000
3000
2000
1000
WAVENUMBER, cm-1
3445 (N-H)
2956 (C-H)
[2254 (CDCl3)]
1678 (C=O)
CF3
O=C
CF3
CH3
H
N
H
H3C

Figure 3. Gas chromatogram (top) and mass spectrum (bottom) of 3-trifluoroacetyl-2,5-dimethylpyrrole.

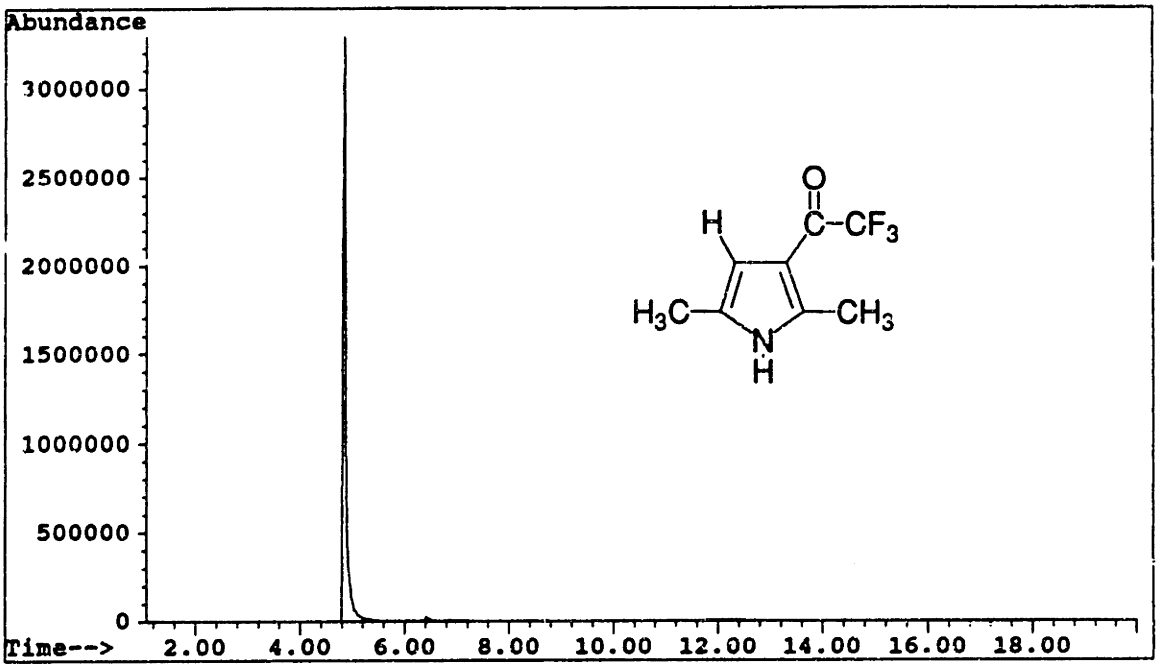
Abundance
3000000
2500000
2000000
1500000
1000000
500000
0
Time-->
2.00
4.00
6.00
8.00
10.00
12.00
14.00
16.00
18.00
O
H
C–CF3
H3C
CH3
N
H

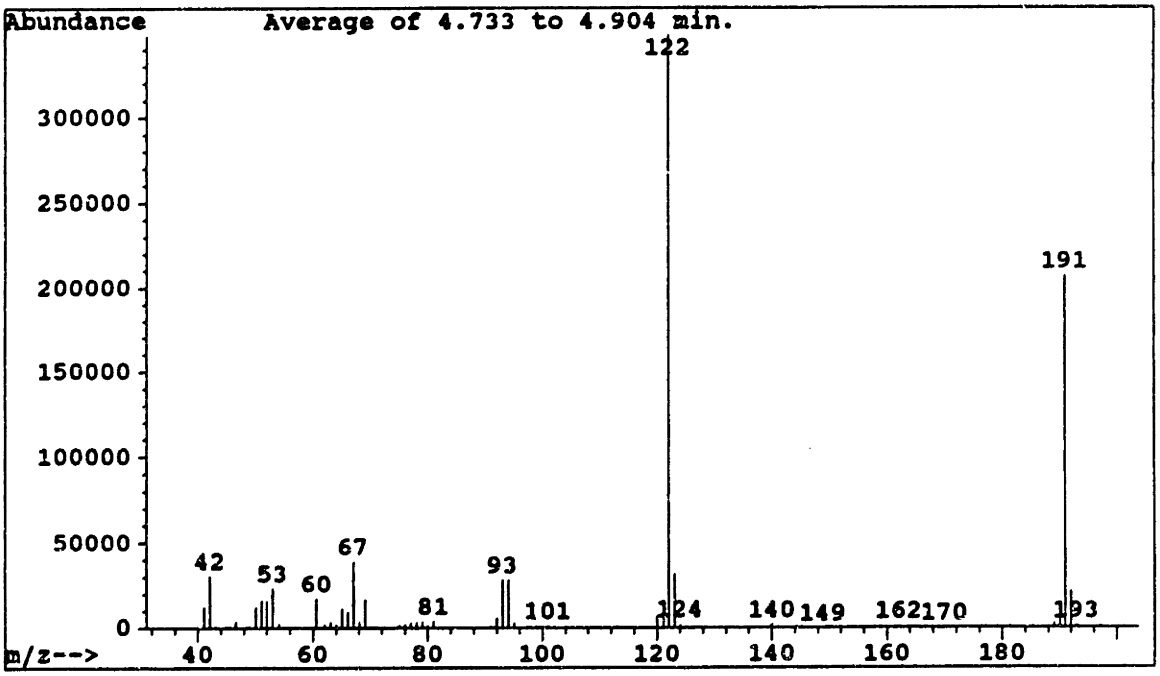
Abundance
Average of 4.733 to 4.904 min.
122
300000
250000
200000
191
150000
100000
50000
42
53
60
67
81
93
101
124
140
149
162
170
193
0
m/z-->
40
60
80
100
120
140
160
180

N-substitution occurred with subsequent loss via basic hydrolysis of the N-trifluoroacetamide during work-up.[14] The case of excess anhydride is important because with an *in-situ* reaction of microelectrode-confined polymer the attacking reagent is always in excess because a very small quantity of polymer is immersed in a comparatively vast solution of reactant. With a five-fold excess of trifluoroacetic anhydride 3-trifluoroacetyl-2,5-dimethylpyrrole was still the major product. A minor product at lower retention time than the 3-trifluoroacetyl derivative was detected by GC/MS that had a mass spectrum consistent with a diacylated product. Since N-trifluoroacetylpyrrole boils 30-40 °C lower than pyrrole, it is not unreasonable that an N,β-diacylated product might have a lower retention time than the β-monoacylated derivative due to loss of hydrogen bonding in the former. The species responsible for the minor peak was apparently unstable and no longer appeared in the GC/MS of the same sample 12 hours later.

Reaction of 1,2,5-trimethylpyrrole with one equivalent of trifluoroacetic anhydride paralleled the behavior of the dimethylpyrrole. In the ^{1}H-NMR the α-methyl resonance split into a pair of singlets further downfield and the N-methyl and β-hydrogen resonances also shifted downfield. While 20 minutes at 0°C resulted in nearly complete consumption of 2,5-dimethylpyrrole by one equivalent of anhydride, a minor fraction of the starting material remained with the trimethylpyrrole. ^{1}H-NMR and GC/MS showed that the reaction proceeded more cleanly with the trimethylpyrrole as compared to the dimethyl substrate. Both reactions are exothermic, and are best carried out below room temperature, especially in the case of 2,5-dimethylpyrrole.

The tetra-substituted pyrrole showed only a small peak in the GC/MS of the reaction mixture and as expected the nitrogen was not found to have low nucleophilicity. It is reported that in the synthesis of N-trifluoroacetylpyrrole that the product can undergo hydrolysis and the aqueous wash step for reaction should be kept short.[14] This precaution was followed in the work-up of the reaction of the tetra-substituted pyrrole also, but hydrolysis of some of the N-acylated product cannot be ruled out.

Reaction of polypyrrole with trifluoroacetic anhydride

The trifluoroacetylation of polypyrrole was carried out on microelectrode-confined films for characterization of electrical properties of the polymer and on macroelectrode-confined films for characterization by specular reflectance Fourier transform infrared spectroscopy (RIR). Polypyrrole, upon exposure to 1 M trifluoroacetic anhydride in CH_3CN at room temperature was found to exhibit a 0.5 V positive shift in the potential of onset of conduction. A polymer-modified microelectrode array was immersed in the anhydride solution for 20 minutes, during which the polypyrrole has held fully reduced and under active potential control, followed by a thorough rinse with water to quench unreacted trifluoroacetic anhydride. The polymer retained 75 % of its initial conductivity. In contrast to what is observed for polypyrrole, the I_D-V_G characteristic of trifluoroacetylated polypyrrole was unaffected by exposure of the polymer to air. (Polypyrrole is rendered permanently conducting by brief exposure to oxygen, displaying only a flat line at constant drain current as its I_D-V_G response.)

To investigate the dependence of the rate of trifluoroacetylation on the oxidation state of polypyrrole, a pair of polypyrrole transistors, deposited side by side on a microelectrode array, were exposed to 1M trifluoroacetic anhydride at 27°C for 20 minutes. One device was held at -0.1 V vs. Ag wire, where polypyrrole is in its reduced state, and the other at +0.5 V vs. Ag wire where polypyrrole is partially oxidized and conducting. The I_D-V_G characteristics of the two transistors before and after exposure to the anhydride are shown in Figure 4. The polypyrrole held reduced showed a +0.5 V shift in onset of conduction. The second polypyrrole transistor, however, showed no shift in its I_D-V_G characteristic although its conductivity actually increased following a very brief exposure to air. Thus, as with polyaniline, the nucleophilicity of polypyrrole can be controlled by adjusting the state of charge of polymer. At +0.5V vs. Ag wire the polymer was found to

Figure 4. I_D-V_G characteristics of polypyrrole before and after exposure to 1M $(F_3CCO)_2O$/0.1 M [*n*-Bu_4N]PF_6/CH_3CN for 20 minutes under active potential control at 0.5 V vs. Ag (top) and -0.1 V (bottom)

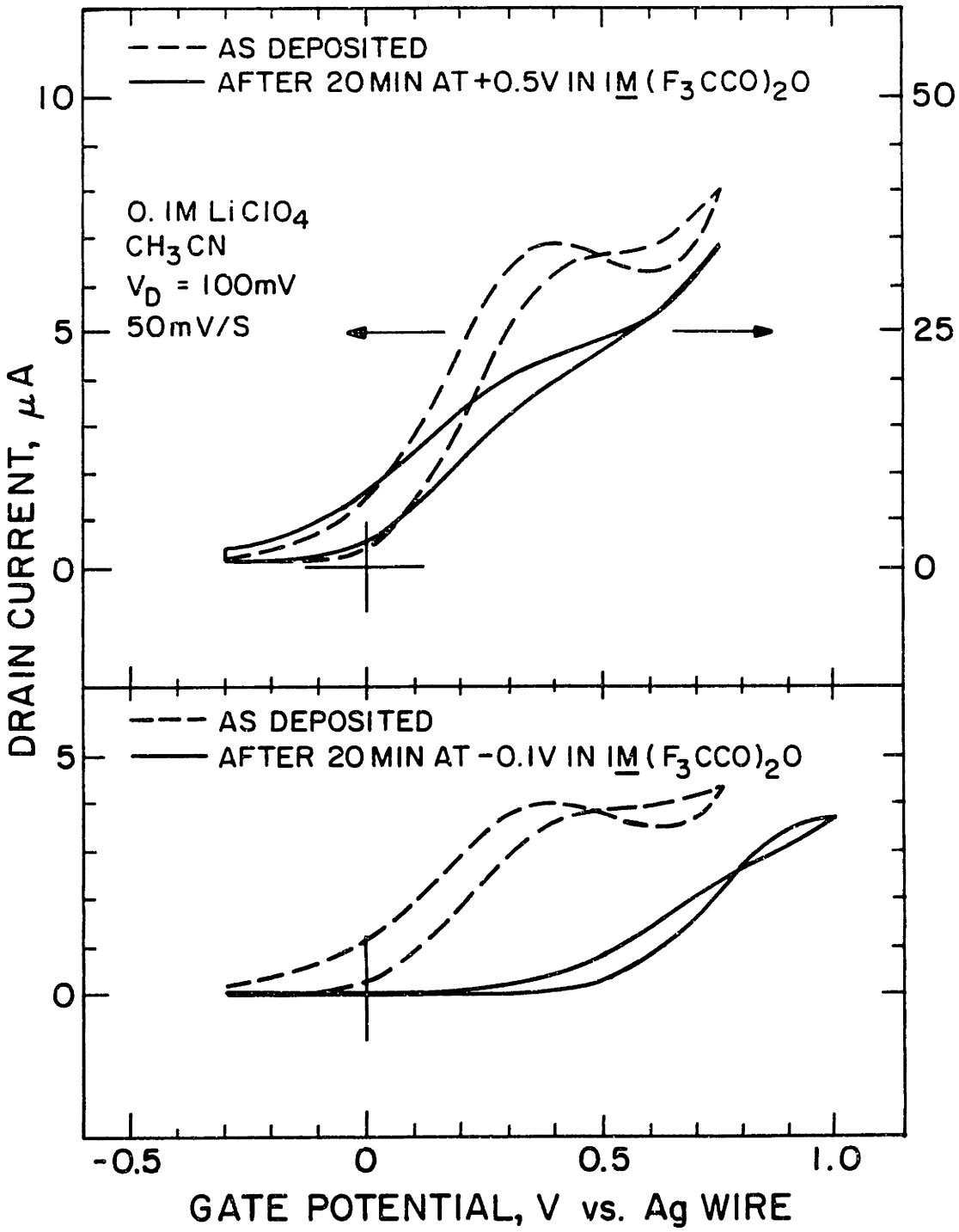
AS DEPOSITED
AFTER 20 MIN AT +0.5V IN 1M $(F_3CCO)_2O$
0.1M $LiClO_4$
CH_3CN
V_D = 100mV
50mV/S
AS DEPOSITED
AFTER 20 MIN AT -0.1V IN 1M $(F_3CCO)_2O$
DRAIN CURRENT, μA
10
5
0
50
25
0
5
0
-0.5
0
0.5
1.0
GATE POTENTIAL, V vs. Ag WIRE

be inert toward trifluoroacetic anhydride over the 20 minute exposure.

The stability to oxygen and large shift in the potential for onset of conduction upon trifluoroacetylation of polypyrrole parallel the effects of substitution described for the pyrrole family in the literature. Pyrrole is sensitive to aerial oxidation and quite reactive but substitution with an electron-withdrawing group results in stability toward oxygen and markedly lower reactivity.[2] The deactivating effect on reactivity of the pyrrole ring caused by an electronegative substituent means a less electron-rich π-system which translates to a more positive potential for oxidation and onset of conduction for a pyrrole polymer.

The trifluoroacetylation of polypyrrole was also carried out on 15 x 40 mm Au electrodes for characterization by specular reflectance infrared spectroscopy (RIR). Because of concern for the sensitivity of polypyrrole to oxygen, the experiment was carried out by two different procedures. In one case, the polypyrrole film was deposited and reacted immediately with the anhydride, then characterized by RIR. Thus, the polymer was not exposed to oxygen until after trifluoroacetylation, at which point it was found above to be stable. RIR of a second electrode derivatized with polypyrrole provided a spectrum of as-deposited polypyrrole. In the second procedure, polypyrrole was deposited, characterized by RIR during which exposure to oxygen was inevitable, reacted with trifluoroacetic anhydride, and characterized again by RIR. Both procedures produced essentially the same RIR spectrum for trifluoroacetylated polypyrrole. Trifluoroacetylation was carried out under an argon atmosphere by immersion of the electrode, under potential control, in a solution of 1M trifluoroacetic anhydride in CH_3CN at 27°C for 20 minutes at -0.2 V vs. Ag. Figure 5 shows the RIR spectrum of a film of freshly-deposited polypyrrole which has not been exposed to trifluoroacetic anhydride. The polymer was undoubtedly conducting due to aerial oxidation when the spectrum was acquired and that probably accounts for the broadening and poor resolution. Figure 6 shows the RIR spectrum of trifluoroacetylated polypyrrole. The important feature is the band at 1666 cm^{-1} assigned as the CO stretch, which has appeared and was not present in the RIR of

Figure 5. Specular reflectance FTIR of electrochemically deposited polypyrrole prior to exposure to trifluoroacetic anhydride.

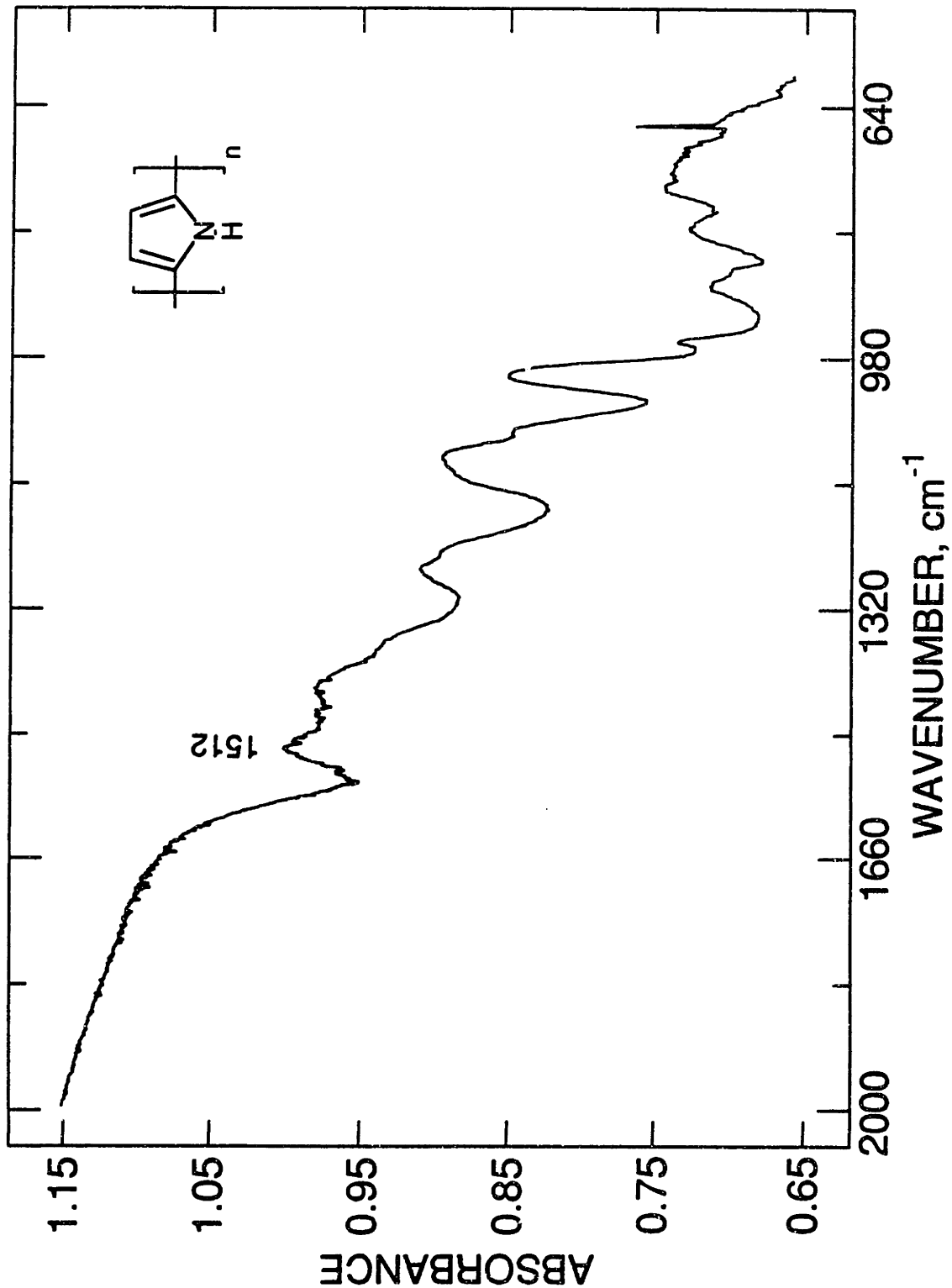
1512
ABSORBANCE
1.15
1.05
0.95
0.85
0.75
0.65
2000
1660
1320
980
640
WAVENUMBER, cm-1
N
H
n

Figure 6. Specular reflectance FTIR of polypyrrole following 20 minutes immersion in 1M $(F_3CCO)_2O$/0.1 M [*n*-Bu_4N]PF_6/CH_3CN at -0.2 V vs. Ag.

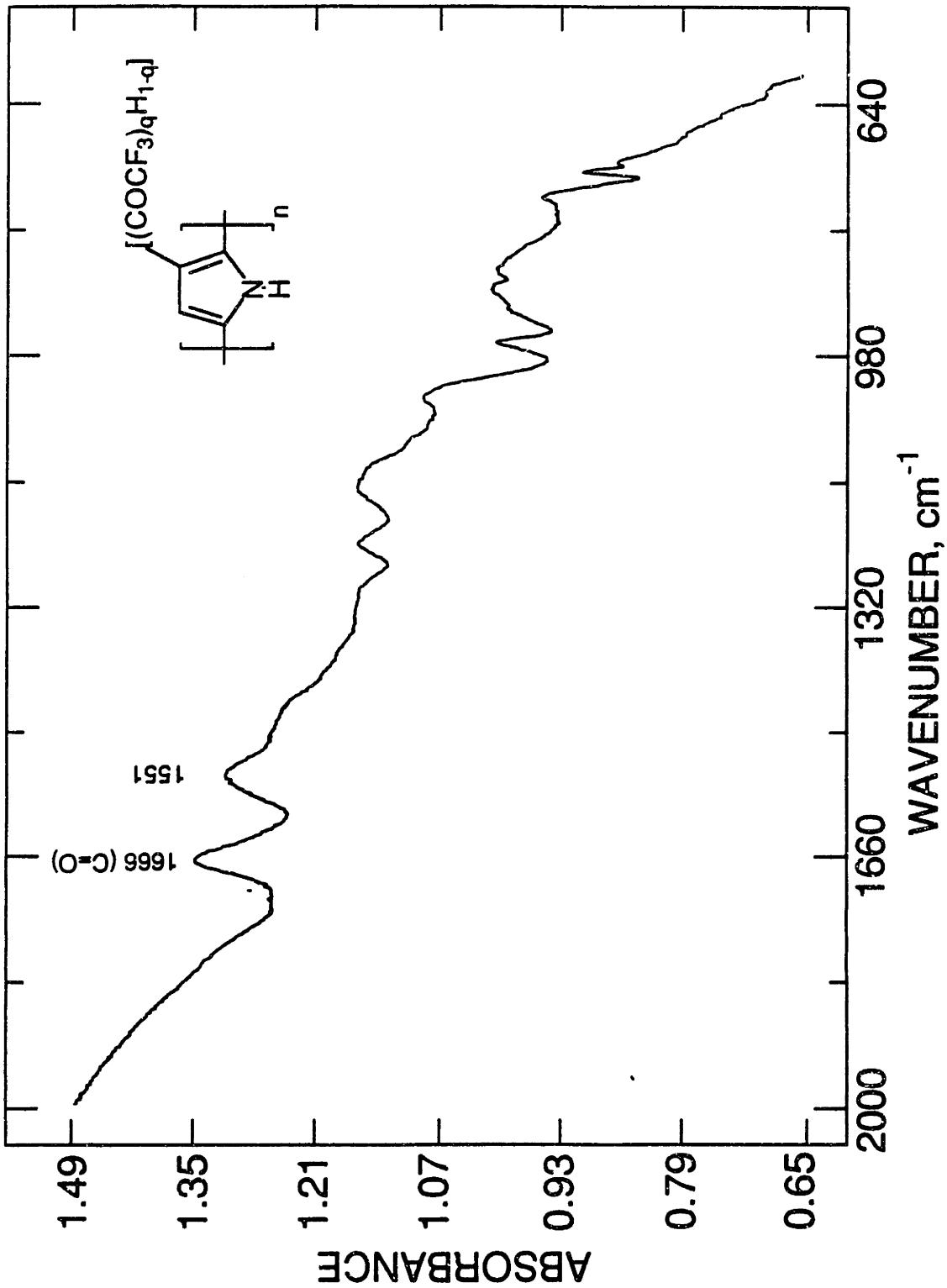
ABSORBANCE
1.49
1.35
1.21
1.07
0.93
0.79
0.65
2000
1660
1320
980
640
WAVENUMBER, cm-1
1666 (C=O)
1551
[(COCF3)qH1-q]n
N
H

polypyrrole prior to exposure to trifluoroacetic anhydride. In 3-trifluoroacetyl-2,5-dimethylpyrrole characterized above the carbonyl stretch occurred at 1678 cm^{-1} while in N-trifluoroacetylpyrrole the carbonyl stretch is reported to be at 1730 cm^{-1}. The presence of a carbonyl band for the polymer at 1666 cm^{-1} is consistent with trifluoroacetylation occurring at β-carbons and not the nitrogens in polypyrrole. That the carbonyl stretch in the polymer comes 12 cm^{-1} lower in energy than for 3-trifluoroacetyl-2,5-dimethylpyrrole is attributed to conjugation of the trifluoroacetyl group with the polymer backbone. Reasonable resonance structures can be drawn for conjugation of the carbonyl group with adjacent rings of the polymer if the trifluoroacetyl group is on a β-carbon but not if it is on nitrogen. Overall, therefore, the 1666 cm^{-1} carbonyl stretch for trifluoroacetylated polypyrrole allows assignment of the product as the 3-trifluoroacetyl derivative, consistent with acylation behavior of the pyrrole family reported in the literature, and with the comparative inertness of nitrogen compared to the β-carbons demonstrated above. It is no surprise, therefore, that the trifluoroacetamide cleavage reagent which regenerated polyaniline from N-acylated polyaniline (section 6.1), did not accomplish such regeneration of polypyrrole. 21 hours immersion in 7% K_2CO_3/5:2 CH_3OH:H_2O resulted only in loss of I_D-V_G response of trifluoroacetylated polypyrrole. A final piece of evidence consistent with β-substitution is the retention of conductivity upon trifluoroacetylation. Since N-substituted pyrroles are several orders of magnitude less conducting than polypyrrole,[1b] the degree of retention of conductivity seen in the I_D-V_G characteristic of the trifluoroacetylated polymer seems incompatible with the assignment of acylation at N. It is concluded that polypyrrole reacts with trifluoroacetic anhydride via attack at the β-carbons of the backbone.

The trifluoroacetylation of poly(N-methylpyrrole) was also studied. The N-substituted polymer is less easily oxidized than polypyrrole and is not oxygen sensitive. Its conductivity is low compared to polypyrrole.[19] Exposure to trifluoroacetic anhydride resulted in a shift of approximately 150 mV in onset of conductivity. Reaction of side-by-side poly(N-methylpyrrole) transistors, one held at 0 V vs. Ag wire and the other at 0.7

resulted in shift in onset of conductivity of the device held at 0 V and retention of onset potential for the device held at 0.7 V, but changes in the electrical characteristics of this polymer were harder to quantify due to its inherently low conductivity. Changes in the I_D-V_G characteristic of poly(N-methylpyrrole) required longer reaction times than for polypyrrole and while the partially oxidized polymer maintained its potential for onset of conduction in the presence of the anhydride it lost about a third of its peak conductivity.

As substrates for reactions conducting polymers are unusual in several respects. Because of extended π-delocalization conducting polymers are considerably easier to oxidize than the monomers from which they are formed, usually by a one or more. Furthermore, the ability to strongly delocalize positive charge which is a fundamental component of conductivity also may activate the β-carbons of the polymer toward electrophilic attack and communicate substituent resonance effects over several rings. As shown in Scheme 2 in the introduction, β-attack results in delocalization of the positive charge onto the adjacent α-carbon and onto nitrogen. In a conducting polymer backbone the α–carbon adjacent to the site of attack is tertiary rather than secondary and, more importantly, strong resonance stabilization of the intermediate can occur, as shown in Scheme 5. In this way the polymer backbone can delocalize the positive charge over several rings. With such delocalization and the more favorable tertiary α-carbon to stabilize the σ-complex, β-attack should be activated in polypyrrole compared to pyrrole itself. The quinoid resonance structure which arises from delocalizing the charge to adjacent rings is significant because of its connection with the theory of charge support and electronic structure of conjugated organic polymers which addresses the extent to which adoption of the quinoid resonance form is energetically favorable.[1c,20,21] In brief, the benzenoid polymer is more favorable for the neutral state, and the quinoid structure is more favorable for support of charge sites (this was discussed in detail in Chapter 3). Given that polypyrrole has been calculated to support a positive charge by a partial distortion to its quinoid resonance form over four rings,[20] it can be postulated that the resonance

stabilization of the intermediate arising from attack of an electrophile results from delocalization of positive charge over approximately four rings adjacent to the site of attack. This is reasonable to the extent that the delocalized σ-complex resembles either a polaron (a radical cation) or a bipolaron (dication), both of which are supported as four-ring delocalizations with a shift to quinoid geometry in polypyrrole.[20]

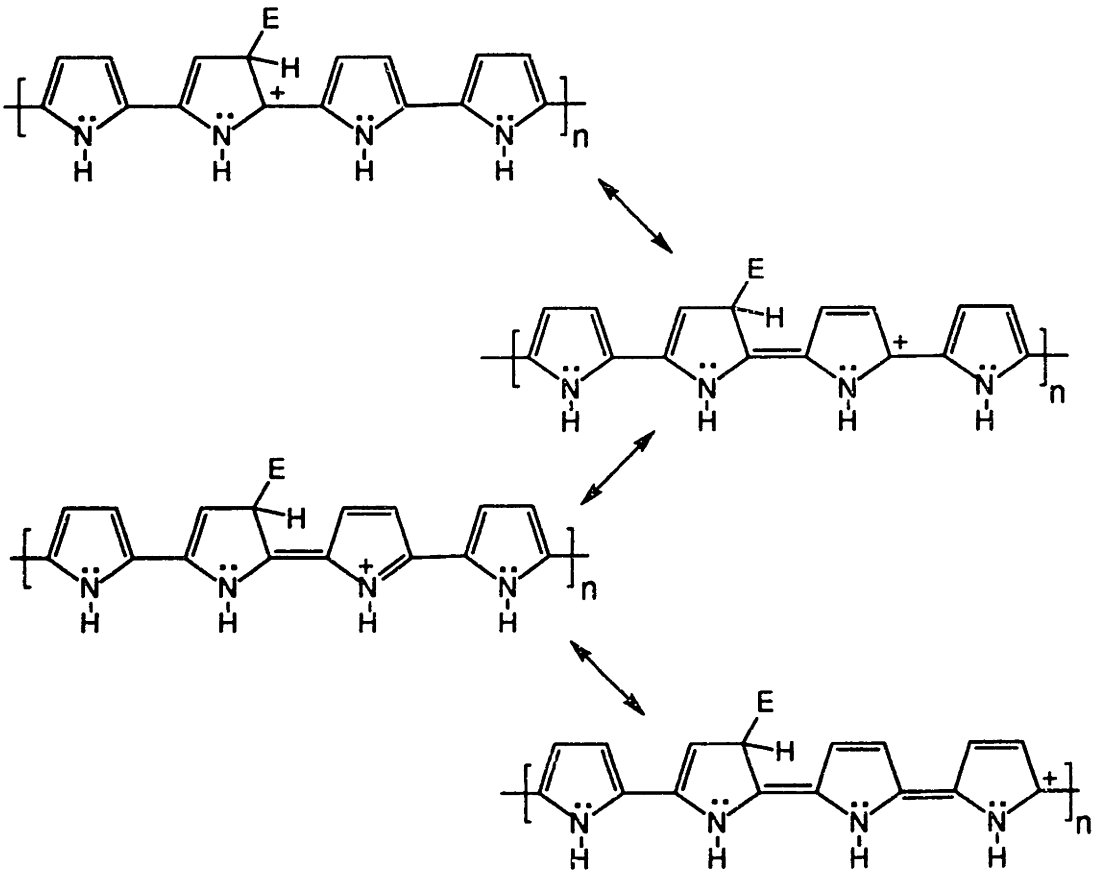

Scheme 5. Resonance stabilization by the backbone of polypyrrole of the σ-complex resulting from electrophilic attack at a β-carbon.

Delocalization further down the chain than four rings would require progressively more adaptation of quinoid form and since the quinoid resonance form is more favorable for support of charge but higher in energy for neutral polymer it would be unfavorable to generate a long section of quinoid units when only a single charge is present. Scheme 5 applies to polyheteroaromatics in general although the contribution of the resonance

structure where the positive charge is on the heteroatom is expected to vary amongst different ring systems. For example, its contribution in polytellurophene should be negligible because of the size mismatch of carbon and tellurium p-orbitals.

The extent over which support of a positive charge induces quinoid distortion is also the distance over which a resonance-withdrawing group such as trifluoroacetyl might be expected to exert a deactivating effect. In the case of trifluoroacetylation, the resonance form in which a negative charge resides on oxygen, the carbonyl carbon is doubly bonded to the β-carbon of the pyrrole ring, and a positive charge resides on an α-carbon on a ring further along the polymer chain may also cover four repeat units in polypyrrole. Since pyrrole is strongly deactivated by electron withdrawing substituents it may be that attack within a few rings adjacent to a trifluoroacetylated ring is made sufficiently unfavorable to preclude substitution to one group per repeat unit.

In summary, polypyrrole is trifluoroacetylated by trifluoroacetic anhydride yielding an air-stable polymer with a potential for onset of conduction 0.5 V positive of polypyrrole itself. The trifluoroacetylated polymer retained 75 % of the conductivity of the starting polypyrrole. Based on the reactivity of model compounds and the appearance of a carbonyl stretch at 1666 cm^{-1} for trifluoroacetylated polypyrrole (compared to 1678 cm^{-1} for 3-trifluoroacetyl-2,5-dimethylpyrrole and 1730 cm^{-1} for N-acetylpyrrole) it was concluded that polypyrrole acylates at the β-carbon sites of the polymer rather than the nitrogen sites as the dominant pathway. Like polyaniline, polypyrrole displayed potential-dependent nucleophilicity by reacting with trifluoroacetic anhydride in the reduced state but not in the partially oxidized state.

Experimental

All materials were used as received from Aldrich Chemical except for pyrrole and trifluoroacetic anhydride, which was distilled prior to use, and tetrabutylammonium hexafluorophosphate which was recrystallized from ethyl acetate. ^{1}H-NMR spectra were obtained on a Varian XL-300 or Bruker AC-250 spectrometer. All infrared spectroscopy was performed on a Nicolet 60SX FTIR spectrometer equipped with a liquid nitrogen-cooled $Hg_xCd_{1-x}Te$ detector. The solution spectra were obtained in a 0.2 mm pathlength CaF_2 solution cell. RIR spectra of the polypyrrole films on Au were acquired with a 74° angle of incidence at 4 cm^{-1} resolution. The IR spectra presented in Figures are shown as-acquired and have not been baseline corrected. Gas chromatography/mass spectrometry was performed on a Hewlett-Packard Model HP5890 Series II Gas Chromatograph equipped with a 5971 Series Mass Selective Detector. A model HP1 non-polar column was used with a three-zone temperature program of 3 min @ 80°C, 20°/min ramp to 200°C, 200°C for the remainder of the program time. Electrochemical measurements were performed using a Pine Instruments model RDE4 bipotentiostat and data were recorded on a Kipp and Zonen model BD90 XY recorder. A silver wire was used as reference electrode and a platinum wire as counterelectrode. A platinum gauze counterelectrode was used for macroelectrode experiments.

Reaction of 2,5-dimethylpyrrole with trifluoroacetic anhydride

30 μL, 0.34 mM, 2,5-dimethylpyrrole was dissolved in 2 grams CD_2Cl_2 and the solution chilled to 0° C in an ice bath. 48 μL, one equivalent, trifluoroacetic anhydride was added and the reaction mixture kept at 0° for 20 minutes and then washed with saturated sodium bicarbonate solution. The organic layer was dried over sodium sulfate. ^{1}H NMR of the reaction mixture showed consumption of most of the starting pyrrole with new peaks appearing at 2.21 and 2.53 ppm (singlets, methyl groups), 6.3 (singlet, slightly broadened), and 8.6 (broad). Analysis of the reaction mixture by GC/MS showed one

major peak and a number of other minor peaks which could not be assigned. The major product had mass spectrum: m/z (relative abundance) 191 (60) M+, 122 (100) loss of CF_3, minor peaks at 94, 93, 67, 60, 53, and 42

Preparation, isolation, and characterization of 3-trifluoroacetyl-2,5-dimethylpyrrole

3 ml CH_2Cl_2 and a magnetic stir bar were placed in an argon-purged 10 ml round bottom flask and chilled to 0°C in an ice bath. 1.0ml 2,5 dimethylpyrrole (9.4 mM) was added by syringe. To the magnetically stirred cold solution of the pyrrole was added 1.47 ml (10.4 mM) trifluoroacetic anhydride dropwise over 2 minutes. The reaction mixture was stirred for an additional 20 minutes and then saturated aqueous sodium bicarbonate was added slowly until gas evolution ceased. The layers were separated and the organic phase dried over sodium sulfate. The solvent was removed by rotary evaporation and the crude product sublimed under vacuum to yield 0.61 g of 3-trifluoroacetyl-2,5-dimethylpyrrole (32%). ^{1}H-NMR (300 MHz, $CDCl_3$): 2.23 (s, 3H, 2-CH3); 2.58 (s, 3H, 5-CH3); 6.29 (s, 1H, 4-H); 9.3 (broad, 1H, N-H). IR ($CDCl_3$, cm^{-1}): 3445, 2956, 1806, 1678, 1538, 1523, 1450, 1362, 1283, 1248, 1203, 1172, 1147. MS: m/z (relative abundance) 191 (60) M+, 122 (100) loss of CF_3, minor peaks at 94, 93, 67, 60, 53, and 42 High resolution MS: calculated 191.05578, found 191.005598. The GC retention time and mass spectrum of the product were identical with that found for the main product of the above reaction. The NMR spectrum, IR spectrum, gas chromatogram, and mass spectrum are shown in Figures 1-3.

Reaction of 1,2,5-trimethylpyrrole with trifluoroacetic anhydride

46 µL, 0.34 mM, 1,2,5-trimethylpyrrole was dissolved in 2 grams CD_2Cl_2 and the solution chilled to 0° C in an ice bath. 48 µL, one equivalent, trifluoroacetic anhydride was added and the reaction mixture kept at 0° for 20 minutes and then washed with saturated

sodium bicarbonate solution. The organic layer was dried over sodium sulfate. ^{1}H-NMR of the reaction mixture showed: 2.21, 2.56 (singlets, 3H for each, α-methyl protons); 3.43 (s, 3H, N-methyl protons); 6.29 (s, slightly split, ring proton). GC/MS of the reaction mixture showed unreacted starting material, a major peak with mass spectrum consistent with trifluoroacetylation of 1,2,5-trimethylpyrrole, and a single side product with high molecular weight and a highly fragmentary mass spectrum. This minor peak could not be assigned.

Reaction of ethyl 3,4-dimethyl-5-methyl-2-pyrrolecarboxylate with trifluoroacetic anhydride

To 0.076g , 0.36mM, of the pyrrole in 2g CD_2Cl_2 was added 48 μL, 0.34mM, trifluoroacetic anhydride. After 20 minutes at room temperature the reaction mixture was washed with saturated aqueous sodium bicarbonate and the organic layer dried over magnesium sulfate Analysis of the reaction mixture by GC/MS showed a main peak for the starting material and a minor peak integrating to < 1% compared to the starting material with mass spectrum consistent with the N-trifluoroacetylated product: m/z (relative abundance) 305(57), 290(6), 260(31), 259(100), 258(32), 216(10), 162(71), 148(89), 134(10), 120(18), 91(14), 77(22), 69(24)

Reaction of polypyrrole with trifluoroacetic anhydride

Due to the sensitivity of polypyrrole to oxygen, all work was carried out in a closed cell under argon and all solutions were degassed by purging with argon prior to transfer into the cell. Polypyrrole was deposited onto platinum microelectrode arrays by anodic polymerization of pyrrole from a solution of 0.20 ml pyrrole in 5 ml 0.1 M [*n*-Bu_4N]PF_6/CH_3CN by scanning positive at 10 mV/S until the characteristic rapid onset of current occurred at which point the potential was held for approximately 0.5 s and then switched back to 0. Reactions with trifluoroacetic anhydride were carried out by

immersion of the derivatized microelectrode array, under electrochemical potential control vs. an Ag reference electrode, into a solution of 1M trifluoroacetic anhydride in 0.1 M [*n*-Bu_4N]PF_6/CH_3CN.

Specular reflectance infrared spectroscopy of polypyrrole and trifluoroacetylated polypyrroles

Polypyrrole was deposited onto 15 x 40 mm electrodes bearing 1000Å of Au on Si wafers by anodic polymerization of pyrrole in a closed cell under argon from a degassed solution of 0.20 ml pyrrole in 5 ml 0.1 M [*n*-Bu_4N]PF_6/CH_3CN by scanning positive from 0 V vs. Ag wire at 10 mV/S until onset of current and holding the potential until a visible film covered the entire electrode. Solutions were transferred in and out of the cell by syringe and cannula techniques. All solutions were degassed with argon prior to use. Trifluoroacetylations were carried out using a solution of 1M trifluoroacetic anhydride in 0.1 M [*n*-Bu_4N]PF_6/CH_3CN with the electrodes held under potential control at -0.2 V vs. Ag. Prior to acquisition of RIR spectra, the electrodes were rinsed with water to quench any anhydride present, then rinsed thoroughly with CH_3CN and dried under a stream of nitrogen.

References

1. a) Diaz, A. F.; Bargon, J. Chapter 3; b) Street, G. B. Chapter 8; c) Chance, R. R.; Boudreaux, D. S.; Brédas, J.-L.; Silbey, R. Chapter 24; in *Handbook of Conducting Polymers*; Skotheim, T. A., Ed.; Marcel Dekker: New York, 1986

2. Jones, R. A., ed. *The Chemistry of Heterocyclic Compounds Pyrroles, Part One* John Wiley & Sons: New York, 1990; a) p. 300 b) p.295 c) p.296 d) p. 448 e) p. 476

3. Jones, R. A.; Bean, G. P. *The Chemistry of Pyrroles* Academic Press: New York, 1977

4. Jones, R. A. "Pyrroles and Their Benzo Derivatives: Reactivity" In *Comprehensive Heterocyclic Chemistry, volume 4*, Bird, C. W.; Cheeseman, G. W. H., ed. Pergamon Press: New York, 1984 a) p.218

5. Marino, G. in *Advances in Heterocyclic Chemistry*, v. 13, Katritzky, A. R.; Boulton, A. J., ed.; Academic Press: New York, 1971 a) p.242

6. Ciamician, G.; Dennstedt, M. *Gazz. chim. ital.*, **1883**, *13*, 445

7. March, J. *Advanced Organic Chemistry, 4th ed.*, John Wiley & Sons: New York, **1992**, chapter 11

8. Chadwick, D. J.; Meakins, G. D.; Rhodes, C. A. *J. Chem. Res.* (S) **1980**, 42

9. Kozikowski, A. P.; Cheng, X.-M. *J. Org. Chem.* **1984**, *49*, 3239

10. Muchowski, J. M.; Naef, R. *Helv. Chim. Acta* **1984**, *67*, 1168

11. Anderson, H. J.; Loader, C. E. *Synthesis* **1985**, 353 (review)

12. Anderson, A. G.; Exner, M. M. *J. Org. Chem.* **1977**, *42*, 3952

13. Katritzky, A. R.; Bird, C. W.; Boulton, A. J.; Cheeseman, G. W. H.; Lagowski, J. M.; Lwowski, W.; McKillop, A.; Potts, K. T.; Rees, C. W. *Handbook of Heterocyclic Chemistry*; Pergamon Press: New York, 1985 a) p. 254

14. Cipiciani, A.; Linda, P.; Savelli, G.; Bunton, C. A. *J. Am. Chem. Soc.* **1981**, *103*, 4874

15. R. Cipiciani, A.; Linda, P.; Savelli, G. *J. Chem. Soc. Chem. Comm.* **1977**, 857

16. Linda, P.; Marino, G. *Ric. Sci.* **1967**, *37*, 424 CAS **1968**, *68*, 39570

17. Nickisch, K.; Klose, W.; Bohlmann, F. *Chem. Ber.* **1980**, *113*, 2036

18. Cooper, W. D. *J. Org. Chem.* **1958**, *23*, 1382

19. Ofer, D.; Crooks, R. M.; Wrighton, M. S. *J. Am. Chem. Soc.* **1990**, *112*, 7869

20. Brédas, J.-L.; Street, G. B. *Accs. Chem. Res.* **1985**, *18*, 309

21. Brédas, J.-L.; Thémans, B.; Fripiat, J. G.; André, J. M.; Chance, R. R. *Phys. Rev. B: Condens. Matter* **1984**, *29*, 6761

Section 6.3

The Chlorination of Poly(3-Methylthiophene)

Abstract

The reaction of Cl_2 with poly(3-methylthiophene) in CCl_4 at -20°C was investigated by microelectrode conductivity measurements, cyclic voltammetry, and X-ray photoelectron spectroscopy. The chlorinated polymer retains electrical conductivity but displays a striking shift in onset of conduction: from 0.43 to 1.18V vs Ag, corresponding to introduction of ≈ 0.65 chlorine atoms per repeat unit, determined by XPS. Chlorine is proposed to substitute at the 4-position of the thiophene ring in poly(3-methylthiophene) based on the XPS results, the known chlorination patterns of the thiophene family, and the behavior upon chlorination of polythiophene and poly(3,4-dimethylthiophene) which were also characterized. Polythiophene exhibited a 450 mV positive shift in onset of conduction while poly(3,4-dimethylthiophene) showed mainly a rapid loss of conductivity with little shift in oxidation potential. This loss of conductivity, also seen in poly(3-methylthiophene) upon excessive chlorination, is proposed to arise from addition of Cl_2 across double bonds, breaking conjugation. The chlorination of polyselenophene was also examined and resulted in a 0.50 V positive shift in onset of conduction but with loss of most of the polymer conductivity. Control of the *in situ* chlorination of surface-confined poly(3-methylthiophene) yields a series of conducting polymers with potentials for onset of conductivity between 0.43 and 1.18V vs Ag wire. The surprisingly large 750 mV shift in onset of conductivity upon chlorination is attributed to the combined steric and electron-withdrawing effects from introduction of a chloro substituent.

Introduction

We present the preparation of a family of electrically conducting polymers based on the *in situ* chlorination of surface-confined poly(3-methylthiophene) where the potential for onset of conductivity is chemically tuned from between +0.43V to +1.18V vs. Ag by controlled introduction of chloro substituents. Poly(3-methylthiophene) is readily chlorinated at -20°C by Cl_2 in CCl_4. The chlorinated polymer, which remains electrically conducting, undergoes a striking shift in the potential for onset of high electrical conductivity from +0.43V to +1.18V vs Ag. This dramatic change arises from introduction of less than one chlorine atom per repeat unit as determined by X-ray photoelectron spectroscopy (XPS). Chlorination is thought to proceed via the expected pathway of substitution at the 4-position of the thiophene ring, equation (1).

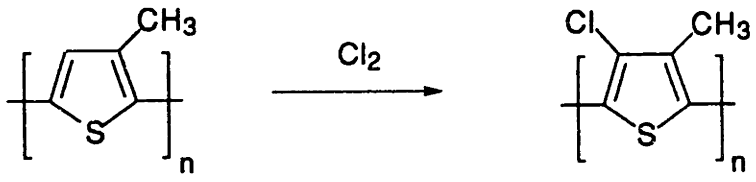

(1)

Thiophene was discovered in 1882 by Victor Meyer whose pioneering investigation[1] into its chemistry included its polymerization[2] and its chlorination. A century later, investigation of the conducting properties of thiophene polymers[3] began. The polythiophene backbone has proven particularly fruitful in the development of conducting polymers, supporting a broad range of substitution and yielding many interesting polymers. Poly(3-methylthiophene) is a particularly highly conducting member of the thiophene family of polymers and is readily synthesized by anodic polymerization 3-methylthiophene. The chlorination of poly(3-methylthiophene) was undertaken as part of the broader study of electrophilic substitution reactions of conducting polymers presented in this chapter Poly(3-methylthiophene) is a polymer substrate which offers high conductivity and stable electrochemistry.[4] It is not plagued by the instability problems which are a drawback of

polyacetylene[5] or the slow kinetics of polypyrrole. Chlorine was chosen as the electrophile for the moderate electron-withdrawing character of a chloro substituent and known reactivity toward thiophene and its derivatives, and was expected to induce a positive shift in the oxidation potential and potential for onset of conductivity of the polymer. Chlorine can be introduced prior to polymerization but with unsatisfactory results. We have observed that 3-chlorothiophene polymerizes poorly yielding a polymer of low conductivity, a problem reported with other 3-halothiophenes.[6,7] This does not, however, preclude chlorination of thiophene-based polymers *after* polymerization. Thiophene itself chlorinates rapidly in the dark at low temperature in the presence or absence of catalyst.[8-11] The reaction leads to 2-chlorothiophene and polychlorinated adducts arising from both substitution and addition reactions. The chlorination of alkylthiophenes[8,9,12-19] has not been investigated as extensively as their bromination but several reactions relevant to the chlorination of thiophene polymers are shown in Scheme I. In the case of alkylthiophenes, ring

Scheme I. Examples of Chlorination of Thiophene Derivatives[8,9,12,14,16,18]

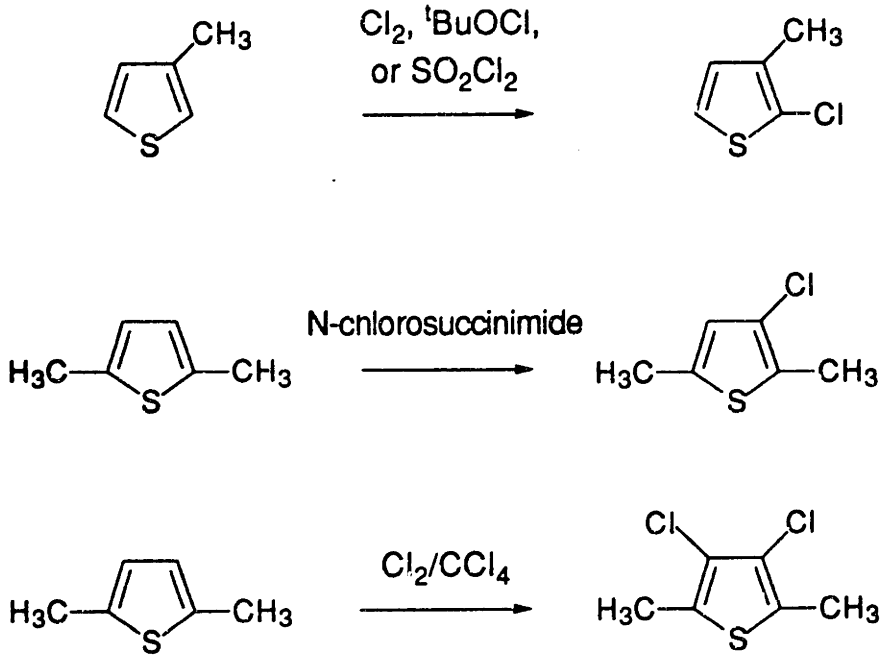

chlorination predominates and chlorination of alkyl side chains does not occur even under conditions where it would be expected.[8,12] In the case of 3-methylthiophene, ring substitution at the 2-position, sometimes including 2,5-disubstitution, is observed for a range of chlorinating agents.[9,12,14] Substitution by chlorine on the methyl group does compete with ring chlorination using PCl_3 under direct sunlight in the presence of PCl_5.[17,8] In an α-linked polyheterocyclic substrate, the more reactive α-hydrogens are no longer available and the chlorination behavior of 2,5-dimethylthiophene is more significant as a model. With both N-chlorosuccinimide[16] and molecular chlorine[18,8,9] substitution occurs at the β-carbons and not the methyl groups. While chlorination of an alkyl side-chain by N-chlorosuccinimide might be expected by analogy with the benzene family, it apparently only occurs in thiophene derivatives when no ring hydrogens are available. A recent report[19] describes the reaction of tetramethylthiophene with N-chlorosuccinimide to give the thenyl chloride which was unstable to work-up and isolated as its adduct with thiophenol. Overall, then, if a ring site is available, chlorination occurs there first, and therefore we expect to obtain a 4-chloro product from the reaction of poly(3-methylthiophene) with chlorine, equation (1). The direct, *in situ* chlorination of poly(3-methylthiophene), polythiophene, poly(3,4-dimethylthiophene), and polyselenophene and its effects on the electrical characteristics of these polymers is now reported.

Results and Discussion

Poly(3-methylthiophene) was deposited onto microelectrode arrays and was chlorinated by immersion in Cl_2/CCl_4. Figure 1 shows the electrochemical characterization of the polymer before and after chlorination. The anodic peak in the cyclic voltammetry of the polymer shifted to more positive potential following chlorination as did the potential of onset of conduction seen in the I_D-V_G characteristic, shifting from an initial value of 0.43 V to a maximum of +1.18 V vs Ag after which further chlorination resulted in loss of conductivity without further change in the potential of onset of conduction. Poly(3-methylthiophene) proved a reactive substrate and the full 750 mV shift in onset of conduction was achieved in under 15 s at room temperature and approximately 100 mM halogen. Chlorine concentrations of 1-20 mM and low temperature are the preferred conditions and allowed more precise control over the extent of chlorination. The same 0.43 to 1.18 V shift in onset of conduction is still observed if the reaction is carried out at room temperature or higher Cl_2 concentrations, but the reaction is rapid and more difficult to regulate. Figure 2 shows the evolution of the I_D-V_G characteristic of a film of poly(3-methylthiophene) over the course of chlorination, starting with 1 mM Cl_2/CCl_4 at -20°C. Cl_2 concentration was raised to 10 mM toward the end of the reaction to maintain a convenient rate of shift in the potential for onset of conduction. Under these conditions the reaction could be halted at any potential for onset of conduction from 0.43 to 1.18 V vs Ag, as shown in Figure 2, yielding a polymer of good conductivity and stable electrochemistry. The graph at the bottom of Figure 2 shows the shift in the potential for onset of conduction as a function of reaction time. The microelectrode array was removed and characterized in blank 0.1 M [*n*-Bu_4N]PF_6/CH_3CN at 13 points over the course of the reaction. For clarity only 7 of the 13 I_D-V_G characteristics are shown at the top of Figure 2. The good stability to +1.5 V vs Ag wire in CH_3CN of the chlorinated polymer was surprising given the high potential for onset of conduction of 1.18V and the lack of rigorously anhydrous conditions, usually critical for polymers which are difficult to oxidize. The same results

Figure 1. Cyclic voltammetry (top) and I_D-V_G characteristic (bottom) of microelectrode-confined poly(3-methylthiophene) before (dashed) and after (solid) chlorination.

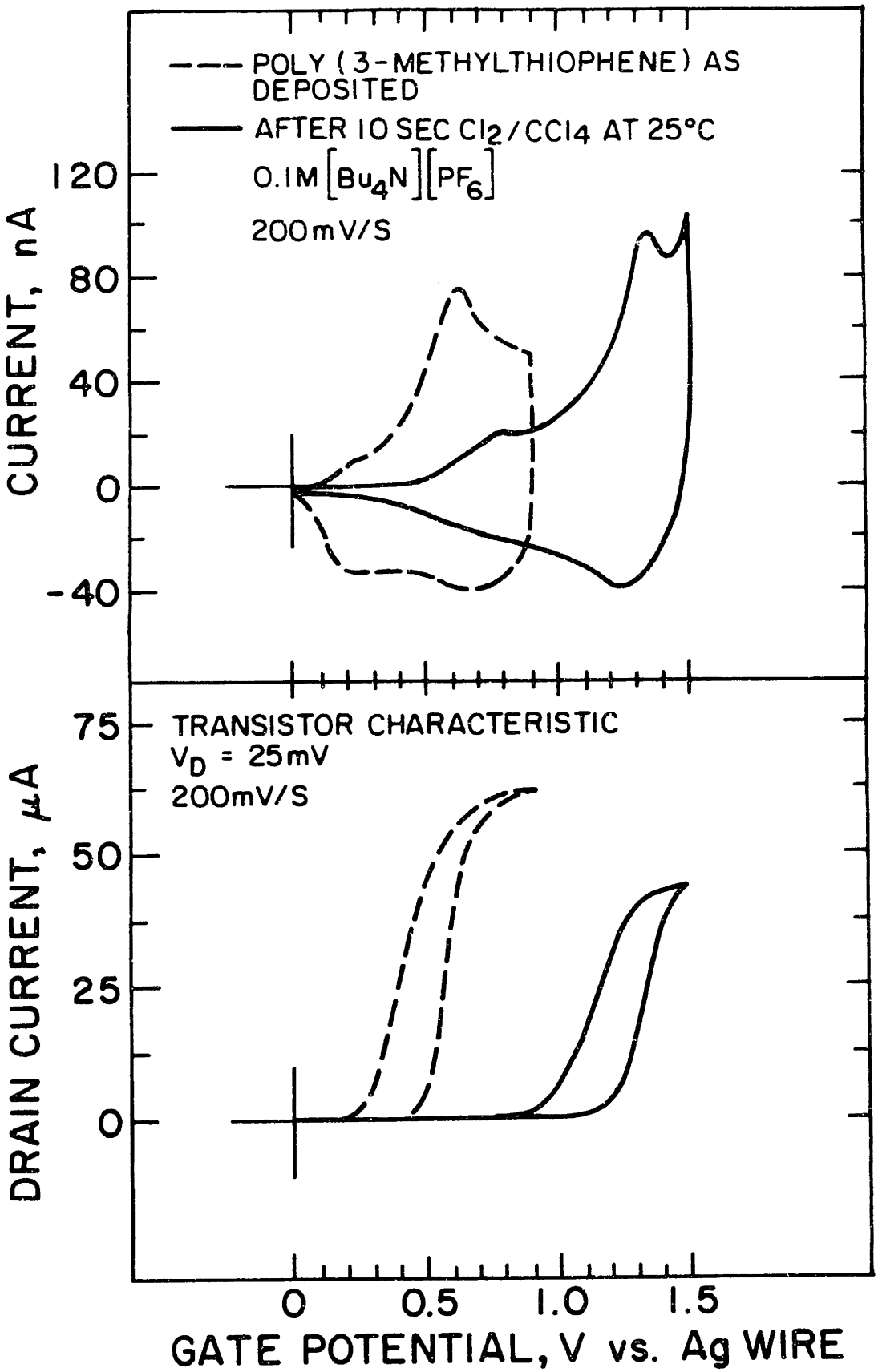
POLY (3-METHYLTHIOPHENE) AS DEPOSITED
AFTER 10 SEC Cl2/CCl4 AT 25°C
0.1M [Bu4N][PF6]
200mV/S
120
80
40
0
-40
CURRENT, nA
TRANSISTOR CHARACTERISTIC
VD = 25mV
200mV/S
75
50
25
0
DRAIN CURRENT, μA
0
0.5
1.0
1.5
GATE POTENTIAL, V vs. Ag WIRE

Figure 2. Chlorination of microelectrode-confined poly(3-methylthiophene) using 1 mM Cl_2/CCl_4 at -20°C until t = 307 s at which point Cl_2 concentration was raised to 10 mM, noted by an asterisk (*) on the figure. The polymer was characterized at 13 points over the 382 s reaction time in 0.1 M [*n*-Bu_4N]PF_6/CH_3CN, V_D = 25 mV, 200 mV/S. The top section shows the progression of the I_D-V_G characteristic to more positive potential for onset of conduction. For clarity only 7 of the 13 characterizations are shown. The bottom graph shows the change in potential for onset of conduction as a function of reaction time for the same poly(3-methylthiophene) film.

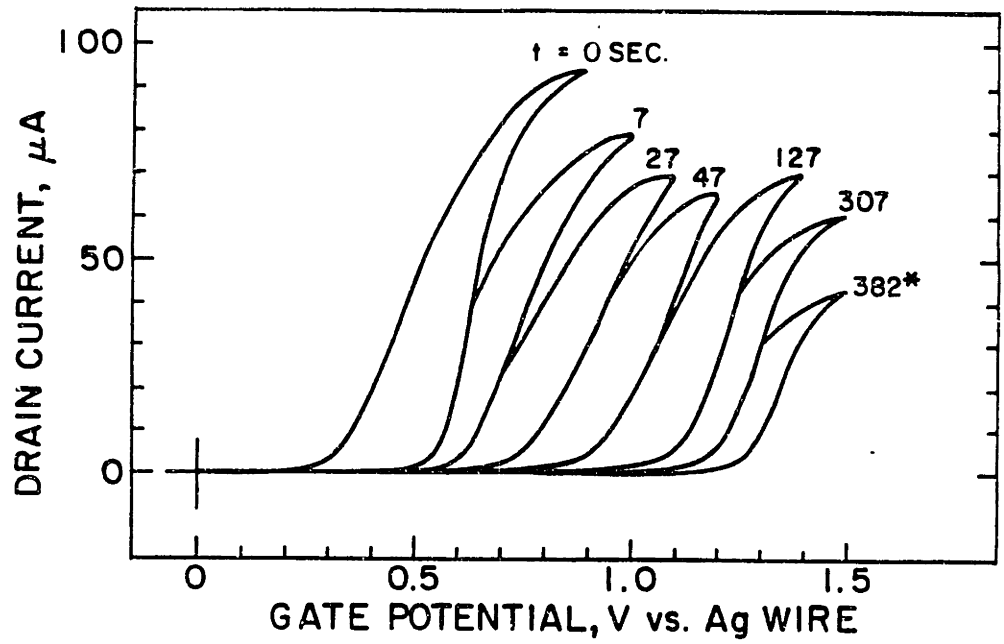
100
50
0
DRAIN CURRENT, μA
t = 0 SEC.
7
27
47
127
307
382*
0
0.5
1.0
1.5
GATE POTENTIAL, V vs. Ag WIRE

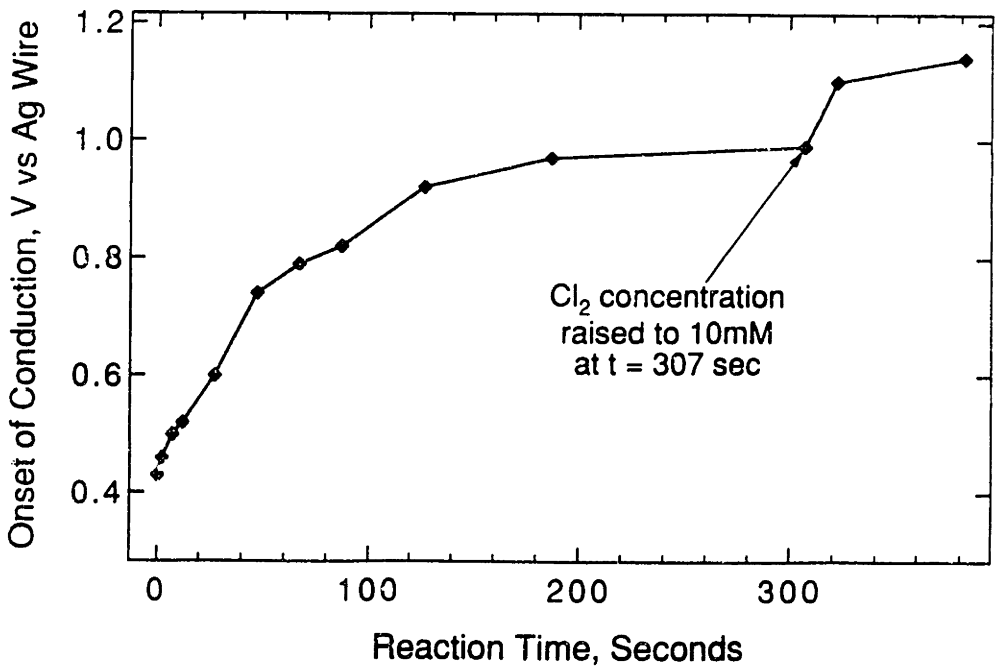
1.2
1.0
0.8
0.6
0.4
Onset of Conduction, V vs Ag Wire
Cl2 concentration
raised to 10mM
at t = 307 sec
0
100
200
300
Reaction Time, Seconds

from chlorination were obtained when the reaction was conducted in complete darkness, ambient room light, or under ultraviolet irradiation.

Polythiophene itself also undergoes reaction with Cl_2. The microelectrochemistry before and after chlorination of polythiophene is shown in Figure 3. Like poly(3-methylthiophene), the parent polymer showed a significant positive shift in the potential for onset of high conductivity, from 0.83 to 1.30 V vs Ag in 0.1 M [*n*-Bu4N]PF_6/CH_3CN. This reaction could also be carried out progressively at low temperature as above to obtain intermediate potentials for onset of conduction between 0.83 and 1.30 V and Figure 3 includes a plot of onset potential as a function of reaction time. The I_D-V_G characteristics in Figure 3 (top) show the polymer at about 65% of the maximum shift in potential for onset of conduction. While poly(3-methylthiophene) retained a surprisingly high fraction of its initial conductivity over the course of the reaction, polythiophene showed a higher rate of loss as the reaction progressed. Figure 4 shows peak drain current plotted as a function of reaction time and also as a function of potential for onset of conduction. Polythiophene still displayed a sharp I_D-V_G characteristic despite the loss in conductivity observed as the polymer became more heavily chlorinated. While the shift in potential for onset of high conductivity was initially rapid in the chlorination of poly(3-methylthiophene), the initial rate was more gradual in the chlorination of polythiophene but then accelerated following the first few reaction intervals, as can be seen in the graph in Figure 3 (bottom).

To determine the extent of chlorination of polymers, and to confirm that chlorine was in fact being introduced, X-ray photoelectron spectroscopy (XPS) was used to analyze chlorinated films of poly(3-methylthiophene) and polythiophene on Au electrodes. The films were chlorinated in a 10 mM solution of Cl_2 under the same conditions used above. To allow more quantitative interpretation of the results, samples of poly(3-chlorothiophene) and poly[3-(4-chlorophenyl)-thiophene][20] were prepared as references of known 1:1 Cl:S content. These two reference polymers gave nearly identical Cl:S ratios, differing by less than 1%. Chlorine content of reacted polythiophene and poly(3-methylthiophene) samples

Figure 3. Chlorination of microelectrode array-confined polythiophene. (top) I_D-V_G characteristic of the polymer before chlorination (dashed), and after chlorination at room temperature had shifted the potential for onset of conduction had shifted approximately 0.3 V positive of its original value. (solid). (bottom) Graph of potential for onset of conduction as a function of reaction time for the chlorination of polythiophene (confined to 4 microelectrodes) at -20°C with 10 mM Cl_2/CCl_4.

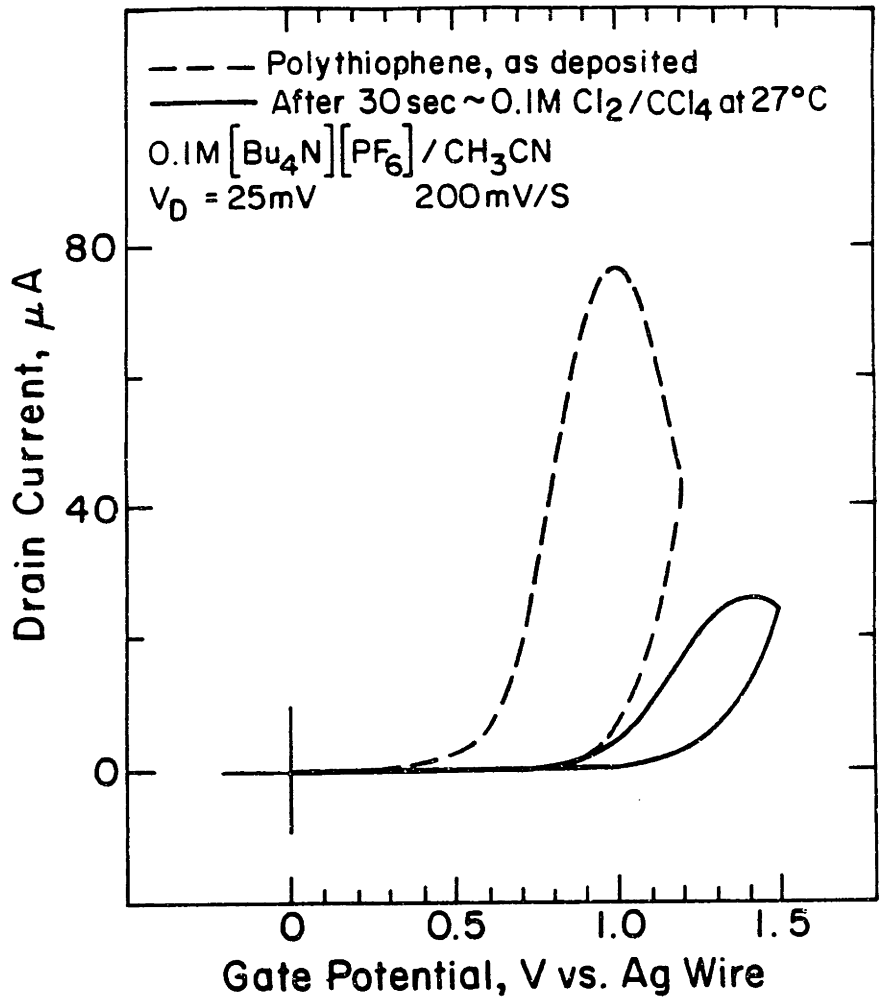
— — — Polythiophene, as deposited
——— After 30 sec ~ 0.1M Cl_2/CCl_4 at 27°C
0.1M $[Bu_4N][PF_6]/CH_3CN$
V_D = 25mV 200mV/S
Drain Current, μA
80
40
0
0
0.5
1.0
1.5
Gate Potential, V vs. Ag Wire

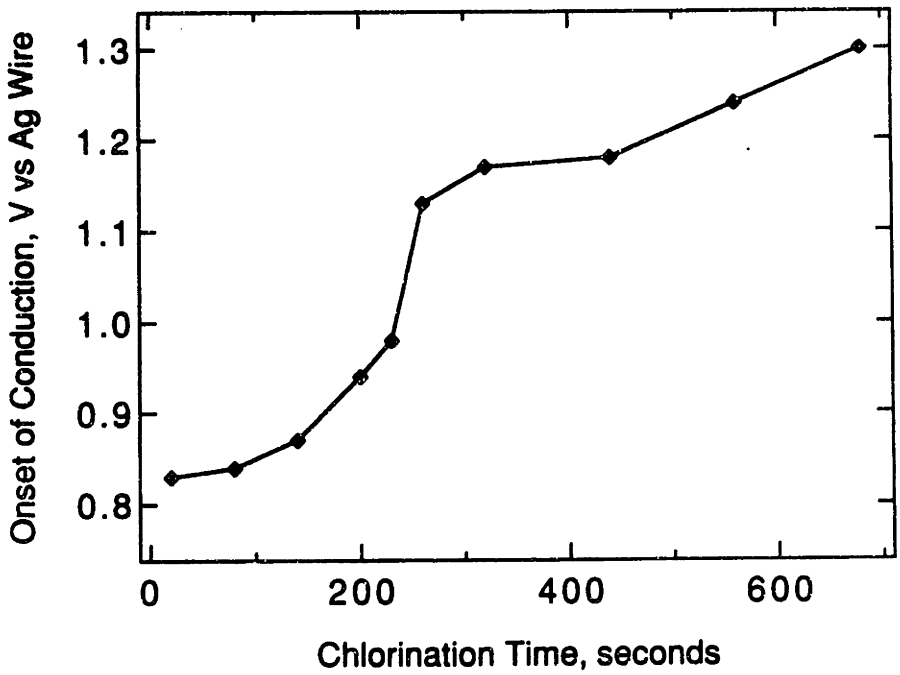
Onset of Conduction, V vs Ag Wire
1.3
1.2
1.1
1.0
0.9
0.8
0
200
400
600
Chlorination Time, seconds

Figure 4. Effects of chlorination on the conductivity of polythiophene. (top) Peak drain current as a function of potential for onset of conduction. (bottom) Peak drain current as a function of reaction time for the same device. See also the graph at the bottom of Figure 3 for a plot of potential for onset of conduction as a function of reaction time for this device. Polythiophene was deposited and characterized on 4 electrodes, thus drain current represents conduction across three interelectrode gaps instead of the usual single gap. Therefore the drain current should be compared to other figures at 1/3 its value.

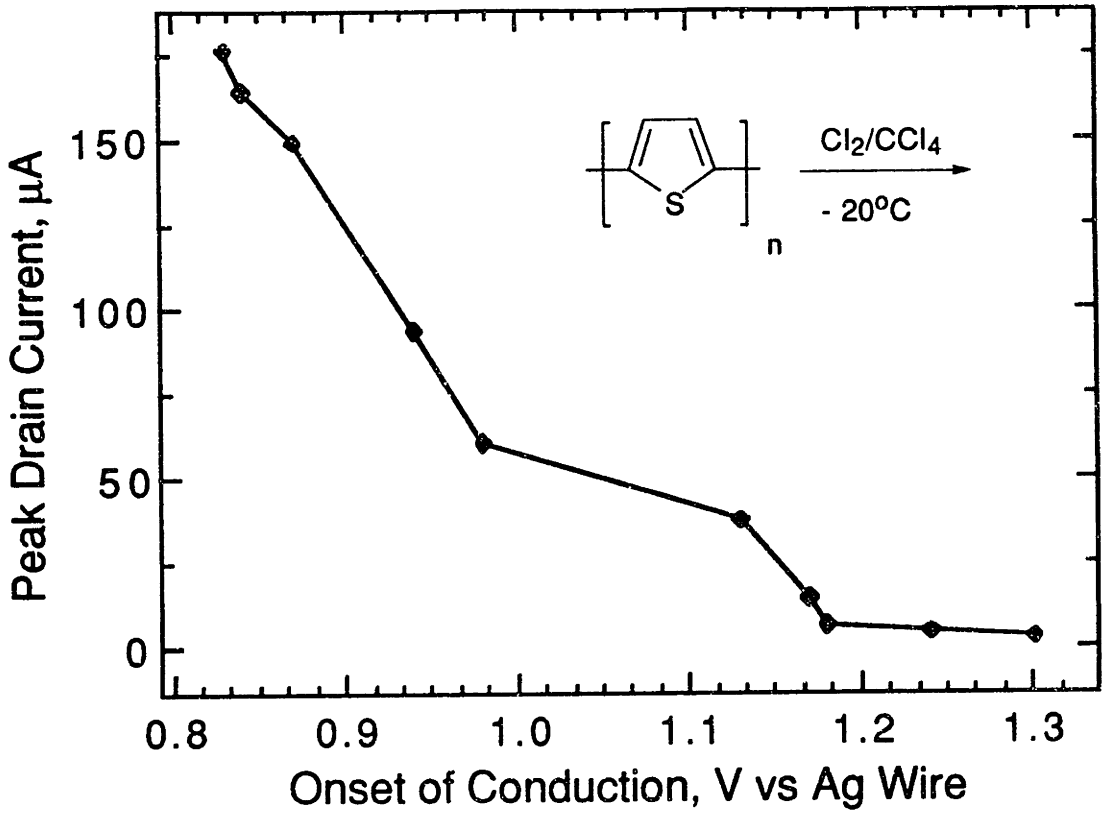
Peak Drain Current, μA
150
100
50
0
0.8
0.9
1.0
1.1
1.2
1.3
Onset of Conduction, V vs Ag Wire
S
n
Cl2/CCl4
- 20°C

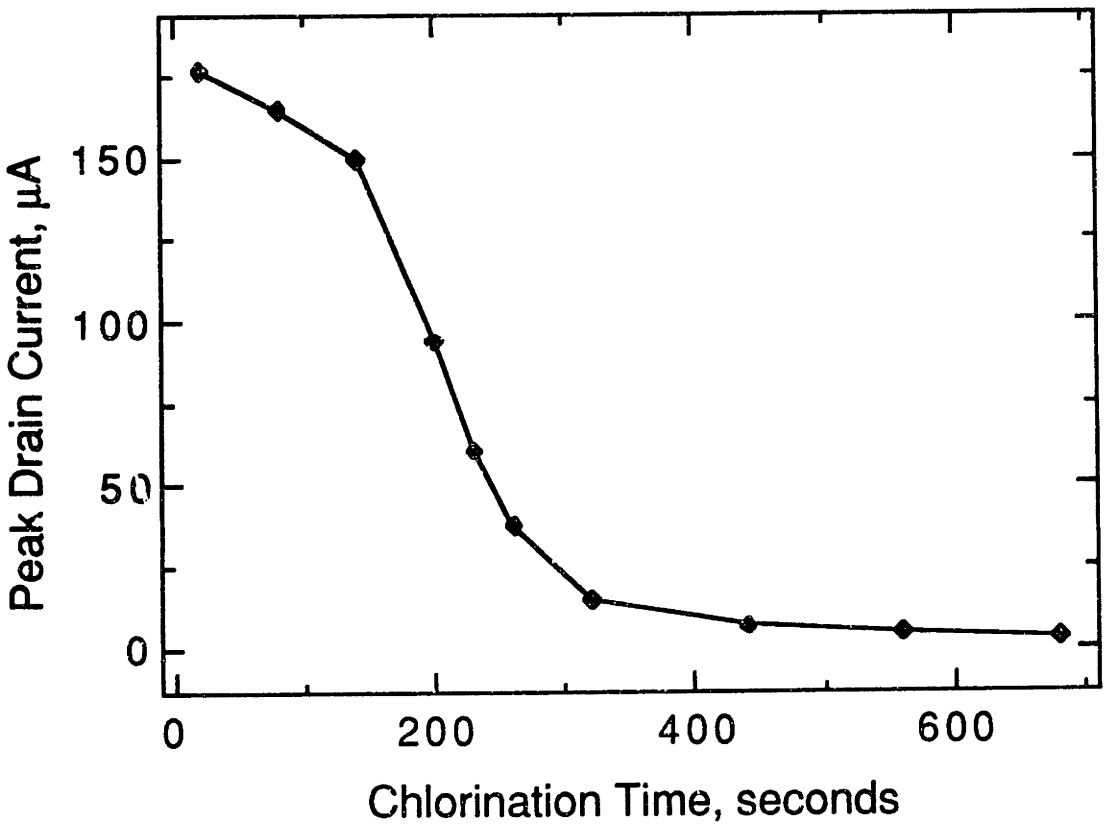
Peak Drain Current, μA
150
100
50
0
0
200
400
600
Chlorination Time, seconds

was calculated using the observed Cl:S ratio of 1.40:1 obtained for the reference samples as indicative of 1:1 Cl:S content. Figure 5 shows the chlorine content of a series of samples of poly(3-methylthiophene) reacted for progressively longer periods. The degree of chlorination leveled off at below one chlorine atom per thiophene ring for poly(3-methylthiophene) and higher levels of halogenation were not observed by XPS. Under more vigorous conditions, 200mM Cl_2 at +27°C for 60 sec, dissolution and loss of most of the polymer film occurred. The XPS data for this sample in Figure 5 were taken on what remained on the electrode of the polymer film which showed 0.73 chlorine atoms per repeat unit.

While both poly(3-methylthiophene) and polythiophene are readily chlorinated, the 3-methyl polymer was the more reactive of the two. The two polymers were deposited onto Au macroelectrodes and chlorinated in 20 mM Cl_2/CCl_4 for 120 sec. Polythiophene was found to chlorinate to 0.26 chlorine atoms per repeat unit, while poly(3-methylthiophene) showed an extent of substitution of 0.64. The greater reactivity of poly(3-methylthiophene) may be due to the expected activating influence of the methyl group toward halogenation. Another interesting difference was that during exposure to the chlorinating solution poly(3-methylthiophene) turned deep blue, the color of its oxidized state,[4] while polythiophene remained red. When carried out on a microelectrode array with the drain voltage left applied during immersion in the chlorination solution substantial drain current, also indicative of oxidation of the polymer, was observed in the case of poly(3-methylthiophene) but not polythiophene. This is interesting from a mechanistic standpoint since oxidation of the polymer can generate radical sites on the backbone,[21,22] so the possibility of a standard free radical chlorination mechanism[23] initiated by the polymer itself cannot be ruled out in the case of poly(3-methylthiophene).

The cyclic voltammetry, like the I_D-V_G characteristic, evolves upon chlorination of poly(3-methylthiophene) and this provides a means of correlating the macroelectrode experiments where XPS was performed with the microelectrode experiments where I_D-V_G

Figure 5. XPS data for the chlorination of poly(3-methylthiophene) on Au electrodes. Chlorine peaks for 6 electrodes chlorinated under the conditions noted. The highest peak corresponds to a sample chlorinated at +27°C in 200 mM Cl_2/CCl_4 for 60 s while the lower five show peaks for samples chlorinated in 10 mM Cl_2/CCl_4 at -20°C for 5, 15, 30, 60, and 180 s. (inset) Plot of chlorine atoms per repeat unit (see text) for the five samples chlorinated in 10 mM Cl_2/CCl_4 at -20°C.

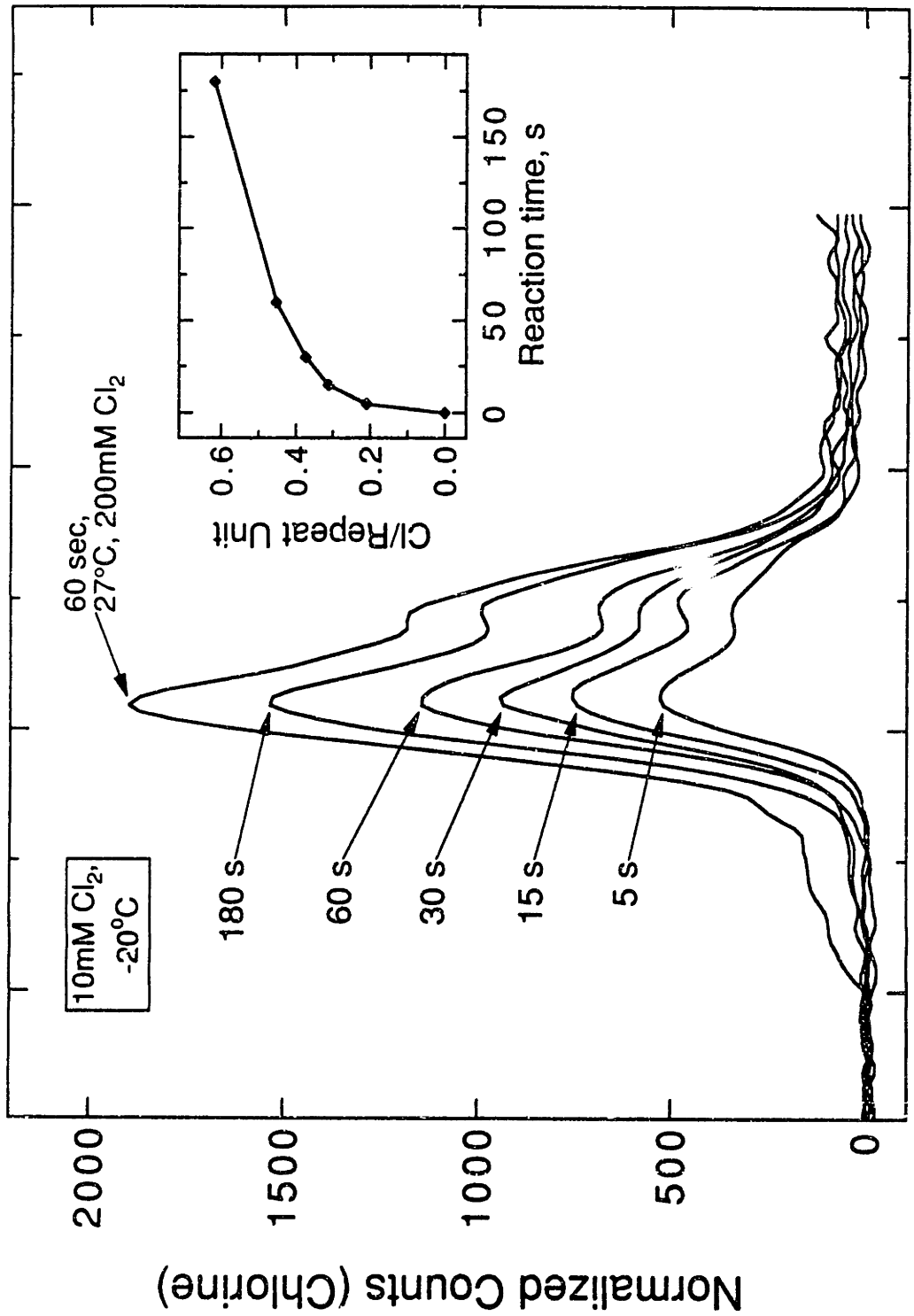
Normalized Counts (Chlorine)
2000
1500
1000
500
0
196
200
204
208
Binding Energy, eV
10mM Cl2, -20°C
180 s
60 s
30 s
15 s
5 s
60 sec, 27°C, 200mM Cl2
Cl/Repeat Unit
0.6
0.4
0.2
0.0
0
50
100
150
Reaction time, s

measurements were made. From this comparison we were able to estimate that for poly(3-methylthiophene) chlorination to the extent of 0.65 chlorine atoms per thiophene ring corresponds to the point at which the potential for onset of conduction reaches the 1.18 V limit. Also, inspection of the graphs in Figures 2 and 5 shows that chlorine content and potential for onset of conduction both increase rapidly at first and then level off, reaching maximum values of 0.73 chlorine atoms per repeat unit and 1.18 V, respectively. We conclude, therefore, that in poly(3-methylthiophene) the shift in the potential for onset of conduction arises from an extent of substitution corresponding to less than monochlorination of each repeat unit.

A more subtle effect on polymer electrical characteristics upon chlorination was an initial decline in maximum transconductance (dI_D/dV_G) from 514 μA/V for as-deposited poly(3-methylthiophene), to 225 μA/V when chlorination had shifted onset of conduction to 0.60 V. However, as the reaction progressed further the trend reversed and maximum transconductance increased to a final value of 349 μA/V when onset of conduction had reached 1.1 V. The trend can be seen upon close inspection of Figure 2. Drain current increases more abruptly for the I_D-V_G characteristics at the extremes of the 0.43 to 1.18 V range of observed onset potential but more gradually in the I_D-V_G characteristics displaying intermediate potentials for onset of conduction. This is seen quantitatively in Figure 6, a plot of maximum transconductance as a function of potential for onset of conduction. Transconductance, a device electrical parameter which is the first derivative of the I_D-V_G characteristic, indicates the magnitude of response of the polymer transistor to a given change in gate voltage, and is a commonly used gain parameter.[24,25] Cyclic voltammetry showed a single anodic peak for poly(3-methylthiophene) prior to, and after, chlorination to the 1.18 V limit of onset of conduction, but two peaks or one broad wave at intermediate points. Both trends are attributable to the progression from a polymer comprised only of 3-methylthiophene units, through a mixed state comprised of non-chlorinated and chlorinated rings, to a state approaching only monochlorinated units. The higher maximum

transconductance of unreacted poly(3-methylthiophene) and of the more heavily chlorinated polymer, and lesser values at intermediate degrees of halogenation, are consistent with the expectation that in a mixed state comprised of two moieties of substantially different oxidation potential, the potential range required to withdraw a fixed quantity of charge from the polymer is widened yielding a more gradual slope in the I_D-V_G characteristic and a broadened, more complex cyclic voltammetric response.

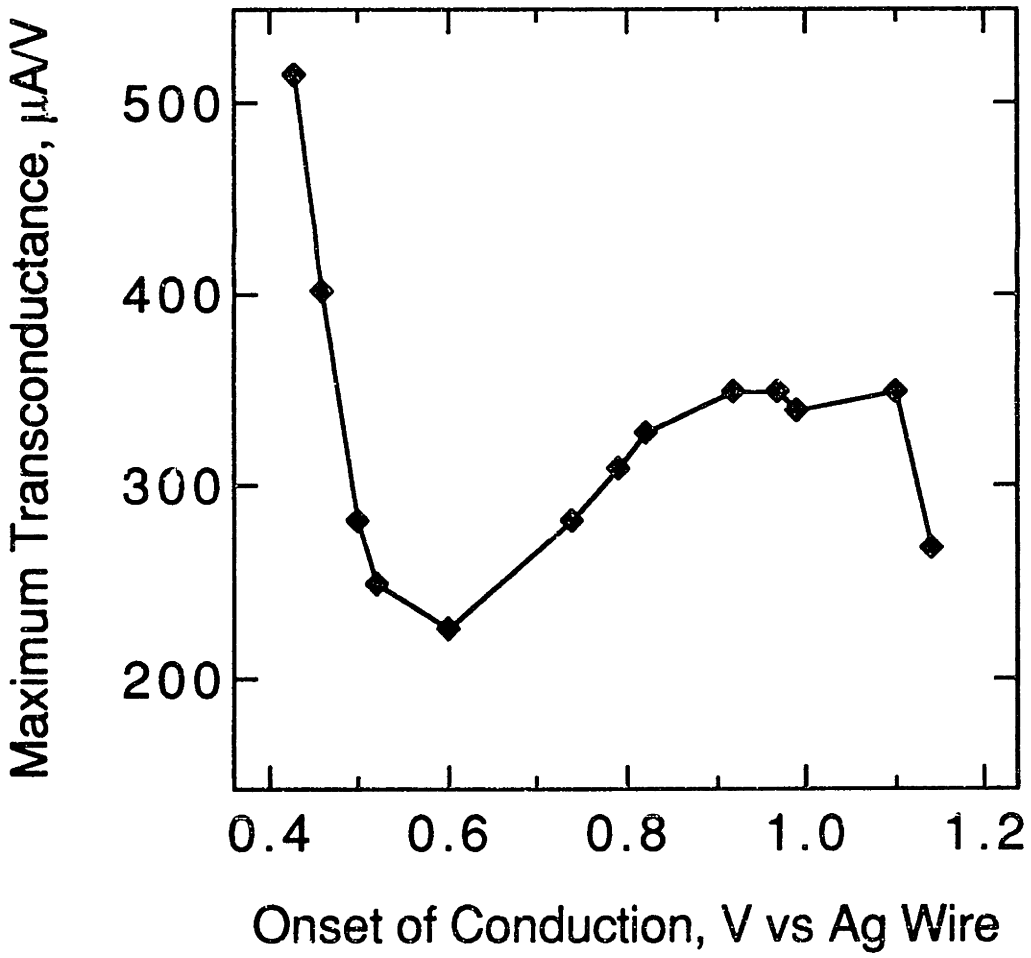

Figure 6. Plot of maximum transconductance (dI_D/dV_G) as a function of potential for onset of conduction for the data shown in Figure 2 for the chlorination of microelectrode-confined poly(3-methylthiophene).

The electrochemical and XPS data for chlorination of poly(3-methylthiophene) and polythiophene were consistent with the expectation that the polymers would react by substitution of a ring hydrogen. XPS analysis indicated that polychlorination of the 3-methylthiophene ring was not occurring in poly(3-methylthiophene), and monochlorination of the methyl group could not give rise to so large a shift in the potential for onset of conduction given that the electronic effect of the chloro substituent would be buffered by a methylene spacer. However, direct evidence of the type presented in sections 6.1 and 6.2 establishing the site of substitution was not provided by the electrochemistry and XPS results from the study of chlorination of poly(3-methylthiophene) and polythiophene. Specular reflectance FTIR (RIR), which proved so useful in the characterization of trifluoroacetylated polyaniline and polypyrrole, was inconclusive here. While the methyl and ring C-H stretches are far enough apart in frequency to be completely resolved in the IR of poly(3-methylthiophene), the C-H region was difficult to observe for polymers by RIR so while the bands for the methyl and ring hydrogens were observable and separate, signal to noise was low. While exposure to the chlorinating conditions used above did result in nearly complete disappearance of the ring C-H band, consistent with the reaction path proposed in equation (1), a general decline in intensity in the C-H region following exposure to Cl_2 did not allow conclusive interpretation of the RIR data.

Seeking further evidence that poly(3-methylthiophene) was reacting by substitution for a β-hydrogen, examination of the chlorination of poly(3,4-dimethylthiophene) was undertaken. This substrate was chosen as a test case because it has methyl hydrogens but no ring hydrogens available which reduces the possible reaction pathways to chlorination at the methyl substituents, and addition of Cl_2 across the double bonds of the ring. These two pathways are distinguishable by the expected contrast in their effects on the electrical characteristics of poly(3,4-dimethylthiophene) and it was for this reason that the polymer was chosen for study. An α–β addition of Cl_2 to poly(3,4-dimethylthiophene) breaks conjugation along the backbone of the polymer and is expected to reduce conductivity as the

reaction proceeds. Chlorination of a methyl substituent on the other hand should render the polymer more difficult to oxidize, and thus raise the potential for onset of conduction, but should not have a large effect on conductivity. Upon chlorination in 10 mM Cl_2/CCl_4 at -20°C, poly(3,4-dimethylthiophene) lost over 90% loss of its conductivity in 12 s but showed little shift in its potential for onset of conduction. The changes upon chlorination in the cyclic voltammetry and I_D-V_G characteristic of the polymer are shown in Figure 7. There was only a minor decline in the cyclic voltammetric response of the polymer and a small shift in the sharp anodic peak in the voltammogram. This behavior, which contrasts sharply to that seen in Figure 1 for the chlorination of poly(3-methylthiophene), is consistent with addition of Cl_2 to double bonds of the ring. Such an addition is expected to have a much smaller influence on the potential for onset of conduction compared to a substitution reaction which leaves conjugation intact because the carbons which get chlorinated no longer contribute to the π-manifold of the polymer, the source of electroactivity and conductivity, and as such no longer participate in charge transport. This is, in essence, equivalent to severing the polymer chain and terminating it with chlorine. The effects of chlorination on poly(3,4-dimethylthiophene) are strikingly similar to the effects of trifluoroacetylation on polyaniline, where substitution at nitrogen breaks conjugation. Applying to both cases is the point put forward in section 6.1 that loss of a minor fraction of the electroactive sites has a minor effect on the cyclic voltammetric response since the majority of redox centers still remain, but can have more severe consequences for conductivity because loss of, say, 5 out of 50 delocalized sites reduces maximum possible conjugation length from 50 to 10 sites. Both polyaniline upon trifluoroacetylation and poly(3,4-dimethylthiophene) upon chlorination show rapid loss of conductivity with little shift in potential for onset of conduction and both polymers show only minor changes in cyclic voltammetric response after loosing over 90 % of their conductivity. This striking similarity in behavior is consistent with poly(3,4-dimethylthiophene) undergoing a loss of extended π-delocalization upon chlorination. The

Figure 7. Change in cyclic voltammetry and I_D-V_G characteristic upon chlorination of microelectrode-confined poly(3,4-dimethylthiophene). Shown after 0, 7, and 12 s in 10 mM Cl_2/CCl_4 at -20°C. V_D = 25 mV

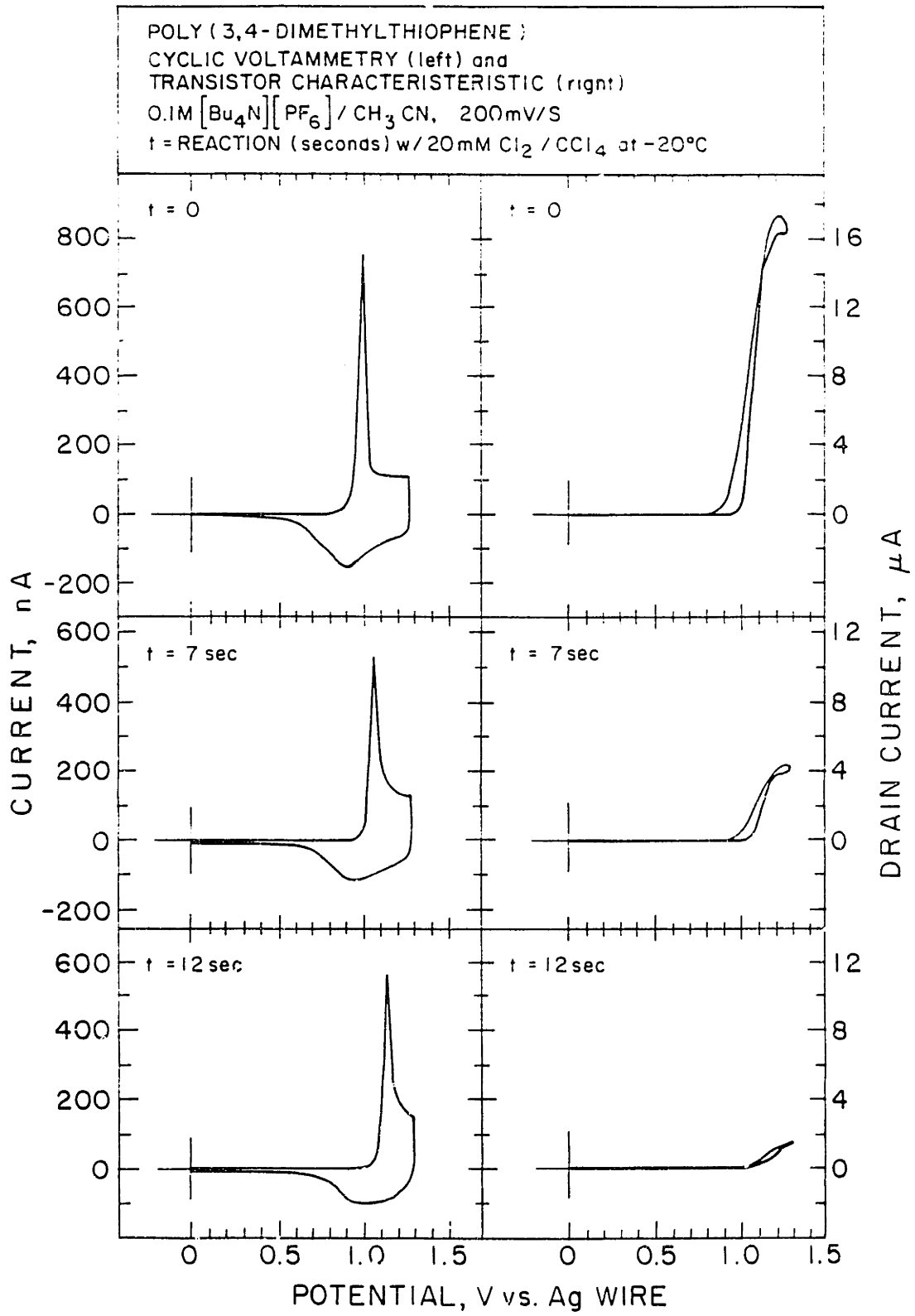
POLY (3,4 - DIMETHYLTHIOPHENE)
CYCLIC VOLTAMMETRY (left) and
TRANSISTOR CHARACTERISTERISTIC (right)
0.1M [Bu4N][PF6] / CH3CN, 200mV/S
t = REACTION (seconds) w/ 20mM Cl2 / CCl4 at -20°C
t = 0
t = 0
t = 7 sec
t = 7 sec
t = 12 sec
t = 12 sec
CURRENT, nA
DRAIN CURRENT, μA
POTENTIAL, V vs. Ag WIRE

behavior of the thiophene family indicates that addition is facile but that substitution at an alkyl side chain is difficult,[8-19] and more importantly that alkylthiophenes will add Cl_2 to ring double without any substitution at the alkyl group.[8] Since our observations are consistent with an addition product and such a reaction pathway is in good accord with relevant precedents in non-polymeric thiophene substrates, it is concluded that poly(3,4-dimethylthiophene) reacts by addition of Cl_2 and not by substitution at the methyl substituents.

It is expected, on the basis of the thiophene chemistry cited in the introduction, that if no ring hydrogens are available for substitution, Cl_2 will undergo an addition reaction to a thiophene double bond in preference to a substitution reaction at an alkyl side chain. The behavior of poly(3,4-dimethylthiophene) certainly indicates that this is also the case for thiophene polymers and that we should not expect the methyl group in poly(3-methylthiophene) to be reactive toward Cl_2. In the chlorination of poly(3-methylthiophene) we determined that the 0.43 V to 1.18 V shift in the potential for onset of conduction came about as a result of at most monochlorination of each repeat unit. Further chlorination resulted only in loss of conductivity, probably due to onset of addition to the double bonds of the ring once most of the ring hydrogens had been substituted. In light of the large magnitude of the shift in potential for onset of conductivity, and the established higher reactivity of ring over side chain hydrogens, chlorination of the methyl group in poly(3-methylthiophene) is not a reasonable reaction path. The changes in electrochemistry upon chlorination, then, of polythiophene, poly(3-methylthiophene), and poly(3,4-dimethylthiophene) are entirely consistent with the reaction pathways expected for each on the basis of the chemistry of monomeric thiophenes. The chlorination products shown in Scheme II are proposed as the dominant initial products for the three thiophene polymers we have examined.

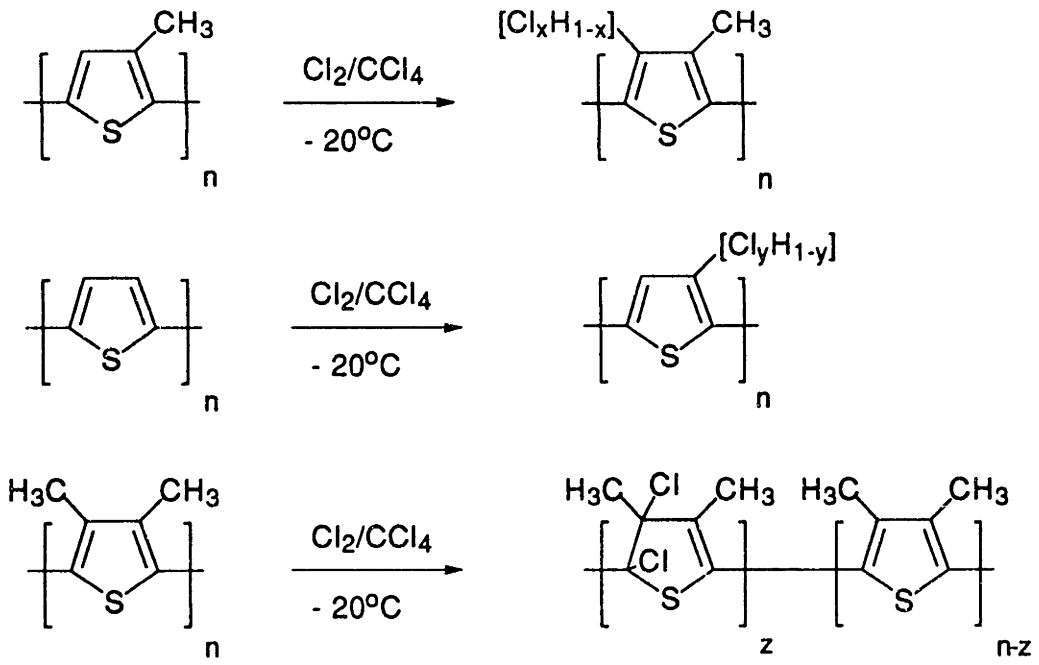

Scheme II. Proposed reactions of chlorine with (top) poly(3-methylthiophene), reacting by substitution for the 4-hydrogen; (middle) polythiophene, reacting by substitution with either the 3 or 4 hydrogen; and (bottom) poly(3,4-dimethylthiophene) with addition across a double bond.

While the shift in potential for onset of conduction in the chlorination of poly(3-methylthiophene) is surprisingly large, it can be understood in terms of the combined steric and electronic effects of introduction of a 4-chloro substituent. In considering the expected potential for onset of conductivity of poly(3,4-dimethylthiophene) compared to that of poly(3-methylthiophene) we expect, on the basis of electronic effects, that the presence of a second electron-donating methyl group will render the dimethyl polymer more easily oxidizable. However, steric considerations also apply and are particularly important in 3,4 disubstituted polythiophenes [26] Poly(3,4-dimethylthiophene), despite bearing a second electron donating group, showed onset of conductivity 550 mV *positive* of poly(3-methylthiophene) (compare Figures 1 and 6). Its surprisingly high oxidation potential has been attributed to steric strain from adjacent methyl groups denying coplanarity of thiophene rings thus attenuating conjugation length. This is borne out by a shift in absorbance maximum from 480 to 330 nm for the 3-methyl to the 3,4-dimethyl polymer.[26] Therefore, if a chloro substituent is introduced at the 4-position of the ring in poly(3-methylthiophene)

it exerts not only an electron withdrawing influence, but also steric strain. Both are expected to result in positive shifts in the potential for onset of conduction and in light of these conspiring substituent effects it is not surprising that chlorination at the 4-position in poly(3-methylthiophene) has such a potent effect on the potential for onset of conduction.

A final substrate which was examined is the less studied polyselenophene, a close relative of polythiophene. Selenophene and thiophene are similar in terms of chemistry and chlorination[27] behavior. Polyselenophene is less conducting than polythiophene and displayed conductivity about two orders of magnitude lower drain current. Figure 8 shows

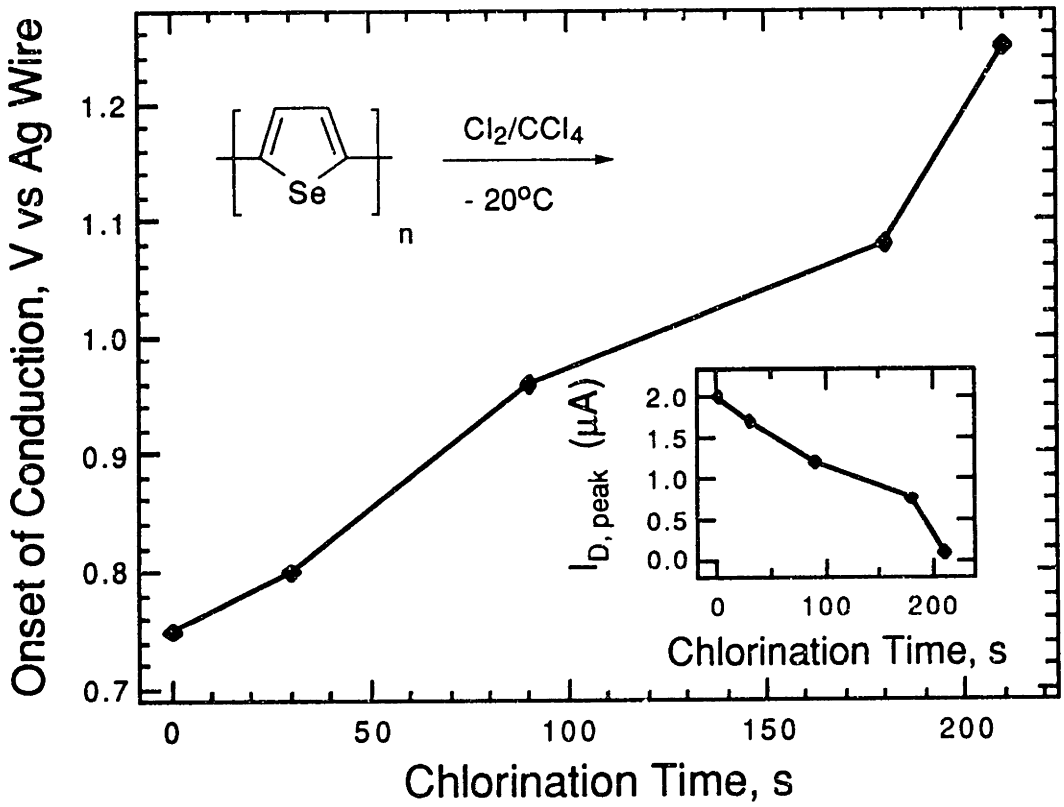

Figure 8. Chlorination of microelectrode-confined polyselenophene at -20 °C in 10 mM Cl_2/CCl_4. Main: Onset of polymer conduction, V vs. Ag wire, as a function of reaction time. Inset: Peak drain current as a function of reaction time. Characterization of I_D-V_G characteristic carried out in 0.1 M [*n*-Bu_4N]PF_6/CH_3CN, V_D = 25 mV, 200 mV/s.

onset potential and drain current as functions of time for polyselenophene chlorinated at -20 °C in 10 mM Cl_2/CCl_4. The potential for onset of conduction shifted 0.50 V, from 0.75 V to 1.25 V vs Ag. Not surprisingly, polyselenophene parallels polythiophene in changes in electrical characteristics upon chlorination. In both polythiophene and polyselenophene the shift in potential for onset of conduction is accompanied by a greater decline in conductivity than observed in the chlorination of poly(3-methylthiophene). Cl_2 addition is certainly a potential side reaction and the greater decline in conductivity may indicate that it competes more favorably with substitution in the chlorination of polythiophene and polyselenophene than in that of poly(3-methylthiophene).

It is interesting to compare the conductivities observed for the chlorinated poly(3-methylthiophene) and polythiophene to those we measured for the polymer obtained by anodic polymerization of 3-chlorothiophene. Poly(3-chlorothiophene), prepared and characterized under the same conditions as the thiophene polymers used above, showed a peak drain current of less than 0.5 μA, compared to 25 μA for polythiophene (Figure 3), and 46 μA for poly(3-methylthiophene) at the level of chlorination corresponding to the full shift in the potential for onset of conduction (Figure 1). It appears that introduction of chlorine after polymerization is the favored route and that a detrimental effect of the chloro substituent on polymerization of 3-chlorothiophene, rather than an inherent incompatibility of chloro substituents with good conductivity, is responsible for the low conductivity observed for poly(3-chlorothiophene).

The good stability and conductivity of poly(3-methylthiophene) even when chlorinated until onset of conduction exceeds one volt vs. Ag wire are unusual when compared to other polymers with very anodic onset potentials such as poly[3-(4-trifluoromethylphenyl)-thiophene] or poly(1,4-dithienyl-2,5-difluorobenzene) which are sensitive to degradation in the conducting state and less conducting than chlorinated poly(3-methylthiophene) [see Chapter 5]. It is significant that poly(3-methylthiophene) retains its desirable characteristics when chlorinated *after* polymerization because an electronegative

substituent, chloro, has been introduced without the ill-effects encountered in the conventional approach of synthesis and polymerization of a substituted monomer.

The range of potentials for onset of conduction accessible with the chlorinated poly(3-methylthiophene) system is of special importance to molecule-based devices. In a device based on two polymers, polyaniline will invariable be one of the pair because of its durability over its entire window of conductivity. The degree of overlap which can be achieved between the I_D-V_G characteristics of polyaniline and chlorinated poly(3-methylthiophene) ranges from a high degree of overlap all the way to complete separation (i.e. polyaniline reaches oxidative turn-off before the chlorinated polymer begins to turn on). While continuum of overlap could also be achieved by the preparation of a relatively large number of monomers of varied substitution (and therefore varied and sometimes unsuitable deposition characteristics and conductivity), this is a less satisfactory approach to the required control over polymer electrical characteristics. The good electrochemical deposition characteristics of poly(3-methylthiophene) and the ease with which any arbitrary potential for onset of conduction between 0.43 and 1.18 V vs Ag can be obtained are valuable assets of the *in situ* chlorination of the polymer. The versatility of chlorinated poly(3-methylthiophene)s as microelectrochemical transistor materials is demonstrated in Section 6.4.

Acknowledgements

X-ray photoelectron spectroscopic characterizations of chlorinated polythiophene and poly(3-methylthiophene films) were carried out in collaboration with Larry Rozsnyai and the author thanks him for his contribution to this research.

Experimental

Cl_2 (Matheson), 3-methylthiophene, thiophene, and selenophene (Aldrich) were used as received. The synthesis of 3,4-dimethylthiophene is described below. [*n*-Bu_4N]PF_6 (Aldrich) was recrystallized from ethyl acetate prior to use, and diethyl ether (Mallinkrodt) was distilled from sodium benzophenone ketyl. ^{1}H-NMR spectra were obtained on a Varian XL-300 or Bruker AC-250 spectrometer. Specular reflectance infrared spectroscopy was performed on a Nicolet 60SX FTIR spectrometer equipped with a liquid nitrogen cooled $Hg_xCd_{1-x}Te$ detector. RIR spectra of the poly(3-methylthiophene) films on Au were acquired with a 74° angle of incidence at 4 cm^{-1} resolution. Gas chromatography/mass spectrometry was performed on a Hewlett-Packard Model HP5890 Series II Gas Chromatograph equipped with a 5971 Series Mass Selective Detector. A model HP1 non-polar column was used with a three-zone temperature program of 3 min @ 80°C, 20°/min ramp to 200°C, 200°C for the rest of the program time.

Electrochemistry

Electrochemical experiments were carried out using a Pine Instruments RDE4 Bipotentiostat with an Ag reference electrode and a Pt counterelectrode. Data were recorded on a Kipp and Zonen BD90 XY or BD91 XYY' recorder. The reference electrode for all experiments was a silver wire. Au macroelectrodes were prepared by thermal evaporation of a 20Å Cr adhesion layer followed by 1000 Å of Au onto silicon wafers using and Edwards Auto 306 thermal evaporator. Prior to use the electrodes were sonicated in acetone followed by isopropanol and blown dry in a stream of nitrogen. Au or Pt microelectrode arrays were cleaned prior to use by etching three times for 3 seconds in 3:1 H_2SO_4:30% H_2O_2 followed by rinsing in deionized water after each etch. Polymers were prepared by anodic polymerization from a 300 mM solution of the monomer in 0.1 M [*n*-Bu_4N]PF_6/CH_3CN. In each case, the potential of the electrode was scanned positive from

0 V at 20 mV/S until the abrupt onset of anodic current at which point the potential was held for 250-500 mS in the case of microelectrode arrays or for several seconds in the case of macroelectrodes (until a visible film covered the electrode). Drain current-gate voltage characteristics were obtained by scanning the potentials of adjacent microelectrodes offset by the drain voltage specified.

Chlorinations

Cl_2 solutions were prepared by condensing 1.0 ml of chlorine (Matheson) in a liquid nitrogen-cooled volumetric tube with an inlet from a Cl_2 tank and an outlet tube terminated in a pipet. The 1.0 ml (20 mmol) of Cl_2 was then allowed to warm to room temperature with the outlet tube pipet immersed in 100 ml of CCl_4 in a 100 ml graduated cylinder where the Cl_2 dissolved readily. This process proceeded smoothly if the liquified Cl_2 was frozen prior to warming and for this reason a liquid nitrogen bath rather than dry ice/isopropanol is recommended as the Cl_2 tended to bump upon warming if it was not frozen first (Caution!). This 0.2 M solution was then diluted with CCl_4 as required to prepare the concentrations specified. Chlorination solutions were prepared in 50 ml Erlenmeyer flasks and either chilled to -20°C with a liquid nitrogen bath or used at room temperature (27°C). Electrodes or microelectrode arrays were immersed for the intervals specified and rinsed with CH_3CN upon removal from the chlorinating solution.

X-ray Photoelectron Spectroscopy

The XPS data were acquired on an SSX-100 spectrometer (Surface Science Instruments) equipped with an Al Kα source, quartz monochromator, concentric hemispherical analyzer, and multichannel detector. Spectra were recorded with a take-off angle of 35° at a 100 eV pass energy, 600 μm spot size, and 100 W electron beam power. Binding energies were referenced to the Au $4f_{7/2}$ peak at 84.0 eV. Gold macroelectrodes with polymer films were prepared and chlorinated as described above. Following

chlorination, the cyclic voltammetric response of the polymer film was recorded in 0.1 M [*n*-Bu_4N]PF_6/CH_3CN and the electrode was then rinsed with CH_3CN and dried with a stream of nitrogen. For the plot in Figure 5 (top) the chlorine region peaks were baseline corrected to zero and then normalized according to number of sulfur counts observed. Two reference samples were included. Poly(3-chlorothiophene) which showed a Cl:S ratio of 1.40:1 and poly(3-(4-chlorophenyl)-thiophene) which showed a Cl:S ratio of 1.41:1. Chlorine atoms per repeat unit for polymer samples were determined from XPS data by dividing the observed Cl:S ratio by 1.405.

3,4-Dimethylthiophene

The thiophene derivative was prepared by the Ni(II)-catalyzed coupling[28] of 3,4-dibromothiophene and methylmagnesium chloride. Into a dry nitrogen-purged 250 ml 3-necked round bottom flask equipped with a stir bar, reflux condenser bearing a gas inlet, and a septum was placed 5.61 g (23 mM) 3,4-dibromothiophene in 20 ml dry ether with 100 mg 1,3-bis(diphenylphosphino)propane nickel(II) chloride (Strem). Methylmagnesium chloride, 3 M in tetrahydrofuran, 24 ml (72 mM, 56% excess), (Aldrich) was added with stirring by cannula. The reaction mixture was stirred and refluxed for 5 days and monitored by GC/MS followed by hydrolysis with 1 M HCl to quench excess Grignard. The phases were separated and the organic layer dried over anhydrous Na_2SO_4. The dried organic layer was worked up by distillation through a short Vigreux column. Solvent was removed at 1 atm and the product, 3,4-dimethylthiophene, was isolated by distillation at reduced pressure. ^1H NMR and MS data were consistent with the literature.[29] Yield was low due to side reactions (probably THF-promoted metal halogen exchange[30] products and thus ether is the preferred solvent). ^1H NMR (Bruker AC-250 NMR spectrometer, 250 MHz, $CDCl_3$): 2.19 (s, 6H, methyl hydrogens; 6.90 (s, 2H, ring hydrogens). MS: *m/z* (relative abundance) [ion]: 111 (100); 112 (71); 97 (59)

References

1. Meyer, V. *Die Thiophengruppe*, Braunschweig: 1888

2. Meyer, V. *Chem. Ber.* **1883**, *16*, 1465

3. Yamamoto, T.; Sanechika, K.; Yamamoto, A. *J. Polym. Sci. Lett.* **1980**, *18*, 9. Lin, J. W.-P.; Dudek, L. P. *J. Poly. Sci. Chem.* **1980** *18*, 2869. Diaz, A. F. *Chem. Scr.* **1981**, *17*, 142. Tourillon, G.; Garnier, F. *J. Electroanal. Chem.* **1982**, *135*, 173. J. Phys. Chem. **1983**, *87*, 3389

4. Ofer, D.; Crooks, R. M.; Wrighton, M. S. *J. Am. Chem. Soc.* **1990**, *112*, 7869

5. Heeger, A. J. In *Handbook of Conducting Polymers*; Skotheim, T. A., Ed.; Marcel Dekker: New York, 1986. Chapter 21

6. Diaz, A. F.; Bargon, J. In *Handbook of Conducting Polymers*; Skotheim, T. A., Ed.; Marcel Dekker: New York, 1986; Chapter 3

7. Roncali, J. *Chem. Rev.* **1992**, *92*, 711 and references therein.

8. Hartough, H. D. *Thiophene And Its Derivatives*; Interscience: New York, 1952

9. Taylor, R. in *Thiophene An Its Derivatives, Part 2*; Gronowitz, S. ed.; Wiley: New York, 1986; pp. 79-117

10. Bird, C. W.; Cheeseman, G. W. H., eds. *Comprehensive Heterocyclic Chemistry, vol. 4*; Pergamon Press: Oxford, 1984; p. 765

11. Eisch, J. J. *Adv. Het. Chem.* **1966**, *7*, 1

12. Campaigne, E.; LeSuer, W. M. *J. Am. Chem. Soc.* **1948**, *70*, 415

13. Davis, M.; Scanlon, D. B. *Aust. J. Chem.* **1977**, *30*, 433

14. McGillivray, G.; ten Krooden, E. *S. Afr. J. Chem.* **1989**, *42*, 113

15. Gronowitz, S.; Frejd, T. *Acta Chem. Scand.* **1975**, B29, 818

16. Usieli, V.; Gronowitz, S.; Andersson, I. *J. Organomet. Chem.* **1979**, *165*, 357

17. Voerman, G. L. *Rec. Trav. Chim.* **1907**, *26*, 293

18. Steinkopf, W.; Köhler, W. *Ann.* **1937**, *532*, 250

19. Nakayama, J.; Kawamura, T.; Kuroda, K.; Fujita, A. *Tet. Lett.* **1993**, *34*, 5725

20. The synthesis and characterization of 3-(4-chlorophenyl)-thiophene and its polymer are described in Chapter 5 of this thesis.

21. Brédas, J.-L.; Street, G. B. *Accs. Chem. Res.* **1985**, *18*, 309

22. Chance, R. R.; Boudreaux, D. S.; Brédas, J.-L.; Silbey, R. In *Handbook of Conducting Polymers*; Skotheim, T. A., Ed.; Marcel Dekker: New York, 1986; Chapter 24

23. March, J. *Advanced Organic Chemistry, 4th ed.*, John Wiley & Sons: New York, **1992**; pp. 689-694

24. Horowitz, P.; Hill, W. *The Art Of Electronics*; Cambridge University Press: New York, 1989; Chapter 3

25. Pierret, R. F. *Field Effect Devices*, Addison-Wesley: Reading, Massachusetts, 1990

26. Tourillon, G.; Garnier, F. *J. Electroanal. Chem.* **1984**, *161*, 51

27. Magdesieva, N. N.; Zefirov, N.S. in *Organic Selenium Compounds: Their Chemistry and Biology*, Klayman, D. L.; Günther, W. H. H. eds.; Wiley-Interscience: New York, 1973. p.442

28. Tamao, K.; Kodama, S.; Nakajima, I.; Kumada, M. *Tetrahedron*, **1982**, *38*, 3347

29. Janda, M.; Srogl, J.; Stibor, I.; Nemec, M.; Vopatrna, P. *Synthesis*, **1972**, 545

30. Zakharkin, L. I.; Okhlobystin, O. Yu.; Bilevitch, K. A. *J. Organomet. Chem.* **1964**, *2*, 309

Section 6.4

Chemically-Tuned Microelectrochemical Electronics: Using Reaction Chemistry in Defining Electrical Function

Abstract

Potential-dependent nucleophilicity of polypyrrole was used to allowed selectively trifluoroacetylate of one of two films of polypyrrole. Polypyrrole and β-trifluoroacetylated polypyrrole, which served as parallel source-drain conduction channels for a microelectrochemical transistor, display onset of conductivity 0.5 V apart resulting in more complex overall I_D-V_G behavior for the device and allowing introduction of a "step" at half of maximum drain current. The polypyrrole/β-trifluoroacetylated polypyrrole transistor demonstrates selective electrophilic substitution as an approach to novel I_D-V_G behavior in microelectrochemical transistors. A microelectrochemical push-pull amplifier based on trifluoroacetylated polyaniline and chlorinated poly(3-methylthiophene) has been prepared. Two I_D-V_G characteristics, chemically tuned to have the appropriate degree of overlap for a push-pull amplifier and to have matched peak drain current, were prepared by direct, *in situ* electrophilic substitution reactions on the two device-active materials. The overlap of I_D-V_G characteristics was established by chlorination of poly(3-methylthiophene) with Cl_2/CCl_4 provided a polymer with onset of conduction at 0.8 V vs. Ag. Trifluoroacetylation of polyaniline under electrochemical potential control was used to match the peak drain current of the polyaniline transistor to that of the chlorinated poly(3-methylthiophene) transistor. The pair of transistors was operated and characterized as a push-pull amplifier driving a 470Ω load resistance. These two results demonstrate the use of reaction chemistry in defining the electrical functions of a 3-state transistor and a push-pull amplifier.

Introduction

The reactivity of conjugated organic polymers in electrophilic substitution demonstrated in the preceding sections of this chapter can be used to tune polymer electrical characteristics. The conductivity of polyaniline and the potential for onset of conduction of polypyrrole can be tuned over a continuos range by the controlled introduction of trifluoroacetyl groups, while the potential for onset of conduction of poly(3-methylthiophene) can be tuned over a wide range by controlled chlorination of the polymer. The range of electrical characteristics accessible with different combinations of electrophiles and conducting polymer substrates is shown in Table 1. Each of the reactions in Table 1 provides a means of tuning the transistor characteristics of a device based on that particular polymer substrate. The chlorination of poly(3-methylthiophene) is particularly successful in this regard offering a wide range of onset potential and good retention of conductivity and stability when more heavily chlorinated to obtain high onset potentials. The trifluoroacetylation of polyaniline is another prime reaction which provides precise attenuation of polymer conductivity to essentially any fraction of its initial value. Trifluoroacetylated polyaniline retains the stability and robust electrochemistry of the parent backbone. The potentials for onset of conduction available from the chlorination of thiophene polymers and the trifluoroacetylation of polypyrrole spans the range of values normally displayed by conjugated organic polymers. This can be seen in Table 2, which includes the onset potentials for most of the polymers characterized over the course of this thesis. The concentration of polymers displaying onset of conduction in the 0.6 to 1.0 V range reflects efforts to develop materials with I_D-V_G characteristics which would overlap to varying degrees with the I_D-V_G characteristic of polyaniline. The preparation of polymers with very positive onsets of conduction by chlorination of polythiophene and poly(3-methylthiophene) is significant because monomers bearing strongly electron-withdrawing substituents do not usually yield good polymers. For more negative potentials for onset of conduction, trifluoroacetylation of polypyrrole leads to a family of materials covering the

-0.1 to 0.4 V range. Since reduced polypyrrole is acylated while the partially oxidized polymer is not, tuning can be carried out selectively as demonstrated below.

Since conducting polymers vary in conductivity from one material to the next, it is convenient that the drain current passed by a polyaniline transistor can be adjusted by reaction of polyaniline with trifluoroacetic anhydride using electrochemical potential control of polyaniline nucleophilicity to regulate the rate of reaction. In this way, drain current of a transistor can be adjusted to match that of another device, or to make a specific contribution of drain current in a transistor based on more than one drain-source channel.

In Chapter 4, unique microelectrochemical device opportunities arising from the finite window of high conductivity displayed by conjugated organic polymers were demonstrated. The reactions shown in Table 1 offer new options for the preparation of molecule-based devices. This is now demonstrated by the preparation of a device with novel I_D-V_G behavior based on the selective trifluoroacetylation of polypyrrole, and a chemically-tuned microelectrochemical push-pull amplifier based on chlorinated poly(3-methylthiophene and trifluoroacetylated polyaniline.

Table 1. Chemical Tuning by Electrophilic Substition: Substrates, Reagents, and Effects

Substrate	Reagent[1]	Reaction	Primary effect	Range
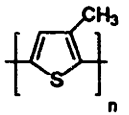	Cl_2	β-chlorination	Anodic shift in onset of conductivity	0.43 - 1.18 V vs. Ag [0.75 V]
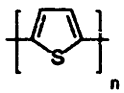	Cl_2	β-chlorination	Anodic shift in onset of conductivity	0.83 - 1.30 V vs. Ag [0.47 V]
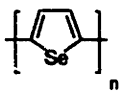	Cl_2	β-chlorination	Anodic shift in onset of conductivity	0.75 - 1.25 V vs. Ag [0.50 V]
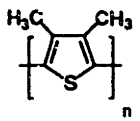	Cl_2	α–β addition	Attenuation of conductivity	> factor of 10^2
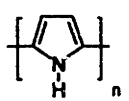	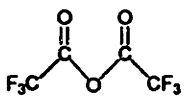	β-trifluoroacetylation with potential-dependent nucleophilicity	Anodic shift in onset of conductivity	-0.1 - 0.4 V vs. Ag [0.5 V]
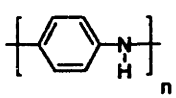	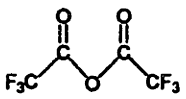	N-trifluoroacetylation with potential-dependent nucleophilicity[2]	Attenuation of conductivity	> factor of 10^4

1. Chlorinations using 1-10 mM Cl_2/CCl_4 @ -20°C. Acylations using 1M $(F_3CCO)_2O/CH_3CN$, with 0.1M $LiClO_4$ (and 0.5 M F_3CCO_2H for polyaniline) if the reaction is to be carried out under potential control.

2. Mono, di, and trichloroacetic anhydride are also suitable electrophiles.

Table 2. Comprehensive compilation of potentials for onset of conductivity for polymers characterized in this thesis. The characterizations were carried out using the same Ag reference electrode as reference in 0.1 M [*n*-Bu_4N]PF_6/CH_3CN for all polymers. Since electrochemistry of polyaniline requires a proton source, 0.5 M F_3CCO_2H was added to the electrolyte medium.

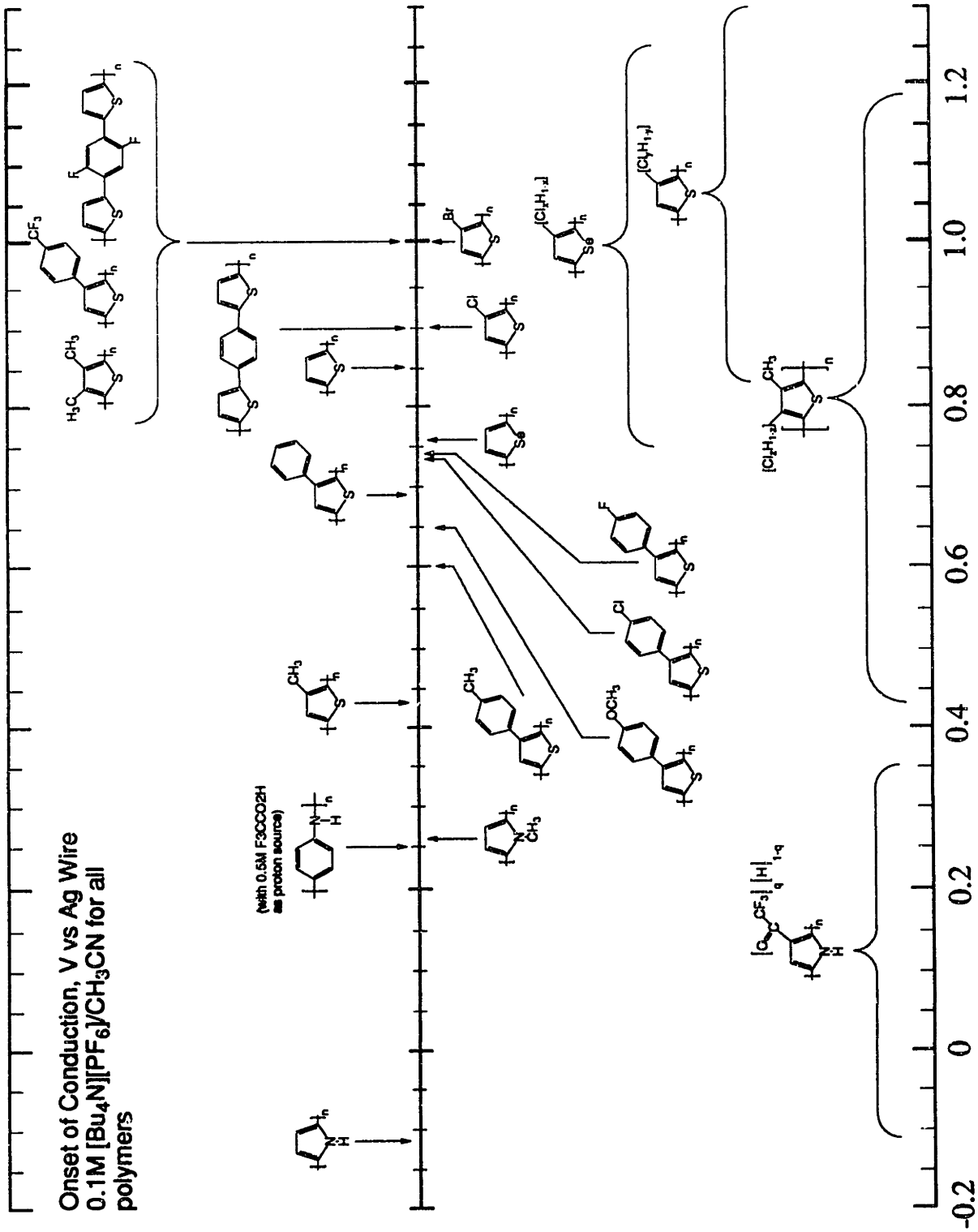
Onset of Conduction, V vs Ag Wire
0.1M [Bu4N][PF6]/CH3CN for all
polymers
(with 0.5M F3CCO2H
as proton source)
-0.2
0
0.2
0.4
0.6
0.8
1.0
1.2

Results

A transistor based on polypyrrole and trifluoroacetylated polypyrrole

It was demonstrated in Chapter 4 that microelectrochemical transistors showing novel I_D-V_G behavior could be prepared based on two parallel source-drain conduction channels which display onset of conductivity at different gate potentials. Such a device was the basis of a ternary logic inverter gate.[1] The potential-dependent trifluoroacetylation of polypyrrole reported in section 6.2 provides one route to a device of more complex I_D-V_G behavior . If the goal is to introduce a step into the I_D-V_G characteristic of a device, two materials of different potential for onset of conduction are needed. While several approaches could be taken to such a device, the pyrrole route was chosen as a further demonstration of selective functionalization of microelectrode-confined polymers using electrochemical control of reactivity.

Scheme I shows how the device was prepared. First, a microelectrode array was functionalized with two independent polypyrrole transistors by anodic polymerization of pyrrole. When connected in parallel, these two transistors function as a single device where drain current flows through two source-drain channels. To obtain a pair of polymers of different potentials for onset of conduction, it is required that trifluoroacetyl groups are introduced into only one of the two polypyrrole channels. Since polypyrrole can be rendered inert toward trifluoroacetylation by holding it in a partially oxidized state, as demonstrated in section 6.2, the reaction can be carried out selectively using electrochemical potential control. Trifluoroacetylation was carried out by immersion of the array in a 1 M solution of trifluoroacetic anhydride in 0.1 M [*n*-Bu_4N]PF_6/CH_3CN with both transistors under active potential control versus an Ag reference electrode. One of the transistors was held at -0.1 V where polypyrrole is in its reduced state and reactive toward the anhydride, while the other transistor has held at 0.5 V to render the polypyrrole of that transistor

partially oxidized and therefore inert to attack by the anhydride. As reported in section 6.2, the reduced polypyrrole underwent a 0.5 V shift in onset of conduction after 20 min

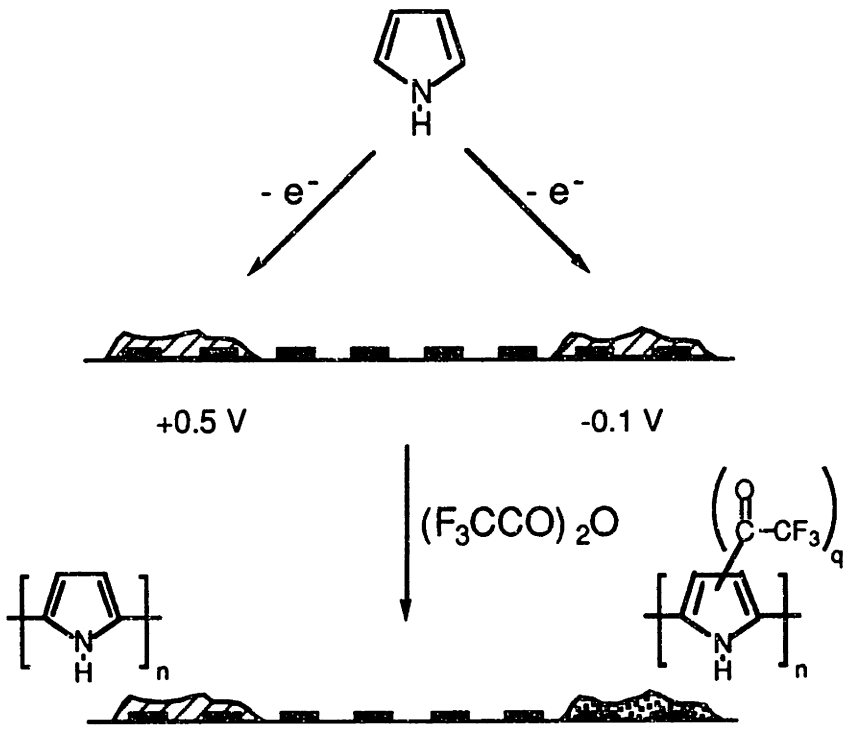

Scheme I. Deposition of two polypyrrole transistors followed by selective acylation of one device by reaction of the two under potential control. At 0.5 V polypyrrole is partially oxidized and non-nucleophilic. At -0.1 V polypyrrole is fully reduced and reacts with trifluoroacetic anhydride.

exposure to 1M trifluoroacetic anhydride. The appropriate electrodes of the array were connected together so that the two individual transistors served as parallel source-drain conduction channels yielding a single transistor device based on two active materials. The overall I_D-V_G characteristic of the transistor device is shown in Figure 1. The resistor determines the relative contribution of the polypyrrole channel to overall drain current. The I_D-V_G characteristic of polypyrrole is broader and more gradual in its increase in conductivity than most other conducting polymers. As a result, the 0.5 V difference in onset of conduction which produced a deep well in the device described in Chapter 4, does

Figure 1. Operation of polypyrrole and trifluoroacetylated polypyrrole transistors in parallel yielding a more complex net I_D-V_G characteristic. The resistor controls the magnitude of the drain current contribution from the polypyrrole device.

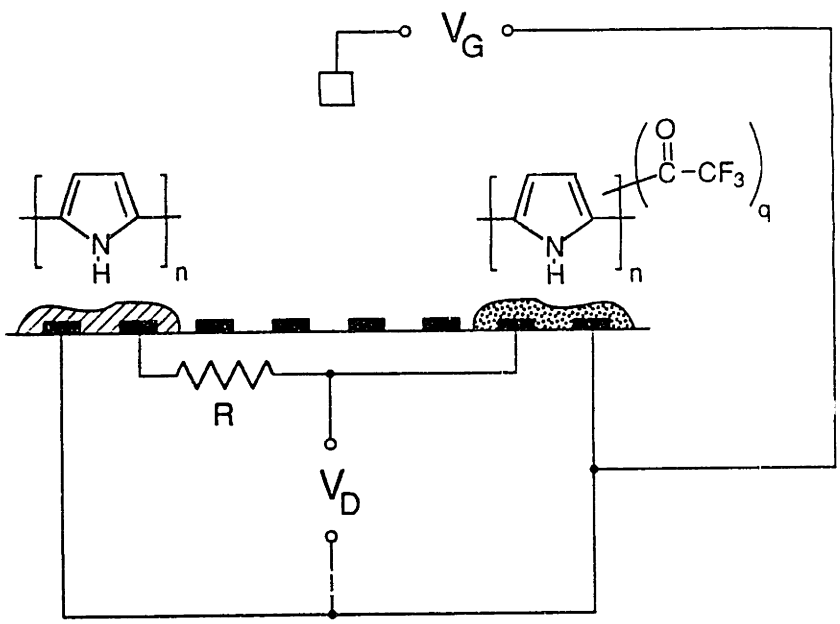
V_G
O
C–CF_3
q
N
H
n
R
V_D

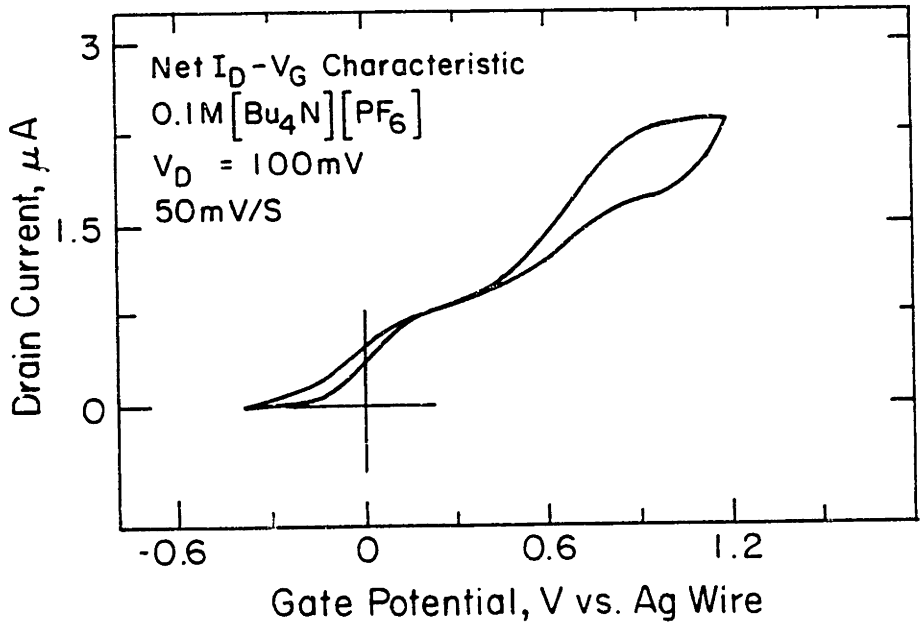
Net I_D–V_G Characteristic
0.1M $[Bu_4N][PF_6]$
V_D = 100mV
50mV/S
Drain Current, μA
3
1.5
0
-0.6
0
0.6
1.2
Gate Potential, V vs. Ag Wire

not produce as sharp a feature in the combined I_D-V_G characteristic shown in Figure 1.

The interesting result is that a new electrical function, a device tailored toward three-state operation, can be created by starting with two identical polymer transistors and selectively altering one of them by a potential-dependent, *in-situ* substitution reaction.

A chemically-tuned push-pull amplifier

Chlorination of poly(3-methylthiophene) and trifluoroacetylation of polyaniline are a versatile combination of reactions. The extent to which the I_D-V_G characteristics of two transistors based on this pair of materials overlap is established by the potential for onset of conductivity in poly(3-methylthiophene). This potential can be tuned over a 0.43 - 1.18 V range by chlorination, providing any degree of overlap ranging from extensive overlap to complete separation, as shown in Figure 2. Further, the drain current displayed by a polyaniline transistor can be adjusted by trifluoroacetylation. With this combination of tunability of both I_D-V_G overlap and relative magnitude, all of the device families developed in Chapter 4 can be prepared from polyaniline and poly(3-methylthiophene), modified by trifluoroacetylation and chlorination, respectively, to obtain the transistor characteristics required for the particular electrical function. To demonstrate implementation of a device using these materials, a push-pull amplifier[2,3,4] was prepared using chlorination of poly(3-methylthiophene) and trifluoroacetylation of polyaniline to establish optimal transistor electrical characteristics.

Polyaniline and poly(3-methylthiophene) are both electrochemical transistor materials with stable electrochemistry in conventional solvents and high drain current density capability. However, the I_D-V_G characteristics of polyaniline and poly(3-methylthiophene) overlap extensively as seen in Figure 2, leaving almost no window of operation for a push-pull amplifier. The optimal overlap for a push-pull amplifier provides a smooth transition between conduction by one transistor and conduction by the other without wasting drain current capability of the transistors. The maximum output current of the

Figure 2. Chemical tuning of the potential for onset of conductivity in poly(3-methylthiophene), and the relationship of the I_D-V_G characteristics obtained to that of polyaniline (dashed line) which has been overlaid. For clarity only the forward scans are shown. The I_D-V_G characteristics of chlorinated poly(3-methylthiophene) are from the work described in section 6.3.

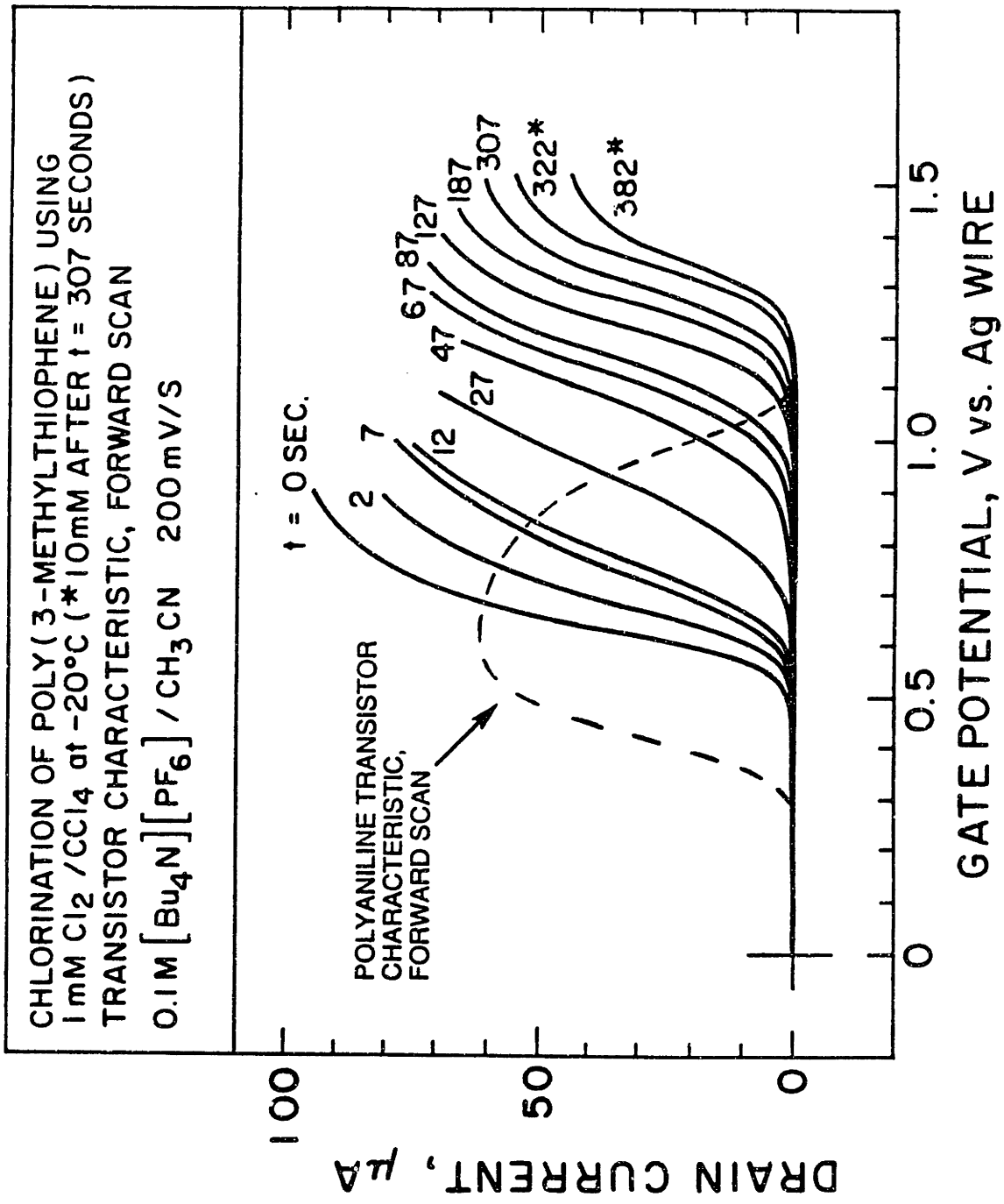
CHLORINATION OF POLY(3-METHYLTHIOPHENE) USING
1 mM Cl_2 /CCl_4 at -20°C (*10mM AFTER t = 307 SECONDS)
TRANSISTOR CHARACTERISTIC, FORWARD SCAN
0.1 M $[Bu_4N][PF_6]$ / CH_3CN 200 mV/S
t = 0 SEC.
2
7
12
27
47
67
87
127
187
307
322*
382*
POLYANILINE TRANSISTOR CHARACTERISTIC, FORWARD SCAN
DRAIN CURRENT, μA
100
50
0
0
0.5
1.0
1.5
GATE POTENTIAL, V vs. Ag WIRE

amplifier is the difference between drain current at the point where the two I_D-V_G characteristics cross (the quiescent current of the amplifier which is not available to the load)[3] and peak drain current of each transistor. Thus, once I_D-V_G overlap is sufficient to prevent crossover distortion, a further increase in overlap only reduces output current capability.

The overlap of the I_D-V_G characteristics of polyaniline and poly(3-phenylthiophene) in the original push-pull amplifier presented in Chapter 4 is a good approximation of optimal overlap but it was more than the minimum required (see Chapter 4, Figure 6). A target potential for onset of conduction of chlorinated poly(3-methylthiophene) of 0.8 V was chosen after close inspection of the overlap of transistor characteristics shown in Figure 6 of Chapter 4. Scheme II shows the steps for preparing the final microassembly of chemically tuned polymers. To avoid exposure of polyaniline to Cl_2, the chlorinated poly(3-methylthiophene) transistor was prepared first. Figure 3 shows the I_D-V_G characteristic of the poly(3-methylthiophene) transistor as deposited and after chlorination until onset of conduction reached 0.8 V vs Ag. A thick film of polyaniline was then deposited onto the array so that the peak drain current of the polyaniline transistor exceeded that of the chlorinated thiophene device. Excess drain current of the polyaniline transistor was provided to allow balancing of the conductivity of the two transistors by trifluoroacetylation of polyaniline, which requires sacrifice of some polyaniline device drain current capability. To demonstrate the precision of attenuation of polyaniline conductivity possible by trifluoroacetylation under potential control, the disparity in peak drain currents has been made deliberately large. The I_D-V_G characteristics of the chlorinated device and polyaniline are shown at the bottom of Figure 3. Note that the overlap of I_D-V_G characteristics is such that there is no dead zone in drain current between the responses of the two transistors. In the final step, shown in Figure 4, the polyaniline device was trifluoroacetylated by cycling at 200 mV/s in 1M trifluoroacetic anhydride between 0.75 V vs. Ag and a lower limit of about 0.2 V to quickly attenuate most of the excess drain current after which the lower limit was

Scheme II

Preparation of a Chemically Tuned Push-Pull Amplifier

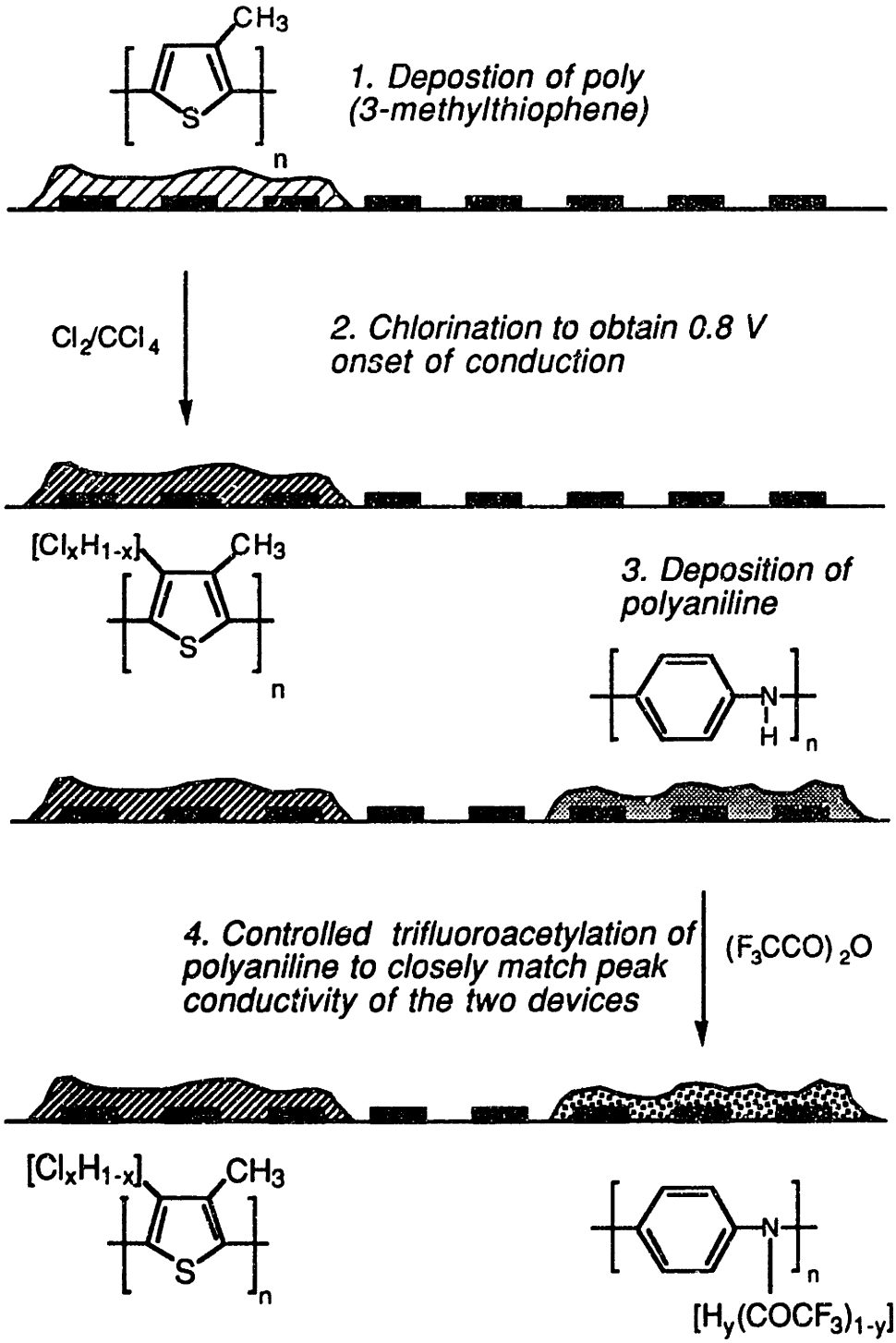

raised to 0.4 V to approach the target end point gradually. The bottom of Figure 4 shows the transistor characteristics of the final matched pair. The peak drain current of the polyaniline transistor now matches that of the chlorinated poly(3-methylthiophene) transistor. Figure 5 shows characterization of the device in the region of V_G for push-pull amplifier operation. The overlap of I_D-V_G characteristics has declined from what is seen at the bottom of Figure 3 as a result of the contraction of the window of conductivity observed in polyaniline upon trifluoroacetylation. The target potential of 0.80 V for onset of conduction for the chlorinated poly(3-methylthiophene) device did not account for this and proved slightly positive of the optimal value for this system. As a result, there is minor crossover distortion in the output waveform of the amplifier, which is shown in Figure 6. The required correction is small, probably less than 100 mV. The preparation of a series of chlorinated poly(3-methylthiophene) devices with onset of conduction in the 0.65 - 0.75 V range is not difficult and would provide a performance profile for the amplifier and allow precise determination of the optimal potential of onset of conduction for the thiophene device of the push-pull amplifier. Importantly, since both the onset potential and relative drain current relationship chosen as the targets were achieved with precision by chemical tuning, it is only necessary to determine what potential for onset of conductivity yields the optimal I_D-V_G overlap for the amplifier in order to prepare a fully optimized device.

Figure 3. Preparation of a chemically-tuned push-pull amplifier. (top) Chlorination of poly(3-methylthiophene) to obtain onset of conductivity at 0.8 V. (bottom) A polyaniline transistor has been deposited onto the array, and the I_D-V_G characteristics for polyaniline and the now chlorinated poly(3-methylthiophene) are shown.

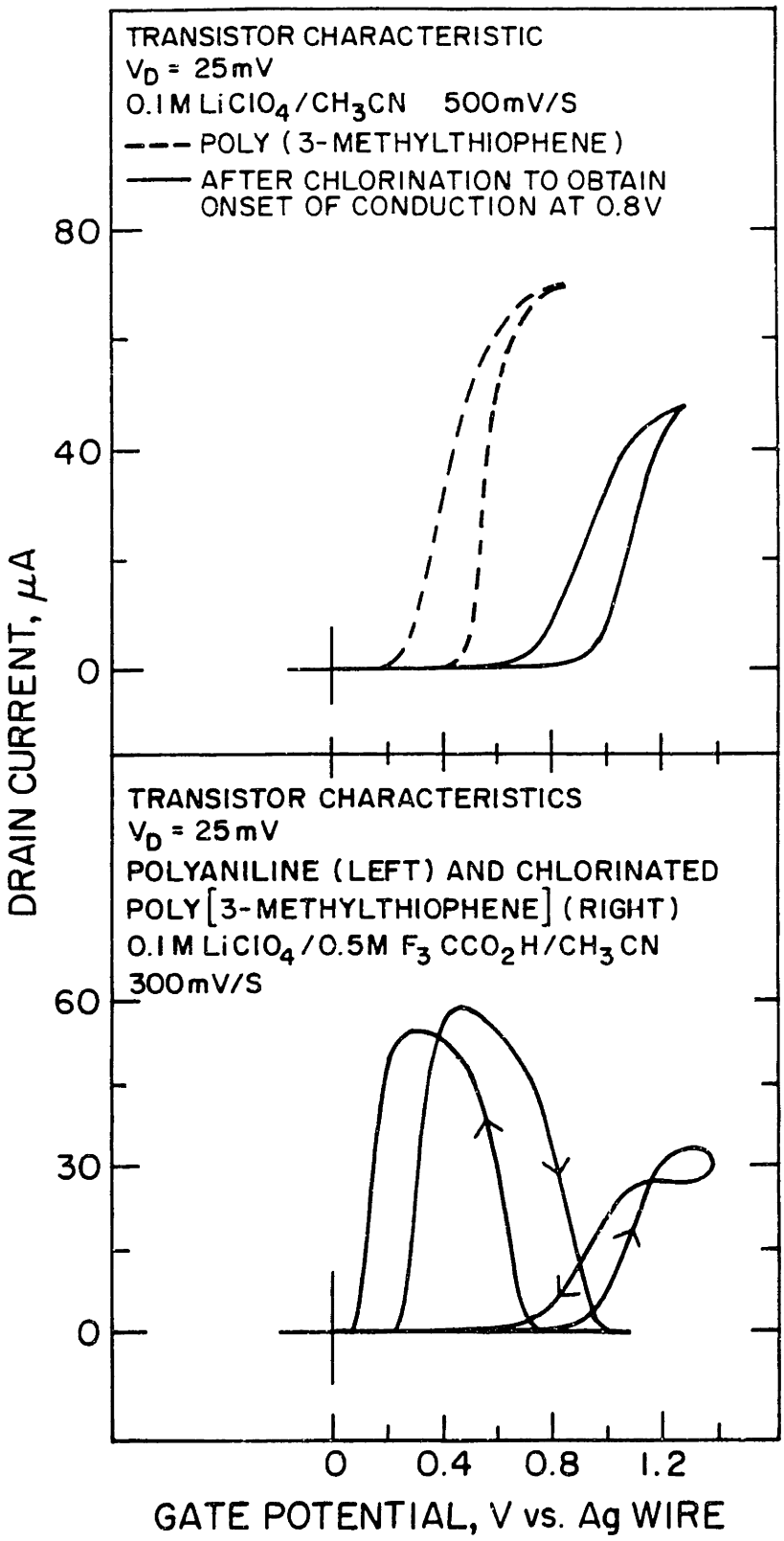
TRANSISTOR CHARACTERISTIC
V_D = 25mV
0.1M $LiClO_4/CH_3CN$ 500mV/S
--- POLY (3-METHYLTHIOPHENE)
—— AFTER CHLORINATION TO OBTAIN ONSET OF CONDUCTION AT 0.8V
80
40
0
TRANSISTOR CHARACTERISTICS
V_D = 25mV
POLYANILINE (LEFT) AND CHLORINATED POLY[3-METHYLTHIOPHENE] (RIGHT)
0.1M $LiClO_4$/0.5M F_3CCO_2H/CH_3CN
300mV/S
60
30
0
DRAIN CURRENT, μA
0
0.4
0.8
1.2
GATE POTENTIAL, V vs. Ag WIRE

Figure 4. Preparation of a chemically-tuned push-pull amplifier. (top) The I_D-V_G characteristics of chlorinated poly(3-methylthiophene) and as-deposited polyaniline. (bottom) The peak drain currents have been matched by controlled attenuation of the conductivity of the polyaniline transistor by trifluoroacetylation.

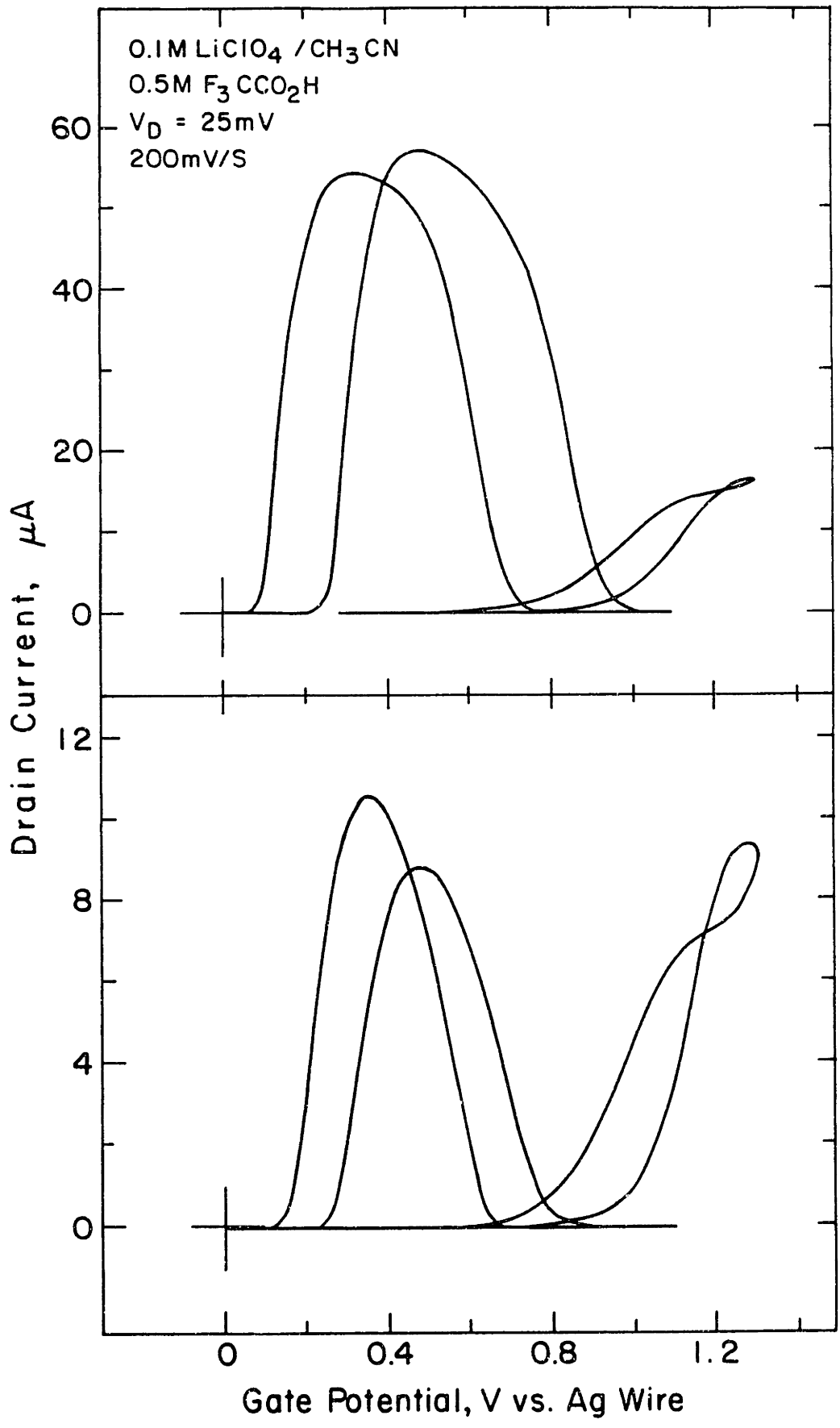
0.1M LiClO4 / CH3CN
0.5M F3CCO2H
VD = 25mV
200mV/S
60
40
20
0
12
8
4
0
0
0.4
0.8
1.2
Drain Current, μA
Gate Potential, V vs. Ag Wire

Figure 5. A chemically-tuned push-pull amplifier based on chlorinated poly(3-methylthiophene) and trifluoroacetylated polyaniline: I_D-V_G characteristics in the range of V_G for amplifier operation.

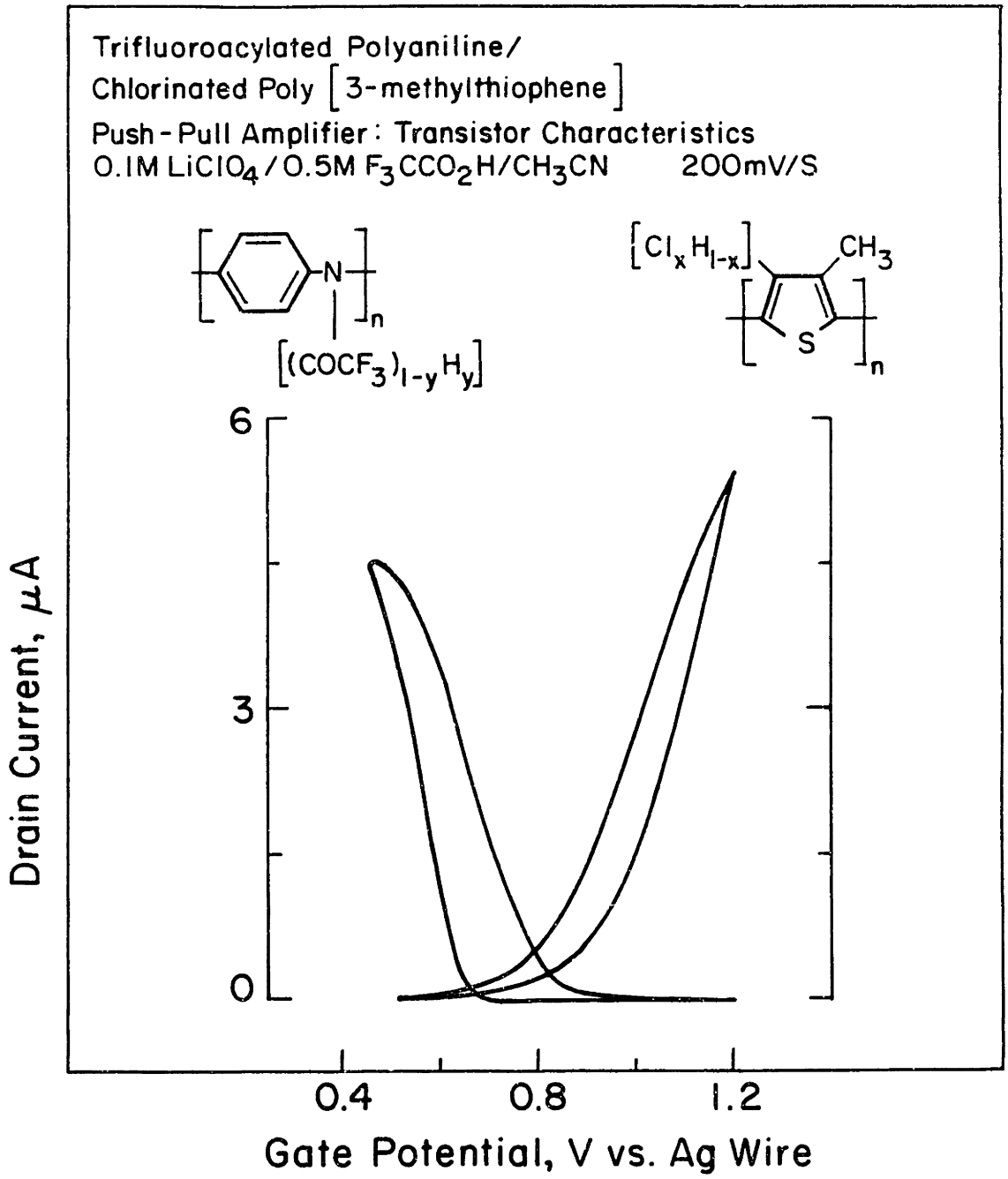
Trifluoroacylated Polyaniline/
Chlorinated Poly [3-methylthiophene]
Push-Pull Amplifier: Transistor Characteristics
0.1M LiClO4 / 0.5M F3CCO2H/CH3CN 200mV/S
[(COCF3)1-y Hy]
[Clx H1-x]
CH3
S
n
6
3
0
Drain Current, μA
0.4
0.8
1.2
Gate Potential, V vs. Ag Wire

Figure 6. Output waveform for the chlorinated poly(3-methylthiophene)/ trifluoroacetylated polyaniline push pull amplifier, driven over it entire operating range.

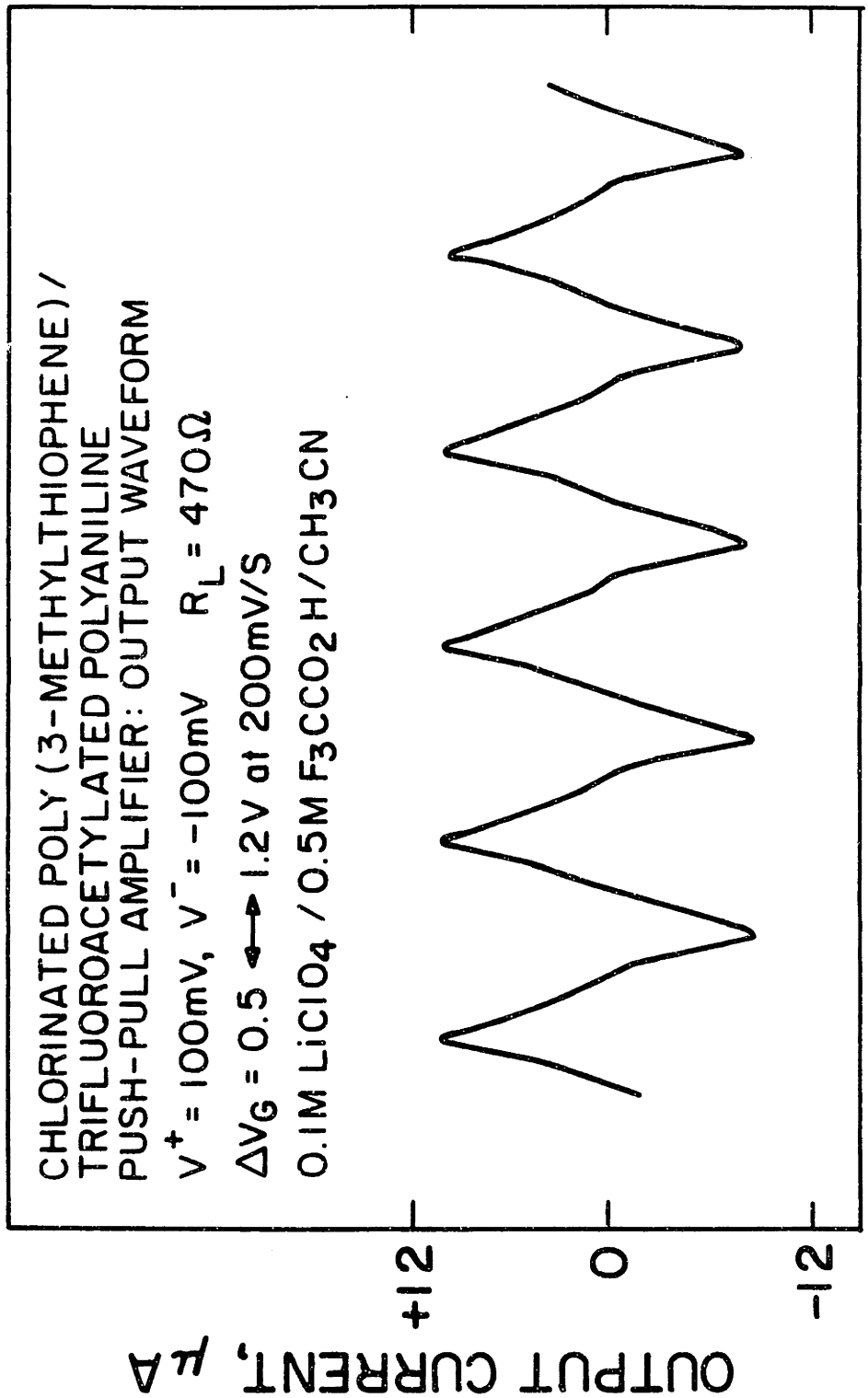
CHLORINATED POLY (3-METHYLTHIOPHENE) /
TRIFLUOROACETYLATED POLYANILINE
PUSH-PULL AMPLIFIER: OUTPUT WAVEFORM
V^+ = 100mV, V^- = -100mV R_L = 470Ω
ΔV_G = 0.5 ⟷ 1.2V at 200mV/S
0.1M $LiClO_4$ / 0.5M F_3CCO_2H/CH_3CN
OUTPUT CURRENT, μA
+12
0
-12
TIME

Discussion

A push-pull amplifier based on chlorinated poly(3-methylthiophene) and trifluoroacetylated polyaniline demonstrates the use of reaction chemistry to introduce electrical function in transistors. The same approach used to prepare the push-pull amplifier can also be applied to the two other families of devices introduced in Chapter 4 using the chlorinated poly(3-methylthiophene)/ trifluoroacetylated polyaniline system because of the wide range over which the complementarity of the two materials can be tuned. The experimental procedure which was outlined in Scheme II is suitable for all three families of devices. What varies from one family to the next is the degree of I_D-V_G overlap and relative drain currents of the two transistors required for the specific electrical function. To prepare a 3-state device in which a plateau or well is designed into the net I_D-V_G characteristic, a higher degree of overlap between two windows of conductivity is required. Poly(3-methylthiophene) itself provides a starting point of high overlap as seen in Figure 2. Because the overall I_D-V_G characteristic is the sum of two contributions, the tunability of polyaniline conductivity by trifluoroacetylation is particularly important in this type of device because the relative drain currents of the two polymers is more critical. Target points for onset potential and relative drain currents for the two polymers are more difficult to judge than was the case for the push-pull amplifier, but the results in Chapter 4 provide a guide.

Another device function introduced in Chapter 4 was a complementary microelectrochemical transistor (CMET) inverter. This device is least demanding in terms of the required I_D-V_G characteristics. A CMET inverter optimally should be based on two I_D-V_G characteristics which do not overlap at all. The magnitude of the gap between them is not critical and the conductivities of the two transistors do not need to be matched. The two transistors function only as switches, and the only drain current requirement is that both transistors provide whatever current is required by the load the inverter drives. To prepare a CMET inverter by the route in Scheme II , chlorination of poly(3-methylthiophene) to the 1.18 V limit of onset of conduction would be carried out followed by deposition of a

polyaniline transistor. Trifluoroacetylation of polyaniline would be an unnecessary refinement for this device. For a wider separation of I_D-V_G characteristics polythiophene, chlorinated for onset of conduction at 1.3 V, could be used in place of chlorinated poly(3-methylthiophene).

In summary, direct reactions on conducting polymers are a versatile and practical approach to preparing materials with predictably altered electrical characteristics for fabrication of microelectrochemical multi-transistor electronic devices. A transistor designed for 3-state operation, a complementary inverter gate, or a push-pull amplifier tuned for maximum output current without crossover distortion, can all be prepared using the versatile combination of controlled *in situ* β-chlorination of poly(3-methylthiophene) and potential-dependent N-trifluoroacetylation of polyaniline which provide the full range of required electrical characteristics.

Experimental

3-State device from two polypyrrole transistors.

The procedure for selective trifluoroacetylation of polypyrrole described in section 6.2 was used. One transistor was acylated to obtain the full 0.5 V shift in onset of conduction. The drain current-gate voltage characteristic was obtained by connection of the two devices in parallel, with a resistor (47 KΩ) in series with one device as shown in Figure 1.

Microelectrochemical Push-Pull Amplifier Based on Trifluoroacetylated Polyaniline and Chlorinated Poly(3-methylthiophene)

Poly(3-methylthiophene) was deposited onto electrodes 1, 2, and 3 of an 8-electrode array and chlorinated such that the reacted polymer displayed onset of conduction at 0.70 V vs Ag in 0.1 M $LiClO_4$/ 0.2 M F_3CCO_2H/CH_3CN, an electrolyte medium suited to both polyaniline and thiophene-based polymers. Electrodes 6, 7, and 8 of the array were cycled in 0.5M H_2SO_4 until a good response was obtained. Polyaniline was deposited onto these electrodes by cycling their potential between 0 and +0.90 V vs SCE in 0.1 M aniline in 0.25 M $NaHSO_4$/ 0.5 M H_2SO_4 until the anodic peak for the polymer (0.2 V) reached 20 nA. The I_D-V_G characteristics of the two polymers were recorded and the polyaniline was trifluoroacetylated by cycling from +0.75 V to +0.3 V vs Ag in 2 M $(F_3CCO)_2O$/ 0.2 M F_3CCO_2H/ 0.1 M $LiClO_4$ while monitoring the I_D-V_G characteristic until the peak drain current of the polyaniline transistor matched that of the chlorinated poly(3-methylthiophene) device. The two transistors were operated as a push-pull amplifier as previously described in Chapter 4.

References

1. Ternary logic is introduced in Chapter 4, section III.

2. McCoy, C. H. and Wrighton, M. S *Chemistry of Materials*, **1993**, *5*, 914

3. Horowitz, P.; Hill, W. *The Art Of Electronics*; Cambridge University Press: New York, 1989; Chapter 2

4. A full description can be found in Chapter 4 of this thesis.

Section 6.5

Investigations of Other Reactions on Conducting Polymers

Abstract

The reactions of polyaniline, polythiophene, and poly(3-methylthiophene) with XeF_2 in CH_3CN, poly(3-methylthiophene) with Br_2 in CH_2Cl_2 under UV irradiation, polyaniline with Cl_2 in CCl_4, and polythiophene under Friedel-Crafts alkylating and acylating conditions were examined. Polyaniline undergoes a decline in conductivity and a contraction of its finite window of conductivity upon reaction with XeF_2 or Cl_2 which closely parallels the effects of trifluoroacetylation on the polymer. Conductivity of chlorinated polyaniline was partially restored upon treatment with CH_3Li. Polythiophene and poly(3-methylthiophene) showed only loss of conductivity upon exposure to XeF_2 in CH_3CN with no change in potential for onset of conduction. Reaction of poly(3-methylthiophene) with Br_2 in CH_2Cl_2 under UV irradiation produced a 400 mV positive shift in onset of conductivity and a broadening of the polymer I_D-V_G characteristic. Reaction of polythiophene under Friedel-Crafts conditions did not produce any evidence of alkylation or acylation in the electrochemistry of the polymer. Attempts to lithiate poly(3-bromothiophene) using alkyllithium reagents and to methylate it with methylmagnesium chloride in the presence of $Ni(Ø_2P(CH_2)_3PØ_2)Cl_2$ were unsuccessful.

Introduction

In the course of examining the reactivity of conducing polymer substrates a number of different reactions were investigated. This section describes the reactions of conducting polymers with several different electrophilic and nucleophilic reagents. Relevant background is provided prior to discussion of each reaction. In each case, the reaction was chosen such that a significant and easily measured change in the I_D-V_G response of the polymer was expected from success of the reaction. Well most of the reagents are conventional sources of electrophilic or nucleophilic groups, certainly the most esoteric electrophile used is xenon difluoride. This powerful oxidative fluorinator became commercially available several years ago and its reactivity toward conducting polymers was examined because of the successful use of this reagent in the fluorination of aromatic substrates.[1]

Results and Discussion

Scheme I shows the results of seven reactions in which a conducting polymer substrate was treated with an electrophilic reagent. In an interesting reaction, it has been reported that xenon difluoride will ring-fluorinate aniline without reaction at the amine group, equation (1), despite the high oxidizing power of the reagent.[1] To see if fluorine

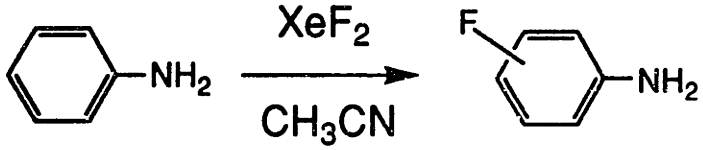

Filler, R. *Isr. J. Chem.* **1978**, *17*,71 (1)

could be introduced onto the backbone of polyaniline, the reaction of XeF_2 with the polymer was examined both at low temperature and at room temperature. A symmetrical contraction of the window of conductivity was observed, resulting in a 100 mV positive

Scheme I

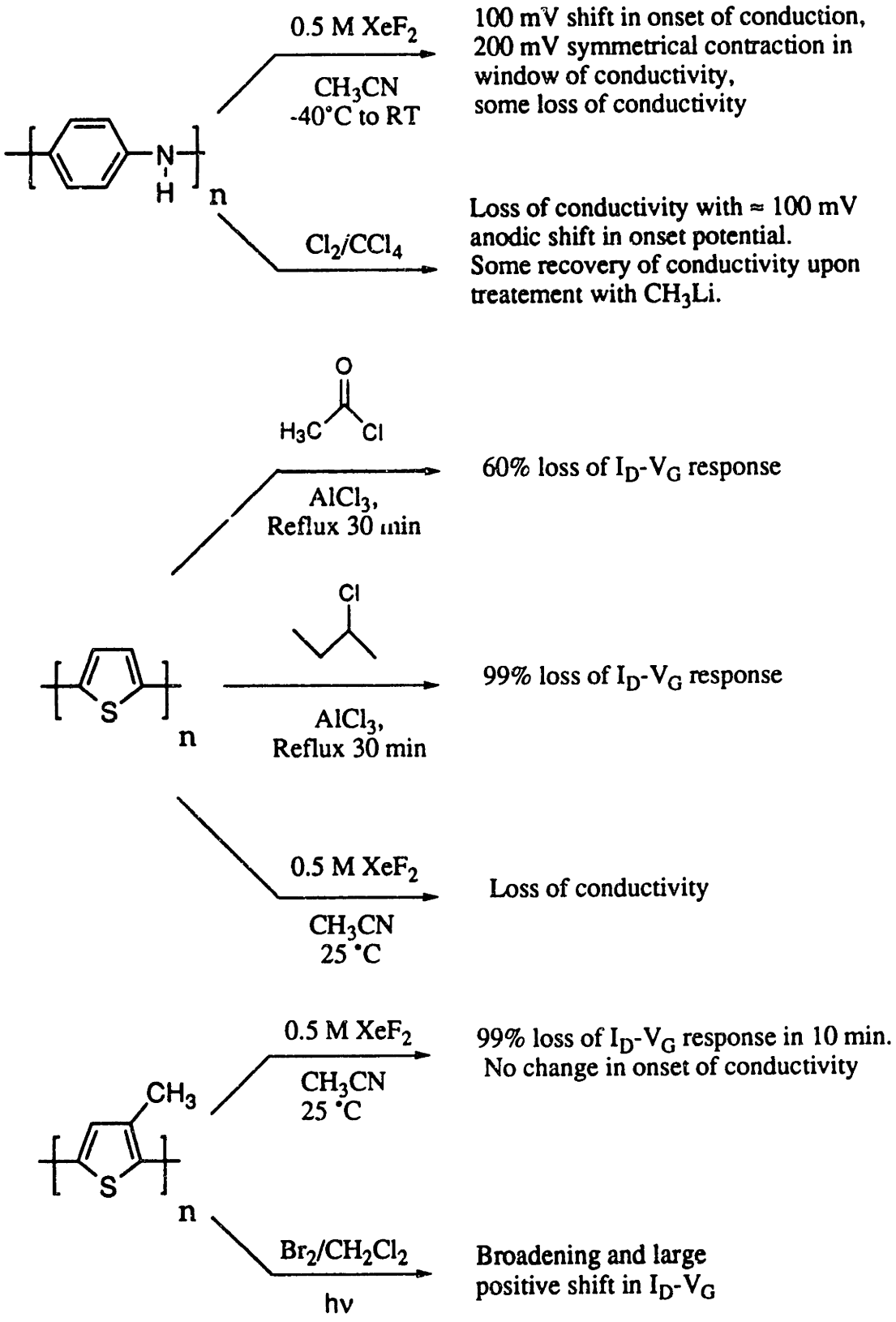
0.5 M XeF2
CH3CN
-40°C to RT
100 mV shift in onset of conduction,
200 mV symmetrical contraction in
window of conductivity,
some loss of conductivity
N
H
n
Cl2/CCl4
Loss of conductivity with ≈ 100 mV
anodic shift in onset potential.
Some recovery of conductivity upon
treatement with CH3Li.
O
H3C
Cl
AlCl3,
Reflux 30 min
60% loss of ID-VG response
Cl
S
n
AlCl3,
Reflux 30 min
99% loss of ID-VG response
0.5 M XeF2
CH3CN
25 °C
Loss of conductivity
0.5 M XeF2
CH3CN
25 °C
99% loss of ID-VG response in 10 min.
No change in onset of conductivity
CH3
S
n
Br2/CH2Cl2
hν
Broadening and large
positive shift in ID-VG

shift in onset of conduction. Reaction times of several minutes at room temperature yielded a polymer which still showed good cyclic voltammetry but only a fraction of the conductivity prior to the reaction. Specular reflectance FTIR was used to examine a film of polyaniline deposited onto a Au electrode and exposed to 0.5 M XeF_2 for 20 min, but no C-F stretch could be observed. Polyaniline turned black, the color of its fully-oxidized state, during exposure to XeF_2, no doubt due to oxidation by the reagent. Reaction under potential control, holding the polyaniline reduced, yielded the same observed changes in electrochemistry. **WARNING:** XeF_2 reacts rapidly with trifluoroacetic acid to produce HF and the explosive and shock-sensitive fluoroxenon(II) trifluoroacetate and xenon(II) bis-trifluoroacetate.[2] Many other acids are known to react similarly, yielding dangerous products.[3] Thus, while polyaniline can be held reduced by potential control, an acid source permitting full redox cycling must not be added. The results from reaction of polyaniline with XeF_2 were not considered promising as a means of tuning potential for onset of conducting since degradation of I_D-V_G response was a major result of exposure of the polymer to the reagent, and only a small shift in onset of conduction was observed. It could not be established whether ring fluorination of the polymer was occurring. Following several further attempts to achieve more revealing results, work in this area was ended.

XeF_2 fluorinates a range of aromatics[1] so it seemed sensible to examine polythiophene and poly(3-methylthiophene) as substrates. Unfortunately, only degradation of I_D-V_G response was observed upon exposure of these polymers to XeF_2 in CH_3CN. While thiophene is an activated substrate compared to benzene, catalysis by anhydrous HF may be a requirement,[1] but this was not examined.

Microelectrode-confined polyaniline exposed to ≈0.1 M Cl_2/CCl_4 was found to display a change in behavior closely paralleling that observed upon trifluoroacetylation and also similar to the effects of reaction with XeF_2. Drain current declined and the window of conductivity for the polymer contracted symmetrically following exposure to Cl_2. A 5 min

exposure resulted in a 95% loss of drain current. Interestingly, partial recovery of conductivity lost from chlorination was effected by immersion of the electrode-confined polymer in 1.6M CH_3Li in ether/hexane followed by immersion in water, presumably via lithium-chlorine exchange.

The Friedel-Crafts alkylation and acylation reactions are classic organic transformations in the chemistry of aromatic compounds and they were undertaken to probe the scope of reactivity of polyaromatic substrates. Shown in Scheme I were the two reactions attempted on polythiophene. In the alkylation, most of the I_D-V_G response of the polymer was lost while in the acylation degradation was not so severe. Had the reactions succeeded, alkylation is expected to result in a negative shift as high as several hundred mV in onset of conduction of the polymer given that poly(3-methylthiophene) turns on 400 mV negative of polythiophene. Acylation should have given rise to a positive shift in onset potential for polythiophene. No change in onset potential was observed in either case so it seems unlikely that either reaction proceeded to a significant extent.

A reaction which showed more promise was the bromination of poly(3-methylthiophene) which resulted in a positive shift in onset of conduction of about 400 mV. A microelectrode array bearing a poly(3-methylthiophene) transistor was immersed for 10 min in a quartz beaker containing 1.5 M Br_2/CH_2Cl_2 under ultraviolet irradiation. Because, unlike in chlorination, 3-methylthiophene can be brominated on the ring in the dark or on the methyl group under free-radical condictions,[4] this reaction is interesting warrants further study. The conditions used were probably excessively aggressive and should be tempered.

One reason for functionalizing a polymer with bromo groups it the possibility of carrying out subsequent synthetic chemistry. There is an example of this in the literature in which N-bromosuccinimide was used to brominate the methyl group of poly(3-methylthiophene) followed by a reaction on the brominated polymer.[5] Along similar lines, reactions of the polymer of 3-bromothiophene were attempted. In this case, nucleophilic

reagents were employed. Surprisingly, treatment of the polymer with CH_3Li, n-C_4H_9Li, and even $(CH_3)_3CLi$, equation (2), had little effect. Both water and iodomethane were

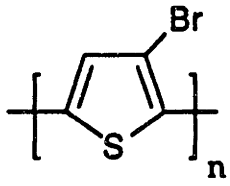

1) n-C_4H_9Li, $(CH_3)_3CLi$, or CH_3Li
-100 to 0°C

2) CH_3I or H_2O (2)

used as quenching reagents since replacement of the bromo group with hydrogen or methyl was expected to result in an observable negative shift in onset of conduction, possibly very large if methylation were successful. Since 3-bromothiophene itself is lithiated easily enough, it was considered strange that no effect on poly(3-bromothiophene) was observed. Degradation of the polymer was not significant after 2 hours exposure to $(CH_3)_3CLi$. Another reaction attempted, equation (3), was the methylation of the polymer using the nickel-catalyzed coupling reaction[6] carried out with 3-bromothiophene in Chapter 5.

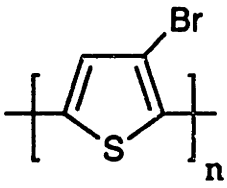

1) CH_3MgCl, $Ni(Ø_2P(CH_2)_3PØ_2)Cl_2$
Et_2O, Reflux 12h

2) CH_3I or H_2O (3)

Reflux for up to 24 hours yielded no evidence of reaction in the electrochemistry of the polymer. One potential problem with this reaction, and also with the Friedel-Crafts reactions, is that a conventional substrate would be in solution whereas the polymer is a separate solid phase. Since both Friedel-Crafts and the Grignard coupling use a catalyst which is itself insoluble until complexed with a reactant, it is may be that polymers are unsuitable substrates for these reactions.

Experimental

XeF_2, dry CH_3CN, $AlCl_3$, 2-chlorobutane, acetyl chloride, 1.6 M CH_3Li in ether/hexane, thiophene, and 3-methylthiophene were used as received from Aldrich Chemical. Cl_2 was purchased from Matheson and CCl_4 and CH_2Cl_2 from Mallinkrodt. Aniline was purified as described in Chapter 2, general experimental section.

Polyaniline, polythiophene, and poly(3-methylthiophene) were deposited onto microelectrode arrays as described previously in this chapter and all reactions were carried out on electrode-confined polymers. For reactions with XeF_2, the reagent was weighed out in a glove box where it was stored in order to keep it dry. 0.5 M solutions of XeF_2 in CH_3CN were prepared under dry argon for the reactions. For reactions requiring reflux, a 25 or 50 ml 3-necked flask with reflux condenser configuration was employed with the microelectrode array suspended from a wire passed through a septum so that is was immersed in the reaction mixture. All reactions were carried out under dry argon except for bromination of poly(3-methylthiophene) which was carried out in an open quartz beaker, and chlorination of polyaniline carried out in a 50 ml Erlenmeyer flask. Electrochemical characterizations were carried out in 0.1 M [*n*-Bu_4N]PF_6/CH_3CN, acidified with trifluoroacetic acid in the case of characterization of polyaniline.

References

1. Filler, R. *Isr. J. Chem.* **1978**, *17*, 71

2. Sladky, F. *Monat. Chem.* **1970**, *101*, 1571

3. Lentz, D.; Seppelt, K. *Prog. Inorg. Chem.* **1982**, 182

4. Hartough, H. D. *Thiophene And Its Derivatives*; Interscience: New York, 1952. Taylor, R. in *Thiophene An Its Derivatives, Part 2*; Gronowitz, S. ed.; Wiley: New York, 1986; pp. 79-117

5. Fabre, P.-L.; Dalger, A. *J. Chem. Research (S)* **1991**, 16 *(M)* **1991**, 0255

6. Tamao, K.; Kodama, S.; Nakajima, I.; Kumada, M. *Tetrahedron*, **1982**, *38*, 3347

Chapter 7

The Effect of Quaternization of Nitrogen on the Charge Transport Properties of Poly(2,5-dithienylpyridine) and a Chemically-Gated Polyaniline Microelectrochemical/Silicon Bipolar Transistor Hybrid Circuit with Very High Gain.

Abstract

The conjugated organic conductor, poly(2,5-dithienylpyridine), reacts with acid or with methyl trifluoromethanesulfonate to render the polymer completely insulating. The effect, presumed to be the result of quaternization of nitrogen, is reversible. Conducting poly(2,5-dithienylpyridine) can be regenerated by treatment of the protonated polymer with pyridine, and treatment of methylated polymer with $Ø_3P$ in refluxing CH_2Cl_2. The conductivity of poly(2,5-dithienylpyridine), confined to microelectrode arrays, was switched off by exposure to 0.1 M F_3CCO_2H/CH_2Cl_2 or to HCl (g) and back on by exposure to 0.1 M pyridine/CH_2Cl_2. The cycle of protonation/deprotonation could be carried out repeatedly. Poly(2,5-dithienylpyridine) showed a decline of greater than a factor of 10^4 in conductivity upon exposure to F_3CCO_2H or HCl (g) for less than 10 s. Continuous scanning of the I_D-V_G characteristic of microelectrode-confined poly(2,5-dithienylpyridine) showed complete loss of response in under three 4 s scans upon introduction of HCl(g), demonstrating a high-gain sensor response. A polyaniline transistor, switched between its conducting and insulating states by O_2 and H_2, respectively, was configured to drive a Si bipolar junction transistor which in turn drove a light emitting diode. The circuit showed an overall gain of 6×10^5, 96% of the gain being provided by the polyaniline transistor. The hybrid circuit demonstrates the compatibility of microelectrochemical transistors with conventional semiconductor devices, and the incorporation of a conducting polymer transistor property, that of chemical sensitivity, into a practical application circuit.

Introduction

The conjugated organic conductor poly(2,5-dithienylpyridine) upon exposure to 0.1M F_3CCO_2H/CH_2Cl_2 or HCl(g) undergoes a transition to an insulator. Conduction is also observed to disappear upon reaction of the polymer with methyl trifluoromethane-sulfonate. Treatment of the protonated polymer with pyridine regenerates conducting poly(2,5-dithienylpyridine), as does treatment of the methylated polymer with $P\emptyset_3$ in refluxing CH_2Cl_2.

Because conjugated organic polymers and redox materials display conductivity which varies as a function of oxidation state and also as a result of interactions with chemical species which alter charge transport properties, microelectrochemical transistors can respond to chemical stimuli.[1-10] In this way, a chemical signal such as the presence of some concentration of a species in solution can give rise to a change in drain current, thereby causing the same effect as gating by an electrical signal. Because a small change in polymer oxidation state gives rise to a large change in conductivity, microelectrochemical transistors can respond to chemical signals with very high gain. As a result, microelectrochemical transistors can be several orders of magnitude more sensitive than potentiometric or amperometric sensors which do not benefit from the amplification afforded by transistor function.[1,2]

Microelectrochemical transistors can exhibit responses to chemical stimuli in several ways. Electron transfer between a partially oxidized conducting polymer and an oxidant or reductant will alter polymer oxidation state and therefore conductivity, manifested as a change in drain current.[1,2] A different mechanism involves a more specific interaction in which a chemical species alters polymer charge transport properties resulting in a change in electrical characteristics.[3-9] Sensitivity to species such as oxidants and reductants,[1,2] protons,[3-7] and metal ions[8,9] have been reported. In these examples, a change in polymer electrical characteristics from which a signal can be derived occurs as a result of the interaction of the particular chemical stimulus with the conducting polymer. While such

effects of chemical species are clearly a possible basis for sensor devices, they also provide a means of probing the fundamental nature of charge transport in conjugated organic polymers. A reaction such as protonation of the nitrogen in poly(2,5-dithienylpyridine), for example, would be expected to alter charge transport along the polymer backbone since the nitrogen would be rendered cationic. Unlike polyaniline, where participation of the nitrogen *p*-orbital is required for a continuous π-manifold, loss of participation of the nitrogen *p*-orbital in poly(2,5-dithienylpyridine) does not *a priori* deprive the polymer of continuos π-delocalization. However, a cationic nitrogen is expected to represent a significant barrier to hole transport in poly(2,5-dithienylpyridine).

Results and Discussion

I. The Effect of Quaternization of Nitrogen on the Charge Transport Properties of Poly(2,5-dithienylpyridine)

2,5-Dithienylpyridine readily underwent anodic polymerization. The polymer was found to be sensitive to water in the oxidized state, so an anhydrous electrolyte medium of 0.1 M *n*-Bu_4NPF_6 in CH_2Cl_2 was prepared for polymer preparation and characterization. The methyl-quaternized monomer, however, did not yield a polymer. Treatment of 2,5-dithienylpyridine with one equivalent of $CH_3OSO_2CF_3$ in refluxing CH_2Cl_2 yielded white crystals of the product which precipitated over the course of the reaction. The methyl-quaternized derivative could not be polymerized onto microelectrodes. A slight reddish film was obtained which displayed no cyclic voltammetric response. Deposition attempts were characterized by an initial, rapid onset of current followed by a decline and disappearance of anodic current. This behavior suggested that poly(methyl 2,5-dithienylpyridinium trifluoromethanesulfonate) was forming at the electrode by was an insulator. Unable to obtain a film of the methyl-quaternized polymer in this way, attention was turned to methyl-quaternization of the polymer instead, Scheme I. Treatment of microelectrode-confined poly(2,5-dithienylpyridine) with methyl trifluoromethanesulfonate rendered the polymer insulating. It is reported[10,11] that N-methylpyridinium salts can be dealkylated with $Ø_3P$. This suggested the interesting possibility of removing the methyl group from the nitrogen in quaternized poly(2,5-dithienylpyridine). The literature procedure[11] called for refluxing at 150°C in dimethylformamide, conditions considered too harsh for the microelectrode array/polymer assembly. Instead, the electrode-confined polymer was immersed in a refluxing solution of $Ø_3P$ in CH_2Cl_2 overnight and this was found to be sufficient. Subsequent characterization of the polymer showed return of conductivity. Thus, the

Scheme I

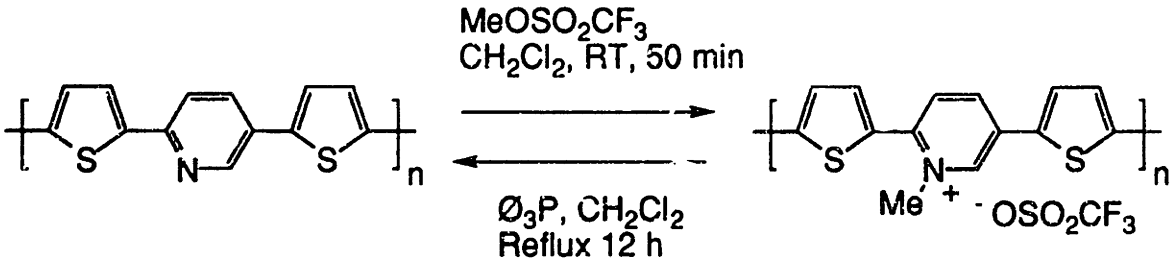

nitrogen of poly(2,5-dithienylpyridine) can be methyl-quaternized resulting in a loss of polymer conductivity, and de-methylated with $Ø_3P$ to restore conductivity as shown in Scheme I.

Poly(2,5-dithienylpyridine) is rendered insulating in acidic environments. Figure 1 shows the I_D-V_G characteristic of the polymer characterized in 0.1 M *n*-Bu_4NPF_6/ CH_2Cl_2 before and after exposure to 0.1 M F_3CCO_2H/CH_2Cl_2 and 0.1 M pyridine/CH_2Cl_2. Exposure to acid for only a few seconds was found to be sufficient to render the polymer completely insulating. The polymer exhibited poor cyclic voltammetric response and no I_D-V_G response to 1.5 V vs Ag following exposure to acid. Exposure to pyridine restored good cyclic voltammetry and I_D-V_G response and the polymer could be taken through successive cycles of protonation and deprotonation illustrating the reversibility of the effect of protonation on conductivity, Figure 1. Because of the apparent sensitivity of the polymer to nucleophilic attack, it was not possible to deprotonate the oxidized polymer with pyridine without onset of rapid degradation. The hindered base 2,6-di-*tert*-butylpyridine was employed in place of pyridine, but it was found to have no effect after 30 minutes on the protonated polymer while subsequent exposure to pyridine quickly restored full conductivity. Apparently, the hindered pyridine is insufficiently basic or too hindered to deprotonate the protonated polymer. Interestingly, following the first exposure of the

Figure 1. I_D-V_G response of poly(2,5-dithienylpyridine) following alternate protonation with F_3CCO_2H and deprotonation with pyridine.

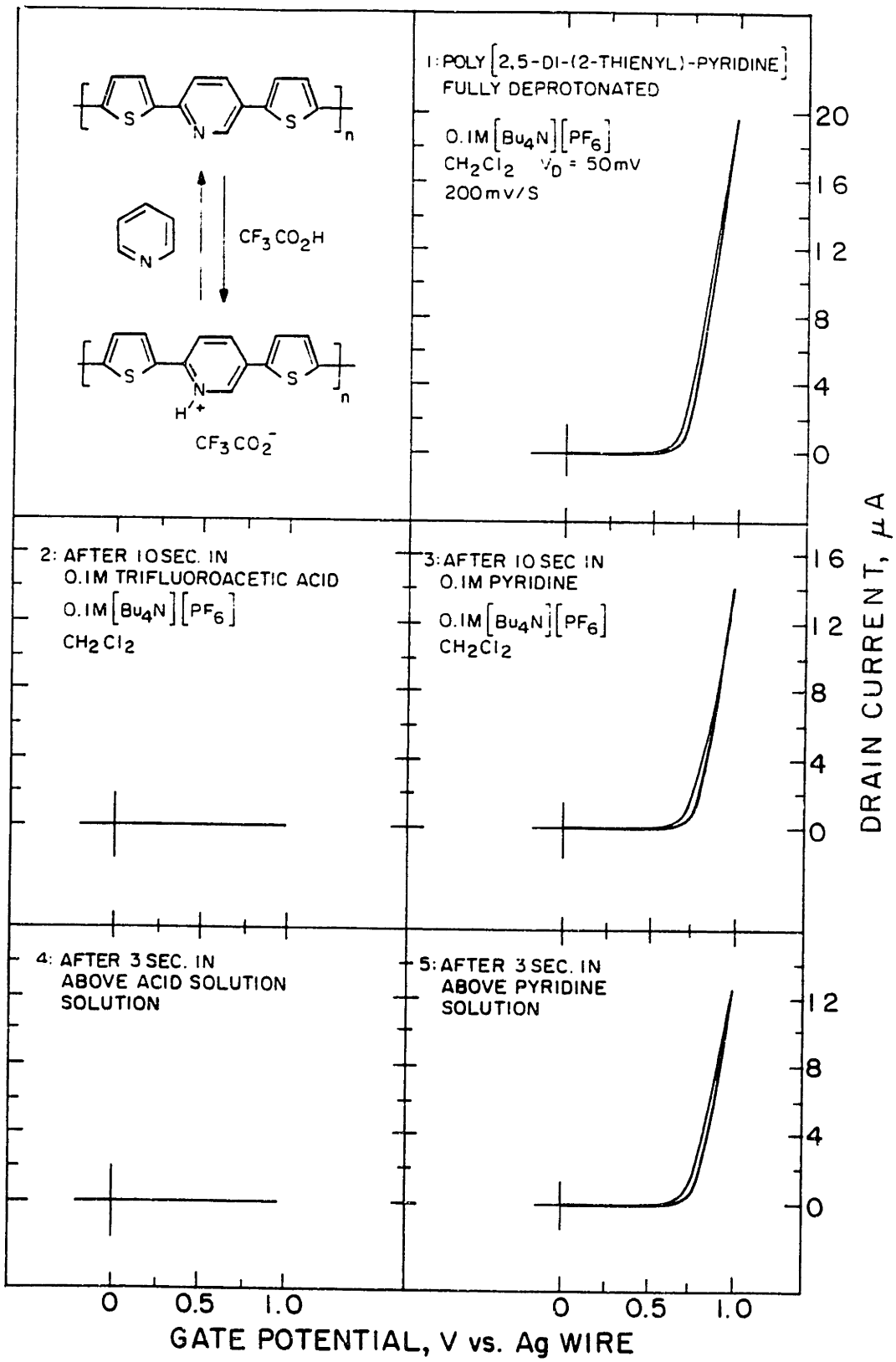
1: POLY [2,5-DI-(2-THIENYL)-PYRIDINE]
FULLY DEPROTONATED
0.1M [Bu4N] [PF6]
CH2Cl2 VD = 50mV
200mv/S
CF3CO2H
H+
CF3CO2-
2: AFTER 10SEC. IN
0.1M TRIFLUOROACETIC ACID
0.1M [Bu4N] [PF6]
CH2Cl2
3: AFTER 10 SEC IN
0.1M PYRIDINE
0.1M [Bu4N] [PF6]
CH2Cl2
4: AFTER 3 SEC. IN
ABOVE ACID SOLUTION
SOLUTION
5: AFTER 3 SEC. IN
ABOVE PYRIDINE
SOLUTION
DRAIN CURRENT, μA
GATE POTENTIAL, V vs. Ag WIRE

polymer to pyridine, its conductivity was found to recover to a value *higher* than that observed for the as-deposited polymer. One device showed an initial peak drain current of 6 μA for as-deposited poly(2,5-dithienylpyridine) which then increased to 30 μA after one cycle of exposure to 0.1 M F_3CCO_2H/CH_2Cl_2 and subsequent treatment in 0.1 M pyridine/CH_2Cl_2. Since the coupling reaction by which anodic polymerization occurs can generate protons,[12,13] it is possible that the polymer deposits in a partially protonated state.

To demonstrate detection of a gas-phase proton source, the I_D-V_G response of a poly(2,5-dithienylpyridine)-modified microelectrode array was characterized before exposing the device to anhydrous HCl for 5 seconds. The I_D-V_G response was recorded subsequent to the HCl exposure and the results are shown in Figure 2. As with trifluoroacetic acid, poly(2,5-dithienylpyridine) is rendered insulating after a few seconds of exposure to the gaseous acid, but conductivity can be restored by subsequent treatment of the polymer with a 0.1 M solution of pyridine in CH_2Cl_2. Figure 3 shows the dynamic response of a poly(2,5-dithienylpyridine) microelectrochemical transistor to the presence of protons. The I_D-V_G characteristic of the device was scanned continuously with the device immersed in 0.1 M *n*-Bu_4NPF_6/ CH_2Cl_2. A stream of HCl was passed above the surface of the solution in a cell consisting of a four-necked round bottom flask with ground glass fittings for the necessary electrodes and gas inlet and outlet. On the first scan of the I_D-V_G characteristic following the introduction of HCl into the cell, the I_D-V_G response was unaffected while the second scan showed a large attenuation of drain current and the third scan was completely flat. Each scan took 4 s. Following exposure of poly(2,5-dithienylpyridine) to acid, the polymer could be deprotonated to repeat the experiment many times.

The demonstration that the loss of conductivity both from reaction with acid or reaction with methyl trifluoromethanesulfonate can be completely restored via a deprotonating or demethylating reagent, respectively, indicates that the polymer remains intact and is not suffering from general degradation. The quaternization of the pyridyl

Figure 2. I_D-V_G response of poly(2,5-dithienylpyridine). Top: before exposure to HCl(g). Middle: After exposure to HCl(g). Bottom: After exposure to 0.1 M pyridine.

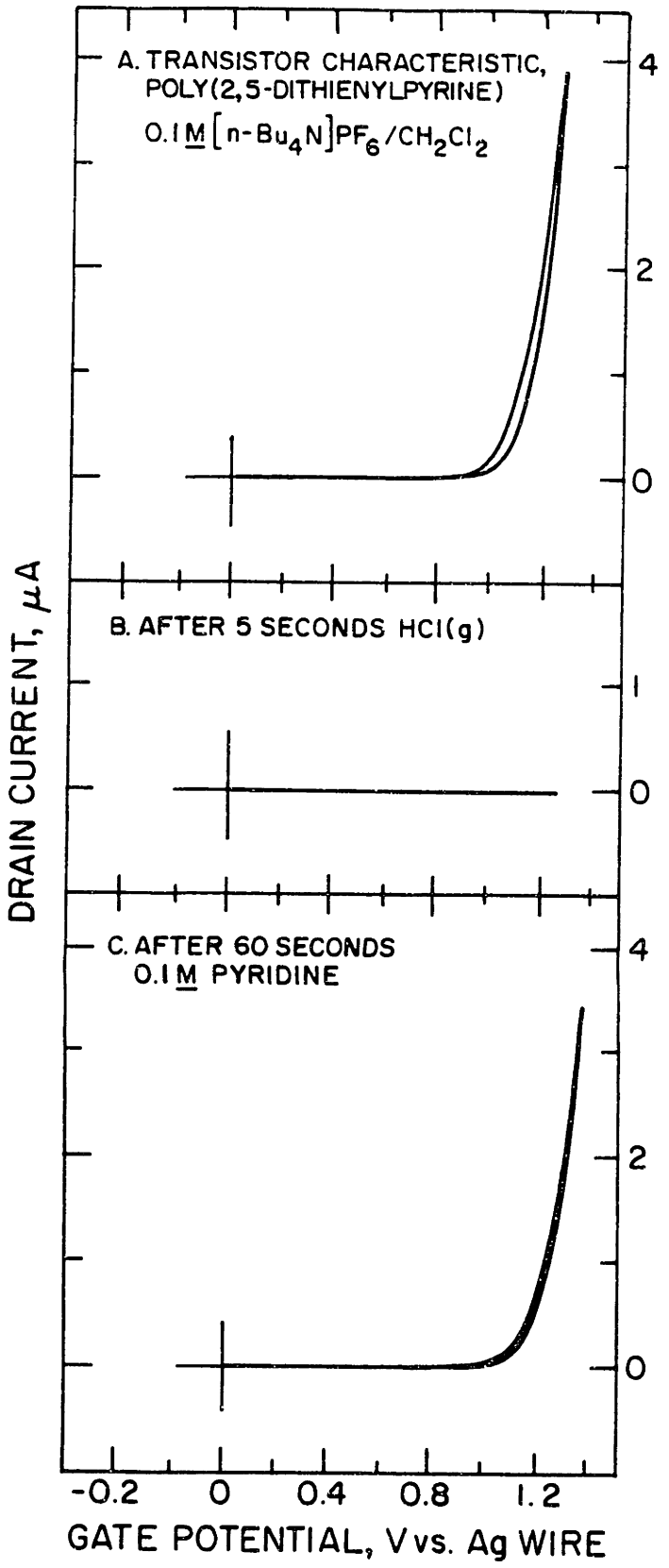
A. TRANSISTOR CHARACTERISTIC,
POLY(2,5-DITHIENYLPYRINE)
0.1 M [n-Bu4N]PF6/CH2Cl2
B. AFTER 5 SECONDS HCl(g)
C. AFTER 60 SECONDS
0.1 M PYRIDINE
DRAIN CURRENT, μA
4
2
0
1
0
4
2
0
-0.2
0
0.4
0.8
1.2
GATE POTENTIAL, V vs. Ag WIRE

Figure 3. I_D-V_G response of poly(2,5-dithienylpyridine) scanned continuously while HCl(g) was passed over the surface of the electrolyte solution.

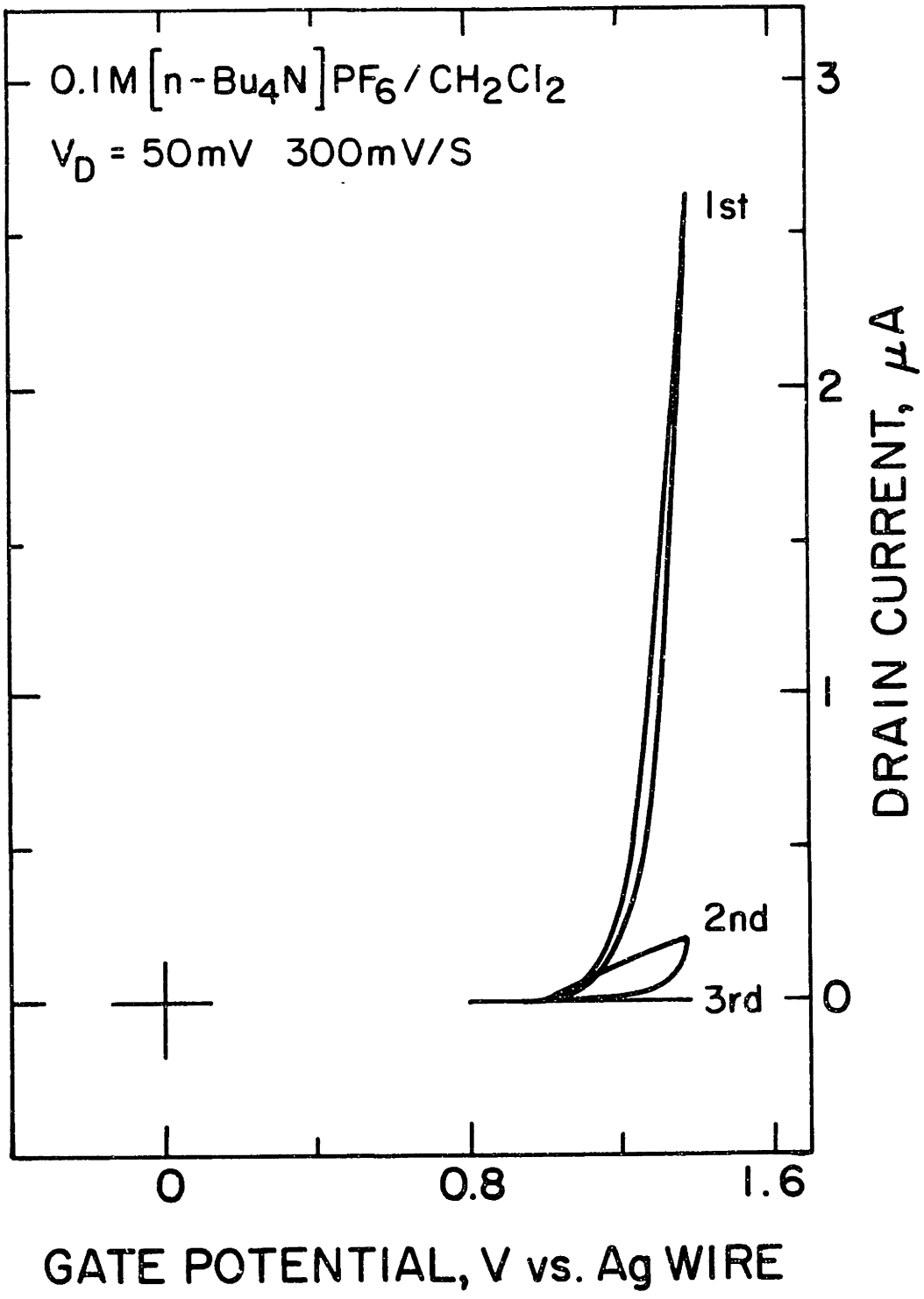
0.1M [n-Bu4N]PF6 / CH2Cl2
VD = 50mV 300mV/S
1st
2nd
3rd
3
2
1
0
DRAIN CURRENT, μA
0
0.8
1.6
GATE POTENTIAL, V vs. Ag WIRE

nitrogen was expected to suppress conduction. The rapid, complete loss of conductivity in the presence of a proton source and the complete return of charge transport after treatment with a base is consistent with the expectation that the protonated pyridyl ring is too difficult to oxidize to allow conduction to occur. Hole transport would require the pyridyl ring to at least partially support a dicationic state. In the fully protonated polymer, Scheme II, each

Scheme II

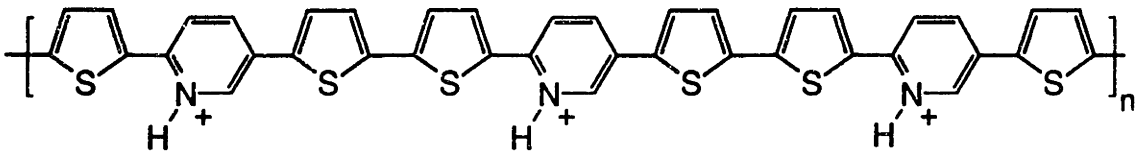

pyridine ring supports one cationic site. Since polyaniline, polythiophene, polypyrrole, and polyacetylene are all known to be rendered insulting when oxidized to the extent of 1 electron per repeat unit,[14,15] it is not expected that the pyridyl rings bearing a localized cationic site as shown in Scheme II will support conduction.

The pyridyl ring in poly(2,5-dithienylpyridine) is thus chemically switchable between its protonated state where it blocks π-conjugation and hole transport, and its non-protonated state where it participates in the π-manifold and allows charge transport in the polymer. Thus, by introducing a chemically sensitive site in the polymer architecture, the interaction between the pyridyl nitrogen lone pairs and protons in solution is translated into a the electrical signal of a change in transistor drain current.

A Chemically Gated Hybrid Circuit Based on One Polyaniline Transistor and One Silicon Transistor.

The sensitivity of microelectrochemical transistors to chemical stimuli was incorporated into a circuit which responded to H_2 and O_2 with overall gain of 6×10^5. Figure 4 shows the circuit schematic and a representation of circuit operation. A polyaniline transistor, if provided with a Pt catalytic surface, can be brought into conduction by exposure to O_2. Partially oxidized, conducting polyaniline can be rendered insulating via reduction by H_2. A polyaniline device was prepared and operated in a cell containing 0.5 M H_2SO_4, with a platinum wire connected to one electrode of the device to provide the required catalytic surface for O_2 reduction and H_2 oxidation. No electrochemical potentiostatic control is necessary since a chemical species sets the oxidation state of the polymer. The polyaniline device was connected to drive the emitter-base junction of a standard Si bipolar transistor. To accomplish that task, a drain voltage exceeding the 600 mV barrier potential of a Si *p-n* junction was required, so drain voltage was set to the unusually high value of 700 mV. A light emitting diode (LED) was chosen as the load for the silicon transistor and required the 3 V supply, V_{CC}, in the silicon transistor leg of the circuit. The Si transistor section of the circuit was characterized independently and it was found that a base current of 10 μA produced reasonable LED brightness, an amount of current well within the capability of a polyaniline microelectrochemical transistor prepared on microelectrodes of the dimensions used. When the polyaniline transistor is exposed to O_2, reduction of O_2 and oxidation of polyaniline occur, bringing the polyaniline transistor into conduction. Drain current then flows, providing base current to the Si transistor, bringing it into conduction. With the Si transistor in the conducting state, current flows through the LED as a result of V_{CC}, and the LED turns on. If oxidized polyaniline is exposed to H_2, H_2 is oxidized, providing the electrons required to reduce polyaniline and return it to its insulating state. Drain current no longer flows, and with no

Figure 4. Schematic (top) and diagram of operation (bottom) of a chemically-gated hybrid circuit based on a polyaniline microelectrochemical transistor and a Si bipolar junction transistor.

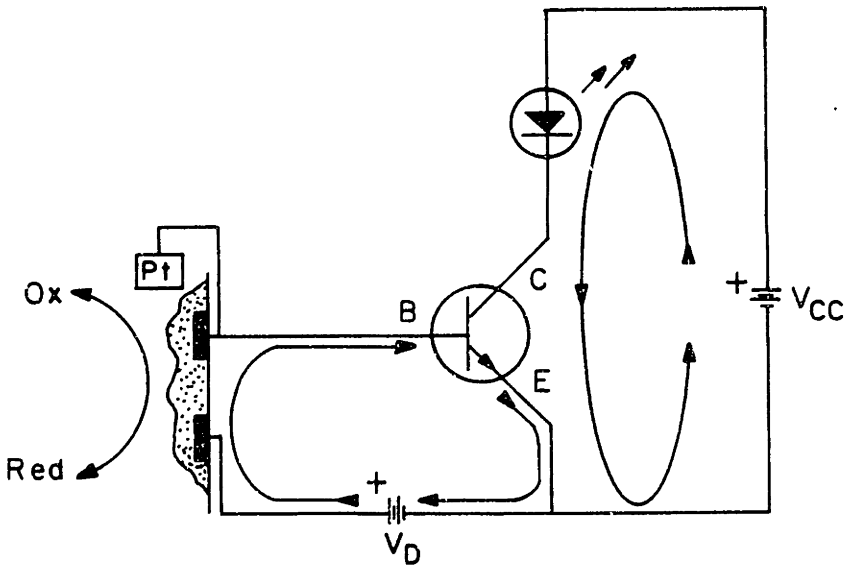
Pt
Ox
Red
B
C
E
+
V_{CC}
+
V_D

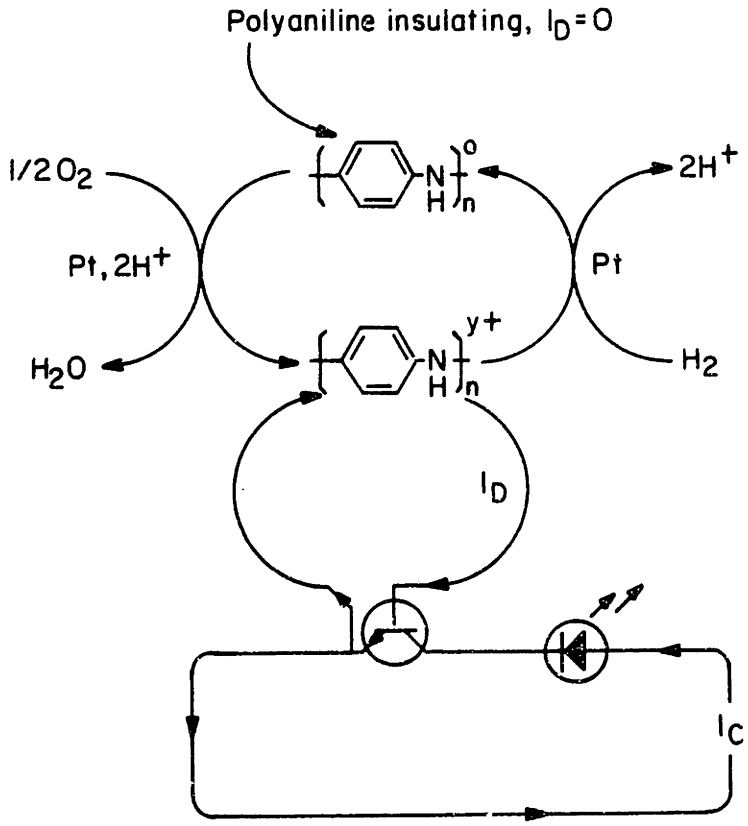
Polyaniline insulating, $I_D = 0$
$1/2O_2$
$Pt, 2H^+$
H_2O
$2H^+$
Pt
H_2
I_D
I_C

Figure 5. Operation of the chemically-gated hybrid circuit shown in Figure 3 showing drain current through the polyaniline device (top) and collector current through the Si device (bottom) as the polyaniline device is alternately exposed to O_2 and H_2.

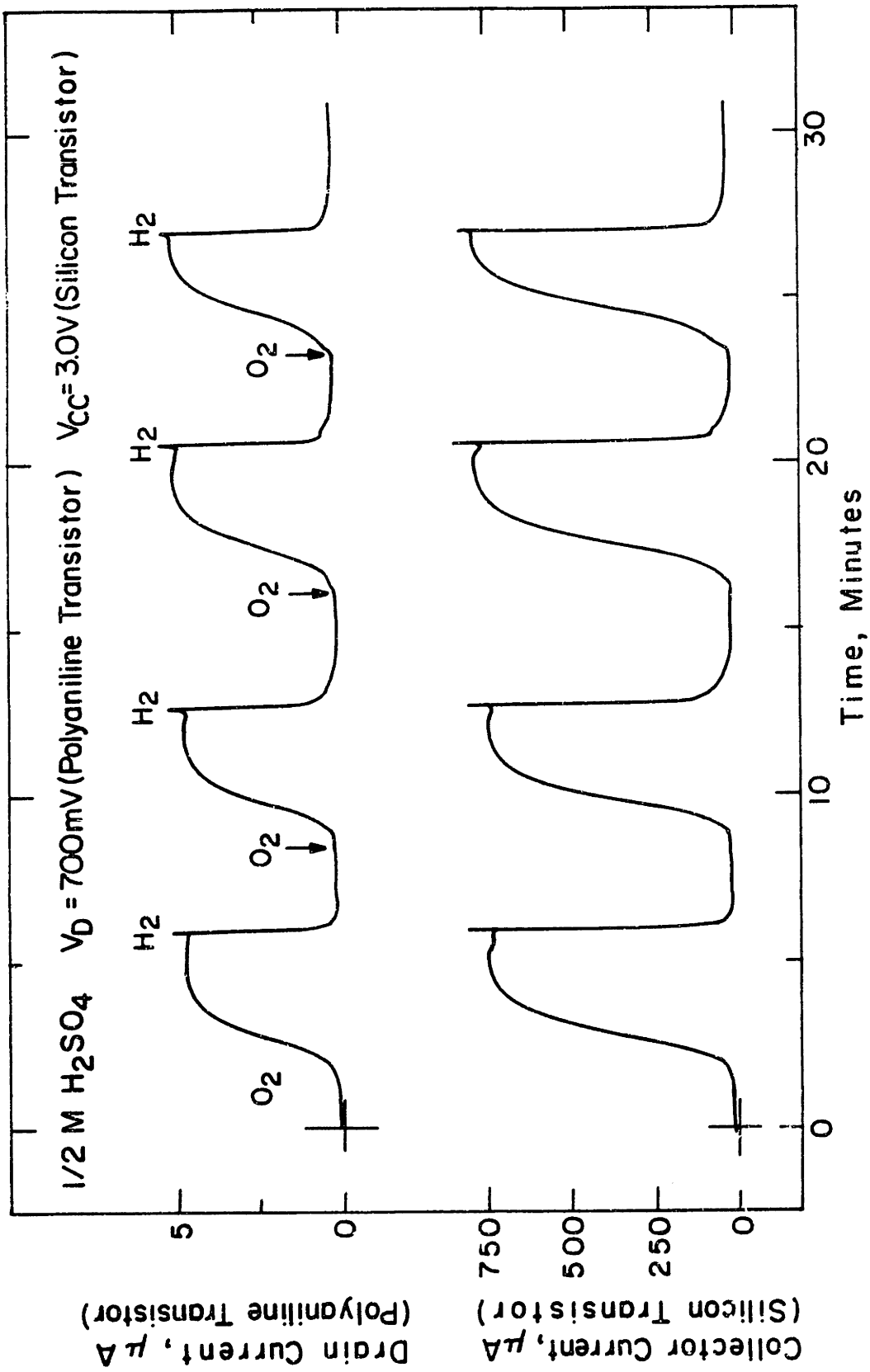
1/2 M H_2SO_4 V_D = 700mV (Polyaniline Transistor) V_{CC} = 3.0V (Silicon Transistor)
O_2
H_2
O_2
H_2
O_2
H_2
O_2
5
0
750
500
250
0
0
10
20
30
Time, Minutes
Drain Current, μA (Polyaniline Transistor)
Collector Current, μA (Silicon Transistor)

current to hold the Si transistor in conduction, it becomes insulating also, and the LED turns off. This can be repeated at will, and the response of the two devices is shown in Figure 5. At the top of Figure 5 is drain current flowing through the polyaniline transistor and driving the Si bipolar transistor. Collector current flowing through the Si transistor is shown at the bottom of Figure 5. It can be seen that the response to H_2 was much more rapid than the response to O_2. The sharp, brief increase in drain current which precedes the decline to zero upon exposure to H_2 is attributed to the characteristic hysteresis in the response of polyaniline in H_2SO_4. The I_D-V_G characteristic of polyaniline shows higher conductivity on the return scan (reduction from the oxidized state) than on the forward scan (oxidation from the reduced state). Thus, when H_2 is introduced, the polymer proceeds to the reduced, insulating state through a higher maximum conductivity than was observed upon oxidation of polyaniline by O_2. This is in complete accord with, and indeed is expected from, the known behavior of polyaniline[14,16]. The gain of this system is high because it is the product of the gains of the polyaniline and Si transistors. The current gain of the Si device was 159, calculated from the data in Figure 5 . The gain of the polyaniline transistor was calculated using the observed drain current, and the gate current determined from the cyclic voltammogram of the polyaniline transistor. Since the response to O_2 took place over a longer period of time, the peak current of the cyclic voltammogram was scaled accordingly assuming a linear reduction in peak current with total time required for the reduction of polyaniline. The current gain of the polyaniline transistor, thus calculated, was 3930. Thus, overall, one electron exchanged between polyaniline and one of the gating chemical species gives rise to a 6.25×10^5 electron change in collector current through the LED.

The hybrid circuit described here demonstrates that a microelectrochemical transistor can function as part of a conventional circuit design. The polyaniline transistor provided the properties of chemical sensitivity and high gain. The Si transistor provided the voltage-handling capability required to drive the LED. At present, microelectrochemical

devices are not able to operate at drain voltages much above 1.5 V. The drain current capability of a polyaniline transistor fabricated on the microelectrode arrays used here is well matched to the general purpose Si transistor used above. The measured current gain of the Si device was 159, while the maximum drain current of a polyaniline transistor on an MS17 microelectrode array is about 5 mA, which is more than adequate to drive a 2N3904 transistor to its maximum rated collector current of 300 mA. While the 700 mV drain voltage required so that the polyaniline transistor could drive the Si device is quite large, the polyaniline transistor proved durable under these conditions and showed no loss of response over the course of the experiment. The LED was chosen as a load to allow a photographic record of circuit operation. However, many other choices of load are also suitable, such as an ammeter to provide a quantitative indicator of response, or a control device which is to be actuated in the presence of O_2. This circuit demonstrates that unique properties of microelectrochemical transistors can be directly incorporated into conventional transistor designs.

Experimental

Materials

CH_2Cl_2 was distilled from P_2O_5 prior to use. [*n*-Bu_4N]PF_6 was recrystallized from ethyl acetate and dried under vacuum for 24 h at 150 °C. $CH_3OSO_2CF_3$, F_3CCO_2H, pyridine, and anhydrous HCl were used as received.

Electrochemistry

Electrochemistry and reactions of poly(2,5-dithienylpyridine) were carried out in dry 0.1 M [*n*-Bu_4N]PF_6/CH_2Cl_2 either in a dry box or in a closed cell consisting of a 4-necked flask with ground glass fittings for the microelectrode array, reference electrode, and counter electrode. Electrochemical measurements were carried out with a Pine Instruments model RDE4 bipotentiostat and data recorded on a Kipp and Zonen model BD90 XY recorder. A silver wire reference electrode and platinum wire counterelectrode were used for all experiments. Poly(2,5-dithienylpyridine) was prepared by electrochemical polymerization of the monomer from an ≈80 mM solution in 0.1 M [*n*-Bu_4N]PF_6/CH_2Cl_2. The electrode-confined polymer was reacted with $CH_3OSO_2CF_3$ in CH_2Cl_2 (220 μl in 5 ml) at room temperature by immersion of the microelectrode array in the solution for 50 min. For dealkylation the microelectrode array was suspended by a wire in a refluxing solution of $PØ_3$ in CH_2Cl_2 overnight. Figure 1 results: Electrochemistry was carried out in a glove box. All I_D-V_G characteristics were obtained in blank 0.1 M [*n*-Bu_4N]PF_6/CH_2Cl_2. The microelectrode array-confined poly(2,5-dithienylpyridine) was immersed in either 0.1 M F_3CCO_2H/0.1 M [*n*-Bu_4N]PF_6/CH_2Cl_2 or 0.1 M pyridine/ 0.1 M [*n*-Bu_4N]PF_6/CH_2Cl_2 as specified followed by a CH_2Cl_2 rinse prior to obtaining the I_D-V_G characteristic of the polymer. Figure 2 and Figure 3 Results: Electrochemistry was carried out in a closed cell. Ar, HCl(g), and the required solutions

were introduced by syringe needle or cannula. Dry CH_2Cl_2 was used to rinse the cell and electrodes after removal of one solution and introduction of the next.

Polyaniline microelectrochemical transistor-Si bipolar junction transistor hybrid circuit.

A polyaniline transistor was prepared as usual (see Chapter 2) and operated in 0.5 M H_2SO_4 in a 4-necked flask equipped with gas inlet and outlet tubes. The inlet tube was connected to an H_2 or O_2 tank as required so that the gas could be introduced into the cell, accomplished via a pipet immersed in the H_2SO_4 solution. The polyaniline device was connected according to the schematic in Figure 4. A 2N3904 NPN Si bipolar junction transistor was chosen, but any general-purpose small-signal device is acceptable. An RDE4 potentiostat was operated as a power supply by shorting the counter and reference electrode terminals together and using K1 to provide +3 V for V_{CC} and K2 to provide +700 mV for V_D.

Synthesis

N-methyl-2,5-dithienylpyridinium trifluoromethanesulfonate

100 mg (0.412 mM) 2,5-dithienylpyridine was dissolved in 3 ml CH_2Cl_2. 100 mg (0.610 mM, 1.48 equiv.) $CH_3OSO_2CF_3$ was added and crystals began to form as the mixture was brought to reflux. After 4h at reflux (the reaction was probably complete in considerably less time than this) a yellow solid, slightly darker in color than the starting material, was collected and rinsed with diethyl ether. The ether rinse induced further precipitation from the mother liquor and a second crop of crystals was obtained. The product was dried under vacuum. Yield, 135 mg (81%).

2,5-dithienylpyridine was provided by Michael Wolf and was synthesized according to the following procedure:

A solution of 2,5-dibromopyridine (2.4 g) and $Pd(P\emptyset_3)_4$ (0.70 g) in diglyme (80 ml) was prepared under argon and stirred for 10 min. A solution of 2-boronothiophene (3.1 g) and 1.0 M $NaHCO_3$ (60 ml) was prepared and added via cannula and the mixture heated at reflux for 24 h. The reaction mixture was cooled and diethyl ether (100 ml) and water (100 ml) added. The organic layer was washed with water (5 x 100 ml) to remove excess diglyme and dried over $MgSO_4$. The solvent was removed in vacuo yielding the crude product which was chromatographed on silica with CH_2Cl_2 / pentane (1:3) to yield pure 2,5-dithienylpyridine (1.84 g, 75%). mp 145 °C. ^1H NMR: (CD_3COCD_3) δ: 8.83 (d, 1H, 2 Hz); 8.03 (dd, 1H, 2 Hz, 8 Hz); 7.88 (d, 1H, 8 Hz); 7.75 (d, 1H, 4 Hz); 7.5-7.6 (m, 3H); 7.2-7.1 (m, 2H). MS (EI), M+ 243. Anal. Calcd. for $C_{13}H_9S_2N$: C, 64.16; H, 3.73. found: C, 64.19; H, 3.74.

References

1. Thackeray, J. W.; White, H. S.; Wrighton, M. S. *J. Phys. Chem.*, **1985**, *89*, 5133.
2. Thackeray, J. W.; Wrighton, M. S. *J. Phys. Chem.*, **1986**, *90*, 6674.
3. Natan, M. J.; Mallouk, T. E.; Wrighton, M. S. *J. Phys. Chem.*, **1987**, *91*, 648.
4. Natan M. J.; Bélanger, D.; Carpenter, M. K.; Wrighton, M. S. *J. Phys. Chem.*, **1987**, *91*, 1834.
5. Bélanger, D.; Wrighton, M. S. *Anal. Chem.*, **1987**, *59*, 1426.
6. Shu, C.-F.; Wrighton, M. S. *J. Phys. Chem.*, **1988**, *92*, 5221.
7. Huang, J.; Wrighton, M. S. *Anal. Chem.*, **1993**, *65*, 2740.
8. Marsella, M. J.; Carroll, P. J.; Swager, T. M. *J. Am. Chem. Soc.* **1994**, *116*, 9347
9. Swager, T. M.; Marsella, M. J. *Mater. Res. Soc. Symp. Proc.* **1994**, *328*, 263
10. March, J. *Advanced Organic Chemistry, 4th ed.*, John Wiley & Sons: New York, **1992.** p.413
11. Deady, L. W.; Finlayson, W. L.; Korytsky, O. L. *Aust. J. Chem.* **1979**, *32*, 1735
12. Diaz, A. F.; Bargon, J. in *Handbook of Conducting Polymers*; Skotheim, T. A., Ed.; Marcel Dekker: New York, 1986. Chapter 3
13. Roncali, J. *Chem. Rev.* **1992**, *92*, 711.
14. Ofer, D.; Crooks, R. M.; Wrighton, M. S. *J. Am. Chem. Soc.*, **1990**, *112*, 7869.
15. Ofer, D.; Park, L. Y.; Schrock, R. R.; Wrighton, M. S. *Chem. Mater.* **1991**, *3*, 573.
16. Chapter 3, this thesis

Chapter 8

Design of Conducting Polymer Electronics: Analog-to-Digital Conversion, Quaternary to Binary Translation, and a Circuit for the Addition of Two Numbers

Abstract

The designs of two circuits based on microelectrochemical transistors are developed based on the results in previous chapters of this thesis. First, a circuit which converts an input voltage into a two-digit binary number is developed based on three partially overlapping finite windows of high conductivity. This circuit is capable of carrying out both analog-to-digital conversion and translation of quaternary logic (4 levels) into binary logic (2-levels). Appropriate polymers for use as the three active materials, provided by the results reported in Chapter 5 and Chapter 6, are selected. Second, a design for a binary adder, capable of adding two one-bit binary numbers, is developed based on conventional logic gates implemented with microelectrochemical transistors. The design of the AND gate as well as the OR gate required by the adder circuit are also developed. The adder design, which uses polyaniline and WO_3 as the active materials, demonstrates a route to a digital function more complex than the single logic gates demonstrated in previous chapters.

Introduction

This chapter presents the design of two microelectrochemical electronic systems which together demonstrate the combination of the chemistry, electrochemistry, and electronics of the previous chapters of this thesis to achieve more the more sophisticated circuit functions of digital-to-analog conversion, quaternary logic to binary logic translation, and the addition of two numbers. The two designs show that circuits of moderate complexity can be developed based on device behavior demonstrated experimentally in the previous chapters, and on the synthetic approaches to conducting polymers developed in Chapter 5 and Chapter 6.

Chapter 4 demonstrated three different molecule-based electrical functions which could be derived in a unique way from the finite window of high conductivity which is characteristic of conjugated organic polymers. The amplifiers, logic gates, and molecule-based approaches to these functions described in Chapters 2, 3, 4, and 6.4 provide a set of building blocks and design approaches which can form the basis of more advanced circuit functions. Chapters 5 and 6 investigated substituent electronic effects and reactivity in conducting polymers, and one aspect of these results was that they provided a wide range of available polymer electrical characteristics through preparation of substituted monomers and by direct, *in situ* chemical tuning via electrophilic substitution reactions. The two designs presented below were not demonstrated experimentally. However, both designs are expected to function as described, since only device electrochemistry and electrical behavior demonstrated experimentally elsewhere in this thesis is invoked.

Results and Discussion

I. Design of An Analog-to-Digital Converter/Quaternary-to-Binary Translator Based on Three Different Finite Potential Windows of Conductivity

Analog-to-digital conversion[1] is the process of converting an analog voltage continuum into numbers, and is thus a means of interfacing the analog to the digital realm. The circuit developed here makes extensive use of the finite window of high conductivity of conducting polymers in its design. The goal chosen was a simple one, that of a 2-bit A/D converter. Such a device converts an analog voltage continuum into a 2-digit binary number. In other words, it assigns an input voltage a binary number of *00*, *01*, *10*, or *11*. The circuit thus requires two output terminals to provide the two-digit binary number, represented as a HIGH output voltage for **1**, and a LOW output voltage for **0**. (See Chapter 3 for a more detailed discussion of logic levels). An approach to this function is shown in Scheme I. The input terminal is the usual gate voltage arrangement which sets the electrochemical potential of all three polymers. The circuit uses transistors which each conduct over different ranges of potential. Thus, the finite window of conductivity is the basis of circuits ability to distinguish one range of input voltage from another, and as demonstrated in Chapter 4, the choice of device-active polymers proves a significant and useful design parameter. Each of the three transistors in the circuit in Scheme I is both a switch and voltage level detector, turning on when input voltage is within the finite potential window of conduction for each specific device. The interconnections of the three polymer-modified sets of microelectrodes provide the desired digital output of two voltages. The voltages are developed as a drop across a resistor when drain current flows through one of the polymers which connects that resistor to V_{DD}, the positive side of the circuit power supply. At input voltage V_1, none of the polymers conduct so no current flows and no voltage is dropped across either of the two resistors, so both outputs A and B

are zero, and the output of the converter, the binary number *BA*, is *00*. At V_2, polymer 1 conducts, and V_{DD}, the power supply voltage, is dropped across resistor R1 and output A is HIGH while output B remains LOW, producing the output *01*. At V_3, polymer 1 is past its potential for onset of oxidative insulation while polymer 2 is conducting, producing the output *10*. To send both outputs high, a third polymer with a high potential for onset of conduction, is configured with two drain electrodes, one connected to each resistor, such that at V_4 where polymer 3 is conducting, drain current flows through both R1 and R2 producing V_{DD} at both outputs for the binary number *11*. It is appropriate to chose a high value for R1 and R2 so that a steep transfer function is obtained. If resistances R1 and R2 are large, slight conduction by a polymer will be sufficient to produce an output voltage of V_{DD}. Thus, as input voltage is scanned from negative of V_1 to positive of V_4, the output of the converter will show the progression *00, 01, 10, 11*. In addition to A/D conversion, the circuit in Scheme I can also carry out translation of quaternary logic,[2] based on four logic levels, to standard two-level binary logic. If the input voltage is a quaternary logic signal, where V_1, V_2, V_3, and V_4 are the logic levels signifying the base 4 digits 0, 1, 2, and 3, respectively, then the circuit correctly translates quaternary *0* to binary *00*, quaternary *1* to binary *01*, quaternary *2* to binary *10*, and quaternary *3* to binary *11*. The circuit would also translate ternary (3-state)[2] logic to binary if ternary 0,1, and 2 were represented by V_1, V_2, and V_3, respectively. Since V_4 would not be required for a ternary input, polymer 3 is required for quaternary to binary translation, but not ternary to binary operation.

This unusual design for analog-to-digital conversion is a further demonstration of device opportunities which arise from the finite window of high conductivity. The circuit shown in Scheme I is relatively simple and requires only a single transistor switching event to carry out a conversion. Only one transistor conducts at any one time, so the circuit consumes minimum power. The basis of the design is the use of different active materials of different finite windows ofconduction.

Scheme I

Design for a Microelectrochemical Analog to Digital Converter Based on Three Different Conducting Polymer Transistors

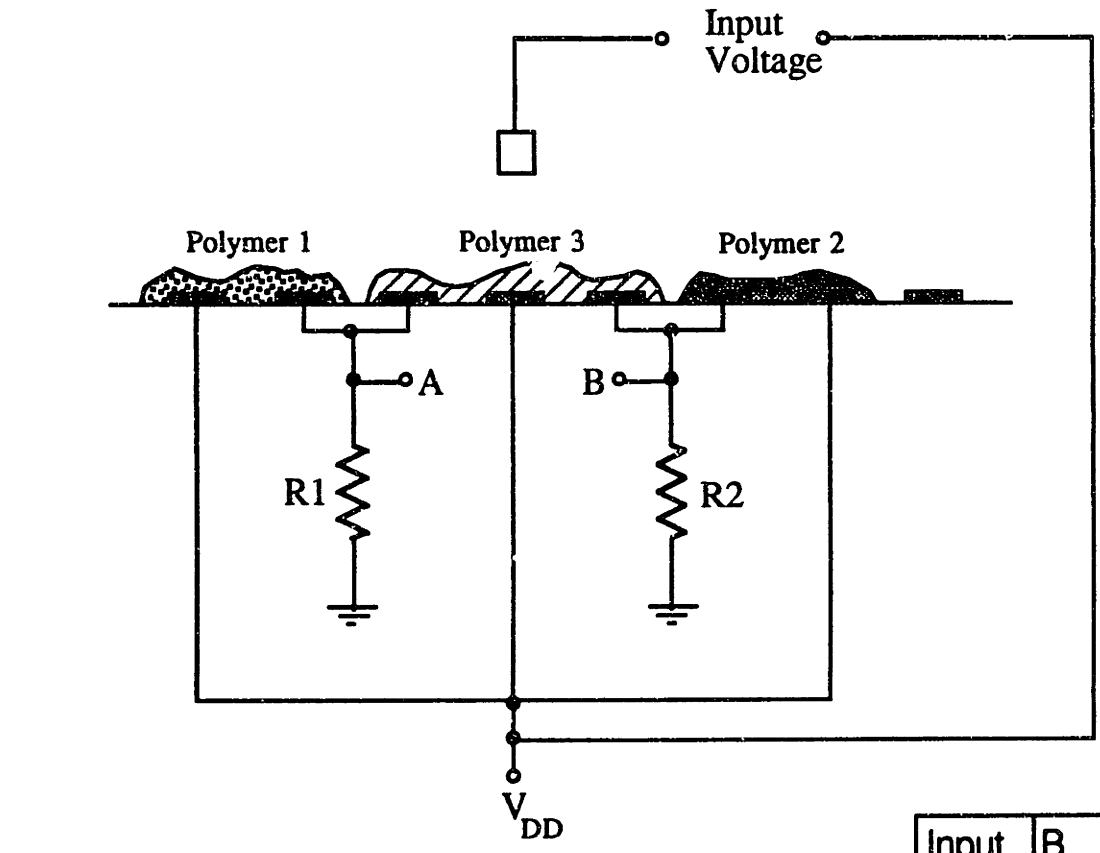

Input	B	A
V_1	0	0
V_2	0	V_{DD}
V_3	V_{DD}	0
V_4	V_{DD}	V_{DD}

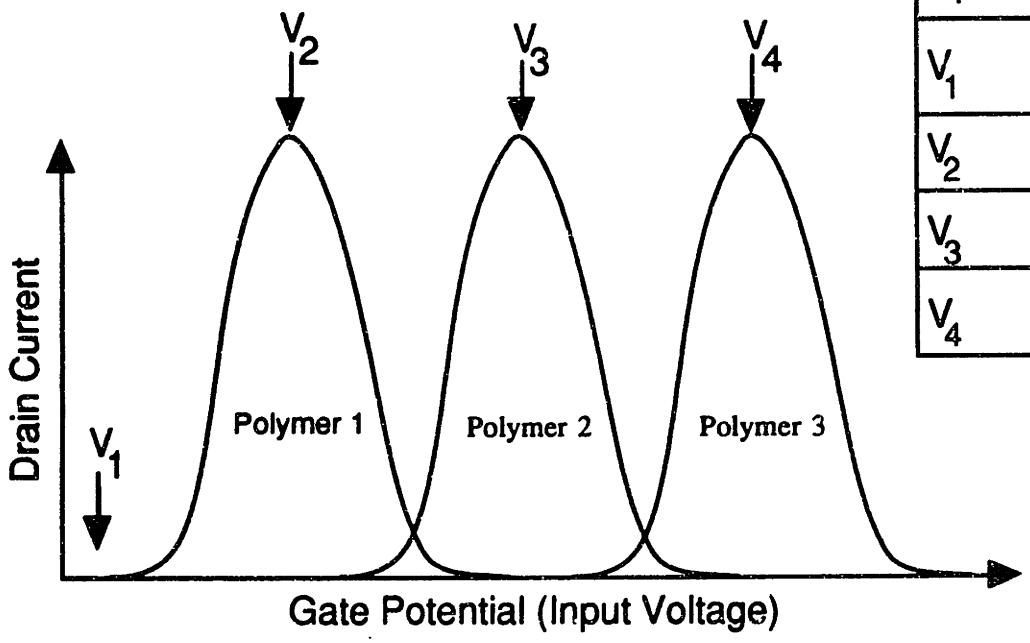

Materials suitable for the device required for realization of Scheme I can be selected. One trio of appropriate polymers for demonstration of the circuit in Scheme I is trifluoroacetylated polyaniline,[3] poly(3-(4-methoxyphenyl)-thiophene),[4] and chlorinated polythiophene[5] (chlorinated to the 1.30 V maximum obtainable for onset of conduction) as polymer 1, 2, and 3, respectively. Scheme II shows the range of potential over which each polymer is conducting. This trio of polymers yields the appropriate overlaps of I_D-V_G

Scheme II

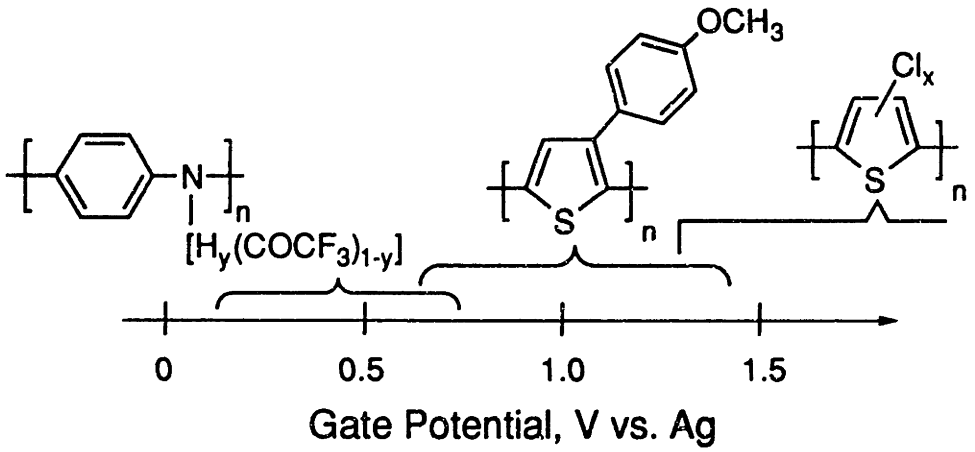

characteristics. Further, all three polymers are of comparable conductivity. Trifluoroacetylated polyaniline was chosen because by controlled, *in situ* acylation its conductivity can be matched to that of the other two polymers, as demonstrated in Chapter 6. Further, Trifluoroacetylation of polyaniline is accompanied by a contraction in the window of conductivity of the polymer with a cathodic shift in potential for onset of oxidative insulation, providing a wider gap between that potential and onset of conduction for chlorinated polythiophene (1.30 V vs Ag). This wider gap makes room for the window of conductivity of poly(3-(4-methoxyphenyl)-thiophene) which shows onset of conduction at 0.65 V vs Ag and onset of insulation at ≈1.4 V vs Ag to serve as polymer 2. While the conductivities of poly(3-(4-methoxyphenyl)-thiophene) and heavily chlorinated polythiophene are not high (10^{-2} S/cm), this is not a critical issue, since large drain currents

are not required. For further details concerning these polymers, see Chapter 5 and Chapter 6. If a device of the type in represented in Scheme I were to be prepared, polythiophene would be deposited first and chlorinated, followed by deposition of poly(3-(4-methoxyphenyl)-thiophene), and finally deposition and trifluoroacetylation of polyaniline.

Design of A Microelectrochemical Transistor-Based Binary Arithmetic Adder.

One function commonly associated with digital logic[1] is the ability to process numbers. The design of a circuit capable of the addition of two numbers based solely on microelectrochemical transistors was undertaken. The task of addition of two one-bit binary numbers was chosen as the goal. The circuit which accomplishes that task must behave in the following way. For addition of two numbers X and Y, Table 1 shows the results in binary (base 2) and decimal (base 10) and the electrical representation as two output levels S2 and S1. S2/S1 is a binary number, S1 being the one's place and S2 being the two's place. As in design of an organic synthesis, it is easiest to develop an

Table 1. Sum of two numbers X and Y in binary and decimal

X	Y	X+Y (binary)	X+Y (decimal)	Digital representation (S2/S1)
0	0	00	0	LOW/LOW
1	0	01	1	LOW/HIGH
0	1	01	1	LOW/HIGH
1	1	10	2	HIGH/LOW

approach starting with the ultimate target and working backwards, analogous to retrosynthetic analysis. Table 1 defines the target, requiring the output shown for S2/S1 given inputs X and Y. First, using standard logic gates,[1a] the design will be defined in a block diagram. It is seen in Table 1 that if either X *or* Y is a 1, then S1 must be 1. An OR

gate provides this relationship. Further, if X *and* Y are 1, then S2 must be 1, a relationship provided by an AND gate. However, when X and Y are both 1, then S1 must be 0 and an OR gate gives a 1 as long as either input is a 1. Thus, a means of setting S1 to zero when X and Y are both 1 must be added to the output of the OR gate. Accounting for this leads to the layout shown in Scheme III as one possible rendition of an adder, based essentially on one AND gate and an exclusive OR gate of which the AND gate is a part. (An exclusive OR gate[1b] is a variation on the OR gate in which the output is HIGH only if *one* of the inputs, but not both, are HIGH). If X and Y are both 0, then the output of both the OR gate and the AND gate are 0. If X or Y (but not both) is 1, then the output of the OR gate is 1 and the output of the AND gate is 0. If both X and Y are 1, the outputs of both the OR gate and the AND gate are 1. This is almost what is required, except that 1 + 1 = 10, not 11 in binary, so the provision must be made to cause S1 to be LOW if S2 is HIGH, giving an overall exclusive OR function. This is represented as and S1 switch, which forces S1 to be LOW if S2 is HIGH. With this provision, the circuit shown in Scheme III should behave as required.

Scheme III

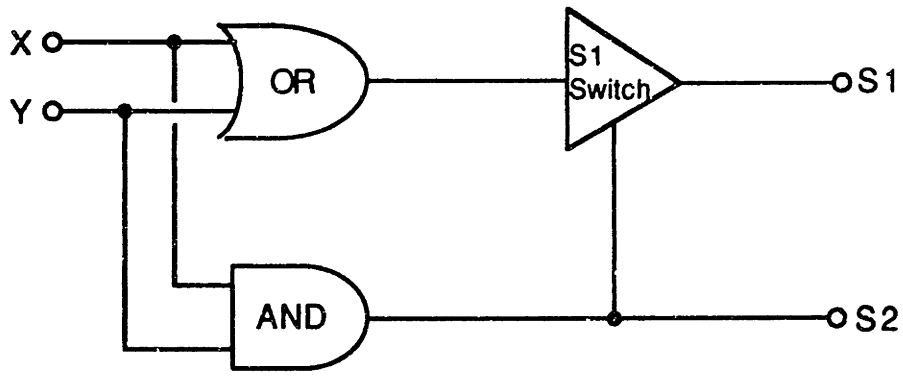

The next step is to implement each of the 3 functions in Scheme III with microelectrochemical transistors. Scheme IV shows a circuit which should provide the OR function. It is based on three WO_3 transistors, labeled Q1,Q2, and Q3. Circuit design and

function are based on the potentiostat-free operation of microelectrochemical transistors demonstrated in Chapter 4 for the complementary microelectrochemical transistor inverter gate, using logic levels of 0 V vs. SCE as LOW and 400 mV vs. SCE as HIGH, with a power supply voltage of 400mV. In the OR gate in Scheme IV, if input A is high, then the source electrode of transistor Q1 is 400 mV negative of SCE where WO_3 is conducting and

Scheme IV. Design for a Microelectrochemical OR Gate

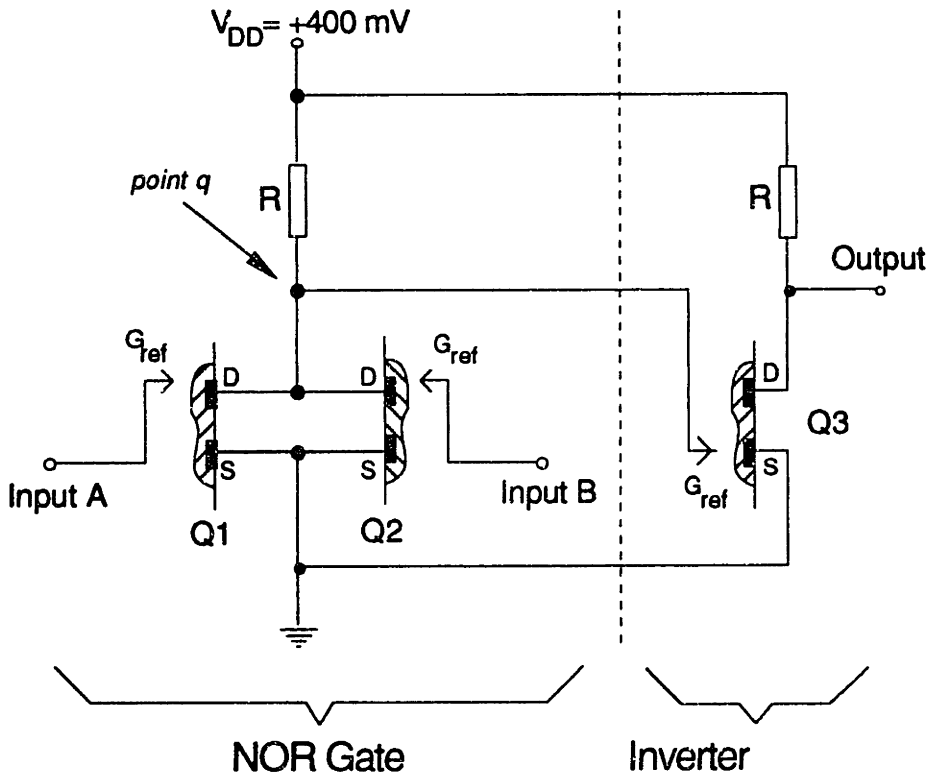

Q1, Q2, Q3 = Tungsten Trioxide METs
Gate Electrode = SCE

drain current flows through Q1. Similarly, Q2 conducts if input B is HIGH. If either Q1 or Q2 is conducting, then point q will be grounded, i.e. LOW. If neither Q1 nor Q2 is conducting, point q will be at 400 mV with respect to ground, i.e. HIGH. Notice that this is the inversion of the OR function so an inverter is added to produce an overall OR

function response. As it turns out, this often happens in gate design and it is common that an inverter is the final stage of the gate.[1a] The value of R should be large compared to the on resistance of the transistors, and 10KΩ is suitable as demonstrated in Chapter 3.

The AND function was developed along similar lines, this time using polyaniline as the device-active material. Scheme V shows the circuit for a microelectrochemical AND gate. The AND function must deliver a HIGH output if and only if both inputs are HIGH.

Scheme V. Design for a Microelectrochemical AND Gate

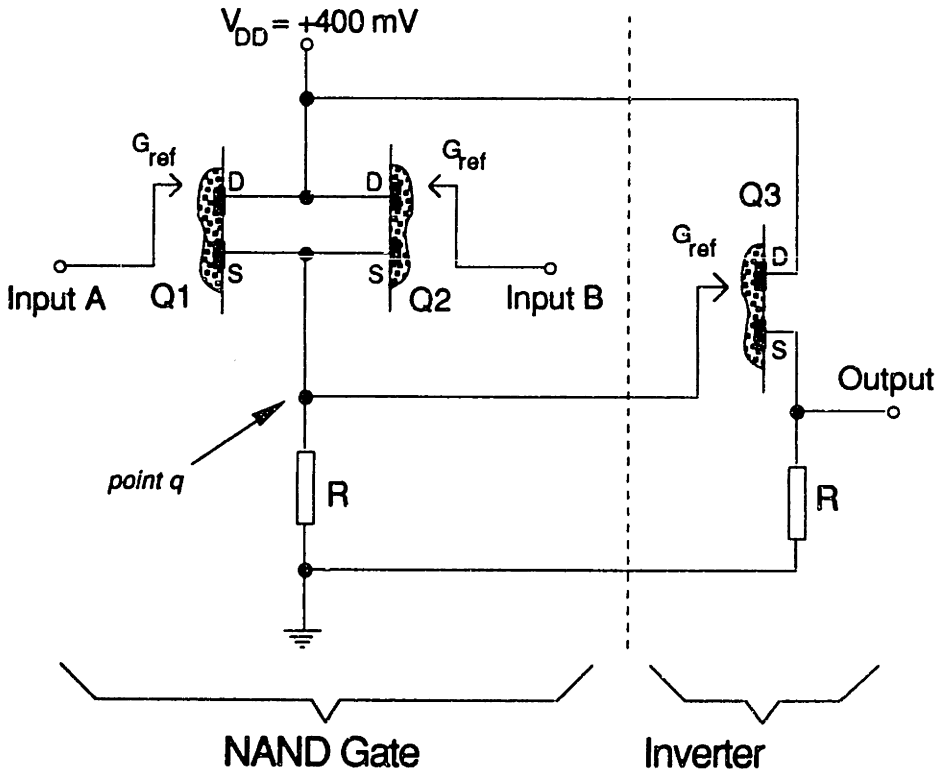

Q1, Q2, Q3 = Polyaniline METs
Gate Electrode = SCE

If input A in Scheme V is LOW, then the drain of Q1 is held 400 mV positive of the SCE reference/counter electrode. Polyaniline is conducting at that potential, so point q in

Scheme V is at 400 mV with respect to ground (HIGH). Similarly, if input B is LOW, Q2 conducts and point q is held at 400 mV vs. ground. Q1 and Q2 with source resistor R constitute a NAND function (the inversion of the AND function) so inverter transistor Q3 is added. If input A and input B are HIGH, both Q1 and Q2 are insulating since both have polyaniline at 0 V vs SCE and point q is at zero vs. ground (logic level LOW). Thus, the SCE counter/reference electrode is at zero and the drain of Q3 is at 400 mV with respect to ground. The polyaniline of Q3 is thus conducting, and the output terminal is at 400 mV, i.e. HIGH. The output is therefore only high when Q1 and Q2 are both insulating which only occurs when both input A and input B are HIGH, thus achieving the AND function.

The final requirement to complete the layout in Scheme III is the provision that when S2 is HIGH, S1 must be low. This is integrated in to the overall design for a binary adder shown in Scheme VI. For simplicity, the microelectrochemical transistors have been given schematic symbols in which a rectangle represents the device-active material to which connections are made (the drain and source electrodes), and a parallel line represents the counter/reference electrode. The arrows indicate the electrode designated as the source, and whether electrons must be injected (as in WO_3) or withdrawn (as in polyaniline) to obtain conductivity. Q1, Q2, and Q3 form an OR gate while Q4, Q5, and Q6 comprise the AND gate. Inputs X and Y drive both gates. Transistor Q7 serves as the S1 switch. When the output of the OR gate (the drain of Q3) is HIGH and the output of the AND gate (drain of Q6/S2) is LOW, then the drain of Q7 is 400 mV positive of its SCE counter/reference electrode and Q7 conducts, allowing the HIGH output of the OR gate through to the S1 output. If, however, the AND gate output is HIGH (which of course requires the OR gate output to be HIGH also) then the source and SCE counter/reference electrodes are both at the same potential, and at 0 V vs. SCE polyaniline is insulating. Further, the drain electrode of Q7 cannot be brought to a potential positive of SCE as long as the SCE counter/reference electrode is HIGH (400 mV) with respect to ground. Under these

circumstances Q7 is insulating, blocking the HIGH output of the OR gate so that S1 is LOW in order to provide the required *10* output for S2/S1 when both X and Y are 1. When Q7 is insulating, it cannot actively hold S1 at ground so a 150 KΩ resistor is provided for that purpose. The large value assures that the resistor will not prevent S1 from achieving a HIGH output, since it is large compared to the 10 KΩ output impedance of the OR gate in the HIGH output state.

While the binary adder of Scheme VI has been designed using both polyaniline and WO_3 devices, an all-polyaniline design would require only that a counter/reference electrode of electrochemical potential slightly positive of the potential for onset of oxidative insulation for polyaniline be used for transistors Q1, Q2, and Q3 to provide the correct function whereby holding the source electrode negative of the counter/reference electrode results in conduction. This option is made possible by the finite window of high conductivity which allows the same microelectrochemical transistor to provide a response analogous to either an *n*-channel or *p*-channel MOSFET. The design in Scheme VI is most appropriately described as a member of the resistor-transistor logic family. However, the binary adder could also have been designed around complementary microelectrochemical transistor (CMET) logic of the type demonstrated in Chapter 4. CMET design is made particularly simple by the fact that conventional CMOS design can be directly translated to CMET gates, as demonstrated in Chapter 4.

In summary, the design of a microelectrochemical circuit for analog-to-digital conversion and quaternary-to-binary translations and of a circuit capable of adding two numbers demonstrates that the results reported in the previous chapters of this thesis provide a sufficient basis for the design of multi-transistor circuits capable of complex functions.

Scheme VI. Design for a Microelectrochemical Binary Adder

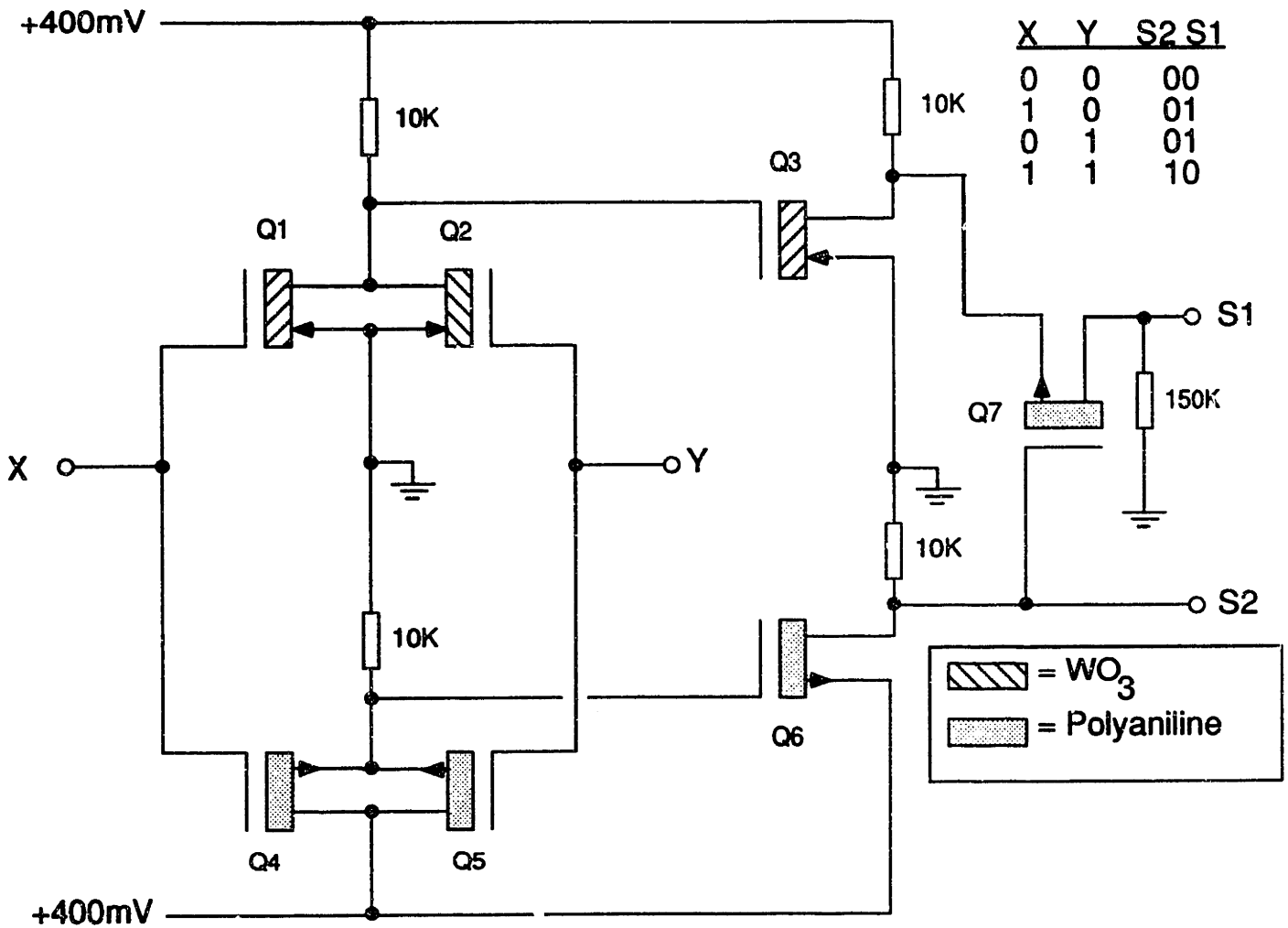

X	Y	S2 S1
0	0	00
1	0	01
0	1	01
1	1	10

References

1. Horowitz, P.; Hill, W. *The Art Of Electronics*; Cambridge University Press: New York, 1989.; a) Chapter 8; b) pp. 479-480

2. *Computer Science and Multiple-Valued Logic: Theory and Applications 2nd ed.*; Rine, D. C., ed.; Elsevier Science Publishing Co.: New York, 1984

3. Chapter 6, sections 6.1, 6.4, this thesis

4. Chapter 5, this thesis

5. Chapter 6, section 6.3, this thesis